NASA TECHNICAL TRANSLATION NASA TT F-16170

WIND ENGINES AND WIND INSTALLATIONS

Ye. M. Fateyev

(NASA-TT-F-16170) WIND ENGINES AND WIND INSTALLATIONS (Kanner (Leo) Associates) 391 p HC $10.25 CSCL 10A
N75-22904
Unclas
G3/44 20751

Translation of "Vetrodvigateli i Vetroustanovki", Moscow, State Publishing House of Agricultural Literature, 1948, pp 1-544

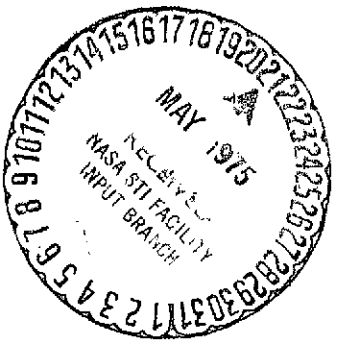

NATIONAL AERONAUTICS AND SPACE ADMINISTRATION
WASHINGTON, D.C. 20546 MARCH 1975

STANDARD TITLE PAGE

1. Report No.	2. Government Accession No.	3. Recipient's Catalog No.
NASA TT F-16170		

4. Title and Subtitle	5. Report Date
WIND ENGINES AND WIND INSTALLATIONS	March 1975
	6. Performing Organization Code

7. Author(s)	8. Performing Organization Report No.
Ye. M. Fateyev, Doctor of Technical Science	10. Work Unit No. NASw-2481
	11. Contract or Grant No.

9. Performing Organization Name and Address	13. Type of Report and Period Covered
Leo Kanner Associates, Redwood City, California 94063	Translation

12. Sponsoring Agency Name and Address	14. Sponsoring Agency Code
National Aeronautics and Space Administration, Washington, D.C. 20546	

15. Supplementary Notes

Translation of "Vetrodvigateli i Vetroustanovki", Moscow, State Publishing House of Agricultural Literature, 1948, pp 1-544

16. Abstract A comprehensive theoretical treatment of aerodynamics precedes the description of wind engines and wind installations. Wind tunnels, the aeordynamic characteristics of wind engines, towers and related equipment, used for testing wind engines, are described in detail. Three methods of adjustment of wind engines to the wind are described, as are several ways for regulating the number of revolutions and the power of wind engines. A chapter on wind engine design ends the first part of the book. Under the heading "Wind Installations," wind energy, anemographs, wind engines working with piston and centrifugal pumps and with various agricultural machines are described. Windmills and windpower stations are discussed. The book ends with a chapter on installation and maintenance of wind engines.

17. Key Words (Selected by Author(s))	18. Distribution Statement
	Unclassified-Unlimited

19. Security Classif. (of this report)	20. Security Classif. (of this page)	21. No. of Pages	22. Price
Unclassified	Unclassified	386	

TABLE OF CONTENTS

INTRODUCTION

1. Development of Wind Utilization 1
2. Utilization of Wind Engines in Agriculture 3

PART I. WIND ENGINES

CHAPTER 1. BRIEF OUTLINE OF AERODYNAMICS 6

3. The Air and its Properties 6
4. The Continuity Equation. The Bernoulli Equation 10
5. The Concept of Turbulent Motion 19
6. Viscosity 28
7. The Law of Similarity 30
8. The Border Layer and the Turbulence 33

CHAPTER 2. MAIN CONCEPTS OF EXPERIMENTAL AERODYNAMICS 38

9. Axes of Coordinates and Aerodynamic Coefficients 38
10. Determination of Aerodynamic Coefficients. Lilienthal's Polar 40
11. Induced Drag of the Wing 43
12. N. E. Zhukovskiy's Theorem on the Lifting Force of the Wing 46
13. Transition from one Wing Span to Another 52

CHAPTER 3. SYSTEMS OF WIND ENGINES 58

14. Classification of Wind Engines According to the Principle of Their Operation 58
15. Advandages and Disadvantages of Various Systems of Wind Engines 65

CHAPTER 4. THEORY OF THE IDEAL WIND ENGINE 68

16. The Classical Theory of the Ideal Wind Engine 68
17. The Theory of the Ideal Wind Engine of Prof. G. Kh. Sabinin 72

CHAPTER 5. THE THEORY OF THE REAL WIND ENGINE OF PROF. G. KH. SABININ 82

18. Work of the Elementary Blades of the Wind Wheel. First Equation of Relation 82
19. Second Equation of Relation 86
20. Moment and Power of the Whole Wind Engine 88
21. Losses of Wind Engines 90
22. Aerodynamic Analysis of the Wind Wheel 93
23. Calculation of the Performance of the Wind Wheel 97
24. The Profiles "Espero" and Their Construction 101

CHAPTER 6. EXPERIMENTAL CHARACTERISTICS OF WIND ENGINES 107

25. Method for Obtaining the Experimental Characteristics 107
26. Aerodynamic Characteristics of Wind Engines 116

27. Experimental Testing of the Theory of Wind Engines 121

CHAPTER 7. EXPERIMENTAL TESTING OF WIND ENGINES 125

28. Equipment of Towers for the Testing of Wind Engines 125
29. Correspondence Between the Performance of the Wind Engine and Its Model 129

CHAPTER 8. ADJUSTMENT OF THE WIND ENGINES TO THE WIND 133

30. Adjustment by Means of the Tail 133
31. Adjustment by Means of Windroses 141
32. Adjustment by Disposition of the Wind-Driven Wheel Behind the Tower 143

CHAPTER 9. REGULATION OF THE NUMBER OF REVOLUTIONS AND OF THE POWER OF WIND ENGINES 145

33. Regulation by Removing the Wind-Driven Wheel from the Wind 146
34. Regulation by Decreasing the Area of the Wings 154
35. Regulation by Rotation of the Blade or Part of it Around the Axis of the Flap 154
36. Regulation by Means of Air Brakes 160

CHAPTER 10. WIND ENGINE DESIGN 162

37. Multi-Bladed Wind Engines 163
38. Rapid (Sparsely-Bladed) Wind Engines 164
39. Weight of the Wind Engine 176

CHAPTER 11. CALCULATION OF THE STRENGTH OF WIND ENGINES 181

40. Wind Load on the Wings and Calculations of the Strength of the Wings 181
41. The Wing Load on the Tail and on the Regulating Lateral Blade 196
42. Calculation of the Head of the Wind Engine 197
43. The Gyroscopic Moment of the Wind-Driven Wheel 200
44. The Power of Wind Engines 202

PART TWO

WIND POWER INSTALLATIONS

CHAPTER 12. THE WIND AS A SOURCE OF ENERGY 212

45. The Origin of the Wind 212
46. Principal Magnitudes Which Characterize the Wind From the Energetic Viewpoint 214
47. The Energy of the Wind 232
48. Accumulation of the Wind Energy 235

CHAPTER 13. CHARACTERISTICS OF WIND POWER UNITS 242

49. Performance of Wind Engines and of Piston Pumps 242
50. Operation of Wind Engines with Centrifugal Pumps 258

51. Operation of Wind Engines with Millstones and Agricultural Machines 278

CHAPTER 14. WIND-DRIVEN PUMP INSTALLATIONS 293

52. Wind-Driven Pump Installations for Water Supply 293
53. Water Tanks and Water Towers in Wind Pump Installations 299
54. Standard Designs of Wind Pump Installations 301
55. Experience with Exploitation of Wind Pump Installations for Water Supply in Agriculture 307
56. Wind-Driven Irrigation Installations 311

CHAPTER 15. WINDMILLS 318

57. Types of Windmills 318
58. Technical Characteristics of Windmills 319
59. Increasing the Power of Old Windmills 322
60. The New Type of Windmill 324
61. Performance Characteristics of Windmills 334

CHAPTER 16. WIND POWER STATIONS 340

62. Types of Generators for Operation With Wind Engine and Voltage Regulator 341
63. Wind Charging Units 345
64. Low-Power Wind Power Stations 347
65. Parallel Operation of Wind Power Stations in a General Circuit with Large Thermic Stations and Hydropower Stations 348
66. Experimental Testing of the Operation of Wind Power Stations Connected Parallel in the Circuit 352
67. High-Power Power Stations Connected in Parallel 359
68. Brief Data on Foreign Wind Power Stations 365

CHAPTER 17. BRIEF DATA ON THE INSTALLATION AND MAINTENANCE OF WIND ENGINES 371

69. Installation of a Low-Power Wind Engine, from 1 to 15 hp 371
70. Maintenance and Servicing of Wind Engines 375
71. Safety Measures During Installation and Servicing of Wind Engines 378

REFERENCES 382

WIND ENGINES AND WIND INSTALLATIONS

Ye. M. Fateyev
Doctor of Technical Sciences

Introduction

/3*

1. Development of Wind Utilization

In our country, the energy of the wind has been widely utilized for a long time, mainly in the rural flour-mill industry. The number of windmills reached 200,000 and in some large villages, there were up to 80 flour mills. These were wooden mills manufactured by the local farmers which had an average power of approximately 5 hp, as a rule; rarely large windmills were found with a diameter of the wheel of 20-24 meters, and a power of 15-20 hp. In such a manner, the homemade mills had an average established power of 1,000,000 hp. The average annual production of such a mill amounted to around 8500 hp hours, consequently, all the existing mills produced 1700 million hp hours per year. Considering that the specific output of a mill was kg/per hp hour, we find that all the windmills of Russia ground around 34 million tons, or 2 billion pood of grain per year.

The construction of wind engines was based merely on the practical experience of many years. The foremen taught the future generations not from books, but from their practical work.

The development of engineering by the end of the nineteenth century has made it possible to create a new type of wind engine with automatic adjustment to the wind and with control of the number of revolutions. The mass production of multi-blade windmotors of metallic construction started to develop.

The development of aviation, the enormous success of which is due to the true creator of modern aerodynamics, the renowned Russian scientist N. Ye. Zhukovskiy, created the conditions for solving anew the theoretical problems of utilization of wind energy. In 1914- /4
1918, N. Ye. Zhukovskiy and his disciples who are now eminent scientists in the USSR, V. P. Vetchinkin, G. Kh. Sabinin, G. E. Proskura and others, elaborated for the first time the theory of wind engines.

The theory and experimental testing of airplane wing and propeller has been applied to the study of phenomena taking place during the passage of the air flow through the wind-driven wheel. In the USSR, in the Central Aerodynamic Institute, the Central Wind Energy Institute and in the All Union Institute for Mechanization and

* Numbers in the margin indicate pagination in the foreign text.

Electrification of Agriculture, several original theoretical and experimental studies have been performed on wind engines and wind-driven installations which to date form the basis of the development of Soviet wind technology.

At the same time an expansion is observed in the field of application of wind engines in the national economy. In addition to flour-mill industry and water supply, they are used for a wider mechanization in agriculture, for example, for the preparation of forage in animal husbandry, the irrigation of fields and vegetable cultures, the lighting of villages, etc.

In the Soviet Union, wind installations have found wide application and are acquiring a growing importance. The favorable wind conditions of the South, which is characterized by high annual averages of wind velocity, make it possible to use the adjustable D-12 wind engine, which gives completely uniform current voltage, and meets the demands of electrical energy.

The energy of the wind can be utilized almost everywhere; therefore, it has special importance among the other sources of energy.

Wind utilization in the USSR has been regarded as an important State problem. As early as 1918, V. I. Lenin considered it imperative to instruct the Acadamy of Sciences to include in its plan of reorganization of the industry and for the economical development /5 of Russia, among other problems, water power and wind engines in general, and their application to agriculture in particular.[1]

The 18th Congress of the VKP, in its resolution based on the report of Comrade V. M. Molotov indicated: "To develop more extensively the construction of small wind-driven electro-stations for purposes of fuel economy."

"To develop widely the construction of small kolkhoz hydro-stations, wind power and gas generator electro-installations based on local fuel."

"To organize mass production of wind engines."[2]

The law on the five-year plan for restoration and development of national economy in the USSR in the years 1946-1950 says: "To ensure mass construction in rural localities of small hydro-electro-stations, wind stations and thermal-electro-stations with portable steam and gas generator engines.

---

1 V. I. Lenin, "Outline of the plan of scientific and technical works" Sochinenya [works], Vol. XXII, 1931, p. 232

2 VKP (b) in resolutions and decisions of congresses, conferences and plenums/" of Tsk, part 2, 1941, pp 735-739

2. Utilization of Wind Engines in Agriculture

The energy of the wind is utilized in various branches of the national economy, but wind installations have received massive development in the agriculture.

In the area of water supply, it is most advantageous and convenient to utilize wind engines. With the aid of a water tower with a container for the storage of water for one or two days, it is possible to supply the farm with water by means of the energy of the wind. By pumping up the water into the reservoir, the wind engine accumulates the energy of the wind in the form of lifted water.

In such a manner it is possible to liberate completely man power, which in many places of the USSR is still widely used for the transport of water. The wind engines acquire an extreme importance in the water supply of animal husbandry in the steppe regions where water is mainly obtained from deep holes and wells. Here, the utilization of wind-driven installations is /6 the most accessible method for the mechanization of water lifting.

Irrigation is one of the main parts of the complex measures in the campaign for high crops. Mechanization of water lifting in irrigation systems meets with serious difficulties due to the lack of local energy resources.

The utilization of wind energy may in several cases solve quite satisfactorily the task of mechanization of irrigation, especially with regard to small parcels with vegetable cultures and fields, where the schedule of watering is not that rigorous. Vegetable cultures require artificial irrigation almost everywhere and not only in dry years. Here, wind engines can be conveniently utilized for lifting the water to a height of 4 to 20 meters. A wind engine with a power of 15 hp can irrigate during a season up to 15-20 hp lifting the water up to 10 m. It is advisable to combine the work of the wind engine, as far as irrigation is concerned, with some other kind of work, for example, electrical lighting or grinding, in those periods when no irrigation is required.

The drying of swampy land is a case in which wind engines have been most conveniently used in agriculture. Here there is no need for storage battery installations, nor for the daily presence of man in order to start and stop the wind engine; the engine can operate and pump up the water from the drainage system all the time, as long as there is wind. The agriculture of Holland is very much indebted to the work of wind engines which transformed swampy lands into fertile fields.

It is not accidental that the grinding of seeds in windmills

has its history of many centuries. Long ago, windmills played the /7
most important role in the rural flour mill industry. This type of work, while quite cumbersome, has a highly flexible schedule of loading. In addition, the possibility of performing the grinding in the stock, makes it possible for the wind engine to operate all the time, as long as there is wind. In this case, it is completely unnecessary to store energy; the energy accumulates in the product of the flour mill industry itself. In such a manner, windmills allow for a fairly complete utilization of wind energy. The windmills in the USSR, can grind, on the average, around 2.5 billions of pood of grain per year. If the same amount of grinding were to be performed with common engines, around 1.3 millions of tons of a nominal 7000-calorie fuel would have to be used yearly. By using wind engines for this kind of work, an enormous amount of fuel is being saved, and at the same time both railway and animal transport are freed of the transportation of this fuel.

The preparation of forage for animal husbandry, such as grinding of seeds and of oil cake, cutting of silo and washing of root crops, make a fairly cumbersome process of production which should be mechanized entirely. The utilization of windmills encounters no difficulties in this respect, since the processing of seeds, of oil cakes, and of straw, can be performed in stock. Complications may arise only when preparing root crops on calm days. However, since one has in reserve horse-drawn actuators, one can always ensure the work of machines for the preparation of root crops.

The charging of storage batteries for electrical lighting, radio and automobile transportation, can be performed anytime during the day. Consequently, the utilization of low-power windmills, ranging from 100 to 1000wWt, as wind charging units encounter no difficulties due to the inconsistency of the wind in the course of time, and should find wide application.

The electrification of the agriculture by means of wind engines forms an essential task. The operation of wind engines with generators, makes it possible to utilize the energy of the wind in almost all kinds of agricultural work and for lighting.

However, a serious handicap in the utilization of wind energy for electrification, especially in those regions where the annual average wind speed is below 5 m/sec, is the necessity of accumula- /8
ting energy in order to obtain a constant voltage current and to ensure the supply of electrical energy on calm days.

Large wind electro-stations, can obviously be efficiently utilized parallel with other electro-stations, such as thermal and hydraulic.

The above presented list of the main branches of agriculture where wind engines are widely and successfully utilized shows the importance and the significance in the development of wind utilization in our socialist economy.

Mechanization of agricultural work by means of wind energy is quite simple and is accessible to the abilities and means of the kolkhozes. In those regions where the annual average wind speed is above 4 m/sec, the cost of production of wind engines is lower than the cost of production of thermal engines under identical conditions. The cost of operation of wind power units is not higher than the cost of operation of thermal and hydraulic engines, and is about 10 times cheaper than the work of horse-drawn gear.

Wind installations are used abroad for various agricultural works; wind-driven pump installations have gained the widest distribution. The wind engines produced for this purpose are of the multi-blade type and are geared to a piston pump.

PART I. WIND ENGINES

Wind engines are engines which transform the energy of /11
the wind into mechanical work. The inconstancy and rarity of this energy determine the construction features of wind engines 1. the presence of devices ensuring the operation of wind engines at high wind speeds, with an approximately constant power and a limited number of revolutions; 2. the awkwardness of wind engines at somewhat higher values of power.

The complexity of scientific and practical problems of utilization of wind energy by means of wind engines, is presently a technical discipline called wind technology.

The main task of wind technology is to create wind engines and wind installations which are capable of providing a motive force which is convenient for utilization and to work with a high output coefficient of wind energy.

Wind technology can be divided into the following parts: 1. the theory and experimental investigation of wind engines; 2. the construction of effective wind engines; 3. the study of the energy problems related to wind; 4. the construction of wind installations and their rational exploitation.

The main section of wind technology is the theory and experimental investigation of wind engines, which are based on aerodynamics -- the science studying air movement and the action of air on the bodies which come in contact with it.

Aerodynamics can be divided into theoretical and experimental. Theoretical aerodynamics is based on the laws of mechanics applied to gas-like bodies; experimental aerodynamics is based on tests performed in wind tunnels and under natural conditions.

We shall be concerned with aerodynamics only insofar as it is directly related to the study of wind engines.

CHAPTER 1. BRIEF OUTLINE OF AERODYNAMICS [55] /12

3. The Air and its Properties

The air blanket surrounding the Earth is called the Earth's atmosphere. The height of the upper limit of the atmosphere has not been established, however, it is known that meteorites catch fire at the height of 200-300 km, while the Northern Lights are observed at even greater altitudes, from 300 to 750 km. This phenomenon attests to to the fact that the Earth's atmosphere has an upper limit of no less than 300 km.

The troposphere. The lower layer of the atmosphere up to an altitude of about 11 km, is called troposphere. With the change in latitude, the average annual altitude of the troposphere changes from 8 km at the poles to 17 km at the equator. It is convenient to consider it equal to an average of 11 km at a latitude of 50° to 60°. The topography and thermal changes of the Earth, as well as solar radiation, influence the state of the troposphere. This is where the vertical flow of the air takes place, clouds are formed, precipitation falls and the wind blows. In such a manner, the troposphere is in a state of constant agitation of its layers, as a result of which, the composition of the air in the troposphere is quite homogeneous. Dry air contains in percentage by volume:

Nitrogen.....N_2	78.03	Carbon dioxide.....CO_2	0.03
Oxygen.....O_2	20.99	Neon.....Ne	0.0012
Argon.....Ar	0.94	Helium.....He	0.0004

and insignificant amount (traces) of krypton and xenon.

By weight, the air contains 23.2% oxygen and 76.8% other gases.

The stratosphere. The layers of the atmosphere situated above the troposphere form the stratosphere. The state of the stratosphere is characterized by the fact that there is almost no vertical dis- /13
placement of layers. The winds are characterized by great constancy; there are neither clouds nor fog; the temperature is almost constant and equals -56.5°.

Investigations of the stratosphere are performed by means of sounding balloons which contain recording meteorological instruments. In the USSR the stratosphere is studied by Prof. Molchanov, by means of radio sounding balloons, which automatically transmit the readings of the instruments to the Earth by radio.

Until today, a layer of the atmosphere with a thickness of 20 km has been investigated. The highest altitude reached by some sounding balloons is 37 km while the height reached by man equals 22 km. In such a manner, the upper layer of the atmosphere has not been studied yet and any conclusions about its state were expounded by various investigators on the basis of theoretical assumptions, by comparing with observed phenomena of nature as for example, the brightness of twilight. The chemical composition of the stratosphere air has not been determined as yet, there are merely assumptions about it. For example, according to Henfry, at a height of 100 km, the percentages by volume are: Nitrogen N_2-2.95, water vapor H_2O-0.04, Oxygen O_2-0.11, Hydrogen H_2-95.58, Helium He-1.31, overall pressure 0.0067 mm Hg, and at the height of 140 km: Nitrogen-0.01, water vapor 0, Oxygen-0, Hydrogen-99.15, Helium-0.84 and overall pressure 0.0040 mm Hg.

The composition of the air remains unchanged, i.e., just like near the surface of the Earth, up to an altitude of about 22 km.

Air pressure. The elasticity of the air is manifested in the pressure it exerts on the bodies which come in contact with it. The pressure of the air on a body is perpendicular to its surface and is the limit of the ratio of the pressure ΔP to the area ΔF:

$$p = \lim \frac{\Delta P}{\Delta F} = \frac{dP}{dF}.$$

In aerodynamics it is convenient to measure the pressure in kilograms per square meters (kg/m^2). In measuring the air pressure by barometer, the magnitude of the pressure is expressed in mm Hg.

The normal pressure of the atmosphere measured by a barometer, at sea level, equals:

$$p_0 = 760 \text{ mm Hg}$$

In the technical system of measurement, this pressure equals:

$$p_0 = 10\,333 \text{ кг/м}^2 = 1{,}0333 \text{ kg/cm}^2$$

The unit of pressure in technical calculations is the atmo- /14
sphere, which equals 1 kg/cm^2.

$$1 \text{kg/cm}^2 = \frac{760}{1{,}033} = 735{,}6 \text{ mm Hg}$$

hence:

$$p \text{kg/cm}^2 = \frac{p \text{ mm Hg}}{735{,}6}.$$

Often it is not the absolute pressure of the atmosphere which is used in calculations, but the excess pressure over the atmospheric one:

$$p' = p - p_0,$$

where p_0 is the atmospheric pressure.

Air temperature. The temperature of the air is usually measured in degrees Celsius. In thermal calculations, the temperature is taken in absolute degrees, which is called the absolute temperature. The zero of the absolute temperature is 273° below the zero of the Celsius scale.

Denoting the absolute temperature by T, we obtain:

$$T = 273 + t.$$

The normal temperature t of the air in the USSR is assumed to be equal to 15° C; in other countries, the standard temperature is convened at 20° C.

The temperature in the troposphere at altitudes lower than 11 km is

$$t_T = 15^\circ - 6.5H, \tag{1}$$

while 6.5 is the average annual change in the temperature of the troposphere per km of increase in altitude H = 11 km.

The pressure at altitudes lower than 11 km is equal to:

$$p_T = p_0\left(1 - \frac{H}{44.3}\right)^{5.256}. \tag{2}$$

The mass density of the air in the vicinity of the Earth:

$$\rho_0 = \frac{\gamma}{g}\ \left[\frac{\text{kg}\cdot\text{sec}^2}{\text{m}^4}\right]$$

where γ is the specific weight of the air, g = 9.81 is the acceleration of the force of gravity.

At a temperature of t_0 = 15°C and a pressure B_0 = 760 mm Hg, /15 the value of the air density near the Earth equals:

$$\rho_0 = \frac{1}{8} = 0.125.$$

Under other conditions, the density equals:

$$\rho = \rho_0 \frac{B}{B_0} \cdot \frac{T_0}{T} = 0.125 \cdot \frac{B}{760} \cdot \frac{288}{273 + t}. \tag{3}$$

The mass density in the troposphere at an altitude of H < 11 km, is determined according to the formula:

$$\rho_T = \rho_0\left(1 - \frac{H}{44.3}\right)^{4.256}. \tag{4}$$

For rapid calculations of the mass density in the region of the troposphere, one can use an approximate formula:

$$\rho_T = \rho_0\left(\frac{20 - H}{20 + H}\right), \tag{4a}$$

where H is the altitude in kilometers.

The pressure and mass density of the air at altitudes above 11 km, are calculated according to Galle's formula:

$$\frac{p}{p_T} = \frac{\rho}{\rho_T} = e^{-\frac{H-11}{6.350}}, \tag{5}$$

where H is the altitude in kilometers.

4. The Continuity Equation. The Bernoulli Equation

The velocity field in the vicinity of a streamlined body. In studying the flow of air around bodies, the movement is examined independently of whether the body moves in the air or whether the air moves around an immobile body, since the forces operating in both cases are similar.

When an air stream flows around a body, the velocity of the particles at a distance from the body are similar everywhere; in the vicinity of the body, the velocity of each particle at various points in the stream will be different both in magnitude and in direction. A so-called velocity field is formed around the body; this illustrates the pattern of the velocities in any given moment in time in a space filled with fluid.

In studying the velocity field, one has to consider the concepts of flow lines of the fluid in movement. The flow line is a line to which the vector of velocity of the fluid is tangent in every point at a given moment. /16

The totality of the flow lines is sometimes called the field of flow.

The flow lines which the fluid forms around a body can be reproduced if a small grain of powder is thrown on the surface of a fluid. Each particle of the powder floating on the surface of the fluid will leave on the photographic film a trace in the form of a drawing. The totality of all the drawings yields the pattern of the flow lines. Their frequency characterizes the magnitude of the velocity in a given part of the field.

If during the movement of a fluid, the velocity, pressure, density, etc, stay constant in time for any point in space, then the pattern of the flow line is also constant. Such a movement is called steady state. The movement where the velocity changes in the course of time, throughout the space occupied or in a part of it, is called non-steady state. The part of the fluid limited by the flow lines, which are drawn through all the points of a small and simple closed contour in the region occupied by the fluid, is called elementary stream tube.

Since the flow lines have the direction of the velocities in all points, the fluid can neither go in nor out through imaginary walls of the tube, and the stream tube can be represented as rigid under steady state movement conditions. The fluid flowing in this tube is called a jet which cannot mix with the neighboring jet. In such a way, each such jet can be represented as being isolated from the mass of the fluid and consequently, the whole flow can be regarded as being composed of individual jets.

The Continuity Equation. Let us distinguish in the general flow of the tube, the flow AB, and let us make two cross sections I and II perpendicular to the axis of the tube (Fig. 1). The mass of fluid passing through section I in one second is equal to

$$m_1 = \rho_1 F_1 V_1 \frac{\text{kg sec}}{\text{m}}$$

At the same time a mass of fluid passes through section II, the size of which equals:

$$m_2 = \rho_2 F_2 V_2$$

where: m-mass
ρ-density
F-area of the cross section of the stream tube
V-velocity through the section.

/17

Under conditions of steady state, the mass of fluid in the examined sector, limited by I and II, can neither increase nor decrease. Otherwise, there would be a change in pressure, density, and velocity of the fluid particles in the section. We can therefore write:

$$m_1 = m_2 = m = \text{Const},$$

or

$$\rho_1 F_1 V_1 = \rho_2 F_2 V_2 = \text{Const.} \qquad (6)$$

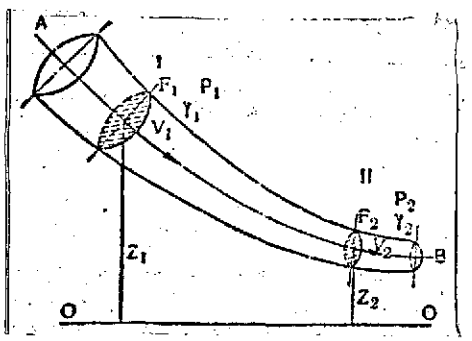

Fig. 1: Stream tube

Expression (6) is called the continuity equation of a jet.

For a noncompressible fluid, $\rho_1 = \rho_2$, and equation (6) can be written in the following form:

$$F_1 V_1 = F_2 V_2 = \text{Const.} \qquad (7)$$

This expression represents the volumetric flow rate of the tube and shows that the volume of fluid coming in the tube must equal the volume of the fluid leaving the tube per unit time.

Bernoulli's equation. Bernoulli's equation is the law of conservation of energy applied to a jet of fluid in steady state movement. For cross sections I and II (Fig. 1) the continuity equation is:

$$\rho_1 F_1 V_1 = \rho_2 F_2 V_2 = m.$$

In the time dt, a column of fluid $V_1 dt$ passes through section I. /18 The volume of this column equals $F_1 V_1 dt$; by multiplying this volume by the mass density, we obtain the mass passing through the section I in time dt.

$$\rho_1 F_1 V_1 dt = m dt.$$

During the same time, a column of fluid $V_2 dt$ passes through the section II. Its volume equals $F_2 V_2 dt$ and its mass:

$$\rho_2 F_2 V_2 dt = m dt.$$

The mass of fluid entering through section I brings a supply of energy which, according to the law of conservation of energy, must be constant between the sections I and II. The total supply of energy to the stream tube through section I is composed of the kinetic energy, i.e., the mass of fluid moving with a velocity and equaling:

$$\frac{m dt V_1^2}{2};$$

potential energy of the pressure of the fluid, equaling the work performed by the particles of the fluid on their pathway at the left of section I. This work equals:

$$p_1 F_1 V_1 dt \qquad (a)$$

where $p_1 F_1$ is the pressure on the column of fluid with section F_1, while $V_1 dt$ is the path which this column has to cross in position I. Multiplying and dividing expression (a) by ρ_1, we obtain:

$$\frac{p_1}{\rho_1} \rho_1 F_1 V_1 dt = \frac{p_1}{\rho_1} m dt,$$

where: p_1 -- pressure,
ρ_1 -- density of the fluid at the left of section I;

potential energy of the weight which equals the potential work of the the fluid crossing section I. This fluid is at a height Z_1, counting from any level, for example, 0 -- 0. The height Z_1 is called the level height.

The potential energy of the weight equals:

$$Z_1 G dt;$$

since the weight of the fluid $G = mg$,

$$Z_1 G dt = Z_1 mg dt;$$

internal energy; for an elastic fluid, i.e., gas, one has to take into consideration the internal thermal energy brought along by the mass mdt through section I in the tube. It is known from thermodynamics that the internal energy of the gas U, is usually expressed in calories per kilogram weight of the gas. Its magnitude is dependent on the temperature of the gas, and consequently, will be different in different sections through the stream tube. /19

The internal energy crossing section I will equal:

$$U_1 mgdt.$$

Since the mechanical equivalent of heat is

$$A = \frac{1}{427} \frac{cal}{kg}$$

the internal energy in kgm will equal

$$\frac{U}{A} mgdt.$$

By the same method one can find the energy of the fluid flowing through section II, i.e., the kinetic energy.

$$\frac{mdtv_2^2}{2}.$$

The potential energy of the pressure:

$$\frac{p_2}{\rho_2} mdt.$$

The potential energy of the weight: $Z_2 mgdt$.
The potential thermal energy:

$$\frac{U_2}{A} mgdt.$$

In the case of flow of a fluid without friction losses and losses of heat through the walls of the tube, the sum of the energies of the flow through section I should equal the corresponding sum of energies through section II.

If mechanical (friction) and heat losses of energy take place in the region between the sections I and II, which could be assigned the magnitude K, than the incoming energy should equal the outgoing one plus the losses K.

Summing up the energy for sections I and II, we obtain the equation of the energy balance: /20

$$\frac{mV_1^2}{2}dt+\frac{p_1}{\rho_1}mdt+Z_1mgdt+\frac{U_1}{A}mgdt=$$
$$=\frac{mV_2^2}{2}dt+\frac{p_2}{\rho_2}mdt+Z_2mgdt+\frac{U_2}{A}mgdt+K.$$

Dividing all the terms of this equation by mgdt -- the weight of the flowing fluid, we obtain:

$$\frac{V_1^2}{2g}+\frac{p_1}{g\rho_1}+Z_1+\frac{U_1}{A}=\frac{V_2^2}{2g}+\frac{p_2}{g\rho_2}+Z_2+\frac{U_2}{A}+\frac{K}{mgdt}.$$

In this equation $g\rho_1 = \gamma_1$; $g\rho_2 = \gamma_2$; denoting the losses through ζ, i.e.

$$\zeta=\frac{K}{mgdt};$$

we finally obtain:

$$\frac{V_1^2}{2g}+\frac{p_1}{\gamma_1}+Z_1+\frac{U_1}{A}=\frac{V_2^2}{2g}+\frac{p_2^2}{\gamma_2}+Z_2+\frac{U_2}{A}+\zeta=\text{Const.} \qquad (8)$$

Expression (8) represents the general form of the Bernoulli equation for any fluid including gases.

After dividing the terms of the given equation by the weight mgdt, we obtained a linear dimension in meters.

The Bernoulli equation for a noncompressible fluid is derived from the general equation (8). Since for a noncompressible fluid,

$$\gamma_1=\gamma_2=\gamma \text{ and } U_1=U_2,$$

equation (8) can be rewritten in the following form:

$$\frac{V_1^2}{2g}+\frac{p}{\gamma}+Z_1=\frac{V_2^2}{2g}+\frac{p_2}{\gamma}+Z_2+\zeta. \qquad (9)$$

Most practical problems are solved by means of this equation.

All the terms of equation (9) have a linear dimension, therefore, they are called heights:

$\frac{V^2}{2g}$ -- velocity height of dynamic pressure;

$\frac{p}{\gamma}$ -- piezometric height;

Z -- level height;
ζ -- height of losses.

If the equation of the balance were to be expressed not per kg, /21 but per meter of fluid, then we could multiply equations (9) by γ and

obtain:

$$\frac{\rho V_1^2}{2}+p_1+\gamma Z_1=\frac{\rho V_2^2}{2}+p_2+\gamma Z_2+\gamma\zeta. \tag{9a}$$

The terms of this equation receive the dimensions of pressure [kg/m^2] and are called:

$\frac{\rho V^2}{2}$ -- dynamic pressure;

p -- static pressure or hydrodynamic pressure;
γZ -- hydrostatic pressure;
$\gamma\zeta$ -- pressure of the losses.

The sum of all the terms in the Bernoulli equation is called total head.

If the equation of Bernoulli is applied to air, then flows which are nearly horizontal are usually examined, consequently Z is very small.

Comparing the small level height Z and the losses ζ with the terms $V^2/2g$, which in modern airplanes are very large, Z and ζ can be disregarded since they are small; we then obtain a simple expression of the Bernoulli equation which is constantly applied in theoretical aerodynamics:

$$\frac{\rho V_1^2}{2}+p_1=\frac{\rho V_2^2}{2}+p_2=\text{Const.} \tag{10}$$

The pressure in the critical point. Let us assume that there is a flow with velocity V_1 around a certain body. If we draw an infinitely small contour abc in section I (Fig. 2), we obtain a jet of an infinitely small cross section which becomes wider and wider as it approaches the body and receives a finite section around the body since the letter has finite dimensions.

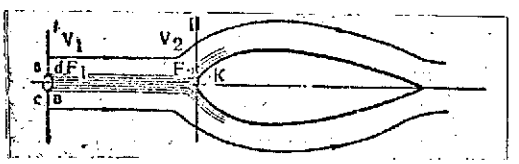

Fig. 2: Flow around a body

Based on the equation of continuity of the jet (7) for sections I and II, we can write: /22

$$\frac{V_2}{V_1}=\frac{dF_1}{F_2}\to 0;$$

since F_2 is very large by comparison with dF_1, the ratio dF_1 over F_2 tends to zero and consequently V_2 also tends to zero.

The point K, where $V_2 = 0$, is called the critical point. According to Bernoulli's equation, we can find the pressure at this point. For sections I and II we have:

$$\frac{\rho V_1^2}{2}+p_1=\frac{\rho V_2^2}{2}+p_2;$$

Hence:

$$p_2 = \frac{\rho V_1^2}{2} + p_1 - \frac{\rho V_2^2}{2}.$$

Since at the critical point $V_2 = 0$, then:

$$p_2 = \frac{\rho V_1^2}{2} + p_1. \qquad (11)$$

In such a manner the pressure at the critical point is the highest to be found in the flow around a body.

Cavitation. The discontinuity of a flowing fluid which is accompanied by the formation of gaps filled with vapor and gases to be found in the fluid is called cavitation. The discontinuity of the flow takes place when the pressure of the fluid becomes negative; in this moment, the pressure changes into tensile stress. The usual fluids can not withstand any tensile stress and tear up.

Let us write the Bernoulli equation for a large reservoir, from which the water is being sucked out by means of a pipe, and let us observe the velocity of the water in the tube at which cavitation sets in. If we take a plane passing through a section of the tube situated below the water level in the reservoir, we shall have:

$Z_2 = 0$ and $p_1 = p_0$, i.e. atmospheric pressure.

The velocity of motion of the water in a large reservoir is very small if compared with the rate V_2 in the pipe which has a small cross section and therefore it can be taken equal to zero, i.e. $V_1 = 0$. The losses ζ due to friction in the reservoir can be disregarded as they are small, and we obtain: /23

$$\frac{p_0}{\gamma} + Z_1 = \frac{V_2^2}{2g} + \frac{p_2}{\gamma};$$

hence:

$$p_2 = p_0 - \frac{\gamma V_2^2}{2g} + \gamma Z_1.$$

This equation shows that the larger V_2, the smaller the pressure p_2. The highest velocity V_2 will be seen at the pressure $p_2 = 0$; under these conditions, the following equation holds:

$$p_0 - \frac{\gamma V_2^2}{2g} + \gamma Z_1 = 0.$$

Hence the limiting velocity of the water in the pipe would be:

$$V_2 = \sqrt{2g\left(Z_1 + \frac{p_0}{\gamma}\right)}. \qquad (12)$$

This velocity will be minimal when the pipe through which the water is sucked out will be close to the water level in the reservoir, i.e. when $Z_1 = 0$.

In this case:

$$V_2 = \sqrt{2g\frac{p_0}{\gamma}}. \tag{12a}$$

For water, γ = 1000 kg/m^2; p_0 = 10330 kg/m^2 and g = 9.81 m/sec.

Substituting these values in equation (12a), we obtain:

$$V_2 = \sqrt{2 \cdot 9{,}81 \cdot \frac{10\,330}{1\,000}} = 14.15 \text{ m/sec}.$$

At this rate of motion of the water, cavitation may set in.

Formula (12) is applicable only at low temperatures. At high temperatures, the discontinuity in the fluid is facilitated by the elasticity of its vapor, and cavitation sets in at a much lower rate.

The equation of Bernoulli for gases. At high velocities, above 100 m/sec, one cannot disregard in Bernoulli's equation the terms containing the value of the internal energy of the gas and therefore, one has to use equation (8).

In most cases of the aviation practice, one deals with high velocities, when the air has no time to exchange heat with the body around which it flows, and consequently the process takes place adiabatically i.e.: /24

$$p_1 V_1^k = p_2 V_2^k = pV^k = \text{Const},$$

where k is the adiabatic exponent.

On the basis of this law, the Bernoulli equation (8) becomes [55]:

$$\frac{V_1^2}{2g} + Z_1 = \frac{V_2^2}{2g} + Z_2 - \frac{k}{k-1} \cdot \frac{p_1}{\gamma_1}\left[1 - \left(\frac{p_2}{p_1}\right)^{\frac{k-1}{k}}\right] + \zeta. \tag{13}$$

For air, k = 1.41, and consequently we can write:

$$\frac{V_1^2}{2g} + Z_1 = \frac{V_2^2}{2g} + Z_2 - 3{,}45\,\frac{p_1}{\gamma}\left[1 - \left(\frac{p_2}{p_1}\right)^{0{,}29}\right] + \zeta. \tag{14}$$

Pressure of the gas in the critical point. Fig. 2 represents a jet which approaches the body in critical point k; let us write equation (13) for this point. Since in the critical point V_2 = 0; $Z_1 = Z_2$, and one can neglect the losses ζ in the jet, this equation can be written in the following form:

$$\frac{V_1^2}{2g} = \frac{k}{k-1} \cdot \frac{p_1}{\gamma_1}\left[1 - \left(\frac{p_2}{p_1}\right)^{\frac{k-1}{k}}\right]. \tag{a}$$

By dividing this equation to kp_1 and multiplying by k-1 and γ, we obtain:

$$\frac{V_1^2}{2}\cdot\frac{\gamma_1}{gkp_1}\cdot(k-1)=-1+\left(\frac{p_1}{p_1}\right)^{\frac{k-1}{k}}. \qquad (b)$$

The formula of the velocity of the sound is well known from physics [1, p.113]:

$$a=\sqrt{k\frac{p}{\rho}}=\sqrt{\frac{gkp}{\gamma}}; \qquad (15)$$

hence

$$a^2=\frac{gkp}{\gamma}, \quad \text{or} \quad \frac{1}{a^2}=\frac{\gamma}{gkp}.$$

Introducing a into equation(b), we obtain:

$$\left(\frac{V_1}{a_1}\right)^2\cdot\frac{k-1}{2}=-1+\left(\frac{p_2}{p_1}\right)^{\frac{k-1}{k}}. \qquad (16)$$

The ratio of the velocity of the gas V in any point to the velocity of the sound k in the same point is called the Mach number -- Ma. /25

$$\mathrm{Ma}=\frac{V}{a}.$$

By substituting this number in equation (16) and solving the equation for p_2/p_1, we obtain:

$$\frac{p_2}{p_1}=\left(1+\frac{k-1}{2}\mathrm{Ma}_1^2\right)^{\frac{k}{k-1}}=(1+0.205\mathrm{Ma}_1^2)^{3.45}. \qquad (17)$$

In such a manner, the pressure of the gas in the critical point depends merely on the initial pressure and on the mach number.

In order to solve the problem, i.e. to find the velocity at which a correction has to be introduced for the compressibility of the air, let us make the following transformation of equation (17):

$$\frac{p_2}{p_1}=\left(1+\frac{k-1}{2}\mathrm{M}_1^2\right)^{\frac{k-1}{k}}=\left[1+\frac{k-1}{2}\left(\frac{V_1}{a_1}\right)^2\right]^{\frac{k-1}{k}}. \qquad (a)$$

Let us expound the right part of this equation into a series according to the binomial theorum, while neglecting the terms of the higher order with regard to V_1/a_1; assuming that $(V_1/a_1)<1$, we obtain:

$$\frac{p_2}{p_1}=1+\frac{k}{2}\left(\frac{V_1}{a_1}\right)^2+\frac{k}{8}\left(\frac{V_1}{a_1}\right)^4+\ldots \qquad (b)$$

Let us change the right hand side of this equation using equation (15) for the velocity of the sound and substituting, instead

of a_1^2, its value $k\,p_1/\rho_1$ in equation (b):

$$\frac{p_2}{p_1}=1+\frac{k}{2}\frac{\rho_1 V_1^2}{k\rho_1}+\frac{k}{8}\cdot\frac{\rho_1 V_1^2}{k\rho_1}\left(\frac{V_1}{a_1}\right)^2=1+\frac{\rho_1 V_1^2}{2\rho_1}+\frac{\rho_1 V_1^2}{8\rho_1}\left(\frac{V_1}{a_1}\right)^2.$$

Hence:

$$p_3=p_1+\frac{\rho_1 V_1^2}{2}+\frac{\rho_1 V_1^2}{8}\left(\frac{V_1}{a_1}\right)^2=p_1+\frac{\rho_1 V_1^2}{2}\left[1+\frac{1}{4}\left(\frac{V_1}{a_1}\right)^2\right]. \qquad (18)$$

Comparing this equation with equation (11) for a noncompressible fluid, we see that these two equations differ in the term $\frac{\rho_1 V_1^2}{2}\cdot\frac{1}{4}\left(\frac{V_1}{a_1}\right)^2$ in the right hand side of equation (18). It follows that the smaller the velocity of the flow by comparison with the velocity of the sound, the lesser the difference in pressure between the compressible and noncompressible flow in the chosen point. Considering the series of velocities V_1, let us see what is the relationship between the pressures of a noncompressible and a compressible fluid.

TABLE 1

Velocity of flow	$V_1=50$	100	150	200
Mach number	$Ma_1=\frac{V_1}{a_1}=0.151$	0.333	0.456	0.603
At sound velocity $a_1=330$ m/sec				
$\frac{(p_3-p_1)\ \text{non-compressible}}{(p_3-p_1)\ \text{compressible}}$	$\frac{1}{1+\frac{1}{4}\left(\frac{V_1}{a_1}\right)^2}=0.994$	0.977	0.95	0.913
$\%=1-\frac{(p_2-p_1)\ \text{non-compressible}}{(p_3-p_1)\ \text{compressible}}\cdot\frac{(p_2-p_1)\ \text{noncompressible}}{(p_2-p_1)\ \text{compressible}}$	100—0.6	2.3	5.0	8.7

where the ratio $\frac{(p_2-p_1)\ \text{noncompressible}}{(p_2-p_1)\ \text{compressible}}$ was obtained by dividing equation (11) by equation (18).

The presented calculation shows that at velocities below 100 m/sec of the flow, on of the body in a quiet flow, the effect of the compressibility of the air on the pressure in the examined point is insignificant.

5. The Concept of Turbulent Motion

Turbulent motion is the movement of fluid in a region which is filled with whirls. This motion can be observed in nature in the form of turbulent dust pillars which sometimes appear in quiet weather or in the form of powerful whirlwinds or typhoons (Fig. 3). Vortexes appear also in the form of rings which can be observed in the exhaust of internal combustion engines for above the pipe of a steam engine.

The most intensive turbulent motion is formed behind a body which moves in a fluid, for example, a ship or a motor boat (Fig. 4).

Demonstration of the vortexes and their properties. If an impeller is introduced along the long axis of a container filled with water and is set in a rapid rotary motion, then /27 a turbulent column is obtained inside the vessel, and the surrounding fluid is subject to a general cyclic movement. The experiment for the formation of a vortex can be performed by means of the instrument illustrated in Fig. 5. A hollow pulley wwith several plane radial partitions which however do not reach the axis, is set in rapid rotational motion by means of a machine. A vat filled with water is placed at the distance of 3 m under the pulley. In order for the experiment to be successful, the water should be slightly heated. In its rotary motion, the pulley twists around a column of air. As a result of the lower pressure in the middle of the newly formed vortex, the water begins to raise and is set in a rotary motion as well. After some time, a water column is formed, in the form of a /28 thin string, which extends from the level of the water to the center of the pulley. Under the pulley, the turbulent string consists of very small drops which are thrown in all directions by the partitions of the pulley. [8].

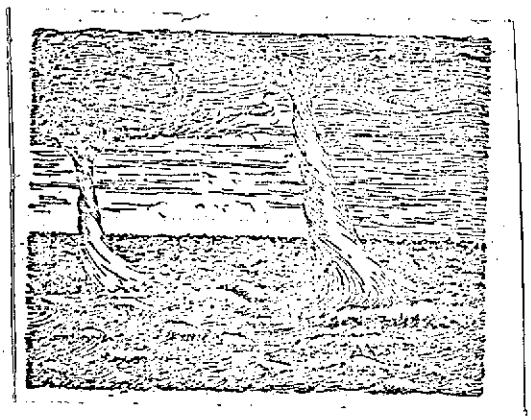

Fig. 3: The typhoon or whirlwind

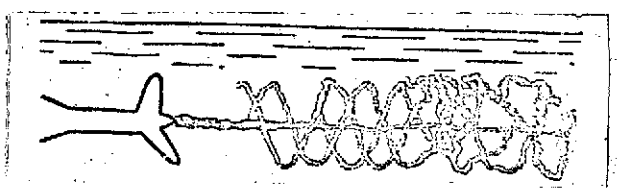

Fig. 4: Vortex formation behind the propeller of a motorboat.

Another interesting experiment on the formation of turbulent rings, can be performed by means of the instrument illustrated in Fig. 6, which is a wooden box. The rear wall of the box is formed by an elastic membrane, while the front wall has a round opening. If we were to fill this box with smoke, then, as a result of knocks produced by means of a small hammer on the rear wall, vortex-like rings would come out through the front wall. Some smokers can let out smoke in the form of similar rings from their mouth. The smoke from the pipes of steam engines sometimes emerges in the form of rings. In calm air the vortex-like rings have their own movement.

It is known from the theory of turbulent motion that the vortex and the velocity field are interdependent, therefore, in the experiments on the formation of vortex-like rings, we see that neighboring parts of the ring act on each point inside it and the ring flies rapidly in the air. An air flow is obtained as a result of

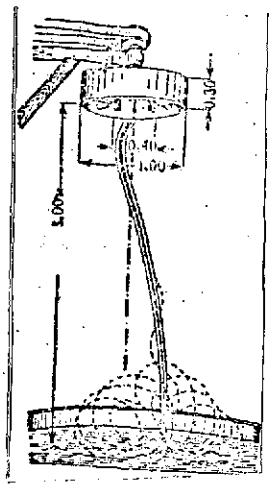

Fig. 5: Instrument for the formation of vortexes.

this, as illustrated in the right side of Fig. 6: the air inside the ring moves forward as a result of which the vortex-like ring carries with it a certain volume of air. This volume of air forms the atmosphere of the ring. /29

If two vortex-like rings are released in succession from the instrument illustrated in Fig. 6, then the rear ring is sucked up by the leading one, is compressed and passes inside it. Later it widens and runs ahead of the first, after which they again change places. The example demonstrates the extreme complexity of turbulent motion.

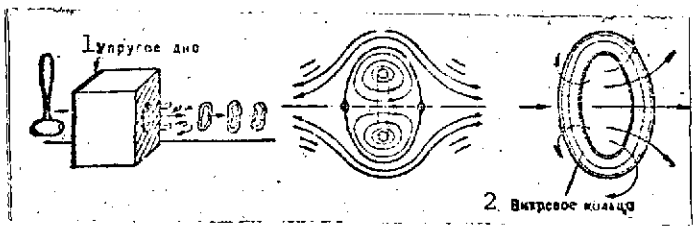

Fig. 6: Instrument for the formation of vortex-like rings

Key: 1. elastic bottom
2. vortex-like ring

The rotation of a fluid is essentially different from the rotation of a solid body. The particles of the rotating solid obey a linear law of the change of velocity with the change of radius, which is expressed by the formula:

$$V = \omega r,$$

where ω is the angular velocity of rotation, while r is the radius.

The particles of the fluid can rotate with various angular velocities. In the same fluid particle the radii can rotate with different angular velocities, different both in magnitude and in size. According to Helmholz, the fluid particle moves forward with the rate of its center of gravity, becomes deformed and rotates.

In presenting the main concepts of aerodynamics only from the point of view of their experimental application, we shall always consider only noncompressible fluids without friction. Such a fluid is called ideal noncompressible. In order to study the motion of a fluid, a few special magnitudes and concepts are introduced, the relationships between which form the theorems of aerodynamics.

The velocity flow. Let us draw an arbitrary line OABC through a flowing ideal fluid (Fig. 7). In any point A of this line, the fluid will have a certain velocity V. Point A can be assumed to be at a distance S from the initial point O along the curve. The

magnitude S can be considered to be positive in the direction of the arrow and negative in the opposite direction.

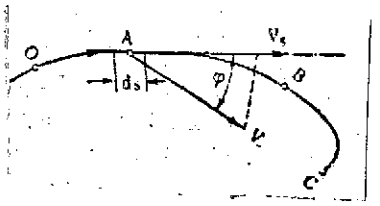

Fig. 7: Circulation of the velocity alongside a contour

Let us single out on this curve the element dS with point A, and let us project the velocity of the flow V to the direction of the tangent to this point. Multiplying the projection V_s of this velocity by the element dS, we obtain the velocity flow dΓ along this element, i.e.: /30

$$d\Gamma = V_s dS. \quad (19)$$

Adding up all the elementary velocity flows along the line OABC, we obtain the velocity flow along the curve:

$$\Gamma_{\infty} = \int_{\infty} V_s dS. \quad (19a)$$

The dimension of the velocity flow is $m^2 sec^{-1}$.

The velocity circulation. The velocity flow in a closed contour is called the velocity circulation. Let us single out in a flowing fluid a closed contour with the circumference S (Fig. 8). In any point of this contour, the fluid will have a certain velocity V. The projection of the velocity V in point A of element dS to the tangent of the curve through this point, multiplied by the element dS, gives the elementary flow:

$$d\Gamma = V_s dS,$$

where V_s is the tangential component of the velocity flow.

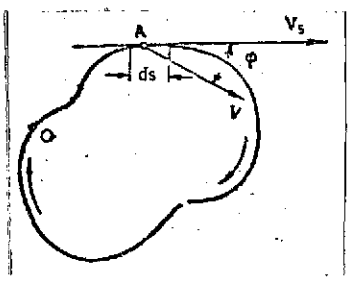

Fig. 8: The velocity circulation in a closed contour

Adding up all the elementary velocity flows on the closed contour, we obtain the velocity circulation:

$$\Gamma = \oint V_s dS; \quad (20)$$

where $\oint$ -- the sign of the integral along a closed contour.

If the contour were to be circumvented in the reverse direction, the sign would change as well.

Denoting the angle between the positive direction of the tangent and the velocity by φ (Fig. 8), the receiving formula can be rewritten in the following form: /31

$$\Gamma = \oint V_s dS = \oint V \cos\varphi dS,$$

where $V\cos\varphi = V_s$ -- projection of the velocity of the fluid to the tangent in point A of element dS.

We can see from equation (19) that the concept of circulation is analogous to the concept of the work of force along any path dS.

The dimension of circulation is $м^2 сек^{-1}$.

Velocity potential. The velocity potential is defined as the function of space $\phi(x,y,z)$, the derivative of which in any direction gives the projection of velocity V to this direction:

$$V_s = \frac{\partial \varphi}{\partial S}. \qquad (a)$$

Equation (a) gives the partial derivative since function ϕ depends upon three coordinates of space and time. The flow with the velocity potential is called potential flow.

If a fixed contour is represented in space, then instead of the partial derivative, the full derivative is written:

$$V_s = \frac{d\varphi}{dS}, \qquad (b)$$

hence:

$$d\varphi = V_s dS. \qquad (c)$$

Integrating once in the limits from point A to point B (Fig. 7) and again along the whole closed contour (Fig. 8), we obtain the following two equalities:

$$\varphi_A - \varphi_B = \int_B^A V_s dS = \Gamma_{AB}, \qquad (21)$$

i.e. the potential difference for two points is equal to the velocity flow along any line uniting these points:

$$\varphi_A - \varphi_A = \oint^A V_s dS = 0, \qquad (21a)$$

i.e. in the case of a single-valued velocity potential of flow, the velocity circulation for any closed contour equals 0.

Consequently, in order to solve the problem whether there is a potential flow in any particular case, it is sufficient to prove/32 that the circulation Γ on any contour is or is not equal to 0.

Basic theorems about vortexes. In analyzing the motion of a particle in any plane which passes through its center of gravity, the concept of the average angular velocity of rotation is used. In order to determine the velocity of rotation of a fluid in point A (9), a plane is passed through this point, the contour k is drawn and the magnitude of the circulation Γ along the contour is determined. Therefore the projection of the average velocity of rotation of the fluid in point A relative to the normal to the area, is the following magnitude:

$$\omega = \frac{\Gamma}{2\sigma}. \qquad (22)$$

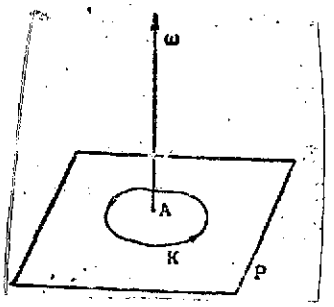

Fig. 9: The vector of the average angular velocity

The smaller the contour taken, the more accurate will the expression be, and in the limiting case we obtain:

$$\omega = \frac{d\Gamma}{2d\sigma}, \qquad (22a)$$

or

$$d\Gamma = 2\omega d\sigma. \qquad (22b)$$

The derivative $\omega d\sigma$ is called the flow of the vortex through the area $d\sigma$; it is analogous to the flow rate $Vd\sigma$.

By rotating the area in all directions around point A, one can find the situation in which ω will have a maximum value.

The magnitude of ω and its direction determine the vorticity of the fluid in point A. The vector ω is called the vorticity vector.

In order to study turbulent motion, several concepts are introduced about the component elements of turbulent motion, which facilitate the formulation of its laws.

The vortex line (Fig 10) is the line to which the vector of turbulent velocity of the fluid is tangent in each point at a given moment.

The surface to which the vector of turbulent velocity of the fluid is tangent in each point at a given moment, is called the vortex surface (Fig. 10) /33

That part of the fluid which is limited by the vortex lines passing through all the points of some small, simple closed contour in the area occupied by the fluid, is called vortex tube. The fluid confined in the vortex tube is called vortex filament.

If ω were to be taken as velocity, then the vortex tube can be considered similar to a jet of fluid with a cross section $d\sigma$. The derivative $\delta d\sigma$ is called, as said above, the vortex flow through the area $d\sigma$. In such a manner formula (22b) shows that the velocity circulation in an infinitely small contour is equal to twice the vortex flow through the area confined by this contour. It should be mentioned that Helmholtz calls the derivative $\omega d\sigma$ the stress of the vortex filament [8].

Stokes theorem. Breaking down an arbitrary surface S, confined by the contour K, (Fig. 11) into infinately small areas, which can be considered plane, this following formula can be written for each of /34 them:

$$d\Gamma = 2\omega d\sigma$$

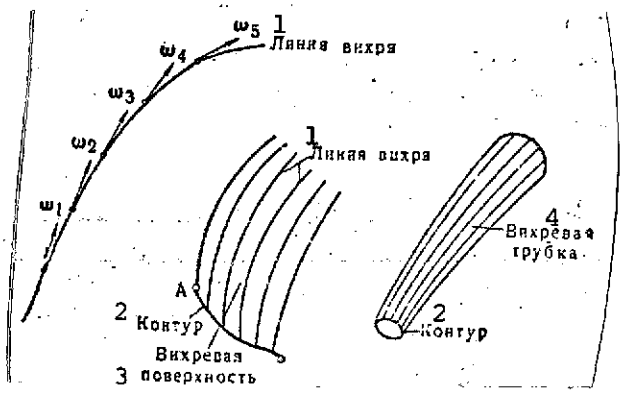

Fig. 10: The vortex line, the vortex surface and the vortex tube

Key: 1. vortex line
2. contour
3. vortex surface
4. vortex tube

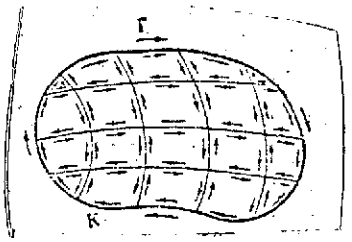

Fig. 11: The contour of the surface

Adding up these expressions for all the elementary areas, we obtain:

$$\iint dI' = 2\iint_{\sigma} s\omega d\sigma$$

It can be seen in Fig. 11 that on each internal side of the rectangles, two circulations in opposite directions are found which annul each other. After reduction and as a result of the addition, in the left part only the derivative $V_s dS$ is left behind, which is related to the element of the contour K. The sum of these derivatives gives the circulation of the velocity along contour K.

$$\Gamma = 2\iint_{\sigma} \omega d\sigma, \qquad (23)$$

i.e. the circulation of the velocity on any contour equals twice the overall flow of the vortex through any area confined by this contour.

According to formula 20, we can also write:

$$\oint V_s dS = 2\iint_{\sigma} \omega d\sigma. \qquad (24)$$

The integral of the area is represented in the right hand side of formula (24), while the integral of the contour is shown in the left hand side. We should note that both the surface and the contour K do not necessarily have to be plane.

The Helmholtz theorem. If we single out on the vortex surface a closed contour Fig(12), then we shall have $\omega = 0$ in any point on the surface. This can be seen from the fact that the vector ω is tangent to the given surface (it can be lateral to the surface of the vortex tube) and the vortex flow through it equals 0, which according to the Stokes theorem gives $\Gamma = 0$, i.e. the velocity circulation on the contour lying on the vortex surface equals 0.

If we draw the contour shown in the right hand side of Fig. 12, on the surface of the vortex tube with infinitely small distances 1-4 and 5-8, then the velocity circulation on this contour will be equal to 0 as shown above (Fig. 12, left). The circulation on the section 1-2-3-4 on the contour equals Γ_1 while on the

section 5-6-7-8 it equals Γ_2; on the portions 5-1 and 4-8 the velocity flows are equal but have opposite directions. Consequently if we /35 denote the circulation in the direction 1-2-3-4-8-7-6-5-1 by Γ_3, in the direction 1-2-3-4-1 by Γ_4, by Γ_5 in the direction 8-7-6-5-8 and by Γ_6 in the direction 8-5-6-7-8, we obtain:

hence:

$$\Gamma_3=0=\Gamma_4+\Gamma_5,$$
$$\Gamma_4=-\Gamma_5=\Gamma_6.$$

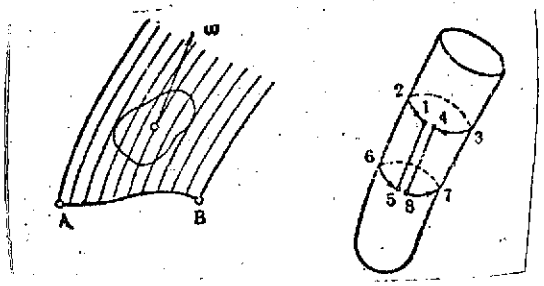

Fig. 12: The closed contour on the vortex surface and the contour on the surface of the vortex tube

In such a manner the velocity circulation on the contour confined by the vortex tube is constant throughout its length.

According to equation (22):

$$\omega=\frac{\Gamma}{2\sigma};$$

consequently, if Γ is constant, then the vector ω should be continuous throughout the space of fluid flow if we neglect the special cases $\sigma = 0$ and $\sigma = \infty$.

Hence, we obtain the Helmholtz theorem: the vortex filaments cannot end suddenly in the fluid; either they extend to infinity or they close into rings or else they lean against the surface of the fluid (Fig. 13).

Vortex strings. If in a fluid with nonturbulent flow, a vortex region is formed, which is confined by a vortex surface in the shape of a tube of finite thickness, then such a tube is called vortex string. The whirlwind observed in nature represents a /36 kind of vortex string of huge dimensions. The simplest type of vortex strings (Fig. 14) are the uniformly turbulent strings, in which ω is constant inside each section; ω can have a different value in another section.

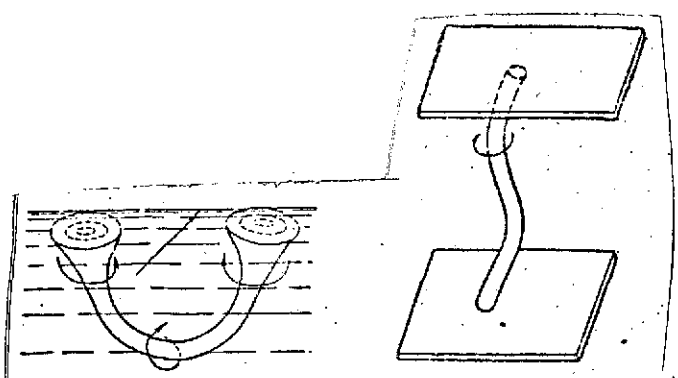

Fig. 13: The shape of vortexes

The flow inside the strength is turbulent while outside it, it is not. Any contour inside the vortex gives a circulation Γ, which is equal, according to Stokes theorem, to twice the vortex flow through the area confined by the contour. The contour lying outside the vortex string has a velocity circulation equal to zero since no vortex flow can pass through it. According to equation 21a, the condition $\Gamma = 0$ indicates

that a velocity potential ϕ exists in the flow, consequently the flow outside the vortex string has a velocity potential, while the flow inside the string has no potential. Hence, the expression "potential flow" which means nonvortex flow in aerodynamics.

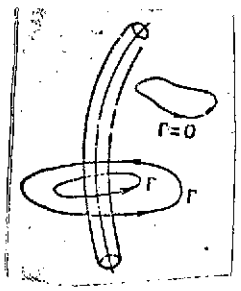

Fig. 14: The vortex string

Since the vortex flow $\omega d\sigma$ is not equal to zero and exists only inside the string, while it equals zero outside it, the vortex flow will be equal to the flow inside the string, regardless of the size and shape of the contour. Consequently, the circulation Γ existing around the /37
vortex string can be taken as a measure of its strength. The velocity circulation in any contour confined by the vortex string is constant and independent of the magnitude and shape of the contour. This can be seen from the fact that regardless of how we draw the contour, the same vortex flow will pass through it, which is equal, according to Stokes theorem to:

$$\Gamma = 2\iint \omega d\sigma = \text{Const.} \qquad (24a)$$

The velocity field appearing in the vicinity of the vortex string is related to its circulation. Let us find the velocity field in the simplest, infinite linear string with a circulation Γ (Fig. 15). If a section with an area p is drawn perpendicular to the axis of the string, then we note that the rate of flow of the fluid particles at equal distances from the axis, will be equal. Let us draw a circle passing through point A with the center on the axis of the string. The velocity V elicited by the string in point A, will be constant and tangent to the surface, consequently the projection of the velocity will be equal to the velocity itself, i.e.

$$V_s = V = \text{Const.}$$

The velocity circulation on this surface will be equal to:

$$\Gamma = \oint V_s dS = V \oint dS = V 2\pi r,$$

hence:

$$V = \frac{\Gamma}{2\pi r}. \qquad (25)$$

In such a manner, the particles of the fluid surrounding the vortex string move with velocities which are inversely related to their distance from the axis of the string. The direction of these velocities coincides with the direction of rotation of the string.

Inside the simplest vortex string, ω = Const and the string rotates like a solid body. The velocity at radius r, can be obtained /38
by the usual formula:

$$V = \omega r,$$

i.e. V will change in a linear fashion. The highest velocity is obtained on the surface of the string. The flow lines, both outside and inside the string form a circle. Outside we shall find a velocity potential but no rotating particles, while inside there will be no velocity potential but there will be rotating particles.

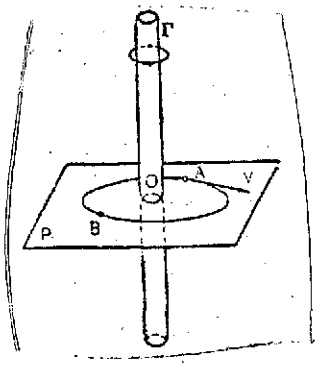

Fig. 15: The velocity field of a vortex string

6. Viscosity

The derivations made in Section 5 refer mainly to an ideal fluid, where no internal forces or friction operate. In reality all real fluids have forces of internal friction which are called viscosity. Therefore, almost all the above presented formulas for the ideal fluid are only approximate for the case of a viscous fluid. The physical importance of viscosity lies in the appearance of forces of inside friction between the layers in a flowing fluid which are produced by the irregular movement of its molecules.

The forces of viscosity tend to retard the rapidly moving parts of the fluid. In a viscous fluid, the vortexes are gradually resorbed and disappear. However, the viscosity can also create vortexes. The strongest vortex formation is observed near the surface of the body around which there is a flow. On the surface of the body itself, the fluid is immobile, as it adheres to the body. At even a small distance from the body, the fluid acquires a large velocity which equals the velocity of the flow.

The thin layer adhering to the surface of the body where the growth in velocity takes place from zero to the velocity which differs by 1% from the velocity of the potential flow around the body is called the border layer. As a result of viscosity, which produces tangential forces, the fluid in this layer is strongly turbulent and therefore is sometimes called the layer of surface turbulence.

The viscosity coefficient. If we single out two elementary areas dS in the border layer (Fig. 16) with the distance between them being δy, then the increase in velocity during the passage from one area to the other will equal $\partial V/\partial y \; \delta y$. Dividing this magnitude by δy, we obtain $\partial V/\partial y$. This magnitude is called the velocity gradient along the normal to the surface of the body. /39

Since the velocities between the areas are different, a force appears between them which is tangent to the surfaces and is produced by the viscosity of the fluid. This force will depend on the velocity gradient and on the area dS:

$$dx = \mu \frac{\partial \gamma}{\partial y} dS. \qquad (26)$$

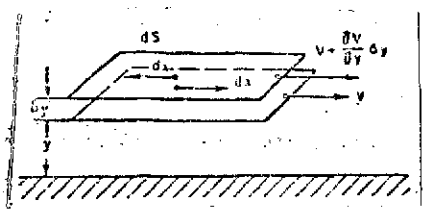

Fig. 16: The interaction between layers due to viscosity

In this equation, μ is called the coefficient of viscosity.

Dividing the force dx to the area dS, will obtain the stress of the force of viscosity τ which is equal to:

$$\tau = \frac{dx}{dS} = \mu \frac{\partial V}{\partial y}. \qquad (27)$$

This stress acts along the surfaces and is called tangential stress.

The dimension of the viscosity coefficient μ is obtained from formula (27):

$$\mu = \frac{\tau}{\frac{\partial V}{\partial y}} = \frac{\frac{kg}{m^2}}{\frac{m}{sec} \cdot \frac{1}{m}} = kg \cdot m^{-2} sec.$$

For the sake of convenience in comparing the viscosity forces, which depend on μ, with the forces of inertia which depend on the mass density ρ, the concept kinematic coefficient of viscosity, ν is introduced:

$$\nu = \frac{\mu}{\rho} [m^2 \cdot sec^{-1}] \qquad (28)$$

We can see that the dimension of ν is the same as in circulation or velocity flow.

The magnitude of the coefficient μ and ν for air at t = 15° and B = 760 mm Hg has the following values: /40

$$\mu_0 = 1.82 \cdot 10^{-6},$$
$$\nu_0 = \frac{\mu_0}{\rho_0} = 1.45 \cdot 10^{-5} m^2 \cdot sec^{-1},$$
or $\nu_0 = 0.145 cm^2/sec.$

The kinematic coefficient of viscosity ν for other atmospheric conditions can be found from the graph of L. Prandtl, which is presented in Fig. 17; on the abscissa the temperature is represented in degrees C, while on the ordinate the coefficient of kinematic viscosity in cm^2 per second.

The coefficient of kinematic viscosity for water at 15° is:

$$\nu = \frac{\mu}{\rho} = \frac{\mu g}{\gamma} = \frac{1.164 \cdot 10^{-4} \cdot 9.81}{1000} = 0.1145 \cdot 10^{-5} m^2/sec.$$

The ratio of the kinematic viscosities of air and water equals:

$$\frac{\nu_{air}}{\nu_{water}} = \frac{1.45 \cdot 10^{-5}}{0.1145 \cdot 10^{-5}} = 12.7.$$

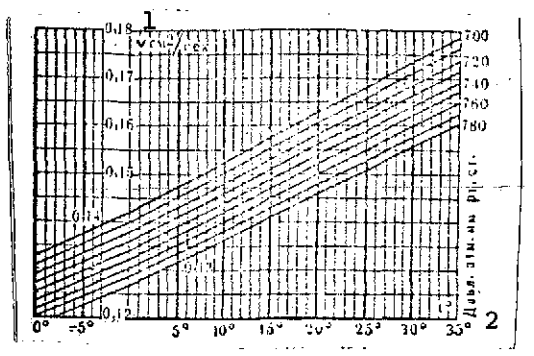

Fig. 17: Graph for the determination of the coefficient of kinematic viscosity of the air

Key: 1. cm^2 per second
2. atmospheric pressure mm Hg

7. The Law of Similarity

Criteria of similarity. Those phenomena in aerodynamics are called similar in which all the characteristics homogeneous physical magnitude, are in identical relation in any point in space [55, 56]. /41

Conclusions on the flying properties of the airplane, on the effectiveness of wind wheels in wind tunnel tests of small models of this machine, either complete or in part, are based on the law of aerodynamic similarity.

The similarity of model and nature is expressed in the proportionality of all the linear dimensions of model and nature and in the equality of the corresponding angles.

The ratio of similar dimensions of model and nature is called the model scale and is expressed by the relationship:

$$k_l = \frac{l_1}{l}.$$

This means that if a section in nature is equal to 1, then the similar factor in the model will be equal to:

$$l_1 = k_l l.$$

Analogically we determine the scale of force, time, density, etc., For example, the ratio of densities in two similar points of comparable phenomena is called the scale of densities:

$$k_\rho = \frac{\rho_1}{\rho},$$

Analogically the scale of viscosity, velocity and force is the following:

$$k_\mu = \frac{\mu_1}{\mu};\ k_V = \frac{V_1}{V} \quad \text{and} \quad k_R = \frac{R_1}{R}.$$

The magnitudes with the index refer to the model.

The linear scale -- k_l, of force -- k_R and of time -- k_t are called the main scale of the phenomena.

The main feature of these scales consists in the fact that in observing their similarities, they appear to be constant throughout the space where the comparable phenomena take place.

We can formulate the following law of aerodynamic similarity, after we presented the concept about the scales of phenomena: two phenomena are called similar if identical scales are obtained for uniform magnitudes in all their compatible points.

If not all the scales fulfill this condition, then one speaks about approximate or partial similarity. /42

It is sufficient to observe the approximate or partial similarity for using the aerodynamic coefficient in solving many practical tasks, as well as for obtaining these coefficients. This means that, let us say, in two phenomena, i.e. in the wind tunnel and in the real airplane, it is sufficient to observe the consistency of the scale of, for example, viscosity or elasticity of the environment, or of the force of the weight, etc., which play in each individual case the most important role, and it is not necessary to have consistency of the scale of all physical magnitudes.

Recent investigations have shown that the aerodynamic coefficient depends not only on the shape of the body and the angles of orientation but also on a number of abstract numbers which have been determined by various scientists. These numbers are called criteria of similarity and they are denoted by the first letters of the names of the authors. Each one of these numbers accounts for a certain factor which affects the flow.

In observing the equality of a certain number of criteria in model and in nature, one can obtain approximate similarity.

In modern wind technology, the following criteria of similarity are used:

The criterion of Reynolds (Re) which evaluates the viscosity of the fluid and of Mach (Ma), which evaluates the elasticity of the fluid. These numbers have the following expressions:

$$\mathrm{Re} = \frac{V_1 l_1}{\nu} = \frac{Vl}{\nu} = \mathrm{Const}, \tag{29}$$

$$\mathrm{Ma} = \frac{V_1}{a} = \frac{V}{a} = \mathrm{Const}, \tag{30}$$

where V and V_1 are the velocities of the flow;
l and l_1 are the linear dimensions of nature and model
ν and ν_1 are the coefficients of kinematic viscosity

The Reynolds number (Re) evalutes the forces of viscosity which retards the motion of the fluid. This magnitude has an extremely important role in solving problems of aero- and aerodynamics.

Under normal conditions, the kinematic viscosity for air is:

$$\nu = 1{,}45 \cdot 10^{-5},$$

consequently, the Reynolds number for air is: /43

$$\mathrm{Re}=\frac{Vl}{1.45\cdot10^{-5}}=69\,000\,Vl.$$

In those cases when the kinematic coefficient of viscosity is similar for model and nature, the following equality holds:

$$V_1\ell_1 = V\ell \tag{31}$$

The derivative $V\ell$ is called the characteristic of the experiment which is used instead of Re in the case of the same ν for model and nature.

In such a manner, the following conditions have to be fulfilled in order to obtain similarity in the presence of viscosity forces:

1. model and nature must be geometrically similar;
2. the orientation of model and nature with regard to the flow should be similar;
3. model and nature should have identical Reynolds numbers.

The transition from model to nature. From the equation $V_1\ell_1 = V\ell = \text{Const}$ we have:

$$\frac{V_1}{V}=\frac{l}{l_1}=\frac{1}{k_l},$$

where $k_1 = \ell_1/\ell$ is linear case.

In such a manner in testing the model in the wind tunnel, where $\sigma_1 = \sigma$ and $\mu_1 = \mu$, similarity will be observed if the velocity in the wind tunnel will be taken equal to:

$$V_1=\frac{1}{k_l}V=\frac{l}{l_1}V,$$

i.e. the velocity V_1 in the model should be greater than the velocity V in nature, by the same factor as the linear dimensions of the model are smaller than in nature.

The fulfillment of this requirement in testing airplane models meets with great difficulty since the velocity of airplanes to date exceeds 100 m/sec. As a matter of fact, in order to obtain a similarity of phenomena for a model at a scale of 1/10, one would have to obtain in the model a flow velocity equal to 1000 m/sec. It is impossible to reach such a velocity in the wind tunnel, since the power for the creation of the flow would have to be several hundred of thousands hp. In addition, at such velocities, the similarity would be destroyed due to the elasticity of the air which strongly affects the flow around bodies already at a velocity similar to that of the sound -- 330 m/sec. In the given case, the effect of the /44 number of Mach will be predominant:

$$\mathrm{Ma}=\frac{V_1}{a}.$$

In order to obtain satisfactory results in the experiments with airplane models, wind tunnels of high pressure or of gigantic dimensions are constructed. The latter make it possible to fly natural-sized airplanes.

It has been established experimentally that at low Reynold's numbers, the coefficient of resistance of bodies is larger, while with the increase in $V_1 l_1$ the resistance decreases, and it stays practically constant at a certain value of $V_1 l_1$.

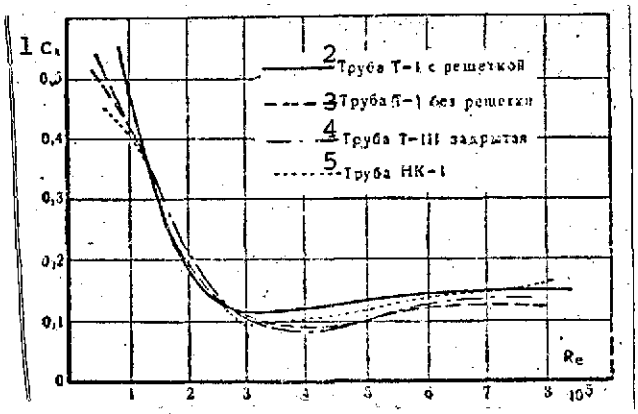

Fig. 18: Change in the coefficient of resistance of a sphere in relation to the number of Reynolds.

Key:
1. R_x
2. tube T_1 with grid
3. tube T_1 without grid
4. tube T_3 closed
5. tube NK-1

Interesting experiments were carried out at TsAGI in various wind tunnels with spheres of various dimensions. The obtained curves of resistance were reconstructed from being dependent on the velocity of the flow to being dependent on the number of Reynolds, and were represented in the form of diagrams as the one shown in Fig. 18. This diagram shows that the coefficient of resistance R_x changes markedly for all experimental curves at Reynold's numbers $Re \leq 3 \cdot 10^5$; as $Re > 3 \cdot 10^5$ the coefficient of resistance stays practically constant.

Hence it can be concluded that in testing models, a Reynold's number which is larger than a certain magnitude has to be obtained. For example, for the wing: /45

$$\frac{V_1 l_1}{\nu} > \mathrm{Re};$$

we see on the graph in Fig. 18. that the smallest resistance is obtained at Reynold's numbers starting with 300,000 and above. Assuming Re = 440, 000, we obtain:

hence:

$$V_1 l_1 > \frac{Re}{\nu} > \frac{440\,000}{145\,000},$$

$$V_1 l_1 > 3 \frac{m^2}{sec}.$$

8. The Border Layer and the Turbulence

During the flow of an object in the air, the air layers in the immediate vicinity of the surface of the body are retarded due to the viscosity of the fluid, and vortexes are formed. These vortexes are carried away with the general flow and are extended irregular turbulent tails (see Fig. 19). The turbulent layer of the air flow in the immediate vicinity of the body, is called the border layer, as was shown in Sec. 6, or the layer of surface turbulence.

In order to demonstrate the vorticity of this layer, let us take the contour abcd (Fig. 19, below) and let us calculate, according to this contour, the velocity circulation. The sides ad and bc have the direction of the flow velocity, while the sides cd and ab are perpendicular to it. Since bc = ad, the circulation will be equal to:

$$\Gamma_{abcda} = V_2\overline{bc} - V_1\overline{ad} = \overline{ad}\,(V_2 - V_1).$$

However V_2 is larger than V_1 and Γ does not equal 0, consequently, the flow is turbulent.

The flow outside the turbulent layer can be considered potential [see equations (21) and (21a)]. The main role in the border layer is played by the forces of viscosity and partly by the forces of inertia. As a result of viscosity, the particles of the fluid are twisted in vortex rings, and are carried away forming behind the body a turbulent tail, while the forces of viscosity play the lesser role.

A clear distinction between the border layer and the external flow does not exist: the velocity increases from 0 on the surface of the body, to the velocity of the flow, at a distance from the body. The thickness of the border layer may be taken to be the distance σ from the surface of the body where the velocity differs from the velocity of the potential current by 1%. Theoretically the thickness of the layer σ changes depending on X according to a parabolic law (Fig. 19, below), where X is the distance of the measured thickness from the leading edge of the body around which the air flows.

/46

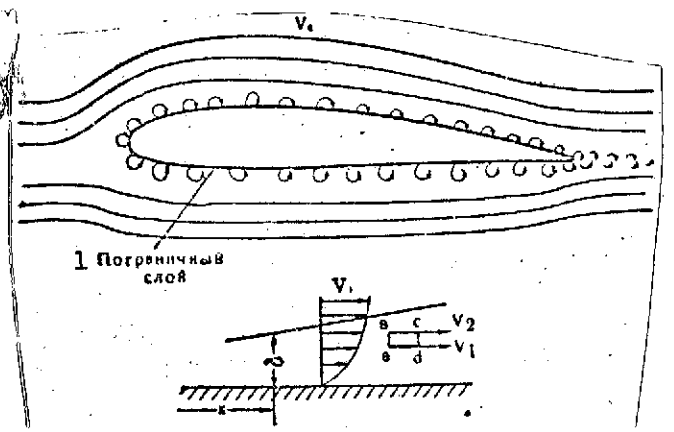

Fig. 19: The border layer

Key: 1. the border layer

At small numbers of Reynolds, the fluid flows in the border layer in the form of nonmixing layers. Such a flow is called <u>laminar</u>.

Investigations have established that in the case of flow around a plate with a length l, situated parallel to the flow, the laminar flow is obtained only for small numbers of Reynolds. When this number increases on a certain length l_k, the flow remains laminar, but later it passes into a strongly churning state which is called <u>turbulent</u> (Fig. 20).

The length on which the flow is laminar is determined by the critical number:

$$\mathrm{Re} \geq 485\,000 = \frac{V_0 l_k}{\nu}.$$

Hence the length of the laminar part will equal: /47

$$l_k = 485\,000 \cdot \frac{\nu}{V_0}.$$

For normal air, we obtain:

$$l_k = \frac{485\,000 \cdot 1{,}45 \cdot 10^{-5}}{V_0} = \frac{7{,}05}{V_0}.$$

The initial turbulence of the flow changes sharply the magnitude of the coefficient obtained in wind tunnels. This takes place as a result of the fact that turbulence has a strong effect on the border layer of bodies surrounded by the flow. For example, if instead of the laminar flow, there was an initial turbulence around the plate illustrated in Fig. 20, then as known from the experiment, the laminar part would be considerably diminished. At large initial turbulence, the laminar part of the border layer can be entirely absent. The resistance of the plate increases under such conditions, since the coefficient of resistance of the plate is larger in the turbulent layer than in the laminar one.

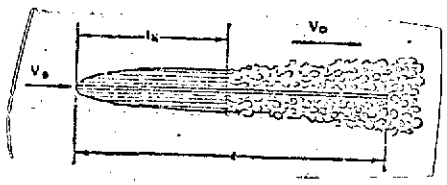

Fig. 20: Transition from laminar to turbulent flow

However, the increase in turbulence increases the coefficient of resistance only in such bodies where the main part of resistance is formed by friction and not by pressure. Examples of such bodies are a plate situated along the flow, wings, air ships and other bodies which have a good aerodynamic shape. (Fig. 21a). In the case of bodies in which the resistance depends mainly on pressure, (sphere, plate perpendicular to the flow, airship placed across the flow, etc.)(Fig. 21b,c), the resistance in the turbulent flow can be smaller than in the laminar flow. The decrease in the magnitude of the coefficient of resistance takes place at the same time with the transition of the border layer of the sphere from laminar to turbulent flow.

Fig. 22 a, b, c shows several consecutive stages of formation of /48 vortexes behind a sphere which is surrounded by flowing air. Fig. 22a illustrate the flow of the air around a sphere immediately after the transition from a state of rest to a state of movement. At this moment, the flow takes place without any disturbance; a high pressure is formed both in front and behind, while a negative pressure is formed on the side. In the next moment the border layer starts to flow from the region with high pressure to the region with low pressure; as a result of this, near the middle section a collision takes place between this flow and the layer flowing in the front (Fig. 22b). As a result of the collision, the flow is disrupted at the surface of the sphere and forms vortexes (Fig. 22c). The pressure behind the sphere becomes negative which causes large /50 resistance. The coefficient of resistance reaches $R_x = 0.48$.

TABLE 2: THE COEFFICIENT OF HEAD RESISTANCE R_X FOR SEVERAL BODIES

The coefficient of head resistance R_x for several bodies.

Serial number	Type of body	Shape of the body and direction of the flow	Surface presumed middle section	Ratio of the size of the surface	Resistance R_x
1	Round plate		$\frac{\pi d^2}{4}$	—	1,11
2	Cone		$\frac{\pi d^2}{4}$	—	0,44
3	Cone with rounded top		$\frac{\pi d^2}{4}$	—	0,22
4	Ellipsoid of revolution-airship		$\frac{\pi d^2}{4}$	—	0,044
5	Rectangular plate		$a \times b$	$\frac{a}{b}$ 1 / 4 / 10 / ∞	1,1 / 1,1 / 1,28 / 1,83
6	Sphere		$\frac{\pi d^2}{4}$	—	0,47
7	Hollow hemisphere		$\frac{\pi d^2}{4}$	—	0,34
8	Cylinder		$\frac{\pi d^2}{4}$	—	0,84
		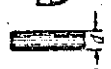		—	0,23
9	Cylinder		$l \times d$	$\frac{l}{d}$ 1 / 5 / 40	0,63 / 0,74 / 1,2

ORIGINAL PAGE IS
OF POOR QUALITY

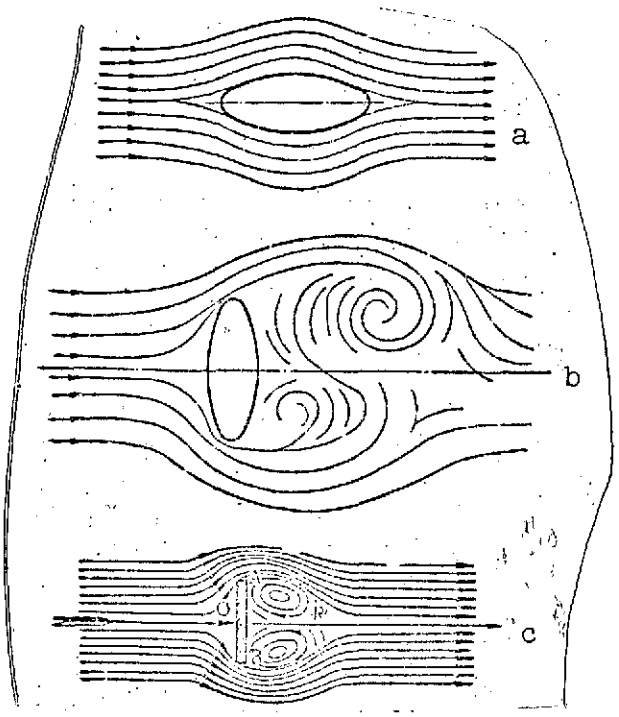

Fig. 21: Vortex configurations behind objects at various positions in the flow

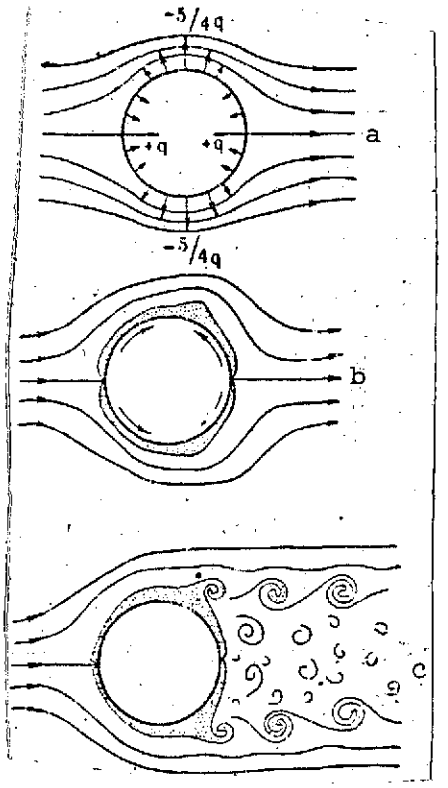

Fig. 22: Formation of vortexes behind a sphere

If the flow around the sphere takes place at large numbers of Reynold, then the border layer passes into the turbulent state. In this case the disruption of the border layer takes place at a point situated farther than in the case of the laminar layer. Due to this fact a smaller potential gradiant is obtained and the coefficient of head resistance decreases down to a value of $R_x = 0.10$, despite the fact that the friction at the surface of the sphere is higher. The turbulent flow in the border layer can be increased by making a ring out of wire on the front side of the sphere; this decreases the coefficient of resistance by approximately 50%.

Table 2 presents the coefficient of the head resistance R_x for a few bodies which were obtained by various authors in investigations on the flow around bodies.

9. Axes of Coordinates and Aerodynamic Coefficients

Three systems of coordinates are used in experimental aerodynamics, terrestrial, flow, and related.

In the terrestrial system of coordinates one of the axes is usually OY_0, is directed vertically upwards, while the other two, OX_0 and OZ_0 are disposed in the horizontal plane. This system of coordinates is used mainly for setting up wind tunnels and for certain models used in the latter.

In the flow system of coordinates the axis OX is directed along a vector of unperturbed flow velocity V; the axis OY is directed in the plane of symmetry of the model; it is the axis of the lifting force; the axis OZ (lateral) is disposed perpendicularly to the axes OX and OY.

The planes formed by the axes of coordinates are called XY -- plane of the flow; XZ -- plane of sliding, and YZ frontal plane.

In testing the flow in wind tunnels, the flow coordinates are truly coincidental with the terrestrial axes of the wind tunnel.

The origin of the coordinate axes of flow for airplane and airship models is placed at the center of gravity of the machines represented by these models while for an isolated wing, at its leading edge.

The axes of coordinate, which during the experiment are considered to be closely related with the model, are called related /52 axes of coordinates or model coordinates.

The origin of these axes of coordinates is usually placed in a point which corresponds to the center of gravity of the natural airplane or in any arbitrary point. The axis OX_1 which is called the long axis, is directed in the plane of symmetry of the model; in the airplane, it is parallel to the center core of the upper wing, while in the airship, it runs parellel to its axis. The axis OY_1 is called normal axis, and it is passed in the plane of symmetry of the model, which is perpendicular to the axis OX_1. The OZ axis is called the transversal axis and it is directed perpendicularly to the axis OX_1 and OY_1.

The plane X_1Y_1 is called the plane of symmetry, the plane X_1Z is called the main plane, while the plane Y_1Z is the transversal plane.

Figure 23 illustrates the disposition of the three systems of coordinates in relation to the model; the vector V represents the velocity of the flow, while the dotted line shows the direction of

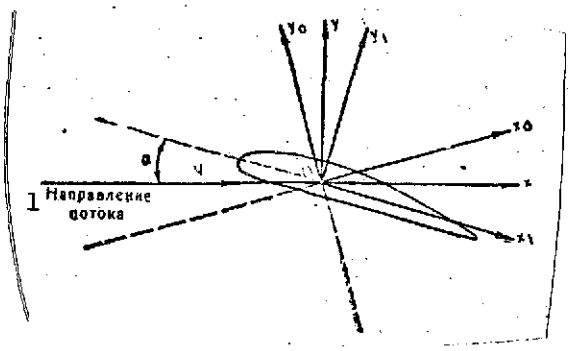

Fig. 23: Coordinate systems

Key: 1. direction of flow

the wing chord.

By rotating the wing around the OZ axis, the angle between the vector of the flow of velocity Z and the plane of the wing X_1Z, will change. This angle is called the true angle of attack, and is noted by α.

Force and moment aerodynamic coefficients. In solving practical tasks, the model is replaced by nature with the aid of aerodynamic coefficients. These coefficients are expressed in abstract numbers. /53

It is convenient for practical purposes to break down into components, according to the flow axes of coordinates, both the total aerodynamic force R, acting on the body around which the flow takes place, and the corresponding coefficient C_R as a result of which the following is obtained (Fig. 24):

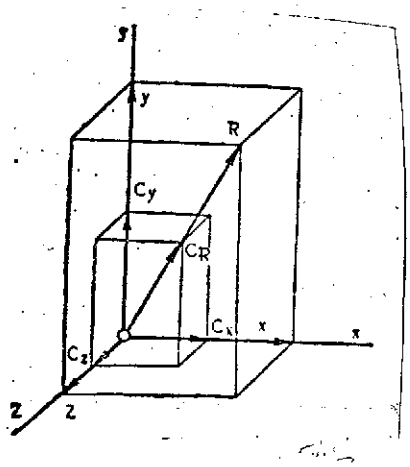

Fig. 24: Resolution of the coefficient C_R according to the coordinates of flow

Head resistance:

Lifting force:

Lateral force:

$$\left.\begin{aligned} X &= C_x S q = C_x S \frac{\rho V^2}{2}, \\ Y &= C_y S q = C_y S \frac{\rho V^2}{2}, \\ Z &= C_z S q = C_z S \frac{\rho V^2}{2}. \end{aligned}\right\} \qquad (32)$$

Here the coefficients C_x, C_y, C_z denote:

C_x -- coefficient of head resistance,
C_y -- coefficient of lifting force,
C_z -- coefficient of lateral force.

It can be seen from Fig. 24, that the force R and the coefficient C_R are the resultants of the corresponding components, i.e.: /54

$$\left.\begin{aligned} R &= \sqrt{X^2 + Y^2 + Z^2}, \\ C_R &= \sqrt{C_x^2 + C_y^2 + C_z^2}. \end{aligned}\right\} \qquad (33)$$

By resolving the moments according to the axes of coordinates, we obtain:

Rolling moment:

Yawing moment:

Pitching moment:

$$\left.\begin{aligned} M_x &= C_{mx} S q L = C_{mx} S L \frac{\rho V^2}{2}, \\ M_y &= C_{my} S q L = C_{my} S L \frac{\rho V^2}{2}, \\ M_z &= C_{mz} S q L = C_{mz} S L \frac{\rho V^2}{2}. \end{aligned}\right\} \qquad (34)$$

The resultant or total moment:

$$\left.\begin{aligned} M &= \sqrt{M_x^2 + M_y^2 + M_z^2}, \\ C_m &= \sqrt{C_{mx}^2 + C_{my}^2 + C_{zm}^2} \end{aligned}\right\} \qquad (35)$$

were C_{mx}, C_{my} and C_{mz} are the coefficients of the moments and are nondimensional numbers.

C_m is called the coefficient of the total aerodynamic moment. In such a manner, the basic formula of aerodynamics for the moment can be written in the following form:

$$M = C_m S L \frac{\rho V^2}{2}, \qquad (36)$$

where S is the area of the wings or another characteristic area of the body, and L is the conditional length.

10. Determination of Aerodynamic Coefficients. Liliental's Polar.

As a result of experimental investigations of the flow of air around bodies in wind tunnels, aerodynamic coefficients are obtained which can be expressed by the following formulas:

/55

$$\left.\begin{aligned} &\text{Coefficient of the resistance force:} && C_x = \frac{X'}{S' \frac{\rho' V'^2}{2}}, \\ &\text{Coefficient of the lifting force:} && C_y = \frac{Y'}{S' \frac{\rho' V'^2}{2}}, \\ &\text{Coefficient of the lateral force:} && C_z = \frac{Z'}{S' \frac{\rho' V'^2}{2}} \end{aligned}\right\} \qquad (37)$$

The corresponding moment coefficients are:

$$C_{mx} = \frac{M'_x}{S'L' \frac{\rho' V'^2}{2}}, \quad C_{my} = \frac{M'_y}{S'L' \frac{\rho' V'^2}{2}}, \quad C_{mz} = \frac{M'_z}{S'L' \frac{\rho' V'^2}{2}}. \qquad (38)$$

The indexes refer to the magnitudes corresponding to the model.

The forces acting on a certain construction are calculated using the following coefficients:

$$\left.\begin{aligned} &\text{Resistance force:} && X = C_x S \frac{\rho V^2}{2}, \\ &\text{Lifting Force:} && Y = C_y S \frac{\rho V^2}{2}, \\ &\text{Lateral Force:} && Z = C_z S \frac{\rho V^2}{2}. \end{aligned}\right\} \qquad (39)$$

The moments:

$$\left.\begin{aligned} M_x &= C_{mx} S L \frac{\rho V^2}{2}, \\ M_y &= C_{my} S L \frac{\rho V^2}{2}, \\ M_z &= C_{mz} S L \frac{\rho V^2}{2}. \end{aligned}\right\} \qquad (40)$$

The action of the force on a body of arbitrary shape is us- /56
ually determined by means of the following equation:

$$P_x = C_x F \frac{\rho V^2}{2}, \qquad (41)$$

where F is the surface of the midsection of the body, i.e. of the projection of the area of the body on a plane perpendicular to the direction of air flow.

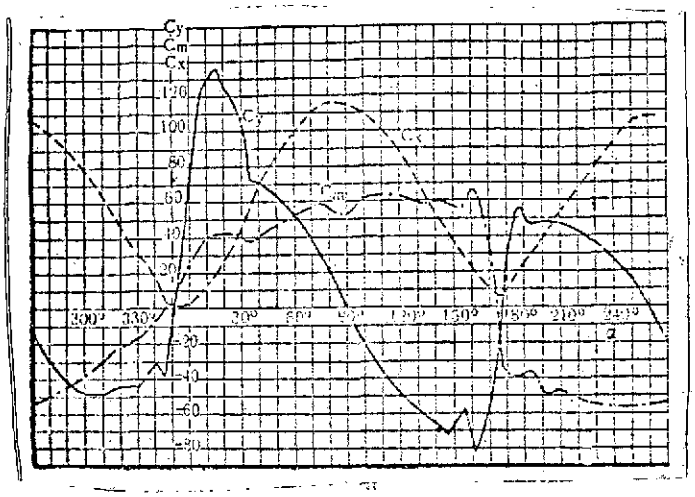

Fig. 25: Characteristics of the coefficients C_y, C_x and C_m of the wing obtained during circular flow.

The change in the aerodynamic coefficients C_y, C_x and C_m in relation to the angle of attack α in the circular flow of the profile of a finite span wing are shown in Fig. 25.

Liliental's polar. The curve characterizing the aerodynamic properties of the wings in general, are called aerodynamic characteristics. The curve illustrating the relations of C_y -- C_x in a rectangular system of coordinates, with marking on the curve of the angles of attack at which these coefficients were obtained is called the curve or polar of Liliental (according to the name of the scientist who suggested this method of illustration of the relationship).

Construction of the polar is performed in the following manner: /57
For each angle of attack α, the values C_y and C_x corresponding to the characteristics $C_y = f(\alpha)$ and $C_x = f(\alpha)$ are introduced into the system of rectangular coordinates C_y -- C_x. For each point, the magnitude of the angle of attack α is marked in degrees (Fig. 26). The value C_x is several times smaller than C_y, therefore, it is convened to take the scale for C_x five times larger than for C_y.

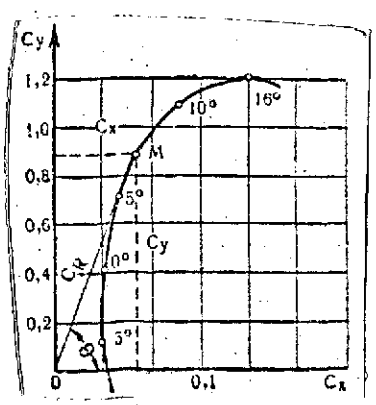

Fig. 26: Liliental's curve

The line drawn from the origin of the coordinate O to any point M on the curve of Liliental marked in the same scale C_y and C_x gives the sector OM which is equal to C_R, the coefficient of the resultant forces of twisting and resistance. The dimensional magnitudes of the forces can be obtained from Liliental's curve by multiplying each coefficient by the measured area S and the dynamic pressure $\rho V^2/2$, i.e.:

$$X = C_x S \frac{\rho V^2}{2}; \quad Y = C_y S \frac{\rho V^2}{2}; \quad R = C_R S \frac{\rho V^2}{2}.$$

The vector C_R makes the angle θ with the axis of the abscissa, the tangent of which is equal to

$$\tan\theta = \frac{C_y}{C_x} = K. \tag{42}$$

The ratio C_y/C_x is called the lift drag ratio. The reverse ratio

$$\frac{C_x}{C_y} = \frac{1}{K} = \mu \tag{43}$$

is called the reverse lift drag ratio.

The best values of lift drag ratios to date are around K = 22.

The center of pressure. The concept center of pressure or /58
in the old terminology, center of the effort of sail area, was created in relation with the study of stability in the symmetric flow around objects. The location of the center of pressure is determined by the coordinate x_1 and is found at the point of intersection of the total aerodynamic force R with the axis OX (Fig. 27). Therefore, the center of pressure is called the point in which the total aerodynamic force intersects the axis OX of the body. The center of pressure is expressed by a nondimensional magnitude since the ratio X_1 to the chord of the wing or the length of the body in general, is:

$$C_g = \frac{X_1}{L}; \tag{44}$$

This ratio is called the coefficient of the center of pressure.

For the wing, C_g is expressed in percent of the chord of the wing b, i.e.:

$$C_g = \frac{X_1}{b} \cdot 100.$$

If the origin of the coordinates is in point O near the leading edge of the wing, (Fig. 27), then C_y and C_x pass through the origin of the coordinates. The total resultant passes through the center of pressure, consequently the moment of the aerodynamic forces relative to the center of pressure should be equal to zero under conditions of equilibrium:

$$M = C_m S \frac{\rho V^2}{2} b - C'_y S \frac{\rho V^2}{2} X_1 = 0,$$

hence:

$$C_m \cdot b = C'_y X_1,$$

or

$$\frac{C_m}{C_y} = \frac{X_1}{b} = C_g.$$

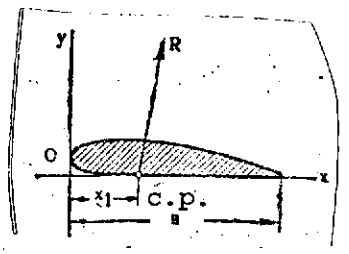

Fig. 27: Determination of the center of pressure

For small angles of attack, up to $\alpha = 20^{\circ}$, $C'_y = C_y$, consequently this equation can be rewritten in the following form: /59

$$C_g = \frac{C_m}{C_y} \quad (44a)$$

The magnitudes C_m and C_y are known from the flow, consequently coefficient C_g can be determined with their aid according to formula (44a).

The coefficients of the moment C_m and of the center of pressure C_g are illustrated in the form of curves on the same graph which contains the curves of Liliental: C_m as a function of C_y and C_g as a function of α, i.e.:

$$C_m = f(C_y); \quad C_g = f(\alpha)$$

11. Induced Drag of the Wing

The resistance force of an infinite span wing appears as a result of the friction of air against the surface and as a result of the breakdown of the flow. The magnitude of this force of resistance, depends on the state of the surface and on the shape of the wing profile. This force is called profile drag.

In the case of a finite span wing, in addition to profile drag, there appear other resistances caused by turbulent strings which are scattered away from the wing. The vortex line or a whole system of vortex lines which pass along the wing span, are called bound vortexes. These vortexes are dragged with the flow and they form behind the wing the vortex sheet. This sheet is unstable and soon after it leaves the wing, it twists into two vortex strings (Fig. 28).

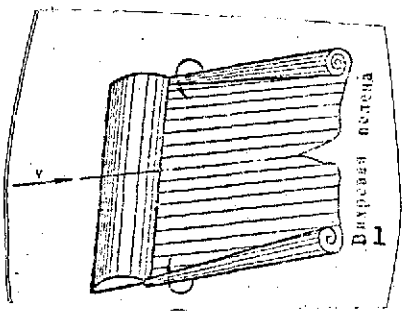

Fig. 28: Vortexes starting at a finite span wing form behind the wing the vortex sheet.

Key: 1. Vortex sheet

As a result of a diminished pressure above the wing, and the increased pressure under it, for a wing of finite span, the mass of the air near the face end of the wing, will tend to go upward and twist into vortexes. /60 These vortexes, as they are not connected with the wing at its tips, are carried away with the general flow and are drawn into vortex strings which go to infinity (Fig. 29). In a viscous fluid, these strings will extinguish and appear finite at a certain distance from the wing, as a result of friction.

The vortex strings running away from the wing elicit the vertical velocity W, which acts on the flow and deflects its direction so to decrease the angle of attack α by a magnitude of $\Delta\alpha$. This angle is called the angle of incidence (Fig. 30). The lifting

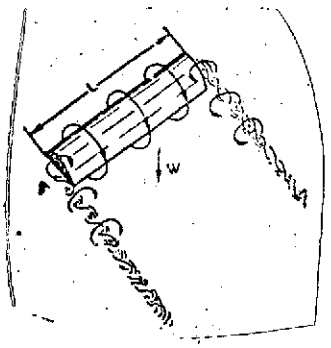

Fig. 29: Vortex strings starting at the tips of a wing of finite span.

force of the wing changes by a magnitude equal to the angle of incidence of the flow $\Delta\alpha$ as compared to the direction which it would take in the absence of the vertical velocity W. With the change in the direction of the lifting force, an additional resistance force appears Q_1 which is called the induced drag.

The angle of incidence has a small value, /61 therefore the resulting velocity V_1 can be taken to be equal to the velocity of the flow V, i.e.

$$V_1 = V,$$

and the angle of incidence of the flow can be calculated in radians according to the formula:

$$\operatorname{tg}\alpha = \Delta\alpha = \frac{W}{V}, \qquad (45)$$

taking the angle and its tangents as equal, due to their small value.

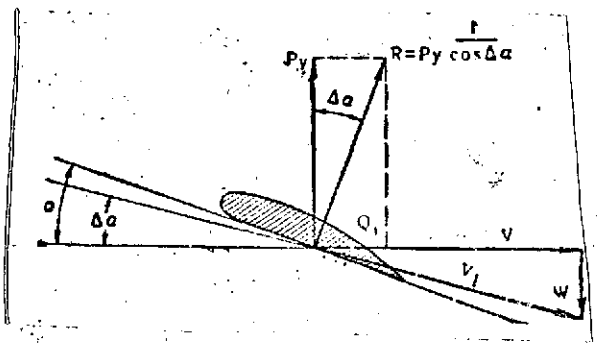

Fig. 30: Graphic illustration of the induced drag.

It is knows from the theory of induction that the average velocity of the slant flow, is determined by means of the formula:

$$W = -\frac{C_y}{\pi\lambda}\cdot V, \qquad (46)$$

where λ is the ratio of the length of the wing ℓ to its width b, i. e.:

$$\lambda = \frac{\ell}{b}, \qquad (47)$$

and is called the relative wingsspan or the aspect ratio.

Substituting the value W in equation (45) we obtain in radians

$$\Delta\alpha = \frac{C_y}{\pi\lambda}, \qquad (48)$$

or in degrees:

$$\Delta\alpha^\circ = \frac{360^\circ}{2\pi}\Delta\alpha = 57{,}3\,\Delta\alpha. \qquad (49)$$

Consequently, the angle of incidence of the flow near the wing will have the following value in degrees:

$$\Delta\alpha^\circ = 57{,}3\,\Delta\alpha = 57{,}3\frac{C_y}{\pi\lambda} = 18{,}23\frac{C_y}{\lambda}. \qquad (50)$$

We can see that, the larger the value of λ -- the aspect ratio, the smaller the angle of incidence of the flow and the larger the true angle of attack α, at a given C_y.

In such a manner, if the flow dashes over a finite span wing at an angle of attack α, then the true angle will be smaller than α, i.e.:

$$\alpha_i = \alpha - \Delta\alpha. \tag{51}$$

For an infinite span wing, λ is equal to infinity, and consequently $\Delta\alpha = 0$, i.e.:

$$\alpha_i = \alpha.$$

The magnitude of the induced drag can be found in Fig. 30. /62

$$Q_i = Y \operatorname{tg} \Delta\alpha = Y \Delta\alpha; \tag{52}$$

Since:

$$\Delta\alpha = \frac{C_y}{\pi\lambda},$$

then:

$$Q_i = Y \frac{C_y}{\pi\lambda}, \tag{52a}$$

but:

$$Y = C_y S \frac{\rho V^2}{2},$$

consequently:

$$Q_i = \frac{C_y^2}{\pi\lambda} \cdot S \frac{\rho V^2}{2}. \tag{53}$$

We can see from equation (53) that the coefficient of the induced drag is equal to:

$$C_i = \frac{C_y^2}{\pi\lambda}. \tag{54}$$

In such a manner, under conditions of air flow over a wing of infinite span the latter is subject to the head resistance X which consists of:

1. the profile drag X_p, which depends only on the wing profile and on the friction of the air against its surface;
2. the induced drag Q_i which depends on the shape and dimensions of the wing in the plane:

$$X = X_p + Q_i = (C_p + C_i) S \frac{\rho V^2}{2} = C_x S \frac{\rho V^2}{2}.$$

The curve C_i of the induced drag is represented on Lilienthal's curve in the form of a parabola, the top of which is at the origin of the coordinates and is called the parabola of the induced drag. In order to obtain the complete picture characterizing the given wing profile, the curve C_y -- α and the curve $K = C_y/C_x$ of the lift drag ratio are drawn on the same diagram (Sec. 13, Fig. 35).

12. N. E. Zhukovskiy's Theorem on the Lifting Force of the Wing.

When the air flows around the wing, a decrease in pressure is obtained above the wing, and an increased pressure below it. The pattern of distribution of pressure above and below the wing is shown in Fig. 31a. /63

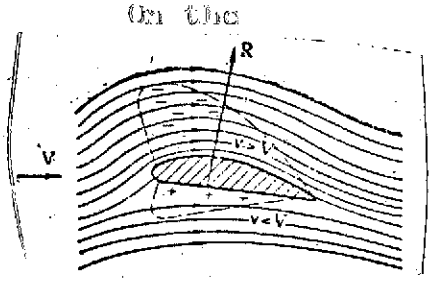

Fig. 31a: Distribution of pressure above and below the wing.

Fig. 31b: Velocity circulation around the wing.

On the basis of Bernoulli's theorem for a noncompressible fluid, this means that the velocity of the jets flowing directly under the wing, is higher than the velocity at a distance from the wing and is lower under the wing. If we draw a contour around the wing (Fig. 31b), then the portion of the contour above the wing will have a higher velocity of flow than the negative flow in the portion below the wing. This indicates that around a wing with a lifting force, velocity circulation exists, and since velocity circulation exists also around a vortex string, N. E. Zhukovskiy suggested to replace in various calculations, the wing by a bundle of vortexes which were called by him, bound vortexes.

N. E. Zhukovskiy's formula of the lifting force of the wing of an infinite span finds wide utilization in laboratory investigations, computations of propellers and wings of airplanes, ventilators and wind engines.

It has the following simple expression:

$$Y = \rho \Gamma V_0 l, \tag{55}$$

where Y is a force perpendicular to the velocity V_0 and acting on a wing sector of length l;

ρ -- mass density

Γ -- velocity circulation

V_0 -- velocity of unperturbed flow.

The direction of the flow Y is obtained according to the following rule: the velocity vector should be turned at a right angle to the side which is opposite to the circulation.

B. N. Yur'yev suggested the following demonstration for this theorem. Let us replace the wing by the bound vortex of a string with circulation Γ, equal to the circulation in the vicinity of the wing, and let us draw around the axis of this vortex a /64

cylinder with length ℓ and a radius R which is very large by comparison with the dimensions of the wing (Fig. 32).

In the velocity field caused by this vortex string, let us represent a forward flow; the overall flow for the distant point will be equivalent to the force around the wing. The force acting on the wing is equal to the force acting on the cylinder detail. Let us find this force. It is composed of the forces of pressure acting on the surface of this cylinder and of the resulting amount of movement which is carried into the cylinder and out of it per second.

Let us now find what pressures are obtained on the surface of the cylinder.

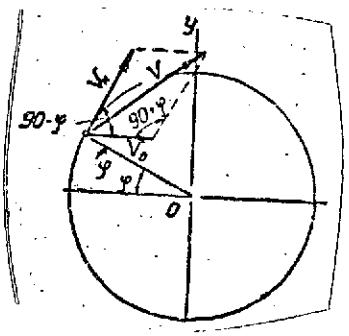

Fig. 32: N. E. Zhukovskiy's theorem

Applying Bernoulli's theorem to any jet of air which intersects the cylinder, the following equation can be written:

$$P_0+\frac{\rho V_0^2}{2}=P+\frac{\rho V^2}{2} \quad \text{or} \quad P_0-P=\frac{\rho}{2}(V^2-V_0^2). \qquad \text{(a)}$$

The velocity V is the geometrical sum of the velocities of the forward moving flow, V_o and the velocity V_k caused by the vortex. The velocity V_o is constant throughout while V_k is also constant and, being directed along the tangents to the cylinder, is variable direction and equal to:

$$V_k=\frac{\Gamma}{2\pi R}.$$

Assuming that the element is situated with reference to the surface of the cylinder at an angle ϕ, the resulting velocity is:

$$V^2=V_0^2+V_k^2-2V_0V_k\cos(90+\varphi);$$

since: /65

$$\cos(90+\varphi)=-\sin\varphi,$$

we can write:

$$V^2=V_0^2+V_k^2+2V_0V_k\sin\varphi.$$

Substituting the value V^2 in equation (a), we obtain equation: (b).

$$P_0-P=\frac{\rho}{2}(V_0^2+V_k^2+2V_0V_k\sin\varphi-V_0^2)=$$
$$=\frac{\rho}{2}(V_k^2+2V_0V_k\sin\varphi). \qquad \text{(b)}$$

Let us now pass to calculation of the lifting force developed by an element of the cylinder with a length on the generating line ℓ

and a circumference of length $Rd\phi$; its area is:

$$dS = lRd\phi$$

The pressure on this element equals $(P_0 - P)$.

Projecting the force acting on this element on the axis OY, perpendicular to the velocity V_0, we obtain:

$$dY_p = (P_0 - P)dS\cos(90 - \varphi) = (P_0 - P)lR\sin\varphi d\varphi,$$

or:

$$dY_p = \frac{\rho}{2}(V_k^2 + 2V_0V_k\sin\varphi)lR\sin\varphi d\varphi = \rho lRV_0V_k\sin^2\varphi d\varphi + \frac{\rho}{2}lRV_k^2\sin\varphi d\varphi.$$

The total lifting force is obtained by adding up all the elementary forces, i.e.

$$Y_p = \rho lRV_0V_k\int_0^{2\pi}\sin^2\varphi d\varphi + \frac{\rho}{2}lRV_k^2\int_0^{2\pi}\sin\varphi d\varphi.$$

The first integral equals π, the second equals 0. Consequently:

$$Y_p = \rho lRV_0V_k\pi.$$

since:

$$V_k = \frac{\Gamma}{2\pi R},$$

then:

$$Y_p = \frac{\rho lV_0\Gamma}{2}.$$

In addition to the forces of pressure, the cylinder is also subjected to pulse forces, for the calculations of which we have to find the total increment in the amount of motion of the fluid in the direction of the axis OY. /66

Let us first find the amount of motion carried in through the same element of the cylinder with an area:

$$dS = lRd\varphi.$$

Let us find the mass per second. The tangential component of the velocity V_k gives no projection perpendicular to the element of the surface. The perpendicular velocity V_n is obtained only on account of the velocity V_0 and equals $V_0\cos\phi$. Consequently, the elementary mass per second is:

$$dm = \rho V_n dS = \rho lRV_0\cos\varphi d\varphi.$$

The amount of movement carried by this mass in the direction of axis OY, will be equal to the elementary pulse lift dY_m. The component of the velocity V_0 gives no projection in this direction -- a projection will be obtained only from the velocity V_k and will equal $V_k\cos\phi$. Consequently:

$$dY_m = dmV_k\cos\varphi = \rho lRV_0V_k\cos^2\varphi d\varphi.$$

The total pulse force is obtained as a result of adding up all the elementary forces, i.e.

$$Y_m = \rho l R V_0 V_k \int_0^{2\pi} \cos^2 \varphi d\varphi = \rho l R V_0 V_k \pi.$$

Replacing V_K by its value $\Gamma/2\pi R$, we obtain:

$$Y_m = \frac{\rho V_0 l \Gamma}{2}.$$

The total magnitude of the lifting force will be equal to:

$$Y = Y_p + Y_m = \rho \Gamma V_0 l. \qquad (55)$$

We see that half of the force was obtained on account of the pressure and the other half on account of the pulse, i.e. creation in the fluid of a certain amount of movement.

It should be noted that the force of resistance in the case of such a flow equals 0. This can be seen from the fact that the velocity in the left and right hand side elements, relative to the axis OY of the cylinder are equal, consequently, the pressures will also be equal.

Therefore, no force of pressure is obtained on the axis OX, in the same way, the amount of movement in the fluid coming in and leaving through these elements of the cylinder, in the direction of the axis OX, are equal. Consequently, the force of the head resistance near a wing in an ideal fluid equals zero. /67

N. E. Zhukovskiy formulated his theorem in the following way: The lifting force acting on an infinite span wing is equal to the density of the fluid multiplied by the circulation, by the velocity of the flow at infinity and by the length of a detailed portion of the wing.

The direction of the force is obtained by turning the velocity vector at a right angle in the direction opposite to the circulation.

For a wing of finite span with vortex strings behind it, a similar derivation to the one suggested by N. E. Zhukovskiy's theorem, can be done by an approximate method (56).

Let us draw a plane at a distance from a wing, perpendicular to the direction of velocity of the flow; this plane intersects the vortex strings(I -- II), and we obtain the picture illustrated in Fig. 33. These vortexes create velocities around themselves which can be calculated by means of the formula (25):

$$V = \frac{\Gamma}{2\pi R}. \qquad (25)$$

Between the vortexes, the fluid acquires a velocity which is directed downward. As a result of this, a part of the fluid i.e.

directed downward

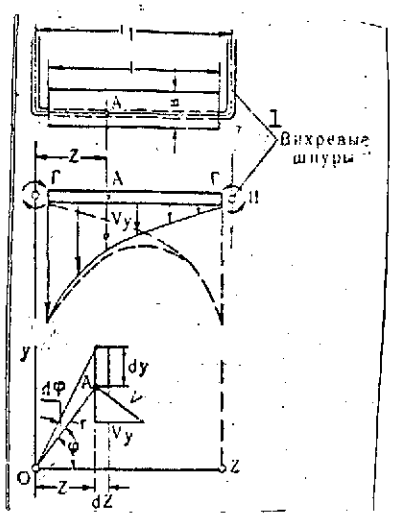

Fig. 33: Induced drag caused by vortexes behind the wing.

Key: 1. vortex strings.

that part situated between the vortexes, receives an increment in the amount of movement in this/68 direction. With regard to the part of the fluid which is situated outside the vortexes, it can be shown that it generally receives an amount of vertical movement from an adjacent vortex which is equal to the amount of movement received from a distant vortex and may have an opposite direction. Consequently, the total increment in the amount of movement for this part of the fluid equals 0. Thus, the action of a finite span wing on the flow of fluid around it consists in the fact, that the part of fluid which is confined between the vortexes receives an increment in the amount of movement in the vertical direction.

If a certain mass of air m is displaced by the wings downward, then the wing presses on it from above, while the fluid presses on the wing from below, causing a lifting force which is equal to the increment in the amount of movement of the displaced mass per unit time.

Let us see what is the value of the amount of movement created by one vortex in an infinitely narrow strip with a weight and length equal to one unit in the direction of the flight.

The vertical component of the velocity elicited in point A, (Fig. 33) by the left vortex, equals:

$$V_y = V\cos\varphi = \frac{\Gamma}{2\pi r}\cos\varphi,$$

where ϕ equals the angle indicated in Fig. 33.

Noting that:

$$r = \frac{Z}{\cos\varphi},$$

we obtain:

$$V_y = \frac{\Gamma}{2\pi Z}\cos^2\varphi.$$

The amount of movement in the parallelepiped which has a length in the direction of the flight equal to 1, a height dy and a width dz, can be written in the following manner:

$$V_y dm = V\rho dZ dy.$$

Here dm -- mass of the parallelepiped
ρ -- mass density of the air

One can see from the figure, that:

$$dy = \frac{rd\varphi}{\cos\varphi} = \frac{Zd\varphi}{\cos^2\varphi}.$$

Substituting this expression in the preceding formula, we obtain: /69

$$V_y dm = \rho \frac{\Gamma}{2\pi} \cdot dZ d\varphi.$$

Let us denote dM, the amount of movement in the whole strip which has a width dZ; then:

$$dM = \int_{-\frac{\pi}{2}}^{+\frac{\pi}{2}} V_y dm = \rho \frac{\Gamma}{2\pi} \cdot dZ \int_{-\frac{\pi}{2}}^{+\frac{\pi}{2}} d\varphi = \frac{1}{2} \rho \Gamma dZ.$$

This expression shows that dM does not depend on the coordinate Y. Consequently, for all strips with a similar width dZ, the amount of movement would be the same. Since we are dealing with two vortexes, their action adds up in the region between them and the amount of movement of this strip doubles and becomes equal to $\rho\Gamma$ dZ; outside, where the vortexes act in the opposite direction, the amount of movement along the vertical equals zero. Consequently, in order to obtain the total amount of movement we have to add up only those strips which lie between the vortexes.

Thus, we find:

$$2M = \int_0^l 2dM = \rho\Gamma \int_0^l dZ = \rho\Gamma l.$$

This expression gives the amount of movement along the vertical of all the strips with width l and a length equal to unity in the direction of the flight. The lifting force of the wing is equal to the amount of movement per second. An air column with a length equal not to one, but to V, passes through the examined plane per second. Substituting V in the previous equation, we obtain the expression of N. E. Zhukovskiy's theorem:

$$\rho\Gamma V l = Y.$$

The equation of relation. In solving practical problems related to the calculation of velocity circulation around the wing, two equations are used: the theoretical formula (55) of N. E. Zhukovskiy:

$$Y = \Gamma \rho V l,$$

and the formula of experimental aerodynamics: /70

$$Y = C_y S \frac{\rho V^2}{2} = C_y S q. \qquad (32)$$

For a rectangular wing S = bl where b is the weight of the wing and l is the span. Substituting the value of S in equation (32), we obtain:

$$Y = C_y \frac{\rho V^2}{2} bl.$$

The lifting force calculated by means of equation (55) (theoretical) should be equal to the lifting force obtained by the experimental formula, i.e.

$$\rho V l = C_y \frac{\rho V^2}{2} b l,$$

hence:

$$\Gamma = \frac{C_y}{2} b V. \qquad (56)$$

Equation (56) is called the equation of relation as it gives the relation between the experimental magnitude C_y and the theoretical Γ.

13. Transition from one Wing Span to Another

In practice one has to replot the Liliental polar obtained in the wind tunnel for a wing with aspect ratio λ_1 and construct another polar for a wing with a new aspect ratio λ_2 or for a wing with infinite span.

In the aerodynamic design of wind engines, the flows are calculated to an infinite span and in the process of the design, the induced drag is taken into consideration.

Since the characteristics of the profiles obtained in the wind tunnel are plotted for wings of finite span, when utilized for the wings of wind engines, the Liliental polar has to be recalculated from a finite span to an infinite one. This recalculation is performed graphically.

Let us assume that we have Liliental's polar for a wing with an aspect ratio $\lambda = 5$ which has to be reconstructed to infinite span $\lambda = \infty$. Since the induced drag of the wing with an infinite span equals zero, by subtracting the induced drag C_i of the given wing from the head resistance C_x we obtain the profile resistance C_p. This subtraction is done by means of the parabola of induced drag for $\lambda = 5$ which is constructed according to formula (54) depending on C_y. Laying out in the diagram (Fig. 34) the result of the calculation, i.e. profile resistance C_p in relation to C_y, we obtain the curve of profile resistance. In practice, this construction can be done as follows: by means of the opening of the compass, the distance between the Liliental polar $\lambda = 5$ and the parabola of the induced drag $\lambda = 5$ is shifted to the left up the ordinate axis. Uniting the obtained points by a dotted line (Fig. 34, left), the characteristic of the profile resistance which is at the same time the Liliental polar for an infinite span wing is obtained. The opening of the angle of attack α has to be laid out on the new Liliental polar, which is performed graphically. Along with the Liliental polar for an infinite span, the curve C_y is drawn in relation to α for $\lambda = 5$ of the profile under discussion (Fig. 34). Further, according to the formula of the flow slant:

$$\Delta\alpha = 57{,}3 \frac{C_y}{\pi\lambda} \qquad (50)$$

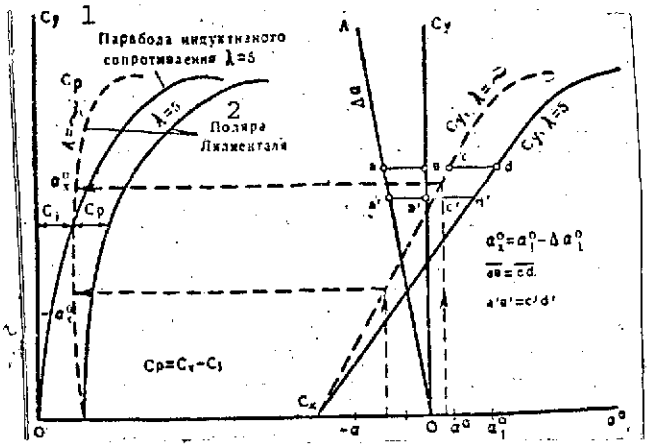

Fig. 34: The shift of Liliental's curve from one wing span $\lambda = 5$ to another $\lambda = \infty$.

Key: 1. parabola of induced drag $\lambda = 5$;
2. Liliental's polar

The magnitude of the flow slant /72 is plotted on the graph; the flow slant is calculated for a certain value, for example $C_y = 1.0$.

The slant of the flow is represented by a straight line O--A which is constructed in the same scale as the angles of attack on the abscissa. Further, curve C_y is drawn at $\lambda = \infty$ for which purpose each magnitude of C_y is shifted to the left by a corresponding segment ab; a'b' etc. which corresponds to the downwash angle $\nabla\alpha$ (Fig. 34). Further, by means of the obtained curve C_y -- α or $\lambda = \infty$, the opening of the angles of attack are placed on Liliental's polar which has previously been constructed on the left. The course of the determination of the angles on the Liliental curve, is shown by a dotted line with an arrow (Fig. 34).

In the transition from one finite span of the wing with an aspect ratio λ_1 to another finite span λ_2, the curve C_y -- α is shifted not by the whole value of the flow slant as in the case $\lambda = \infty$, but by the difference in the flow slant between the two cases, i.e. by the magnitude:

$$\Delta\alpha_1 - \Delta\alpha_2 = C_y\left(\frac{1}{\pi\lambda_1} - \frac{1}{\pi\lambda_2}\right)57.3. \quad (57)$$

In this case one calculates on Liliental's curve not the total induced drag, but the difference between the induced drags of the two wings with aspect ratio of λ_1 and λ_2:

$$C_{i_1} - C_{i_2} = C_y^2\left(\frac{1}{\pi\lambda_1} - \frac{1}{\pi\lambda_2}\right). \quad (58)$$

We can see that the recalculation from a wing with span to another is performed by means of two curves of the characteristics of the wing's profile -- Liliental's curve and the C_y -- α curve.

Table 3 presents the numeric values of the aerodynamic characteristics of profiles, which can be used for wings of wind engines. The graphic illustration of the characteristics of these profiles is given in Fig. 35 -- I, II, III, and IV. The ordinates of the profiles are given in Table 4 [54]. A certain profile is chosen, depending on the construction of the wind wheels. In Tables 3 and 4 and in Fig. 35, the number of profiles correspond to the number of experimental series in the given laboratory.

TABLE 3. AERODYNAMIC CHARACTERISTICS OF THE PROFILES OF FINITE SPAN WINGS

Profile 909 TsAGI				Profile 910 TsAGI				Profile 730 MAI				Profile 796 MAI			
α	c_y	c_x	c_m	α	c_y	c_x	c_m	α	c_y	c_x	c_m	α	c_y	c_x	c_m
−10	−28,00	2,30	1,00	−10	−82,80	4,00	−1,20	1	2,60	1,02	2,80	−8	−31,20	2,30	0,00
− 8	−13,80	1,70	4,00	− 7	−12,60	1,40	3,40	0	9,40	0,76	4,40	−6	−18,60	1,57	2,64
− 6	0,20	1,30	7,30	− 4	6,30	1,10	8,00	2	25,20	0,98	7,60	−4	−5,60	1,22	5,50
− 4	14,00	1,30	10,70	− 2	21,00	1,20	11,20	4	39,80	1,58	11,00	−2	7,40	1,16	8,60
− 2	26,60	1,54	13,60	0	34,50	1,60	14,40	6	54,20	2,46	14,40	0	20,50	1,34	11,50
0	40,00	2,00	16,80	2	47,40	2,20	17,80	8	68,40	3,74	17,60	2	33,60	1,74	14,60
2	53,00	2,80	20,20	4	60,40	3,20	21,00	10	81,20	5,24	20,40	4	46,46	2,42	17,80
4	65,50	4,00	23,70	6	74,00	4,56	24,40	12	91,00	7,20	22,80	6	60,50	3,44	21,20
6	79,50	5,38	27,20	9	93,0	5,96	29,00	14	98,00	12,18	24,80	8	74,20	4,66	24,40
9	99,50	7,80	32,20	10	—	—	—	16	97,80	21,36	27,80	10	87,40	6,04	27,20
12	118,00	10,82	36,60	12	112,00	9,70	33,75	18	95,80	27,60	—	12	99,20	7,56	29,20
15	133,00	14,20	39,90	15	126,00	13,20	37,20	20	90,00	—	—	14	110,40	9,24	31,38
17	141,00	17,50	42,80	18	130,40	18,80	40,00					16	120,20	11,66	33,20
18	143,00	19,30	43,40	19	129,40	21,20	40,80					18	126,50	13,24	34,60
19	141,60	21,30	43,90	20	127,60	23,90	41,00					20	128,20	16,20	35,46
20	139,20	23,50	44,40	22	122,00	24,40	—					22	125,60	20,06	36,00
				24	115,20	36,80	—					24	119,20	24,20	36,40
				−12	—	8,00	—								
				−14	−47,60	13,70	−10,00								

TABLE 4: ORDINATES FOR THE CONSTRUCTION OF PROFILES

Abscissa (in % of the length of the profile)	Number of Profile I — 909		II. — 910		III — 730		IV — 796	
	Ordinate in % of the length of the chord							
	upper	lower	upper	lower	upper	lower	upper	lower
0	2,95	2,95	2,50	2,50	0	0	3,50	3,50
1,25	5,55	1,11	4,70	1,00	—	—	6,10	1,40
2,5	6,60	0,80	5,63	0,51	2,22	−0,70	7,21	0,76
5,0	8,26	0,20	7,00	0,17	3,19	−1,03	8,86	0,03
7,5	9,50	0,05	8,33	0,05	—	—	10,01	−0,50
10	10,51	0	8,90	—	4,42	−1,43	10,89	−0,87
15	11,86	0	10,5	0	—	—	12,17	−1,38
20	12,60	0	10,66	0	5,65	−1,88	12,96	−1,57
30	13,00	0	11,0	0	6,00	−2,20	13,35	−1,65
40	12,50	0	10,56	0	5,64	−2,21	13,00	−1,60
50	11,30	0	9,53	0	5,25	−2,03	11,95	−1,48
60	9,73	0	8,22	0	4,46	−1,84	10,44	−1,29
70	7,73	0	6,56	0	3,46	−1,55	8,39	−1,04
80	5,43	0	4,60	0	2,34	−1,19	5,95	−0,73
90	2,86	0	2,42	0	1,17	−0,75	3,20	−0,40
95	1,47	0	1,25	0	—	—	1,75	−0,25
100	0,00	0	0,00	0	0,00	0,00	0,14	−0,01

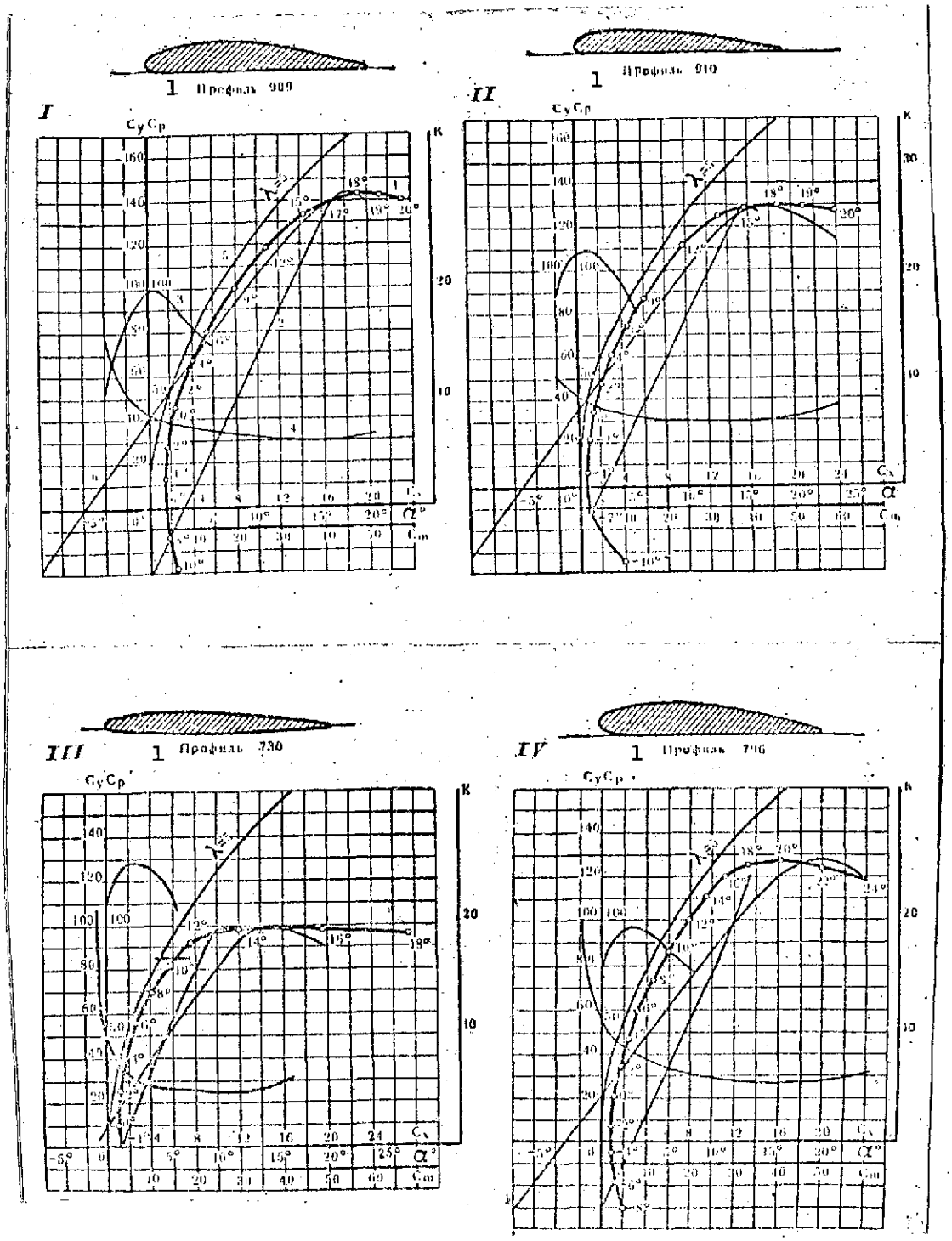

Fig. 35: Complete aerodynamic performance [illegible] of the wing. [Legend illegible]

Key: 1. Profile

Since the induced drag of the wing is calculated in the aerodynamic design of windwheels by means of formulas, in using the above profile for wind wheels, the characteristics of the /76
selected profile have to be reconstructed for the characteristics of an infinite span. Thise reconstruction has to be done according to Fig. 34.

Example. Let us recalculate the characteristics presented in Fig. 35 -- IV of the profile 796 with an aspect ratio $\lambda = 5$ to an infinite span and $\lambda = \infty$. Recalculation is done using the above presented method.

By means of equation (54), let us calculate C_i for various values of C_y, the magnitudes of which are written in Table 3.

$$C_i = \frac{C_y^2}{\pi\lambda} = 0{,}0637 C_y^2.$$

$\alpha = 0°$; $C_{i_0} = 0.0337 \cdot 0{,}205^2 = 0{,}00268$ in the scale of the graph $C_i = 0{,}200$

$\alpha = 2°$; $C_{i_2} = 0.0337 \cdot 0{,}336^2 = 0{,}00715$ » » » $C_i = 0{,}715$

$\alpha = 3°$; $C_{i_3} = 0.0337 \cdot 0{,}465^2 = 0{,}01370$ » » » $C_i = 1{,}370$

$\alpha = 14°$; $C_{i_{14}} = 0{,}0337 \cdot 1{,}104^2 = 0{,}07800$ » » » $C_i = 7{,}800$

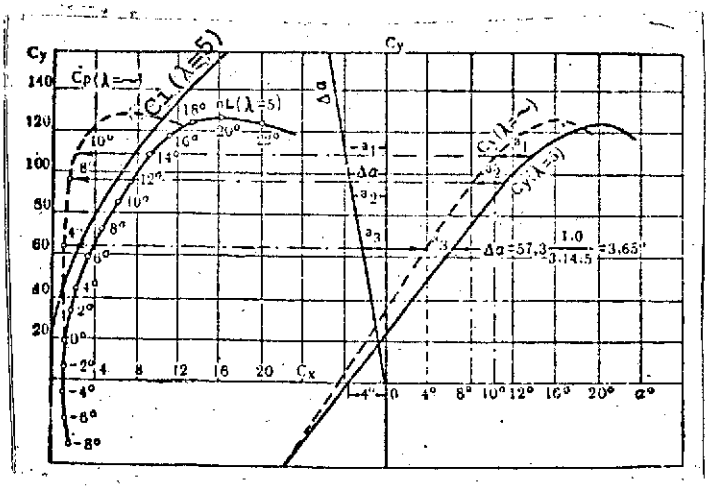

Fig. 36: Graphic representation of the characteristics of an infinite span wing (example).

The points obtained for C_i /77 are plotted on the graph in Fig. 36, and through them, curve C_i is drawn -- the parabola of the drag. On the same graph, let us draw Liliental's curve, i.e. C_y and C_x at the corresponding angles α which are given in Fig. 35 -- IV. By means of these two curves, let us construct the curve of the profile resistance $C_p(\lambda = \infty)$.

The plotting of the point is done either by recalculation using equations $C_p = C_x - C_i$, where C_x and C_i have to be taken at the corresponding C_y, or by shifting the segment taken between the curves C_y and πL on the graph up to the axis of the ordinate, by means of the opening of the compass. This plotting is done on the graph to the left of the dotted curve C_p ($\lambda = \infty$).

Further, let us plot in the right hand side of the graph, curve $C_y(\lambda = 5)$ -- α, which is given in Fig. 35 -- IV, and let us construct the downward angle $\Delta\alpha$.

The magnitude of this angle at $C_y = 1.0$ is equal to: /78

$$\Delta\alpha = 57.3\frac{C_y}{\pi\lambda} = 57.3\frac{1.0}{3.17.5} = 3.65^\circ.$$

The segment in the scale of the angles on the abscissa for angle $\Delta\alpha = 3.65^\circ$ is equal to 1.62 x 3.65 = 5.92 mm. This segment is laid out on the horizontal to the left of axis C_y, against $C_y = 100$ and through its end we draw the oblique line $\Delta\alpha$ passing through the origin.

By shifting the curve ($\lambda = 5$) to the left by the magnitude of the segment a_1, a_2, a_3 etc., we obtain the curve of $C_y(\lambda = \infty)$, which is shown by the dotted curve.

The size of the angles on Liliental's curve plotted for infinite span $C_p(\lambda = \infty)$, is shown on the graph by means of dotted lines.

It is suggested to do the recalculation of the other characteristics presented in Fig. 35 to an infinite span wing as an exercise.

14. Classification of Wind Engines According to the Principle of Their Operation

The existing systems of wind engines can be divided into three catagories according to the type of construction of their wheel and it position in the wind stream.

The first category includes those wind engines in which the wind wheel is situated in the vertical plane; the plane of rotation is perpendicular to the direction of the wind and consequently the /80 axis of the wind wheel is parallel to the flow. Such wind engines are called winged.

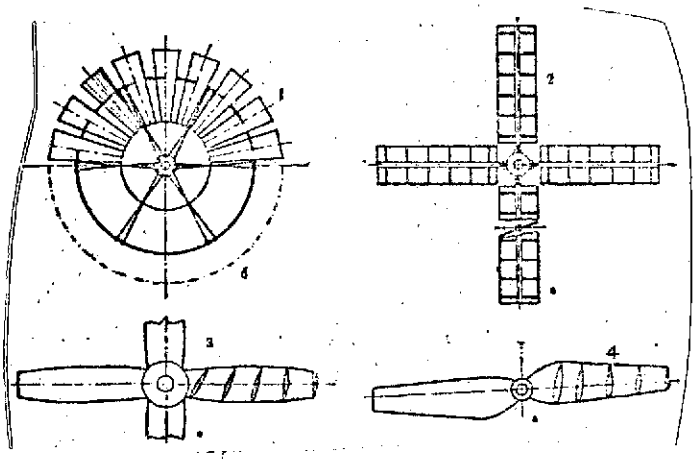

Fig. 37: Diagrams of the wheels in winged wind engines: 1 -- multi-bladed wing wheel; 2, 3, and 4 -- sparsely bladed wind wheels.

According to Gost 2656-44, depending on the type of wind wheels and on their rapidity, winged wind engines are divided into three groups (Fig. 37).

Rapidity is the ratio of the circular velocity of the blade's ends to the velocity of the wing:

$$z=\frac{\omega R}{V}. \qquad (59)$$

Group 1 -- comprises wind engines which are multi-bladed low speed with a rapidity $Z_n \leq 2$.

Group 2 -- wind engines which are sparsely bladed low speed and of simple wood-metal construction comprising wind-mills with a rapidity $Z_n > 2$.

Group 3 -- wind engines which are sparsely bladed and rapid, $Z_n \geq 3$.

The second category comprises systems of wind engines which have a vertical axis of rotation of the winged wheel. They can be divided into groups according to the type of their construction:

Rotating in which the nonoperational blades are either covered with a screen or are situated with their arms against the wind (Fig. 38);

Rotor type Savonius wind engines (Fig. 39).

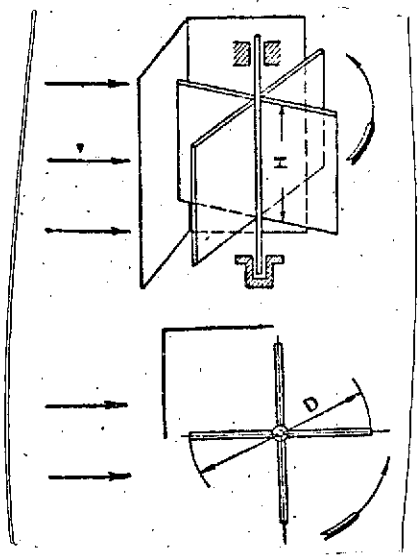

Fig. 38: Diagram of the rotating wind engine

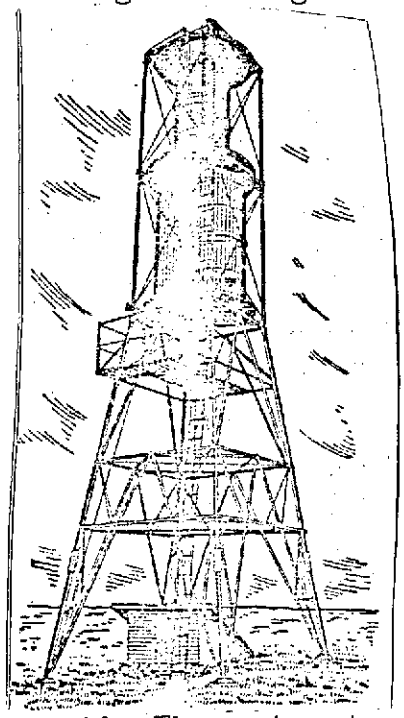

Fig. 39: The rotor type wind engine

To the third category belong those wind engines which operate by the principle of the watermill wheel and are called drum type. In these wind engines, the axis of /81 rotation is horizontal and perpendicular to the direction of the wind (Fig. 40).

There are in existence other types of wind engines as well, however, they have not received practical application and have remained in the realm of suggestions of their inventors.

With regard to the above presented classifications let us examine the main principles of operation of the wind forces elicited by wind engines.

Work of the surface acted on by the wind. A wind stream with cross section F possesses kinetic energy which is determined by the expression:

$$\frac{mV^2}{2}. \qquad (60)$$

The mass of air flowing through cross-section F with a velocity V is equal to: /82

$$m = \rho FV. \qquad (61)$$

Substituting in the expression of the kinetic energy ρFV instead of m, we obtain:

$$\frac{mV^2}{2} = \frac{\rho FV^3}{2}, \qquad (62)$$

hence, the energy of the wind changes proportionally to the cube of its velocity.

Let us see what is the percentage of wind energy which can be transformed into useful work by a surface situated perpendicularly to the direction of the wind and moving in the same direction, as, for example, in wind engines of the rotatory type.

The work per second or the power T is determined by the product of the force P by the velocity V:

$$T = PV.$$

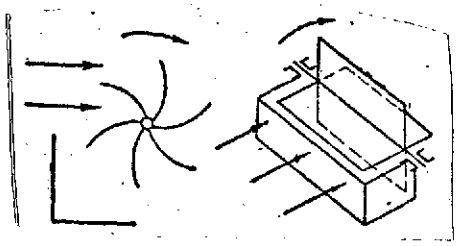

Fig. 40: Diagram of the drum type wind wheel.

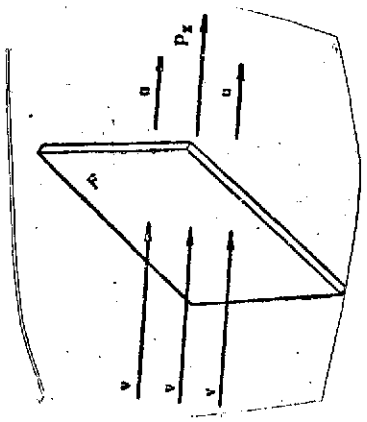

Fig. 41: Action of the wind force on the surface.

The same work can be obtained either on account of a large force at low speed of displacement of the working surface, or contrarily on account of a small force and consequently a small surface, but with a corresponding increase in the velocity of its displacement.

Let us assume that surface F is situated perpendicularly to the direction of the wind. Due to its retardation by the surface, the air flow is dammed and will flow around it and produce a pressure with a force P_X. As a result of the action of this force, the surface is displaced in the direction of the flow with a certain velocity U (Fig. 41); the work under these conditions will equal the product of the force by the velocity U, with which the surface F is displaced. i.e.: /83

$$T = P_X U, \qquad (a)$$

while P_X is the drag, which according to equation (41), equals:

$$P_x = C_x F \frac{\rho}{2}(V-U)^2. \qquad (b)$$

In this case the wind dashes over the surface with a relative velocity which is equal to:

$$W = V - U \qquad (c)$$

substituting the value of P_X from equation (b) into equation (a), we obtain:

$$T = C_x F \frac{\rho}{2}(V-U)^2 U. \qquad (d)$$

The energy of the wind flow dashing over this surface, as determined by equation (62), equals:

$$\frac{F\rho V^3}{2}.$$

Let us determine the ratio of the work produced by a moving surface and expressed by equation (d) to the energy of the wind stream which has a cross section equal to the surface, i.e.:

$$\xi = \frac{C_x F \frac{\rho}{2}(V-U)^2 U}{F\frac{\rho V^3}{2}} = C_x (V-U)^2 \frac{U}{V^3}.$$

After transformations we obtain:

$$\xi = C_x \left(1 - \frac{U}{V}\right)^2 \frac{U}{V}. \qquad (63)$$

The magnitude ξ is called the output coefficient of the wind energy.

We can see from equation (63) that ξ depends on the velocity of displacement of the surface in the direction of the wind. At a certain value of the velocity U, the coefficient ξ receives its maximum value, which we shall now determine.

Denoting the ratio U/V by e and substituting in equation (63), we obtain:

$$\xi = C_x (1 - e)^2 e. \qquad (63a)$$

In order to find e, at which ξ is maximal, we shall make the first /84 derivative of the equation (63a) equal to zero:

$$\xi = C_x (1 - e)^2 e = C_x e - 2C_x e^2 + C_x e^3.$$
$$\frac{d\xi}{de} = C_x - 4C_x e + 3C_x e^2 = 0.$$

Hence:

$$3e^2 - 4e + 1 = 0.$$

In solving this equation with regard to e, we obtain two roots: $e_1 = 1/3$ and $e_2 = 1$, at $e = 1$ $\xi = 0$. Consequently we have to take:

$$e = \frac{U}{V} = \frac{1}{3}.$$

In such a manner, in order to obtain maximal ξ, the surface has to move with a velocity:

$$U = 1/3V. \qquad (64)$$

Such a result is obtained on the basis of the following argument. If the velocity of displacement of the surface equals zero, U = 0, then the work of the wind also equals zero. If U = V, i.e., the surface is displaced with the velocity of the wind, then the work will also be equal to zero. Since there is no drag on account of which the work is performed, it follows that the value of the velocity U is confined within the limits U = 0 and U = V. In order to find the value of the velocity U at which maximum ξ is obtained, let us give various values to the ratio of the velocity of displacement of the surface to the velocity of the wing from 0 to 1, and substituting these values in equation (63a), let us find at what ratio U/V this maximum obtained.

Plotting the calculated figures on the graph, we obtain the characteristic curve of the power for surface F which works with drag (Fig. 42).

Examining the curve, we see that the maximum value: /85

$$\frac{\xi}{C_x} = 0{,}148$$

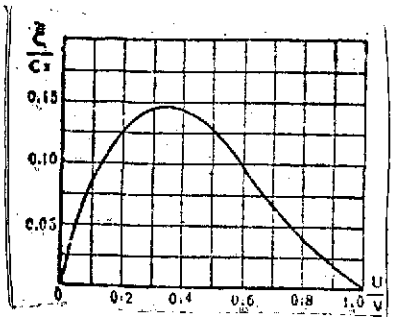

Fig. 42: Characteristics of the ideal output coefficient of the wind energy by a surface displaced in the direction of the wind.

is obtained when the velocity of displacement of the surface amounts to 1/3 of the velocity of the wind, i.e. when

$$U = 0.33V, \quad \xi = 0.148 C_x.$$

The coefficient of the head resistance C_x for surfaces situated perpendicularly to the wind flow, according to Table 1, equals about 1.30, consequently we can write

$$\xi_{max} = 0.148 \cdot 1.30 = 0.192,$$

i.e. the maximum output coefficient of the wind energy under conditions of the work of the surface with drag, cannot be more than:

$$\xi = 0.192.$$

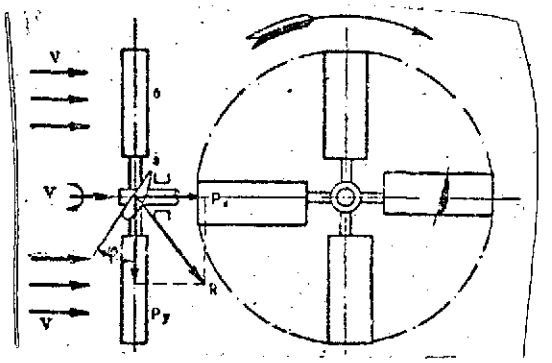

Fig. 43: Construction diagram of the winged wind wheel

Work of the wind wheel in winged wind engines. Winged wind wheels operate on account of a slightly askew impact under conditions of movement on the blade, perpendicularly to the direction of the wind velocity, as opposed to the direct impact which we examined in the previous case. The construction of such a wheel is shown in Fig. 43.

The wings are attached to the horizontal shaft. The number of the wings in modern wind engines vanes from 2 to 24, and generally does not exceed 24. The /86
wing of the wind wheel is made of the flap a and the blade b which is attached to the flap in such a manner that it forms with the plane of rotation a certain angle ϕ. This angle is called the rigging angle of the blade (Fig. 43). An air stream with a relative velocity W dashes over its elements under an angle α, which is called the angle of attack, and with a force R. The angles ϕ and α determine to a significant extent the effectiveness of the wings. The force R is distributed between the forces P_x and P_y (Fig. 44a). The forces P_x produce a pressure in the direction of the wind which is called head pressure. The forces P_y act in the plane y -- y of the rotation of the wind wheel and create a torque.

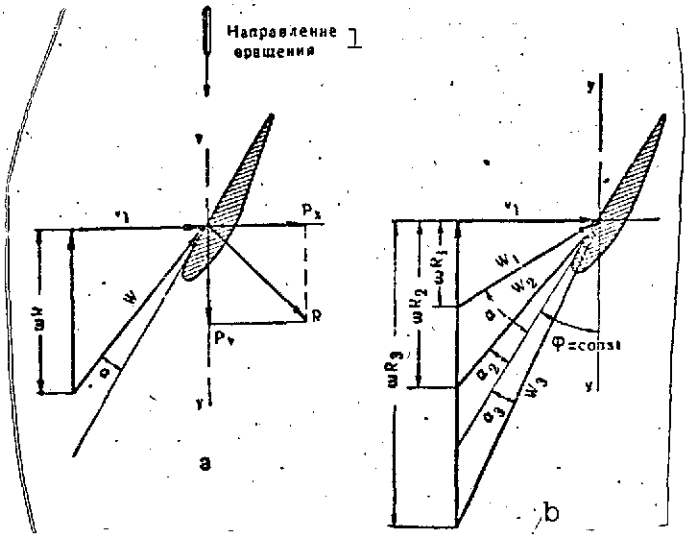

Fig. 44: a--diagram of action of the forces of the air stream on an element of the blade; b--graphic representation of the relative stream dashing over the elements of the blade, situated at various radii of the wind wheel; 0

Key: 1. direction of rotation

The maximum forces which cause the rotation of the wheel, are obtained at a certain value of the angle of attack α, i.e. the angle of the slope of the relative stream to the surface of the blade. In view of the fact that the /87 circular velocity is not uniform along the length of the wing, but rather increases as its elements are farther away from the axis of rotation of the winged wheel, the relative velocity W of the flow dashing over the blade, also increases. At the same time the angle of attack α decreases and at a certain circular velocity ωR, where ω is the angular velocity, this angle becomes negative (Fig. 44b). Consequently, not all the elements of the wing have maximal lifting force.

If we decrease the angle ϕ of each element of the blade as it becomes removed from the axis of rotation, so that the most convenient angle of attack α is maintained more or less constant, then we obtain conditions under which almost all the elements of the blade operate with the same maximal lifting force. A blade with a variable rigging angle ϕ assumes the shape of a propeller surface.

The correct rigging angles of the blade under conditions of inadequate lift-drag ratio, and of a width corresponding to the given rapidity, ensure a high output coefficient of the wind energy. For example, in high performance models, it reaches 46%.

Concerning the lifting force of the rotating cylinder. In addition to the above described two principles of the work of the wind during its action on the surface, one must recall the force elicited on a cylinder which rotates in the air stream. The work of the wind in this case can be performed on account of this force.

If the cylinder is situated in the flow of an ideal fluid, perpendicular to its direction, then the filament dashing over the cylinder is subdivided surrounds the cylinder and again closes up behind it. In front of and behind the cylinder, two critical points A and B are obtained on its surface, where the velocities are equal to 0,

(Fig. 45), while in points C and D, the velocities will be maximal and equal between themselves.

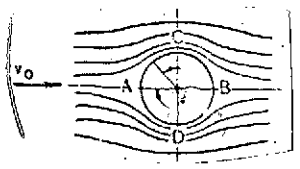

Fig. 45: Diagram of the flow of an air stream around a cylinder at rest.

If a cylinder placed in the air stream rotates around its own axis, then it will drag with it particles of the fluid situated closest to the walls of the cylinder; the flow of the latter will be coincident with the direction of rotation of the cylinder. Thus we obtain two flows. One, which is the main flow surrounding the cylinder and another which is induced by the rotation of the cylinder, which is analogous to the flow surrounding a vortex string. The velocity of this flow decreases as the distance from the cylinder increases (see Sec. 8). /88

Under conditions of a clockwise rotation of the cylinder, and a movement of the main flow from the left to the right and upward (Fig. 46), the velocities of both flows add up and give a large combined velocity, while below, the velocities of the two flows are subtracted and give a comparatively small resultant velocity.

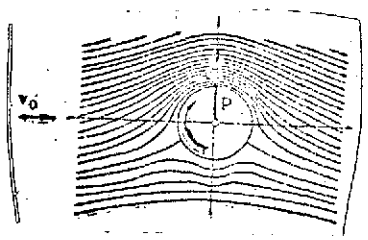

Fig. 46: Diagram of formation of the lifting force on a cylinder rotating in the airstream.

Examining the spectrum of the stream lines around the cylinder (Fig. 46), we see that the stream lines above the cylinder are disposed very closely, while, on the contrary they are disposed very sparsely below the cylinder. Using Bernoulli's equation for the range of the flow outside the border layer, we see that above the cylinder a decrease in pressure takes place, while below it, an increase. This phenomenon causes force P, which acts on the cylinder from above and perpendicular to the flow.

The magnitude of this force, in the particular case of N. E. Zhukovskiy's theorem (equation 55), is equal to:

$$P = \rho \Gamma V_0 l.$$

Since the lifting force is proportional to the circulation Γ, it depends to a large extent on the ratio of the circular velocity of the cylinder U to the velocity of the main stream V_0, i.e. on U/V_0.

Experimental curves showing the dependence of C_y, the coefficient of the lifting force, and of C_x, the coefficient of the head drag on the ratio U/V, where U is the circular velocity of the rotating cylinder and V is the velocity of the stream, are shown in figures 47-48; the C_y and C_x of these curves are /89

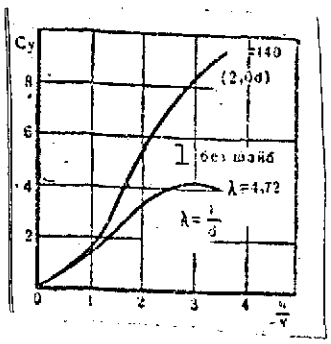

Fig. 47: Characteristics of the rotor

$C_y = f(U/V)$ according to flow.

Key: 1. without rings

calculated according to the formula:

$$C_y = \frac{P_y}{F\frac{\rho V^2}{2}} \quad \text{и} \quad C_x = \frac{P_x}{F\frac{\rho V^2}{2}},$$

where F = dl; d -- diameter of the cylinder, l -- its length.

The air-blast cylinders had discs at each end, which were called rings. The presence of rings in the cylinders considerably increased the lifting force.

The first engines with rotating cylinders instead of blades, were suggested in 1925, however, the experiments performed at that time did not give positive results.

Since the drag of the cylinders is extremely high, as compared to the lifting force, their lift-drag ratio is very low. It is known from experiments, that in the best case the lift-drag ratio of cylinders at a certain ratio of circular velocity to the velocity of the airstream, receives its maximal value around 7, i.e. 1/3 of the value in the case of the wing. However, the circular velocity of displacement of the cylinders in the plane of rotation of the wind wheel changes proportionally to its radius. Consequently the best ratio will be at a single distance of the section of the /90 cylinder from the axis of the winged wheel. As a result of this, the latter can not give an adequate effect on the whole. However, the construction of the winged wheel with the rotating cylinder near the axis of the flap, is extremely complicated as compared to the winged wind wheel.

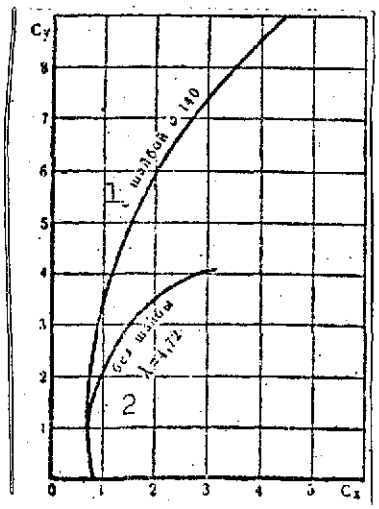

Fig. 48: The polar of the rotor of Fig. 47.
Key: 1. with ring
2. without ring

15. Advandages and Disadvantages of Various Systems of Wind Engines

Wind engines of the second and third categories (rotating and drum type) are distinguished by a very simple diagram of the work of the wind wheel. In rotating wind engines, the airstream dashing over the wind wheel presses on the blades on one side of the axis of rotation, while on the other side, it meets either the screen covering those blades which go against the wind, or else the arms of the blades, if they are revolving, as a result of which, the pressure of the stream on them is rather small. As a result of this, the force obtained in the plane of rotation creates the torque of the wind wheel. An analogous phenomenon takes

place in drum type wind engines. However, in rotating wind engines, the position of the wind wheel in the wind stream is more favorable; it is always in the working position from whatever side the wind blows. In drum type wind engines, as in the winged type (the first category), a special device is needed in order to adjust the wind wheel to the wind with each change of its direction.

The main shortcomings of rotating and drum type wind engines, result from the principle of disposition of the working surfaces of the wind wheel in the wind stream, i.e.:

1. Since the working blades of the wing are displaced in the direction of the airstream, the wind load does not act simultaneously on all blades, but does so in succession. As a result, each blade is subjected to a discontinuous load, the magnitude of which equals for a blade oriented in the direction of the wind.

$$P = C_R F \frac{\rho}{2}(V-U)^2,$$

where: C_R -- the coefficient of the force P, acting in the direction of rotation;
U -- the velocity of displacement of the blades.

The blades of the opposite side of the wind wheel, if they are covered with a screen (Fig. 38), are subjected to a drag, which is /91 equal to:

$$P_1 dr = C_x F \frac{\rho U^2}{2}.$$

If they go with the arms to the wind:

$$P' dr = C'_x F_p \frac{\rho (V+U)^2}{2}$$

(here, F_p is the lateral surface of drag of the arms; C'_x is the coefficient of the drag.)

The torque of the wind wheel is the difference between the torque of these forces. As a result, the output coefficient of wind energy is rather low, and does not exceed 10% under the most favorable conditions, as determined by experimental investigations.

The output coefficient of wind energy, in the case of rotating wind engines, can be increased by improving the surfaces and the combination of their disposition in the wind stream. However, due to elaborate construction, such a wind engine becomes more complicated than the winged engine.

2. The movement of the surfaces of the wind wheel, in the direction of the wind, prevents the development of large revolutions, since the surfaces cannot move faster than the wind.

3. The dimensions of the utilized part of the wind stream (the marked-off surface), are small by comparison to the dimensions of the wheel itself, which considerably increases its weight per unit of the established power of the wind engines.

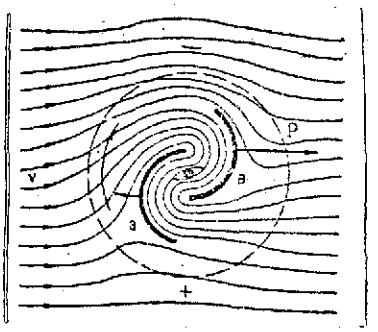

Fig. 49: Diagram of the movement of the airstream around the Savonius type rotor.

In the Savonius type wind engine (Fig. 39), the wind wheel also rotates in a horizontal plane, but the flow through the marked-off surface takes place quite differently than in the rotating and drum type wind engines. In the given case, the wind wheel creates the lowest damming to the wind stream. /92

The wind stream which is directed as shown in figure 49, glides past the convex surface a and acts with full force on the surface b, which it surrounds and creates an additional force which sets the rotors in motion. Those drags which were found in rotating wind engines, are not found here. Therefore, the output coefficient of wind energy by the Savonius type wind engines, is approximately twice higher than in the rotating engines. The highest output coefficient of wind energy, $\xi = 18\%$, was found with the Savonius model rotor in a wind tunnel.

As confirmed by both theory and practice winged wind engines are to a considerable extent, free of the above enumerated shortcomings of rotating and drum type wind engines.

The good aerodynamic properties of winged wind engines, the possibility of constructing them at high power (above 1000 hp in one unit), the relatively light weight per unit power, all these are the main advantages of winged engines of these categories. Therefore, they have now found widest distribution. The plants in USSR and in other countries, manufacture to date exclusively winged wind engines.

CHAPTER 4: THEORY OF THE IDEAL WIND ENGINE /93

The theory of the ideal wind engine was first elaborated in 1914 by V. P. Metchinkin, on the basis of the theory of the ideal screw propeller. In this work, he established the concept of the output coefficient of winded energy by the ideal wind engine.

In 1920, Prof. N. E. Zhukovskiy, elaborated the theory of "Windmill NEZh" where he derived the output coefficient of the wind energy by the engine [7].

Analogous theories were later elaborated, again in our country, by Prof. G. Kh. Sabinin and academician G. F. Proskura.

The theory of the ideal wind engine of Prof. N. E. Zhukovskiy, is a classical theory. It establishes that the maximal coefficient of utilization of the wind energy by an ideal wind engine is equal to 0.593.

From the point of view of the practical application, the theory of the ideal wind engine was elaborated more completely by Prof. G. Kh. Sabinin, according to him, the output coefficient of the wind energy for an ideal wind engine equals 0.687.

Ideal wind engine is called the wind wheel in which:

1. the axis of rotation is parallel to the velocity of the wings;
2. there is an infinitely large number of blades of small widths;
3. the profile drag of the wing equals zero, and the circulation along the blade is constant;
4. the velocity of the airstream on the wind wheel is constant throughout the marked-off area of the wind engine;
5. the angular velocity tends to infinity.

16. The Classical Theory of the Ideal Wind Engine /94

Let us represent a uniform wind stream dashing over an ideal wind wheel with a velocity V across section AA' (Fig. 50). In the section BB', the velocity of the winged wheel will be $V_1 = V - v_1$, while at a certain distance behind the wind engine, in section CC', the velocity will be $V_2 = V - v_2$.

The rotating wind wheel creates a damming effect, as a result of which the velocity of the stream decreases as the distance to the wind engine for, and behind, some time diminishes the wind engine, as shown by curve I in Fig. 50. At the same time, the pressure of the air p increases as the distance to the wind engine decreases,

(curve II), and it decreases markedly during the passage through the marked-off area. Behind the wind engine, a certain negative pressure $p_0 - p_2$, is formed, which asymptotically approaches 0 as the distance from the wind engine increases, i.e. the normal pressure is restored (curve III).

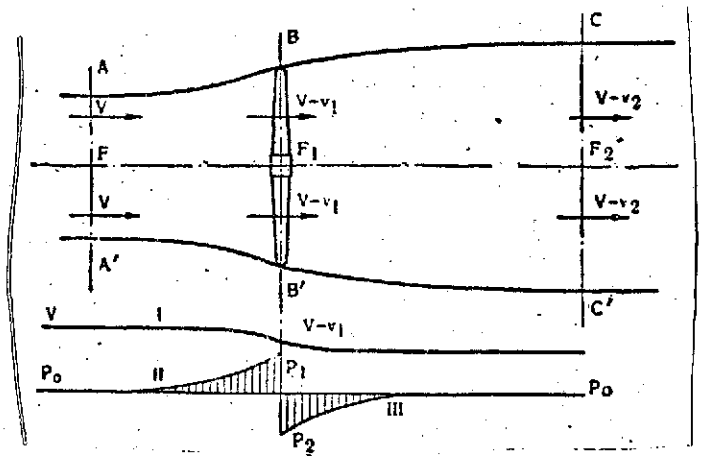

Fig. 50: Characteristics of air flow through wind wheel

The loss in velocity behind the ideal wind engine, can be determined by means of Bernoulli's equation:

$$p_2 + \frac{\rho V_2^2}{2} = p_0 + \frac{\rho V^2}{2}.$$

Since $p_2 < p_0$, $V > V_2$.

The kinetic energy of the wind in front of the wind engine, equals $mV^2/2$, while behind the wind engine, it is $m(V - v_2)^2/2$. The difference between these energies is spent on the wind wheel and in the absence of losses, it can be obtained as useful work:

$$T_1 = \frac{mV^2}{2} - \frac{m(V - v_2)^2}{2}. \qquad (a)$$

Transforming the right hand side of equation (a), we obtain:

$$\frac{m}{2}[V^2 - (V - v_2)^2] = \frac{m}{2}(2Vv_2 - v_2^2) = mv_2\left(V - \frac{v_2}{2}\right).$$

consequently:

$$T_1 = mv_2\left(V - \frac{v_2}{2}\right). \qquad (b)$$

The energy T_1, perceived by the wind wheel, can be expressed as the product of the force of pressure of the wind T, by the velocity in the plane of the wind engine $(V - v_1)$, i.e.:

$$T_1 = P(V - v_1). \qquad (c)$$

The head pressure P is equal to the increment in the movement of the jet passing through the marked-off area, i.e.:

$$P = mv_2.$$

Substituting the value of P in the equation (c), we obtain

$$T_1 = mv_2(V - v_1). \qquad (d)$$

Comparing equations (b) and (d), we find that:

hence:

$$mv_2\left(V-\frac{v_2}{2}\right)=mv_2(V-v_1),$$

or:

$$v_1=\frac{v_2}{2}$$

$$v_2=2v_1. \qquad (65)$$

The equality (65) shows that the loss of velocity in the airstream takes place not only in the section of the wind wheel, but also at a certain distance behind the wind engine, while the total loss in velocity is twice larger than the loss on account of the wind wheel.

A mass of air m, passes through marked-off area F of the wind /96
wheel, the amount of which per second equals:

$$m=\rho FV. \qquad (61)$$

Substituting the value of the air mass into the expression of the kinetic energy of the wing in front of the wind wheel, we obtain:

$$\frac{mV^2}{2}=\frac{\rho FVV^2}{2}=\frac{\rho FV^3}{2},$$

which corresponds with the equation (62) and Sec. 14.

Taking the ratio of the work per second, perceived by the ideal wind wheel:

$$T_1 = P(V - v_1)$$

to that energy of the wind which would correspond to a cross section equal to the area marked-off by the wind engine:

$$\frac{\rho FV^3}{2},$$

we obtain the ideal output coefficient of the wind energy ξ_i.

$$\xi_i=\frac{P(V-v_1)}{F\frac{\rho V^3}{2}}. \qquad (66)$$

Let us transform this equation:

$$\frac{P(V-v_1)}{F\frac{\rho V^3}{2}}=2\frac{P}{F\rho V^2}\cdot\frac{V-v_1}{V}.$$

The expression $2P/F\rho V^2$ is called the coefficient of loading per marked-off area or the coefficient of frontal pressure, and is denoted by the B, i.e.:

$$B=\frac{2P}{F\rho V^2}. \qquad (67)$$

Substituting in this equation, $P = \rho F (V - v_1) v_1 = \rho F (V - v_1) 2v_1$ and denoting $v_1/V = e$, we obtain after reduction:

$$B = \frac{2\rho F (V - v_1) 2v_1}{\rho F V^2} = \frac{4 (V - v_1) v_1}{V^2} = 4e (1 - e). \tag{68}$$

Proceeding in the same way with equation (66), we obtain for ξ_1:

$$\xi_1 = \frac{F\rho (V - v_1)^2 2v_1}{F \frac{\rho V^2}{2}} = \frac{4 (V - v_1)^2 v_1}{V^3} = \frac{4 (V - v_1)}{V} \cdot \frac{(V - v_1)}{V} \frac{v_1}{V} = \tag{69}$$

$$= 4e (1 - e)^2.$$

The ratio $v_1/V = e$ is called the drag coefficient. /97

Let us determine the value of e, at which ξ_1 will have the maximal value. For this purpose, let us take the first derivative and make it equal to 0, i.e.:

$$\frac{d\xi_1}{de} = \frac{d}{de} [4e (1 - e)^2] = \frac{d}{de} (4e - 8e^2 + 4e^3) = 0,$$

or:

$$\frac{d\xi_1}{de} = 4 - 16e + 12e^2 = 0,$$

hence:

$$3e^2 - 4e + 1 = 0.$$

Solving this equation, we find that ξ has its maximal value when $e = 1/3$, but

$$\xi_1 = 4 \cdot \frac{1}{3} \left(1 - \frac{1}{3}\right)^2 = \frac{16}{27} = 0{,}593.$$

From equation (66) let us find B, the coefficient of loading per marked-off area at maximal ξ_1:

$$B = 4 \left(1 - \frac{1}{3}\right) \frac{1}{3} = \frac{8}{9} = 0.888.$$

In such a manner, the following main assumptions can be derived from the classical theory of the ideal wind engine.

1. The maximum output coefficient of wind energy of the ideal wind wheel equals $\xi_1 = 0.593$.

2. The loss of velocity in the plane of the wind wheel equals 1/3 of the velocity of the wind:

$$v_1 = \frac{1}{3} V.$$

3. The total loss in the velocity of the wind behind the wind wheel is twice larger than the loss in the velocity of the wind in the plane of the wind wheel:

$$v_2 = \frac{2}{3} V.$$

In such a manner, the velocity of the wind behind the wind wheel amounts to 1/3 of the velocity of the wind in front of the wind wheel.

4. The coefficient of loading per marked-off area of the wind wheel equals B = 0.888.

Assuming the drag coefficient $e = v_1/V$ varies in the limits from 0 to 1 and calculating by means of equation (66) and (68), we obtain the following values for coefficient ξ_i and B: /98

$e = \frac{v_1}{V}$	0,1	0,2	0,333	0,4	0,5	0,6	0,7	0,8	0,9	1,0
ξ_i	0,324	0,512	0,592	0,576	0,500	0,384	0,252	0,128	0,036	0
B	0,360	0,640	0,888	0,960	1,000	0,960	0,840	0,640	0,360	0

17. The Theory of the Ideal Wind Engine of Prof. G. Kh. Sabinin

The difference between this theory and former theories consists in the fact that in determining the axial force of pressure of the stream on the wind wheel, the pulse of the force is calculated according to the turbulent solenoid in that place where it has assumed a steady state cylindrical shape, and not at the time of its formation, as was assumed by the previous theories. Since the solenoid in the cylindrical part has an area of the cross section which is larger than the area marked-off by the wind wheel, the axial force and the output coefficient of wind energy, according to the theory of G. Kh. Sabinin, will be somewhat larger.

As a consequence of the conditions accepted for determining the ideal wind engine (Sec. 16), we obtain the following: the axial velocities are constant throughout the section of the stream, which results from the turbulent theory of the screw propeller of N. E. Zhukovskiy: the circulation around any closed contour inside the drifting stream equals 0, and consequently, the flow is not turbulent and the tangential velocities are equal to 0. The circulation in the plane of rotation of the wind engine equals 0, and there is only a pressure jump. The tip losses are equal to 0, as they are inversely proportional to the number of blades and to the angular velocity of rotation.

Let a homogeneous flow with a velocity V, dash over the wind engine as shown in Fig. 50. Let us draw through the circle described by the tips of the blades, the flow lines forming a bottle shaped surface AA'BB'CC', which we shall call "boundary surface".

As the distance from the wind engine grows, the boundary surface gradually passes into a cylindrical surface. That part of the stream which is enclosed in the boundary surface is called working flow. The boundary surface BB'CC', which is situated behind the wind engine, is a surface of division formed of an infinitely thin vortex layer, consisting of a series vortex strings of infinitely low intensity, which start off at the tips of the blades and are wound in the shape of a coil with infinitely small pitch on the surface of the division (Fig. 51). In such a manner, the surface of the division is a vortex solenoid. The vortex layer of the solenoid, can be schmatically represented as consisting of a series of vortex strings, the /99

diameter of which equals the thickness of the vortex layer. The external particles of such a vortex have a velocity which is similar to the velocity of the adjacent nonturbulent layer. The velocities decrease toward the center of the vortex, if we imagine that the vortex rotates like a solid body.

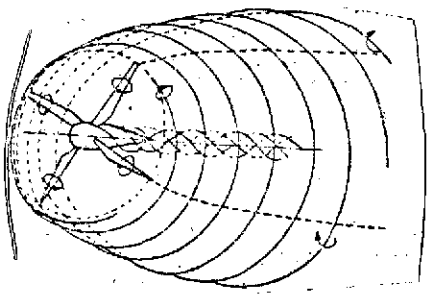

Fig. 51: Formation of a vortex solenoid behind the wind wheel.

Such an infinitely thin vortex layer requires no formation of energy, since its kinetic energy is infinitely small as a result of the infinitely small mass of the layer, while its maximal velocities are finite.

Assuming that at a sufficient distance from the wind engine, the vortex solenoid assumes a cylindrical shape and drifts into infinity, we obtain that the streams both inside and outside the solenoid are parallel and the pressures are constant in all the points of the flow which are sufficiently removed from the wind engine.

The deformation of the flow caused by the ideal wind engine results in the application of velocities produced by the vortex solenoids on a homogeneous flow, while the velocities caused by the solenoids are directed in the reverse direction with respect to the velocity of the flow. /100

The increase in the amount of movement of the fluid caused by the wind engine equals the amount of movement caused by the newly formed cylindrical part of the solenoid.

Figure 52 represents the diagram of the air flow through the wind wheel. In a section A -- A', infinitely far from the wind engine, the flow has a velocity V and a surface F. In the section B -- B', in the plane of the wind wheel, the axial velocity of the flow equals $V - v_1$, where v_1 is the velocity caused by the vortex selonoid at its end; the marked-off area is F_1.

In the section C -- C', infinitely far away from the wind engine, the velocity in the cylindrical part of the solenoid amounts to $V - v_2$, where v_2 is the velocity caused by the solenoid at a sufficient distance from the wind engine. The velocity of the flow outside the cylindrical part of the solenoid will be V, since the solenoid causes no velocity in the external flow.

The velocity of movement of an infinitely long vortex solenoid with respect to the flow, has been assumed by Prof. G. Kh. Sabinin to be equal to half the velocity caused by the solenoid inside it, i.e. equal to $v_2/2$. Since the solenoid is carried by the flow with the velocity V, the absolute velocity of the solenoid will be

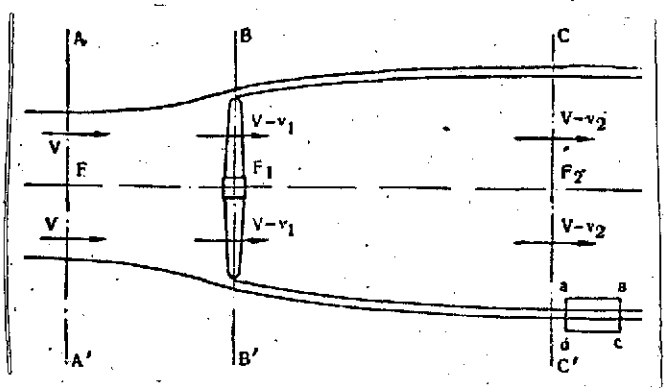

Fig. 52: Diagram of the flow through of the airstream through the wind wheel.

$V - v_2/2$; this is the velocity/101 of formation of the vortex solenoid.

Let us determine the circulation of the velocity of the vortex solenoid per unit of its length, for which purpose let us describe a rectangular contour abcd in such a manner that its sides ab and cd will be parallel to the axis of the stream, while the sides bc and da will be perpendicular to it (Fig. 52). Going around the contour in clockwise direction, the circulation on the side ab, according to equation (19), would be $\overline{ab}\,(V - v_2)$, since the velocity $V - v_2$ is parallel to ab. The circulation along cd will be $\overline{cd}V$; the circulation along the sides bc and da will be equal to 0, since these sides are perpendicular to the velocity V and $V - v_2$; the circulation at the side where these sides intersect the vortex solenoid is also equal to 0 since the vortex layer is infinitely thin while the circular velocity of rotation of the particles of the vortex layer is finite. The circulation throughout the contour will be:

$$\overline{ab}(V - v_2) - \overline{cd}V,$$

since:

$$\overline{ab} = \overline{cd},$$

the circulation along the contour abcd will equal:

$$-\overline{ab}\cdot v_2.$$

The circulation per unit length of the solenoid will be:

$$\Gamma = -\frac{\overline{ab}v_2}{\overline{ab}} = -v_2. \qquad \text{(a)}$$

Let us calculate the pulse of the force required for the formation of the vortex solenoid and for this purpose, let us use the following theorem. The pulse of the force $P\Delta t$ required for the formation of the vortex ring, equals the area of the vortex ring F multiplied by the circulation of the velocity Γ around the vortex and multiplied by the density of the fluid ρ:

$$P\Delta t = \rho F\Gamma. \qquad \text{(b)}$$

Here the pulse of the force is in a direction perpendicular to the plane of the vortex ring.

If we were to break down the splenoids into elementary rings with a length along the axis of the solenoid of dz, then per unit length of solenoid there will be 1/dz vortex rings. /102

The force pulse for the formation of a single vortex ring of the solenoid amounts to:

$$\rho F_2 d\Gamma, \tag{c}$$

where $d\Gamma$ is the circulation of the velocity of one ring;
F_2 is the area of the cross section of the cylindrical part of the solenoid.

Since the length of the solenoid increases in time dt by:

$$\left(V-\frac{v_2}{2}\right)dt,$$

over the same interval of time, the following rings are formed:

$$\left(V-\frac{v_2}{2}\right)\frac{dt}{dz}. \tag{d}$$

The pulse of the force and the wind engine in term dt will be numerically equal to the sum of the pulses required for the formation of the vortex rings appearing during the same time. On the basis of equations (c) and (d), this sum will amount to:

$$Pdt=\rho F_2 d\Gamma\left(V-\frac{v_2}{2}\right)\frac{dt}{dz}. \tag{e}$$

Let us rewrite this equation in the following manner:

$$Pdt=\rho F_2\frac{d\Gamma}{dz}\left(V-\frac{v_2}{2}\right)dt, \tag{f}$$

but:

$$\frac{d\Gamma}{dz}=\Gamma \tag{f1}$$

is the circulation of the velocity per unit length of the solenoid, which, according to equation (a) equals v^2. Therefore, reducing equation (e) by lower dt and substituting in it, instead of Γ its value v_2, we obtain:

$$P=-\rho F_2 v_2\left(V-\frac{v_2}{2}\right).$$

Let us transform this equation by representing it in the form of two components:

$$-P=[\rho F_2(V-v_2)]v_2+\rho F_2\frac{v_2^2}{2}. \tag{70}$$

The expression in the square brackets of the first term in the right hand side of the equation is the mass of the air passing through the marked-off area per unit time, while the whole first term i.e.:

$$[\rho F_2(V-v_2)]v_2,$$

is the increment in the amount of movement of this mass which we shall denote by m_1. The second term is in its dimension the same increment in the amount of movement per unit time. It cannot be broken down to two factors so that a certain mass of fluid would correspond to one factor, while a certain velocity which would be /103

the same for all particles of this mass, would correspond to the second factor, since we do not know the characteristics of that process in which the formation of the amount of movement represented by

$$\rho F_2 \frac{v_2^2}{2}$$

takes place.

For the sake of convenience in subsequent reasoning, let us multiply and divide this expression, i.e. the second term of equation (70), by v_2:

$$-P = [\rho F_2 (V - v_2)] v_2 + \left[\frac{\rho F_2 \frac{v_2^2}{2}}{v_2}\right] v_2. \tag{70a}$$

The fraction in the square brackets cannot be reduced by v_2, since in its physical essence, the numerator of this fraction is an integral:

$$\rho F_2 \frac{v_2^2}{2} = \int dm v_1,$$

where the law of formation of function m and v is not known to us.

The expression

$$\frac{\rho F_2 \frac{v_2^2}{2}}{v_2}$$

is called the bound mass and is noted by m_2. Let us note that:

$$\rho F_2 (V - v_2) = m_1.$$

Equation (70a) can be rewritten in the following manner:

$$-P = (m_1 + m_2) v_2. \tag{71}$$

The sum (m_1 + m_2) is called the drag mass, while velocity v_2 is called the velocity of traction. In such a manner, equation (71) can be formulated in the following way: the frontal pressure caused by the flow on the wind engines, equals the product of the drag mass by the velocity of the traction with opposite sign. The diagram of the formation of the bound mass m_2 is shown in Fig. 53. The particles of the airstream which in the first moment are situated in the plane of rotation of the wind engine AA and outside the sphere of influence of the wind engine, move to a distance $v\Delta t$ after a certain interval of time Δt and assume a position A'A'. The particles of the air which in the beginning are situated inside the marked-off area and represent the beginning of the stream passing through the wind engine, cross a distance $(V - v_2)\Delta t$ after a time Δt, and assume the position CC. In this minute the vortex solenoid will extend from the wind engine to the section bb and have a length of $(V - v_2/2)\Delta t$. In such a manner, the length of the solenoid formed during the time Δt will be longer by $v_2/2\Delta t$ than the column of fluid passing through the wind engine. The part of the solenoid cc -- bb will be filled with the air sucked by the solenoid from the end bb. This mass of air is the bound mass. /104

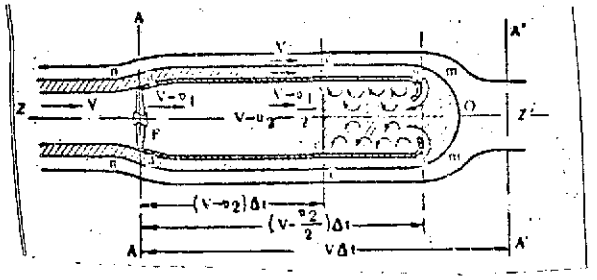

Fig. 53: Formation of the bound mass.

In reality, the increment in the amount of movement of the mass over the time Δt can be written:

$$\rho F_2 \frac{v_2}{2} \Delta t v_2.$$

and related per unit time:

$$\left[\rho F_2 \frac{v_2}{2}\right] v_2,$$

where the expression in square brackets is the mass of air confined in the section of the solenoid cc, bb, and v_2 is the increment in the velocity of this mass or the velocity of traction.

The layer of fluid with a ringed-shaped section enclosed between the surfaces ommccnn and aa bb, which is hatched in Fig. 53 and forms the walls of the bottle, is used for the formation of the bound mass. In reality, the phenomenon is not as simple; in its movement the solenoid breaks down to individual vortex wings which gradually extinguish, but the amount of movement caused by them will be preserved. /105

Let us write the balance of the energy of the air flowing through the wind wheel per second. The energy imparted by the flow equals:

$$(m_1 + m_2)\frac{V^2}{2}.$$

the energy perceived by the wind engine: $P(V - v_1)$.

the energy carried by the flow in the form of kinetic energy:

$$(m_1 + m_2)\frac{(V - v_2)^2}{2}.$$

The losses related to the formation of the bound mass, calculated by the velocity of the traction [32]:

$$m_2 \frac{v_2^2}{2}.$$

The equation of the balance of energy will have the following form:

$$(m_1 + m_2)\frac{V^2}{2} = P(V - v_1) + (m_1 + m_2)\frac{(V - v_2)^2}{2} + \frac{m_2 v_2^2}{2} \qquad \text{(a)}$$

Substituting in the equation (a) the value $P = (m_1 + m_2)v_2$ and dividing by $(m_1 + m_2)$, we obtain:

$$V^2 = 2(V - v_1)v_2 + (V - v_2)^2 + \frac{m_2 v_2^2}{m_1 + m_2}. \qquad \text{(b)}$$

Substituting the values of m_1 and m_2, in equation (b), obtain:

$$m_1 = \rho F_2 (V - v_2) \text{ и } m_2 = \rho F_2 \frac{v_2}{2},$$

$$V^2 = 2(V - v_1)v_2 + (V - v_2)^2 + \frac{\rho F_2 v_2 \cdot v_2^2}{2\left[\rho F_2 \left(V - v_2 + \frac{v_2}{2}\right)\right]}.$$

oor:

$$V^2 = 2(V - v_1)v_2 + (V - v_2)^2 + \frac{v_2 \cdot v_2^2}{2V - v_2}. \qquad (c)$$

Solving equation (c) relative to v_2, we find: /106

$$v_2 = \frac{2v_1}{1 + \frac{v_1}{V}}. \qquad (72)$$

This is the first velocity relation which differs from the analogous one in the classical theory.

Let us write the equation of the flow assuming that a flow with a velocity V dashes over a wind engine staying in one place (Fig. 50):

$$FV = F_1(V - v_1) = F_2(V - v_2),$$

hence:

$$\frac{F}{F_1} = 1 - \frac{v_1}{V}$$

and

$$\frac{F_2}{F_1} = \frac{V - v_1}{V - v_2} = \frac{1 - \frac{v_1}{V}}{1 - \frac{v_2}{V}}.$$

Substituting from equation (72), the value v_2/V, we obtain:

$$\frac{F_2}{F_1} = \frac{1 - \frac{v_1}{V}}{1 - \frac{2\frac{v_1}{V}}{1 + \frac{v_1}{V}}} = \frac{\left(1 - \frac{v_1}{V}\right)\left(1 + \frac{v_1}{V}\right)}{1 + \frac{v_1}{V} - 2\frac{v_1}{V}},$$

or, reducing:

$$\frac{F_2}{F_1} = 1 + \frac{v_1}{V}. \qquad (73)$$

Setting the expression F/F_1 and F_2/F_1, we obtain:

$$F_1 = \frac{F + F_2}{2}, \qquad (74)$$

i.e. The marked-off area is the arithmetical average of the areas of the working stream in front of and behind the wind engine.

Determination of the magnitude of the drag mass $(m_1 + m_2)$, is given by the theorem: The mass of fluid dragged by the wind engine or by its grid, does not depend on the conditions of the wind engine and on the permeability of the grid, and is equal to the volume corresponding to the area marked-off in the flow, multiplied by the density of the fluid.

Let us use equation (71), divide both its parts by v_2 and replace m_1 and m_2 by their values: /107

$$m_1 + m_2 = \frac{P}{v_2} = [\rho F_2(V - v_2)] + \left[\rho F_2 \frac{v_2}{2}\right] = \rho F_2\left(V - \frac{v_2}{2}\right).$$

Substituting the value of v_2 from equation (72) and F_2 from equation (73), we obtain:

$$m_1 + m_2 = \rho F_1\left(1 + \frac{v_1}{V}\right)\left(V - \frac{v_1}{1 + \frac{v_1}{V}}\right) = \rho F_1 \frac{\left(1 + \frac{v_1}{V}\right)(V + v_1 - v_1)}{1 + \frac{v_1}{V}};$$

after reduction, we obtain:

$$m_1 + m_2 = \rho F_1 V = \text{Const.} \tag{75}$$

The frontal pressure on the wind engine, is obtained from equation (71), substituting the value $m_1 + m_2$ from equation (75):

$$P = (m_1 + m_2) v_2 = \rho F_1 V v_2. \tag{76}$$

The load on the marked-off area is:

$$B' = \frac{P}{F_1 \rho \frac{V^2}{2}} = \frac{\rho F_1 V v_2}{F_1 \rho \frac{V^2}{2}}, \tag{77}$$

or:

$$B' = 2\frac{v_2}{V}.$$

Substituting the value v_2 from equation (72), we obtain:

where:

$$B' = \frac{4\frac{v_1}{V}}{1 + \frac{v_1}{V}},$$

consequently:

$$\frac{v_1}{V} = e,$$

$$B' = 4\frac{e}{1+e}. \tag{77a}$$

Taking into consideration equation (77), we obtain that the frontal pressure P is equal to:

$$P = \rho \frac{V^2}{2} F_1 B' = \rho \frac{V^2}{2} \cdot F_1 \frac{4e}{1+e}. \tag{78}$$

The power of the shaft of the wind engine is, according to equation/108 (in Sec. 16), equal to:

$$T = P(V - v_1).$$

Substituting the value P from equation (78), we obtain:

$$T = \rho F_1 \frac{V^3}{2} \cdot 4e\frac{1-e}{1+e}.$$

The coefficient of utilization of the wind energy is equal to:

$$\xi = \frac{T}{F_1 \rho \frac{V^3}{2}} = \frac{F_1 \rho \frac{V^3}{2} \cdot 4e\frac{1-e}{1+e}}{F_1 \rho \frac{V^3}{2}};$$

after reduction:

$$\xi = 4e\frac{1-e}{1+e}, \tag{79}$$

or:

$$\xi = B'(1-e). \tag{79a}$$

Assuming that the first derivative of expression (79) is equal to zero, we obtain:

$$\frac{d\xi}{de} = \frac{d}{de}\left[4e\frac{1-e}{1+e}\right] = 4\frac{(1-2e)(1+e) - (e-e^2)(+1)}{(1+e)^2} = 0,$$

hence:

$$e=-1+\sqrt{2}=0{,}414,$$

i.e. the maximum of ξ is obtained when:

$$e=\frac{v_1}{V}=0{,}414,$$

and not 0.333, as in the classical theory.

Substituting the value e in equation (79), we obtain:

$$\xi_{max}=4\cdot 0{,}414\frac{1-0{,}414}{1+0{,}414}=0{,}687. \qquad (80)$$

The load on the marked-off area amounts to:

$$B_{max}=4\frac{0{,}414}{1+0{,}414}=1{,}172. \qquad (81)$$

Table 5 presents for the sake of comparison, characteristic magnitudes of the ideal wind wheel obtained according to the classical theory of N.E.Zhukovskiy and according to the theory G. Kh. Sabinin.

TABLE 5

	Total velocity of the wind lost behind the wind wheel.	Coefficient of loading on the marked-off surface B^1.	Drag coefficient of the air-stream v_1/V at ξ_{max}	Load B at ξ_{max}	Maximal output coefficient of the wind energy ξ_{max}
Classical theory	$v_2=2v_1$	$4\frac{v_1}{V}\left(1+\frac{v_1}{V}\right)$	0,333	0,888	0,593
Theory of G. H. Sabinin	$v_2=\frac{2v_1}{1+\frac{v_1}{V}}$	$\frac{4\frac{v_1}{V}}{1+\frac{v_1}{V}}$	0,414	1,172	0,687

In order to compare the two theories, Fig. 54 shows the depen- /109
dence of ξ on the function v_1/V.

In conclusion, let us present the main assumption of the classical theory and of the theory G. Kh. Sabinin.

1. According to the classical theory, the loss in the velocity of the wind behind the wind wheel equals twice the loss in the velocity of the wing in the plane of the wind engine, i.e. /110

$$v_2 = 2v_1.$$

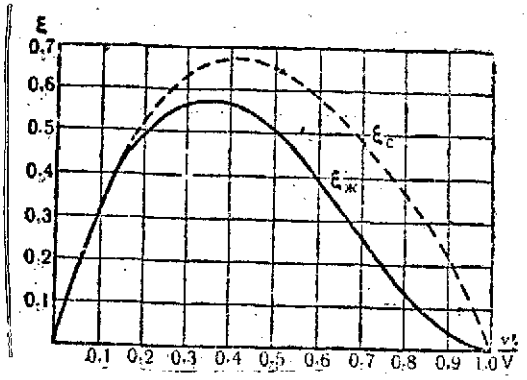

Fig. 54: Relationship between the output coefficient of wind energy and v_1/V.

According to the theory of G. Kh. Sabinin, the decrease in the velocity of the wind behind the wind engine, is expressed by the relation:

$$v_2 = \frac{2v_1}{1+\frac{v_1}{V}}.$$

2. The axial pressure according to the classical theory:

where:

$$P = m_1 v_2,$$
$$m_1 = F_1 \rho (V - v_1).$$

According to the theory of Prof. Sabinin, in addition to the mass of air flowing through the area marked-off by the wind wheel, the mass of air m_2 sucked into the vortex solenoid from the surrounding stream, is taken into consideration. The axial pressure equals: $P = (m_1 + m_2) v_2$.

The mass dragged by the wind engine equals:

$$m_1 + m_2 = F_1 V = \text{Const.}$$

In practice, it is not possible to build a wind engine with an infinitely large number of blades which would make an infinitely large number of revolutions and would work without losses, as in the case of the ideal wind engine. In reality, we are dealing with a real wind engine, which has a finite number of blades (from 1 to 24), makes a finite number of revolutions and works with losses.

CHAPTER 5. THE THEORY OF THE REAL WIND ENGINE OF PROF. G. KH. SABININ

18. Work of the Elementary Blades of the Wind Wheel. First Equation/111 of Relation.

Let us single out in the blades of the wind wheel, two concentric circles with radii r and r + dr, the winged surface $dF = 2\pi r dr$. This ring cuts sections with the length dr in the wings, which are called elementary blades (Fig. 55). Let us draw the flow lines through all the points of both surfaces, which form two bottle shaped surfaces ABC, A'B'C' (Fig. 56). The fluid enclosed between these surfaces is called elementary ring jet.

Let us assume, as is commonly done in analysis theories, that the difference between the pressure on both sides of the winged wheel acting on the area of the wing, which is obtained from the intersection of the area marked-off by the elementary jet, is perceived by the elementary blades.

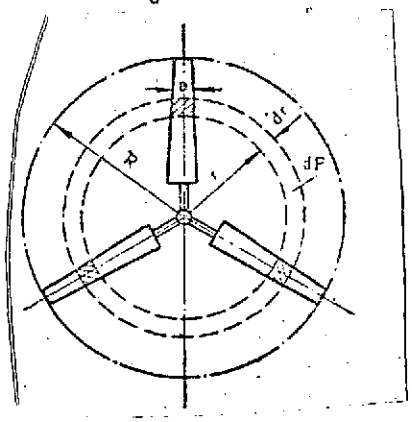

Fig. 55: Elementary blades singled out in the wind wheel.

On the basis of this assumption, we can/112 write the first equation of relation:

$$2\pi r dr\,(p_1 - p_2) = i\,(dY \cdot \cos\beta + dX \sin\beta), \qquad (82)$$

where Y -- the lifting force of the wing perpendicular to the flow;
X -- the drag force of the wing (head drag of the wing) directed along the flow;
β -- the angle between the plane of rotation of the winged wheel and the direction of the air flow dashing over the wing;
i -- the number of blades of the winged wheel.

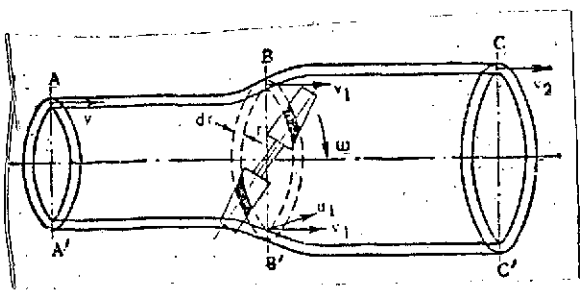

Fig. 56: Elementary annular jet.

In order to determine the direction of the forces acting on the elementary blade, let us draw its section in Fig. 57, where the Z axis is directed along the axis of the wind wheel, while the x -- x axis in the plane of its rotation; V -- direction of the wind velocity; W -- direction of the velocity of the relative flow, dashing over an element of the blade.

Let us break down the force dR, acting on the elementary blade,

into two forces: dX, acting in the direction of the flow, and dY, directed perpendicular to the flow. The force dX induces the drag of the wing element; dY induces the circular effort of the wing element which is called lifting force.

As a result of the rotation of the winged wheel in the plane x --x, the air flow dashes over the winged wheel not with the velocity of the wind V, but with a relative velocity W, which is composed geometrically of the velocity of the wind V and the circular velocity ωr, where ω is the angular velocity and r is the distance of the blade element from the axis of rotation of the winged wheel.

The velocity of the flow dashing over an element of the blade /113 in a relative motion is equal to:

$$W=\sqrt{V_1^2+(-\omega r-u_1)^2}, \tag{83}$$

where $V_1 = V - v_1$ is the velocity of the wind in the plane of the wind engine.

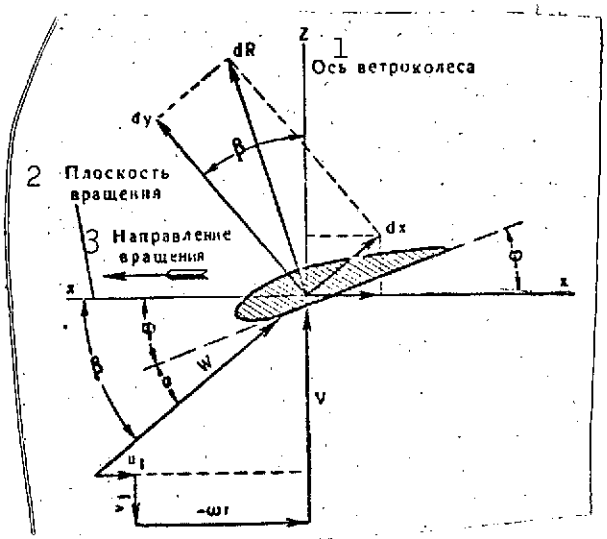

Fig. 57: Diagram of the velocities of an air flow dashing over an element of the blade.

Key: 1. axis of the wind wheel
2. plane of rotation
3. direction of rotation

The velocity u_1 is obtained as a reaction of the torque developed by the blades. This velocity has an opposite direction to the torque; its magnitude is taken as the average for the whole region in which the blades operate. In reality this velocity is equal to zero in front of the wind wheel and to u_2 immediately behind it. Since the law of the change of this velocity is unknown, we can assume as a first approximation that it is equal to:

$$u_1=\frac{u_2}{2}. \tag{84}$$

According to equation (39) /114 in Sec. 10, the forces dY and dX can be expressed as follows:

$$dY=C_y b dr \frac{\rho}{2} W^2, \tag{85}$$

$$dX=C_x b dr \frac{\rho}{2} W^2, \tag{86}$$

where b is the width of the blade element on the chord.

In addition, we can write on the basis of equation (76):

$$p_1-p_2=\frac{P}{F_1}=\rho V v_2. \tag{87}$$

Substituting for dY, dX and $p_1 - p_2$ their values in equation (8 (82), we obtain equation:

$$2\pi r dr_2 V v_2 = i\left(bdrC_y \frac{\rho}{2} W^2 \cos\beta + bdrC_x \frac{\rho}{2} W^2 \sin\beta\right); \tag{88}$$

after reductions, we obtain:

$$2\pi r V v_2 = ibC_y \frac{W^2}{2} \cos\beta \left(1 + \frac{C_x}{C_y} \operatorname{tg}\beta\right), \tag{88a}$$

or:

$$4\pi r V v_2 = ibC_y W^2 \cos\beta \left(1 + \frac{C_x}{C_y} \operatorname{tg}\beta\right).$$

On the basis of Figat57n we can denote:

$$\operatorname{ctg}\beta = \frac{\omega r + u_1}{V - v_1} = z_u, \tag{89}$$

which is called the number of relative modules.

From equation (89) we have:

$$-\omega r - u_1 = -z_u (V - v_1),$$

or:

$$(-\omega r - u_1)^2 = z_u^2 (V - v_1)^2,$$

and knowing that $V_1 = V - v_1$, equation (83) can be rewritten in following way:

$$W = \sqrt{(V - v_1)^2 + z_u^2 (V - v_1)^2} = (V - v_1)\sqrt{1 + z_u^2}. \tag{90}$$

Let us substitute:

$$\sin\beta = \frac{V - v_1}{W} = \frac{V - v_1}{(V - v_1)\sqrt{1 + z_u^2}} = \frac{1}{\sqrt{1 + z_u^2}}, \tag{91}$$

$$\cos\beta = \frac{\omega r + u_1}{W} = \frac{\omega r + u_1}{(V - v_1)\sqrt{1 + z_u^2}} = \frac{z_u}{\sqrt{1 + z_u^2}}, \tag{92}$$

$$\operatorname{tg}\beta = \frac{1}{z_u}, \tag{93}$$

$\frac{C_x}{C_y} = \mu$ reverse lift drag ratio (94)/115

and substitute them in equation (88):

$$4\pi r V v_2 = ibC_y (V - v_1)^2 (1 + z_u^2) \frac{z_u}{\sqrt{1 + z_u^2}} \left(1 + \frac{\mu}{z_u}\right).$$

Introducing into this equation $e = v_1/V$, and replacing v_2 by its value from equation (72), we obtain:

$$ibC_y = 8\pi r \frac{e}{(1 + e)(1 - e)^2} \cdot \frac{1}{(z_u + \mu)\sqrt{1 + z_u^2}}. \tag{95}$$

This equation is called the equation of relation; it relates the width of the blade and the coefficient of the lifting force with the deformation of the flow characterized by magnitude e.

Adding up the projections of the forces of the blade element on the tangent to the circle on which it moves, we obtain the

circular effort developed by the elementary blade:

$$dQ = ibdr\frac{\rho}{2}W^2(C_y\sin\beta - C_x\cos\beta).$$

Substituting the value of W, sin β and cos β and introducing $C_x = \mu C_y$, we obtain:

$$dQ = ibdr\frac{\rho}{2}(V-v_1)^2(1+z_u^2)C_y\frac{1-\mu z_u}{\sqrt{1+z_u^2}}. \qquad (96)$$

Substituting the value ibCy from equation (95) and reducing, we obtain:

$$dQ = 4\pi r\frac{e}{(1+e)(1-e)^2}\times$$
$$\times\frac{1}{(z_u+\mu)\sqrt{1+z_u^2}}dr\rho(V-v_1)^2\sqrt{1+z^2}(1-\mu z_u),$$
$$dQ = 4\pi rdr\rho\frac{e}{1+e}V^2\frac{1-\mu z_u}{z_u+\mu}. \qquad (97)$$

The moment relative to the axis of the wind engine is equal: /116

$$dM = dQr = 4\pi r^2dr\rho\frac{e}{1+e}V^2\frac{1-\mu z_u}{z_u+\mu} \qquad (98)$$

The work of the elementary blades per second is:

$$dT = dM\omega = 4\pi rdr\frac{e}{1+e}\rho V^3\frac{1-\mu z_u}{z_u+\mu}z. \qquad (99)$$

The energy per second at a distance from the wind engine, enclosed in the flow, the cross section area of which is determined by the area of the ring marked-off by the elementary blade, is equal to:

$$dT_0 = 2\pi rdr\rho\frac{V^3}{2}.$$

Dividing the work per second of the elementary blades by this energy, we obtain the elementary output coefficient of the wind energy:

hence:

$$\xi = \frac{dT}{dT_0} = \frac{4\pi rdr\frac{e}{1+e}\rho V^3\frac{1-\mu z_u}{z_u+\mu}z}{2\pi rdr\rho\frac{V^3}{2}},$$
$$\xi = \frac{4e}{1+e}\cdot\frac{1-\mu z_u}{z_u+\mu}z. \qquad (100)$$

Multiplying and dividing the expression (100) by (1 - e) we obtain:

$$\xi = 4e\frac{1-e}{1+e}\cdot\frac{1-\mu z_u}{z_u+\mu}\cdot\frac{z}{1-e}.$$

Since the expression 4e 1 -ee/1 + e represents the ideal output coefficient of the wind energy, we can write equation (

(101)

where:

$$\xi = \xi_i\frac{1-\mu z_u}{z_u+\mu}\cdot\frac{z}{1-e} = \xi_i\eta, \qquad (102)$$
$$\eta = \frac{1-\mu z_u}{z_u+\mu}\cdot\frac{z}{1-e}$$

is called the relative efficiency of the elementary wind engine.

In the case of a large number of modules one can consider with some approximation:

$$\frac{z}{1-c} \cong z_u,$$

and then:

$$\eta = \frac{1-\mu z_u}{1+\frac{\mu}{z_u}}. \tag{102a}$$

Let us remember that the number of modules or rapidity of the wind engine, is the ratio of the circular velocity of the blade tip to the velocity of the wind. /117

$$Z = \frac{\omega R}{V}. \tag{59}$$

The number of modules of the blade element per radius r equals:

$$z = \frac{\omega r}{V}. \tag{103}$$

The number of modules for any radius r of the wind engine with a known rapidity Z, can be expressed:

$$z = Z\frac{r}{R}, \tag{104}$$

where R is the radius of the wind wheel.

19. Second Equation of Relation

The moment relative to the axis of the wind engine of the aerodynamic forces acting on the elementary blade, is equal in magnitude and opposite in sign, to the moment of the amount of movement acquired by the elementary jet dragged with the wind wheel. It is assumed that in this process, the bound mass also takes part, since otherwise the theory of Helmholz about vortex preservation would not hold (Fig. 13).

The second equation of relation is derived from Fig. 57.

$$i(dY\sin\beta - dX\cos\beta)r = d(m_1 + m_2)2a_1 r. \tag{105}$$

but:

$$d(m_1+m_2)=2\pi r dr\rho V. \tag{75}$$

Substituting the values of dY and dX from equations (85) and (86), and the value of $d(m_1 = m_2)$ from equation (75), in equation (105), we obtain:

$$ibdr\,(C_y\sin\beta-C_x\cos\beta)\frac{\rho}{2}W^2r=2\pi r dr\frac{\rho V}{u_1}2u_1r. \tag{105a}$$

Substituting in this equation sin β and cos β by their values from equation (91) and (92) and reducing, we obtain: /118

$$ib\left(C_y\frac{1}{\sqrt{1+z_u^2}}-C_x\frac{z_u}{\sqrt{1+z_u^2}}\right)W^2=8\pi rVu_1.$$

Substituting $\mu = C_x/C_y$ from equation (94) and $W^2 = (V - v_1)^2 (1 + z^2_u)$ from equation (90), we obtain:

$$ibC_y\frac{1-\mu z_u}{\sqrt{1+z_u^2}}(V-v_1)^2(1+z_u^2)=8\pi rVu_1.$$

From this equation, let us find the ratio u_1/V, for which purpose we divide the right and left part by $8\pi rV^2$ and we replace the ratio v_1/V by its value e.

$$\frac{u_1}{V}=\frac{ibC_y}{8\pi r}(1-e)^2(1-\mu z_u)\sqrt{1+z_u^2} \tag{106}$$

Substituting the value $ibC_y/8\pi r$, from equation (95), we obtain:

$$\frac{u_1}{V}=\frac{e}{(1+e)(1-e)^2}\cdot\frac{(1-e)^2(1-\mu z_u)\sqrt{1+z_u^2}}{(z_u+\mu)\sqrt{1+z_u^2}}.$$

After reduction we obtain:

$$\frac{u_1}{V}=\frac{e}{1+e}\cdot\frac{1-\mu z_u}{z_u+\mu}. \tag{107}$$

Transforming equation (89), we find the relation between z_u and z:

$$z_u=\frac{\omega r+u_1}{V-v_1}=\frac{\omega r}{V}\cdot\frac{V}{V-v_1}+\frac{u_1}{V}\cdot\frac{V}{V-v_1}=\frac{z}{1-e}+\frac{u_1}{V(1-e)}.$$

Substituting the value u_1/V from equation (106):

$$z_u=\frac{z}{1-e}+\frac{e}{1-e^2}\cdot\frac{1-\mu z_u}{z_u+\mu}; \tag{108}$$

$$z=z_u(1-e)-\frac{e}{1+e}\cdot\frac{1-\mu z_u}{z_u+\mu}. \tag{109}$$

Let us solve this equation relative to z_u:

$$z_u^2+\mu z_u-\frac{z_u z}{1-e}-\frac{\mu z}{1-e}-\frac{e}{1-e^2}+\frac{e}{1-e^2}\mu z_u=0;$$

$$z_u^2-z_u\left(\frac{z}{1-e}-\mu-\frac{e}{1-e^2}\mu\right)-\frac{e}{1-e^2}-\mu\frac{z}{1-e}=0;$$

$$z_u=\frac{1}{2}\left[\frac{z}{1-e}-\mu\left(1+\frac{e}{1-e^2}\right)\right]\pm$$

$$\pm\sqrt{\frac{1}{4}\left[\frac{z}{1-e}-\mu\left(1+\frac{e}{1-e^2}\right)\right]^2+\frac{e}{1+e^2}+\mu\frac{z}{1-e}}. \tag{110}$$

Since μ has usually a small value, equations (109) and (110) can be simplified, taking μ = 0: /119

$$z = z_u(1-e) - \frac{e}{z_u(1-e)}; \tag{109a}$$

$$z_u = z\frac{1+\sqrt{1+\frac{4e}{z^2}\cdot\frac{1-e}{1+e}}}{2(1-e)} = z\frac{1+\sqrt{1+\frac{z_u}{z^2}}}{2(1-r)}. \tag{110a}$$

Equations (95), (103) and (110) make it possible to do a complete aerodynamic calculation of the wind wheel for the given ωR and V, as well as of the shape of the wing profile. The diagram C_y and C_x is used for this purpose, which was constructed for the given profile.

Assuming that e varies between 0.28 and 0.35, for the most convenient angle of attack, according to the diagram C_y and C_x for the given profile, the following is obtained: $\mu = C_x/C_y$.

Substituting the values of z, e, and μ in equation (110), the number of the relative modules z_u is found. Further, using equation (95), the total width of the blade ib is found:

$$ib = \frac{8\pi r}{C_y}\cdot\frac{e}{(1+e)(1-e)^2}\cdot\frac{1}{(z_u+\mu)\sqrt{1+z_u^2}} \tag{111}$$

Finally, the rigging angle of the blade φ with radius r is determined:

$$\varphi = \operatorname{arc\,ctg} z_u - \alpha. \tag{112}$$

C_y is found from the diagram C_y -- α, which was constructed on the basis of experimental data.

20. Moment and Power of the Whole Wind Engine

The moment of the whole wind engine is obtained by integrating equation (98) from r_0 to R, were r_0 is the distance from the axis of the wind engine to the origin of the blade, and R is the distance from the axis of the wind engine to the edge of the blade.

$$M = \int_{r_0}^{R} dM = \int_{r_0}^{R} 4\pi r^2 \rho \frac{e}{1+e} V^2 \frac{1-\mu z_u}{z_u+\mu} dr. \tag{113}$$

This moment is expressed in abstract numbers and is denoted by $\overline{M}$. The right and left part of equation (113) is divided by $\pi R^3 \rho V^2/2$ and the expression $\overline{r} = r/R$ is introduced which is called the relative radius: /120

$$\overline{M} = \frac{M}{\pi R^3 \rho \frac{V^2}{2}} = \int_{\overline{r}_0}^{\overline{R}} 8\frac{e}{1+e}\cdot\frac{1-\mu z_u}{z_u+\mu}\overline{r}^2 d\overline{r}. \tag{114}$$

Equation (114) is basic for calculating the moment characteristics. It can be used with variable values of e along r, if one

assumes that the elementary jets do not influence each other, which is acceptable in practice under conditions of smooth changes of e.

For a wind engine with a constant e along the radius, e can be written outside the sign of the integral:

$$\overline{M} = 8\frac{e}{1+e}\int_{\overline{r_0}}^{\overline{R}} \frac{1-\mu z_u}{z_u+\mu}\overline{r}^2 d\overline{r}. \qquad (115)$$

This integral can be solved if the torsion of the jet is neglected, which is permissible in rapid wind engines.

Consequently, we can take $u_1 = 0$, and the relative number of modules z_u from equation (89) can be expressed as follows:

$$z_u = \frac{\omega r + u_1}{V - v_1} \cong \frac{\omega r}{V - v_1} = \frac{\omega r}{V(1-e)} = \frac{z}{1-e}. \qquad (116)$$

For the edge of the blade, one can write:

$$z_u \cong \frac{\omega R}{V - v_1}. \qquad (117)$$

Dividing equation (116) by (117), we obtain: /121

$$\frac{r}{R} \cong \frac{z_u}{Z_u}; \qquad (118)$$

$$\frac{dr}{R} = \frac{dz_u}{Z_u}. \qquad (119)$$

With a series of transformations made for equation (115) and neglecting the small value μ^2 and $z^3 u_0 / Z^3 u$, we obtain:

$$\overline{M} = \frac{4e}{(1+e)Z_u}\left[(1+\mu)\left(1-\frac{r_0^2}{R^2}\right) - 2\mu\left(\frac{Z_u}{3}+\frac{1-\frac{r_0}{R}}{Z_u}\right)\right]. \qquad (120)$$

Substituting the value of z_u from (116), we obtain:

$$\overline{M} = \frac{4e}{Z}\cdot\frac{1-e}{1+e}\left[\left(1-\frac{r_0^2}{R^2}\right) - 2\mu\left(\frac{Z_u}{3}+\frac{1-\frac{r_0}{R}}{Z_u}-\frac{1-\frac{r_0^2}{R^2}}{2}\right)\right] \qquad (121)$$

The power developed by the wind engine is equal to the $M\omega$, and since from equation (114) the moment is equal to:

$$M = \overline{M}\pi R^3 \frac{\rho V^2}{2}, \qquad (114a)$$

the power developed by the wind engine can be written as follows:

$$T = M\omega = \overline{M}\pi R^3 \rho \frac{V^2}{2}\omega. \qquad (122)$$

Substituting here $Z = \omega R/V$, instead of $\omega = ZV/R$, we obtain:

$$T = \overline{M}\pi R^2 \rho \frac{V^3}{2} Z. \qquad (122a)$$

Replacing $\overline{M}$ by its value from equation (121), we obtain:

$$T = 4\varepsilon \frac{1-\varepsilon}{1+\varepsilon}\left[\left(1-\frac{r_0^2}{R^2}\right) - 2\mu\left(\frac{Z_u}{3}+\frac{1-\frac{r_0}{R}}{Z_u}-\right.\right.$$
$$\left.\left.-\frac{1-\frac{r_0^2}{R^2}}{2}\right)\right]\pi R^2 \rho \frac{V^2}{2}. \qquad (123)$$

Dividing the power of the wind engine by the energy of the flow per second, we obtain the output coefficient of the wind energy: /122

$$\xi = \frac{T}{\pi R^2 \rho \frac{V^2}{2}} = 4\varepsilon \frac{1-\varepsilon}{1+\varepsilon}\left[1-\frac{r_0^2}{R^2}-\right.$$
$$\left.-2\mu\left(\frac{Z_u}{3}+\frac{1-\frac{r_0}{R}}{Z_u}-\frac{1-\frac{r_0^2}{R^2}}{2}\right)\right]. \qquad (124$$

Since:

$$4\varepsilon \frac{1-\varepsilon}{1+\varepsilon} = \xi_i \quad \text{и} \quad \xi = \xi_i \cdot \eta,$$

then:

$$\eta = 1-\frac{r_0^2}{R^2}-2\mu\left(\frac{Z_u}{3}+\frac{1-\frac{r_0}{R}}{Z_u}-\frac{1-\frac{r_0^2}{R^2}}{2}\right). \qquad (125)$$

In deriving this equation, no consideration was given to the losses which occur as a result of the formation of vortexes which start off at the tip of the blade, and the torsion of the drifting jet was taken equal to 0, which is permissible in rapid wind engines.

Consequently, the output coefficient of wind energy, calculated according to formula (124), is considerably higher than the one which can be obtained in practice. We shall deal with the correction for losses below (Sec. 21).

21. Losses of Wind Engines

The losses of wind engines can be divided into four groups [35].

1. Blade-tip losses, which occur due to the formation of vortexes starting at the blade tip. These losses are determined on the basis of the theory of induced drag. A part of these losses was accounted for by deriving the ideal output coefficient of wind energy ξ_i; the part which was not accounted for is expressed by the formula (126):

$$\overline{T} \cong \frac{\varepsilon}{1-\varepsilon}\left[\frac{8\sqrt{1+\left(\frac{1-\varepsilon}{Z}\right)^2}}{(1+\varepsilon)iZ} - \frac{1}{\sqrt{1+\left(\frac{iZ}{\pi\left(1-\frac{\varepsilon}{2}\right)}\right)^2}}\right]. \qquad (126)$$

2. Profile losses which are caused by the friction of the air/123 jet against the surface of the wing and depend solely on the profile of the blades.

The power absorbed by the profile drag of the elementary blade of length dr, at a radius r of the wind engine, equals:

$$dT_p = iC_p b dr \frac{\rho}{2} W, \tag{127}$$

where C_p is the coefficient of the profile drag which is equal to C_x for a wing of infinite span, i.e.:

$$C_p = C_x .$$

Since $C_x/C_y = \mu$, or $C_x = \mu C_y$, $C_p = \mu C_y$. Substituting the value C_p which is equal to μC_y and

$$W = (V - v_1)\sqrt{1 + z_u^2}$$

in equation (127), we obtain:

$$dT_p = ibC_y \mu dr \frac{\rho}{2} (V - v_1)^2 (1 + z_u^2) \sqrt{1 + z_u^2}.$$

Substituting the value ibC_y from equation (95), let us transform this equation:

$$dT_p = 4\pi r \frac{e}{(1+e)(1-e)^2} \times \frac{1}{(z_u + \mu)\sqrt{1 + z_u^2}} \mu dr \frac{\rho}{2} (V - v_1)^2 (1 + z_u^2) \sqrt{1 + z_u^2}$$

$$dT_p = \frac{4\pi r dr e}{(1+e)(1-e)^2} \rho (V - v_1)^2 \frac{1 + z_u^2}{z_u + \mu} \mu.$$

Let us substitute:

$$r = z\frac{V}{\omega}; \quad dr = \frac{V}{\omega} dz; \quad z_u \cong \frac{z}{1-e};$$

and let us neglect μ in the denominator as being a small value by comparison with z_u:

$$dT_p \cong 4\pi \frac{V^2}{\omega^2} z dz \frac{e}{(1+e)(1-e)^2} \rho V^2 (1-e)^2 \frac{1 + \frac{z^2}{(1-e)^2}}{\frac{z}{1-e}} \mu,$$

$$dT_p \cong 4\pi \rho \frac{V^3}{\omega^2} \cdot \frac{e(1-e)^2}{1+e} \mu \left[1 + \frac{z^2}{(1-e)^2}\right] dz.$$

Integrating in the limits 0 to Z, we obtain: /124

$$T_p \cong 4\pi \rho \frac{V^3}{\omega^2} \cdot \frac{e(1-e)^2}{1+e} \int_0^Z \mu \left[1 + \frac{z^2}{(1-e)^2}\right] dz.$$

The profile losses at the blade tip exist in the form of flap drag which is thus approximately taken into account. As a result of integrating, we obtain the profile losses for the whole wind engine:

$$T_p \cong \pi R^2 \frac{\rho V^2}{2} \cdot \frac{4e(1-e)^2}{1+e} \cdot \frac{V^2}{\omega^2 R^2} 2\mu' \left[Z + \frac{Z^3}{3(1-e)^2}\right],$$

where $\mu' = C_x/C_y$ is the average value for the whole blade. Since $\frac{4e(1-e)}{1+e} = z_1$ and $\frac{V}{\omega R} = \frac{1}{Z}$, substituting the values of these

expressions in the given equation and deriving the latter by expression $\pi R^2 \rho \frac{V^3}{2} \xi_i$, we obtain the final formula for the profile losses in a dimensionless form:

$$\bar{T} \cong \frac{T_p}{\pi R^2 \frac{\rho V^3}{2} \xi_i} = 2\mu' \left[\frac{1-e}{Z} + \frac{Z}{3(1-e)} \right]. \qquad (128)$$

3. The losses due to torsion of the jet behind the wind engine are equal to the kinetic energy of the tangential velocities of the twisting jets. The magnitude of these losses is obtained by integrating the kinetic energy from the tangential velocities of all the elementary jets v_2 in the limits r_0 to R:

$$T_m = \int_{r_0}^{R} (2\pi r dr \rho V) \frac{u_2^2}{2}. \qquad (129)$$

Let us replace in the given expression u_2 by its value which is equal to $2u_1$.

Since, on the basis of equations (106) and (102):

$$\frac{u_1}{V} = \frac{e}{1+e} \cdot \frac{1-\mu z_u}{z_u+\mu} = \frac{e}{1+e} \cdot \frac{1-\mu z_u}{\left(1+\frac{\mu}{z_u}\right) z_u},$$

$$z_u \cong \frac{z}{1-e} \text{ и } \eta = \frac{1-\mu z_u}{1+\frac{\mu}{z_u}},$$

we obtain:

$$u_1 \cong \frac{e}{z} \cdot \frac{1-e}{1+e} \eta V,$$

consequently:

$$u_2 = 2u_1 \cong 4e \frac{1-e}{1+e} \eta \frac{V}{2z},$$

hence:

$$u_2 = \frac{V}{2Z} \cdot \xi_i \eta,$$

or:

$$u_2 = \frac{V}{2Z} \cdot \frac{R}{r} \xi_i \eta. \qquad (130)$$

Substituting the value u_2 in equation (129), we obtain:

$$T_m = \int_{r_0}^{R} \pi r dr \rho V^3 \frac{R^2}{r^2} \cdot \frac{\xi_i^2 \eta^2}{4Z^2}.$$

Placing the constants outside the sign of the integral and replacing η by some value η_1, which is average for the whole radius r, we obtain:

$$T_m = \pi R^2 \rho \frac{V^3}{2} \cdot \frac{\xi_i^2 \eta_1^2}{2Z^2} \int_{r_0}^{R} \frac{dr}{r} = \pi R^2 \frac{\rho V^3}{2} \cdot \frac{\xi_i^2 \eta_1^2}{2Z^2} \ln \frac{R}{r_0}.$$

Deriving both parts of this equality by the power of the ideal wind engine: $T_i = \pi R^2 \frac{\rho V^3}{2} \xi_i$,

we obtain the abstract magnitude for the losses due to the torsion of the jet behind the wind engine:

$$\bar{T}_m = \frac{\xi_i \eta_1^2}{2Z^2} \ln \frac{R}{r_0}. \qquad (131)$$

4. Losses due to incomplete utilization of the whole marked-off area are accounted for by the relation: $\left(\frac{r_0}{R}\right)^2$.

The useful power developed by the wind engine is obtained by subtracting all the losses from the power of the ideal wind engine:

$$T = T_i\left(1 - \frac{r_0^2}{R^2}\right) - T_j - T_p - T_m.$$

Dividing by T_i we obtain: /126

$$\frac{T}{T_i} = 1 - \frac{r_0^2}{R^2} - \frac{T_j}{T_i} - \frac{T_p}{T_i} - \frac{T_m}{T_i},$$

Hence:

$$T = T_i\left(1 - \frac{r_0^2}{R^2}\right) - \bar{T}_j - \bar{T}_p - \bar{T}_m. \qquad (132)$$

Dividing the right and the left part of this equation by the expression of the wind energy $\pi R^2 \gamma \frac{V^3}{2}$,

we obtain the output coefficient of the wind energy for the real wind engine:

$$\xi = \xi_i\left(1 - \frac{r_0^2}{R^2}\right) - \bar{T}_j - \bar{T}_p - \bar{T}_m. \qquad (133)$$

Since according to equation (101), $\xi = \xi_i \eta$, we find that the relative efficiency η of the wind engine equals:

$$\eta = 1 - \frac{r_0^2}{R^2} - \bar{T}_j - \bar{T}_p - \bar{T}_m. \qquad (134)$$

22. Aerodynamic Analysis of the Wind Wheel.

The diagram of the construction of a four-blade wind wheel is given in Fig. 58. The following data are required for the analysis

1. The power N in hp which has to be obtained from the wind engine;

2. The velocity of the wind V at which the wind engine should develop this power; since

3. The number of modules or rapidity Z of the wind engine at the maximum output coefficient of the wind energy for the given type of wind engine;

4. The output coefficient of the wind energy ξ.

The analysis is started by determining the diameter of the wind wheel D, based on the equation of the power of the wind engine in hp units, which is obtained by dividing equation (62) by 75 and multiplying by the output coefficient of the wind energy ξ, i.e.:

$$N = \frac{\xi F V^3 \gamma}{2 \cdot 75}, \qquad (135)$$

where $\gamma = 0.125 \left[\frac{kg/sec^2}{m^4}\right]$ -- the mass density of the air is taken at a temperature t = 15° C and atmospheric pressure B_0 = 760 mm/Hg.

Substituting the value ρ = 0.125 in equation (135), we obtain/127 the power of the wind engine, expressed in relation to the area marked off by the wind wheel of any type, for the conditions t - 15° and B_0 = 760 mm/Hg.

$$N=\frac{\rho FV^3\xi}{2\cdot 75}=\frac{0,125\cdot FV^3\xi}{150}=0,000833\,FV^3\xi. \quad (136)$$

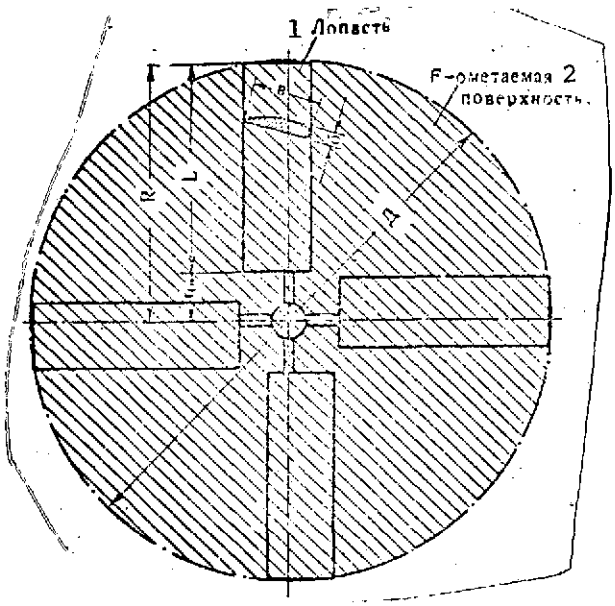

Fig. 58: Diagram of the wind wheel.

Key: 1. blade
2. F -- marked-off area

Since, for a winged wind engine, the marked-off area F (Fig. 58) equals: $F=\frac{\pi D^2}{4}=0,785\,D^2,$

The power of the winged wind engine can be expressed in relation to its diameter D.

$$N=0,000833\cdot 0,785\,D^2V^3\xi=0,000654\,D^2V^3\xi \quad (137)$$

or $N=\frac{D^2V^3\xi}{1530}.$

The power of the wind engine /128 in kW is written as follows:

$$N=0,000481\,D^2V^3\xi\ \text{kWt}. \quad (138)$$

The diameter of the windwheel for the given power in hp units, equals:

$$D=\sqrt{\frac{N}{0,000654\,V^3\xi}}=\sqrt{\frac{1530\,N}{V^3\xi}}. \quad (139)$$

For another temperature t and pressure B, the power should be determined for the corresponding mass density ρ, which is determined by formula 3.

Introducing this correction into the equation of the power, we obtain:

$$N_\alpha=N\frac{B}{B_0}\frac{(273+15)}{(273+t)}=\frac{NB\,288}{760\,(273+t)},$$

and correspondingly the diameter of the wind wheel will be equal to:

$$D=\sqrt{\frac{1530\,N}{V^3\xi}}\cdot\sqrt{\frac{760\,(273+t)}{B\,280}}. \quad (139a)$$

The velocity of the wind V at which the wind wheel should develop the power given in the analysis, is usually taken as being equal to 8 -- 14 m/sec. (see chapt. IX).

The number of modules Z is easily assumed or determined, if the number of revolutions of the wind wheel n is known:

$$Z=\frac{\omega R}{V}=\frac{\pi nR}{30V},$$

hence:

$$n=\frac{30ZV}{\pi R}. \quad (140)$$

Further, on the basis of construction considerations and experimental data, the thickness of the blade profile is selected. The blade tip should have a profile of a thickness of $\delta = 0.1\ b$ to $0.15\ b$, where b is the width of the blade. Towards the bush, the thickness of the profile δ increases, reaching in wind engines with rotatory blades 0.2 b to 0.35 b near the flap axis.

In order to solve the equation which determines the shape of the blades, their number and the output coefficient of wind energy are given by several values of the drag coefficient e, for example, e = 0.3; 0.35; 0.40, and the ideal output coefficient of wind energy $\xi_i = 4e\frac{1-e}{1+e}$ is determined. Consequently ξ is determined by means of equations (126), (128), (131) and (133) and the curve of the relationship ξ -- e is plotted, wherefrom /129 the e corresponding to ξ_{max} is chosen. The computation table, Table 6, is then set up where the main formulas are presented in the upper part.

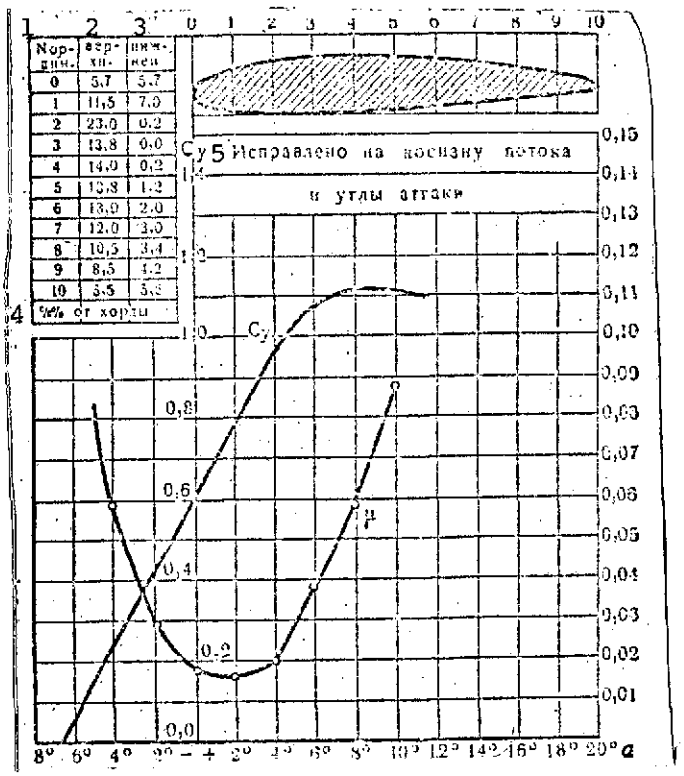

Нор-дин.	верх-ня	ниж-ня
0	5,7	5,7
1	11,5	7,0
2	23,0	0,2
3	13,8	0,0
4	14,0	0,2
5	13,8	1,2
6	13,0	2,0
7	12,0	3,0
8	10,5	3,4
9	8,5	4,2
10	5,5	5,5

% от хорды

Fig. 59: Curve for the determination of C_y and μ in relation to α.

Key: 1. Serial number
2. upper
3. lower
4. from the chord
5. corrected to the obliqueness and angle of attack.

Column 1 presents the radii of the cross sections of the blade in relative units $\bar{r} = r/R$. Each horizontal line in the table with the figures, represents the data for a certain cross section of the blade with radius $\bar{r} = r/R$.

The first line in Table /132 6 contains the partial formulas according to which the computation is performed.

In the first columns in Table 6, 2-5, z_u is computed by means of formula (110a); if great accuracy is desired, then equation (110) should be used. In columns 6-10, the expression ib C_y/R is computed by means of (95). In columns 11-14, the values of C_y, μ and b are introduced on the basis of the diagram of values C_y and μ as a function of α (Fig. 59) which is set up for the given example. In columns 15-17, α is introduced, and the rigging angle of the blade $\phi = \beta - \alpha$ is calculated.

After the selection of the profile, the angle of

TABLE 6. COMPUTATION OF THE MODEL OF A WIND ENGINE

$D=0{,}36$; $Z=3{,}5$; $i=4$

$\xi_i=4e\,\frac{1-e}{1+e}$	$e=0{,}30$ $\xi_i=0{,}646$	$e=0{,}35$ $\xi_i=0{,}674$	$e=0{,}40$ $\xi_i=0{,}687$
$\xi=\frac{i}{2}\left[1-\left(\frac{r_0}{R}\right)^2-\bar{T}_f-\bar{T}_p-\bar{T}_m\right]$	$\xi=0{,}646\,(1-0{,}4-0{,}113-0{,}075-0{,}034)=$ $=0{,}476$	$\xi=0{,}674\,(1-0.04-0.135-0{,}079-0{,}036)=$ $=0{,}478$	$\xi=687\,(1-0{,}04-0{,}085-$ $-0{,}158-0{,}036)=0{,}467$
$\bar{T}_f\cong\frac{e}{1-e}\left[\frac{8\sqrt{1+\left(\frac{1-e}{z}\right)^2}}{(1+e)\,iz}-\right.$ $\left.-\frac{1}{\sqrt{1+\left[\frac{iz}{\pi\left(1-\frac{e}{2}\right)}\right]^2}}\right]$	$\frac{0{,}3}{1-0{,}3}\left[\frac{8\sqrt{1+\left(\frac{1-0{,}3}{3{,}5}\right)^2}}{(1+0{,}3)\,4\cdot3{,}5}-\right.$ $\left.-\frac{1}{\sqrt{1+\left[\frac{4\cdot3{,}5}{\pi\,(1-0{,}15)}\right]^2}}\right]=0{,}113$	$\frac{0{,}35}{1-0{,}35}\left[\frac{8\sqrt{1+\left(\frac{1-0{,}35}{3{,}5}\right)^2}}{(1+0{,}35)\,4\cdot3{,}5}-\right.$ $\left.-\frac{1}{\sqrt{1+\left[\frac{4\cdot3{,}5}{\pi\,(1-0{,}175)}\right]^2}}\right]=0{,}135$	Analogically we find: $\bar{T}_f=0{,}158$
$\bar{T}_p\cong 2i'\left[\frac{1-e}{z}+\frac{z}{3\,(1-e)}\right]$	$2\cdot0{,}02\left[\frac{1-0{,}3}{3{,}5}+\frac{3{,}5}{3\,(1-0{,}3)}\right]=0{,}075$	$2\cdot0{,}02\left[\frac{1-0{,}35}{3{,}5}+\frac{3{,}5}{3\,(1-0{,}35)}\right]=0{,}079$	Analogically we find: $\bar{T}_p=0{,}085$
$\bar{T}_m\cong\frac{\xi_i\bar{r}_0^2}{2\bar{z}^2}\ln\frac{R}{r_0}$	$\frac{0{,}646\cdot0{,}9^2}{2\cdot3{,}5^2}\cdot2{,}3\lg\frac{1}{0{,}2}=0{,}034$	$\frac{0{,}674\cdot0{,}9^2}{2\cdot3{,}5^2}\cdot2{,}3\lg\frac{1}{0{,}2}=0{,}036$	Analogically we find: $\bar{T}_m=0{,}036$
$z=$ $=Z\frac{r}{R}$	$z_a=\frac{z}{2\,(1-e)}\times$ $\times\left[1+\sqrt{1+\frac{\xi}{z^2}}\right]$	$i=\frac{R\,[i\bar{b}C_y]}{b\;C_y}$ $b=\frac{R\,[i\bar{b}C_y]}{iC_y}$	$\varphi=\operatorname{arc\,ctg} z_a-\alpha$

1	2	3	4	5	6	7	8	9	10	11	12	13	14	15	16	17
$\frac{r}{R}$	z	$2(1-e)$	$1+\sqrt{1+\frac{\xi}{z^2}}$	Z_a	$8\pi\frac{r}{R}$	$z_a+\mu$	$\frac{e}{(1+e)\,(1-e)^2}$	$\sqrt{1+z_a^2}$	$\bar{ib}C_y$	C_y	μ	Number of Profile	b	α	$\varphi=\operatorname{arc\,ctg}z_a$	$\varphi=\varphi-\alpha$
1	3,5	1,3	2,026	5,46	25,08	5,48	0,614	5,55	0,508	0,654	0,016	Inversion of the ellipse thickness	0,035	0°30′	10°23′	9°53′
0,8	2,3	1,3	2,042	4,40	20,19	4,42	0,614	4,52	0,618							
0,6	2,1	1,3	2,072	3,35	15,08	3,37	0,614	3,50	0,788	0,696	0,016	1/5	0,040	0°54′	12°48′	11°54′
0,4	1,4	1,3	2,160	2,33	10,06	2,35	0,614	2,53	1,046	0,788	0,017	1/5	0,045	2°46′	16°39′	13°53′
0,2	0,7	1,3	2,540	1,57	5,02	1,39	0,614	1,70	1,304	0,942	0,025	1/5	0,050	3°55′	21°23′	17°28′
										1,066	0,047	1/5	0,055	6°08′	36°08′	30°00′

attack corresponding to the smallest μ is calculated by means of the diagram (Fig. 59), and C_y is found.

Assuming the number of blades is i, the thickness of the blades b is found:

$$b=\frac{[i\bar{b}C_y]}{C_y}R; \tag{141}$$

Finding the value for b, the finite value C_y is calculated:

$$C_y=\frac{[i\bar{b}C_y]}{ib}R; \tag{142}$$

According to the diagram (Fig. 59), μ and α, corresponding to the value C_y are found, and they are introduced into the columns 11, 12 and 15 of Table 6.

Such computations are done also for the cross section $\bar{r} = 0.2$ of the blade. In this section, a thicker profile $\delta/b = 0.3$ to 0.35 is taken in order to increase the strength of the flap. In this case, C_y is also chosen large since otherwise the width of the blade would have to be excessively large. The width of the blade at the level of the bush, is taken equal to:

$$\bar{b}_{0,2} = 1.3 \text{ до } 2.0\bar{b}_1 \qquad (143)$$

Determining the width of the blade at the tip and at the bush, the width of the blade for any section can be found assuming it has the shape of a trapezoid:

$$b_k = b_1 + \frac{b_{0,2} - b_1}{n-1}(k-1), \qquad (144)$$

where n is the number of sections of the blade; /133
k is the serial number of the section counting from the tip of the blade.

Also determining b, C_y is found by means of equation (142), and then μ and α from the curve (Fig. 59) and finally, φ. If, as a result of constructional elaborations the thickness proves to be insufficient, i.e. the flap of the wing cannot be placed in the contour of the profile, then increasing the thickness makes it necessary to recalculate starting with the 11th column of Table 6.

In this table an example of calculation is presented for a 4-blade wind wheel with D = 0.36 m and a number of modules Z = 3.5.

23. Calculation of the Performance of the Wind Wheel

The performance of a wind engine is the dependence of the relative moment of the wind wheel M and of the output coefficient of the wind energy ξ on the number of modules Z. These characteristics are necessary in order to find the main parameters of the wind wheel. In sections 26, 27 and 29, these are discussed in more detail; here we shall present the method of calculation of the performance of a wind wheel, theoretically.

The characteristics are calculated for each section of the blade; an example is presented in Table 7, where the characteristics for each section of the blade are calculated in the horizontal line. Column 1 comprises the radii of the sections, column 2 -- the rigging angles of the blades, column 3 -- the total width of the blade in an abstract form, column 4 -- the angles of attack, as an independent argument. For the sake of convenience in calculations, the

value of the angles is given in whole degrees. The formulas, by means of which the calculation is performed are presented in the same table in the corresponding columns, on page 97.

In order to obtain the full performance, the angles α have to be taken starting with the angle at which C_y is very small or equal to 0, and up to $\alpha = 90 - \phi$. However, not always diagrams C_y -- μ for testing the profiles are available for all the angles of attack; in this case, one has to limit oneself to the construction of a part of the characteristics up to the angles of attack corresponding to C_y = max. This part of the characteristics is in fact the working part which is the most interesting.

TABLE 7. PERFORMANCE OF A WIND ENGINE

$p = 0{,}36$; $i = 4$; $Z = 3$

							$\frac{c}{(1+\bar{c})(1-\bar{c})^2} = C_y \frac{(z_a+\mu)\sqrt{1+z_a^2}}{\frac{8\bar{r}}{ib}}$						$\Delta\bar{M} = \frac{8\bar{r}^3}{\frac{1+\bar{c}}{\bar{c}}} \cdot \frac{1-\mu z_a}{z_a+\mu}$					$z = z_a(1-\bar{c}) - \frac{1}{z_a \frac{1+\bar{c}}{\bar{c}}}$			$Z = \frac{z}{\bar{r}}$
1	2	3	4	5	6	7	8	9	10	11	12	13	14	15	16	17	18	19	20	21	22
$\bar{r}$	$\varphi°$	$i\bar{b}$	$\alpha°$	$\beta = \varphi + \alpha$	$z_a = c\operatorname{tg}(\varphi+\alpha)$	μ	C_y	$\frac{8\bar{r}}{i\bar{b}}$	$z_a+\mu$	$\sqrt{1+z_a^2}$	$\frac{\bar{c}}{(1+\bar{c})(1-\bar{c})^2}$	$\bar{c}$	$8\bar{r}^3$	$\frac{1+\bar{c}}{\bar{c}}$	$1-\mu z_a$	$z_a+\mu$	$\Delta\bar{M}$	$z_a(1-\bar{c})$	$z_a \frac{1+\bar{c}}{\bar{c}}$	z	Z
			— 5°	6,2	0,21	0,109	0,150		0,32	1,05	0,143	0,245		5,12	—0,001	9,32	—0,0005	6,970	0,021	6,950	6,95
			— 4	7,2	7,91	0,058	0,250		7,97	7,96	0,422	0,279		4,59	0,540	7,97	0,1184	5,700	0,028	5,670	5,67
1	11,2	0,67	— 2	9,2	6,17	0,029	0,440	67,70	6,20	6,25	0,482	0,292	8,00	4,42	0,821	6,26	0,2400	4,360	0,037	4,320	4,32
			+ 2	13,2	4,26	0,016	0,780		4,42	4,38	0,401	0,270		4,70	0,932	4,42	0,3590	3,110	0,050	3,060	3,06
			6	17,2	3,23	0,037	1,010		3,28	3,39	0,313	0,288		5,40	0,880	3,28	0,3980	2,500	0,057	2,440	2,44
			8	19,2	2,87	0,058	0,110		2,93	3,04	0,262	0,201		5,98	0,833	2,93	0,3810	2,290	0,058	2,230	2,23
			— 6°	8,1	7,03	0,232	0,056		7,33	7,10	0,107	0,096		11,44	—1,050	7,33	—0,0640	6,370	0,012	6,360	7,94
			— 4	10,1	5,61	0,058	0,250		5,67	5,70	0,296	0,229		5,55	0,674	5,67	0,1100	4,380	0,032	4,350	5,43
0,8	14,1	0,74	— 2	12,1	4,07	0,029	0,440	27,20	4,70	4,77	0,363	0,253	5,12	4,95	0,895	4,70	0,1910	3,485	0,043	3,440	4,30
			+ 2	16,1	3,46	0,016	0,780		3,48	3,60	0,359	0,251		4,98	0,945	3,48	0,2800	2,590	0,058	2,530	4,20
			6	20,1	2,72	0,037	1,030		2,77	2,91	0,315	0,256		5,34	0,899	2,77	0,3110	2,103	0,069	2,030	2,54
			8	22,1	2,47	0,058	1,110		2,53	2,65	0,275	0,209		5,79	0,857	2,53	0,3000	1,954	0,070	1,884	2,36
			— 6°	12,3	4,59	0,232	0,056		4,88	4,68	0,068	0,064		16,60	—0,340	4,88	0,0121	4,300	0,013	4,290	7,15
			— 4	14,3	3,92	0,058	0,250		3,97	4,04	0,215	0,172		6,81	0,773	3,97	0,0823	3,240	0,037	3,200	5,33
0,6	18,3	0,81	— 2	16,3	3,42	0,029	0,440	18,64	3,44	3,56	0,288	0,216	2,88	5,63	0,901	3,44	0,1340	2,685	0,052	2,633	4,38
			+ 2	20,3	2,70	0,016	0,780		2,72	2,88	0,329	0,237		5,21	0,957	2,72	0,1940	2,054	0,071	1,993	3,32
			6	24,3	2,21	0,037	1,060		2,25	2,42	0,311	0,227		5,40	0,918	2,25	0,2170	1,706	0,084	1,622	2,70
			10	28,3	1,85	0,089	1,120		1,94	2,11	0,246	0,161		6,23	0,835	1,94	0,1990	1,500	0,086	1,414	2,36
			— 6°	17,2	3,23	0,232	0,056		2,53	3,38	0,059	0,056		18,9	0,057	3,53	0,0011	3,050	0,016	3,030	7,57
			— 4	19,2	2,87	0,058	0,250		2,93	3,04	0,197	0,160		7,25	0,833	2,93	0,0503	2,415	0,048	2,367	5,92
0,4	23,2	0,89	— 2	21,2	2,58	0,029	0,440	11,30	2,61	2,77	0,281	0,212	1,28	5,70	0,925	2,61	0,0795	2,030	0,068	1,962	4,90
			+ 2	25,2	2,12	0,016	0,780		2,14	2,35	0,347	0,245		5,09	0,936	2,11	0,1140	1,605	0,092	1,513	3,78
			6	29,2	1,79	0,037	1,060		1,83	2,05	0,352	0,247		5,04	0,934	1,83	0,1303	1,347	0,111	1,236	3,09
			10	33,2	1,53	0,089	1,120		1,62	1,83	0,295	0,210		5,57	0,864	1,62	0,1239	1,195	0,117	1,078	2,69
			— 6°	27,9	1,89	0,232	0,056		2,19	2,14	0,046	0,045		23,50	0,448	2,19	0,0028	1,800	0,023	1,777	8,88
			— 4	29,9	1,74	0,058	0,250		1,80	2,01	0,160	0,136		8,36	0,809	1,80	0,0192	1,504	0,069	1,435	7,18
0,2	33,9	0,89	— 2	31,9	1,61	0,029	0,440	5,66	1,64	1,90	0,242	0,189	0,32	6,30	0,953	1,64	0,0295	1,305	0,099	1,206	6,03
			+ 2	35,9	1,38	0,016	0,780		1,40	1,70	0,329	0,236		5,23	0,978	1,40	0,0426	1,054	0,138	0,916	4,58
			6	39,9	1,20	0,037	1,060		1,23	1,56	0,360	0,252		4,93	0,956	1,23	0,0501	0,895	0,168	0,727	3,63
			10	43,9	1,04	0,089	1,120		1,13	1,44	0,323	0,234		5,28	0,907	1,13	0,0487	0,796	0,182	0,614	3,07

The first three columns contain the initial data characterizing /136 the shape of a wind engine. In columns 4-8 the angles of attack α are calculated, the inflow $\phi + \alpha$, the number of the relative modules and of the magnitude C_y and μ, which are found from the curve plotted for the given profile. In columns 9-13, the expression $\frac{e}{(1+e)(1-e)^2}$ is calculated from formula (95) and the magnitude of e is determined. This is done graphically from the curve which expresses the functional dependence of the above expression, on e, which can be plotted using a small number of points. In columns 14-18, the specific moment is calculated in an abstract form by means of: $\frac{e}{(1+e)(1-e)^2}$

$$\Delta\bar{M} = S\frac{e}{1+e}\cdot\frac{1-\mu\frac{c_a}{r_a}}{\frac{r_a}{c_a}+\mu}\bar{r}^2\Delta\bar{r}. \qquad (145)$$

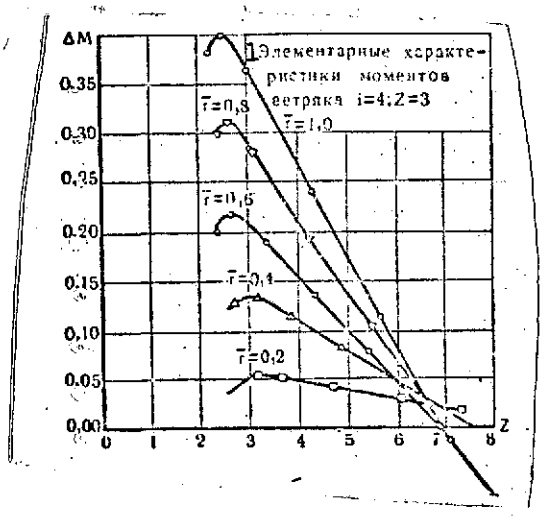

Fig. 60: Characteristics of the abstract moment for each section of the wing.

Key: 1. elementary characteristics of the moments of the wind engine

In the last four columns 19-23, the number of modules related to the blade tip is calculated.

The characteristics of the abstract moments for each section are plotted from /137 the calculated data (Fig. 60); here the number of the modules from columns 22 (Table 7) are plotted on the abscissa, while on the ordinate -- the abstract moment for each element of the blade from column 18.

Subsequently, the diagram of the distribution of the moment along the blade is plotted; for this purpose, in Fig. 60 the ordinate is drawn for the given number of modules, the intersection of which with the curve gives the magnitude of the moments for all the sections. Transferring these values to the graph (Fig. 61), the magnitudes of the moment along the blade are obtained.

Each curve in Fig. 61 corresponds to a certain number of modules Z. In such a manner, the graph (Fig. 61) is in fact a solution of the integral of the equation (115).

The area circumscribed by the abscissa and the curve of the moment is equal to the integral taken between the limits $\bar{r} = 0.2$ to $\bar{r} = 1.0 = R$. If the given area were replaced by an isometric square, the base of which would be equal to $\bar{r} = 1$, then its height in the ordinate scale would express the magnitude of moment.

Fig. 61: Change in the abstract moment along the blade in relation to Z.

Key: 1. distribution of the moment of the blade.

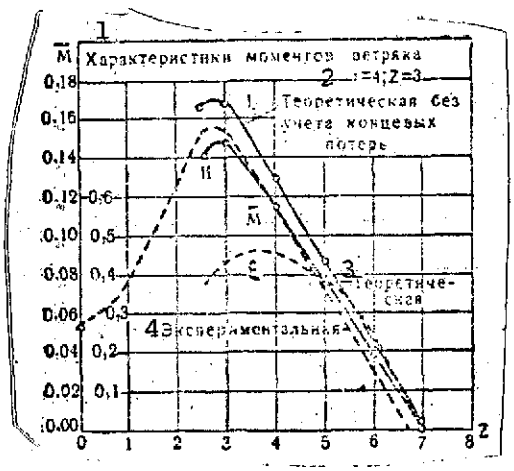

Fig. 62: Calculated aerodynamic characteristics of the whole wind wheel.

Plotting on the ordinate the height of the squares taken in Fig. 61, and on the abscissa -- the number of modules, we obtain the aerodynamic performance of the entire wind engine, shown in Fig. 62.

The characteristics of the moment in Fig. 62, are plotted on the basis of equation (115) which does not take into account the tip losses. If we express these losses by the moment of the losses, then we can substract them from the theoretical moment and correct the characteristics.

Dividing the power T_j of the tip losses by the angular velocity, we obtain the /138 moment of the blade tip losses:

$$M_j = \frac{T_j}{\omega}. \qquad (146)$$

Since:

$$T_j = \pi R^2 \rho \frac{V^3}{2} \xi_i \bar{T}_j,$$

Then:

$$M_j = \bar{T}_j \frac{\pi R^2 \rho \frac{V^3}{2} \xi_i}{\omega}.$$

Dividing this moment by the expression: $\pi R^3 \rho \frac{V^2}{2}$, we obtain it in an abstract form:

$$\bar{M}_j = \frac{M_j}{\pi R^3 \rho \frac{V^2}{2}} = \frac{T_j V}{\omega R} = \bar{T}_j \frac{\xi_i}{Z} \qquad (147)$$

Substituting here the value of T_j from equation (126) and ξ_j from equation (79), we obtain:

$$\bar{M}_j = \frac{4e^3}{Z(1+e)} \left[\frac{8 \sqrt{1 + \left(\frac{1-e}{Z}\right)^2}}{(1+e)iZ} - \frac{1}{\sqrt{1 + \left[\frac{iZ}{\pi\left(1-\frac{e}{2}\right)}\right]^2}} \right]. \qquad (148)$$

The calculation of $\bar{M}_j$, the moment of /139 the blade tip losses of this wind engine, is done in Table 8. By setting out in the scale of the moment, the blade tip losses below curve I in Fig. 62, we obtain curve II of the characteristic of the moment which accounts for the blade tip losses and is in such a manner the final characteristic of the moment.

TABLE 8. CALCULATION OF THE MOMENT OF THE BLADE TIP LOSSES (EQUATION 148)

1	2	3	4	5	6	7
Z	e	$\frac{2\sqrt{1+\left(\frac{1-e}{Z}\right)^2}}{Z(1+e)}$	$\frac{1}{\sqrt{1+\left(\frac{1Z}{\pi\left(1-\frac{1}{2}\right)}\right)^2}}$	Column 3 + Column 4	$\frac{k_M}{Z(1+e)}$	M_i
2,5	0,23	0,684	0,248	0,426	0,0685	0,0287
3	0,26	0,545	0,222	0,323	0,072	0,0231
4	0,285	0,397	0,166	0,231	0,063	0,0145
5	0,28	0,315	0,134	0,181	0,049	0,0089
6	0,27	0,265	0,112	0,153	0,0363	0,0059
7	0,26	0,228	0,098	0,130	0,0302	0,0040

Multiplying the value of the moment $\bar{M}$ by the corresponding magnitude of the number of modules Z, we obtain the output coefficient of the wind energy $\xi = \bar{M}Z$. This coefficient, when plotted on the same graph, gives the characteristic of the power of the wind engine shown by a dotted curve (Fig. 62).

24. The Profiles "Espero" and Their Construction.

The profile of the wing plays a most important role in obtaining a high efficiency of the wind wheel. Numerous profiles of wings are utilized in the practice; among them, an important place is occupied by the "Espero" profile. This profile was elaborated on at Ts AGI by engineer B. V. Korostelev, who named it "Espero". A series of these profiles was tested in the wind tunnel of Ts AGI at velocities of the airstream of approximately 30 m/sec. The angles of attack were taken from $\alpha = -14^\circ$ to $\alpha = 90^\circ$. The dimensions of /140 the handle were 750 x 150 mm. The obtained results were calculated for an infinite span and are presented in the form of graphs in Fig. 63, 64.

Fig. 63 gives the value of C_y as a function of $\alpha = -14^\circ$ up to $\alpha = 10^\circ$, while Fig. 64 -- for angles $\alpha = 10^\circ$ to $\alpha = 90^\circ$. On the abscissa, the thicknesses of the profile in fractions of the chord are plotted, while on the ordinate -- the coefficients of the lifting force of the wing $C_y = \frac{Y}{\rho\frac{v^2}{2}S}$. Each thick curve corresponds to a certain angle of attack α in the given period. The angles α are denoted at the end of the corresponding curve. The thinner curves which intersect the thick ones represent the curve at μ = const. i.e. each curve corresponds to a given μ of the series. The value of μ is shown in the middle of the curve. The curve C_y and μ are constructed for a profile thickness of $\delta/b = 0.1$ to 0.5.

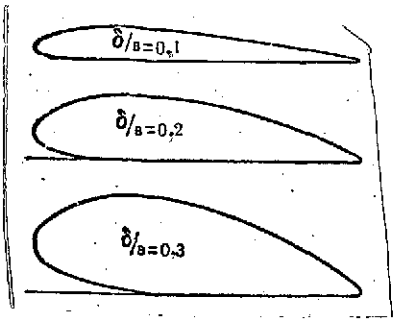

Fig. 65: Profile "Espero" for the thickness δ/b = 0.1, 0.2, and 0.3.

Example 1. Find C_y and μ for a profile "Espero" with thickness 0.21 at an angle of attack $\alpha = -1^\circ$.

Solution. On the abscissa we find the point δ/b = 0.21; starting from it, we go along a vertical line until the intersection with the thick curve denoted -1° and we calculate the magnitude of the ordinate on the left scale; it will be equal to $C_y = 0.827$.

The magnitude of μ is found by interpolating visually the distance of the point (δ/b = 0.21; $C_y = 0.827$) from the nearest thin curve μ = 0.01 and μ = 0.015. The unknown μ is found to be equal to μ = 0.012.

Using the graph 64, it should be kept in mind that the area circumscribed between the curve α = 10 and $\alpha = 28^\circ$, gives the values of C_y and μ rather inaccurately, since this region corresponds to the /142
angles of attack at which the jet is disrupted and forms vortexes.

Fig. 65 gives the profile "Espero" for a thickness δ/b = 0.1, 0.2 and 0.3, while Fig. 66 presents two graphs by means of which an "Espero" profile of any thickness can be constructed. On the abscissa, the thicknesses of the profile expressed in fractions of the chord for the abscissa of the profile which is indicated at the end of each curve, is presented. The left graph -- a gives the ordinate of the head of the profile for the abscissa from 0 to 0.3; the first graph -- b gives the ordinates of the tail for the abscissas from 0.4 to 1.0. The plotting of the profile is done in the following manner (Fig. 67). The axes of the coordinates are plotted, and the values of abscissas obtained by multiplying the length of the profile chord of the projected wing by the number at the end of the curve are plotted on the abscissa (Fig. 66).

Example 2. Find the ordinate of the profile of the projected blade with a chord equal to 1000 mm and thickness δ/b = 0.3 for abscissa 0.2.

Solution. Let us find the magnitude of the ordinate according to the curve at the end of which the number 0.2 is written. There are two such curves on the left diagram in Fig. 66: the upper curve, the ordinate of which gives a magnitude of the ordinate of the back edge of the profile equalling 0.289, and the lower curve, the ordinate of which equals 0.0272, gives the magnitude of the ordinate of the lower part of the profile. Multiplying the obtained coordinates by the length of the chord we obtain for the abscissa of the projected profile, $x = 0.2 \cdot 1000 = 200$ mm and for the ordinate, $y = 0.289 \cdot 1000 = 289$ mm and $y = 0.0272 \cdot 1000 = 27.2$ mm.

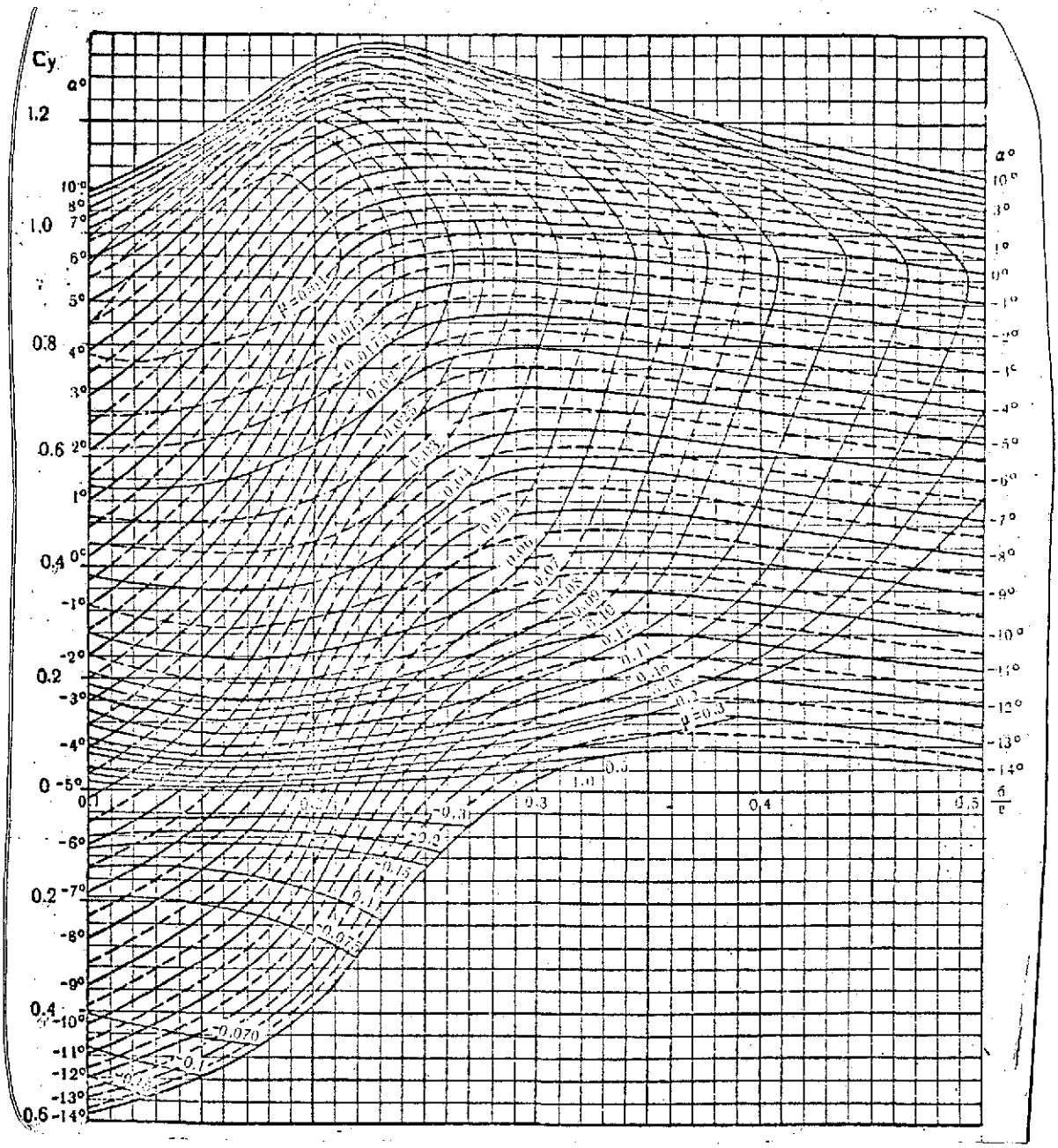

Fig. 63: Graph for the determination of C_y and μ of wings with an infinite span for "Espero" profile in relation to α = 14 up to 10°.

ORIGINAL PAGE IS
OF POOR QUALITY

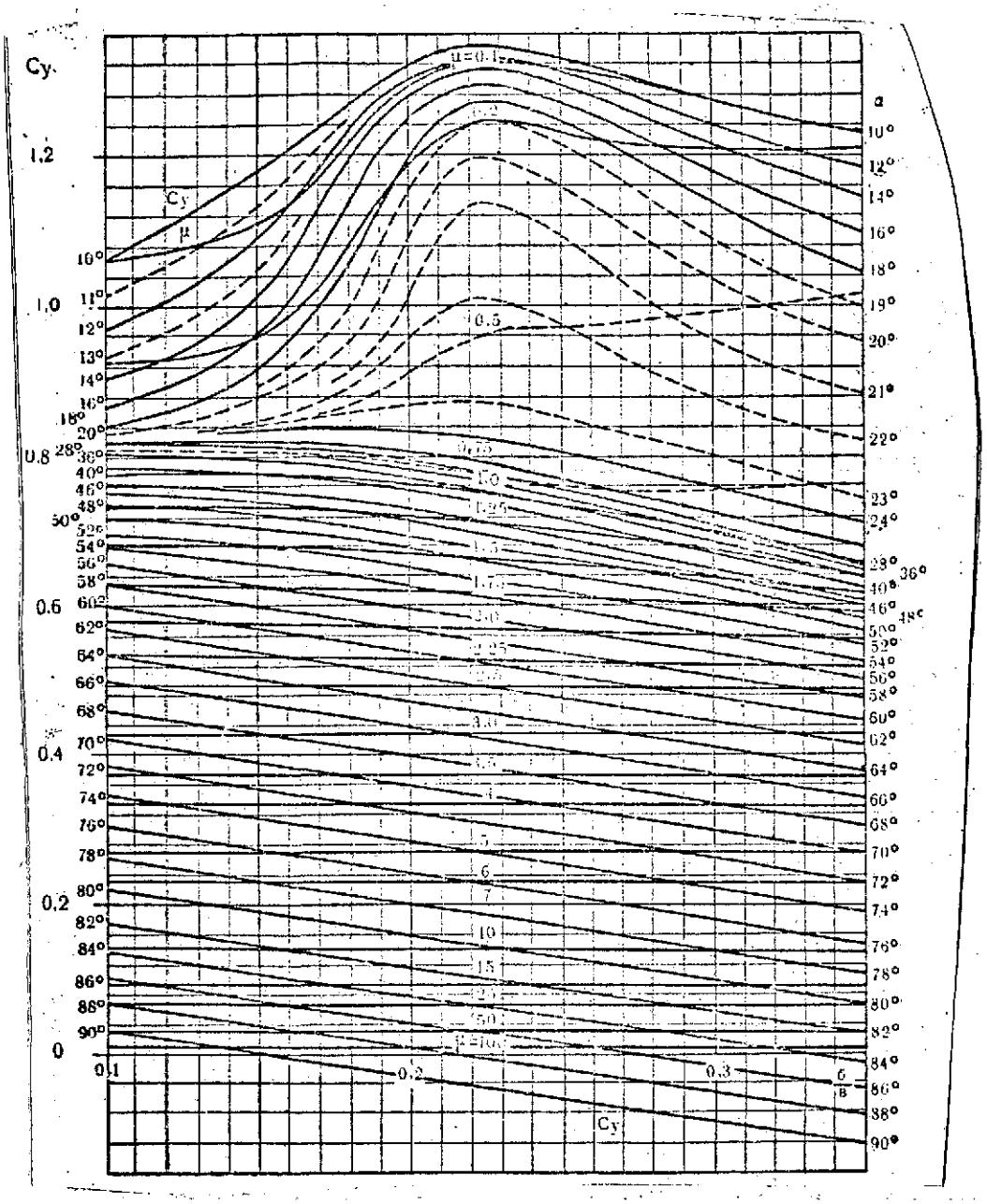

Fig. 64: Graph for determination of C_y^{φ} and μ of wings of infinite span with "Espero" profile, in relation to α = 10 to 90°.

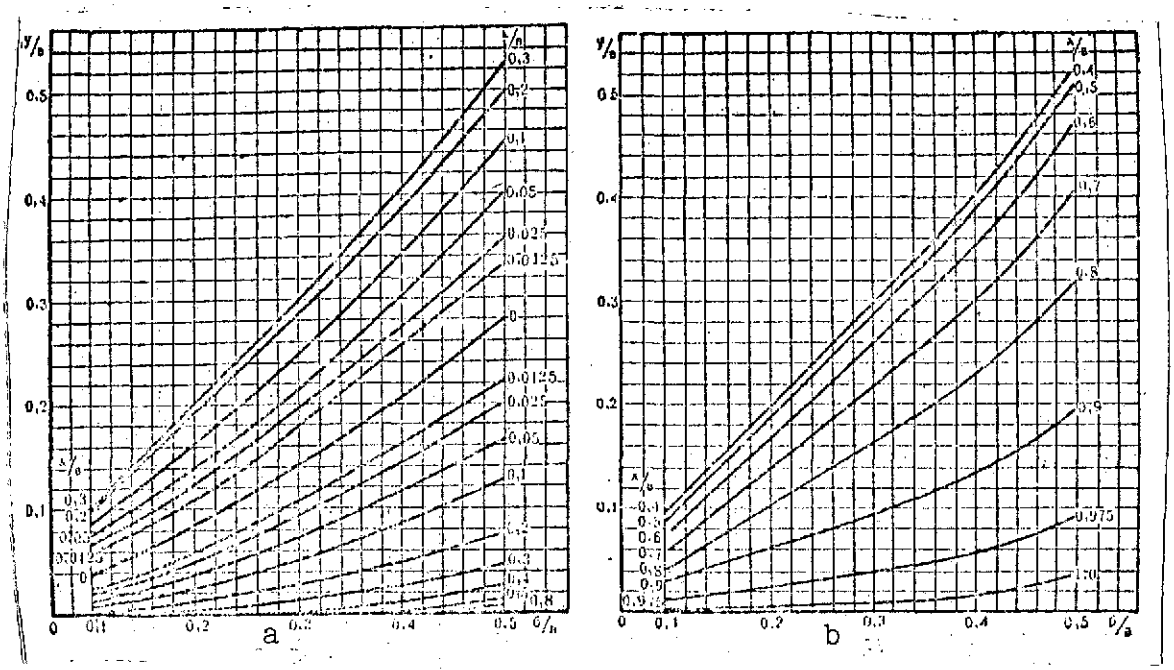

ORIGINAL PAGE IS
OF POOR QUALITY

Fig. 66: Graph of the ordinates of the "Espero" profile, a. spout of the profile; b. tail of the profile.

The remaining coordinates are determined in a similar manner, the pointsoare plotted, they are united by means a French curve and the profile of the wing is obtained.

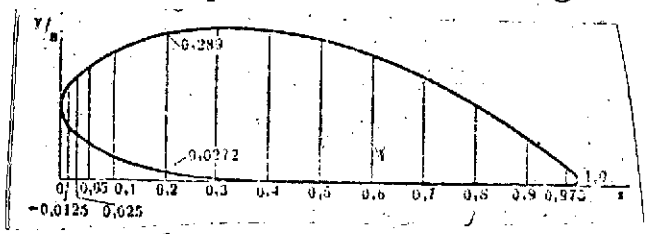

Fig. 67: Plotting of the "Espero" profile

25. Method for Obtaining the Experimental Characteristics.

The experimental characteristics of wind engines are obtained either in the wind tunnel, where an airstream is artificially created, or under natural conditions in a wind power laboratory with a tower which is equipped with special instruments.

Fig. 68 represents the diagram of a wind tunnel with a diameter of 1.6 m set up in one of the laboratories of the USSR.

The main instruments for testing models of wind engines in the wind tunnel are the following:

1. A micromanometer working with alcohol and with a TsAGI tube for measuring the dynamic pressure of the airstream in the tube;
2. a recorder with a chronograph for recording the revolutions of the wind wheel model;
3. a barometer for determining the atmospheric pressure;
4. a thermometer for determining the temperature during the experiment.

The experimental characteristics of wind engines are obtained according to the inertia method of the Aerodynamic Institute in Kuchino.

This method is based on the law of inertia of a revolving mass. In order to confer a known angular acceleration to a body revolving about its own axis, a torque has to act on the body, which should be equal in magnitude to the movement of inertia of the body, in this case the wind wheel, relative to the axis of its rotation multiplied by /145 the angular acceleration, i.e.:

$$M = I\frac{d\omega}{dt} \tag{149}$$

where M -- torque;
I -- moment of inertia of the revolving body;
dω/dt -- angular acceleration.

In such a manner, knowing the angular acceleration at each moment in time and the moment of inertia of the model of a revolving wind wheel, we can determine the torque of the models $M = M_{aer}$, caused by the external forces, i.e. by the airstream in the wind tunnel.

Determining the value of the angular velocity ω, for each moment in time, the number of the modules;

$$Z = \frac{\omega R}{V}$$

corresponding to the obtained torque of the wind engine M_{aer} is found, and subsequently the characteristics $M_{aer} = f(Z)$ are plotted. The diagram of wind wheel testing of a wind wheel is illustrated in Fig. 69.

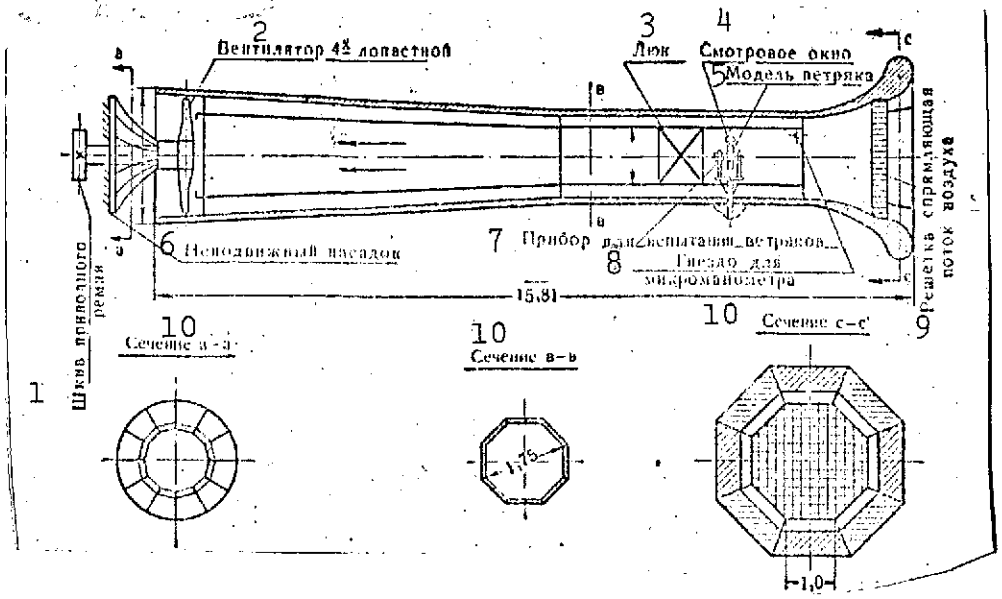

Fig. 68: Diagram of the wind tunnel.

Key:
1. belt pulley
2. four-bladed ventilator
3. hatch
4. peep hole
5. model of the wind engine
6. fixed nozzle
7. device for testing wind engines
8. container for the micromanometer
9. screen for rectifying the airstream
10. cross section

The model of the wind engine 1 is placed in a wind tunnel 2, where an airstream is created by means of ventilator 3. On the shaft of the model, there is an electric contact 9 which once in the course of a revolution of the shaft closes the circuit by making contact with the circuit of the electromagnet 4, which sets in motion pen 10 of chronograph 6. The revolving of the chronograph drum takes place due to a small synchronal electromotor 7 via transmission 8. Recording of the readings is made on paper blackened with the smoke of a kerosene lamp, which covers the drum of the chronograph. The recording has the shape of white tracings on a black background. The drum must have a constant number of revolutions.

The velocity of the airstream created by the ventilator should be 10 to 12 m/sec. As soon as a homogeneous stream is established in the wind tunnel, the mechanical stop which maintains the wind

engine model in a stationary state, is suddenly pulled back. Under the action of the wind stream, the wind engine is set in motion and picks up speed; after a certain interval of time, it reaches a maximum number of revolutions which are called synchronal. As the current reaches a steady state, the number of revolutions does not change any more.

At the time that the wind engine picks up speed, the two pens 10 and 11 start writing on the blackened paper; pen 10 marks its tracing after each revolution of the shaft of the wind engine model, /147 while pen 11 marks the time each second. This pen is connected with a clock mechanism in the following manner: the pendulum of 12 o'clock, touches mercury drop 13 in its lowest position and establishes contact closing the circuit of electromagnet magnet 5, and setting in motion the second pen 11.

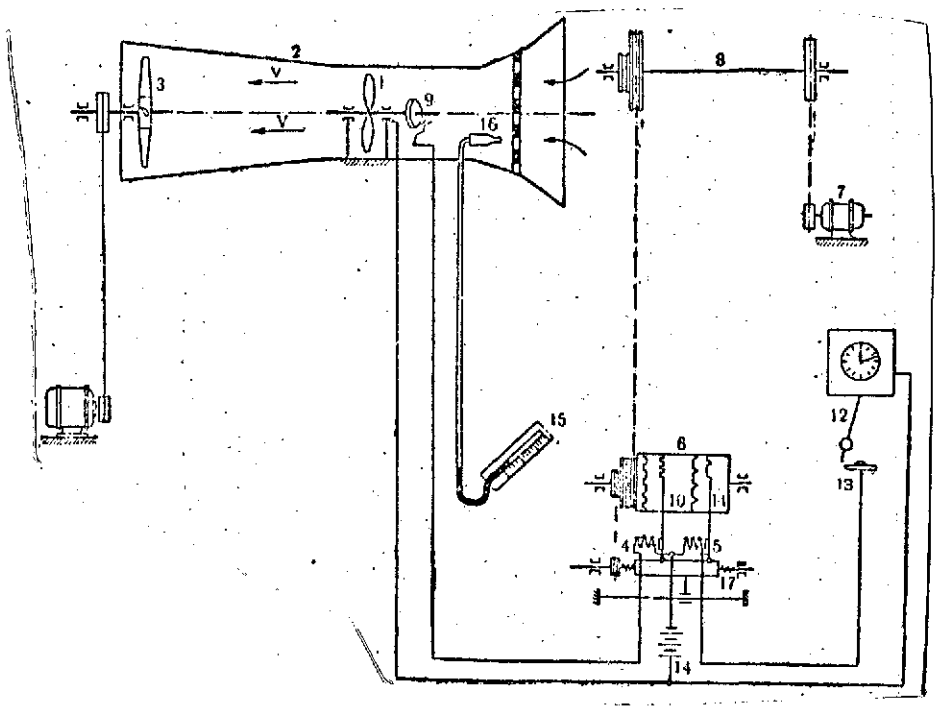

Fig. 69: Diagram of the devices for model testing in a wind tunnel.

At the same time, by means of micromanometer 15 which is connected to tube 16, the dynamic pressure of the airstream in the tunnel is measured in order to determine subsequently the velocity. The carriage with pen 10 and 11 is displaced parallel to the axis of the chronograph drum by means of screw 17. The instrument receives electrical current from the storage battery 14.

The experiment is stopped when the wind wheel reaches a synchronal number of revolutions, which requires no more than 15 seconds.

After the experiment, the paper is removed from the chronograph and placed in a solution of shellac which after drying fixes the soot on the paper and prevents the recording from being erased. The diagram of the recording is shown in Fig. 70.

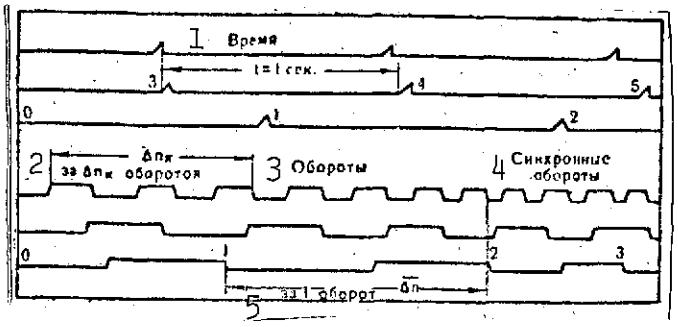

Fig. 70: Diagram of the recording of revolutions and time.

Key: 1. time
2. after Δn_k revolutions
3. revolutions
4. synchronal revolutions
5. after one revolution

Processing of the experimental results. On the paper removed from the chronograph, it can be found at what time in seconds t_p from the beginning of the rotation, did the wind engine reach synchronal revolutions. The seconds are denoted by figures 0, 1, 2, 3, 4, 5, etc. above on the diagram. Synchronal revolutions are characterized by equal length of the segments Δn of the recording between two adjacent tracings of revolutions. On the diagram %148 these are denoted by the figures 0, 1, 2, 3 above the tracings.

By measuring the length of the segment for each second of the time of take-off, the average length l_{av} is found which was traced by the pen during one second.

$$l_{av} = \frac{\Sigma l}{t_p},$$

where t_p is the number of seconds in the course of which the wind engine took off.

For determining the angular velocity of the take-off of the model, the length of the segment Δn between the tracings of the first, second, third, etc. up to the sixth or eighth revolutions is measured. Further the segments of two revolutions are measured at the same time, then of three, etc. gradually increasing the measured part Δn after Δn revolutions. The smaller the difference between two segments of neighboring revolutions, the closer are the revolutions to being synchronal.

The time Δt_k, in the course of which the wind engine made Δn revolutions on the singled out segment Δn_k should be equal to:

$$\Delta t_k = \frac{\Delta n_k}{l_{av}} \cdot \frac{[\text{мм}]}{[\text{мм}]},$$

where k -- serial number of segments Δn_k on which Δn revolutions were performed (Fig. 70);

l_{av} -- length of the segment corresponding to 1 second.

The average angular velocity developed by the wind engine which makes Δn_k revolutions corresponding to a given Δn_k segment, is obtained from the equation;

$$\omega_k = \frac{2\pi \Delta n_k}{\Delta t_k} \left[\frac{\text{rad}}{\text{sec}}\right]$$

It is commonly considered that the average angular velocity ω_k of the wind engine is reached by the latter in the middle of the time interval Δt_k. Consequently, the average angular velocity ω_k is developed by the wind engine in the following time:

$$t_k = \Sigma_{\Delta t}^{k-1} + \frac{\Delta t_k}{2} \text{ [sec]}$$

After determining the value ω_k and t_k for all the individual segments Δn, counting from the beginning of the motion and up to the onset of synchronal revolutions, the curve of the take-off $\omega = f(t)$ is plotted (Fig. 71).

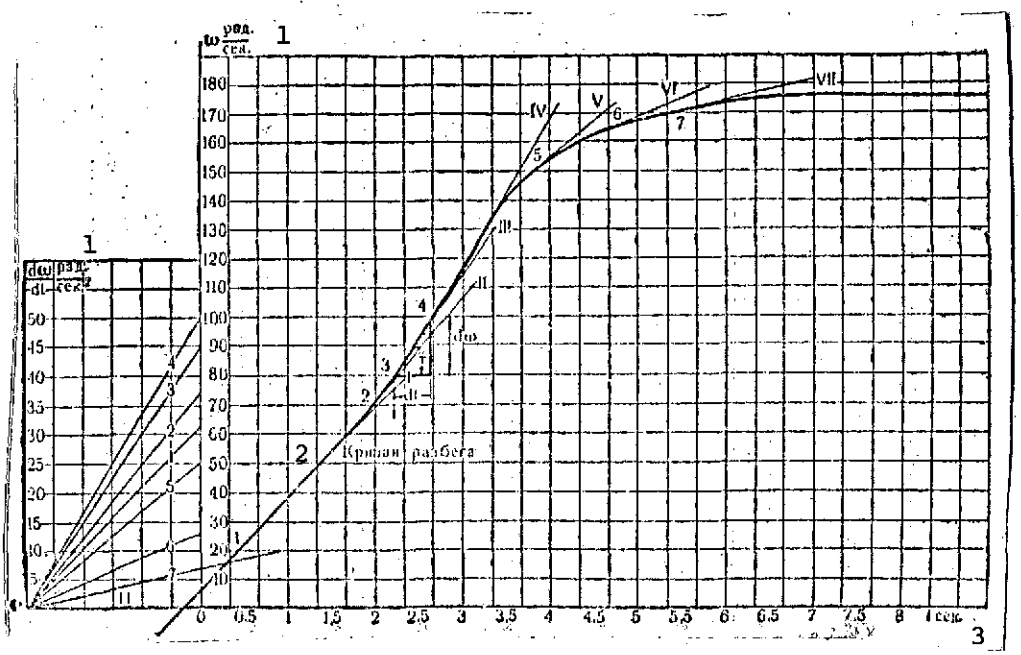

Fig. 71: Curve of a wind wheel take-off model in a wind tunnel and plot of the tangents for determination of the angular acceleration.

Key: 1. Rad./sec.
2. take-off curve
3. sec

It should be mentioned that the shaft of the wind engine up to /150 the first closing of the circuits by means of contact 9 which acts on on pen 10, passes an interval of time Δt, the magnitude of which depends on the initial mutual position of the revolving contact 9 of the shaft and contact 13 of the clock mechanism (Fig. 69).

Therefore, at t = 0 (origin of the coordinates), the angular velocity may assume a certain value, as shown in Fig. 71. The magnitude of the angular velocity in the same interval of time is determined on the ordinate axis by the course of the left part of the take-off curve, which should pass slightly above the origin of the coordinates, without disturbing its smooth course.

From the take-off curve, it is possible to determine graphically the angular acceleration dω/dt, corresponding to the selective values of time t and angular velocity ω. For the sake of convenience in calculating the number of modules Z = ωR/V, the magnitude dω/dt is determined for round values of ω = 10, 20, 30, 40, etc.

Fig. 71 is an example for graphic determination of the angular acceleration from the take-off curve ω = f(t). Let us select on the curve points 1, 2, ...7 through which tangents I, II, ...VII are drawn. On the continuation of the horizontal axis at the left, let us lay out segment OP = H which is called the polar distance, while point P is called the pole. Let us draw rays P -- 1, P -- 2, ... P -- 7, from point P, which are parallel to tangents I, II,... VII. We can see from figure 71 that segments 01, 02, 03, 04, etc. on the axis ω are proportional to the angular accelerations in the points of the graph 1, 2, ... 7, since it can be seen from the plot that all these are proportional to the tangens of the slopes ϕ of the tangents, i.e.:

$$\overline{01} = H \operatorname{tg} \varphi_1;\ \overline{02} = H \operatorname{tg} \varphi_2 \quad \text{etc.}$$

In addition, the real angular accelerations are also proportional to the tangens of the slopes of the tangents on the graphs of the angular velocity.

We can therefore take segments $\overline{01}$, $\overline{02}$ ... etc. as scaling values of the angular accelerations in the corresponding points. The relation between real angular and the scaling ω is determined by:

$$\omega = k_\omega \bar{\omega},$$

analogically

$$t = k_t \bar{t}.$$ /151

Differentiating the expressions, we obtain: $\begin{cases} d\omega = k_\omega d\bar{\omega}, \\ dt = k_t d\bar{t}, \end{cases}$

where $\overline{d\omega}$ is the elementary scaling displacement, while $\overline{dt}$ is the elementary scaling of time, k_ω and k_t -- scales of the angular velocity and time.

Since dω/dt = tgϕ (Fig. 71), then $\frac{d\omega}{dt} = \frac{k_\omega d\bar{\omega}}{k_t d\bar{t}} = \frac{k_\omega}{k_t} \operatorname{tg} \varphi.$

Let us determine the scale of the angular acceleration.

From the plots (Fig. 71) for the scaling angular acceleration, for example, in point 1:

$$\frac{d\omega}{dt} = H \operatorname{tg} \varphi_1, \quad \text{(a)}$$

since:

$$\frac{d\omega}{dt} = \frac{k_\omega}{k_t} \operatorname{tg} \varphi \quad \text{(b)}$$

and

$$\frac{d\omega}{dt} = k_s \frac{d\bar{\omega}}{dt}, \quad \text{(c)}$$

solving equations (a), (b) and (c) relative to $k_{[illegible]}$, we obtain the unknown scale:

$$k_s = \frac{k_\omega}{H k_t}. \quad \text{(d)}$$

In order to determine the aerodynamic moment of the wind wheel, the moment of its inertia relative to the axis of rotation should be known.

This moment is determined by means of a three-thread hanger according to the method suggested by Prof. V. P. Vetchinkin. The hanger is a three-blade symmetrical wooden star wheel, which is suspended by means of three threads (Fig. 72). The point of attachment of the threads to the starwheel form an equilateral triangle; thus, the threads of the hanger form a circular cylinder with a vertical axis. There is an opening in the center of the star wheel in which the shaft is placed, with the model of the wind wheel attached to it; the axis of the shaft coincides with the axis of the cylinder. It should be kept in mind that after it is blast off, the model does not move on the shaft of the instrument, and the angle $\varphi_r = 1$ does not change. The system of the hanger (threads -- model + star wheel) is likened to a body suspended on an elastic bar; the star wheel is carefully rotated around its vertical axis at a small angle and then released. The system undergoes oscillations around its vertical axis in a horizontal plane, the period of which is determined by the following: $T_c = \frac{\Sigma t_c}{n_c}$, /152

where Σ_{tc} is the time in the course of which the system makes n_c full oscillations.

Subsequently the system is deflected at a small distance to one side at a small angle and then released; the star wheel starts to describe flat oscillations. The period of these oscillations, analogically to the previous case, is equal to: $T_d = \frac{\Sigma t_d}{n_d}$.

After obtaining the periods of the oscillations, the radius of the inertia is determined by means of the following equation: $\rho = r \frac{T_d}{T_d}$,

where r is the distance from the center of the star wheel to the point of attachment of the thread.

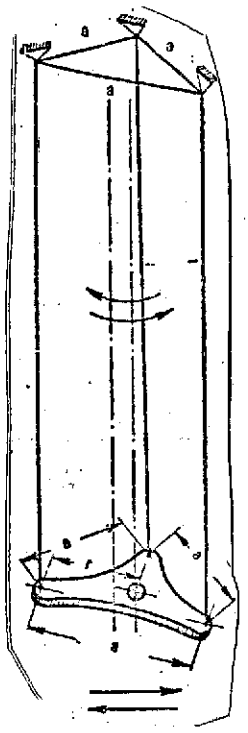

Fig. 72: Three-thread hanger

This expression was obtained on the basis of th the following conclusion. In his work "Method for the Experimental Determination of Inertia Moment of Solid Bodies by Means of a Mutliple-Thread Hanger", V. P. Vetchinkin, gives the formula for determining the period of oscillation of the suspended system for the case when all the threads are situated about the vertical /153 axis of a circular cylinder with a parallel axis passing through the center of gravity:

$$T_c = 2\pi \sqrt{\frac{I_0 l}{Mg(r^2 - c^2)}}, \qquad \text{(a)}$$

where r is the radius of the cylinder formed by the threads of the hanger with a length l;
c is the distance between the center of gravity of the body and the axis of the cylinder.

If the center of gravity of the body is situated on the axis of the threads, then c = 0, as is the case with our 3-thread hanger, and equation (a) assumes the aspect:

$$T_c = 2\pi \sqrt{\frac{I_0 l}{Mgr^2}}; \qquad \text{(b)}$$

hence the moment of inertia:

$$I_0 = \frac{T_c^2 Mgr^2}{4\pi^2 l}. \qquad \text{(c)}$$

Let us transform the expression $\frac{Mgr^2}{4\pi^2 l}$ in equation (c) and write it in the following form:

$$\frac{Mgr^2}{4\pi^2 l} = Mr^2 \left(\frac{1}{2\pi}\sqrt{\frac{g}{l}}\right)^2.$$

The expression in parentheses is one divided by the period of oscillation of a mathematical pendulum, i.e:

$$\frac{1}{2\pi}\sqrt{\frac{g}{l}} = \frac{1}{2\pi\sqrt{\frac{l}{g}}} = \frac{1}{T_d},$$

consequently

$$\frac{Mgr^2}{4\pi^2 l} = Mr^2 \frac{1}{T_d^2}.$$

Substituting the right part of this equality in equation (c), we obtain:

$$I_0 = Mr^2 \frac{T_c^2}{T_d^2}, \qquad \text{(d)}$$

in addition:

$$I_0 = M\rho^2, \qquad \text{(e)}$$

where ρ is the radius of the inertia.

From equations (d) and (e) we find: /154

$$Mr^2\frac{T_c^2}{T_d^2}=M\rho^2,$$

or

$$r^2\frac{T_c^2}{T_d^2}=\rho^2,$$

consequently, the radius of the inertia is equal to:

$$\rho=r\frac{T_c}{T_d}.$$

The moment of inertia of the hanger system is equal to:

$$I_{mod+stw}(M+m)\rho^2=(M+m)\left(r\frac{T_c}{T_d}\right)^2,$$

where M is the mass of the model;
m is the mass of the star wheel;
r is 0.0801 m for the star wheel of the Aerodynamic Laboratory in Kuchino.

The moment of the inertia of the model should be equal to the moment of inertia of the hanger system with the model minus moment of inertia of the star wheel, i.e.:

$$I_{mod} = I_{mod + stw} - I_{stw}.$$

For the Aerodynamic Laboratory in Kuchino, I_{stw} is known and equal to:

$$I_{stw}=0{,}0000269\ kgf\ m\ sec^2$$

Since the relative aerodynamic moment of the wind engine, according to equation (114), is equal to:

$$\overline{M}=\frac{M_{aer}}{\pi R^3\rho\frac{V^2}{2}},\quad M_{aer}=I\frac{d\omega}{dt},$$

then:

$$\overline{M}=\frac{I_{mod}\frac{d\omega}{dt}}{\pi R^3\frac{\rho V^2}{2}}=\overline{I}\frac{d\omega}{dt},$$

where $\overline{I}=\frac{I_{mod}}{\pi R^3\frac{\rho V^2}{2}}$ is the relative moment of inertia of the model of the wind engine.

Multiplying all the values of $d\omega/dt$ by the magnitude $\overline{I}$, we obtain a series of values for the relative aerodynamic moment $\overline{M}$. /155

In determining the velocity of the airstream on the basis of the micromanometer readings, the atmospheric pressure and air temperature have to be taken into account, as well as the correction factors of the micromanometer:

$$V=\sqrt{\frac{2L\frac{\Delta C_n}{\Delta b}C\zeta}{\rho_0}},\qquad (150)$$

where C is the correction coefficient of the given micromanometer = 0.106;

ρ_0 = 0.132 -- mass density of the air at 0° and 760 mm atmospheric pressure;

ΔC_n -- correction factor for alcohol;

Δ_b -- correction factor for temperature and atmospheric pressure; $\Delta b = \frac{273 B}{760 T}$;

ζ -- coefficient tube of the micromanometer 0 = 1.02;

L -- height of the fluid in the micromanometer above 0;

$$L = L' - L_0,$$

where: L' is the height of the column of fluid in the micromanometer at the moment of take-off;

L_0 is the height of the fluid in the micromanometer prior to the creation of pressure.

After determining the velocity of the air flow, the number of modules Z is found for each given ω, corresponding to the acceleration $d\omega/dt$ found according to graph 71: $Z = \frac{\omega R}{V}$.

Having $\bar{M}$ and its corresponding Z, it is easy to plot the characteristic $\bar{M} = f(z)$; further, by means of the equality $\xi = \bar{M}Z$, the characteristic is readily plotted:

$$\xi = f(Z).$$

The tests are performed in duplicate and the average values of two determinations are taken for plotting the characteristics of a given model. /156

26. Aerodynamic Characteristics of Wind Engines

The curve describing the relationship between the diverted moment and the output coefficient of the wind energy on one hand, and number of modules on the other hand, are called aerodynamic characteristics of wind engines.

The main magnitude characterizing a wind engine from the aerodynamic point of view are, in the opinion of G. Kh. Sabinin, the following (Fig. 73):

Z_n -- normal velocity or normal number of modules at which ξ = max. The magnitude Z_n is situated on the abscissa opposite the point of intersection with the horizontal line with characteristic ξ.

$\bar{M}_n$ -- normal relative torque developed by the wind engine with a normal number of modules.

$\bar{M}_0$ -- initial relative moment or moment of pickup therewith Z = 0.

$\bar{M}_{max}$ -- maximal relative moment which can be developed by the wind engine. The ratio $\bar{M}_{max}/\bar{M}_n$ is called the overloading of the wind engine.

Z_0 -- the synchronal velocity is that number of modules at which $\bar{M} = 0$.

The aerodynamic characteristics of the wind wheel change depending on the number and the shape of the blades as well as on the position of the blade in the wind flow.

The change of the characteristics of the wind wheel at various rigging angles ϕ of the propeller blade can be seen in Fig. 74, /157 which presents the characteristic of a 18-blade wind wheel model obtained in three experiments with the following rigging angles ϕ of the blades:

Number of experiments	Distance from the axis $\bar{r}=\frac{r}{R}$		
	1.0	0.75	0.33
I	17°	26°	45°
II	20°	29°	48°
III	25°	34°	53°

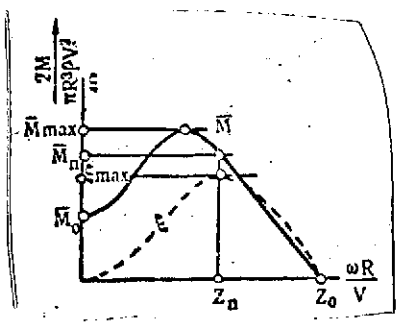

Fig. 73: Plotting of of the aerodynamic characteristic of the wind wheel.

The model of the wind wheel has:

$\frac{r_0}{R}=0,33$ and $\frac{b_1}{b_2}=0,62.$

The continuous lines in Fig. 74 show the curves $\bar{M}$, while the dotted lines are the ξ curves for all three experiments I, II and III correspondingly.

The best parameters of the characteristics were obtained with smallest rigging angles (see curves $\bar{M}$ and ξ, Fig. 74 and table).

The effect of the wing shape on the characteristics of the wind wheel is shown by the curve in Fig. 75, obtained in a wind tunnel for two models of wind wheels of a four-winged windmill. Model I had flat blades with a constant width b = 0.283 R and a constant rigging angle:

$$\phi = 14^{\circ};\ r_0/R = 0.2;$$

Model II with propeller blades, width b = 0.357, R = const; the rigging angles are presented in the following table.

The continuous lines in Fig. 75, illustrate the curves $\bar{M}$, while the dotted lines show the ξ curves.

Wing wheel I gives a maximal output coefficient of the wind energy at $\xi = 0.17$; wind wheel II gives $\xi = 0.316$.

Consequently, the blades with a variable rigging angle and a bent profile, have an almost twice larger ξ as compared to the flat blades of a windmill with constant rigging angle.

The shape of the wings affect strongly the magnitude of ξ. /158
The streamline profile of the wing of the wind wheel increases ξ to a larger extent than the variable rigging angle.

Figure 76 shows the characteristics of a four-blade wind engine, with flat blades and streamlined profile at a constant rigging angle $\phi = 14^{\circ}$, obtained during model testing in a wind tunnel. Comparing this characteristic with the characteristic of a four- /159
blade windmill in which the blades have a constant rigging angle $\phi = 14^{\circ}$ (see curves I in Fig. 75), we find that the output coefficient of wind energy of the wind wheel with streamlined profile of the wings, is 2.3 times larger than in the same wind engine with blades in the form of plates attached to the flap.

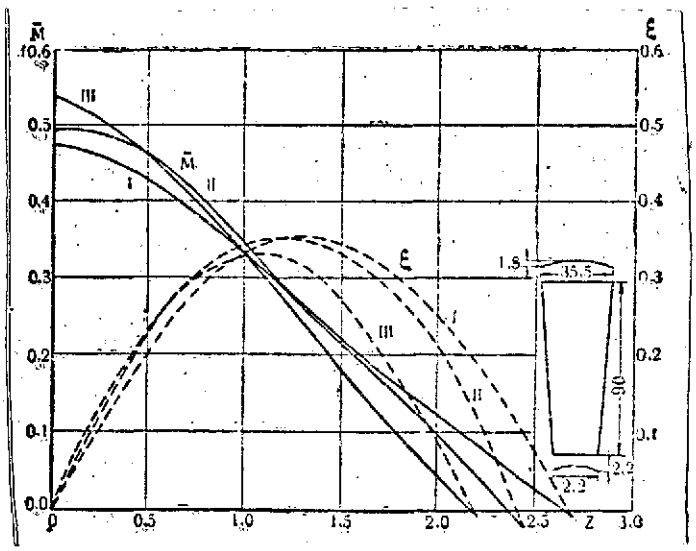

Fig. 74: Aerodynamic characteristic of an 18-blade wind wheel

Table to Figure 74.

Parameter	Experiments		
	I	II	III
Maximal coefficient of utilization of wind energy	0.35	0.35	0.33
Number of modules Zn	1.30	1.20	1.05
Initial torque M_0	0.48	0.50	0.54
Synchronal rapidity Z_0	2.80	2.40	2.10

Tests of wind wheel models of a rural windmill with three different profiles of the wings showed that the wing of this mill with a streamlined profile increases ξ almost two-fold, even if it does so only from the rear side (Fig. 77). This is explained by the fact that the more streamlined the /161
body the smaller the drag which breaks the rotation of the wind wheel. In addition, the streamlined shape of the wing in the rear side, makes it possible for the stream in this part to flow with a higher speed without turbulence, which causes a larger lifting force.

Let us establish further the effect of the number of blades and of the coefficient of charge k_3 on the characteristics. This coefficient represents the ratio of the area of the blade to the surface marked off by the wind wheel.

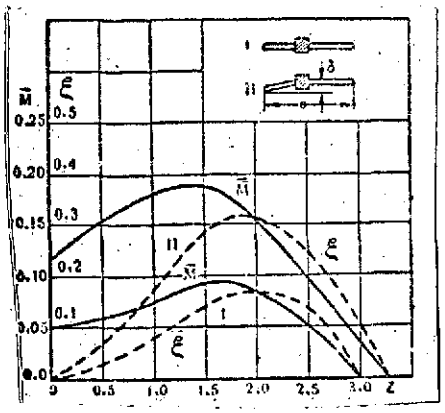

Fig. 75: Characteristic of a 4-blade windmill I -- with flat blade and rigging angle $\phi = 14^{\circ} = \text{const}$; II -- with propeller blade.

Table (to Figure 75)

Notations	Distance from the axis $\bar{r} = \frac{r}{R}$				
	0.2	0.4	0.6	0.8	1.0
axis ϕ	29°15'	25°57'	22°23'	18°11'	15°15'
errors of deflection $\frac{\delta}{\phi}$	0.0535	0.0367	0.0268	0.0214	0.0168

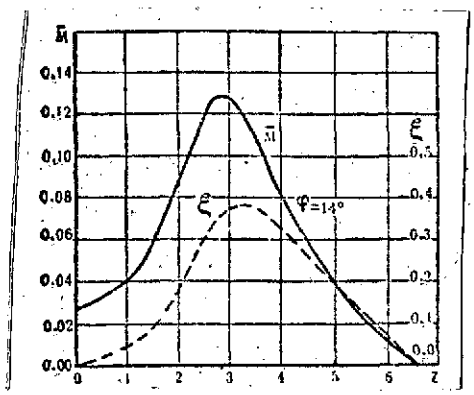

Fig. 76: Characteristic of the 4-blade wind wheel with streamlined flat blades. Rigging angle $\phi = 14^{\circ} = \text{const}$.

Denoting the coefficient of charge by k_3, the area of the blades by S, and the area marked off by F, we obtain:

$$k_3 = \frac{S}{F}.$$

G. Kh. Sabinin performed experimental investigations of four models with different numbers of blades and different coefficients of charge of the marked off area, i.e.:

Number of blades	2	3	4	6
Coefficient of charge k_3	0.096	0.15	0.208	0.295

The profiles of the tested blades are shown in Fig. 80. The experimental characteristics for this wind engine are presented in Figs. 78 and 79.

Examining the obtained characteristics, we see that the number of blades affect little the coefficient of charge of the wind energy. Some increase in ξ is observed only in the 6-blade wind engine. However, this increase cannot be attributed to the large number of blades. This increase could be caused by other circumstances, which are hard to account for in the experimental model. Hence it follows that the power of the wind engine does not depend on the number of blades of the wind wheel; it depends only on the diameter of the wind wheel, the shape of the blades and their position in the wind flow. The change in the number of blades affects strongly the rapidity and the initial moment of the wind wheel. For example, according to Fig. 78, the 6-blade wind engine has a normal rapidity of $Z_n = 2.7$ and an initial

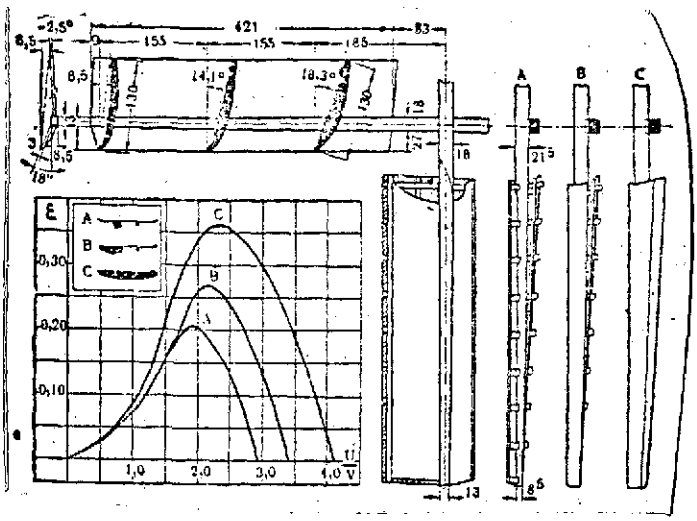

Fig. 77: Characteristic of a rural windmill wind wheel, various profiles of the wing bl blades:

a. with flat blades;
b. with streamlined spout;
c. with streamlined back of blade

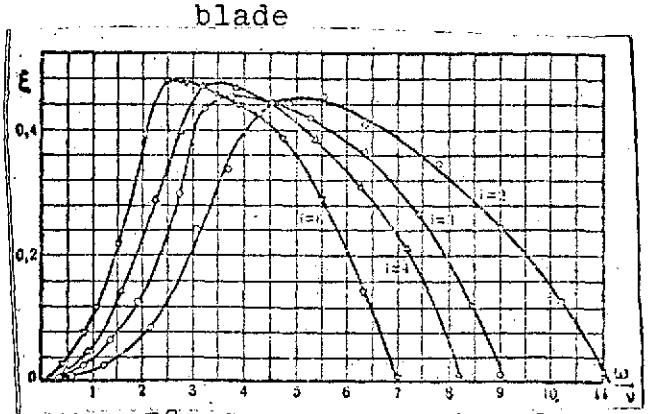

Fig. 78: Characteristic of wind wheels with various numbers of blades.

moment $\bar{M}_0 = 0.067$, while the 2-blade engine has a rapidity/163 $Z_n = 5$ (Fig. 79) and $\bar{M}_0 = 0.01$. In such a manner, the 6-blade wind engine has a rapidity which is equal to approximately 1/2.5 of the same magnitude in the 2-blade wind wheel, while the initial moment is 6.7 times larger. If we compare the acceleration of these wind engines which represent the ratio of the initial moment to the normal one $\bar{M}_0/\bar{M}_n$, we obtain for the 6-blade engine

$$\frac{\bar{M}_0}{\bar{M}_n} = \frac{0.067}{0.18} = 0.37,$$

while for the 2-blade engine

$$\frac{\bar{M}_0}{\bar{M}_n} = \frac{0.01}{0.09} = 0.11.$$

In such a manner, the acceleration is 3.3 times larger in the 6-blade engine than in the 2-blade wind engine.

An even larger difference is observed between the initial moment of multiple-blade wind engines and that of sparsely-bladed ones. For example, in a 18-blade wind engine $\bar{M}_0 \approx 0.5$, in the 2-blade wind engine $\bar{M}_0 = 0.1$, i.e. it is 1/50 of the value in the multi-blade engine. Knowing the aerodynamic characteristics and the effect of various factors on their main magnitudes, we can give the correct solution to several problems of construction of the wind wheel under definite conditions of operation of the wind engine. For example, a sparsely-bladed wind engine which is characterized by great rapidity and a small moment of pickup is most suited for working with a generator which has a small moment of pickup and works with a large number of revolutions. A multiple-bladed wind engine is more suited for working with a rotary piston pump which loads the engine with a large moment of pickup and requires few revolutions.

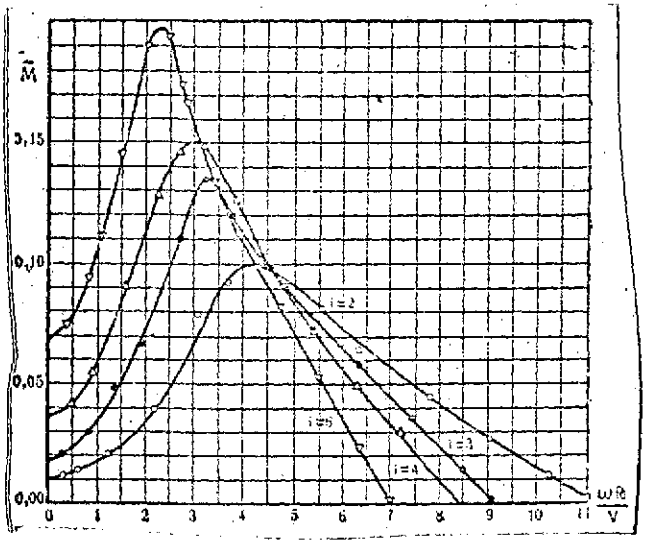

Fig. 79: Characteristics of the moment of wind wheels with various numbers of blades.

27. Experimental Testing of the Theory of Wind Engines.

The theory of wind engines was tested by G.Kh. Sabinin [36]. Preliminarily the aerodynamic characterization of a series of wind engines with number of blades i = 2, 3, 4 and 6, was performed according to the classical theory and according to the theory of G. Kh. Sabinin. The models were designed with an "espero" blade profile and with an increasing thickness of the blade from the end to the bush i.e. $\delta/b = 0.12$ to $\delta/b = 0.24$. The drag coefficient for a 2-blade wind engine was assumed to be $v_1/V = 0.3$, for the /166 remaining ones it was $v_1/V = 0.35$. For each element along the blade v_1/V was taken const. The construction of the models and their dimensions are presented in Fig. 80. As a result of testing the model, the characteristics presented in Fig. 81, 82, 83, and 84 were obtained, where the thick line 3 represents experimental characteristics of the moments, the thin line 1 was obtained by calculations according to the classical theory and the thin line 2 was obtained by calculating according to the theory of G. Kh. Sabinin.

Examination of the above presented characteristics shows that the curve obtained according to the theory of G. Kh. Sabinin, in all cases at $\omega R/V < 4$, i. e. in the right part of the graph, are above the experimental curves, while the curves obtained according to the classical theory are below them, with the exception of the 2-blade wind engine, in which both theoretical curves are below the experimental one at a number of modules which is similar to the synchronal number.

Let us note further that the theoretical characteristics according to both G. Kh. Sabinin and the classical theory differ from the experimental ones to a large extent. The experimental curve at /168 $\omega R/V \geq 4$ seems to be the average curve drawn between the curves calculated by the two theories.

Examining the curves at $\omega R/V < 4$, the left part of the graph, we see a completely different picture. Both theoretical curves almost coincide, while they are much below the experimental curve.

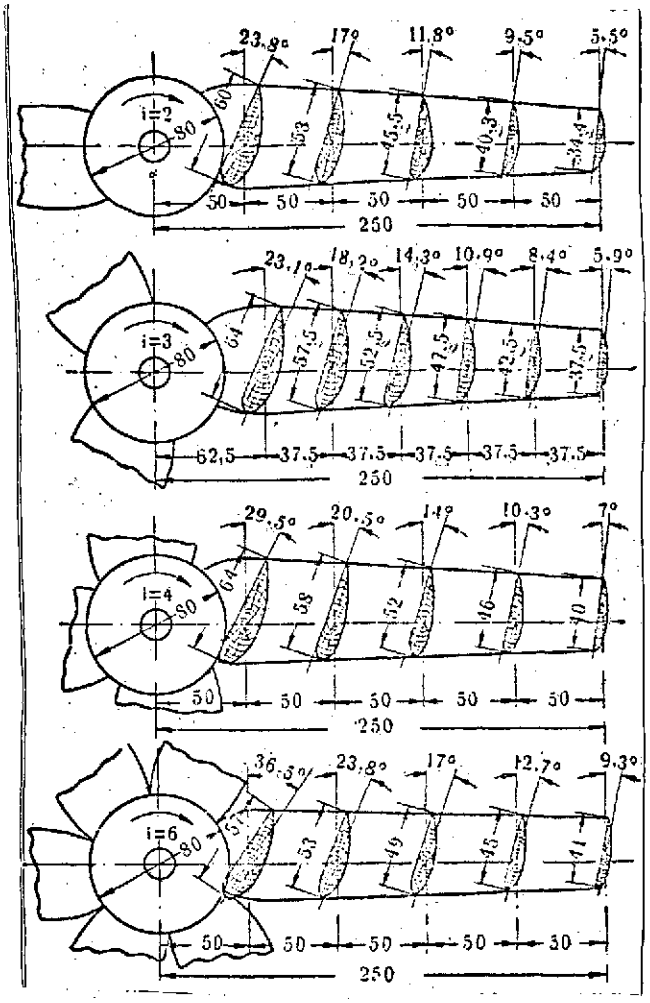

Fig. 80: Models of wind wheels with various numbers of blades.

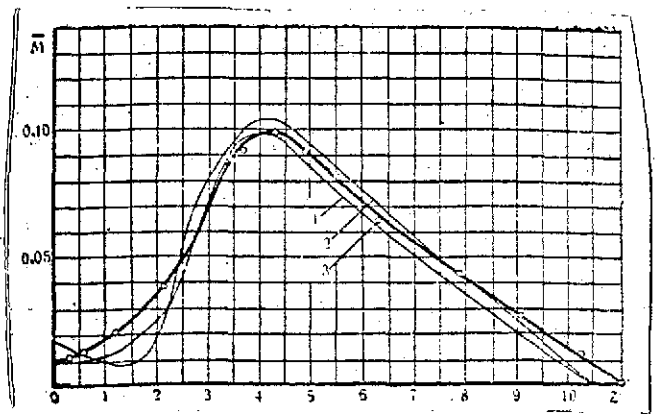

Fig. 81: Characteristics of theoretical and experimental moments for 2-bladed models of wind wheels.

Analogous experiments were performed in the wind tunnel D = 6 m with two models of wind engines of larger dimensions: one model of a 3-bladed wind wheel had D = 2.2 m and Z_n = 4.5; the other -- also 3-blade, but with narrow blades and more rapid, had D = 2.5 m and Z_n = 7. These experiments are interesting in that, in addition to the characteristics of the moment, experimental characteristics of the axial pressure of the stream on the wind wheel were obtained. The experimental and theoretical characteristics of these wind engines, are presented in Fig. 85 and 86, where the thin curves were obtained by G. Kh. Sabinin's theory, while the thick dotted lines were obtained experimentally. Fig. 86 illustrates the circles of the experimental characteristic of the model D = 0.5, a copy of which is the model with D = 2.2 m. These points show that the experimental characteristics of both models in the right part are similar and are very close to the theoretical curve, while in the upper and left part of the graph, they are markedly divergent. The same is noted for curve of coefficients B, characterizing the axial pressure.

/169

$$B = \frac{2P}{\pi R^2 \rho V^2}$$

where P -- is the force of the axial pressure; this magnitude is also called frontal pressure, while B is the coefficient of loading. These experiments are interesting in that they

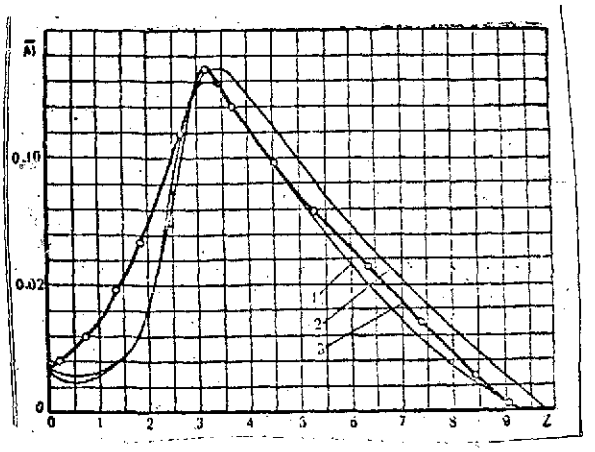

Fig. 82: Characteristics of the moments for 3-bladed models of wind wheels.

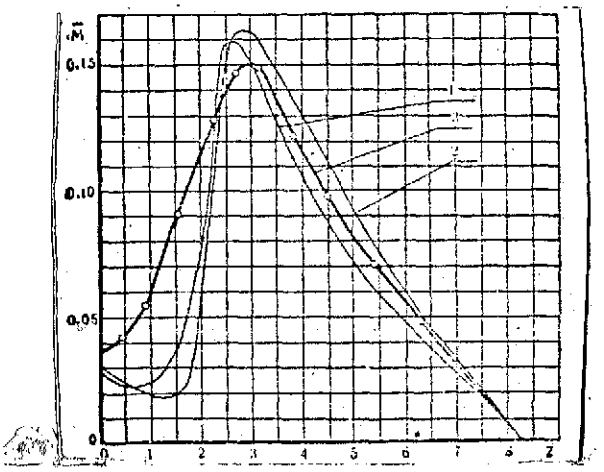

Fig. 83: Characteristics of the moments for 4-bladed models of wind wheels.

confirm the correctness of both G. Kh. Sabinin's theory as well as of the classical theory. The discrepancy between experiment and experiment [sic] in certain characteristics, leaves no doubt as to the correctness of these theories, since the discrepancies are so insignificant, that they are practically negligible.

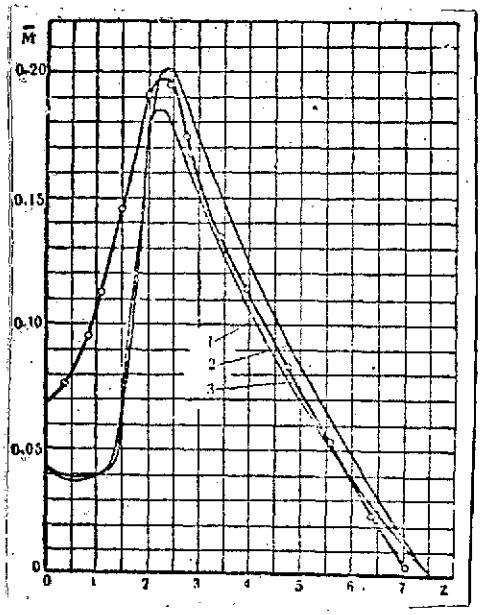

Fig. 84: Characteristics of the moments for a 6-bladed wind wheel.

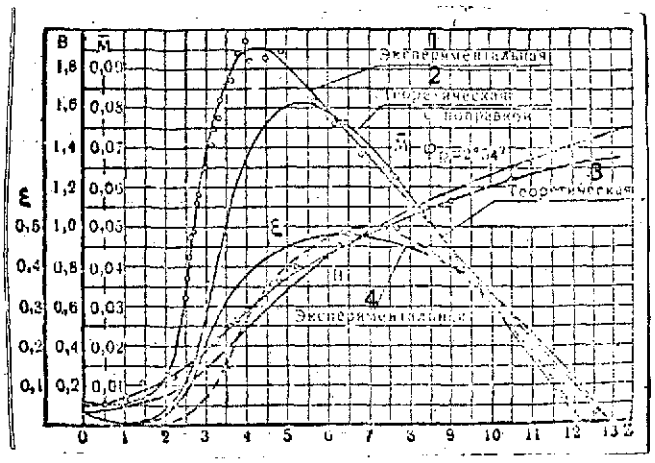

Fig. 85: Experimental and theoretical characteristics of the wind engine D = 2.5 m; Z_n = 7; i = 3.

Key: 1. experimental
2. theoretical with correction
3. theoretical
4. experimental

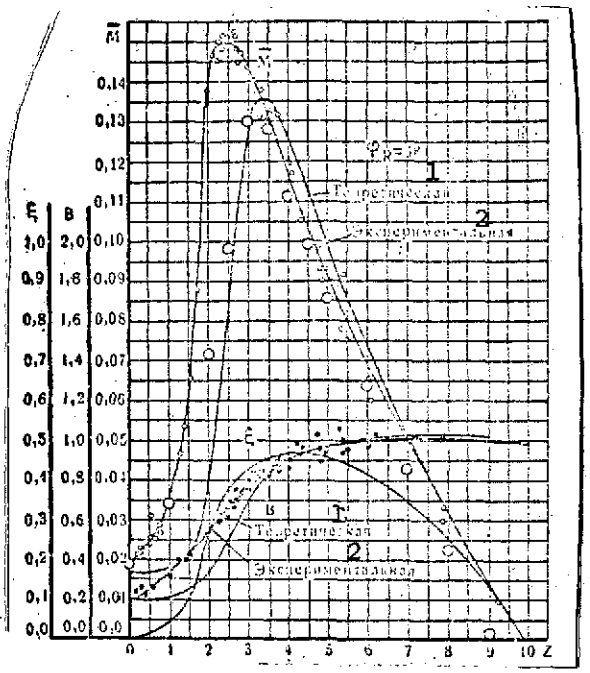

Fig. 86: Experimental and theoretical characteristics of wind engine D = 2.2; Z_n = 4.5; i = 3.

Key: 1. theoretical
2. experimental

The experimental testing of real wind wheels on towers with measured wind flow, is valuable and necessary because the result obtained under these conditions illustrate most truly the operation of wind engines. The airstream in a wind tunnel, acts on the model with a velocity which is constant in magnitude and direction, while the wind flow dashing over the wind wheel under real conditions changes both in velocity and in its direction. In addition, wind wheels have various details on their wings, whose purpose is to regulate the number of revolutions, and certain things which it is not always possible to carry out on a model.

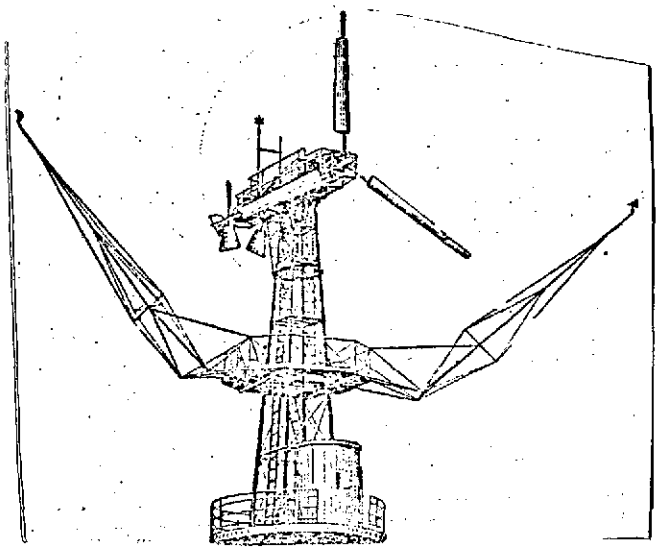

Fig. 87: General view of the upper part of an experimental tower.

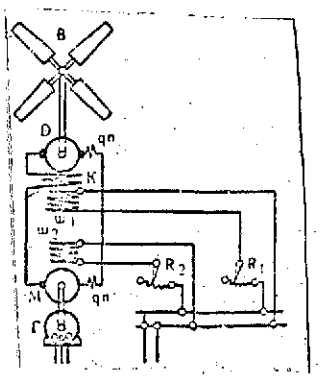

Fig. 88: Diagram of the electrical equipment.

28. Equipment of Towers for the Testing of Wind Engines.

The testing of wind engines under natural conditions, is performed on towers equipped with special instruments and devices.

Fig. 87 illustrates the upper part of the experimental tower of the Windpower Laboratory TsAGI, in which the axis of the wind wheel is situated at the height of 45 m [52].

Such experimental towers have a wind engine which consists of a head of lattice construction, as well as various electric, measuring and recording devices.

The diagram of the electric machinery of an experimental tower is shown in Fig. 88. The DC generator with a power of 1.75 to 4.75 kW, at 900 to 1275 rpm, the voltage /171
230 V, has additional poles with independent excitation and a differential compound winding K which can be switched over to a compound winding. The motor generator with a power of 5.5 kW, 1425 rpm, consists

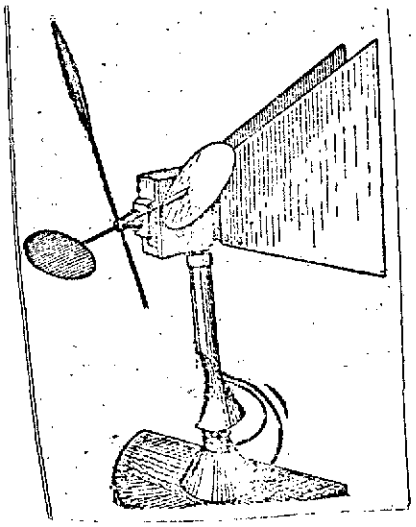

Fig. 89: Electro-anemometer of the system designed by Prof. Sabinin.

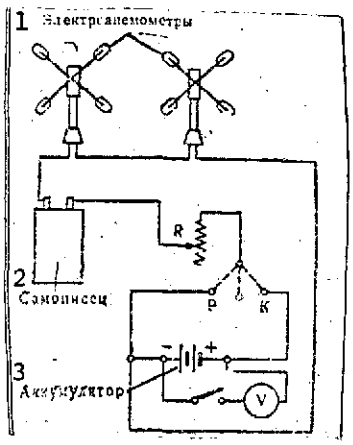

Fig. 90: Diagram of measurement of wind velocity by means of two electro-anemometers.

Key: 1. electro-anemometers
2. recorder
3. storage battery

of a DC generator with independent excitation of 230 V and a 3-phase asynchronal motor of 220 V connected to the electrical circuit. The wind engine B sets in motion dynamo D. The obtained electrical current goes through a switchboard to motor generator M. This machine works as a motor and sets in motion the asynchronal generator Г which supplies the current to the circuit /172 Such a diagram makes it possible to regulate the power and the number of revolutions of the wind wheel within the limits from 0 to any value. The regulation is performed by means of excitation rheostats of the dynamo of wind engine R_1 and motor-generator R_2.

The measuring equipment of the experimental tower is selected so as to obtain a complete aerodynamic performance of the wind engine. During the testing, the following parameters have to be measured: instantaneous and average wind velocities, torque and number of revolutions of the wind engine.

The wind velocities are measured by means of two electro-anemometers of the system of Prof. Sabinin, which are built on the principle of a DC generator (Fig. 89). The recording of the velocities is performed on a recording volt meter. In order to avoid interference with the readings of the anemometers by the wind engine, the anemometers

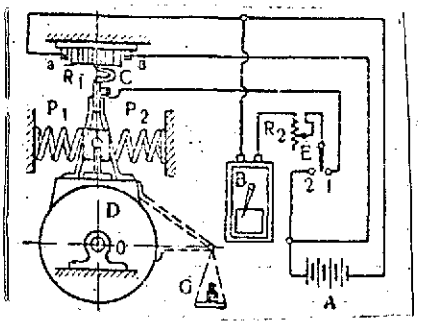

Fig. 91: Schematic of electrodynamometer.

are situated on poles in the plane of the wind wheel at a distance of 20 m from each other, on both sides of the axis of the wind wheel, at equal distance from it.

The system of measurement of the wind velocity by means of two electro-anemometers is shown in Fig. 90. Both instruments are connected in series to the same recorder. The reference reading of the recorder is obtained when the electro-anemometers have their blades removed. Voltmeter V serves for determination of the voltage of the battery. When voltmeter V is disconnected and the switch is positioned on clamp p, both anemometers will give their total electro-motive force to the recorder.

The measurement of wind velocity in two points gives a more reliable result. Since the energy of the wind is proportional to the cube of its velocity, the error in the determination of the power increases to the same degree. For the sake of greater accuracy, the velocity of the wind should be measured not in two but in many points, however, the measurement is extremely complicated. /173

For measuring the torque, an electro-dynamometer is used (Fig. 91). The dynamo-starter and the gear casing are made of one unit and they can revolve in their bearings. A pin is attached to the gear casing which is connected by means of washers to springs P_1 and P_2. In addition, brush C is connected on a support to the dynamometer; the brush glides along the winding of the reostat-rheometer R_1. Under the effect of the magnetic field, the starter turns to reverse, and it compresses either spring P_1 or P_2 depending on the direction where the starter turns. In this moment, brush C moves along rheometer R_1 which receives the current from battery A through clamps a and b. The milliammeter B with recorder is connected by means of a clamp to the clamp of rheostat a, and by means of the other clamp through regulating rheostat R_2 and switch E to brush C. When the switch is positioned on clamp 1, the recorder shows a certain voltage reading. The greater the compression of the spring, the larger the deflection of the brush and the larger the reading on the recorder. The switch is set on clamp 2, in order to check the reference reading of recorder and circuit. /174

In order to soften the strokes and to obtain a more smooth recording, an oil-damper is attached to the starter by means of a by-pass valve. Calibration of the springs P_1 and P_2 is performed by means of a weight suspended to the lever which is attached to the starter. The shorter of the levers is 1.385 m in length, its weight varies from 1 kg to 45 kg.

The number of revolutions of the wind wheel is recorded by means of a tachometric machine, the diagram of which is represented in Fig. 92.

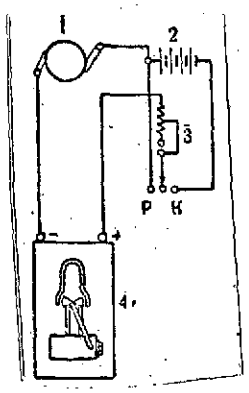

Fig. 92: Diagram of a tachometric machine.

The tachometric machine 1 is connected by means of a belt-drive with the shaft of the wind engine by means of one of the intermediate shafts of the reduction gear. Recorder 4 records the revolutions. Battery 2 and rheostat 3 serve for reference tests.

In such a manner, the recording of the wind velocities, torques and of the number of revolutions during the test, is performed simultaneously on the recorders of the electro-anemometers, electro-dynamometer and tachometric machine.

The processing of the recordings of the three observed magnitudes is performed each minute. The average values of the readings of the instruments are determined by means of a planimeter and written on forms which contain the formulas by means of which the unknown magnitudes $\overline{M}$ and ξ are calculated. This processing yields one point of performance.

Under conditions of large fluctuations in the rotation of the wind engine perminute, a correction is introduced for the increment in kinetic energy of the rotating mass, determined by the formula:

$$\Delta\overline{M} = \frac{I_c}{2t}\cdot\frac{\omega_2^2-\omega_1^2}{\omega}, \qquad (151)$$

where: I_c -- moment of inertia of the wind wheel;
ω_1 and ω_2 -- angular velocities of rotation in the beginning and end of each minute;
ω -- average angular velocity of the wind engine in minutes; /175
t -- time of the experiment in minutes.

The increment in moment $\Delta\overline{M}$ is the average moment of aerodynamic forces per minute spent on the increase in kinetic energy of the rotating wind wheel.

The barometric pressure and the temperature on which the mass density of the air is dependent, are taken into consideration in processing the observations, and in calculations of the performance.

29. Correspondence Between the Performance of the Wind Engine and Its Model.

The testing of the theoretical performance of the wind engine is performed by testing a wind wheel under natural conditions and its model in the wind tunnel. Comparing the theroetical performance of a wind engine with the experimental performance, the degree of discrepancy between these performances is revealed.

In accurate tests, a correctly calculated wind wheel should give experimental performances which are near the theoretical ones.

The discrepancy between these performances may be caused first of all by the fact that the wind wheel operating under natural conditions differs from the model tested in the wind tunnel. There are various devices for regulating the number of revolutions and power on the wings of the real wind engine, as well as fastenings which insure its strength; these details are usually not reproduced on the model.

Such a comparative test was performed at TsAGI. A 3-blade wind wheel was built with a diameter D = 8 m, and a module number $Z_n = 4.5$, with a rigging angle $\phi = 6^\circ$ at the outer tip of the blade.

The profile of the wing was calculated for six sections situated along the propeller line and without any steering devices on the blade.

The construction of the wing is shown in Fig. 93, while Fig. 94 shows the congruency of its sections; this gives the picture of the disposition of the blade sections relative to each other.

The main data of the aerodynamic analysis of a wind engine (according to the theory G. Kh. Sabinin) are presented in Table 9.

TABLE 9

$\frac{r}{r}$	z	α°	φ°	$\varphi+\alpha$	Profile "espero" $\frac{}{b}$	c_y	k	$\frac{m}{b}$
1.0	4.50	2°15′	5°55′	0.60	0.12	0.698	0.0137	0.35
0.85	3.82	1°05′	8°26′	0.68	0.15	0.74	0.014	0.35
0.7	3.15	0°23′	11°05′	0.76	0.17	0.765	0.013	0.35
0.55	2.47	0°33′	14°17′	0.84	0.19	0.834	0.01	0.35
0.4	1.80	0°45′	18°05′	0.92	0.21	0.983	0.01	0.35
0.25	1.12	4°15′	23°05′	1.00	0.22	1.208	0.021	0.35

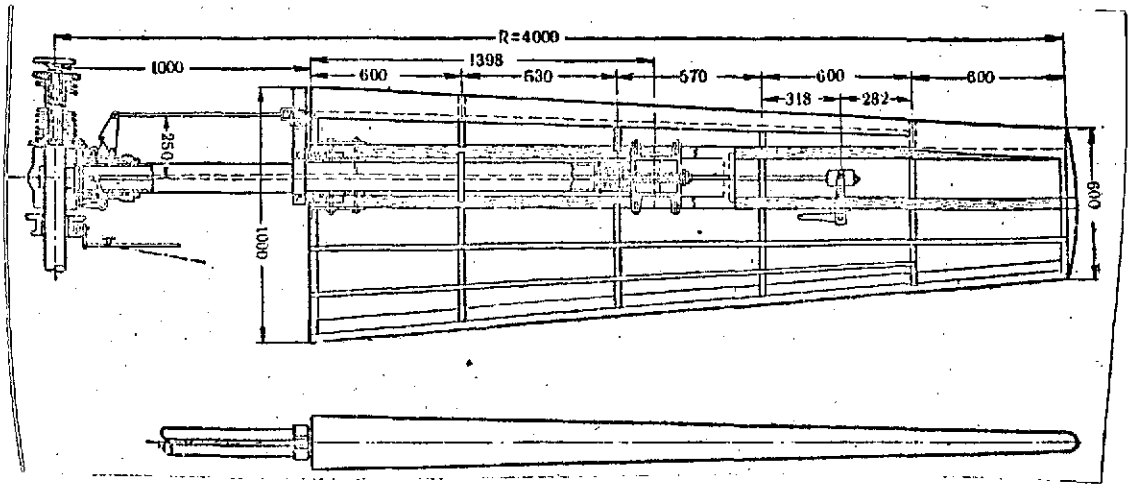

Fig. 93: Construction of the wing of an experimental wind wheel D = 8 m, Z_n = 4.5, i = 3, m/b = 0.35.

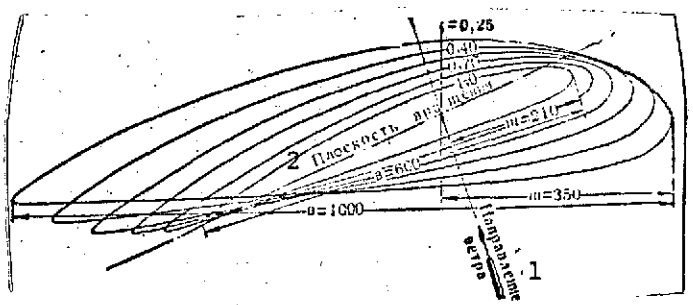

Fig. 94: Congruency of the sections of the wing blade, shown in Fig. 93.

Key: 1. direction of the wind
2. plane of rotation

The aerodynamic performance of this wind engine, obtained by testing under natural conditions, is shown in Fig. 95. /177

In addition, the model of such a wind engine was tested in a wind tunnel. The model showed complete similarity to the wind engine D = 8 m, tested under natural conditions.

The performance obtained by calculation and by testing of the wind engine under natural conditions and of its model in a wind tunnel, are presented in Fig. 96, where I is the theoretical curve (dots); II is the thick continuous curve obtained in the wind tunnel, and III is the same curve obtained during the test of the wind wheel under natural conditions.

Comparison of the curves shows a fairly good agreement /178 between the theoretical and model performances and the full-scale wind engine yields ξ_{max} = 0.497; testing of the model in the wind tunnel gives ξ_{max} = 0.47 while under natural conditions ξ_{max} = 0.40. As we see, the discrepancies are small, which confirms the correctness of the method of aerodynamic analysis according to the given theory.

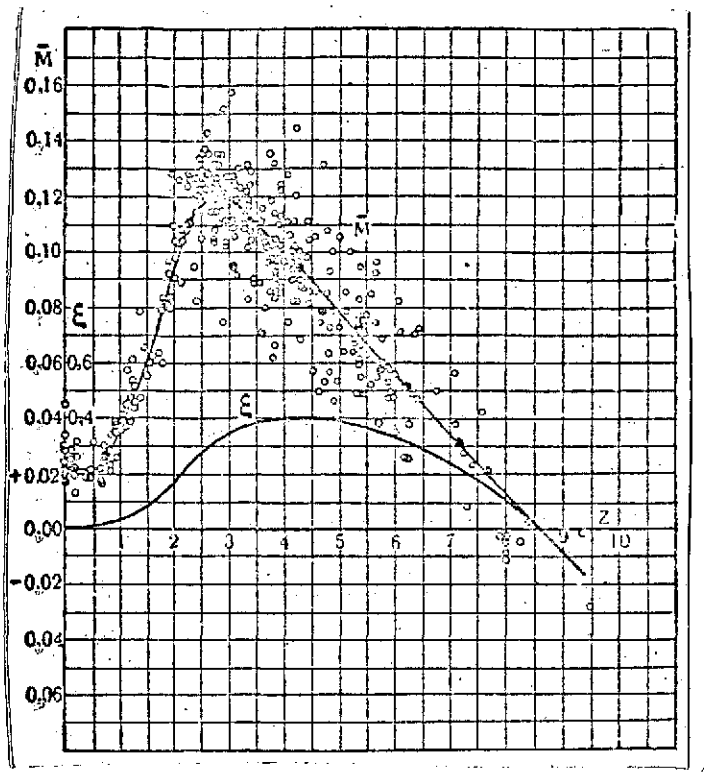

Fig. 95: Experimental performance of the wind wheel (see Fig. 93).

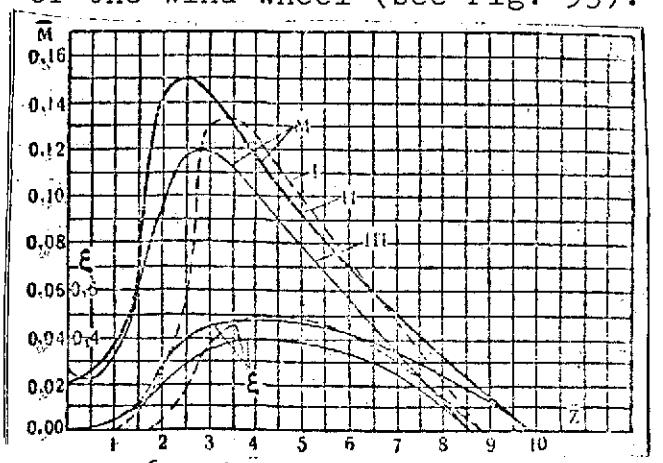

Fig. 96: Characteristics of the wind wheel D = 8 m; Z_n = 4.5; i = 3: I-theoretical curve; II-curve obtained in the wind tunnel; III-curve obtained by testing under natural conditions.

In order to explain the influence of the rigging angle ϕ on the performance, tests were performed at various rigging angles ϕ of the blade of this wind engine, under natural conditions. The obtained characteristics in relation to the rigging angle of the blade ϕ are shown in Fig. 97. /179

The method used in agriculture for testing wind engines differs somewhat from testing wind engines under laboratory conditions. In agriculture, an entire wind power unit is usually tested for a definite type of work. The task of these tests are obtaining the performance of agricultural machines in relation to the revolutions and the search for the most convenient conditions of exploitation of the wind power unit for a given type of work.

As a result of the tests, guidelines have to be elaborated for the exploitation of the given machine with the wind engine.

The following points should be included in the program of the tests:

1. examination of the conditions of agricultural exploitation of the wind installation;

2. compilation of its technical performance;

3. preparation of a wind power unit for tests corresponding to local conditions;

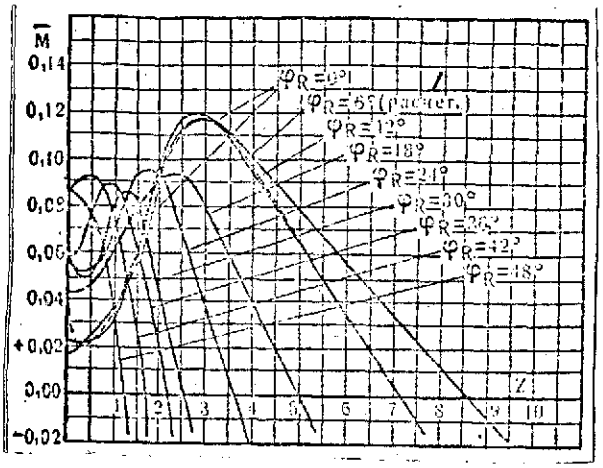

Fig. 97: Performance of a wind wheel D = 8 m, Z_n = 4.5, i = 3, tested at various rigging angles of the blade.

Key: 1-calculated

4. testing of the wind installations with determination of: /180

a. the performance of the wind engine while working with band brake or brake block if the local conditions permit it,

b. wind velocities at which the wind engine starts to operate, is regulated and stops,

c. losses due to friction in the wind engine and in the transmission to the power tool,

d. output of the wind power unit depending on the wind velocity and the revolutions of the wind wheel,

e. performance of the power tool connected to the wind engine.

The results of the test are entered in protocols, summarizing tables are set up and the performance of the wind installation is plotted, on the basis of which conclusions are made on the advisability of using a wind engine for the work with a given machine.

The details of the performance test of wind engines are exposed in the author's book Metodika ispytaniya vetrodvigateley, rabotayushchikh s tsentrobezhnymi nasosami i s sel'skokhozyaystvennymi mashinami [Method for testing wind engines operating with centrifugal pumps and with agricultural machines], 1959.

CHAPTER 8. ADJUSTMENT OF THE WIND ENGINES TO THE WIND /181

The wind constantly changes its direction, mainly in the horizontal plane. The wind engine operates most effectively at a time when the velocity of the wind is directed perpendicularly to the plane of rotation of the wind wheel. Hence it follows, that the wind wheel should be made by appropriate means to follow all the changes in the direction of the airstream.

These movements which follow the direction of the wind are called adjusment of the wind engine to the wind.

In the simple wind engine, the home-made adjustments of the wind wheel to the wind is made by hand, while in the factory-made improved model, the wind wheel is automatically adjusted to the wind.

The manual adjustment to the wind is performed by either by means of an ordinary lever which is fastened to the rotating part of the mill, or by means of a gearing. This question is discussed in more detail in the section on windmills (sections 58 and 61).

The automatic adjustment to the wind is performed by the following four methods: 1-by means of a tail which acts analogically to a wind vane; 2-by means of small wind engines called windroses, which act on the rotating part of the wind engine through gearing; 3-disposition of the wind wheel behind the tower of the wind engine by the principle of adjustment to the wind by means of the tail; 4-adjustment to the wind by means of an electrical motor. All of these methods of adjustment to the wind are applied in practice.

30. Adjustment by Means of the Tail. /182

In low-power wind engines, up to 15 hp, the wind wheel is adjusted to the wind by means of a tail which acts like a wind vane.

When the wind is directed perpendicularly to the wind wheel (direction 1 in Fig. 98), no forces which shifts the tail to any side appear on the surface. As soon as the wind changes its direction (direction 2 in Fig. 98), a lateral force P_{tl} appears on the surface of the tail which turns it and along with it the head of the wind engine around the vertical axis. This rotation continues until the tail becomes parallel, while the plane of rotation of the windmill becomes perpendicular to the direction of the wind.

The following forces act on the system which rotates around its vertical axis (Fig. 99 and 100):

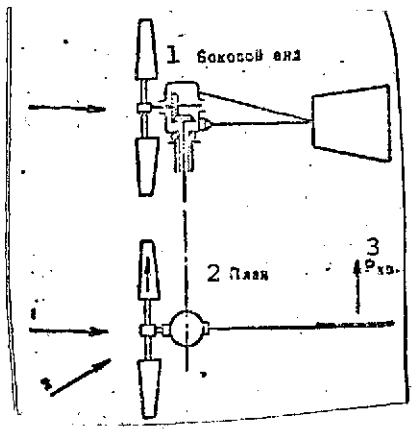

Fig. 98: Diagram of the adjustment of the wind wheel to the wind by means of the tail.

Key: 1. lateral view
2. top view
3. P_{tl}

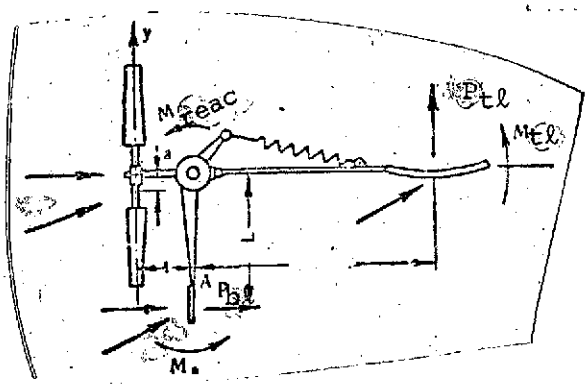

Fig. 99: Diagram of the action of forces on a wind engine with a lateral blade.

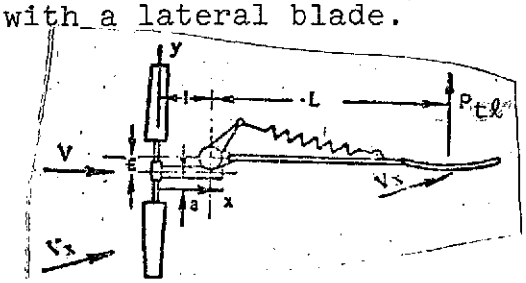

Fig. 100: Diagram of the action of forces on a wind engine, the axis of which is shifted relative to the vertical axis of the tower.

1. a force acting on the surface of the tail during deviations of the wind up to $\varphi = \pm 20°$, which is equal to:

$$P_{tl} = C_a F_a \frac{\rho V^2}{2} \left(\frac{1-e}{1+e}\right)^2, \qquad (152)$$

where: $\left(\frac{1-e}{1+e}\right)^2$

is the coefficient which accounts for losses in velocity of the airstream behind the wind wheel;

2. aerodynamic forces acting on the wind wheel;

$$Y = \bar{y} \pi R^2 \rho \frac{V^2}{2}, \qquad (153)$$

$$X = \bar{x} \pi R^2 \rho \frac{V^2}{2}, \qquad (154)$$

where R is the radius of the wind wheel;

$\bar{y}$ and $\bar{x}$ are coefficients of the aerodynamic forces which are adjusted experimentally during the testing of the whole wind wheel. This coefficient is analogous to the coefficients C_y and C_x which are obtained by testing the blade. /183

In Fig. 101 and 102 the graphs showing the changes in y and x are shown for a multiple-bladed and a sparsely-bladed wind wheel, while Figs. 103 and 104 present the graphs for the determination of the point of application of forces X which are directed parallel to the axis of rotation of the wind wheel. These curves were plotted on the basis of an experimental investigation in a wind tunnel performed by I. V. Smirnov, and may serve as a guide for calculating the aerodynamic forces acting on a wind wheel.

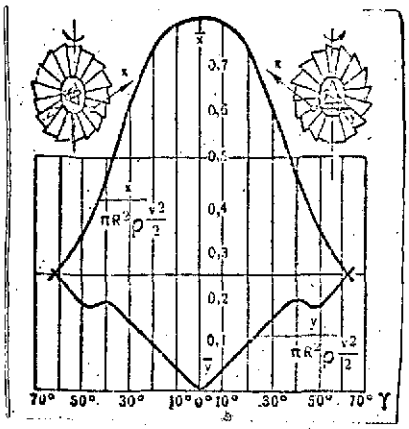

Fig. 101: Curves of the coefficients Y and X of the aerodynamic forces acting on a multiple-bladed wind wheel in relation to the angle of rotation of the wind engine formed with the normal position, M = const, n = 624 rpm Z_n = 1.4.

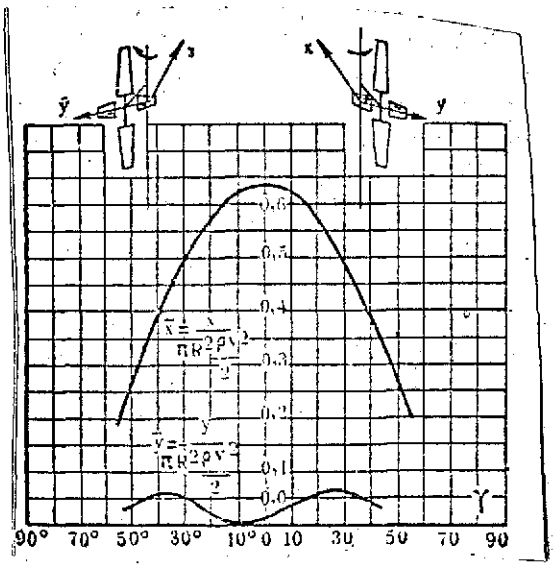

Fig. 102: Curve of the coefficients $\bar{Y}$ and $\bar{X}$ of the aerodymanic forces for model "Syur" 4-blade wind engine without tail, with load, in relation to the angle of rotation of the wind engine formed with the normal position in the wind; n = 1860 rpm, Z_n = 5.

The force on the surface attached from the side behind the wind wheel for purposes of regulation (for regulation see sec. 33, Fig. 119), equals: /186

$$P_{b\ell} = C_R F_{b\ell} \frac{\rho V^2}{2} \qquad (155)$$

In equations (152) and (155), C_R is the coefficient of the drag force which is the resultant of the lifting and drag forces appearing on the surfaces, under the action of the flow which forms with it an angle α.

The magnitude of the coefficient of the resultant force is equal to: $C_R = \sqrt{C_y^2 + C_x^2}$ (156)

The coefficients C_y and C_x for the plates, can be taken from the curve in Fig. 105.

In solving equations (152) and (155), we assume that the direction of the resultant forces of drag P_{tl} and $P_{b\ell}$ is perpendicular to the surface, which is not entirely true. The resultant force of the surface resistance, which is inclined at an angle α° with respect to the flow, forms a certain angle θ° with the perpendicular to the surface (at angles α > 110°, the angle of deflection of the resultant R does not exceed θ = 1°). /187

Further, it should be mentioned that the point of application of this force, changes with the change in the angle of attack. Its position on the surface is determined by means of equation (44a) and Fig. 106, where the curves of the change in the center of pressure are presented for blades with various ratios of length ℓ of the plate to its cord b ($\lambda_\gamma = \ell/b$ = 1; 3; 6; 1/3; 1/6).

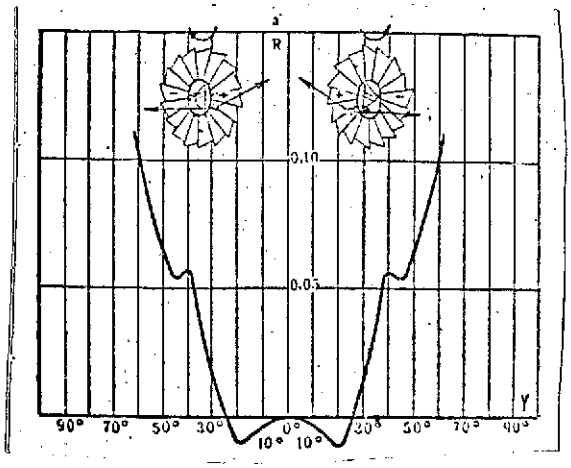

Fig. 103: Curves of the centers of pressure $\bar{a} = a/R$ of a 18-blade wind engine, to Fig. 101.

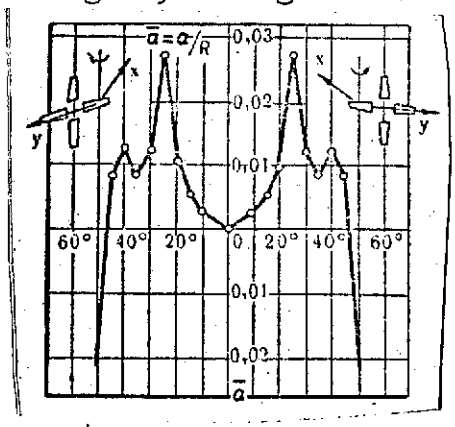

Fig. 104: Curves of the centers of pressure $\bar{a} = a/R$ of a 4-blade "Syur" wind engine without tail with load in relation to the angle γ. The revolutions of the model n = 1860 = const; Z = 5; to Figure 102.

Forces P_{tl}, Y, X and P_{bl}, which are expressed by equations (152), (153), (154), and (155), create moments relative to the vertical axis, which maintain the system in equilibrium:

$$M_{tl} = P_{tl} L. \quad (157)$$

$$\left.\begin{aligned} M_{bl} &= P_{bl} L' \\ M_y &= Yl \\ M_x &= Xa \end{aligned}\right\} \text{(according to Fig. 99)} \quad (158)$$

$$M_x = X(\varepsilon \pm a) \text{ (According to Fig. 100)} \quad (159)$$

where a is the distance from the center of pressure to the axis of rotation of the wind wheel; it is taken with a + sign when the center of pressure is situated to the right of the axis of rotation of the wind wheel and with a - sign when it is situated to the left of the axis of rotation of the wind wheel; ε is the magnitude of displacement of the axis of the wind wheel relative to the axis of the tower (Fig. 100); L and L' are the distance from the axis of rotation of the head to the center of pressure of the surface corresponding to the tail and to the blade. /188

In wind engines with vertical rotating shafts, the moment of the reactive force of the pinion piece on the vertical shaft exerts a great influence on the position of the wind-driven wheel relative to the direction of the wind. This moment is called the reactive moment. It tends to turn the head of the wind engine, relative to the vertical axis (Fig. 107).

The circular force which sets the pinion in motion, causes a reactive force P_p, which acts on the arm r relative to the vertical axis. This force creates a torque of the whole head, which is able to turn around the vertical axis. The magnitude of the reactive moment is determined by means of the equation:

$$M_p = 716{,}2 \frac{N}{n} \text{ kg m}, \quad (160)$$

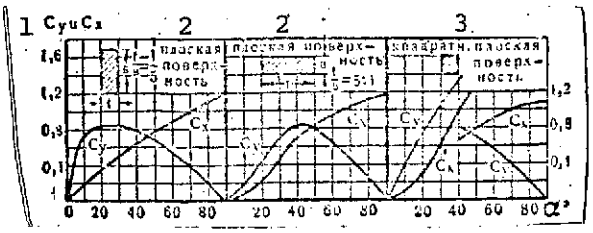

Fig. 105: Changes in the coefficient C_y and C_x of the blades in relation to the angle α.

Key: 1. C_x and C_y
2. flat surface
3. square flat surface

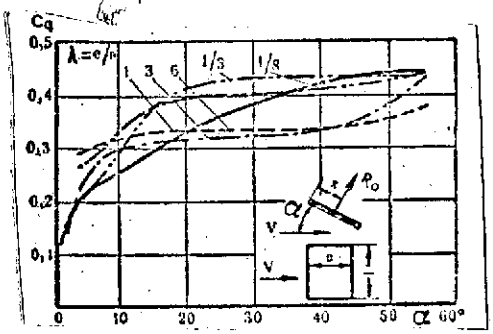

Fig. 106: Curves of the center of pressure of flat plates according to Eiffel.

where N is the power of the wind engine in hp;

n is the number of revolutions per minute of the vertical shaft at a given power.

We can see from equation (160) that the reactive moment is equal to the torque of the shaft of the wind engine.

Our system will be in equilibrium when the sum of the moment of the forces acting on it relative to the vertical axis Z - Z will be equal to zero, i.e.

$$\Sigma M_{zz} = M_{xe} + M_A - M_y + M_x - M_p = 0$$

for the system shown in Fig. 99, and

$$\Sigma M_{zz} = M_{xe} - M_y + M_x = 0$$

for the system shown in Fig. 100.

From these equations, we can obtain the moments of the tail for the system shown in Fig. 99 and 100.

$$M_{xe} = M_y + M_p - M_A - M_x, \quad (161)$$

$$M_{xe} = M_y - M_x. \quad (162)$$

The forces causing these moments are given by equations (152), (153), (154) and (155).

One can follow the effect of the position of the system in the wind flow from the magnitude of the moment caused by the action of the wind on the surface of the tail and the wind-driven wheel, in the experimental data obtained by I. V. Smirnov. %189

Fig. 108 gives the experimental curve of the moments for those cases when the wind-driven wheel does not change its initial position, i.e. the tail is rigidly connected to the head of the wind engine.

Fig. 109 and 110 show the curves made of the relative moments for wind engines regulated by the "Eklips" system with blades and without it (on regulation see section 33).

These curves represent the change in the magnitude of the moment, which rotate the head relative to the vertical axis, in relation to the angle γ formed between the axis of rotation of the wind-driven wheel and the direction of the wind. The relative (nondimensional) moment $\bar{M}_Z$ is called the ratio of the dimensional moment M_Z found

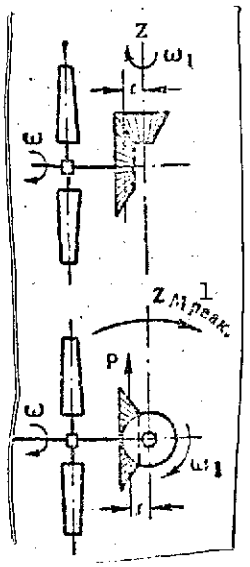

Fig. 107: Diagram of the action of the reactive moment of transmission.

Key: 1. M_{react}

experimentally to the area marked off by the wind-driven wheel πR^2, the radius of the wind-driven wheel R and the dynamic pressure $\rho V^2/2$, i.e. /190

$$\overline{M}_z = \frac{M_z}{\pi R^3 \frac{\rho V^2}{2}}, \tag{163}$$

where M_Z is the dimensional magnitude of the moment in kgm;

R is the radius of the wind-driven wheel in m.

It follows from equation (163) that the dimensional moment is equal to:

$$M_z = \overline{M}_z \pi R^3 \frac{\rho V^2}{2}. \tag{164}$$

The curve of the moment shown in Fig. 108, 109 and 110 were obtained for models with the following ratio of the construction dimensions of the system:

Sweep of the wind-driven wheel -- ℓ/D = 0.125 for the curves in Fig. 108

Likewise -- ℓ/D = 0.167 for the curves in Fig. 109 and 110

Sweep of the surface of the tail from the axis of rotation to the external tip of the surface -- L/D = 1.0 for all the curves.

Eccentricity between the axis of rotation of the wind-driven wheel and the axis of rotation of the head -- ε/D = 0 for the curves in Fig. 108.

Eccentricity between axis of rotation of the wind-driven wheel and the axis of rotation of the head -- ε/D = 0.04 for the curves in Fig. 110.

A ratio of the surface of the tail f to the area marked off by the wind-driven wheel F -- f/F = 0.129 for all the curves.

In Fig. 108 and 110, curve I represents the aerodynamic moment $\overline{M}_Z$ of the wind-driven wheel, curve II represents the total moment $\overline{M}$ of the wind-driven wheel and of the tail, and curve III is the moment of one tail (depending on the angle γ between the direction of the wind and the axis of rotation of the wind-driven wheel). In Fig. 109, we have the curve of the total moment M_Z of the wind-driven wheel, of the tail and of the lateral blade with a square surface (the sides of the square are 0, 177 D).

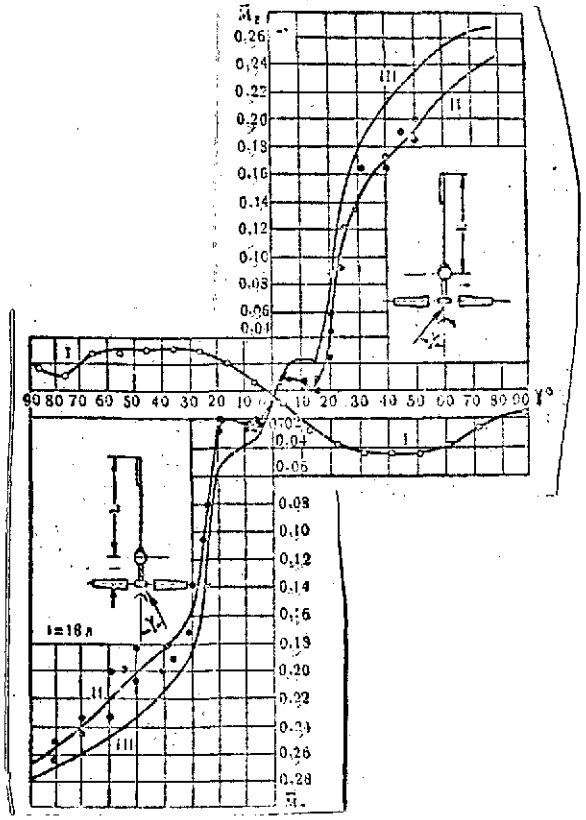

Fig. 108: Curve of the moments of the forces acting on the wind engine system during changes in the direction of the wind.

Comparison of the curves in Fig. 108 with the curves in Fig. 109 and 110, shows that the wind-driven wheel is in the most favorable position with regard to the wind, when the wind engine has no additional devices for envisaging the deflection of the wind-driven wheel for purposes of regulation (Fig. 108). In this case, when the wind is deflected by even a small angle, a moment is created which makes it possible for the system to turn and place the wind-driven wheel into the wind (see curve III). /191

In the presence of a surface or of eccentricity between the vertical axis and the axis of the wind-driven wheel, a moment appears which deflects the wind-driven wheel from the direct action of the wind upon it. In this case, the total curve II of the moments, does not pass through the origin of the coordinates (Fig. 109 and 110). At the angle $\gamma = 0$, there is a negative moment which deflects the wind-driven wheel. Only at an angle $\gamma = 20^{\circ}$ does the total moment become positive (Fig. 110) and the system acquires a stable position. In order to compensate for the negative moment, the surface of the tail is given the shape of a handle with the convexity to the side of the regulating surface or of the eccentricity. Such a tail makes it possible to compensate to a certain extent for the negative moment, and to decrease the angle of deflection of the wind-driven wheel. For this purpose, in practice the tail is made at a certain angle of deflection ϕ (5 to 6°) relative to the axis of the wind-driven wheel on the opposite side with regard to the direction of the regulating surface of the eccentricity (Fig. 111). /192

Let us note that this measurement compensates also for the reactive moment M_p, which takes place in wind engines with rotating vertical shafts. /193

A characteristic feature of the tail adjustment to the wind in the wind-driven wheel, is that the tail reacts rapidly to all the changes in the direction of the wind. In such a manner, it is possible for the wind-driven wheel to be under the direct effect of the

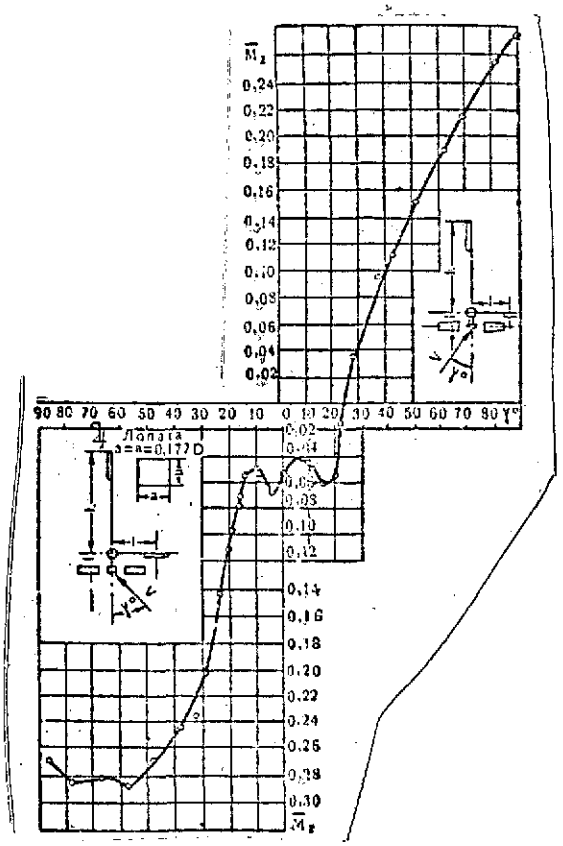

Fig. 109: Curves of the moments of the forces acting on the wind engine system during changes in the direction of the wind. Wind engine with lateral blade.

Key: 1. Blade

airstream for a longer time in the process of operation. This has an extremely great importance, since the wind engine can develop its full power only when the wind flow is directed perpendicularly to the plane of rotation of the wind-driven wheel.

However, the rapid reaction of the tail to all changes of direction of the wind has also a negative aspect. As the head of the wind engine turns on the wings of the wind-driven wheel, gyroscopic forces appear during the rotation of the wheel. These create a bending moment which in the practice of wind power utilization is called gyroscopic moment [34]. This moment bends the flaps of the wings and the axis of the wind-driven wheel (Fig. 112).

In the course of one revolution, the moment which bends the wind flap becomes zero twice, when the flap assumes the horizontal position, and acquires a maximal value twice, when the flap assumes a vertical position (Fig. 113). Its magnitude is equal to: /194

$$\left.\begin{aligned} M_y &= 2I\omega\omega_1 \text{ — relative to axis Y} \\ \text{and} \quad M_z &= I\omega\omega_1 \text{ — relative to axis Z} \end{aligned}\right\} \qquad (165)$$

where: I is the moment of inertia of the wing relative to the axis of rotation of the wind-driven wheel;
ω is the angular velocity of the wind-driven wheel;
ω_1 is the angular velocity of rotation of the whole system relative to the vertical axis.

Gyroscopic moments will be treated in more detail in Section 43.

The magnitude ω_1 depends on the length of the tail. From the point of view of the principle of work of a surface, the maximal work is performed by the surface when it is displaced with a velocity U = 1/3 V. Since the surface of the tail is displaced around a circle with a radius equal to the length of the tail L, which is taken

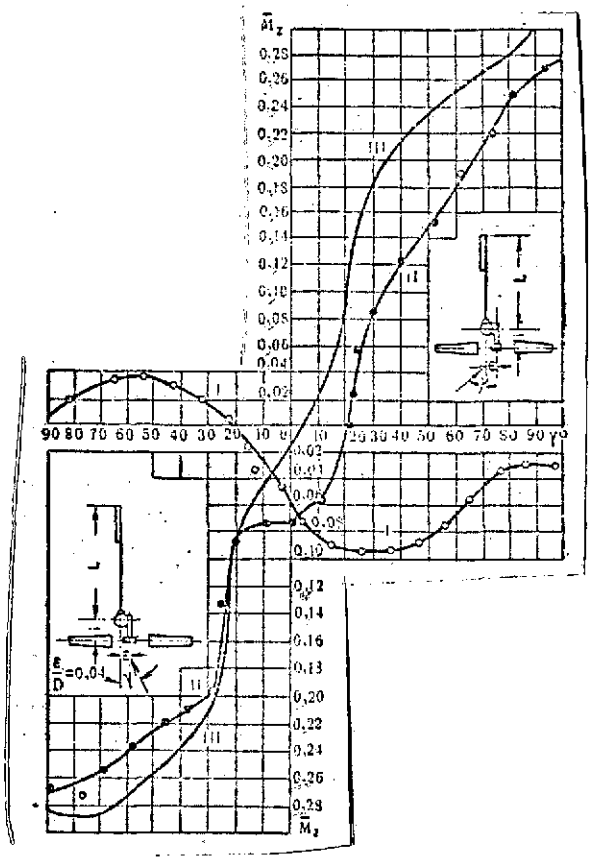

Fig. 110: Curves of the moment of the forces acting on the wind engine system during changes in the direction of the wind. The wind engine is removed from the wind by means of displacement of the axis of the wind-driven wheel relative to the axis of the tower.

from the vertical axis to the center of effort of the sail area, we can write:

$$U=\frac{2\pi nL}{60}=\frac{\pi n}{30}L=\frac{1}{3}\cdot V;$$

here

$$\frac{\pi n}{30}=\omega_1$$

consequently:

$$\omega_1 L=\frac{1}{3}\cdot V$$

hence

$$\omega_1=\frac{1}{3}\cdot\frac{V}{L} \qquad (166)$$

31. Adjustment by Means of Wind Roses. /195

The diagram of adjustment by means of wind rotors is presented in Fig. 114. At a certain sweep in distance behind the wind-driven wheel, two small wind engines are mounted called windroses, the plane of rotation of which is perpendicular to the plane of rotation of the wind-driven wheel and parallel to the direction of the wind. As soon as the wind changes direction (arrows V_x in Fig. 114), the windroses start to turn. The torque of the wind rotors is perceived by the transmission, which consists of conical and cylindrical pinions. The cylindrical pinions of the last pinion couple is engaged in a large geared wheel which is firmly attached to the crown of the tower. During the rotation of the windroses the pinion revolves on the immobile gearwheel and drags with it the whole system of the head, turning it in a horizontal plane. This displacement continues until the windroses stop which takes place when they become parallel to the flow, consequently, at this moment in time, the wind wheel is parallel to the direction of the wind.

While in the case of tail adjustment to the wind, the velocity of rotation of the system around the vertical axis in the case of squalls threatens a rapid wind engine with breakage, the latter is less likely in the case of windroses. This is due to the possibility of selecting any gear ratio between the windroses and the pinions on the tower. Consequently, the angular velocity of deflection of the wind engine

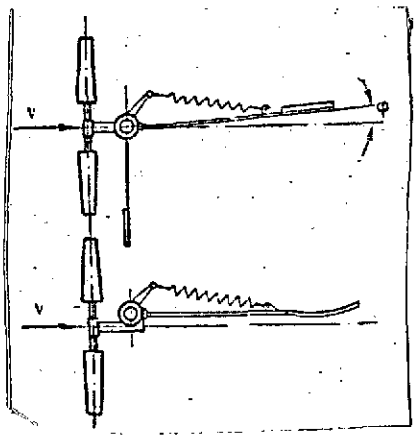

Fig. 111: Deflection of the tail relative to the direction of the wind for purposes of compensation of the moment from the lateral blade and the wind-driven wheel.

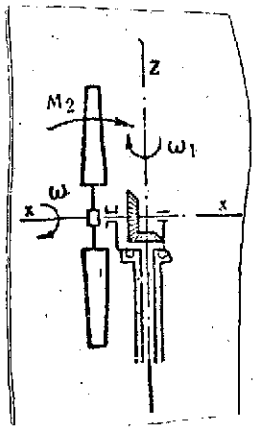

Fig. 112: Diagram of the action of the gyroscopic moment on the wind driven wheel.

ω_1 which is a multiplier in the equation (165), depends on the selection of the transmission and not on accidental breakage by the wind.

The adjustment to the wind by means of windroses is used in certain wind engines, the power of which exceeds 15 hp.

The angular velocity of rotation of the system around the vertical axis is determined by equation: /196

$$\omega_1 = \frac{\omega_0}{i}, \quad (167)$$

where: i is the gear ratio of the transmission from the windroses to the gear pinion, attached to the upper crown of the tower;
ω_0 is the angular velocity of the wind rotors, the magnitude of which is determined by the equation:

$$\omega_0 = \frac{2Z_0 V}{D}, \quad (168)$$

where Z_0 is the synchronal number of modules of the wind rotors; this magnitude is taken from experimental characteristics (Fig. 115); for other conditions, the characteristics of wind rotors are presented in Section 42, Fig. (184);
D is the diameter of the windroses;
V is the velocity of the wind.

The diameter of windroses is taken from 0.15 to 0.2 of the diameter of the wind-driven wheel. The dimensions of the blades of the wind rotors are chosen depending on the diameter of the wind rotors D, i.e.: the width at the external tip $a = D/3$, the width at the internal tip $b = D/6$, length $\ell = D/3$.

The number of blades in windroses is usually 4, 6 or more.

Using the characteristics in Fig. 115 and equations (167) and (168), the transmission can be selected in such a way that the gyroscopic moment will not be dangerous for the solidity of the construction of the wind engine. The value of ω_1 is taken to be approximately equal to 0.05.

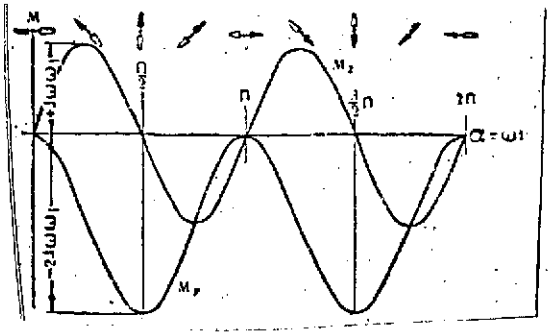

Fig. 113: Characteristics of the gyroscopic moment of a 2-bladed wind driven wheel.

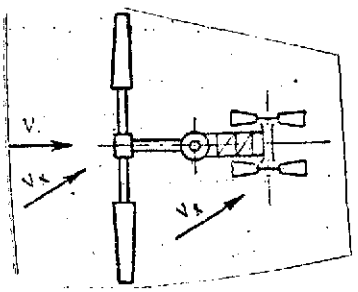

Fig. 114: Diagram of wind wheel adjustment to the wind by means of windroses.

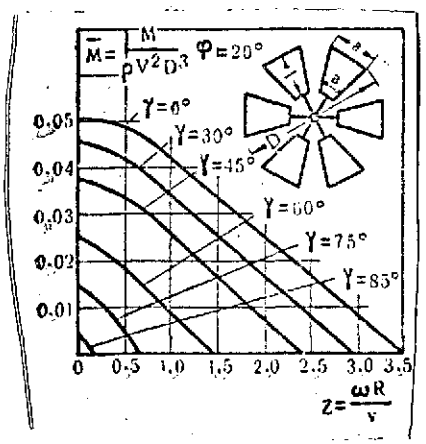

Fig. 115: Characteristics of the torque of windroses for various angles between the direction of the wind and the plane of rotation.

32. Adjustment by Disposition of the Wind-Driven Wheel Behind the Tower. /197

If the wind-driven wheel is disposed behind the tower at a sufficiently large distance, then an aerodynamic moment, the characteristic of which is shown by the curves in Fig. 108 and 110, will act on the system. The action of this moment will cause the wind-driven wheel to adjust itself behind the tower in the direction of the wind, since the wind-driven wheel itself would play the role of a wind vane (Fig. 116).

Since the magnitude of this moment, shown by curve 1 in Fig. 108 and 110, depends on the ratio ℓ/D, for a 18-bladed wind engine it will be obviously possible to use this curve for finding the required aerodynamic moment which will adjust the wind-driven wheel in the direction of the wind.

Let us denote the relative moment known from experiments, by $\bar{M}_z$ and its corresponding ratio ℓ/D by a; the moment which is required in order to maintain the wind-driven wheel in the direction of the wind, will be denoted $\bar{M}'_z$ and correspondingly $\ell'/D' = a'$; then:

$$\frac{\bar{M}'_z}{\bar{M}_z}=\frac{a'}{a},$$

or /198

$$\bar{M}'_z=\bar{M}_z\frac{a'}{a}. \qquad (169)$$

Consequently, the required aerodynamic (dimensional) moment can be approximately determined by equation:

$$M'_z=\bar{M}_z\frac{a'}{a}\pi R^3\rho\frac{V^2}{2}. \qquad (170)$$

If such curves M_z are not available for determining the rapidity of

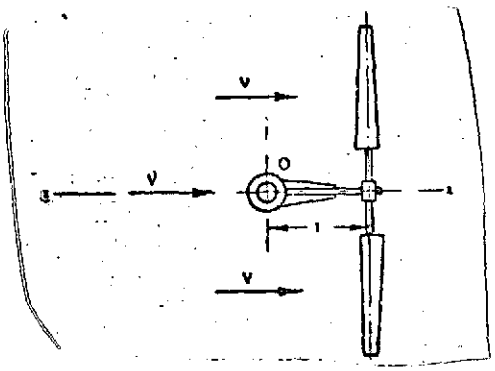

Fig. 116: Adjustment to the wind by disposition of the wind-driven wheel behind the tower.

wind engines, experimental curves of the aerodynamic forces X and Y shown in Fig. 102 can be used. Calculating the force Y by means of equation (153) and multiplying it by the sweep of the wind-driven wheel l', we obtain the aerodynamic moment necessary in order to keep the wind-driven wheel in the direction of the wind:

$$M_{a_{op}} = Y \cdot l = \bar{y}\pi R^2 \rho \frac{V^2}{2} l. \qquad (171)$$

This method of adjustment to the wind which is simple from the point of view of design, has serious shortcomings, i.e.:

1. since the sweep of the wind-driven wheel which in the given case plays the role of a tail surface, is several times smaller than the drift of the tail surface from the vertical axis, on the basis of equation (166), the angular velocity ω_1 of the turn of the head will be several times larger than the angular velocity of the turn of the head by means of the tail; consequently, the gyroscopic moment will be several times larger than in wind engines adjusted by means of the tail;

2. the center of gravity of the rotating system is shifted to one side relative to the vertical axis, which causes an overload of the bearing on the support.

In wind engines with a power of 100 hp and more, which are used in wind power electrical stations, the adjustment to the wind is usually performed by means of an electrical motor. As soon as the direction of the wind performs a certain angle relative to the axis of rotation of a wind-driven wheel, a contact device connects the electrical motor which sets in motion the transmission, rotating the system around the vertical axis. At the time when the wind-driven wheel becomes perpendicular to the direction of the wind, the contact switches the electrical motor off automatically. The transmission from the electrical motor to the pinion attached to the tower is performed in the same manner as in the adjustment by means of windroses.

CHAPTER 9. REGULATION OF THE NUMBER OF REVOLUTIONS AND OF THE POWER/199 OF WIND ENGINES

The lack of consistency of the wind energy, complicates to an extreme degree the technique of utilization of this energy. If the velocity of the wind changes 2 to 3 times per minute, the energy changes 8-27 times during the same period. Cases are known, from anemograph tracings, when the velocity of the wind changed more than 4 times in the course of one minute, which means that the wind energy changed more than 64 times. However, certain power tools attached to the wind engine require a certain power and number of revolutions which have to stay constant throughout the time of operation of these tools. In order to fulfill this requirement, the wind engine has to be regulated, i.e. it has to have a constant number of revolutions at a given power, which is independent of the velocity of the wind.

The transformation of wind energy into mechanical energy should naturally tend to complete utilization of the wind energy passing through the wind-driven wheel. If it were possible to perceive the whole power of the wind by the wind engine at all possible velocities up to storm, the highest annual production would be obtained. However, in this case it would be necessary to build such a strong wind engine, which would be able to bear the load at maximum wind velocity occurring in a given region. The weight of such a wind engine would be enormous, while the service life with maximal load would be extremely short, as follows from the data on [illegible] occurrence [illegible] (see Chapter 12, section 46). Moreover, the energy is needed by the consumer daily and in approximately the same amount. Consequently, the maximal/200 energy which the wind installation can supply in a short period of time may appear quite useless. Finally, the working tools selected for the wind engine at its maximal power, have a very low output coefficient at low velocities of the wind. Therefore, for the beginning of regulation and for insuring the strength of power tool parts, the calculated velocity of the wind is chosen according to the annual averages of wind velocities. In practice, the calculated wind velocity for determining the power of wind engines, is taken V_y = 8 m/sec for regions with annual average velocities up to 5 m/sec, V_y = 10 m/sec for regions with annual average wind velocities up to 7 m/ sec and finally V_y = 14 m/sec, for regions with annual average wind velocities about 7 m/sec.

The power of the wind engine, determined for wind velocities V_y is called the adjusted power N_y. It is optimal for regions with a given average wind velocity.

The regulation of wind engines consists in changing the position of the wind-driven wheel or of its blades in the wind flow, in order to obtain approximately constant power and revolutions.

The available methods of regulation of wind engines used in practice can be divided into two main groups according to the nature of action of the regulating mechanism.

The first group comprises those systems of regulation in which the main regulating mechanism is a centrifugal regulator of a certain kind. In this case certain systems of regulation can have bilateral action of the external forces on the change in the position of the blade or of the wind-driven wheel in the air flow: on one side -- centrifugal forces of regulating flyweights, on the other side -- the force of the wind.

In wind engines with such regulation, the number of revolutions of the wind-driven wheel increases in the process of operation with the increase in the force of the wind, as a result of which there is an increase in the centrifugal forces of the regulating flyweights, which change the position of the blades. Consequently, the lifting force is diminished and the revolutions decrease down to their normal value.

The action of the wind force on the blade in relation to the /201
construction of the regulation system, can be either added up to the centrifugal forces of the regulating flyweights or, subtracted, since the point of application of the resultant wind force (center of pressure) on the blade, may be either to the right or to the left of the axis of rotation of the blade.

The second group comprises the systems of regulation in which the change in the position of the blade or of the entire wind-driven wheel is performed under the action of the wind force.

The correct determination of all the forces acting in a given system of regulation is the task of the designer. The quality of the regulation depends on how this task is fulfilled.

33. Regulation by Removing the Wind-Driven Wheel From the Wind.

This method of regulation is the simplest and is based on the fact that the smallest quantity of air flows through the wind-driven wheel when the direction of the wind is oblique to the direction of the wheel. In addition, the lifting force changes due to the change of the angle of attack on the wings during rotation. Both these factors make it possible to limit the power of the wind engine at wind velocities exceeding 8 m/sec.

In the simplest type of wind engines such as the goat-skin and the tent-shaped wind-mill, removal of the wind-driven wheel is performed manually; in the improved, modern wind engine, it is done automatically by means of regulating devices.

The automatic regulation by removing the wind-driven wheel from the wind, is used in multi-bladed low power wind engines. In this system regulation is performed by two methods: first,

by means of a lateral surface -- a so called blade which is fixed to the head of the wind engine behind the wind driven wheel to the right or left side of its axis of rotation; second, by the displacement of the axis of rotation of the wind-driven wheel to a certain distance (50 to 100 m) to the right or left of the vertical axis of rotation of the head of the wind engine.

The diagram of regulation of the wind pressure on the lateral blade is shown in Fig. 117.

In the second case, the deflection of the wind-driven wheel takes place due to the moment of frontal pressure of the wind on the wheel relative to the vertical axis; the arm of the moment is equal to ε (Fig. 118) at $\gamma = 0$.

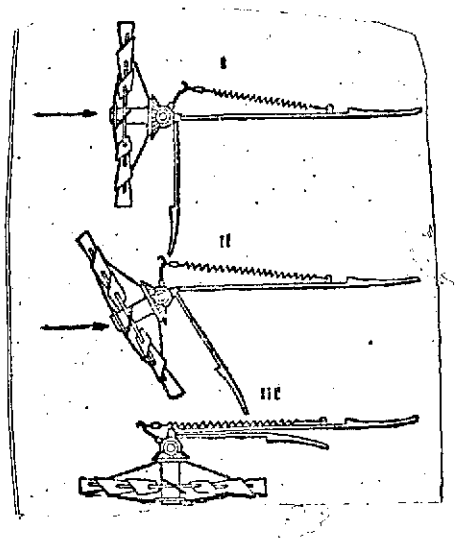

Fig. 117: Diagram of regulation by removal of the wind-driven wheel from the wind by means of a lateral blade.

In Fig. 117 and 118, the wind engine is in the operating position, in position I, at a wind velocity below 8 m/sec; in position II -- during regulation at wind velocity exceeding 8 m/sec, and in position III, at a wind velocity exceeding 12 m/sec, at which it stops. /202

In the examined system of regulation, the force of the wind acting on one side of the vertical axis, is balanced by means of a spring which is attached at one end to the tail of the wind engine, and at the other to the lever attached to its head.

Due to its simplicity, regulation by removal of the wind-driven wheel from the wind has found wide application in multi-bladed low power wind engines, which are mainly used for lifting water in agriculture.

Let us examine the action of the forces in the given system of regulation.

Moments created relative to the vertical axis of the system act on a wind wheel which is disposed perpendicularly to the direction of the wind.

In wind engines with vertical rotating shafts and with lateral blades, this moment is equal to:

$$M_{b\ell} = P_{b\ell}L - M_{reac} \qquad (a)$$

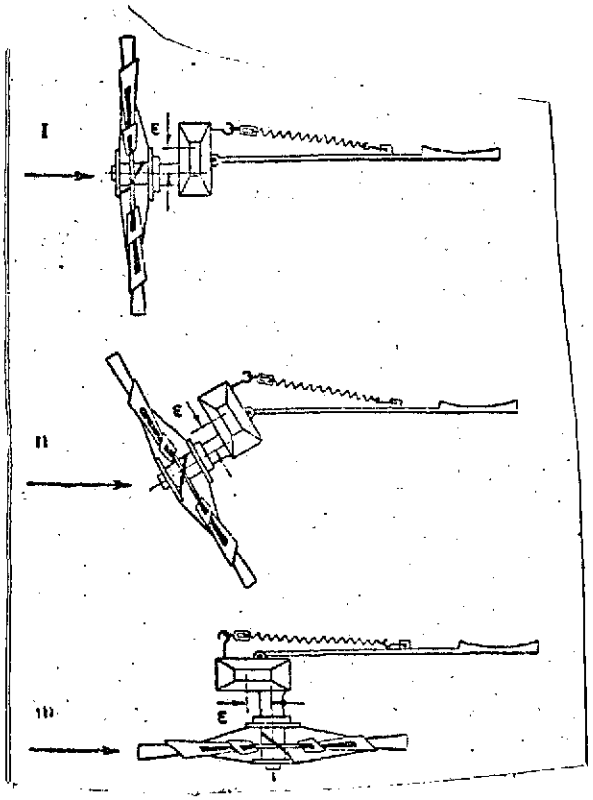

Fig. 118: Diagram of regulation by means of removal of the wind-driven wheel from from the wind by shifting the wind-driven wheel axis relative to the axis of the tower.

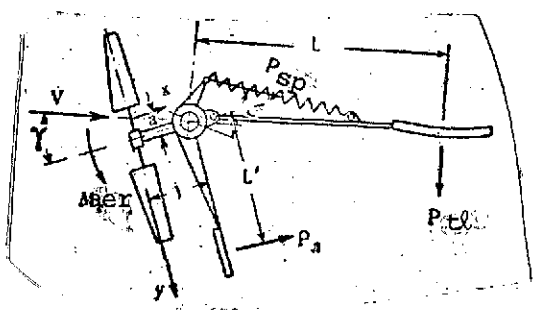

Fig. 119: Diagram of the regulation of the wind force in a wind engine system regulated by means of a lateral blade.

If the deflection of the wind-driven wheel is performed on ac- /203
count of eccentricity ε, then according to equation (158), the moment is equal to:

If the $M_a = X\varepsilon.$ (b)

If the wind-driven wheel forms a certain angle γ with the direction of the wind, then the following forces act on the system (Fig. 119 and 120): force X, perpendicular to the plane, and force Y which acts in the plane of the wind-driven wheel. These forces as well as the force on the lateral blade create during /204
the regulation a moment relative to the axis of rotation of the head, the magnitude of which is equal to:

$$M_{aer} = Yl + PL' \pm Xa - M_{reac}; \quad (c)$$

$$M_{aer} = Yl + X(\varepsilon \pm a). \quad (d)$$

The internal force of the spring P_{sp} with the arm relative to the axis of the system r_x balances this moment. Consideration is given to the fact that all these forces cannot remove the tail from the position parallel to the wind, i.e.:

$$P_{sp}L = Yl + PL' \pm Xa - M_{reac}; \quad (e)$$

$$P_{sp}L = Yl + X(\varepsilon \pm a). \quad (f)$$

In the presented equations, /205
a plus sign should be put before a when the center of effort of the sail area passes on the side of the blade or of the eccentricity, and a minus sign -- when it passes through the opposite side of the blade.

In the process of regulation, under the action of the examined forces, the system turns somewhat relative to the axis of the tower. As a result of this, the tail

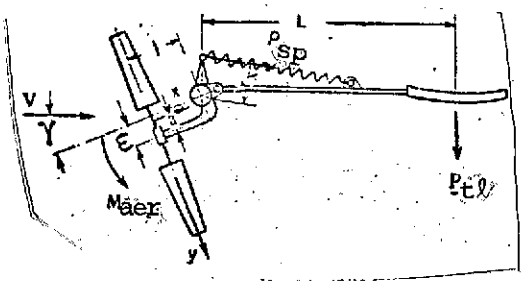

Fig. 120: Diagram of the action of forces on the wind engine system regulated by removing the wind-driven wheel from the wind by shifting the fitting of the axis of the wind-driven wheel relative to the axis of the tower.

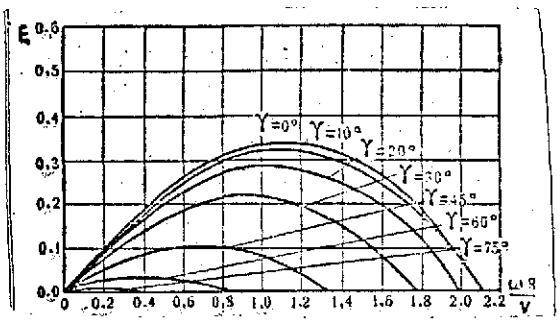

Fig. 121: Characteristic of a 18-bladed wind-driven wheel in relation to the deflection angle γ of the axis of rotation from the direction of the wind.

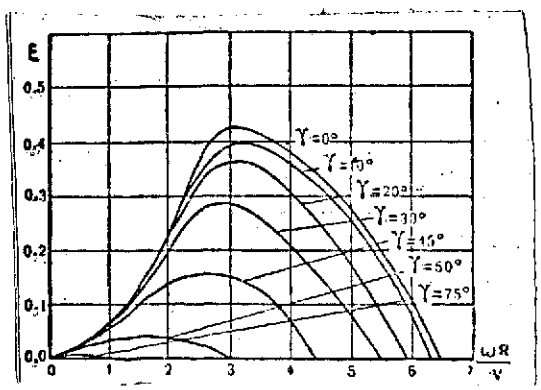

Fig. 122: Characteristic of a 4-blade wind engine in relation to deflection angle γ of the axis of the wind engine formed with the direction of the wind.

forms an angle which is larger than prior regulation. Due to this fact, an equilibrium is formed between all the forces which fix the system in a certain position in the air-flow stream at each velocity of the wind.

The spring should be calculated in such a manner, that the moment formed by its internal force, acting with arm r_x, should be equal to the moment created by the aerodynamic forces acting on the wind-driven wheel and on the blade, i.e.:

$$M_{sp} = M_{aer}$$

In equations c, d, e, and f, the distance a from the center of effort of the sail area to the axis of the wind-driven wheel is determined by the relation $\frac{a}{R} = \bar{a}$, $a = \bar{a}R$,

where $\bar{a}$ is taken for multi-bladed wind-driven wheels from Fig. 103, while for wind-driven wheels with only a few blades -- from Fig. 104; the values a/R which lie above the abscissa have a minus sign, while those lying below the abscissa have a plus sign. This is explained by the fact, that the arm of force X decreases during the passage of the center of effort of the sail area to the left of the axis of rotation of the wind-driven wheel, and increases by the magnitude a during the passage of the center of effort of the sail area to the right. This refers to the case when the axis of the wind-driven wheel is shifted to the right relative to the axis of the tower. For example, for multi-bladed wind-driven wheels, when $\gamma < 27^\circ$, the ratio a/R should be positive while at large angles γ, the curve passes above the abscissa and consequently, in this case a/R should be negative. This means that at large angles γ, the center of effort of the sail area is shifted to the

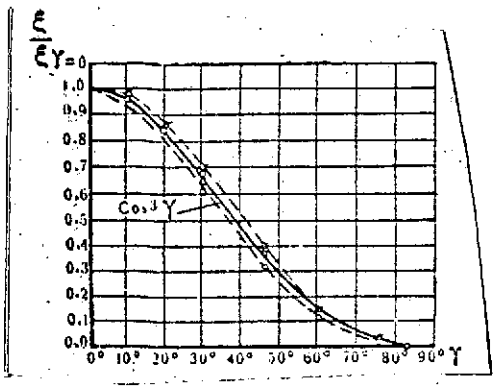

Fig. 123: Characteristic $\xi/\xi_{\gamma=0}$ in relation to the angles of the wind-driven wheel.

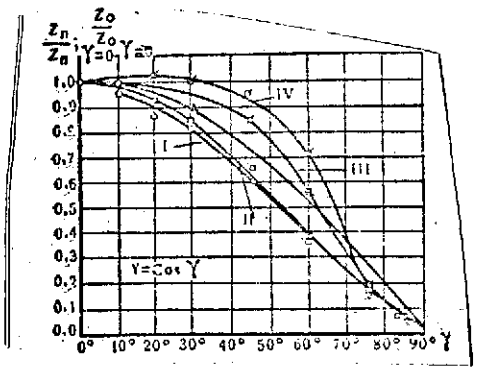

Fig. 124: Characteristic of normal and synchronal velocity of rotation of wind-driven wheels.

other side of the axis of rotation of the wind-driven wheel, i.e. to the left of its axis. Forces X and Y are taken from the right side of the graphs in Fig. 101 and 102.

Forces X, Y, and $P_{b\ell}$ change proportionally to the square of the wind velocity and of the coefficients $\bar{x}$, $\bar{y}$, C_y and C_x determined from the graphs in Fig. 101, 102, and 105.

Characteristics of the wind-/206 driven wheel at various deflection angles γ formed between the axis of rotation and the direction of the wind, the velocity of which does not change [33]. In Fig. 121 the curves of the change in the output coefficient of the wind energy ξ in relation to Z are presented for various angles of a slow 18-bladed wind engine, while Fig. 122 presents the curves of a rapid 4-bladed wind engine. The curves show that the output coefficient of the wind energy ξ decreases to an insignificant extent at angles γ varying from 0 /207 to 20°, while it decreases sharply at angles exceeding 20°. The change in ξ, in relation to the deflection angle γ of the wind-driven wheel from the direction of the wind is shown in Fig. 123, where the curves are plotted for the ratios ξ to $\xi_{\gamma=0}$ for 4 models of wind-driven wheels: 18-bladed, 4-winged mill, 4 bladed and 2 bladed.

For practical purposes it is entirely possible to consider that the power of a wind engine during its removal from the wind changes proportionally to the cube of the cosine of the angle of deflection of the wind wheel from the direction of the wind, i.e. $\xi = \xi_{\gamma=0} \cos^3 \gamma$, which is seen from the curve $\cos^3 \gamma$ in Fig. 123.

Let us denote $\xi_{\gamma=0} = \xi_n$; $N_{\gamma=0} = N_n$ etc.: then $N = f(\gamma)$ will be equal to:

$$N = N_n \cos^3 \gamma \tag{172}$$

The change in the velocity of rotation of the wind-driven wheel is shown in the graph of Fig. 124. Curve I refers to an 18-bladed engine; II -- to a 4-bladed mill; III -- to a 4-bladed wheel and IV -- to a 2-bladed wheel. The curve cos γ almost coincides with the curve describing the relationship between the synchronal velocity of these wind engines and the angle γ, i.e. it can be considered/208 that :

$$\frac{Z_0}{Z_{0n}} = \cos\gamma,$$

or

$$Z_0 = Z_{0n} \cos\gamma.$$

At a constant velocity of the wind, Z changes proportionally to the angular velocity of the wind-driven wheel, i.e.:

$$\omega = \omega_n \cos\gamma,$$

hence:

$$n = n_n \cos\gamma.$$

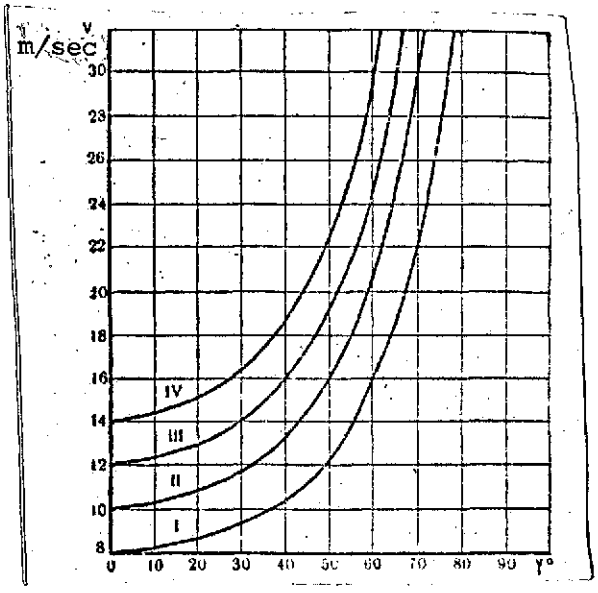

Fig. 125: Curves of the changes in the angles in relation to the wind's velocity at which N = const and ω = const.

Consequently, the synchronal revolutions of a wind-driven wheel change proportionally to cos γ at V = const.

In practical calculations of the regulation of removal of a wind-driven wheel from the wind, it is important to know the angle γ at which the wind-driven wheel is supposed to deflect during the increase in wind velocity, in order to preserve the revolutions and the power developed at the particular wind velocity where these were taken as constant in the calculation of regulation i.e. it is important to know the relation connecting the angles with the wind velocity at which the revolutions and the power will be constant. From equations (135) and (172) it follows:

hence:

$$N = N_n \frac{V^3}{V_n^3},$$

$$N = N_n \cos^3\gamma,$$

$$\cos\gamma = \frac{V_n}{V}. \tag{173}$$

Assuming that V_n is the velocity of the wind at which the wind engine should be removed from the wind, and the working velocities of the wind $V >> V_n$, let us find the cosine of the angles, and subsequently the angle corresponding to these velocities. After calculating a series of points and plotting them on the graph (Fig. 125), we obtain the curve of the angle at which the wind-driven wheel showed a deflection at the wind velocities $V > V_n$, in order to preserve N and ω constant. Curve I was calculated for V_n = 8 m/sec; II -- for V_n = 10 m/sec; III -- 12 m/sec and IV -- 14 m/sec. These curves refer to any wind-driven wheel. /209

It is simpler to determine the angles γ graphically (Fig. 126). On the straight line OB let us lay out in the scale of wind velocity V_n, V_1, V_2 etc.; further, let us draw the arc CD with a radius V_n; from the ends of the pinions V_1, V_2, V_3, etc. let us draw the tangents. Each radius drawn from O perpendicular to the corresponding tangent will be deflected from the straight line OB by an angle γ which is necessary in order to have constant revolutions and power of the wind-driven wheel at various velocities of the wind $V > V_n$. /210

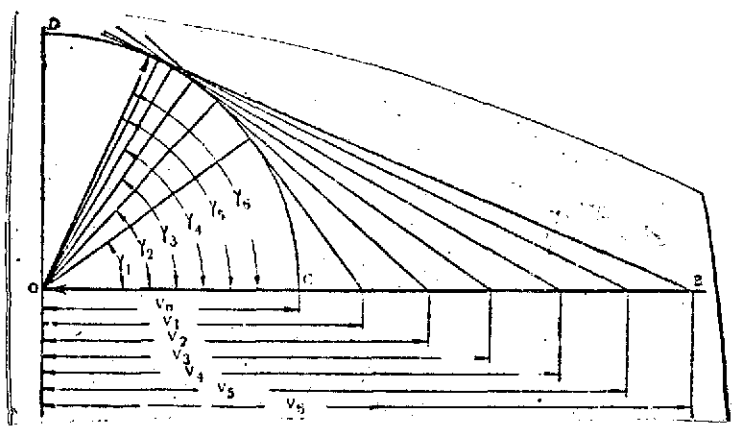

Fig. 126: Graphic determination of the angle γ.

From Fig. 126 we have:

$$V_n = V_1 \cos\gamma_1 = V_2 \cos\gamma_2 \text{ etc.},$$

hence, it follows:

$$\cos\gamma = \frac{V_n}{V},$$

which was also obtained above -- equation (173).

In final account, calculation of regulation by removing the wind-driven wheel from the wind amounts to finding the relation between the change in the moment of the spring, which insures its present position of the wind-driven wheel with regard to the direction of the wind at an angle γ corresponding to a given power N = const and ω = const. For this purpose, let us first plot the curve of the aerodynamic moment in relation to γ for various wind velocities (Fig. 127) according to equation:

$$M_{aer} = Yl + Pl' \pm Xa - M_{react} \qquad (a)$$

for a wind engine, which is deflected on account of its lateral blade, and

$$M_{aer} = Yl + X(\varepsilon \pm a) \qquad (b)$$

for a wind engine which is deflected on account of eccentricity ξ.

Subsequently, using this graph and curves $V = f(\gamma)$ (Fig. 125), /211 let us plot in Fig. 127 the points corresponding to the given wind velocity and the angle γ which should be found on the curves of aerodynamic moment at the given wind velocity opposite the corresponding angles γ (Fig. 125). Uniting the points thus found by a line, we obtain curve A which shows how the moment of the spring should change in various positions of the wind-driven wheel relative to the direction of the wind. The vertical hatching below, shows the magnitude of the reactive moment M_{react} = const.

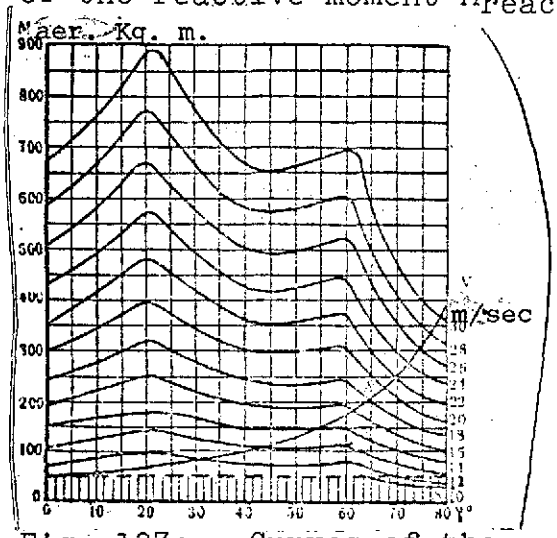

Fig. 127: Curves of the aerodynamic moment of the TV-8 wind engine.

Fig. 127 shows a graph plotted for a TV-8 wind engine; it can be used in calculating the regulation of the wind engine of the same type and power. For another type of wind engine, a different graph has to be plotted by the presented method.

For a problem-free action of the system of regulation by removal of the wind wheel from the wind, the friction in the supports should be as small as possible. The friction in /212 the supports influences the regulation in the sense that the wind-driven wheel is late in coming out from the wind during its increase in velocity and is returning to the wind during the decrease in wind velocity. The larger the friction in the supports, the coarser the regulation. The regulation by removal of the wind-driven wheel from the wind in rapid wind engines is inconvenient because it increases the effect of the gyroscopic moment. As a matter of fact, during regulation by this system, the head with the wind-driven wheel is in constant movement around the vertical axis, on one hand on account of the work of the tail, and on the other hand, on account of the deflection of the wind-driven wheel according to the conditions of the given regulation. As they have the same direction, these two movements will give a large angular velocity ω_1 as a result. Since in equation (165) of the gyroscopic moment, the angular velocity of the wind-driven wheel is a term which in rapid wind engines is also large, the resultant gyroscopic moment may threaten the durability of the wind engine. This is why, in practice, regulation is mainly used for low-speed multi-bladed wind engines. Exceptionally, rapid wind engines with this type of regulation are found, in view of the simplicity of the design of this system.

34. Regulation by Decreasing the Area of the Wings.

This method of regulation is used in the old tent-shaped windmills. Under conditions of low wind, the wings work with their whole surface; if the wind increases to the extent that the number of revolutions of the wind-driven wheel starts to increase rapidly, the area of the blades is decreased. In the simplest homemade wings this decrease is done manually by removing from the wings a certain part of the boards which compose its surface. In sail wings, the sail which covers the net of the wing is rolled up manually. Such a method of regulation is understandably, extremely imperfect, and at the same time, it is attended with great difficulty.

When the velocity of the wind changes rapidly, it is difficult to perform in time the necessary operation, and the wind engine may break before the area of the wing can be diminished.

In more recent designs of windmills which are regulated by the /213
examined principle, the surface of the wing is manufactured of either longitudinal or transversal folds which have the aspect of venetian blinds. When the wind-driven wheel develops a higher number of revolutions than is necessary for normal operation, the folds or blinds open up and openings appear in the working surface of the wings as a result of which the effect of the wind force on the wings decreases and the number of revolutions of the wheel becomes smaller. The folds/214
as well as the blinds are opened manually by means of a linkage mechanism, while in improved models -- automatically by means of centrifugal flyweights which are placed on the wings, or by means of a special centrifugal regulator.

Fig. 128 shows a wind engine with automatic regulation: a -- wind engine prior to regulation; b -- with open blinds during a hold. The adjustment to the wind is accomplished by means of windroses.

The main drawback of this regulation consists in the fact that a wing with blinds can be given no streamlined profile; this causes large drag and leads to a low output coefficient of the wind energy. Moreover, the numerous hinges on which the blinds rotate complicate the manufacture of the wings. This regulation is not used in modern wind engines.

35. Regulation by Rotation of the Blades or Part of it Around the Axis of the Flap.

Any change in the slope of the blade relative to the wind, causes a change in the lifting force and consequently, in its component which acts in the direction of rotation of the wind-driven

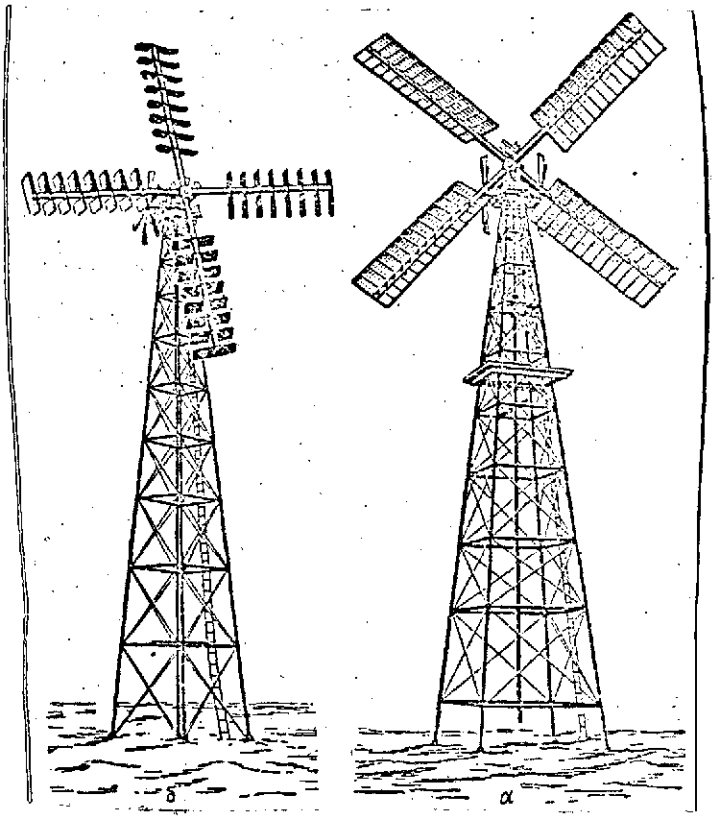

Fig. 128: Wind engine which is regulated by decreasing the area of the wings.

wheel. This pattern lies at the basis of regulation by rotation of the blade or of part of it around the axis of the flap.

The rotation of the blade around the axis of the flap is performed by two methods. First, by the direct action of the wind on the wing which, being freely sitted on the axis of the flap which passes near the start of the wing, is deflected by the pressure of the wind and, as it is maintained in balance by means of the flyweight, it allows regulation of the revolutions to be made. Second, the rotation of the blade is performed by means of centrifugal forces developed either by a normal centrifugal regulator or by flyweights situated on the wings of the wind-driven wheel. As the revolutions of the wheel increase, the flyweights are displaced along the axis of the flap under the action of centrifugal forces and set in motion the rods which are connected by means of a linkage mechanism with the blades; the latter are turned to decrease the angle of attack. Consequently, the lifting force on the wing decreases and the torque and revolutions of the wind-driven wheel are diminished. During the regulation, balance is maintained/215 between the regulator spring and the centrifugal force of the flyweights.

Prof. G. Kh. Sabinin suggested a system of regulation in which the turning of the blade is performed by the action of the wind force on the stub-wing attached to the axis at the rear edge of the wing. This stub-wing is called stabilizer, and the regulation is called stabilizing (Fig. 129). N. V. Krasovskiy completed this regulation by means of a rod passing through the center of the flap tube.

The process of regulation takes place in the following manner. In the resting state, blade one and stabilizer two are on a line

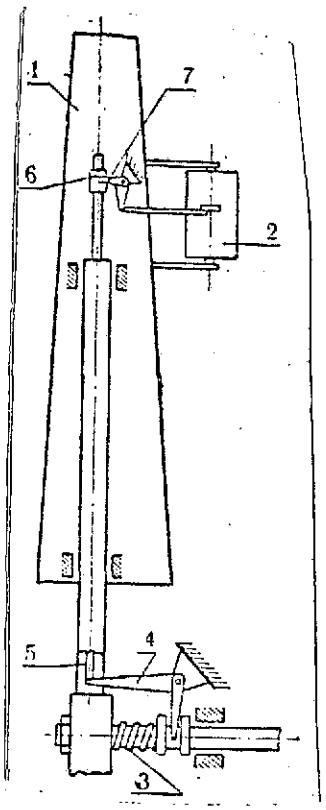

Fig. 129: Diagram of regulation by turning the blades around the flap axis by means of a stabilizer:
1. blade
2. stabilizer
3. spring
4. arm
5. rod

comforming to the direction of the wind (position I, Fig. 130). As the wind engine is turned on, spring 3 which was tight until then is now released, and acting through arm 4 and rod 5, it shifts the stabilizer 2 by a certain angle relative to the chord of the wing (position II, Fig. 130) and at the same time places it at a certain angle to the direction of the wind. As a result of this a lifting force appears on the surface of the stabilizer which turns the wings relative to the axis of the flap with the following moment:

$$M_{cm} = C_r f \frac{\rho V^2}{2} r, \qquad (174)$$

where: f -- surface of the stabilizer in m;
r -- distance from the center of ef- /216
fort of the sail area of the stabilizer to the axis of the flap;
C_r -- coefficient of the lifting force.

Under the action of this moment, the blade will turn around the axis of the flap as long as there is an equilibrium between the moment of the aerodynamic forces acting on the surface of the stabilizer and the blade of the wing; the cord of the blade will form with the direction of the relative flow, a certain angle α. At the same time, lifting forces are developed on the blade which leads to the rotation of the wind-driven wheel (position III, Fig. 130). In this case, the airstream will dash over the wing and the stabilizer with a relative velocity W, which is equal to:

$$W = \sqrt{V^2 + \omega^2 r^2}.$$

As a result of the increase in angle β of the relative flow, the moment of the stabilizer increases and the blade turns as long as a balance sets in again between the aerodynamic forces on the wing and the stabilizer, and as long as angle α is not equal to the initial angle. In such a manner, the blade maintains a constant angle of attack with the direction of the flow, at a constant angle of rotation of the stabilizer β, under all conditions of operation of the wind engines ($Z = \omega R/V$) to the limit of /217 regulation; the stabilizer lies in the plane of the blade.

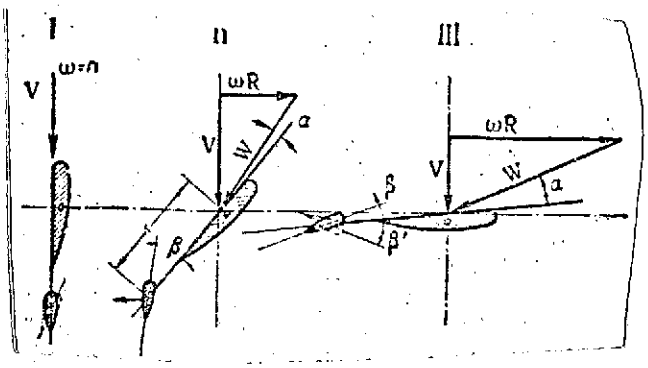

Fig. 130: Position of the wing during the regulation by means of stabilizers.

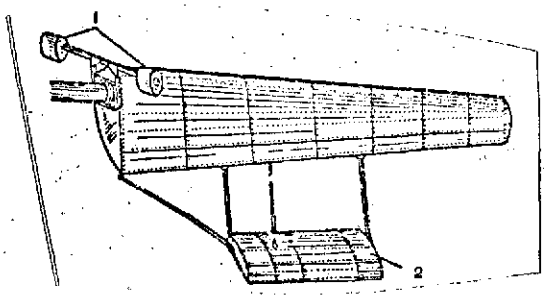

Fig. 131: Wing with stabilizer and compensating flyweights:
1. compensating flyweights;
2. stabilizer.

When the number of revolutions increases above the calculated one under the action of centrifugal forces, flyweight 6 is displaced on the axis of the wing and by means of arm 7, it turns the stabilizer 2 by another angle β' (position III). The balance which had existed until then between the moment of the stabilizer and of the blade, is disturbed, i.e. the moment of the stabilizer becomes slightly larger than the moment of the blade relative to the axis of the flap, and consequently, the blade turns in the reverse direction decreasing the angle of attack α. At the same time the lifting force of the wing decreases and the number of revolutions of the wind-driven wheel is reduced down to a w value which is slightly below the initial one.

In addition to the moment from the aerodynamic forces acting on the blade relative to the axis of the flap, centrifugal forces of the mass of the blade and of the stabilizer appear during the movement of the wind-driven wheel. The components of these forces also produce a moment relative to the axis of the flap in all positions of the wing, in addition to the position which coincides either with the plane of rotation of the wind-driven wheel, or with the plane which is perpendicular to it. This moment hinders the turning of the blade on account of aerodynamic forces. Therefore, in order to compensate for the moment from the mass forces, additional flyweights, which have been calculated accordingly, are attached in front of the spout of the wings, (see 1 in Fig. 131). The centrifugal forces of these flyweights

[Pages 218 and 219 missing in original copy]

a dynamic equilibrium so that in addition to the forces of gravity, centrifugal forces also act on the wings. /220

Let us examine the method of calculation of Prof. G. Kh. Sabinin for the dynamic equilibrium of the blade [31].

Let a flat wing, which can rotate freely on axis OZ coinciding with the geometric axis of the flap, rotate on the shaft XX' with an angular velocity ω (Fig. 134). Let us take point A on the wing with mass m and find the moment of the centrifugal force relative to the axis OZ, obtained from the rotation of the shaft XX'. Let us drop a perpendicular AD from point A to OZ and another perpendicular AC to the plane XOZ. Joining C and D, we obtain the right angle ACD. Let us denote the projection of the centrifugal force R on direction AC by the letter Q; the moment of centrifugal force relative to the axis OZ will be expressed:

$$M = Q\overline{CD} \qquad (a)$$

Since the two triangles AQR and O'AC are similar, we can write:

$$\frac{Q}{R} = \frac{AC}{AO'}; \qquad (b)$$

but:

$$R = m\omega^2 AO' \qquad (c)$$

and:

$$AC = AD \sin\alpha, \qquad (d)$$

$$CD = AD \cos\alpha, \qquad (e)$$

where α is the angle formed between AD and CD.

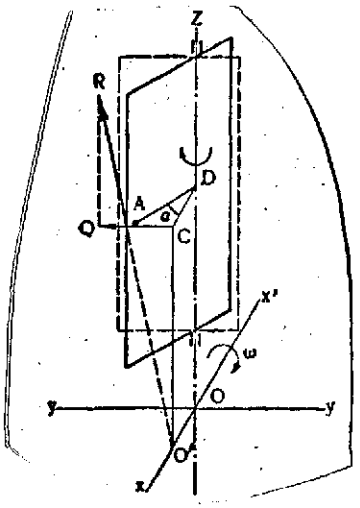

Fig. 134: The forces acting on a rotating blade.

Substituting the values Q and CD from (b), (c), (d) and (e) into (a), we obtain after reduction:

$$dM = dm\omega^2 AD \sin\alpha \cos\alpha; \qquad (f)$$

where AD is the distance between the point A and the axis OZ. Assuming that the blade is sufficiently thin and flat, we can consider angle α as being constant in all the points of the blade. The moment of the centrifugal forces rotating the blade will be equal to: /221

$$M = \omega^2 \sin\alpha \cos\alpha \int A\overline{D}^2 dm, \qquad (g)$$

but

$$\int A\overline{D}^2 dm = I, \qquad (h)$$

where I is the moment of inertia of the blade relative to the axis OZ.

Consequently:

$$M = I\omega^2 \sin\alpha \cos\alpha, \qquad (i)$$

or:

$$M = I\omega^2 \frac{\sin 2\alpha}{2}. \qquad (175)$$

This moment tends to turn the blade in the direction of the arrow so that the blade will be perpendicular to the shaft as shown by the dotted line in Fig. 134. The moment zero becomes at $\alpha = 0°$ and $\alpha = 90°$; the first position is unfavorable. The maximum value is assumed by the moment at $\alpha = 45°$ and $\sin 2\alpha = 1$, consequently:

$$M_{max} = \frac{1}{2} I\omega^2. \qquad (176)$$

Hence, we can see that in order to obtain the least possible unbalance, the moment of inertia I of the wing relative to the axis of the flap should be decreased as far as possible.

In wind engines regulated by rotation of the blade under the action of the stabilizer, the moment of inertia is composed of the moment of inertia of the wing, I_w, and the moment of inertia of the stabilizer with its fastenings I_{st}:

$$I = I_w + I_{st}. \qquad (177)$$

The moment of inertia of the stabilizer reaches 75% of the total moment of inertia of the wing. It is therefore necessary to tend to decrease the moment of inertia of the stabilizer in particular. This can be obtained by decreasing the weight of the stabilizer and of its fastenings. In order to obtain a dynamic equilibrium of the blade relative to the axis of the flap, compensating flyweights are mounted in front of the spout of the wing, as was said earlier (Fig. 131). /222
In wind engines which are regulated by rotation of the blade tips by means of a stabilizer, a flyweight is mounted on the spout of the rotating part of the blade in order to reach dynamic equilibrium.

If the weight of the compensating flyweight is taken slightly above the weight necessary for complete compensation, overcompensation can be obtained. In this case the blade will tend to turn in the same direction in which it should turn under the action of the regulator in the given case of the stabilizer.

The effect of overcompensation was used by engineer V. S. Shamanin, who suggested a system of regulation based on the principle of the dynamic unbalance of a rotating wing or part of it. In order for the blade to be able to turn in a reverse direction relative to the moment of the dynamic forces of the blade, the above author suggested a rod to pass through the axis of rotation of the blade (Fig. 135). The centrifugal flyweight a, situated at the end of rod b, tends to stay in the plane y -- y during the rotation of the wind-driven wheel under the action of centrifugal forces. A moment appears under these conditions which turns the blade in the direction shown by arrow M.

The magnitude of this moment is determined by equation (175).

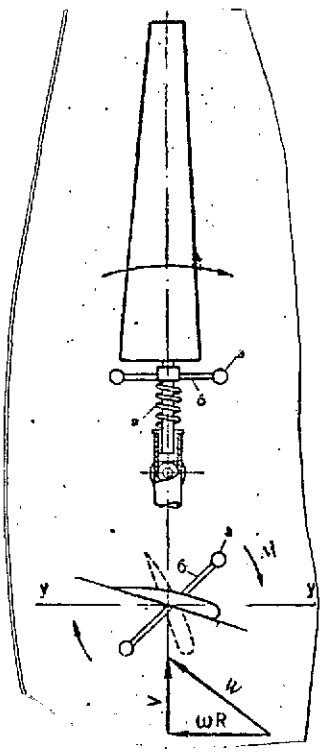

Fig. 135: Diagram of the regulation according to V. S. Shamanin.

In order to obtain a regulating effect, it is sufficient to have the moment of inertia of the compensating flyweight 30% larger than the moment of inertia of the blade, i.e.:

$$I_{comp} = 1.3I_{bl}$$

The author of this book suggested to use as a /223 regulating factor, the forces of inertia of the blade which turn it in the plane of rotation of the wind-driven wheel. The magnitude of the moment of these forces can be determined by means of equation (175).

When the blade is situated at an angle ϕ_1 to the plane of rotation of the wind-driven wheel, a lifting force Y acts on it, the projection of which on the plane X -- X is directed in the sense of rotation of the wind-driven wheel (Fig. 136, a). The projection of this force will decrease with the decrease ϕ and when the blade assumes the position shown by the dotted line, the projection of force Y will be minimal. /224 In order to continue the deflection of the blade until the point where it reaches a position with negative angle ϕ_2 (Fig. 136,b), one has to add flyweight A with mass m situated on arm r. The moment of inertia of this mass will turn the blade in the same direction in which it turned prior to the position shown by the dotted line in Fig. 136,a. As a result, the component of the lifting force Y' will act in the reverse sense causing breakage of the wind-driven wheel.

Under conditions of a normal number of revolutions, the blade is adjusted at an angle ϕ to the plane of rotation of the wind-driven wheel by means of the spring.

The first experimental testing of this regulation system was performed at the polygon of VIME, which showed that this regulation can be applied just like other analogical systems. A shortcoming of this regulation is the high frontal pressure, since it is the plane of the blade rather than its arm which is adjusted to the wind during the regulation.

36. Regulation by Means of Air Brakes.

During the rotation of the wind-driven wheel, a lifting force and a drag force appear on its blades. One of the components of the lifting force turns the wheel, while the drag brakes this rotation.

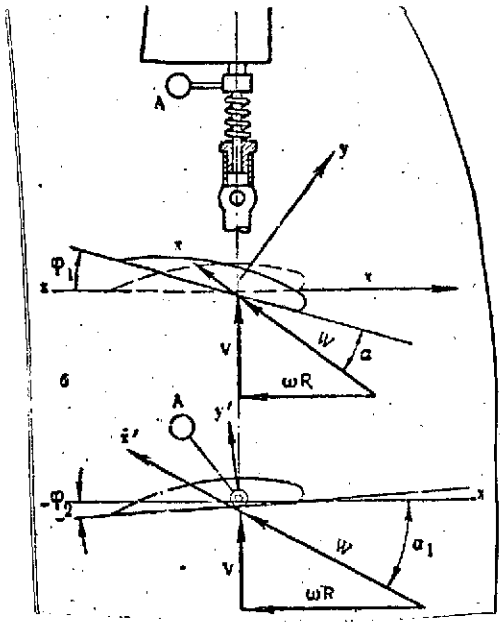

Fig. 136: Inertia type regulation of E. M. Fateyev.

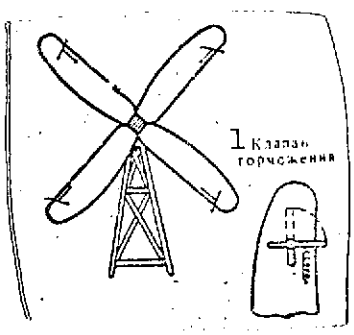

Fig. 137: Diagram of Bilau's system of regulation by means of air brake.

Key: 1. brake valve

If it were possible to change the drag by means of a certain device, so that it would hinder the increase in the number of revolutions of the wind-driven wheel, such a braking device could be used as a regulator.

The diagram of regulation by means of air brakes, is shown in Fig. 137. Turning valves are mounted on the blade of the wind-driven wheel, which are parallel to the direction of the circular velocity of the wheel and cause almost no drag under conditions of a normal number of revolutions. In this normal situation, the valves are contained by the spring. As the number of revolutions increases, the centrifugal forces turn it in a direction perpendicular to the direction of rotation. In this position, the valves are displaced with a large circular velocity and increase the drag to such an extent, that the excess torque of the wind-driven wheel is surmounted by the drag and the wind-driven wheel is slowed down.

This same valves can be mounted on the blade in a different place. For example, engineer S. V. Perli placed them at the tips of the wings in wind engines designed by him.

The author of this book suggested to design an air brake in the form of a bi-plan or tri-plan by dividing the general surface into several stub-wings. This makes it possible to use air brakes for wings of large dimensions D = 16 (Fig. 297).

CHAPTER 10. WIND ENGINE DESIGN

/226

The design of modern winged wind engines has been in accordance with the technical requirements of the conditions of their exploitation in the agricultural production. For example, in order to lift water by means of wind engines from a hole at a depth of 100 m and more, the rotary system pump of single action is widely used, which is characterized by a large moment of pickup and a small number of piston strokes. According to this characteristic, the multi-bladed low-speed wind engine was designed which has a large moment of pickup and a small speed (Fig. 74), and responds entirely by its technical requirements to lifting water from deep holes by means of a rotary system pump.

With the development of the mechanization of production processes in agriculture, the motorforce was required not only for milling and water supplies, but also for the preparation of forage, the irrigation of vegetable cultures, electrification of economic and daily life's needs, sawing of lumber, etc. The power tools of these processes require a large number of revolutions and do not need a large moment of pickup, since their start is idle. In order to satisfy the new technical requirements, rapid wind engines were designed which are convenient in the work with machines requiring large numbers of revolutions.

Wind engines of the rapid type with a small number of blades, have a small initial moment (Fig. 79), therefore they are more convenient for the work with those machines which are distinguished by a large number of revolutions and a small moment of pickup/227 such as generators, centrifugal pumps, etc.

According to the main technical requirements of production processes in agriculture, in general, two types of wind engines have been developed -- the rapid and the slow types, which have different dimensions, designs of the transmission mechanisms and systems of regulation. According to GOST 2656, the wind engines can be divided into three groups. The first group comprises the multi-bladed engines with a diameter of the wheel of 3.5 and 8 m; the second group comprises the engines with a small number of blades with the number of modules Z_n from 2 to 3, the diameter of the wind-driven wheel from 8 to 16 m (windmills), and the third group -- the rapid ones, with the number of modules Z_n from 4 to 7.5, and the diameter of the wind-driven wheel 1.5; 3; 5; 10; 12 and 18 m.

The types of wind engines built in the USSR have been elaborated in the Central Aerodynamic Institute and the Central Wind Energy Institute and later in the All Union Scientific Research of Mechanization and Electrificaton of the Agriculture (VIME), in the All Union Institute

of Agricultural Engineering (VISKhOM) and in the Ukranian Scientific Research Institute for the Mechanization of Agriculture.

Multi-bladed low-speed wind engines were released under the brand names TV-5 (low-speed wind engines with the diameter of the wind-driven wheel of 5 m) and TV-8, while the rapid wind engines were released under the brand names VIME D-12, VISKhOM D-3.5, VIME-GUSMP D-18 (VIME and the Main Directorate of the Northern Maritimes), UNDIM D-10, etc.

37. Multi-bladed Wind Engines.

The multi-bladed wind engine TV-5 (Fig. 138) is intended for work with piston pumps only.

The wind-driven wheel has a diameter of 5 m and consists of 24 blades with a variable rigging angle along the blade. The cord of the blade at the internal tip makes, with the plane of rotation, an angle of 45°, while at the external tip, the angle is 17°.

The head of the wind engine (Fig. 139) is an iron cast crankcase in which a crank operated mechanism is mounted. The crank makes it possible to adjust the rod of the pump to 300 and 400 mm, for which purpose two openings are made in the large gear wheel under the pins of the connecting rod; one has a radius of 150 mm, and the other has the radius of 200 mm. /228

The adjustment to the wind is performed by means of a tail which is built in the form of a triangular girder made of iron carbide with a trapezoid tail, the dimension of which is 2.82 m^2, made of plates of galvanized iron. The surface of the tail is concave at the side of the regulating spring, the purpose of which is to compensate for the aerodynamic moment of the wind-driven wheel, which appears as a result of the displacement of the axis of rotation of the wind-driven wheel relative to the vertical axis of rotation of the head.

The wind engine is mounted on a four-legged steel tower with a height of approximately 15 m. At the base of the tower, a horse-drawn winch is situated which sets in motion the piston pump on calm days. /229

Regulation of the wind engine is performed by removing the wind-driven wheel from the wind (Fig. 118). The wind engine starts its operation and is stopped below, by means of a manual winch attached to the leg of the tower. A cable goes from the winch upward and is attached to stop clutch 13 (Fig. 139) which moves longitudinally along the support tube 14. Clutch 13 contains ring 15 which can turn around the clutch and at the same time move longitudinally. The ring has

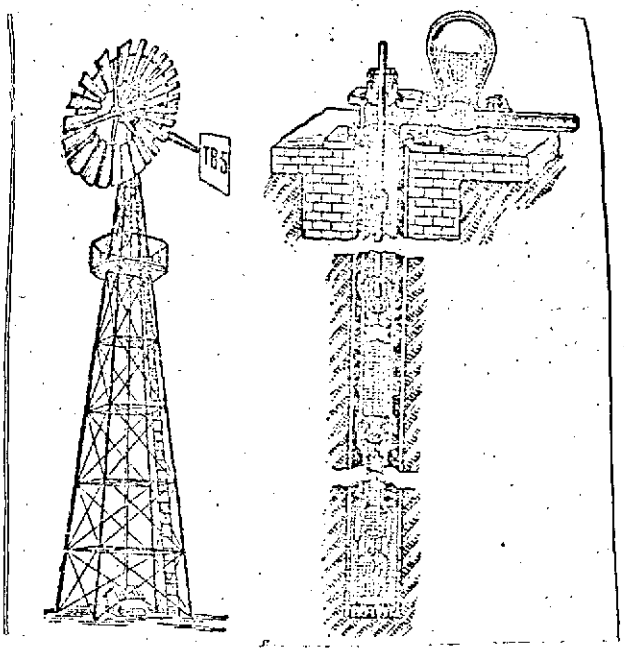

Fig. 138: Multi-bladed wind engine TV-5.

a cut on one side which contains/230 bracket 16 made of round iron, which is attached to the head of the wind engine. As it turns around the vertical axis, the head turns the directional clamp and the ring while clutch 13 does not turn due to a key which is welded to the wall of support tube 14.

The power of the wind engine at a wind velocity of 8 m/sec equals 2.5 hp; the number of revolutions of the wind-driven wheel at full load is 40 rpm. The output for lifting water with a pressure head of 10 m amounts to 10 m^3 at a wind velocity of 8 m/sec.

The multi-bladed TV-8 wind engine is intended for work with agricultural machines in animal husbandry in kolkhozes and sovkhozes.

The general view of such a wind engine is presented in Fig. 140.

A wind-driven wheel with a diameter of 8 m has 18 blades made of plates of galvanized iron with a thickness of 1.25 mm, which are attached to three wings, interconnected by means of spokes made of iron carbide 45x45 mm. The blades are mounted with a variable rigging angle, i.e. at the external ring, the angle between the cord of the blade and the plane of rotation of the wind-driven wheel equals 22°, while at the internal ring, this angle equals 47°. The length of the blade is 2,450 mm, its width at the external ring is 674 mm, while at the internal one it is 410 mm. The spokes are attached to flanges of the hub of the wind-driven wheel by means of two bolts each.

The head of the wind engine (Fig. 141) is the shaped elongated cast iron 5, into the root of which axis 2 is pressed under an angle 6.5° to the horizontal. This deflection is made in order to bring the wind-driven wheel nearer to the tower and avoid touching the leg of the latter with the blades. Two conical roller bearings are fitted to this axis, which carry the hub of the wind-driven wheel. The rim of the conical gear wheel 3 is attached to the rear flange of the hub; wheel 3 is engaged with conical pinion 4 which is fitted on the vertical shaft 12 of the wind engine. The number of teeth of the large wheel $Z_1 = 63$, at the pinion $Z_1 = 17$. The lower base of the head is fitted to tube 6, which rotates freely in two supports. In the upper support 7, it turns on ball bearings which are placed

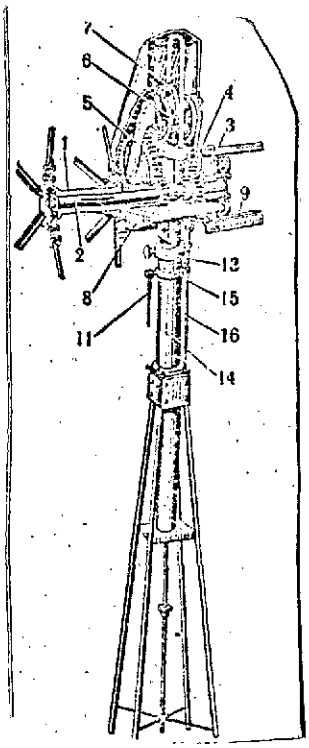

Fig. 139: Head of wind engine TV-5: 1-hub of the wind-driven wheel; 2-shaft of the wheel; 3-small driving pinions; 4-large pinions with crank mechanism; 5-connecting rods; 6-rollers; 7-guide arc for the roller; 8-crank case; 9-girder of the tail; 10-bracket for regulating the spring; 11-cable; 12-bumper; 13-stop clutch; 14-support tube; 15-ring of the stop clutch; 16-bracket.

on a self-aligning circular pivot. The /232 cast iron shell of the lower support 8 is attached by means of bracing wires to the legs of the tower. Through its center passes the sharp tip of the support tube which, with its fitted head turns freely in the support; this takes place upon starting, stopping and regulation of the wind engine.

The tail for adjusting the wind engine to the wind consists of girder 11 which has a length of 7,370 mm. The end of this girder has the shape of a trapezoid and a surface made of galvanized iron is attached to it. The area of the surface $f_{t\ell}$ is equal to 4.85 m^2, which amounts to $f_{t\ell}/F = 0.097$, where F is the surface marked off by the wind-driven wheel.

The wind engine is mounted on a metallic lattice construction on tower 13 with a height of 14.85 m. The winch (Fig. 141) at the base of the tower perceives the work of the vertical shaft and transmits it either to a piston pump, or to an agricultural machine -- straw-cutter, oil cake breaker, root cutter, cornmill, millstone, etc.

In the absence of wind, the same winch can be used to set in motion a piston pump which is either horse-drawn or tractor-driven; the vertical shaft of the engine is disconnected from the winch by means of ddog-tooth clutches on the upper and the lower compartments of the vertical shaft.

Regulation of the wind engine by removing the wind-driven wheel from the wind, is performed by means of a lateral blade (Fig. 117). The area of the blade equals 1.95 m^2, which amounts to 3.9% from the area marked off by the wind-driven wheel.

The wind engine is started and stopped by means of a manual winch, situated below, which is fastened to the leg of the tower at its base. Cable 14, which goes from the winch upward, is connected at its two ends to clutch 9 which moves longitudinally along the support tube. The clutch has an arm with a slit which contains iron

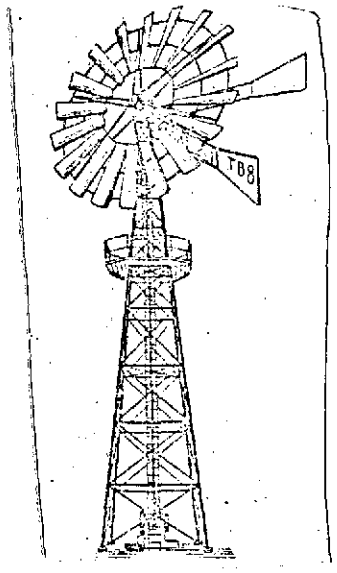

Fig. 140: The TV-8 wind engine.

rod 10, fastened at one end to the upper support, and at the other end to the lower one. This rod serves as a guide during the upward and downward displacement of the clutch.

The upper end of the stop cable is fastened to the tail wherefrom, it passes via two rollers through the support tube where it is connected to a rod; the latter has a salient on its lower end, which goes into the longitudinal slit of the support tube. Out-/233
side the tube, this salient seizes up the base of the clutch which is carried by the support tube. In such a manner a connection is established between the mobile head of the wind engine and the stoppage mechanism, which can only move forward along the support tube.

The power of the wind engine at the wind velocity of 8 m/sec equals 6.5 hp on the shaft of the wind-driven wheel, while the number of its revolutions at full load is 25 rpm.

38. Rapid (Sparsely-bladed) Wind Engine.

The wind engine VIME D-12 (Fig. 142) has a three-bladed wind-driven wheel with a diameter of 12 m. The blades of the wings have a streamlined profile and are made of wood and metal; they are attached to the steel tubes of the flap.

The head of the wind engine (Fig. 143) is shaped like an iron cast crankcase which contains the support of the horizontal shaft 2 as well as a couple of conical gear pinions 3-5, which transmit the rotation of the wind-driven wheel 1 to the vertical shaft 5. The crankcase of the head is attached to support tube 6 which rotates around a vertical axis in two supports: the upper 7, which is a roller support, and the lower 8 which is ball-shaped.

The grease is poured from the upper transmission into the crank-/235
case of the head up to a certain level.

The stoppage and starting of the wind engine is performed by means of a winch which is mounted to the leg of the tower by means of a screw. The screw is connected to stop clutch 14 by means of cable 16. As the cable is tightened by the screw, the lever of shifting device 17 displaces clutch 10 around the horizontal shaft; clutch 10 act on clutch 9 by a kinematic link. The latter clutch

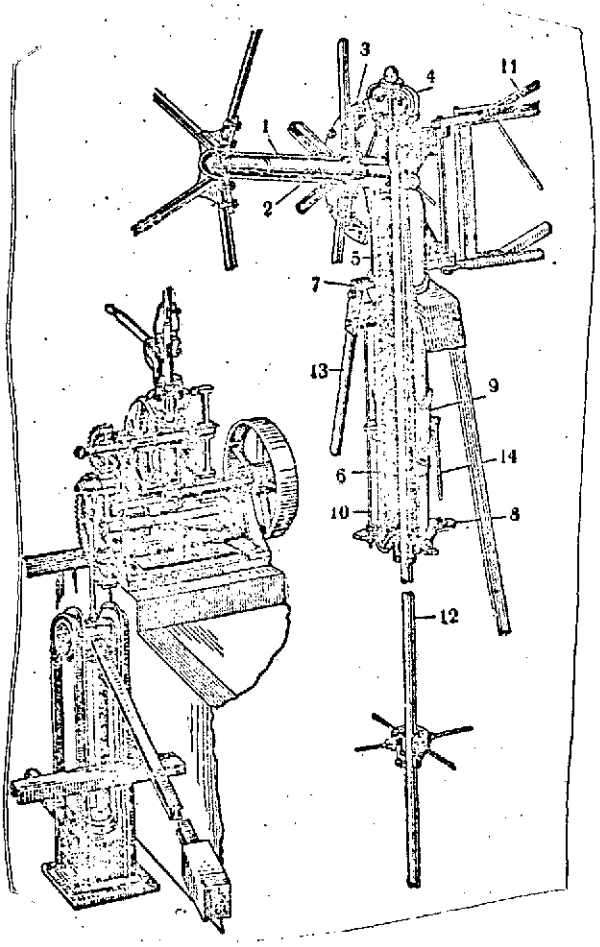

Fig. 141: Head of the TV-8 wind engine: 1-hub of the wind-driven wheel; 2-axis of the wind-driven wheel; 3-conical gear wheel; 4-conical pinion; 5-conus of the head; 6- supporting tube; 7-upper support of the head; 8-lower support of the head; 9-stop clutch; 10-guide for clutch 9; 11-tail girder; 12-vertical shaft; 13-tower; 14-stop cable.

acts on stabilizer 19 by means of cranks 11 and rod 12 which pass inside the flaps, and adjusts the stabilizer at a large negative angle. Due to this fact, a negative moment which is transmitted to the main shaft appears on the revolving part of blade 20. This moment balances the positive moment of the rigidily fixed part of the blade 18, and the wind engine stops.

Cable 16 is released upon stopping the wind engine, and by the action of spring 13 and rod 21 with a lever mechanism, the stabilizers are automatically adjusted at a certain angle of attack which was determined during the design for a given set of conditions of operations. Under the action of the wind, the stabilizers are displaced relative to the axis of the flap and adjust the blade tips in the working position. The wind engine starts to work at a velocity of the wind around 4 m/sec.

Due to the fact that wind engines of this design work with an almost constant number of revolutions, they are suitable for small wind-driven power stations. They can be equally used for setting in rotation machine tools in workshops of agricultural machine parts as well as driving agricultural machines and centrifugal pumps for irrigation.

At a wind velocity of 8 m/sec, /237 the VIME D-12 wind engine can develop a power of approximately 15 hp on the shaft of the wind-driven wheel. The normal number of revolutions of the wind-driven wheel is 55-60 rpm.

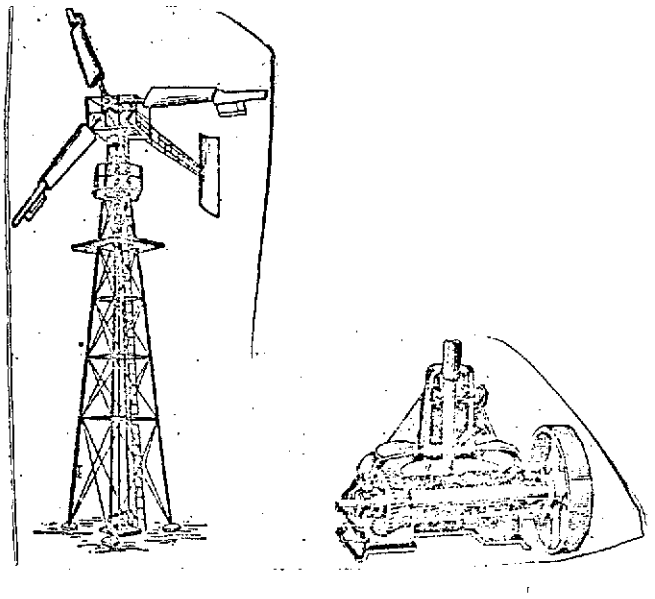

Fig. 142: The rapid VIME D-12 wind engine.

The VIME D-5 wind engine has a three-bladed wind-driven wheel with a diameter of 4 m (Fig. 144). The rotation of the wind-driven wheel is transmitted to the vertical shaft which is connected to the reducing gear at the base of the tower, by means of a couple of conical gear pinions. The regulation is achieved by the rotation of the blade around the axis of the flap. The power of the wind engine at a wind velocity of 8 m/sec equals 2.7 hp on the shaft of the wind-driven wheel. The normal number of revolutions of the wind-driven wheel is n = 180 rpm. The head (Fig. 145) has a cast crankcase just like wind engine VIME D-12, with the only difference that the cover of the crankcase is made above and it contains the support of the upper bearing of the vertical shaft. /238

The reducing gear mounted at the base of the tower has two pulleys which can set in motion a centrifugal pump or low-power agricultural machines as well as a generator.

Wind engine PD-5. This wind engine is intended for operation with a power pump. The two-bladed wind-driven wheel of wood and metal construction turns the main shaft, which has two supports with ball-bearings (Fig. 146). The rotation of the wind-driven wheel is transmitted through a couple of conical wheels to the vertical shaft. The transmission ratio of the revolutions of the wind-driven wheel to the revolutions of the vertical shaft equals 1:2.5. Regulation is performed by means of a lateral blade and of valves which are placed on the tips of the blades of the wind-driven wheel. The valves work like air brakes and prevent the wind-driven wheel from separating during the shedding of the load.

Below, in the upper compartment of the vertical shaft, a centrifugal clutch is mounted (Fig. 147), which at certain numbers of revolutions connects the lower compartment of the shaft, joined with a power-driven winch, which has worm gearing. The crank-driven mechanism of the winch sets in forward motion a yoke which is joined with the rod of the pump. This wind installation is experimental and serves to find the potential of operation of a rapid wind engine with power pump.

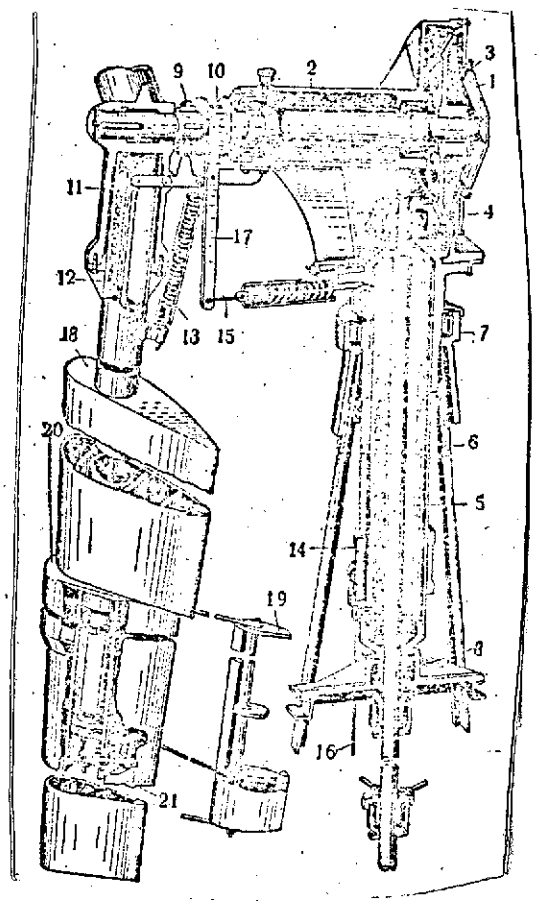

Fig. 143: Head of the VIME D-12 wind engine: 1-crankcase of the head; 2-stop of the wind-driven wheel; 3-conical wheel; 4-conical pinion; 5-vertical shaft; 6-support tube; 7-upper support; 8-lower support; 9-stop clutch; 10-second stop clutch; 11-lever of stoppage and regulation; 12-rod of stoppage and regulation; 13-regulating spring; 14-clutch for start and stoppage; 15-rod for setting the clutch 9 in motion; 16-stop cable; 17-lever for starting and stopping the wind engine; 18-rigid part of the blade; 19-stabilizer; 20-rotating part of the wing; 21-centrifugal flyweight.

The wind engine starts to work idly, therefore, it is set in motion at low wind velocities.

The VIME-GUSMP D-18 wind engine is a rapid wind engine of all-metallic construction with a tower of a height of 19 m (Fig. 148). /239

The wind-driven wheel has a diameter of 18 m and has three wings with streamlined blades (Fig. 149). Regulation of the revolutions of the wind-driven wheel, is performed by Prof. G. Kh. Sabinin and N. V. Krasovskiy's system, by turning the terminal part of the wing which amounts to [fraction illegible] of the length of the wing. /240

The head of the wind engine consists of a metallic frame on which the reducing gear with a transmission ratio of 1:3 is placed, as are a mechanical brake block and a mechanism for adjustment to the wind by means of a hand wheel and windroses. The head is fastened to the support tube 325x9 mm (Fig. 150) which turns on rollers in a ring attached to the upper part of the tower; the lower end of the tube, turns in a support with a ball bearing. /241

The start and stopping of the wind engine is performed like in the VIME D-12 wind engine, by means of a manual winch which passes to the foot of the tower.

The windroses which adjust the wind-driven wheel to the wind, are 18-bladed wind-driven wheels with a diameter of 2.7 m. The blades of the windroses are made of pine wood planks with a thickness of 10 m. The rotation of the shaft of the windroses is transmitted through a conical gear to

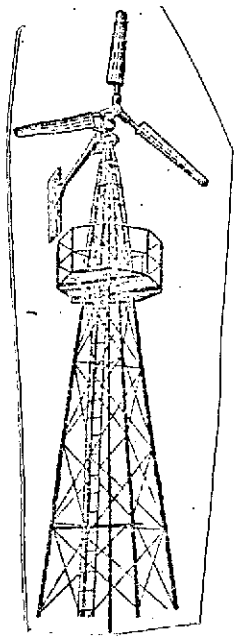

Fig. 144: VIME D-5 rapid wind engine.

the axial horizontal shaft and further through a worm gearing to the lantern wheel ring fixed to the upper belt of the tower. The overall transmission ratio equals 1:500.

The tower of the wind engine has a height of approximately 19 m and consists of a lower riveted pyramidal part with the side of the square at the base equalling 4.8 m and an upper prismatic all-rounded construction with the side of the square equalling 0.735 m (Fig. 151). The tower is constructed of iron carbide 100 x 100 x 14 mm and 60 x 60x 8 mm.

The vertical shaft has a diameter of 70 mm and it turns in three spherical ball bearings mounted on the center of the tower on horizontal bracing wires. Below, the vertical shaft is attached to a reducing gear (Fig. 152) with a transmission ratio of 1:3. Two pulleys, 800 mm diameter each, are fitted on the horizontal shaft of the reducing gear, from where the generator can be set in motion and the transmission of the movement to the machinery can be performed. /242

The legs of the tower are built in a foundation with rough walling at a depth of 2.4 m.

Wind engine of the system Ufimtsev-Vetchinkin D-10 (Fig. 153). The aerodynamic analysis was performed on the basis of the turbulence theory of N. E. Zhukovskiy under the leadership of Prof. V. P Vetchinkin; the electrical machinery and the automation were elaborated by A. G. Ufimtsev.

The distinctive feature in the design of this wind engine is the small weight per kw power. The wind-driven wheel has three blades of wooden-metallic construction, with an aerodynamic profile, /243 similar to a wing of the aerodynamic type with an inverted parabolic airfoil, suggested by N. E. Zhukovskiy and S. A. Chaplygin. The blades are rigidly attached to the tubular flaps which rotate freely on ball bearings fastened to a special trilling, which is carried on the horizontal shaft of the wind engine.

The regulation of the power is performed by turning the blades around the axis of the flap in the direction of the wind. For this purpose, the flaps are passed in the vicinity of the spout of the blades, in such a manner that the center of effort of the sail area is displaced relative to the axis of rotation of the wing to the rear edge.

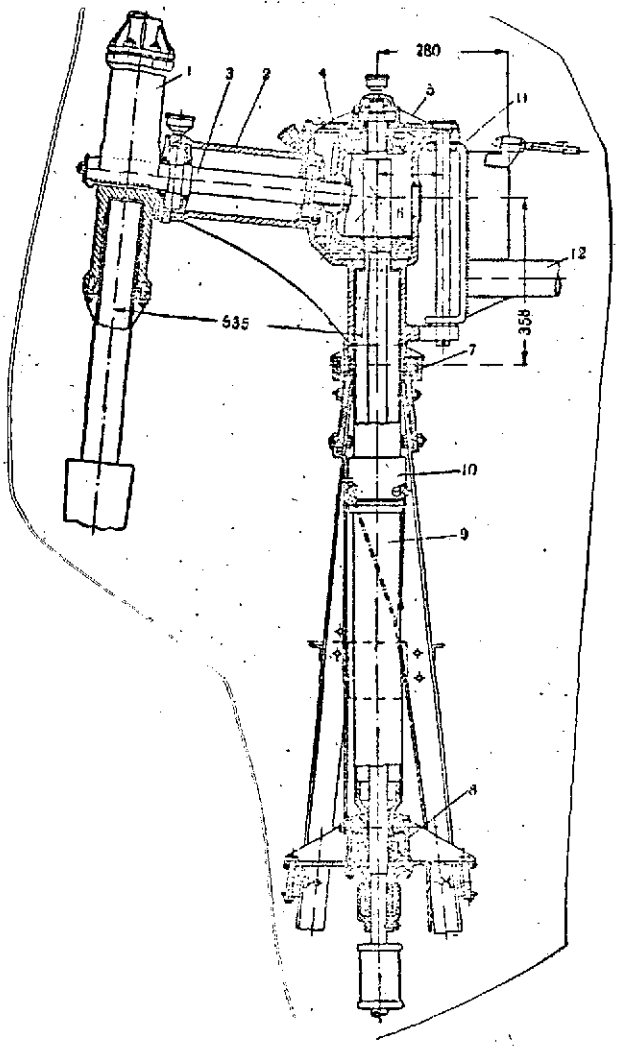

Fig. 145: Head of the VIME D-5 wind engine: 1-flap of the wind-driven wheel; 2-crankcase; 3-shaft of the wind-driven wheel; 4-conical wheel; 5-conical pinion; 6-vertical shaft; 7-upper support; 8-lower support; 9-support tube; 10-stop clutch; 11-axis of the tail; 12-tube of the tail; 13-guide rollers and stop cable.

The rotation of the wind-driven wheel is transmitted to a vertical shaft through a couple of conical teeth with a transmission ratio of 1:3.5. On the vertical shaft below, a large wooden pulley is placed, wherefrom the rotation of the dc generator is transmitted with a transmission ratio of 1:10 by means of a belt drive. A pulley is fitted to the shaft of the dc generator, which has a free pace so that it can lag behind when the shaft of the generator is rotated by means of another motive force. This is caused by the fact, that the shaft/244 of the generator is a continuation of the shaft of the flywheel in A. G, Ufimtsev's system. As the number of revolutions of the wind engine decreases, the flywheel rotates the generator for 2-3 minutes, due to the given system of transmission; the lag of the wind engine is not reflected in the work of the flywheel. In such a manner, this design makes it possible to iron out the number of revolutions of the generator for short intervals of time, under conditions of pulsed wind.

The dc generator has a nominal power of 3.5 kw, 1750 rpm, 220 V, 17 A. It was possible to increase the voltage to 350 V when the wind velocity increased.

Due to the presence of the flywheel, which abolishes the rapid transition from one set of conditions of operation of the installation to another, the wind-driven power station could be regulated manually by one of three methods i.e.: 1-by the change of the angle of attack of the blade by means of the manual stop winch; 2-by decreasing or increasing the current of excitation in the magnets by means of the shunt rheostat;

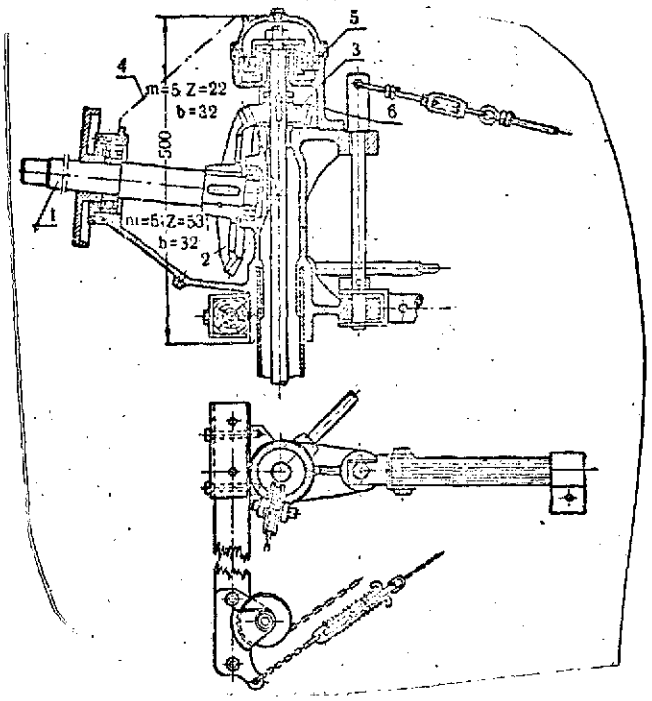

Fig. 146: Head of the PD-5 wind engine; 1-shaft of the wind-driven engine; 2-conical wheel; 3-conical pinion; 4-crank of the head; 5-ball bearing of the vertical shaft; 6-upper support.

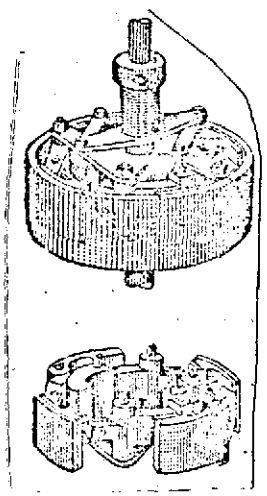

Fig. 147: Centrifugal clutch to wind engine PD-5 designed by engineer S. B. Perli.

3-by increasing or decreasing the load on the station which was done by connecting additional lamps and motors.

The adjustment of the wind-driven wheel to the wind is performed by means of a tail of lattice construction which has a biplane unit mounted on its end (this is why such a tail is called biplane).

The tail unit is slightly arched in order to compensate for the reactive moment of the vertical shaft, which appears during engagement of the upper transmission. Without this, the wind engine could not stand exactly in the direction of the wind during its operation. Besides, a curved surface has greater strength.

The tower with a height of 40 m is of lattice construction with indentical square sections throughout its height; it is maintained in vertical position by means of bracing wires.

The wind engine Ts AGI D-18. The project of this wind engine (Fig. 154) was elaborated under the direction of Prof. V. P. Vetchinkin, according to the system of the Ufimtsev-Vetchinkin D-10 wind engine.

Distinctive features of the Ts AGI D-18 wind engine are the following: 1-connection of a flywheel of the proper type with a capacity of 10 minutes to the vertical shaft of the wind engine; 2-the considerable height of the tower -- 40 mm; 3-regulation by turning the blade /245 according to the Ufimtsev system

The wind-driven wheel has three blades which rotate around the axis

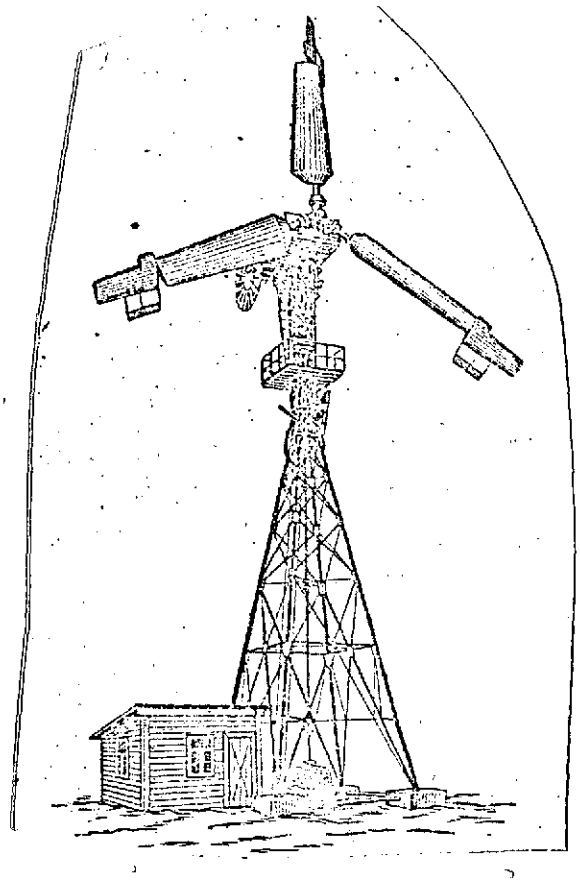

Fig. 148: The VIME-GUSMP D-18 wind engine.

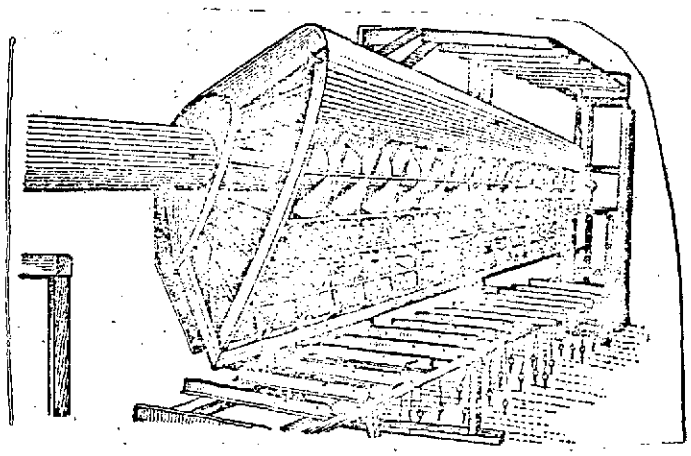

Fig. 149: Wing with partially removed casing.

of the flaps; their axes pass in the spout of the wing in such a manner, that the resultant force of the airstream which passes close to the central axis of the blade, creates a moment relative to the axis of the flap. This moment rotates the blade with its arm towards the wind, which is counteracted by the flyweight suspended to the system of levers of the regulation mechanism. When the wind engine is addressed, the flyweight is raised, and the wings are freely adjusted with the spout towards the wind just like wind winch rings, which makes it possible to have small loads on the wheel at rest.

The flywheel (Fig. 155) is built by the same diagram as the wind engine of Ufimtsev-Vetchinkin described above, and differs from it only in its weight. The disc of the flywheel weighs approximately 1.25 tons; the number of revolutions is 2500-3500 per minute.

In order to decrease the resistance of the air, the disc is placed on a rotating housing. This decreases the drag approximately 3.5 fold.

The tower is all metallic /246 of welded construction and has a height of 40 m. With such a high tower, the wind engine can work more hours per year than with a low tower.

The adjustment to the wind is performed by means of a triplane tail, which is done in order to decrease the angular velocity of rotation of the tail during side gusts.

The weights of the wind engine's parts are: for the tower-7.5 tons,

ORIGINAL PAGE IS OF POOR QUALITY

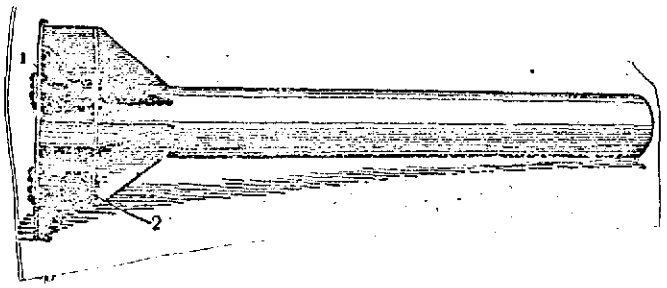

Fig. 150: Support tube: 1-support under the frame of the head; 2-rollers.

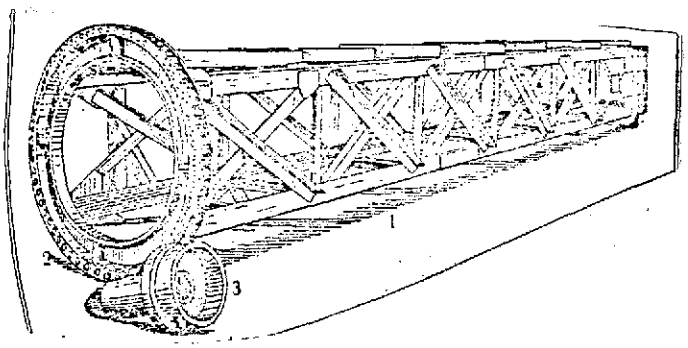

Fig. 151: The prismatic part of the tower; 1-girder; 2-ring with latern pinion; 3-pintle to the support tube shown in Fig. 150.

head of the wind engine-3.5 tons; flywheel-1.5 tons, overall weight-12.5 tons.

[Pages 248 and 249 are missing from the original text. Figures 157, 158, and 159 are also missing.]

in one of the guides. The oil is collected by means of a pump from the oil vat of the crank. The wind engine has roller bearings and automatic lubrication. /252

The compact transmission mechanism of the Fairbanks wind engines, is manufactured according to diagram IV (Fig. 156). A wall is fitted to the shaft of the wind-driven wheel (Fig. 160), which is engaged with a worm wheel; a connecting rod mechanism is mounted on the rim of the worm wheel.

The transmission mechanism of multi-bladed wind engines "Aeromotor" is built according to diagram VI (Fig. 156). The crank mechanism of multi-bladed wind engines "Hercules" and "Climax" in England, are built according to the same diagram. The design of the head of wind engine "Aeromotor" is shown in Fig. 161, while that of "Hercules" is shown in Fig. 162. The difference between them consists only in the mechanism of starting and stopping. In the first, this mechanism consists of a series of levers connected with the clutch which rotates on the support tube and is displaced longitudinally along it (Fig. 161), while in the second, two guide rollers replace the levers; a chain is thrown over the two rollers, which, at its upper end is fastened to the tail, while its lower end passes inside the support tube and is fastened to the clutch which can only glide along the support tube upwards and downwards (Fig. 162).

The design of the transmission mechanism in the "Gigant" wind engine is quite simple (Fig. 163). The forward movement is communicated by the connecting rods to the rod of the pump; the connecting rod in its turn is connected to a yoke, one end of which is hinged to an immobile support (diagram VII, Fig. 156). /253

ORIGINAL PAGE IS
OF POOR QUALITY

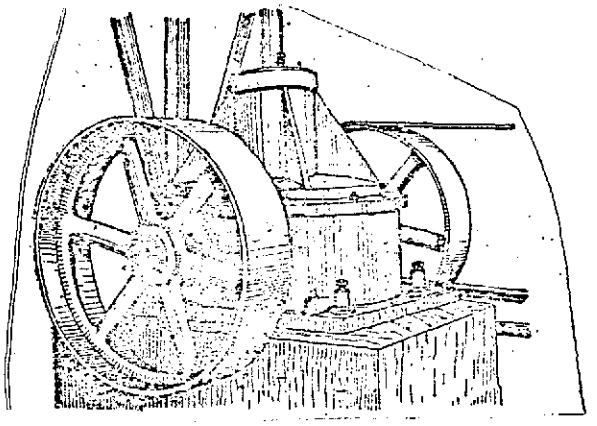

Fig. 152: Reducing gear for the D-18 wind engine.

Technical Characteristics

Power of the wind engine at the wind velocity of 8 m/sec.....38 hp
Normal number of revolutions of the wind-driven wheel.....42 rpm
Revolutions of the body of the reducing gear.....378 rpm
Weight of the individual units of the wind engine:

wind-driven wheel	2250 kg
head, regulation, mechanism for stoppage and turning to the wind	3025 kg
tower	4825 kg
reducing gear with vertical shaft	2400 kg
Total weight	12,500 kg

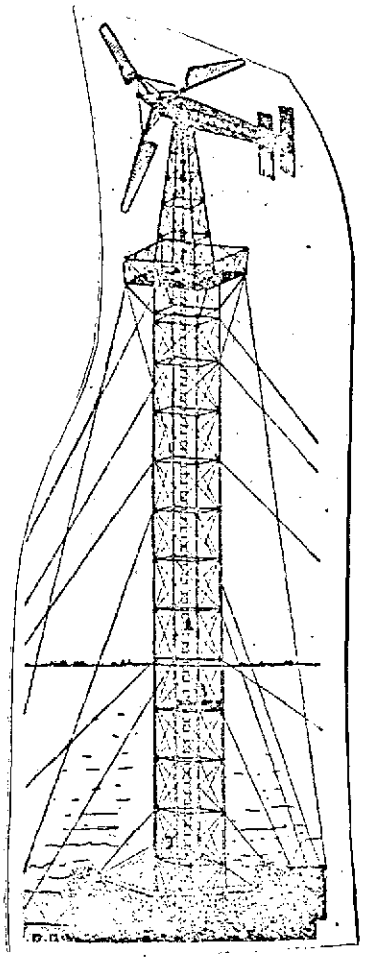

Fig. 153: Wind engine of the system Ufimtsev-Vetchinkin D-10.

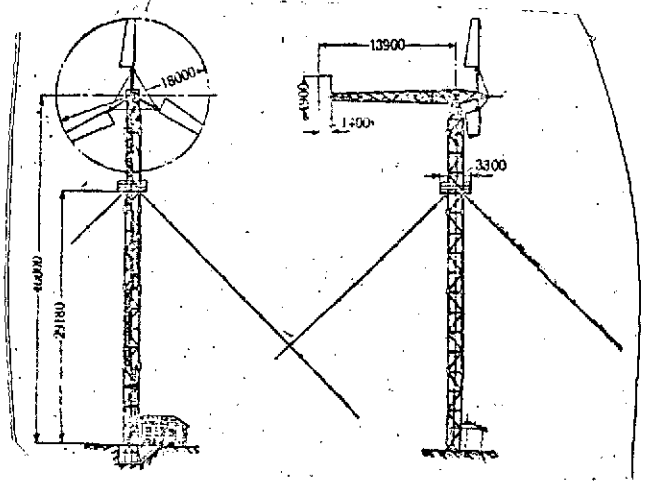

Fig. 154: The wind engine TsAGI D-18 according to the system of Prof. Vetchinkin.

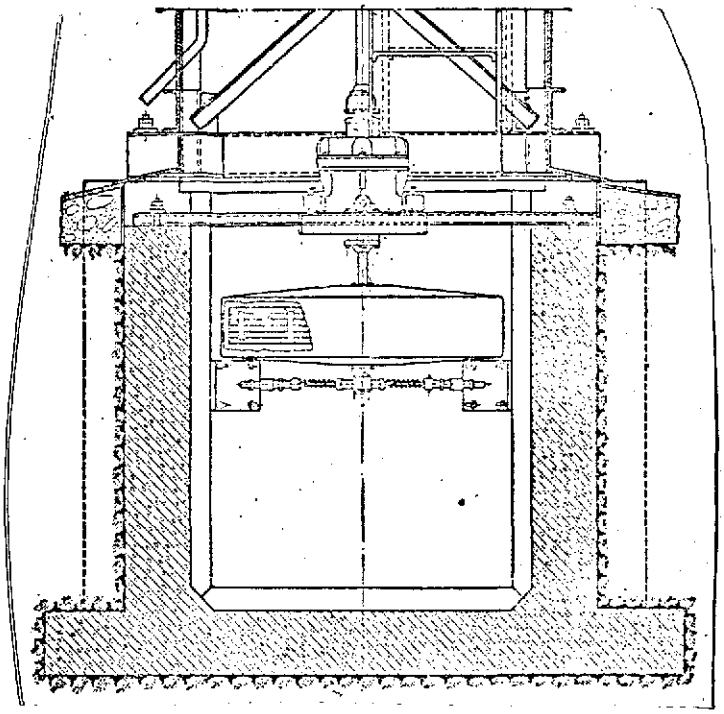

Fig. 155: The flywheel of the TsAGI D-18 wind engine.

The wind engine "IZI" has a transmission mechanism with internal toothed gearing (diagram VIII, Fig. 156). The general aspect of the head of this engine and the cylindrical transmission with internal gearing, are shown in Fig. 164.

Among the rapid wind engines for electrical installations, we shall mention the six-bladed wind engines with a diameter of the wind-driven wheel varying from 5 to 12.5 m of the Danish firm "Agrico" (Fig. 165). The wings of these wind engines have flaps made of steel pipes. The regulation is performed by turning the blades of the wings around the axis of the flaps. All six blades are kinematically interconnected so that they turn simultaneously in the process of regulation.

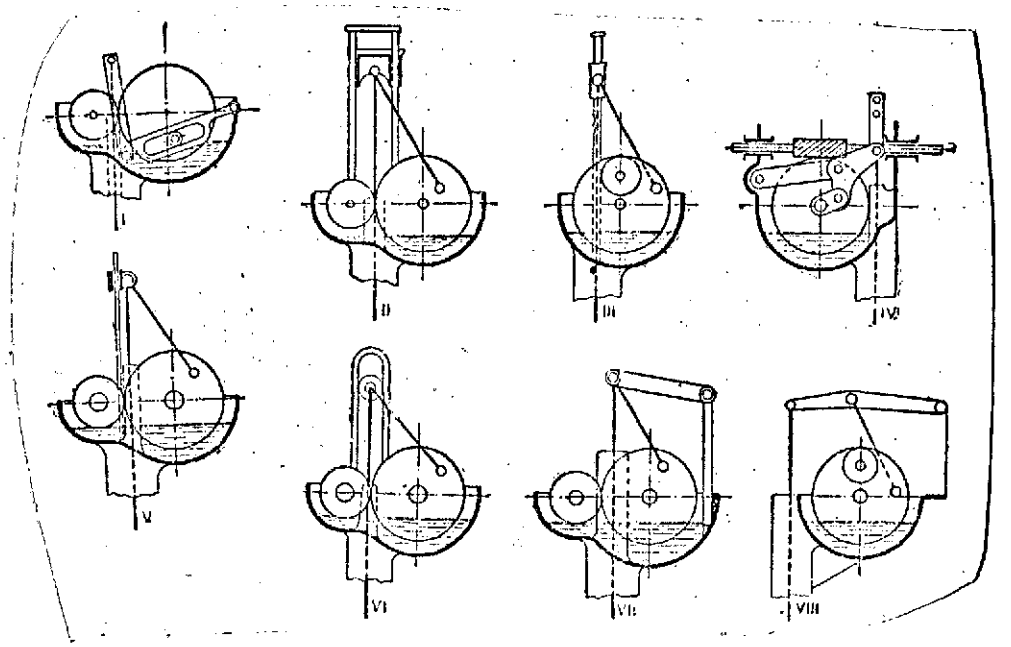

Fig. 156: Diagram of the transmission mechanism of wind engines, working with piston pumps.

ORIGINAL PAGE IS
OF POOR QUALITY

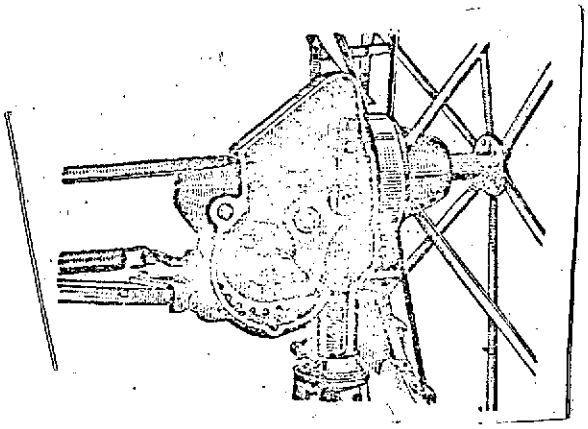

Fig. 160: Head of the wind engine "Fairbanks".

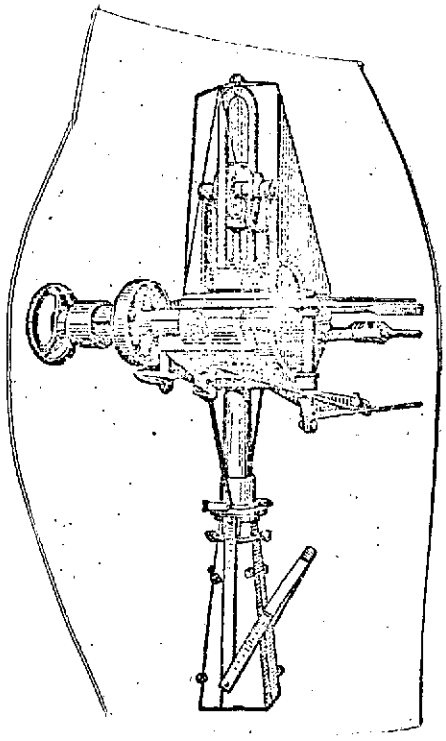

Fig. 161: Head of the wind engine "Aeromotor".

ORIGINAL PAGE IS
OF POOR QUALITY

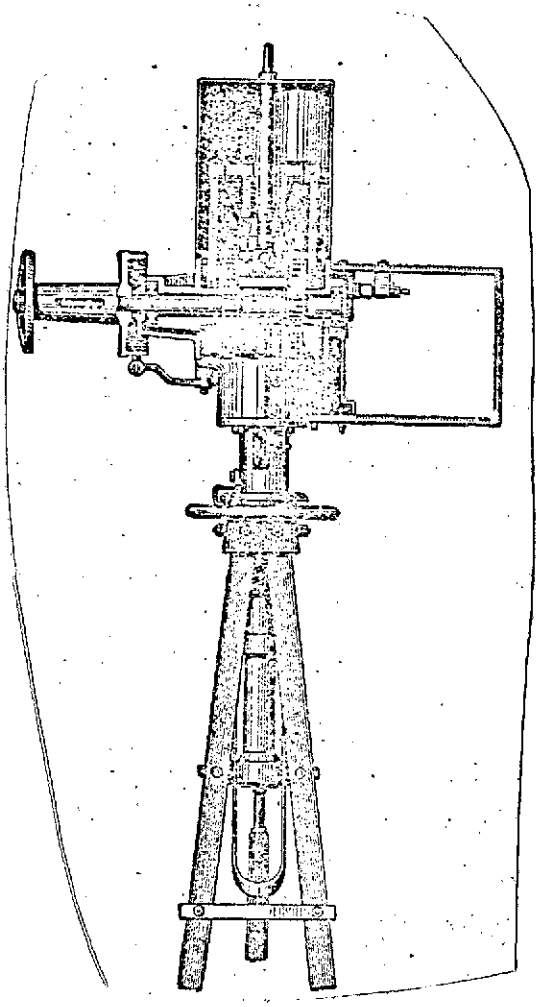

Fig. 162: Head of the wind engine "Hercules".

For small wind-driven power installations, the American firm "Roralight" releases the model "1000" with a 3-bladed wind-driven wheel, diameter 3.45 m. The number of revolutions is limited by turning the blade by means of a centrifugal regulator mounted on the shaft of the wind-driven wheel (Fig. 166). Power -- 1 kWt at 300 rpm; four-pole shunt generator -- 1 kWt, at 32-40 V, with maximal number of revolutions 1200 rpm, displaced behind the wind-driven wheel. /255

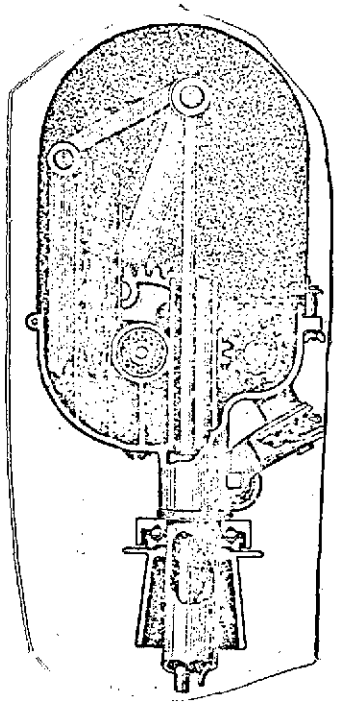

Fig. 163: Head of the "Gigant" wind engine.

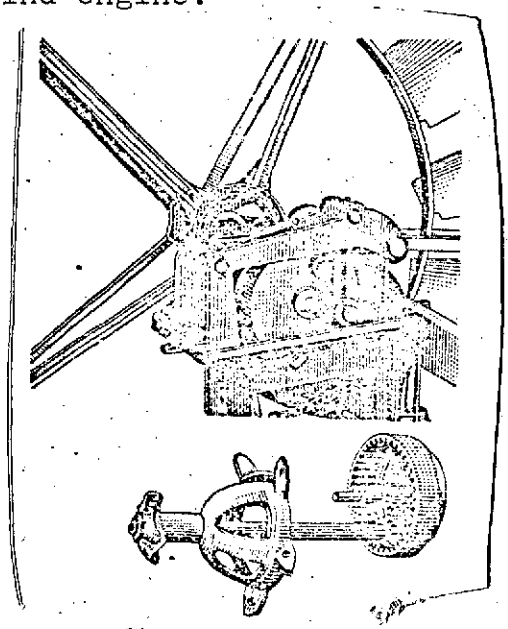

Fig. 164: Head of the wind engine "IZI" and the transmission mechanism.

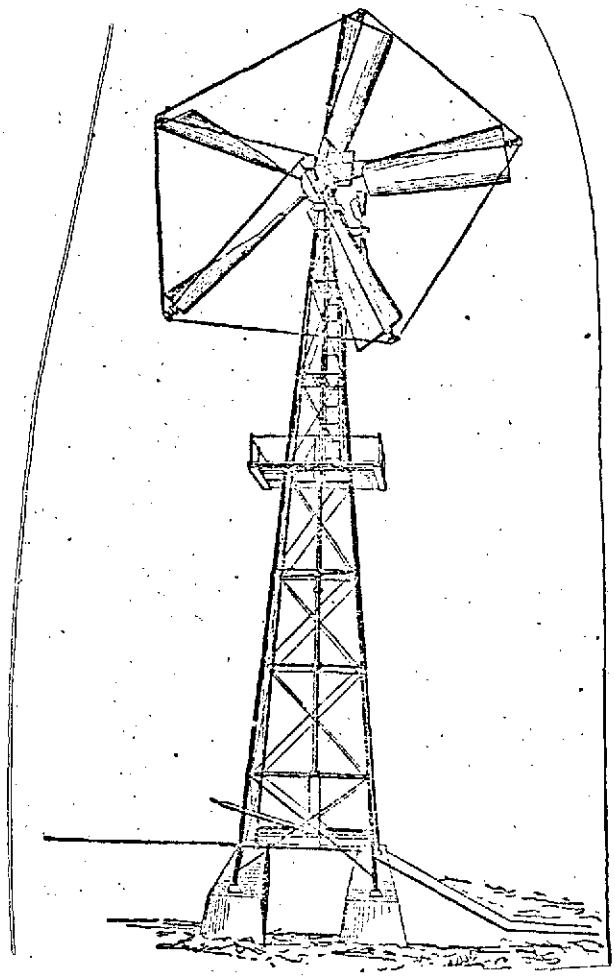

Fig. 165: Wind engine "Agrico".

39. Weight of the Wind Engine

The main element in the design of a wind engine is the creation of a wind engine which would have the lowest weight with high performance. This requirement is derived from the necessity of metal savings, as well as saving in the transportation of the excessively heavy wind engines to the site of their exploitation. Generally speaking,

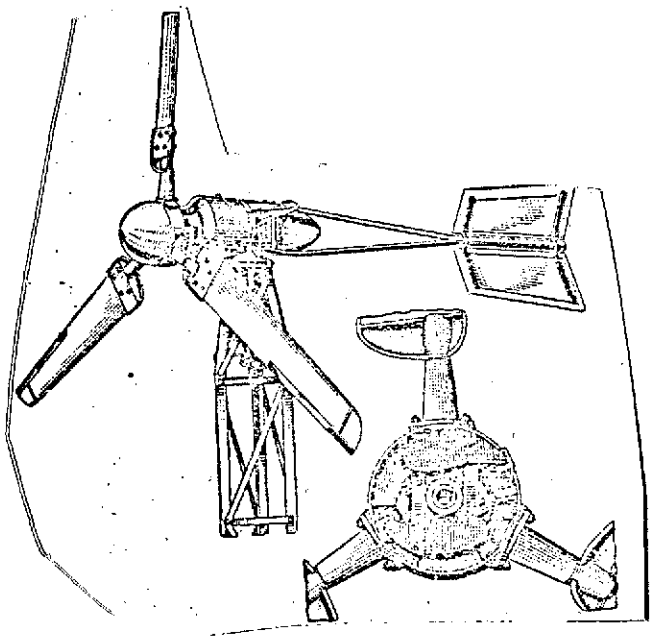

Fig. 166: Wind-driven electrical engine "Roralight".

wind engines have an extremely high metal content. The weight of rapid wind engines averages /256 from 300-400 kg per 1 hp, while of the low speed engines -- from 500-800 kg per 1 hp.

Table 10 presents the weight of wind engines of Soviet and foreign production.

Let us note in this table the values of column 10 which contains the weight of engines related to unit area marked off by the wind-driven wheel. It appears that the multi-bladed wind engines, which belong to the group of low-speed engines, are almost twice heavier than the rapid engines with a small number of blades.

The curves in Figs. 167 and 168 present a comparison between the weight of wind engines produced in the USSR. In Fig. 167, the weight of the low- and high-speed wind engines are given, taking into account the weight of the tower, while Fig. 168 presents the curve of the weight of the wind engine without accounting for the weight of the tower. These curves show that the low-speed wind engines are 30-65% heavier than the rapid ones when the weight of the tower is taken into account, and from 80-125% heavier when the weight of the tower is not considered.

The curve in Fig. 169 illustrates the change in the relative /257 weight of rapid wind engines VIME D-5, VIME D-12, VIME D-3 and TsVEI D-50 with similar aerodynamic parameters, constructed and designed in Soviet plants.

Hence, we see that the specific weight of wind engines, i.e. /260 the weight related to unit area marked off by the wind-driven wheel, increases markedly with the increase in the diameter of the wind-driven wheel. This indicates that one should not be carried away by the large dimensions of wind engines.

Fig. 170 presents the weight curves in relation to the diameter of the wind-driven wheel in foreign wind engines with multiple blades: I--for the English wind engine "Hercules"; II--for the American wind engine "Samson"; III-American wind engine "Aeromotor";

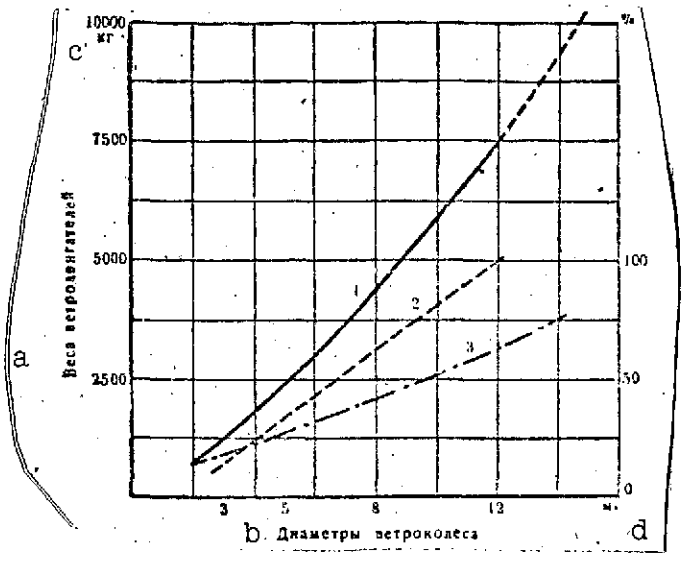

Fig. 167: Curves of the overall weight of wind engines: 1-weight of low-speed wind engines; 2-weight of high-speed wind engines; 3-curve of the excess weight of low-speed wind engines above the weight of rapid ones in %.

Key: a-weight of the wind-engine
b-diameter of the wind driven wheel
c-kg
d-m

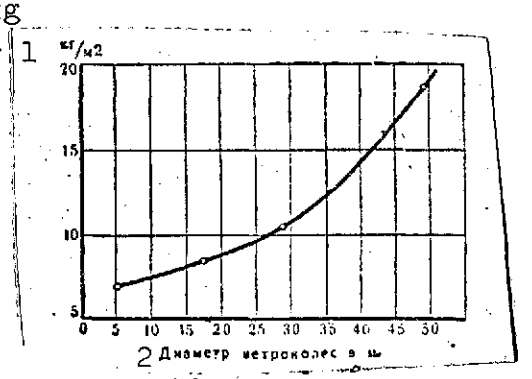

Fig. 169: Characteristics of the weight of wind-driven wheels per square m of the marked off area in rapid wind engines.

Key: 1-kg/m^2
2-diameter of the wind-driven wheel in m.

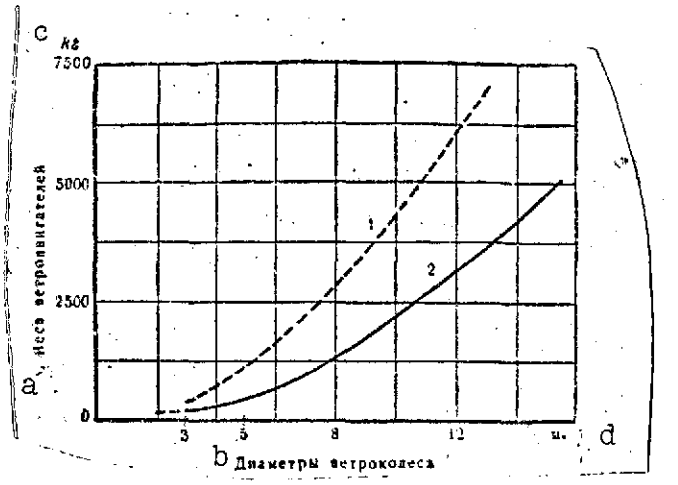

Fig. 168: Weight curves of wind engines without the tower: 1-weight of low-speed wind engines; 2-weight of rapid wind engines.

Key: a-weight of the wind engine
b-diameter of the wind-driven wheel
c-kg
d-m

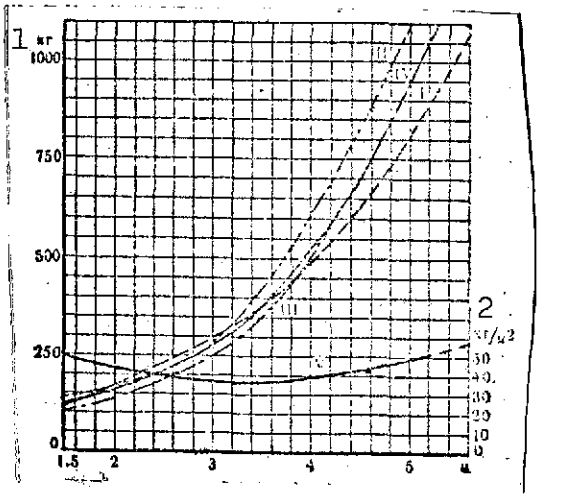

Fig. 170: Characteristic of the weight of wind engines.

Key: 1-kg
2-kg/m^2

ORIGINAL PAGE IS
OF POOR QUALITY

TABLE 10: DATA ABOUT THE WEIGHT OF WIND ENGINES.

Name of the wind engine	Diameter of wind driven wheel (in M)	No. of blades	Marked off area (in sq m)	Wt. of individual parts of wind engines (kg): Wind-driven Wheel	tail	head	reducing gear	Wt. of wind engine without tower (in kg)	Wt. of engine related to unit marked off area (in kg)	Wt. of tower (in kg)	Ht. of tower (in m)
1	2	3	4	5	6	7	8	9	10	11	12
Soviet Production											
Multi-bladed (TV-5)	5	18	19,6	344	92	535	320	1 291	66	1 198	15
TV-8	8	18	50,3	820	160	580	380	1 950	38,8	1 900	15
Rapid VIME D-12	12	3	113,0	796	195	1 220	230+ shaft 308	2 755	24,3	1 682	16
VIME D-5	5	3	19,6	135	65	165	210	575	29,4	1 300	15
VIME D-30	30	3	707	7 526	—	10 125	7 949	25 600	36,2	16 134	24
VIME D-3, wings made of aviation mat.	3	3	7,07	7	2,4	25	—	44,4	6,25	15,3	4
Rapid Ts VEI D-12	12	3	113	1 129	794	1 021	—	2 944	26,0	2 553	12
Crimean TsAGI D-30	30	3	707	—	—	—	—	33 900	48	15 170	25
Superpower TsVEI D-50 (project)	50	3	1 960	37317	—	73 000	Included in wt. of head	108 000	55	52 000	50
Rotor TsVEI F=13,D=2m N=6.5	Span of the rotor 10	2+2	13	850	—	—	—	850	65	1 763	13,5
Wind Engine of Ufimtsev-Vetchinkin	3	3	78,5	420	250	960	Vertical shaft 323	1 958	25	—	40
Wind Engine PD-3 (Made of dural)		2	7,07	9	4	13	—	26	2,7	Tube 14	4
Multi-bladed Foreign											
"Samson" USA	3,05	18	7,3	—	—	—	—	237	35,6	—	—
	4,9	24	18,8	—	—	—	—	1 010	54	—	—
"Stover"	3,05	18	7,3	—	—	—	—	252	34,5	—	—
"Star" USA	4,3	18	14,5	—	—	—	—	772	53,0	—	—
"Aeromotor"	3,05	18	7,3	—	—	—	—	262	36,0	495	16,2
	4,9	18	18,8	—	—	—	—	950	50,5	1 090	16,2
"Hercules" England	3,05	18	7,3	—	—	—	—	254	35	640	15,2
	4,9	18	18,8	—	—	—	—	920	49	980	15,2
	5,5	18	23,7	—	—	—	—	1 000	42	1 040	15,2

IV-curve of the average weight of the wind engine in relation to the diameter of the wind-driven wheel, which was plotted on the basis of curves I, II, and III; V-curve of the average weight of the wind engine per square m of area marked off by the wind-driven wheel.

The last curves shows that multi-bladed wind engines with a diameter of 3 to 3.5 m have the minimal weight.

The calculation of the strength of a mechanism or structure is determined by the magnitudes load and permissible stress. The methods presented below make it possible to determine the magnitude of the load; standardization of the stress related to calculations of wind engines is presently extremely difficult due to the insufficient experience with this method.

40. Wind Load on the Wings and Calculations of the Strength of the Wings.

The load on an elementary area of the blade with a width b and length dr, is equal, according to equation (85), to: $dP = C_y b dr \frac{\rho W^2}{2}$,

where: C_y is the coefficient of the lifting force of the wing;
ρ is the density of the air;
W is the relative velocity of the airstream which dashes over an element of the blade;
r is the distance of the blade from the axis of rotation of the wind-driven wheel.

The relative velocity of the airstream:

$$W = \sqrt{\omega^2 r^2 + V^2},$$

where: ωr is the circular velocity of an element of the blade;
V is the velocity of the wind.

Consequently:

$$dP = C_y b dr \frac{\rho}{2} (\omega^2 r^2 + V^2). \quad (a)$$

Assuming that $C_y b$ are constant throughout the length of the wing and /262 integrating, we obtain the total load on the wings:

$$P = C_y b \frac{\rho}{2} \int_{r_0}^{R} (\omega^2 r^2 + V^2) dr = \quad (b)$$

$$= C_y b \frac{\rho}{2} \left[\frac{\omega^2}{3} (R^3 - r_0^3) + V^2 (R - r_0) \right].$$

Placing $(R - r_0)$ in front of the bracket, we obtain:

$$P = C_y \frac{\rho}{2} b (R - r_0) \left[\omega^2 \frac{R^2 + R r_0 + r_0^2}{3} + V^2 \right]. \quad (c)$$

Let us note: $b(R - r_0) = S$ -- area of the blade,

$\frac{R^2 + R r_0 + r_0^2}{3} = r_m^2$ -- hypothetical radius of the wings. (178)

Substituting S and r_m in equation (c), we obtain the over-all load on the wing:

$$P = C_y \frac{\rho}{2} S (\omega^2 r_m^2 + V^2). \quad (179)$$

During wind gusts which come with high velocities and to which the wind-driven wheel cannot instantaneously adapt, the wings may be overloaded. The ratio of the maximal possible load on the wings P_{max} which appears during wind gusts to the working load at a calculated velocity of the wind P_p is called the coefficient of overloading.

$$n = \frac{P_{max}}{P_p}. \tag{180}$$

Let us denote the velocity of the wind during a wind gust V_n and let us write the equation of the load on the wings as V and V_n:

$$P = C_y S \frac{\rho}{2} (\omega^2 r_m^2 + V^2), \tag{179}$$

$$P_{max} = C_{yn} S \frac{\rho}{2} (\omega^2 r_m^2 + V_n^2), \tag{179a}$$

where C_{yn} is the coefficient of the lifting force during a wind gust.

Taking the ratio of the equation (179a) to (179), we obtain the expression for the coefficient of overload in the following form:

$$n = \frac{P_{max}}{P} = \frac{C_{yn} (\omega^2 r_m + V_n^2)}{C_y (\omega r_m^2 + V^2)}.$$

Since forces P and P_{max} are calculated at a maximal value $C_y = C_{yn}$, we can assume: /263

$C_{yn}/C_y = 1$; consequently:

$$n = \frac{\omega^2 r_m^2 + V_n^2}{\omega^2 r_m^2 + V^2}. \tag{d}$$

Let us note:

$$k = V_n/V$$

and $z_m = \frac{\omega r_m}{V}$ -- hypothetical number of modules at $r = r_m$.

Substituting these values in equation (d) and dividing the numerator and denominator of the right side by V^2, we obtain:

$$n = \frac{\frac{\omega^2 r_m^2}{V^2} + \frac{V_n^2}{V^2}}{\frac{\omega^2 r_m^2}{V^2} + \frac{V^2}{V^2}} = \frac{z_m^2 + k^2}{z_m^2 + 1}; \tag{181}$$

the value of C_y in equation (179) should be taken as maximal.

In determining the internal force on the bearings as well as on the tower, P_f (i.e. the overall frontal pressure on the wind-driven wheel should be known. The magnitude of this pressure is obtained by multiplying equation (179) by the number of blades i and by the coefficient of overloading n, i.e.:

$$P_f = C_y S \frac{\rho}{2} (\omega^2 r_m^2 + V^2) in. \tag{182}$$

The maximal load on the wings:

$$P_{max} = \frac{P_{\Sigma}}{i}. \qquad (183)$$

Let us examine two cases of operation of the wind-driven wheel: 1-under load and 2-without load. In both cases, the direction of the wind is perpendicular to the plane of rotation of the wind-driven wheel.

Case I. The wind engine is under load. The equation of pressure on the blade:

$$P = C_y S \frac{\rho}{2} (\omega^2 r_m^2 + V^2), \qquad (179)$$

where C_y -- maximal coefficient of the lifting force, the value of which for multi-bladed wind engines is presented in the table below.

Width of the blade / height of the arch $\frac{b}{l}$	8	10	14	16	20	25	60	∞
C_y maximum values	1.56	1.46	1.36	1.26	1.12	0.98	0.80	0.74

For a rapid wind engine with "espero" profile, the value of C_y is taken from the graph (Fig. 171) where the value of C_y was obtained for an angle of attack $\alpha = 10$. For other profiles, C_y should be selected according to their wind tunnel tests. The characteristics of certain profiles were presented in Fig. 35, I, II, III and IV in Chapter 2. /264

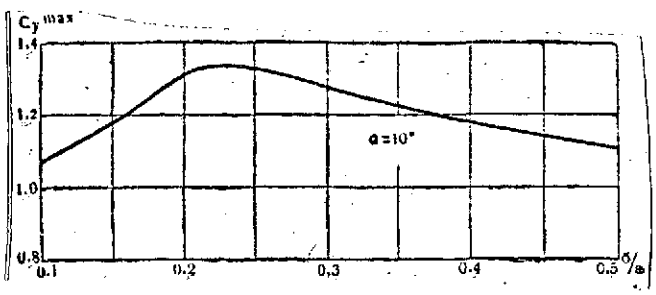

Fig. 171: Graph of C_y in relation to δ/b for an "espero" profile.

Case II. The wind-driven wheel stands in the plane of rotation perpendicular to the wind flow at a working velocity V; the load of the working machine is excluded:

$$P_{max} = \frac{X}{i}, \qquad (184)$$

Where: X is the frontal pressure on the wind-driven wheel measured in Kuchino's wind tunnel; is the number of blades.

$$X = \bar{x}\pi R^2 \rho \frac{V^2}{2}. \qquad (154)$$

The values of $\bar{x}$ -- coefficients of the frontal pressure, when the wind engine is without any load:
Multiple bladed wind-driven wheel with cylindrical arch $\bar{x} = 0.642$ /265
Four bladed "Syun" wind-driven wheel with aerodynamic profile $\bar{x} = 0.412$

Example 1. Determine the frontal pressure and the load on the wing of the wind engine at a wind velocity V = 10 m/sec.

The wind-driven wheel has a diameter D = 16 m; $r_0 = 0.1\ D = 1.6$ m; the width of the blade at the level of the section which is nearest to the center of the wind-driven wheel is $b_1 = 1.8$ m, while at the external end it is $b_2 = 0.8$ m; $\delta/b = 0.16$. The number of modules $Z_n = 3$ and the number of blades i = 4.

The frontal pressure equals, according to equation (182):

$$P_A = C_y \frac{\rho}{2} S (\omega^2 r_m^2 + V^2) in.$$

$C_y = 1.2$ -- maximum coefficient of the lifting force which is found from the graph in Fig. 171 at $\delta/b = 0.15$.
$\rho = 0.125$ -- mass density of the air at 15^0 and 760 mm Hg.

$$S = \frac{1.8+0.8}{2}(8-1.6) = 8.3\ м^2$$

-- area of the blade.

$$\omega = \frac{Z_n V}{R} = \frac{3 \cdot 10}{8} = 3{,}75\ -$$

-- angular velocity of the wind-driven wheel.

$$r_m = \sqrt{\frac{R^2 + R r_0 + r_0^2}{3}} = \sqrt{\frac{8^2 + 8 \cdot 1{,}6 + 1{,}6^2}{3}} = 5{,}14\ -$$

-- hypothetical radius of the wing.

Here

$$n = \frac{Z_m^2 + k^3}{Z_m^2 + 1} = \frac{1{,}93^2 + 1{,}5^3}{1{,}93^2 + 1} = \frac{5.97}{4{,}72} = 1{,}26$$

$$k = \frac{V_n}{V} = 1{,}5;$$

$$Z_m = \frac{\omega r_m}{V} = \frac{3{,}75 \cdot 5{,}14}{10} = 1{,}93.$$

Substituting numerical values in equation (182), we obtain:

$$P_A = 1{,}2 \cdot \frac{0{,}125}{2} \cdot 8{,}3 (3{,}75^2 \cdot 5{,}14^2 + 10^2) \cdot 1{,}26 \cdot 4 = 1\,990\ kg.$$

The load on the wing is found from the equation (183): /266

$$P_{max} = \frac{P_A}{4} = \frac{1\,990}{4} = 498 kg.$$

Distribution of the wind load on the wing. The load is distributed along the length of the blade proportionally to the distances of the blade's sections from the axis of rotation of the wind-driven wheel. It is common usage to represent this load graphically in the form of a line which forms a certain angle with the axis of the flap. The load is distributed on the cord of the wing in the shape of a triangle (Fig. 172).

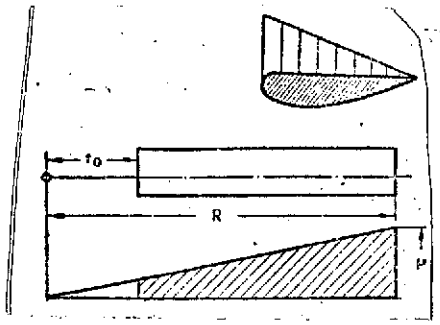

Fig. 172: Distribution of the load along the length and the cord of the blade.

The load on the blade is determined by the method of A. I. Makarevskiy, who represented it as the volume of a trihedral cut pyramid, with its tip directed towards the center of the wind-driven wheel (Fig. 173).

The volume of such a pyramid is equal to:

$$V=\frac{h}{3}(f+F+\sqrt{fF});$$

According to the notation in Fig. 173, we have:

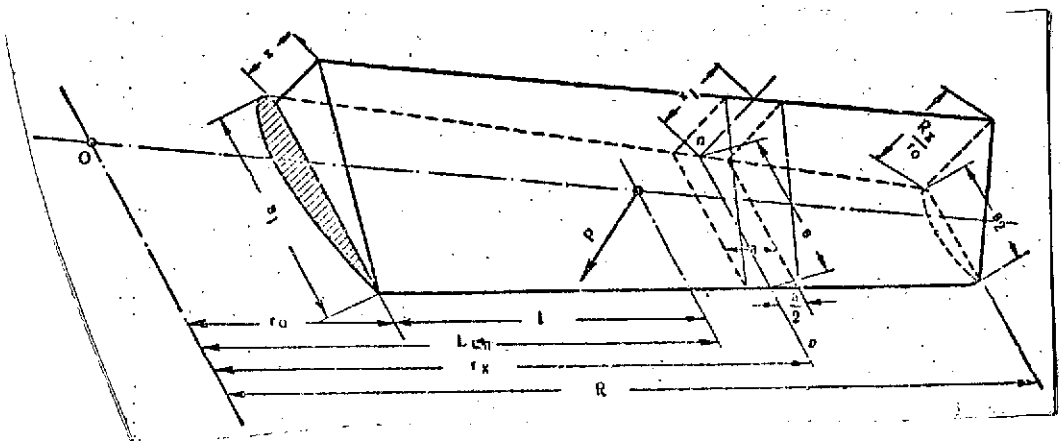

Fig. 173: Volumetric load on the blade.

$h=R-r_0$ -- height of the pyramid;

$f=\frac{b_1 x}{2}$ -- base of the pyramid, nearest to the center of the wind-driven wheel;

$F=\frac{b_2 x \frac{R}{r_0}}{2}$ -- base of the pyramid, removed from the center.

Substituting these expressions, we obtain:

$$V=\frac{R-r_0}{3}\left(\frac{b_1 x}{2}+\frac{b_2 x\frac{R}{r_0}}{2}+\sqrt{\frac{b_1 x}{2}\cdot\frac{b_2 x\frac{R}{r_0}}{2}}\right)=$$
$$=\frac{x(R-r_0)}{6}\left(b_1+b_2\frac{R}{r_0}+\sqrt{b_1 b_2\frac{R}{r_0}}\right).$$

Let us replace the subradical expression b_1 by its value, obtained from relation: /268

$$\frac{b_1}{b_2}=\frac{r_0}{R},$$

hence: $b_1 = b_2 \frac{r_0}{R}$.

Substituting under the radical, we obtain:

$$V = \frac{x(R-r_0)}{6}\left(b_1 + b_2\frac{R}{r_0} + \sqrt{b_2\frac{r_0}{R}\cdot b_2\frac{R}{r_0}}\right) = \frac{x(R-r_0)}{6}\left[b_1 + b_2\left(\frac{R}{r_0}+1\right)\right].$$

Assuming that the ordinate x = 1 m, we obtain:

$$V = \frac{R-r_0}{6}\left[b_1 + b_2\left(\frac{R}{r_0}+1\right)\right] \text{ m}^3. \qquad (185)$$

If we consider the volume of the load in the shape of a prismatoid with two parallel sides, we can write the following formula for such a volume: $V = \frac{h}{6}(f + F + 4M)$,

where, according to Fig. 173, we have:

$h = R - r_0$ -- height of the prismatoid;

$f = \frac{b_1 x}{2}$ -- area of the first bases of the prismatoid;

$F = \frac{b_2 x}{2}\cdot\frac{R}{r_0}$ -- area of the second bases, parallel to the first;

$M = \frac{b_1 + b_2}{2}\cdot\frac{x + x\frac{R}{r_0}}{2}\cdot\frac{1}{2}$ -- area of the middle section, which is equidistant from the parallel bases.

Substituting the values of h, f, F and M in the equation of the volume of the prismatoid, we obtain:

$$V = \frac{R-r_0}{6}\left(\frac{b_1 x}{2} + \frac{b_2 x\frac{R}{r_0}}{2} + 4\frac{b_1+b_2}{2}\cdot\frac{x + x\frac{R}{r_0}}{2}\cdot\frac{1}{2}\right).$$

After transformation of this equation for x = 1, we obtain:

$$V = \frac{R-r_0}{6}\left[b_1\left(1 + \frac{R}{2r_0}\right) + b_2\left(\frac{1}{2} + \frac{R}{r_0}\right)\right]. \qquad (186)$$

Equation (185) is recommended for wings with a trapezoid shape of the blade, which narrows towards the center of the wind-driven wheel, used in multi-bladed wind engines. Equation (186) is more suitable for wings with a trapezoid shape of the blade, which narrows towards the center of the wind-driven wheel, as used in rapid wind engines. /269

Specific load. The ratio of the load on the wing to the volumetric load is called specific load, the magnitude of which is:

$$p = \frac{P_{max}}{V} = \frac{P_{max}}{\frac{R-r_0}{6}\left[b_1 + b_2\left(\frac{R}{r_0}+1\right)\right]} \text{ kg/m}^3 \qquad (187)$$

for blades, which narrow towards the center, and

$$p = \frac{P_{max}}{V} = \frac{P_{max}}{\frac{R-r_0}{6}\left[b_1\left(1 + \frac{R}{2r_0}\right) + b_2\left(\frac{1}{2} + \frac{R}{r_0}\right)\right]} \text{ kg/m}^3 \qquad (188)$$

for blades which widen towards the center.

The position of the center of effort of the sail area or of the resultant load P, is found in the following way, using the notations in Fig. 173.

The cord of any section at a distance l from the base of the blade is expressed by the equality:

$$b_l = b_1 - \frac{(b_1 - b_2)}{(R - r_0)} \cdot l. \qquad \text{(a)}$$

The largest load at the level of the spout of the blade for the same section is equal to:

$$x_l = x\left(1 + \frac{l}{r_0}\right). \qquad \text{(b)}$$

The elementary volume of the load is:

$$dV = \frac{b_l \cdot x_l}{2} dl = \frac{x}{2}\left(b_1 - \frac{b_1 - b_2}{R - r_0} \cdot l\right)\left(1 + \frac{l}{r_0}\right) dl. \qquad \text{(c)}$$

Let us write the general expression for the position of the center of effort of the sail area:

$$L_{yn} = r_0 + \frac{\int_0^{R-r_0} dVl}{V},$$

where V -- the over-all volumetric load on the wing.

Solving the integral and dividing the results by V, which is /270 known from equation (186), we obtain L_{yn}.

$$\int_0^{R-r_0} dVl = \int_0^{R-r_0} \frac{b_l x_l}{2} dl \cdot l =$$

$$= \int_0^{R-r_0} \frac{x}{2}\left(b_1 - \frac{b_1 - b_2}{R - r_0} \cdot l\right)\left(1 + \frac{l}{r_0}\right) l \cdot dl =$$

$$= \frac{x}{2}\left[b_1 \frac{(R-r_0)^2}{2} + \left(\frac{b_1}{r_0} - \frac{b_1 - b_2}{R - r_0}\right)\frac{(R-r_0)^3}{3} - \frac{(b_1 - b_2)}{(R-r_0)r_0} \cdot \frac{(R-r_0)^4}{4}\right] =$$

$$= \frac{x}{2}(R-r_0)^2\left[\frac{b_1}{2} + \frac{b_1}{3r_0}(R-r_0) - \frac{b_1 - b_2}{3} - \frac{b_1 - b_2}{4r_0}(R-r_0)\right] =$$

$$= \frac{x}{2} \cdot \frac{(R-r_0)^2}{12}\left[b_1 + b_2 + b_1\frac{R}{r_0} + 3b_2\frac{R}{r_0}\right].$$

Dividing this expression by the right hand side of equation (186) and taking $x = 1$, we obtain: L'_{yn} at the base of the blade:

$$L'_{yn} = \frac{R - r_0}{2} \cdot \frac{\left(b_1 + b_2 + \frac{b_1 R}{r_0} + 3b_2\frac{R}{r_0}\right)}{\left(2b_1 + b_2 + b_1\frac{R}{r_0} + 2b_2\frac{R}{r_0}\right)}. \qquad (189)$$

Adding up r_0, we obtain L_{yn} from the axis of rotation of the wind wheel:

$$L_{yn} = r_0 + \frac{(R - r_0)}{2} \cdot \frac{\left(b_1 + b_2 + b_1\frac{R}{r_0} + 3b_2\frac{R}{r_0}\right)}{\left(2b_1 + b_2 + b_1\frac{R}{r_0} + 2b_2\frac{R}{r_0}\right)}. \qquad (190)$$

The dimension of the wing is usually radius $r_0 = 0.2R$ for almost all wings, the rapid wind engines have a width $b_2 \approx 1/2\ b_1$; in the wing of windmills $b_2 = b_1$, while in multi-bladed wind engines, $b_2 \approx 2b_1$. Substituting these values in equations (186) and (190), we obtain simple expressions for a rapid calculation of the volumetric load V and for the position of the center of effort of the sail area L_{yn} for different wings.

For rapid wings with a narrow tip of the blade:

$$V = 0.833Rb_1 \quad \text{(a)}$$

$$L_{yn} = 0.648R. \quad \text{(b)}$$

For multi-bladed wings: /271

$$V = 1.74Rb_1, \quad \text{(c)}$$

$$L_{yn} = 0.724R. \quad \text{(d)}$$

For the wings of windmills:

$$V = 1.2Rb_1, \quad \text{(e)}$$

$$L_{yn} = 0.688R. \quad \text{(f)}$$

Load on the rib of the wings. Let us take the distance between the ribs equal to a, consequently, the load over this distance is distributed between the two ribs in such a manner that one part of it over distance a/2 corresponds to one rib, while another part over distance a/2 corresponds to the other. The magnitude of the load on the rib is found by multiplying the specific load [see equation (187) and (188)] by the volume ΔV of the areodynamic load on the rib.

Let us determine the volume ΔV by integrating:

$$dV = \frac{1}{2} b \cdot x \cdot dr_x = \frac{1}{2}\left(b_1 - \frac{b_1 - b_2}{R - r_0}\right)(r_x - r_0)\frac{r_x}{r_0} \cdot dr_x =$$

$$= \frac{1}{2r_0(R - r_0)}(b_1 R - b_1 r_0 - b_1 r_x + b_1 r_0 + b_2 r_x - b_2 r_0) r_x dr_x =$$

$$= \frac{1}{2r_0(R - r_0)}[(b_1 R - b_2 r_0) \cdot r_x - (b_1 - b_2) r_x^2] dr_x.$$

If we denote the distance between the center of the wind-driven wheel and the rib by r_x, the unknown volume will be between the limits from $r_x - a/2$ to $r_x + a/2$, i.e.:

$$\Delta V = \int_{r_x - \frac{a}{2}}^{r_x + \frac{a}{2}} dV$$

Substituting here the value of dV and integrating, we obtain the volume of the load on one rib:

$$\Delta V = \frac{a}{2r_0(R-r_0)}\left[(b_1R - b_2r_0)r_x - (b_1-b_2)\left(r_x^2+\frac{a^2}{12}\right)\right] \text{ м}^3.$$

Multiplying the specific load p by this volume, we obtain the load on one rib: /272

$$Q_x = p\cdot\Delta V = \frac{Pa}{2r_0(R-r_0)}\left[(b_1R - b_2r_0)r_x - (b_1-b_2)\left(r_x^2+\frac{a^2}{12}\right)\right] \text{kg}, \quad (191)$$

where: a -- distance between the ribs;
r_x -- distance from the rib to the axis of the wind-driven wheel;
b_1 -- width of the blade at the tip which is turned towards the center of the wind-driven wheel;
b_2 -- width of the blade at the external tip;
p -- specific load on the blade which widens towards the center of the wind-driven wheel [equation (188)].

Those blades which rise towards the external circumference are used only in the multi-bladed wind-driven wheels of small diameters, and usually have no ribs.

Example 2. Determine the load on the rib of a wing of previous example 1, if the distance between the ribs and the axis of the wind-driven wheel r_x = 5 m; the distance between the ribs is a = 0.6 m.

r_0 = 1.6 m; R = 8 m; b_1 = 1.8 m; b_2 = 0.8 m (Fig. 173).

Solution. The load on the wing, according to example 1, is equal to P_{max} = 498 kg.

Let us find the volume of the load on the wings, according to equation (186):

$$V = \frac{R-r_0}{6}\left[b_1\left(1+\frac{R}{2r_0}\right)+\left(\frac{1}{2}+\frac{R}{r_0}\right)\right] =$$
$$= \frac{8-1.6}{6}\left[1{,}8\left(1+\frac{8}{2\cdot 1{,}6}\right)+\left(\frac{1}{2}+\frac{8}{1{,}6}\right)\right] = 11.5 \text{ м}^3.$$

The specific load p is found according to equation (188):

$$p = \frac{P_{max}}{\frac{R-r_0}{6}\left[b_1\left(1+\frac{R}{2r_0}\right)+\left(\frac{1}{2}+\frac{R}{r_0}\right)\right]} = \frac{498}{11{,}5} = 43.5 \text{ kg/m}^3$$

The load on the rib of the wing at a distance r_x = 5 m from the axis of the wind-driven wheel, is equal, according to equation (191), to:

$$Q_x = \frac{p \cdot a}{2r_0(R-r_0)}\left[(b_1R - b_2r_0)\,r_m - (b_1 - b_2)\left(r_x^2 + \frac{a^2}{12}\right)\right] =$$
$$= \frac{43.5 \cdot 0.6}{2 \cdot 1.6\,(8-1.6)}\left[(1.8 \cdot 8 - 0.8 \cdot 1.6)5 - \right.$$
$$\left. - (1.8 - 0.8)\left(5^2 + \frac{0.6^2}{12}\right)\right] = 51.7 \text{ kg}.$$

The load on the rigidly attached part of the wing during regulation by rotation of the blade tip. /273

The rigidly attached part of the wing is subjected to the highest load during a storm. Therefore, in determining the load on this part of the wing, the maximum velocity of the wind V_{st} for regions with annual average wind velocity

up to 5.5 m/sec.....40 m/sec,
from 5.5 to 7 m/sec.....50 m/sec,
and above 7 m/sec.....60 m/sec.

The frontal pressure on the rigid part of the blade is equal, according to equation (179), to:

$$P_{ri} = C_y S_{ri} \frac{\gamma}{2}\left(\omega^2 r_m^2 + V_{st}^2\right),$$

where: $C_y = 1.28$ -- coefficient of the lifting force;
S_{ri} -- area of the rigid part of the blade;
r_m -- hypothetical radius of the wing, which is determined by means of equation (178), where R is taken from the center of the wind-driven wheel to the tip of the rigid part of the blade.

The load on the rotating part of the blade. When the wind engine operates under a storm, the moment of the rotating part of the blade M_{ro} acts in the opposite direction and balances the excess moment M_{ex} developed by the rigid part of the blade M_{ri}, i.e.:

$$M_{ex} = M_{ro} = M_{ba} - M_{ri},$$

where M_{ba} is the moment developed by the blade when the power of the engine is balanced [see equation (193)].

Hence, the force applied at the rotating part of the blade will be equal to:

$$P_{ro} = \frac{M_{ba} - M_{ri}}{R_x} \quad (192)$$

where:

$$M_{ba} = \frac{75 \cdot N_{ba}}{\omega}; \quad (193)$$

$$M_{ri} = \frac{75 \cdot N_{ri}}{\omega}; \quad (194)$$

R_x -- distance of the point of application of force P_{ro} to the axis of rotation of the wind-driven wheel. /274

The power of a wind-driven wheel which has a diameter D_{ri} between the limits of a circumference which passes through the tips of the rigid part of the blade, equals, according to equation (137):

$$N_{ri}=0.000654\,D_{ri}^{2}V_{st}^{3}\xi_{st} \qquad (137a)$$

here ξ_{st} should be determined on the basis of the number of modules according to the aerodynamic characteristic of the given wind-driven wheel.

$$Z_{st}=\frac{\omega R_{ri}}{V_{st}},$$

where:

$$R_{ri}=\frac{D_{ri}}{2}.$$

Let us find ξ_{st} on the basis of a given Z_{st} according to the characteristic and let us substitute it in equation (137a). The normal power N_{ba} is found at ξ_{max}. Having the numerical values of N_{ri} and N_{ba}, let us find M_{ri} and M_{ba} and, finally, P_{ro} [see equations (192), (193) and (194)].

After determining the pressure P_{ro} on the rotating part of the wing, let us find C_y by means of equation (179):

$$C_y=\frac{2P_{ro}}{S_{ro}\rho(\omega^2r_m^2+V^2)}. \qquad (195)$$

After we obtain C_y for a given ratio δ/b, let us find from the graph in Fig. 63, the angle of attach α, which should be expected to be negative.

The load on the turning blade stabilizer is equal to:

$$Q_{st}=C_y\frac{\rho}{2}S_{st}(\omega^2r_{st}^2+V^2), \qquad (196)$$

where: C_y is the maximal coefficient of the lifting force;
$C_y = 0.9$ at $\delta/b = 0.17$;
S_{st} is the area of the stabilizer;
ω is the angle of velocity of the wind-driven wheel;
r_{st} is the radius of the stabilizer, which is equal to the distance from the center of effort of the sail area of the stabilizer to the axis of the shaft of the wind-driven wheel;
V is the working velocity of the wind in m/sec, at which the engine develops its full power.

The distribution of the load along the length of the turning power of the wing is homogeneous while the distribution along the cord is triangular. /275

The load on the flap. Two cases of loading are examined in this calculation of the strength of the flap.

Case 1. The axis of the flap has a horizontal position; O and D are supports of the flap; E and K are supports of the wing (Fig. 174).

The flap is subjected to the action of a moment of the weight forces M_g, the moment of the aerodynamic forces M_a and the elongation caused by the centrifugal forces C:

$$M_g = G(L_{cg} - \ell),$$

Where G is the weight of the wing determined by its outline;

L_{cg} is the distance between the center of gravity of the wind and its axis of rotation; it is assumed to be $L_{cg} = 0.48$ R;

ℓ distance from the axis of rotation to the dangerous section; $\ell = 0.2$ up 0.25 R.

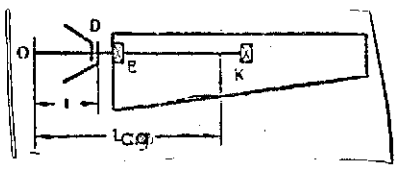

Fig. 174: Diagram of the wing for calculation of the flap in its horizontal position.

The moment in the dangerous section equals:

$$\begin{aligned} M_g &= G\cdot(0.48R - 0.25R) = G\,0.23R, \\ M_a &= P_{max}(L_{cg} - l), \end{aligned} \qquad (197)$$

where: L_{cg} is the distance from the center of effort of the sail area to the axis of rotation of the wind-driven wheel;

P_{max} is the load on the wing, which is determined by means of equations (182) and (183); the calculated moment:

$$M = \sqrt{M_g^2 + M_a^2}, \qquad (198)$$

the centrifugal force:

$$C = m\omega^2 r = \frac{G}{9.81}\omega^2 L_{um} = \frac{G}{9.81}\omega^2 0.48R = 0.049 G_{sp}\omega^2 R. \qquad (199)$$

the stress in the dangerous section of the flap:

$$k = \frac{M}{W} + \frac{C}{F}, \qquad (200)$$

where: F is the area of the section of the flap;
M is the overall moment which bends the flap.

Case 2. The axis of the flap has a vertical position; the wing/276 points downward.

The flap is subjected to the action of: 1-the moment of the aerodynamic forces M_a; 2-the moment of the gyroscopic forces M_g; 3-the moment of centrifugal forces M_{cf} and 4-the weight forces of the wing G.

$$\begin{aligned} M_a &= P_{max}(L_{cg} - l) \\ M_g &= \left[\int_l^R dmr^2 - l\int_l^R dmr\right] 2\omega\omega_1, \end{aligned} \qquad (201)$$

where the difference between the integrals inside the brackets is equal to:

I -- the moment of inertia of the wing relative to the axis of rotation of the wind-driven wheel;

ω -- angular velocity of rotation of the wing;

ω_1 -- angular velocity of rotation of the head with the wind-driven wheel relative to the axis of the tower.

Consequently:

$$M_g = I 2\omega\omega_1. \tag{201a}$$

The stress in the dangerous section of the flap:

$$\sigma = \frac{M_a + M_g}{W} + \frac{G + G}{F}. \tag{202}$$

In calculating the spars of the wing, the gyroscopic moment is not accounted for, since the mass of the spars themselves is a very small value. In calculating the flap, the gyroscopic moment cannot be neglected, since this moment is determined by the entire mass of the wing (spars, ribs, supports, regulating flyweights, ect.).

The stress which appears on account of the moment of centrifugal forces has to be added to the stress in the dangerous section of the flap. The magnitude of this moment can be found by means of equation (175):

$$M_{cf} = I_w \frac{\omega^2 \sin 2\varphi}{2},$$

where: I_w is the moment of inertia of the wing with the stabilizer relative to the axis of the flap;

φ is the rigging angle.

The ratios of the moments of inertia of the blade and of the stabilizer are of approximately equal.

$$I_{st} = 0{,}75\, I_w, \quad I_b = 0{,}25\, I_w.$$

Calculation of the strength of the wings with stabilizers is performed in the following sequence. /277

First, the calculated load on the wing is estimated from equation (179):

Second, the strength of the flap is calculated from equation (202) and

Third, using the obtained dimensions of the flap, the δ/b of the profile is determined based on the disposition of the flap, after which one can proceed to design the wing; a tracing is made of the matched sections of the wing and the spars are placed in it.

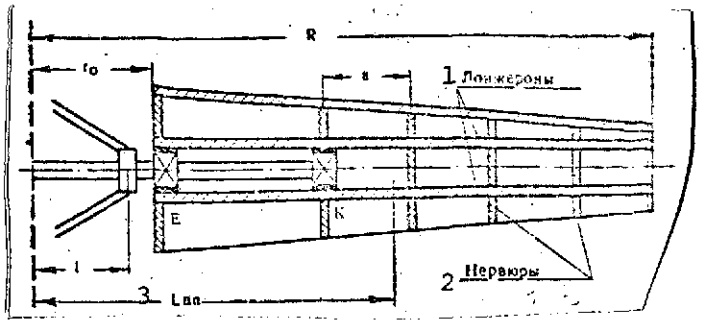

Fig. 175: Diagram of a two-spar wing.

Key: 1-spar
2-rib
3-Lcg

After having obtained the design shape of the wing, the spars are calculated.

We shall present the calculation of a two-spar wing (Fig. 175 and 176). The wind load on the blade causes forces P_1 and P_2 on the spar:

$$P_1=\frac{Q_x}{l}\left(m+\frac{l}{2}-\frac{1}{3}b\right);\quad P_2=\frac{Q_x}{l}\left[\frac{1}{3}b-\left(m-\frac{l}{2}\right)\right].$$

These formulas are derived according to Fig. 176. The force Q_x -- the load on the ribs, is determined by means of equation (191).

The spars are calculated as cantilever beams on two supports E and K (Fig. 175). The concentrated forces P_1 and P_2 are applied at the sides of attachment of the ribs (Fig. 176).

Calculation of the stabilizer. The load on the stabilizer of rapid wind engines is determined according to equation: /278

$$Q=C_{y\,max}f_{st}\frac{\rho}{2}(\omega^2r_{st}^2+V_p^2).$$

This load, which is distributed uniformly along the length of the spar and as a triangle along its cord, bends the spar with a moment:

$$M_u=\frac{Ql_{st}}{8}, \qquad (203)$$

where: l_{st} is the length of the stabilizer (Fig. 177).

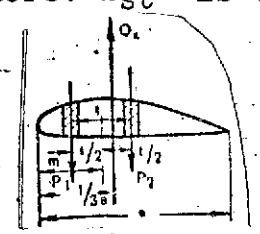

Fig. 176: Section through a two-spar wing.

In addition, the torque M_t which appears as a result of the shift in the center of effort of the sail area relative to the axis of the spar, acts on the spar of the stabilizer. Since the load is distributed in the shape of a triangle on the cord, the center of effort of the sail area is at a distance of 1/3 of the cord from the spout of the stabilizer, consequently:

$$M_t=Q\left(\frac{1}{3}b_{st}-m_{st}\right), \qquad (204)$$

where b_{st} and m_{st} are given in Fig. 177.

When the ratio of the permissible stress of flection $k_{f\ell}$ to k_t of the torsion is $k_{f\ell}/k_t \approx 1.3$, the over-all stress on the torsion of the spar equals: /279

$$\sigma=0.35\sigma_{f1}+0.65\sqrt{\sigma_{f1}^2+4\tau_t^2}, \qquad (205)$$

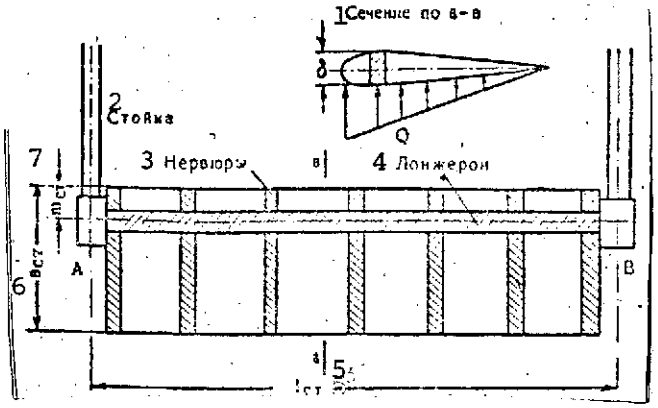

Fig. 177: The load on the stabilizer.

Key: 1-section across б-в
2-stanchion
3-ribs
4-spar
5-ℓ_{st}
6-b_{st}
7-m_{st}

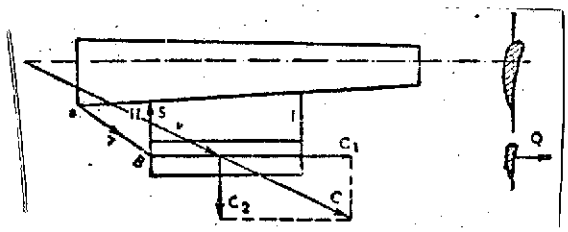

Fig. 178: Action of the forces on the stabilizer.

where $\sigma_{fl}=\frac{M_{us}}{W_{us}}$ and $\sigma_t=\frac{M_t}{W_t}$;

$W_{f\ell}$ and W_t are respectively the moment of flection and the torque. The load on the rib of the stabilizer equals:

$$Q_n=\frac{Q}{n-1}, \qquad (206)$$

where n is the number of ribs.

For calculation of the flection, the rib is considered to be a beam with sealed ends. The flection moment is equal to :

$$M_n=Q_n\left(\frac{1}{3}b_{st}-m_{st}\right). \qquad (207)$$

The stanchions of the stabilizer are subjected to flection by force Q and to centrifugal force C (Fig. 178). Stanchion I is subjected to flection by the aerodynamic force Q/2 and to elongation by the force $C_2/2$.

Stanchion II is subjected to flection by force Q/2, to compression by force S, which is obtained by resolution of force C_1 to the direction aB of the guide rope and of stanchion II, and to elongation by force $C_2/2$ (Fig. 178).

The guide rope aB is calculated as being subject to elongation by force T which is obtained as a component of the resolving force C_1 into the direction of stanchion II and of guide rope aB. /280

The loads on the wing of the rapid wing engine without regulation, which is connected in parallel, is determined on the basis of its performance.

The performance of wind engines with Z = 6 and higher, under conditions of n = const; N = f(V) is given in Fig. 179, where V_p = the velocity of the wind at which the wind-driven wheel works with maximal power; V_{lim} is the limiting velocity of the wing at which the engine stops.

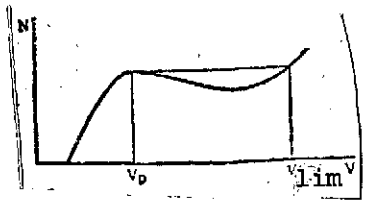

Fig. 179: Performance of a wind engine working without regulation.

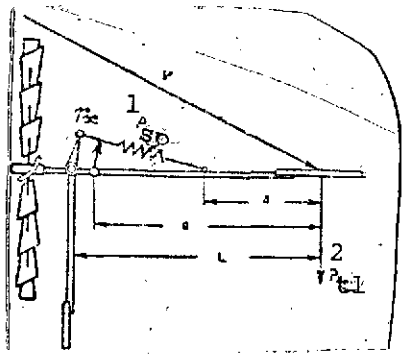

Fig. 180: The load on the tail hinged to a spring.

Key: 1-P_{sp}
2-$P_{t\ell}$

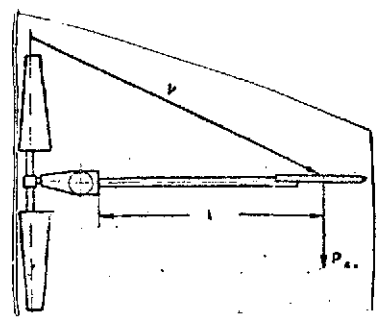

Fig. 181: The load on the tail with rigid attachment to the head of the wind engine.

Examples of calculation for the wing.

a-The engine works at a wind velocity V_{lim}. The load on the wing is:

$$P = C_{y\,max} \frac{\rho}{2} S (\omega^2 r_m^2 + V_{lim}^2) \quad (208)$$

the frontal pressure will be:

$$P_h = C_{y\,max} \frac{\rho}{2} S (\omega^2 r_m^2 + V_{lim}^2) \sin n. \quad (209)$$

Cymax is taken from the curve in Fig. 171.

The load is distributed throughout the length of the wing, according to Fig. 173.

b-The engine is at rest. Velocity of the wind during a storm:

$$V_s = 40 - 50 \text{ m/sec}$$

The load on the wings:

$$P_s = 0.08 S V_s^2 \quad (210)$$

The load is distributed on the length of the wing proportionally to the cord. The load on the cord is distributed uniformly.

41. The Wing Load on the Tail and on the/281 Regulating Lateral Blade.

The folding tail (Fig. 180) has to be calculated on the basis of the internal force of the spring, the dimensions of which are determined as shown in Chapter VIII on regulation (section 33).

Drawing the perpendicular r_x from the point of torsion of the tail to the direction of the force P_{sp}, we can write the following equation:

$$P_{sp} r_x = P_{t\ell} b; \quad (211)$$

$$P_{t\ell} = \frac{P_{sp} r_x}{b} = \frac{M_{sp\,max}}{b}. \quad (212)$$

The stress in the tail rod caused by force $P_{t\ell}$:

$$k = \frac{P_{t\ell} a}{W} \quad (213)$$

(r_x, a and b see Fig. 180).

The stress caused by the weight of the tail unit G; $k_1 = \frac{Gb}{W}$.

The lateral regulating blade. $M_{sp} = M_{bla}$; $k = M_{bla}/W$. The area of the lateral regulating blade, is usually taken in the limits from 0.01 to 0.03 F; where F is the area marked off by the wind-driven wheel.

The unfolding (rigid) tail (Fig. 181) should be calculated by the lateral force, which is determined by equation:

$$P_{tl} = C_y f \frac{\rho V^2}{2}, \qquad (214)$$

where C_y = 1.0 to 1.2; f is the area of the tail in m^2 which is assumed on the basis of statistical data f ≈ 0.03 to 0.06F, where F is the area marked off by the wind wheel. /282

The stress caused by the aerodynamic force P_{tl}:

$$k = \frac{M_{tl}}{W} = \frac{P_{tl} L}{W}. \qquad (215)$$

The load caused by the weight of the tail G:

$$k_1 = \frac{GL}{W}. \qquad (216)$$

42. Calculation of the Head of the Wind Engine.

Girder of the head. The following load acting on the girder of the head should be known in order to calculate it (Fig. 182).

1. Frontal pressure P on the wind-driven wheel, which can be calculated for stabilizers of wind engines according to equation (182), and for engines without regulation by means of equation (209).

2. Weight load, acting on the girder, i.e. G_w weight of wind-driven wheel and G_{tl} weight of the tail.

The moment caused by the gyroscopic forces of the entire wind-driven wheel $M_g = I_0 \omega \omega_1$ (Sec. 43) for a wind engine with a number of blades higher than 2; $M_g = 2I_0 \omega \omega_1$, for a two-bladed wind engine.

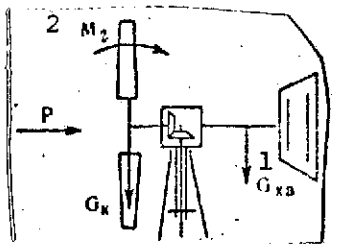

Fig. 182: Load on the head of the wind engine.

Key: 1. G_{tl}
2. M_g

The horizontal shaft is subjected to the action of:

a. the torque M_w = 716.20 = N/n kg;

b. a deflecting moment caused by the weight of the wind-driven wheel and

c. a moment caused by the gyroscopic forces of the entire wind-driven wheel.

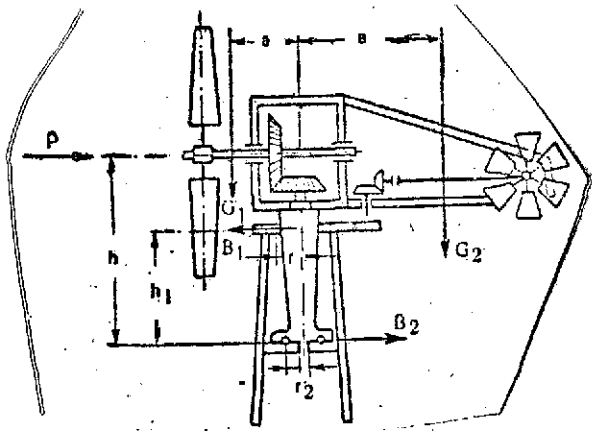

Fig. 183: Diagram of the head for determination of the forces of friction.

Determination of the forces of friction in the supports of the head during adjustment of the wind-driven wheel to the wind by means of windroses. Let us compare the equation of the sum of the moment and of the projection of the forces according to the notation given in Fig. 183. For determining the reactions B_1 and B_2, we obtain the following equality:

$$\begin{aligned} -G_1 a - B_1 h_1 + Ph + G_2 b = 0; \\ P + B_2 - B_1 = 0. \end{aligned}$$

Hence: /283

$$B_1 = \frac{Ph + G_2 b - G_1 a}{h_1}, \qquad (217)$$

and

$$B_2 = B_1 - P,$$

$$B_2 = \frac{Ph + G_2 b - Ga}{h_1} - P. \qquad (218)$$

The moments of friction are caused by the force G -- weight of the head, B_1 and B_2. Let us note:

M_1 -- moment of friction from the weight of the head;

M_2 -- moment of friction from forces B_1 and B_2; $M_1 = \mu G r_2$; $M_2 = \mu (B_1 r_1 + B_2 r_2)$;

$$M_1 + M_2 = M_{hf}.$$

The windroses and their main dimensions are determined by the characteristics of small wind engines (Fig. 184). The characteristics indicate that most convenient are the small wind engines with trapezoid blades and a rigging angle $\phi = 20^\circ$ and 30°.

The moment of friction in the bearings of the windroses:

$$M_{w0} = \mu' G_w \frac{d}{2},$$

where $\mu' = 0.10$ -- coefficient of friction of metal against metal; /284

G_w -- weight of the windroses;

d -- diameter of the shaft of the wind rotors.

During adjustments of the wind-driven wheel to the wind, this moment of friction should be surmounted by the aerodynamic moment of the wind rotor, which can be found be means of the characteristics in Fig. 184.

The moment developed by the windroses, is equal to:

$$M_w = \overline{M}_w \rho (0.4 V_0)^2 D^3, \qquad (219)$$

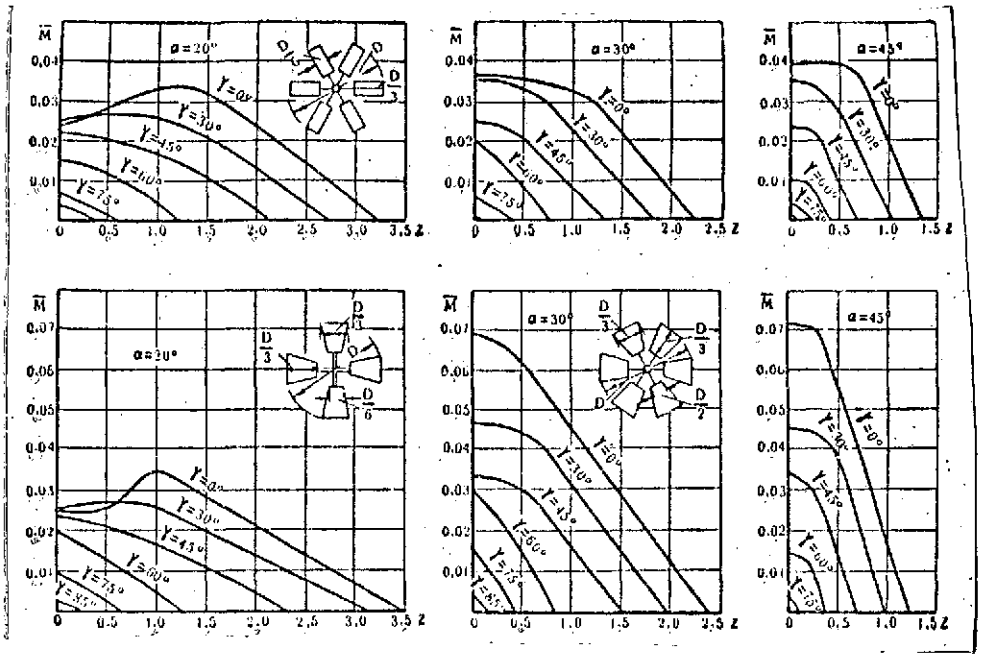

Fig. 184: Characteristics of windroses

where $\overline{M}_W$ is taken from the characteristic in Fig. 184 at an angle $\lambda = 75^\circ$ and $Z = 0$;

$\rho = 0.125$ -- mass density of the air;

V_0 -- average annual velocity of the wind in the given region;

0.4 -- coefficient which accounts for the decrease in wind velocity behind the wind-driven wheel;

D -- diameter of the wind rotors.

After reductions, we obtain for one windrose:

$$M_W = 0{,}02\,\overline{M}_W \rho V_0^2 D^3. \tag{220}$$

The gear ratio of the wind rotors:

$$i = \frac{\overline{M}_W \eta f r}{\eta (M_W - M_g)}, \tag{221}$$

For two wind rotors:

$$i = \frac{\overline{M}_W \eta f r}{2\eta (M_W - M_g)}, \tag{222}$$

where η is taken equal to 0.9 for conical and cylindrical transmissions and 0.45 -- for worm gearing. The transmission should correspond to ω_1 (see Sec. 43).

43. The Gyroscopic Moment of the Wind-Driven Wheel

During the rotation of the head around the axis of the tower z' -- z' (Fig. 185), in addition to the aerodynamic forces, centrifugal and gyroscopic forces act on the wings of the rotating wind-driven wheel. Let us take on the blade point A with mass m and let us write the expression for these forces: $Q = m\omega^2 r$ -- the centrifugal force appearing as a result of the rotation of the wind-driven wheel around its axis; $Q = m\omega_1^2 \ell$ -- the centrifugal force appearing during the rotation of the head around the axis z' -- z'. The force of acceleration of Coriolis: /286

$$P = 2m\omega_1 U \sin\beta_1,$$

where ℓ is the distance of point A from the axis z' -- z'. The force Q_1 is directed from axis z' -- z' parallel to ℓ; $U = \omega r$ is the relative velocity, which in a given case is equal to the circular velocity of rotation of point A around the axis X -- X. The direction of the force P is perpendicular relative to velocity U and the axis of rotation of the entire system z' -- z'. Angle β_1 is formed by velocity U and the axis z' -- z'. These forces cause moments M_x, M_y and M_z relative to the axes OX, OY and OZ.

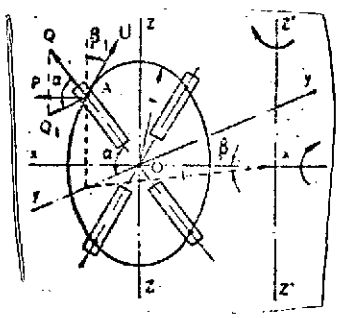

Fig. 185: Action of the gyroscopic moment on the wind-driven wheel.

The over-all moment which breaks the flap at the bush is equal to [34]

$$M_g = 2I\omega\omega_1 \sin\omega t, \qquad (223)$$

where I -- moment of inertia of the wing relative to the axis OX.

The calculated maximal moment, which bends the flap, when the flap is vertical:

$$M_g = 2I\omega\omega_1. \qquad (224)$$

The shaft is bent by the gyroscopic moment of the entire wind-driven wheel. It is obtained by the summation of the moments of all the flaps (for three or more blades)

$$M_y = I_0\omega\omega_1, \qquad (225)$$

where I_0 is the moment of inertia of the entire wind-driven wheel relative to the axis OX.

For a 2-bladed wind engine,

$$M_y = 2I_0\omega\omega_1. \qquad (226)$$

The angle of velocity ω is found by means of equation:

$$\omega = \frac{\pi n}{30},$$

where n is the number of revolutions of the wind-driven wheel per minute.

The head of the wind engine turns with an angular velocity /287
which is equal to:

$$\omega_1 = \frac{Z_0 V}{iR_0}, \quad (227)$$

where:

$Z_0 = \omega_0 R_0 / V$ -- synchronal number of modules of the wind (228)
rotors which is found according to the characteristics in Fig. 184;

i -- gear ratio of the transmission from the wind rotors to the pinions on the tower;

R_0 -- radius of the wind rotors;

ω_0 -- angular velocity of the wind rotors.

On the basis of equation (224) and (227), the moment which bends the flap is equal to:

$$M = 4I \frac{V Z_0 \omega}{Di}. \quad (229)$$

The stress in the flap

$$\sigma = \frac{M100}{W} = \frac{42IV Z_0 n}{WDi} \text{ (kg/cm}^2\text{)}, \quad (230)$$

where: W -- moment of the drag of the flap at the bush;
D -- diameter of the wind rotors;
V -- velocity of the wing in m/sec;
Z_0 -- number of synchronal modules of the wind rotors.

The stress on the shaft of the multi-bladed wind engine

$$\sigma = \frac{21 I_0 V Z_0 n}{WDi} \text{ kg/cm}^2, \quad (231)$$

Determination of the angular velocity of rotation ω_1 of the wind engine relative to the axis of the tower. The angular velocity ω_1 for the rotation of the windroses is determined under the following conditions:

a. the velocity of the wind 20 m/sec;

b. direction perpendicular to the plane of rotation of the windroses ($\gamma = 0$);

c. the windroses are considered as working with a synchronal number of modules:

$$\omega_0 = \frac{2Z_0 V}{D}, \quad (232)$$

where: Z_0 -- synchronal number of modules taken from wind tunnel tests (Fig. 184);
V -- velocity of the wind taken equal to 20 m/sec at the head;
D -- diameter of the windroses.

$$\omega_1 = \frac{\omega_0}{i},$$

where i -- gear ratio of the transmission from the small wind engines /288
to the pinion on the tower.

The measurement of the strength of winds is performed under the same conditions under which the value of ω_1 was determined.

44. The Power of Wind Engines

The wind engine consists of two main parts: the head of the wind engine with all the machinery and the tower on which the head is mounted.

In winged wind engines, the towers play an extremely important role; they make it possible to raise the wind-driven wheel to any height, as required by the local topographical conditions. Different kinds of obstacles on the surface of the ground may disturb the linear motion of the airstream causing turbulence. The tower makes it possible to raise the wind-driven wheel beyond the limits of this turbulence.

Since the power of the wind engine changes proportionally to the cube of the wind velocity, i.e.

$$N = N_0 \left(\frac{V}{V_0}\right)^3,$$

we can write the equation of the power of the wind engine as a function of height, using equation (248) (Sec. 46):

$$N = N_0 \left(\frac{H}{H_0}\right)^{0.6}, \tag{233}$$

where: N_0 -- power at the height H_0;
N -- power at the height H.

The approximate characteristic of the power of the wind engine in relation to the height of the wind-driven wheel above the ground is shown in Fig. 186a.

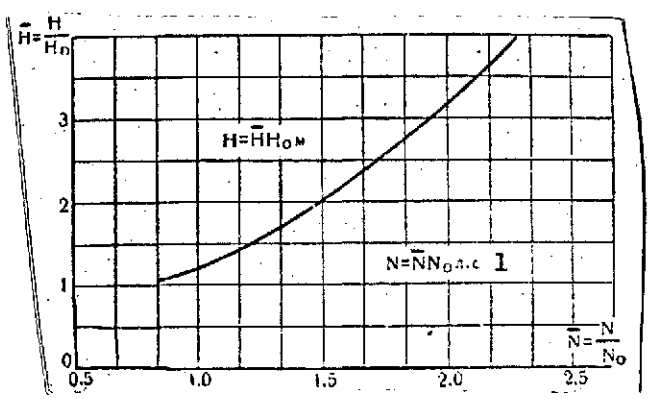

Fig. 186a: Characteristic of the power of the wind engine in relation to the height of the tower.

Key: 1. hp

However, in selecting the height of the tower, it is important to pay attention to the technical possibilities and the conditions of exploitation of the wind installation.

The minimal height of the tower should be equal to (Fig. 186b)

$$H = h + c + R, \tag{234}$$

where: h -- height of the obstacles in the vicinity of the wind installation;

c -- distance from the top of the obstacle to the lowest point on the marked-off area, assumed to be 1.5 to 2 m;
R -- radius of the wind-drivenwwheel.

The opening between the legs of the tower with a height above 10 m /289

$$B=0.22H \text{ to } 0.25H.$$

For towers below 10 m, B = 0.30 H m.

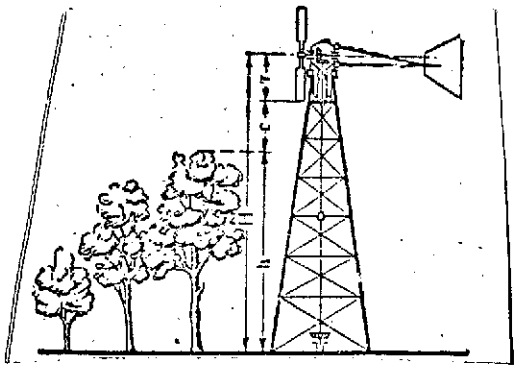

Fig. 186b: Determination of the height of the tower.

The distance between neighboring wind engines with the same height of the tower and diameter of the wind-driven wheel, is assumed to be equal to 15 D, where D is the diameter of the wind-driven wheel.

The construction diagrams of towers for windwengines are shown in Fig. 187 and 188.

The first three diagrams of /291 type A tower are usually used for wind engines with a power up to 10 hp:

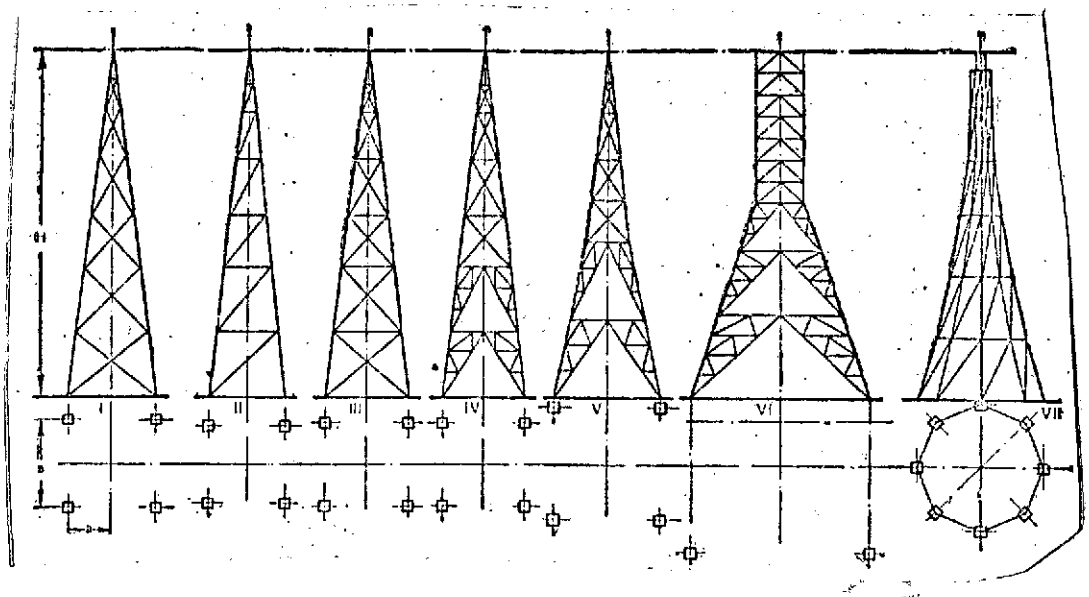

Fig. 187: Construction diagram of type A towers.
I -- VIII refer to type A, IX refers to type B, and X -- XI refer to type C.

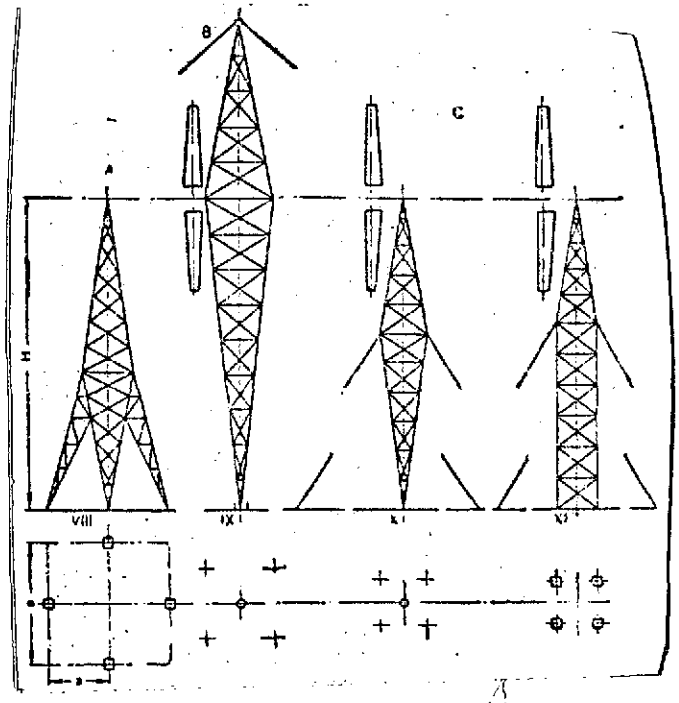

Fig. 188: Construction diagram of types A, B, and C towers.

the other diagrams of towers of this type are used for wind engines of higher power. The type B and C towers, according to the diagrams, are used in the construction of towers with bracing wires. The ratio of the weights of these towers is presented in the graph of Fig. 189, where the curves describing the relationship between the weight of the tower and the ratio H/R are presented: /292
GIX/GA -- ratio of the weight of type IX rotating tower to the weight of any of the group A non-rotating towers;
GXI/GA -- ratio of the weight of group C towers to the weight of group A towers;
GX/GA -- ratio of the weight of type X towers -- rotatory, to the weight of the group A towers.

These curves show that with the increase in the relative height H/R, the weight of the rotating towers is considerably smaller than the weight of Group A towers. Towers with bracing wires have a smaller weight than the group A tower. However, the towers of group A are more convenient and more reliable in the exploitation.

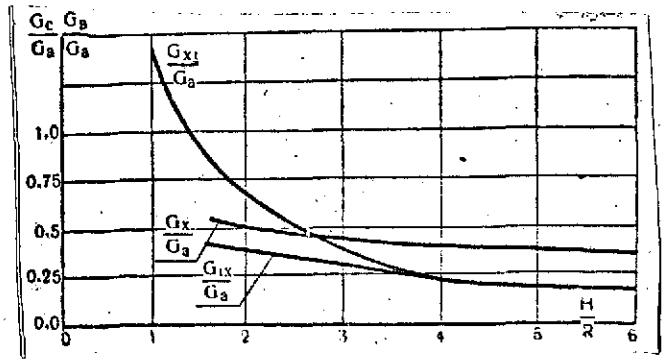

Fig. 189: Graph of the relative weights of towers

The preliminary weight of the type A tower, constructed according to diagrams I, II, III and IV, can be calculated by means of an equation which was derived by the author on the basis of statistical data according to metallic towers of this type, i.e.:

$$G = (16{,}5HR^2 + 0{,}723H^3 + 5{,}3R^3)\frac{K}{10}, \quad (235)$$

where: H is the height of the tower in m;
R is the radius of the wind-driven wheel in m;
K is the coefficient accounting for the weight of

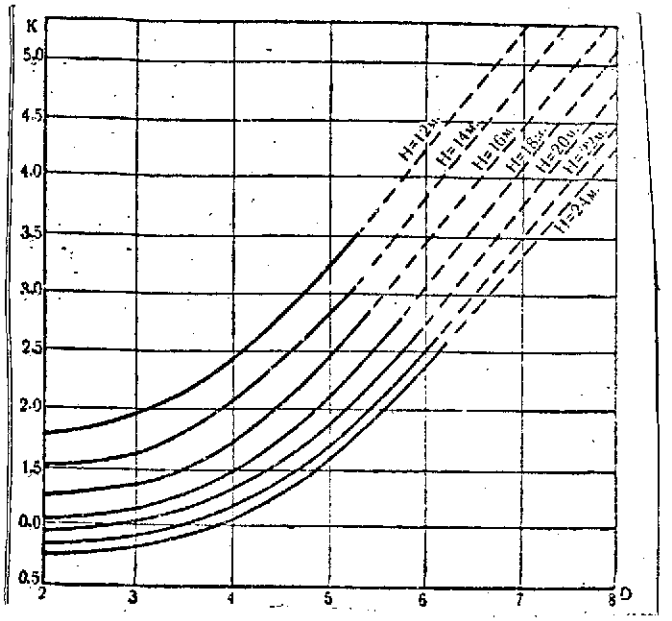

Fig. 190: Graph of the coefficient K for determination of the preliminary weight of the tower.

the construction and is taken in relation to D and H from the graph in Fig. 190.

The expression $16.5\ HR^2$ accounts for the flection moment caused by the action of the wind force on the head of the wind engine; expression $0.723\ H^3$ is the/293 flection moment caused by the pressure of the wind on the tower and expression $5.3\ R^3$ is the moment caused by the weight of the tail.

If the wind engine is removed from the wind by means of a blade, then instead of expression $5.3\ R^3$, $6.4\ R^3$ should be substituted in equation (235).

Example. Determine the weight of a tower with a height H = 15 m of a multi-bladed wind engine D = 5 m.

From the graphs in Fig. 190, we find the value k = 2.6; substituting the values of the other magnitudes in equation (235), we obtain the weight of the tower:

$$G=(16{,}5\cdot 15\cdot 2{,}5^2+0{,}723\cdot 15^3+5{,}3\cdot 2{,}5^3)\,\frac{2{,}6}{10}=1\,050\ \text{kg}$$

The wind loads on the towers of wind engines are determined according to an equation obtained experimentally at TsAGI for the models shown in Fig. 191: /294

$$P=R_x\left(\frac{H}{H_{mod}}\right)^{\frac{2}{7}}V^2, \qquad (236)$$

where: V = 40 m/sec for regions with an annual average wind velocity up to 5.5 m/sec;

R_x -- coefficient of the head pressure, taken from Table 11;

H -- measured height of the tower in m;

H_{mod} -- height of the tower model in m.

Assuming V = 40 m/sec. and H_{mod} = 0.486 m and substituting /295 these values in equation (236), we obtain:

$$P = 6770R_xH^2. \qquad (237)$$

For a four-legged lattice tower R_x = 0.00085 and

$$P = 5.75\ H^2\ \text{kg}. \qquad (238)$$

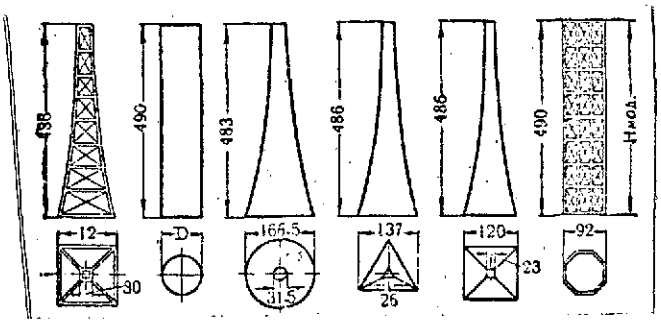

Fig. 191: Types of tower models tested in the wind tunnel.

TABLE 11

Type of Model (Fig. 191)	Coefficient of head pressure R_x	Distance of the point of application of the resultant from the base x/H (in %).
4-legged lattice tower	0.00085	42.8
Cylindrical solid	0.00105	—
Conical solid	0.0013	41.2
Trihedral solid disposed with the edge towards the wind	0.0017	32.1
Trihedral solid disposed with the sides towards the wind	0.0029	28.5
Tetrahedral solid disposed with the edge or the side towards the wind	0.0024	29.8
Cylindral lattice tower	0.0014	49.4

Hence, we see that the load in kg per 1 m height of the tower amounts to 5.75 H.

Analogically to the previous case, we obtain for a cylindrical solid tower:

$$P = 7{,}1 K H^2 \text{ kg} \qquad (239)$$

K -- correction coefficient for cylindrical solid tower, determined from the graph in Fig. 192, in relation to H/D, while D is the diameter of the cylindrical tower.

For calculation of the towers, the head pressure on the wind-driven wheel has to be determined. On the basis of experimental data, the following formulas are derived for wind loads on a multi-bladed wind-driven wheel (Fig. 193):

$$P_x = \bar{x} F \rho \frac{V^2}{2}; \qquad (240)$$

$$P_y = \bar{y} F \rho \frac{V^2}{2}. \qquad (241)$$

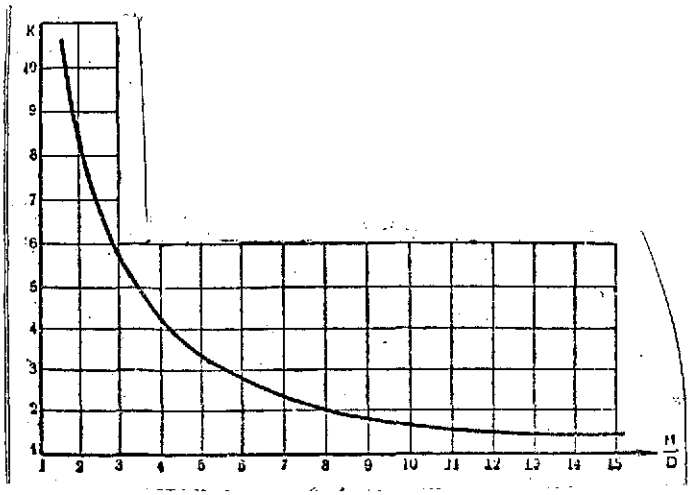

Fig. 192: Relationship between the coefficient K of cylindrical towers and the ratio of height H to diameter of the tower.

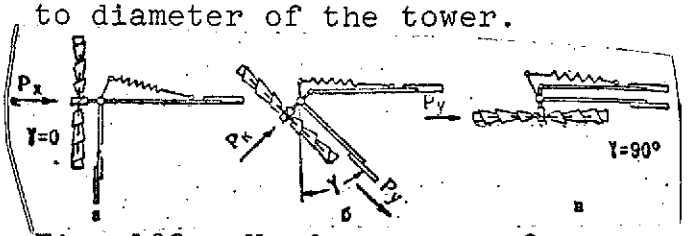

Fig. 193: Head pressure for different positions of the wind-driven wheel.

$\bar{x}$ and $\bar{y}$ -- load coefficients /296 obtained experimentally and presented in Table 12:
ρ -- mass density of the air (at a barometric pressure of 760 mm Hg and 15° C, $\rho = 0.125$);
$F = \pi R^2$ -- the area marked off by the wind-driven wheel;
V -- velocity of the wind in /297 m/sec, which, depending on the angle γ is assumed to be equal to 8-30 m/sec, according to the curve in Fig. 125.

Example. Determine the forces P_x and P_y, acting on a wind-driven wheel D = 5 m of the multi-bladed type, in the case of operation with load, V = 10 m/sec, regulation according to curve I, Fig. 125. According to Fig. 125, the wind-driven wheel should deflect at an angle $\gamma = 40°$ at a wind velocity of 10 m/sec. In Table 12, in column of $\gamma = 40°$, in the two lower lines, we find $\bar{x} = 0.475$ and $\bar{y} = 0.20$. Substituting the numerical values of

TABLE 12. VALUES OF $\bar{x}$ AND $\bar{y}$ FOR MULTI-BLADED WIND ENGINES.

Type of operation	Load coefficient of the wind	Angle of rotation γ of wind-driven wheel				
		0	10°	20°	30°	40°
Idle operation	$\bar{x}$	0.625	0.610	0.575	0.510	0.374
	$\bar{y}$	0.000	0.075	0.130	0.180	0.220
With loading of power tool	$\bar{x}$	0.780	0.760	0.730	0.625	0.475
	$\bar{y}$	0.000	0.050	0.100	0.150	0.200

Type of operation	Load coefficient of the wind	Angle of rotation γ of wind-driven wheel				
		50°	60°	70°	80°	90°
Idle operation	$\bar{x}$	0.250	0.150	0.078	0.060	—
	$\bar{y}$	0.225	0.220	0.180	0.150	0.140
With loading of power tool	$\bar{x}$	0.350	0.275	0.180	0.100	—
	$\bar{y}$	0.180	0.240	0.260	—	—

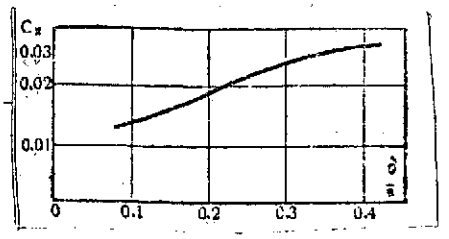

Fig. 194: Values of the coefficient C_x in relation to δ/b.

the given magnitudes in equations (240) and (241), we obtain:

$$P_x = \bar{x}F\frac{\rho V^2}{2} = 0.475\frac{\pi 5^2}{4}\cdot\frac{0.125\cdot 40^2}{2} = 59\ \text{kg}.$$

$$P_y = \bar{y}F\frac{\rho V^2}{2} = 0.20\frac{\pi 5^2}{4}\cdot\frac{0.125\cdot 40^2}{2} = 24.6\ \text{kg}$$

In determining the head pressure in rapid wind engines, equation (182) has to be used, since in a given case, the airstream dashes over the wind-driven wheel perpendicularly to the plane of rotation of the wind-driven wheel, and this has to be taken into consideration.

The forces P_b in rapid wind engines, with only a few blades, and P_x and P_y in multi-bladed wind engines, which are regulated by the removal of the wind-driven wheel from the wind, create moments which deflect the tower relative to its base or the belt, where the bracing wires are fastened in type X and XI towers (Fig. 188).

The wind loads on the tower of wind engines with stabilizer are determined by the following procedure.

1. The head pressure on the wings and head:

$$P = iC_x S\frac{\rho}{2}V_s^2 + 0.08FV_s^2 \qquad (242)$$

C_x -- aerodynamic coefficient of the wing at an angle of attack corresponding to $C_y = 0$ (Fig. 194);
V_s -- wind velocity in the storm (40 m/sec);
F -- area of the middle section of the head in m^2. /298

2. Pressure of the wind on the girder of the tower, according to formula (237), is equal to:

$$P_t = 4{,}25R_x H^2 V_t^2 \qquad (243)$$

(refers to the whole tower); 2/3 of P_t are assumed to act on the frontal side of the tower, while 1/3 of P_t acts on the rear side of the tower.

The load is assumed to be uniform throughout the height of the tower. H -- height of the tower; V_t = 40 m/sec; R_x -- for a four-legged tower = 0.00085, for a cylindrical tower = 0.0014.

3. Moment caused by the gyroscopic forces. The maximal gyroscopic moment relative to the y -- y axis for a three-bladed wind engine and for the multi-bladed engine, according to equation (225):

$$M_y = I_0\omega\omega_1.$$

For two-bladed wind engines, according to equation (226):

$$M_g = 2I_0\omega\omega_1.$$

The calculated overall moment: $M = M_a + M_g$,

where M_a is the moment caused by the aerodynamic forces on the wind-driven wheel.

The moment caused by the weight forces on the wind engine, obtained due to the lack of balance between the part of the head relative to the axis of the tower (Fig. 195):

$$M_e = Rl.$$

The tower is subjected to weight loads:
a. weight of the engine: $Q = Q_{ww} + Q_{tl} + Q_{tr}$,

where: Q_{ww} -- is weight of the wind-driven wheel;
Q_{tl} -- weight of the tail;
Q_{tr} -- weight of the upper transmission with crank house;
b. the tower's own weight Q_t.

The foundation under the tower of the wind engine, should satisfy the following main requirements: 1. it should be sufficiently strong in accounting for the static and dynamic load; 2. the foundation should give no large sediment, especially not a homogeneous one which could cause slanting of the construction. Sediments are most likely to appear when the foundation of the tower foot is built on sand of small or average density. In order to abolish the slant of the tower, the center of gravity of the entire mass of the foundation of the foot tower should be on the same vertical line. /299

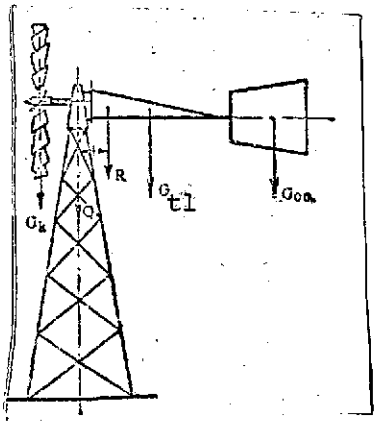

Fig. 195: Weight load on the tower.

The allowable specific pressures of weak soils (clay, and loam in the ductile state, sandy loam of average density and powdered sand saturated with water, as well as ground with interlayers of silt or peat) are up to 1.5 kg/cm^2. For the same soil of average density, the allowable specific load should be assumed to be 1.5 to 3.5 kg/cm^2, while for strong soils -- from 3.5 to 6 kg/cm^2.

In determining the allowable pressures on various soils, OST 90004-38 should be used (Table 13).

The depth at which the foundations are laid are taken 0.1 to 0.25 m deeper than the depth of freezing in a given region. The first number corresponds to humid, sandy soil, while the larger number corresponds to water-permeable clay soil.

The depth of freezing in the European part of USSR is assumed to be:

For the northern and eastern regions .....2.0 m
For the northwestern region.....1.6 "
For the central region.....1.5 "
For the western region.....1.3 "
For the southern region.....1.1 "

The foundations under the foot of the tower, are built of brick or stone on cement mortar. The bending loads caused by /300 the head pressure of the wind on the tower and the wind engine, cause at the base of the tower, a moment $M = P_h H + PH_t$, where H and H_t are the distances between the point of application of the forces and the base of the foundation (Fig. 196).

TABLE 13. ALLOWABLE PRESSURE (IN kg/cm^2) ON THE FOUNDATION SOIL AT A DEPTH OF THE BASE 2 M BELOW THE DAY

Name of soil	solid	average
I. Sandy and gravelly soils		
1. dry sandy loam	2.5	2.0
2. humid sandy loam	2.0	1.5
3. powdered dry sand	2.5	2.0
4. humid dry sand	2.0	1.5
5. fine dry sand	3.0	2.0
6. fine humid sand	2.5	1.5
7. average sand regardless of humidity	3.5	2.5
8. rough and gravely sand regardless of humidity	4.5	3.5
9. gravel and pebbles regardless of humidity	6.0	5.0
	in hard state	in docile state
II. Clay soils		
1. clay	6.0—2.5	2.5—1.0
2. loam	4.0—2.5	2.5—1.0

The compression forces are the weight of the wind engine and of the tower Q; the weight of the foundation G_ϕ.

The maximal internal forces on the legs are encountered when the wind blows diagonally through the tower: under these conditions the following equality holds:

$$M = P_M \cdot 1{,}4B,$$

hence

$$P_M = \frac{M}{1{,}4B},$$

where 1.4B -- distance between the foundations along a diagonal line.

The calculated force on the frontal leg equals:

$$P_1 = \frac{Q}{4} + G_\phi - P_M, \qquad (244)$$

on the hind leg:

$$P_2 = \frac{Q}{4} + G_\phi + P_M. \qquad (244a)$$

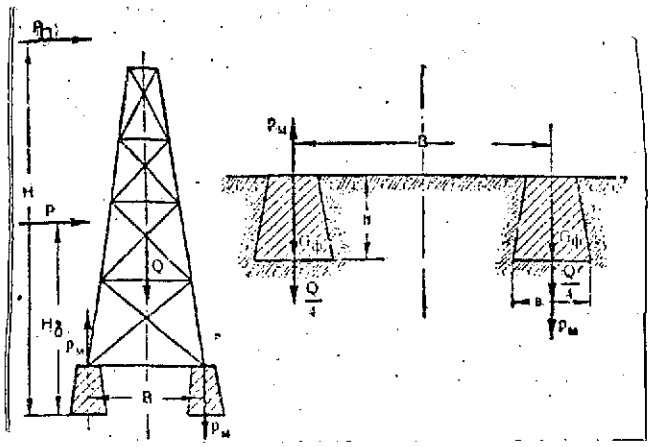

Fig. 196: Foundations under the feet of the tower.

Assuming that the area at the base of the foundation in cm^2 is F, the pressure on the ground is determined:

$$k = \frac{P_1}{F} kg/cm^2 .$$

PART TWO

WIND POWER INSTALLATIONS

CHAPTER 12. THE WIND AS A SOURCE OF ENERGY /305

45. The Origin of the Wind

The main cause of the formation of wind is the uneven heating of the Earth's surface by the sun.

Let us assume that as a result of the uneven heat given by the sun's rays, segment AF on the horizontal surface of the Earth has been warmed up to a greater extent than segment FB (Fig. 197). The air which comes in contact with the Earth is warmer about AF than above the segment FB. The air column above segment AF widens while above segment FB, it is compressed. At the same time, at a certain level CD, the pressure on segment CE becomes greater than before, while on segment ED, it decreases. Therefore, the air flows in the direction CED. At the level AFB, i.e. on the Earth's surface, the pressure above segment AF decreases as a result of the displacement of the air; the pressure above the colder segment FB increases. Therefore, the air flows from segment FB to segments AF below, i.e. in a direction opposite to the displacement above. As a result, the circulation of air illustrated in Fig. 197 by means of arrows is obtained.

The uneven distribution of heat between various regions of the Earth determines the circulation of the air in the Earth's atmosphere.

The Earth's surface is irregular; the dry land, oceans, mountains and forest cause variable heating of the surface at the same latitude. The revolution of the Earth also causes deviations in the air flow. All these causes complicate the general circulation of the atmosphere. A series of individual circulations appear, which are to some extent, related to each other.

A calm zone with weak variable winds is found at the equator /306
near the Earth's surface. Eastern winds of considerable strength blow in the upper layers above this zone. To the north and to the south of the calm zone are situated the zones of the trade winds, which as a result of the revolutions of the Earth from west to east, are deviated to the west. In such a manner, constant winds blow in the Northern Hemisphere from the northeast, while in the Southern Hemisphere they blow from the southeast, as shown in the diagram in Fig. 198. The trade winds extend approximately to the 30th degree northern and southern latitudes and are distinguished by the regularity of the airstreams as far as direction and velocity are

concerned. The average velocity of the southeastern trade winds in the Northern Hemisphere reaches near the surface of the Earth 6-8 m/sec. In the vicinity of the large continents, these winds are disturbed by the strong annual fluctuations in temperature and pressure above the continents. Above the layer of trade winds, there is a layer of variable winds, and beyond that layer we have the zone of the counter-trade winds which blow in a direction opposite to that of the trade winds. The height of the layer of counter-trade winds varies from 4-8 km, depending on the time of the year and on the region. /307

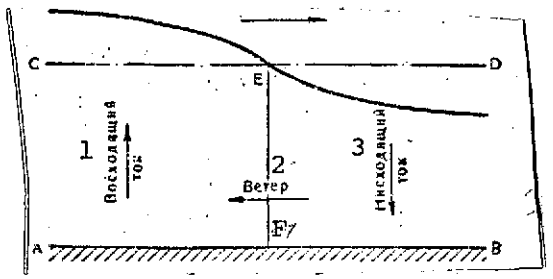

Fig. 197: Diagram of formation of airstreams.

Key: 1. upward current
2. wind
3. downward current

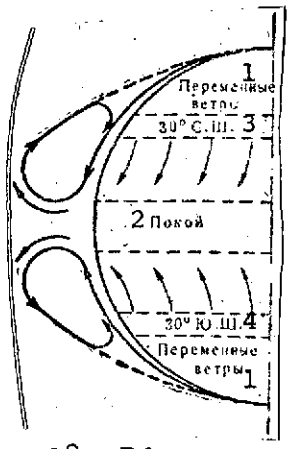

Fig. 198: Diagram of the general circulation in the Earth's atmosphere.

Key: 1. variable winds
2. calm
3. 30° Northern latitude
4. 30° southern latitude

In the subtropical latitudes, the zones of the trade winds are replaced by calm regions in the belts of high pressure. To the north and to the south of these regions, approximately up to 70°, the winds blow at all altitudes between the western and southwestern points in the northern hemisphere, and between the western and the northwestern points in the southern hemisphere. In addition, at these latitudes, turbulent movements appear and disappear continuously and complicate the simple diagram of the general circulation of the atmosphere shown in Fig. 198.

Local winds. The particular local topographic conditions of the Earth's surface (seas, mountains, etc.) cause local winds.

Breezes. As a result of the changes in day and night temperature, sea winds are formed on the shores which are called breezes.

During the day, in sunny weather, the land warms up to a greater extent than the surface of the sea, therefore the warm air becomes less dense and flows upwards. At the same time the cold sea air flows towards the land forming a seashore wind. The air lifted above the land flows towards the sea in the upper layer and subsides at a certain distance from the shore.

In such a manner, a circulation of the air sets in which is directed below to the seashore and above, from the land to the sea. At night the air above the land is cooled to a greater extent than the air above the sea and therefore, the direction of the circulation changes: below, the air flows to the sea and above, from the sea to the land. The zone of the breeze extends approximately 40 km towards the sea and 40 km towards the land. The height of the breezes extends in our latitude to 200 -- 300 m. In tropical countries, breezes are observed almost throughout the year, while in the moderate zone, only in hot weather during the summer. In our country, breezes are observed in the summer near the shores of the Black and Caspian Seas.

The monsoons. The annual changes of temperature near the shores of large seas and oceans cause a circulation which is analogous to the breezes but has an annual cycle. This circulation which has larger dimensions than the breezes is called monsoon. The monsoons appear due to the following reasons. In the summer the dry land is heated to a greater extent than the surrounding seas and oceans; due to this fact, a low-pressure is formed above the land, and below, the air /308 flows from the oceans towards the land while above on the contrary, from the land to the surrounding ocean. These winds are called sea monsoons. In the winter, the lands are much colder than the surface of the sea; a region of high-pressure is formed above the lands as a result of which the lower layer of the air assume a direction from the land towards the ocean, while the upper layer, on the contrary, from the oceans to the land. These winds are called continental monsoons.

Strong monsoons can be observed on the southern shores of Asia -- in the Indian Ocean and Arabian Sea, where they have a southwestern direction in the summer and a northeastern direction in the winter. Monsoons are also observed near the eastern shores of Asia. Strong northwestern continental winds blow during the winter; during the summer, southwestern and southern humid sea winds are observed. These winds effect considerably the climate of the far eastern regions.

46. Principal Magnitudes Which Characterize the Wind From the Energetic Viewpoint.

The velocity of the wind and its measurement. The velocity of the wind is defined as the distance in m which is passed by a mass of air in the course of 1 second. The velocity of the wind changes constantly in magnitude and direction. The cause of this change is the uneven heating of the Earth's surface and the irregularity of the local topography.

The velocity of the wind is the most important characteristic of the technical properties of the wind. It is measured by means of

special instruments which are called anemometers. Various types of instruments are in use by means of which the velocity and the direction of the wind are determined. All these instruments can be divided into two groups according to the method of determination of the magnitudes.

1. Instruments which indicate or record the instantaneous velocity and direction of the wind;
2. Instruments which indicate or record the velocity and direction of the wind during a certain time interval.

Wild's wind vane indicates the instantaneous velocity and direction of the wind. This instrument is utilized in many meteorological stations. Its general view is shown in Fig. 199. /309

The wind vane has a metallic board suspended on an axis, perpendicular to the indicator of the wind direction in such a manner, that during the revolutions of the vane, its plane is constantly disposed towards the direction of the wind, which deflects it by a certain angle. The magnitude of this angle depends on the velocity of the wind. During its deflections, the board passes along sector B with 8 pins numbered from 1 to 8 which indicate the magnitude of the wind velocity in a given moment. The magnitude of the wind velocity corresponding to each pin, for a wind vane with a 200 g, 150 x 300 mm board, is presented in Table 14.

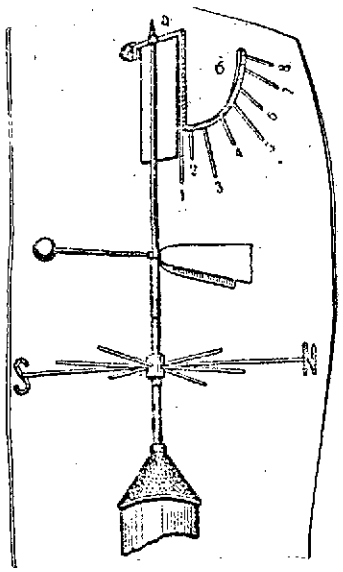

Fig. 199: Wild's wind vane.

In addition, the velocity of the wind can be determined from the readings of a Wild wind vane with a 200 g board by means of the following equation which are varied for deflections of the board up to pin 7:

$$V = 2N_{\ell} - 1 \qquad (a)$$

$$V = 2(N - 1), \qquad (b)$$

where: N_{ℓ} is the number of the lower pins of the two between which the board moves at the time of the observation; /310

N -- number of the pins around which the board moves at the time of observation.

Equations (a) and (b) have been suggested by the author for use when no conversion table is available.

The wind vane with a 200 g board is used in regions which have low wind velocities. Wherever the velocities are large, a wind vane with a 800 g board is used, as shown in Table 15.

TABLE 14. DETERMINATION OF THE WIND VELOCITY BY MEANS OF WILD'S WIND VANE WITH A 200 G BOARD

No. of the pins	1	1-2	2	2-3	3	3-4	4	4-5	5	5-6	6	6-7	7	7-8	8	above 8
Velocity of the wind in m/sec.	0	1	2	3	4	5	6	7	8	9	10	12	14	17	20	above 20

TABLE 15. DETERMINATION OF THE WIND VELOCITY BY MEANS OF WILD'S WIND VANE WITH A 800 G BOARD

Number of pins	1	1-2	2	2-3	3	3-4	4	4-5	5	5-6	6	6-7	7	7-8	8	8 and above
Velocity of the wind in m/sec.	0	2	4	6	8	10	12	14	16	18	20	24	28	34	40	40 and above

The advantage of Wild's wind vane consists in the fact that due to the simplicity of its design, it is not expensive and has a great durability.

Readings by means of the wind vanes, are usually taken 3-4 times a day. Comparison of the readings obtained on an hourly basis with the usual readings taken 3-4 times a day, show that the latter are sufficiently reliable for preliminary calculations. For example:

$$V_3 = 0.93\,V_{24},$$
$$V_4 = 0.99\,V_{24},$$

where V_3, V_4 and V_{24} are the average velocities of the wind obtained from the readings of a Wild wind vane, 3, 4 and 24 times a day respectively.

We can see that the readings taken four times a day give an average daily wind velocity with an error of 1% as compared to the average wind velocity obtained on the basis of 24 readings per day.

Observations of the instantaneous wind velocities at various meteorological stations can be quite inaccurate, since the recording of the observations on wind velocity in a given case, depend entirely on the observer who is susposed to estimate the velocity of /311 the wind by the average position of the wind vane board in an interval of two minutes.

Anemometers. The average velocity of the wind can be determined accurately by means of an anemometer. The main part of this instrument is a fly which consists of a crosspiece with

hemispheres at its ends. On one side of the axis of rotation, the wind encounters the convexity while on the other -- the concavity of the hemisphere. The uneven shape of the surfaces causes pressure differences between the two sides of the vertical axis of the crosspiece, as a result of which it turns; the hemispheres are subjected to the following pressures of the wind:

$$P_1 = C_1 \frac{F\rho}{2}(V+U)^2, \quad (a)$$

$$P_2 = C_2 \frac{F\rho}{2}(V-U)^2, \quad (b)$$

where: P_1 and P_2 -- pressure of the wind corresponding to the convex hemisphere into the wind and the concave hemisphere in the direction of the wind;

C_1 and C_2 -- drag coefficients of the hemisphere;

ρ -- mass density of the air;

F -- projection of the surface of the hemisphere on the plane perpendicular to the direction of movement;

V -- velocity of the wind;

U -- circular velocity of displacement of the hemisphere.

Since the friction of the axis of the crosspiece during its rotation with the hemisphere is insignificant as compared to the acting forces, the right hand side of equations (a) and (b) can be rewritten:

$$C_1 \frac{F\rho}{2}(V+U)^2 = C_2 \frac{F\rho}{2}(V-U)^2. \quad (c)$$

After reduction, we obtain:

$$C_1(V+U)^2 = C_2(V-U)^2, \quad (d)$$

or:

$$C_1\left(1+\frac{U}{V}\right)^2 = C_2\left(1-\frac{U}{V}\right)^2. \quad (e)$$

Substituting in this equation the values of the drag coefficient obtained experimentally, $C_1 = 0.34$ and $C_2 = 1.32$, we find that the circular velocity of the hemisphere amounts to approximately 1/3 of the velocity of the wind, i.e.:

$$U \approx \frac{1}{3}V. \quad (245)$$

Expression (e) shows that the ratio of the linear velocity of /312 the wind does not depend on the density of the air, and consequently, the number of revolutions of the crosspiece with the hemisphere is proportional to the velocity of the wind.

This simple relationship facilitates the determination of the transmission mechanism of the anemometer. It should be mentioned, however, that $U = 1/3V$ is obtained on the assumption that the ratio $C_1/C_2 = \text{const}$ throughout the path of displacement of two diametrically opposed hemispheres of the anemometer. In reality, the ratio U/V changes somewhat with the change in the wind velocity V. However, these changes are so insignificant that they are practically negligible.

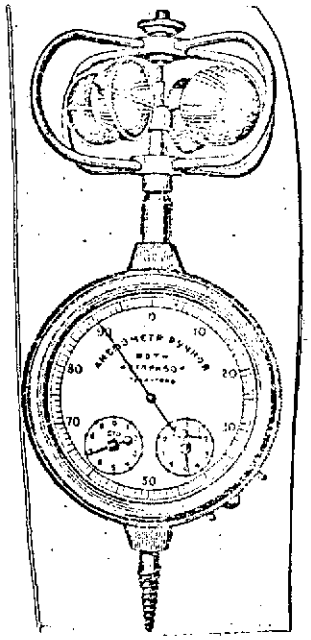

Fig. 200: Anemometer produced by "Metpribor".

The most widely distributed anemometer is the "Metpribor" hand anemometer (Fig. 200), which consists of a crosspiece with cups-hemispheres at each end and of a box with a counter which indicates the path in meters passed by the airstream during a given time interval. Calculation of the time is performed by means of a stop watch or by means of a watch which has a second hand. The counter of the anemometer and the stop watch are started at the same time or else the time on the watch is noted, and after the elapse of the desired time interval, the stop watch and the anemometer are stopped at the same time or the time at the end of the observation is noted on the watch. The numbers on the face of the anemometer show the number of meters by which the airstream was displaced during the period of the observation. Dividing this number by the time of observation in seconds, we obtain the value of the average /313 wind velocity in m/sec for the time interval of the observation.

In measurements of wind velocity, the face of the anemometer should be placed at an angle of 45° to the direction of the wind, which is extremely important when calibrating this instrument. The investigations of Prof. G. Kh. Sabinin and I. V. Smirnov at the Kuchino wind tunnel established that a change of +4.4 to -9.4% is observed in the readings depending on the position of the anemometer with regard to the stream, as shown in Fig. 201.

Before utilization, the anemometers have to be calibrated, as a result of which, tables or graphs are obtained for the conversion of the wind velocities, obtained according to the readings of the anemometer, to real velocities which are determined by calibrations using another accurate and tested instrument.

The electroanemometer is used for instantaneous determinations of wind velocities. A crosspiece with hemispheres turns a small dc generator. The elaborated electrical current is fed to a volt meter, the scale divisions of which indicate directly the magnitude of the /314 wind velocity in a given moment.

Anemographs. Anemometers, the readings of which are recorded are called anemographs. This is the most convenient instrument for recording wind velocities; if it is well calibrated, the velocity values recorded by it are of course more accurate than those determined by the eye.

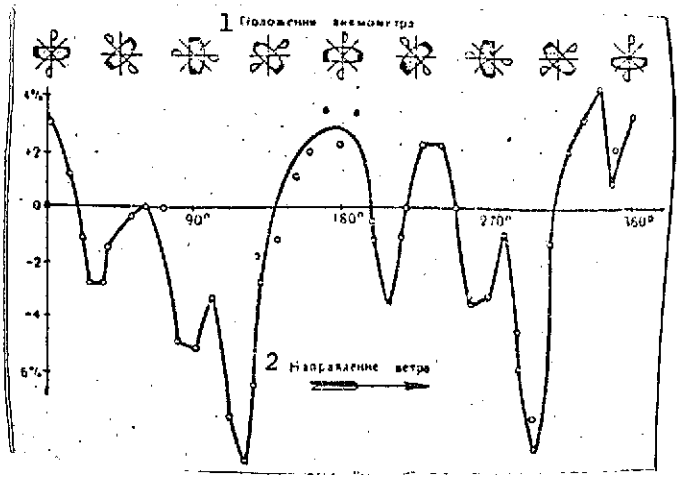

Fig. 201: Change in the readings of the anemometer in relation to its different positions in the wind stream.

Key: 1. position of the anemometer
2. direction of the wind

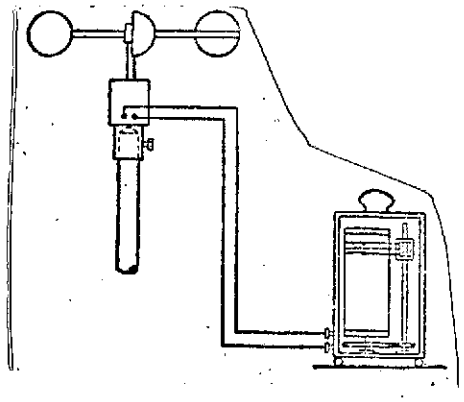

Fig. 202: Contact anemometer with recorder.

Two types of electroanemometers with recorder, are in existence; 1. an electroanemometer with voltage dependent operation, and 2. a contact anemometer and recorder which are fed from an electrical storage battery. In the first case, the recording is a smooth and continuous curve while in the second -- it is a straight interrupted line. A contact anemometer with recorder is shown in Fig. 202. A line with transversal streaks recorded by the pin at the time of the contact is seen on the paper which covers the drum of the recorder. Each distance between the two streaks corresponds in this recorder to a certain path S passed by the wind. If a segment on the line ℓ mm corresponds to t seconds, then it is easy to determine the average velocity of the wind per t seconds by calculating the number of n i.e., of the intervals between the streaks on a portion of the line of ℓ mm: $V = \frac{Sn}{t}$ m/sec

A more accurate determination of the velocity of the airstream, can be performed by means of Pito's tube. This tube is mounted with the open end of the wind vane into the wind. The dynamic pressure of the wind stream causes a pressure on the air /315 inside the tube. A diagram of the Pito tube is shown in Fig. 203. It consists of two tubes: an internal one which is thin with an open front end where the airstream exerts its pressure, and an external tube which is fixed and forms a closed airspace united with the atmosphere of the lateral openings in the front part of the tube. The rear end of the thin tube is connected either directly or via a rubber tube (depending of the design of the instrument) with the tube of a liquid-column pressure gauge; the other end of the latter is connected with the air space of the thick tube. The pressure of

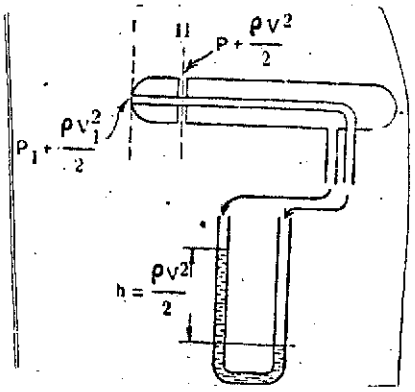

Fig. 203: Pito's tube.

the airstream in the thin tube is transmitted by the liquid in the U-shaped tube of the pressure gauge, as a result of which, the level of the liquid in this tube is establised at different heights. For this purpose, colored alcohol is usually utilized. The pressure of the airstream is determined from the difference of height between the levels of the liquid while the velocity of the wind in a given moment is determined by means of Bernoulli's equation.

In section I (Fig. 203), the air pressure in the thin tube is equal to p_1 and the velocity is V_1; in section II, the pressure is p while the velocity is V.

Consequently, for these two sections, Bernoulli's equation is written in the following manner:

$$p+\frac{\rho V^2}{2}=p_1+\frac{\rho V_1^2}{2}. \qquad (a)$$

since the velocity in the same tube is equal to zero ($V_1 = 0$), we can write:

$$p_1=p+\frac{\rho V^2}{2}, \qquad (b)$$

or:

$$p_1-p=\frac{\rho V^2}{2}. \qquad (c)$$

/316

This pressure difference causes the difference in the position of the liquid levels in the tube of the pressure gauge. Consequently, we can write:

$$\frac{\rho V^2}{2}=h\gamma. \qquad (d)$$

Hence, we obtain:

$$V=\sqrt{\frac{2h\gamma}{\rho}}, \qquad (246)$$

where: ρ -- mass density of the air;
h -- height of the column of liquid in mm;
γ -- specific weight of the liquid in the pressure gauge.

The relationship between the mass density of the air ρ, the temperature t and the barometric pressure is given by equation (3) (see first chapter).

Substituting ρ in equation (246) by its value from equation (3), we obtain:

$$V=\sqrt{\frac{2h\gamma}{0.0474\frac{B}{273+t}}}=\sqrt{\frac{42.2h\gamma(273+t)}{B}}=$$
$$=6.5\sqrt{\frac{h\gamma(273+t)}{B}}.$$

The specific weight of the water $\gamma_w = 1$, while that of alcohol is 0.79. Expressing h in mm water, and substituting the numerical values of the specific weight, we obtain:

for the water column pressure gauge:

$$V = 6.5\sqrt{\frac{h(273+t)}{B}};$$

for the alcohol pressure gauge:

$$V = 6.5\sqrt{\frac{0.79h(273+t)}{B}}.$$

Under normal conditions, t = 15° C, B = 760 mm Hg. Substituting these values, we obtain the following simple expressions:

for the water column pressure gauge:

$$V = 4\sqrt{h}; \quad (247)$$

for the alcohol pressure gauge:

$$V = 3.55\sqrt{h}. \quad (247a)$$

Anemograph. An instrument which records not only the velocity /317 of the wind but also its direction is called anemograph.[1] The recording made by this instrument gives a clear representation of the specific pattern of changes in the velocity and direction of the wind.

The general view of the receiving part of the anemograph is shown in Fig. 204, where 1. is a worm gearing with contact for tracing the velocity of the wind; 2. is a box with an electrical device which perceives the direction of the wind. The tracings are transmitted via an electric conductor to a recorder which is mounted in the building of the meteorological station.

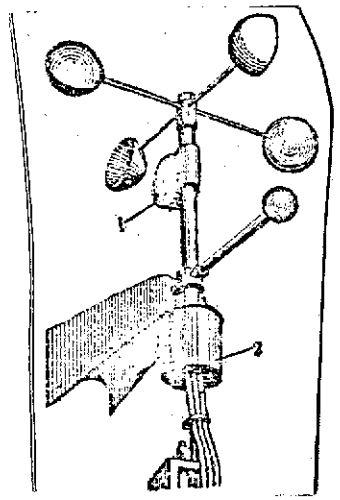

Fig. 204: Anemograph.

Micromanometer. At low velocities of the airstream which are measurable by means of Pito's tube, the height h in a normal manometer is too small, which hinders accurate readings. A more sensitive instrument for use with Pito's tube is the micromanometer [26].

Fig. 205 illustrates the diagram of the commonest micromanometer with tilted tube. In the newest design, it is possible to change the slope of the tube, which is convenient for changing the sensitivity of the micromanometer depending on the experimental conditions.

Closed vessel A, which is connected by means of tubing B with Pito's tube,

1. [Translator's note: A different word is used in Russian from the word in the heading of the previous section, which however, has the same meaning in English.]

usually contains alcohol. Due to the difference in pressure -- dynamic pressure between the side of Pito's tube and the surface pressure on the side of the open tilted tube C, the level in the tube assumes a certain position above the level in vessel A at a height h. Measuring the length of the liquid column ℓ in the tilted tube at a known angle α of tilting and a specific weight of the liquid γ we obtain:

$$h = \ell \sin \alpha \gamma \qquad (a)$$

The slope of the tube in micromanometers of this type is made /318 in such a way that the $\sin \alpha$ is a proper fraction: 1/2; 1/4, etc.

Example. At the slope of the tube $\sin \alpha = 1/10$ and a displacement in the meniscus inside the tilted tube $\ell = 5$ mm, specific weight of the alcohol $\gamma = 0.8$, we obtain: $h = 5 \cdot 1/10 \cdot 0.8 = 0.4$ mm water column

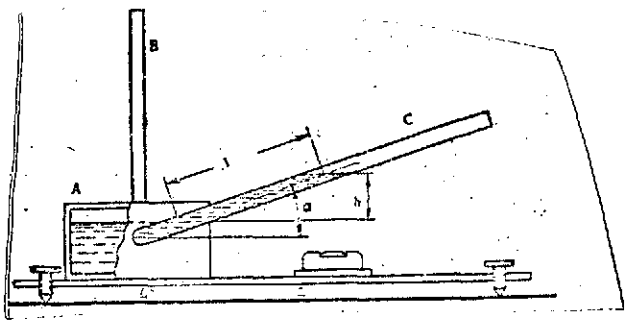

Fig. 205: Diagram of a micromanometer.

Since we adjusted the height of the alcohol column to that of the water column, the obtained value h can be substituted in equation (247); the obtained velocity is:

$$V = 4\sqrt{0.4} = 4 \cdot 0.63 = 2.53 \text{ m/sec.}$$

Avereage monthly and average annual wind velocities. The average velocity of the wind is called the average arithmetic magnitude composed of several observed velocities over a given interval of time. For example, 6 measurements of wind velocity were performed every 10 minutes in the course of an hour, consequently, the average velocity of the wind for this time interval equals:

$$V_{av} = \frac{\Sigma V}{6}.$$

This method of calculating the average wind velocity gives an approximate value. The average velocity of the wind can be obtained more accurately by means of anemometers. The average velocity of the/319 wind determined by means of the anemometer is obtained by dividing the number of meters shown by the anemometer, by the time in seconds of operation of the anemometer. For example, in the beginning of the observation, the point of the anemometer counter indicated the number 425 m; after 1 hour of operation the anemometer showed the number 18,784 m. Consequently, the average velocity of the wind per hour equaled in this hour:

$$V_{av.hr.} = \frac{18,784 - 425}{3,600} = \frac{18,359}{3,600} = 5,1 \text{ m/sec.}$$

If we add up the average wind velocities per hour observed in the course of every hour for one day and divide by 24, we obtain the average daily wind velocity, i.e.:

$$V_{av.hr.} = \frac{\Sigma V_{av.hr.}}{24}.$$

In an analogical way, the average annual velocity of the wind is determined by the expression: $V_0 = \frac{\sum V_{av.mo.}}{12}$.

On the basis of recordings of average daily velocities of the wind, performed by meteorological stations in the course of several years, tables are compiled of the average monthly and average annual velocity of the wind. These tables are of great practical interest, not only for wind technology, but also for many other branches of the national economy.

According to the data of meteorological stations obtained from observations performed for many years, general conclusions can be made about the distribution of the average velocities of the wind. The daily course of the wind velocity is characterized by the fact that the maximal velocities are usually observed in the middle of the day, from 11 AM to 3 PM, with a maximum at 1 PM. The annual course of the average monthly wind velocities is characterized for most regions in the USSR by a minimum in the summer months and a maximum in spring and in the fall.

On the contrary, in the Northern Ural and Nothern Siberia, the maximal wind velocity is observed in the summer.

In the plains, the velocities of the wind are highest during the day and lowest at night; in the highlands, on the contrary; the night wind velocities are greater than those reported during the day. In the winter, the velocity of the wind is similar at night and during the day.

As a rule, the regions situated near the seashores are distinguished by the strongest winds, for example, the coastlands of the Arctic and Pacific Oceans, of the Black and Caspian Seas, and of the Baikal and Balkhash Lakes. /320

In the mainlands, the regions with comparatively large wind velocities are our semi-arid regions in the southeastern European part of USSR.

The lowest velocities of the wind are observed in regions of the central part of Yakutia. Comparatively weak wind velocities are observed in the northeastern regions of the European part of the USSR, where the effect of forest areas is felt. The highest wind velocities are observed in the central regions of the Central Asian part of the USSR.

It is common usage to judge on the possible amount of wind energy which passes in a certain region in the course of the year from the annual average velocities of the wind. The latter however, may give entirely different amounts of energy because they are similar for regions which are situated at a certain distance from one another. This is explained by the fact that the annual average

velocities of the wind are arithmetical averages of the values of numbers to the first power, while the energies of the wind are sums of the cubes of these numbers. The sum of the cubes of a series of numbers with small fluctuation in their values is smaller than of a series of numbers with marked variations in their values, which give the same sum as the first series when taken to the first power.

The effect of obstacles on the wind velocity. When the airstream flows around an obstacle, a part of it is transformed from a linear movement into an irregular turbulent one. The air jets which flow around the edge of obstacles, in their immediate vicinity, are broken and form vortexes which are dragged away into the direction of the airstream. New vortexes appear at the sites of the streams which have been carried away, and so forth. This turbulence which starts at the sides of the obstacle is gradually extinguised at a distance from it, and disappears completely at a distance of approximately 15 times the height of the obstacle.

Investigations in the wind tunnel showed that the velocity of the airstream which passes above the roof of a house is markedly increased and consequently, an anemometer placed in the vicinity of /321 the tip of a roof, if the latter stands in an entirely open area, gives excessively high values of wind velocity for the given region. Behind the obstacle the velocity of the airstream decreases, not only at the level of the obstacle, but even at a slightly greater height.

The data obtained in the Kuchino wind tunnel about the movement of an airstream around models of individual houses, as well as groups of houses are shown in Fig. 206. The drawing shows that an anemometer placed in the vicinity of buildings cannot give true values of the wind velocity.

The underlying surface and the local topography exert a great influence on the velocity of the wind. An anemo-reconnaissance instrument has established that, at the height of 10-20 m, the velocity of the wind in plain-steppes changes, depending on local topography. The velocity of the wind above mountain tops in open mountain chains with regular streamlined slopes without any sudden change in topography increases 1.5-2 fold. If the elevation does not have regular slopes or the relief is disrupted by precipices, ravines, etc, the velocity of the wind is usally low.

Elevations with steep, precipitous, stony slopes cause very low wind velocities; a decisive effect belongs here to the ascendant and descendant streams.

The local topography creates the so-called local winds. If the airstream encounters an isolated top, then under certain conditions it can surround it and blow in the valley, and not above its reach. In the valley between the elevations, a kind of gangway is formed where the airstream is forced through. In such a manner, local winds

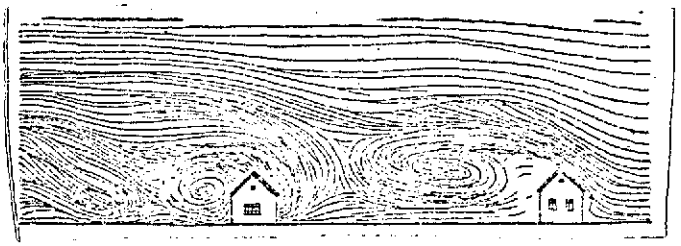

Fig. 206: Aerodynamic spectrum around houses models.

are created which sometimes /322 reach great strength under conditions where the velocities of the wind are comparatively low in the neighboring open part. The velocity of the wind also increases when the airstream surrounds hills with a more of less regular outline of their surface.

Anemo-reconnaissance. Most meteorological stations perform recordings of wind velocities according to the indications of Wild's wind vane and only 3 times per day, at 7 AM, 1 PM and 9 PM local time; the accuracy of this data is insufficient for thorough technical calculations. Therefore, in those cases when complete information is needed about the wind resources of a certain region, an expedition is sent out for anemometric reconnaissance. These expeditions study the structure of the wind, at the same time performing observations on the velocity and direction in several sites of the selected region.

Anemometric reconnaissance establishes: 1. the degree of uniformity of the airstream, 2. the effect of topographical conditions and various obstacles in a given region on the velocity and direction of the wind, 3. the dependence of the velocity and direction of the wind on the height above regions with changing configuration. In addition, parallel observations performed in various places of the same region and in the neighboring meteorological stations, facilitate the finding of conversion coefficients for the approximate determination of the average wind conditions in each of the sites of reconnaissance on the basis of corresponding average data about the velocities at other meteorological stations. The data of anemometric reconnaissance serve as a basis for selecting the site of construction of wind-driven installations as well as other structures which are related to a certain extent with the wind conditions of a given locality, for example, meteorological stations, airports, bases of airships, new towns, etc.

Interesting information was obtained for example, by the anemometric expedition in the mountainous regions of Crimea. The observations were performed by means of an anemometer with hemispheres fastened to rods with a length of 4 m. The duration of the readings on the anemometer was from 30-60 minutes. In the course of 45 days, /323 1400 separate observations were made; the following was found.

The velocity of the wind in valleys decreases considerably as compared to the general flow. In those places where the valley loses its steep slopes, the extinguishing effect disappears and the winds reach almost normal velocities. In the valleys of rivers, the wind stream loses 50-60% of its speed when directed across the valley.

In mountainous crossing points, high wind velocities were observed on the most streamlined tops which had regular outlines; tops with large stony precipices slackened the wind.

Regions of high plateaus are characterized by high velocities of the wind; the increase in velocity above the normal flow reaches 100%. Despite their higher position with regards to the center plateau, those points on the elevation which have wooded slopes also have lower wind velocity.

Recurrence of the wind. The wind recurrence is defined as the sum of the hours in the course of which wind with the same velocity blows in a certain place at different times.

The recurrence is the main magnitude characterizing the wind from an energetic viewpoint. In view of the inconsistency of the wind, the study of its recurrence is a very difficult task. Science has dealt with this matter for a long time. On the basis of long term investigation, several scientists have given mathematical relations which make it possible to find the theoretical magnitude of wind recurrence in a given region with a certain degree of accuracy. As early as 1889, Prof. Sreznevskiy derived the mathematical relation which gives a relatively close coincidence of the theoretical recurrence of the wind with the practical one, for Leningrad.

M. M. Pomortsev was the first to determine the relation which gives values of wind recurrence close to the real ones, for regions with annual average velocities not exceeding 5 m/sec. He arrived at the conclusion that this relation is characteristic and yields a normal Gaussian probability curve: $\tau = \frac{dt}{dV} = A \cdot e^{-B(V-V_0)^2}$,

where the parameters A and B can be determined either by the method of the least squares from actual observations, for whole values of V_0, or from a theoretical relation which is derived from Pomortsev's assumption on the applicability of Gauss's law to the given case. /324

$$A = \frac{\sqrt{B}}{\sqrt{\pi}} = \frac{\sqrt{n-1}}{\sqrt{\pi} \cdot \sqrt{\Sigma (V-V_0)^2}}; \quad B = \frac{n-1}{\Sigma (V-V_0)^2}.$$

V -- velocity of the wind;
V_0 -- average velocity of the wind in the examined time interval;
n -- number of components.

The recurrence curves of the winds according to Pomortsev are presented in Fig. 207, while Table 16 illustrates the recurrence in hours [27].

More recent theoretical data on wind recurrance was suggested by Gullen.

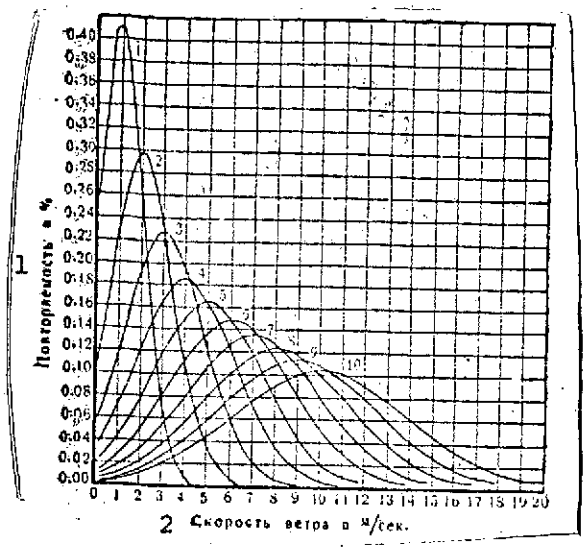

Fig. 207: Curves of wind recurrence according to M. Pomortsev.

Key: 1. recurrence in %
2. wind velocity in m/sec.

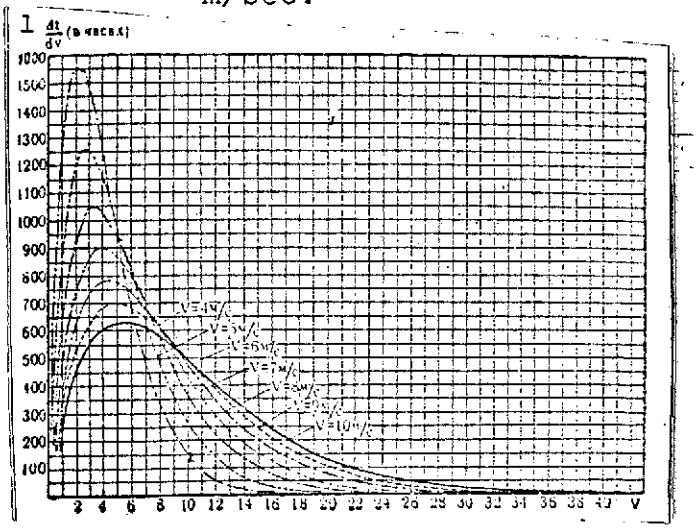

Fig. 208: Curves of wind recurrence according to Gullen.

Key: 1. in hours

The curves of wind recurrences according to Gullen elaborated by S. L. Rozentul are presented in Fig. 208; Table 17 gives the recurrence corresponding to these curves in hours. /325

For a comparison of the theoretical recurrence with the recurrence of the winds observed in nature, Fig. 209 and 210 illustrate the recurrence curves according to Gullen, Pomortsev and according to actual data. /326

Examination of these curves leads to the conclusion that in order to determine the recurrence of various wind velocities it is quite possible to use the curves and tables of Gullen and M. M. Pomortsev. It is recommened to use Gullen's curves for the determination of the recurrence of wind velocities in regions with average velocities from 6 m/sec above, while Pomortsev's curves need more accurate values of recurrence in regions with average wind velocities below 6 m/sec.

Change in wind velocity with altitude. The given obstacles on the Earth's surface effect considerably the velocity and direction of airstreams. As the altitude above the Earth's surface increases, this influence diminishes and it disappears almost completely at a certain altitude.

Fig. 211 presents the changes in the velocity of the wind, recorded by a special instrument which was mounted in a kite, in an Aerological observatory in the USSR. Curve a shows the change in the velocity of the wind in a short time period at an altitude of 250 m, while curve b shows the wind velocity during the same time intervals in the vicinity of the Earth's surface. These graphs /327

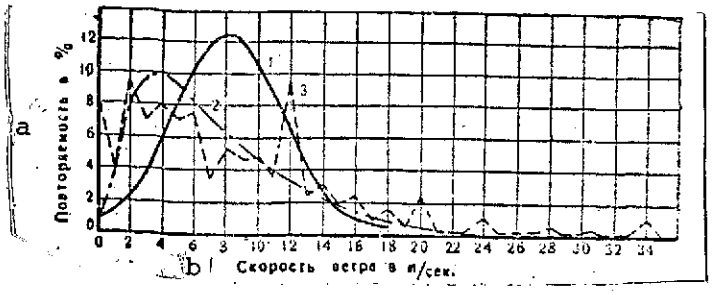

Fig. 209: Comparison of the recurrence curves according to Pomortsev and according to Gullen with the rear recurrences in nature: 1-recurrence according to Pomortsev; 2-according to Gullen; 3-according to tracings.

Key: a. recurrence in %
b. wind velocity in m/sec.

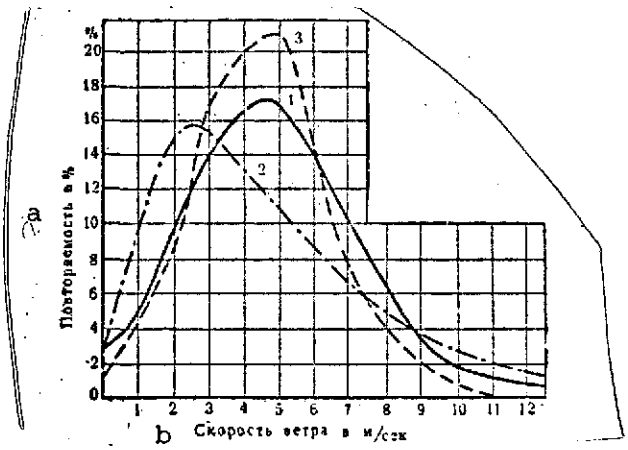

Fig. 210: Comparison of the recurrence curves according to Gullen and according to Pomortsev with the actual recurrences for Moscow: 1-recurrence according to Pomortsev; 2-according to Gullen; 3-according to recordings.

Key: a. recurrence in %
b. wind velocity in m/sec.

show that the flow of airstreams in the upper layers of the atmosphere takes place with less pulsations than below, in the vicinity of the Earth's surface. Observations on the changes in the wind velocity with altitude, above various kinds of underlying surfaces, show that the greatest decrease in velocity in the vicinity of the Earth's atmosphere is caused by urban development, even in the plains. When the underlying surface is an open plain, the velocity of the wind decreases in the vicinity of the Earth's surface. The lowest radiants of decrease in wind velocity is observed above a convex surface with a smooth out- /329
line of its relief; here there is even a slight increase in wind velocity in the vicinity of the surface. For example, in Novorossiysk, there is an increase in wind velocity in the vicinity of the Earth's surface which amounts to 1/1/2 fold as compared to the general stream flowing above the Earth's surface in the Markhotsk Pass. Fig. 212 give curves obtained according to observations performed in the Aerological observatory in the USSR which gives the values of wind velocity during the winter and during the summer; it can be seen that in the layers above 1000 m, there is a slight change in wind velocity with altitude while at an altitude of about 500 m the wind velocity decreases with an increase in altitude. This phenomenon should probably be related with the circumstance that on calm days, when the Earth's surface is sufficiently heated by the sun, air currents of a local character resembling

TABLE 16. RECURRENCE OF THE WIND ACCORDING TO M. M. POMORTSEV

Wind velocity, in m/sec	Average annual wind velocities (in m/sec)									
	1	2	3	4	5	6	7	8	9	10
	Hours of wind recurrence									
0	2 230	876	500	307	175	87	52	44	18	0
1	3 600	2 020	1 030	630	376	228	149	88	62	18
2	2 190	2 590	1 700	1 070	684	420	262	187	140	70
3	653	2 020	1 990	1 445	1 003	700	462	334	228	180
4	87	873	1 710	1 610	1 310	963	700	492	350	280
5	—	330	1 050	1 445	1 445	1 210	930	685	500	394
6	—	51	525	1 070	1 310	1 320	1 100	876	700	520
7	—	—	193	640	1 050	1 228	1 180	1 030	840	684
8	—	—	62	315	700	1 000	1 120	1 100	980	788
9	—	—	—	152	376	700	963	1 033	1 000	876
10	—	—	—	52	183	438	720	886	960	896
11	—	—	—	26	70	262	500	700	850	876
12	—	—	—	—	52	131	312	516	700	796
13	—	—	—	—	26	52	170	350	520	688
14	—	—	—	—	—	26	70	220	368	520
15	—	—	—	—	—	—	36	115	250	420
16	—	—	—	—	—	—	18	61	157	290
17	—	—	—	—	—	—	16	26	87	193
18	—	—	—	—	—	—	—	17	52	131
19	—	—	—	—	—	—	—	—	18	79
20	—	—	—	—	—	—	—	—	—	61

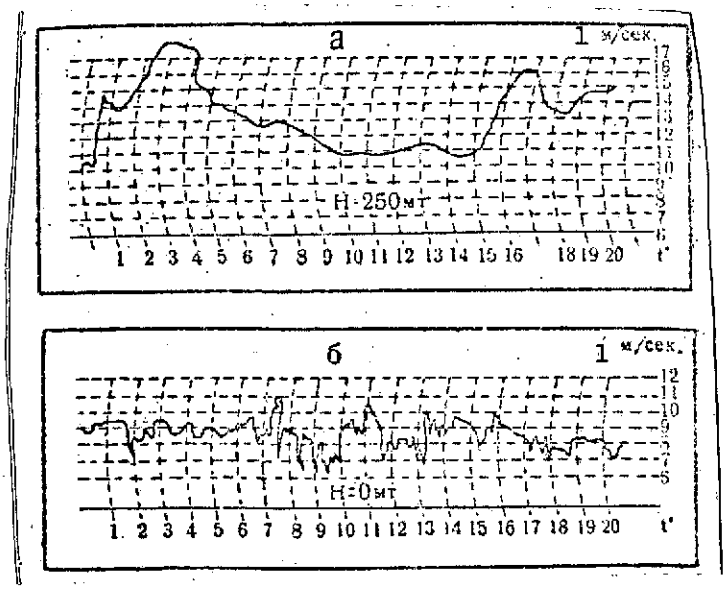

Fig. 211: Characteristic of the wind: a-at an altitude of 250m; b-on the surface of the Earth.

Key: 1-m/sec

the breezes are formed near the Earth, which increase the/330 general movement of the air during the day. When the velocity of the general circulation is low, these local winds can of course considerably increase the wind in the vicinity of the Earth's surface. The effect of the local wind is quenched under conditions of increase in the winds of the general circulation, and what comes to the fore are effects of a general order [23]. In the lower layers and up to 500 m above the Earth's surface, a marked increase in wind velocity is observed with increasing distance from the ground. A comparison of the velocities between winter and summer shows that the change in wind velocity with altitude is much /331 less expressed in the summer than in the winter, which is explained by lower values of the vertical temperature gradient in winter time as compared to the summer.

TABLE 17. RECURRENCE OF THE WIND ACCORDING TO GULLEN

Wind velocity in m/sec	Average annual wind velocities in m/sec						
	4	5	6	7	8	9	10
	Hours of wind recurrence						
Up to ½	365	245	172	130	103	83	65
1	1 200	850	630	475	400	300	250
2	1 540	1 200	930	750	620	520	450
3	1 450	1 250	1 040	870	736	620	550
4	1 220	1 150	1 020	900	775	680	605
5	930	950	930	860	770	700	630
6	660	780	810	780	740	670	620
7	470	630	680	700	675	650	600
8	330	480	650	600	600	600	570
9	220	350	450	520	530	550	540
10	150	260	360	460	475	490	490
11	90	200	280	350	410	440	450
12	50	140	220	280	345	380	400
13	36	100	170	230	290	330	360
14	20	60	140	190	240	280	320
15	17	40	100	150	200	240	280
16	10	30	70	125	170	200	240
17	—	22	60	100	140	175	210
18	—	13	40	75	120	150	180
19	—	10	30	58	99	130	150
20	—	—	20	36	75	110	130
21	—	—	18	27	60	85	110
22	—	—	15	22	50	75	100
23	—	—	10	17	35	60	80
24	—	—	5	15	25	50	70
25	—	—	—	10	22	40	60
26	—	—	—	6	18	35	50
27	—	—	—	4	15	30	40
28	—	—	—	—	12	22	32
29	—	—	—	—	10	18	28
30	—	—	—	—	—	12	22
31	—	—	—	—	—	10	17
32	—	—	—	—	—	9	15
33	—	—	—	—	—	7	14
34	—	—	—	—	—	6	10
35	—	—	—	—	—	3	6
36	—	—	—	—	—	—	5
37	—	—	—	—	—	—	4
38	—	—	—	—	—	—	3
39	—	—	—	—	—	—	2
40	—	—	—	—	—	—	2

On the basis of the given observations on wind velocity in relation to altitude, several investigators derived general formulas for determining the velocity of the wind according to altitudes.

Of these formulas, the simplest relation for a height of 5 m and above is the following expression:

$$V = V_0 \left(\frac{h}{h_0}\right)^{\frac{1}{5}}, \tag{248}$$

where: V_0 and h_0 -- are correspondingly the velocity and the height, measured in the vicinity of the ground;
V -- velocity determined for a height h.

The shortcoming of this formula is that it does not account for the effect of the underlying surface on wind velocity, as well as for the turbulence seen in the vicinity of the ground. D. L. Laykhtman took into consideration the effect of these factors and admitting

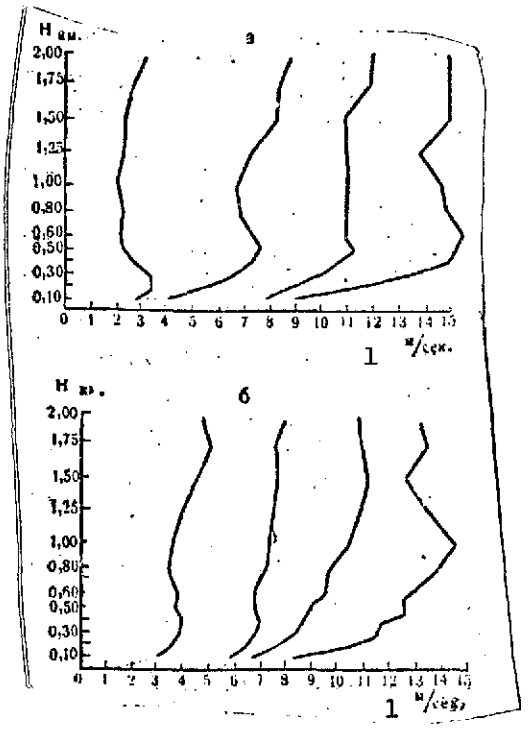

Fig. 212: Characteristic of the change in wind velocity in relation to altitude: a-winter at 1 AM; b-summer at 1 PM

Key: 1. m/sec

that at a certain height h_0, the velocity of the wind V = 0, he obtained the following formula:

$$V = V_1 \frac{\ln \frac{h}{h_0}}{\ln \frac{h_1}{h_0}},$$

where V -- unknown velocity of the wind at h; V_1 -- known velocity of the wind at h_1; h_0 -- height at which the velocity of the wind is equal to 0. Usually h_0 is regarded as a measure of the roughness of the underlying surface; its magnitude equals 6.7 cm in the case of a sugar-beet field; 3.2 cm in the case of a field covered with low grass, and 0.5 cm, if the underlying surface is covered with snow.

A comparison of this equation with the results of direct observations which include the air layer close to the ground starting with several cm, confirmed the validity of this equation for calculating the changes in wind velocity in relation to altitude under conditions of an adiabatic gradient (Laykhman, "Wind profile and interchange in the atmospheric layer close to the ground", Izvestiya Akademii nauk USSR 8(1) (1944).

The change in wind velocity in the layer extending from 1-5 m above the surface of the ground, according to the observations of Rykachev performed in 1917 and published in the collection Yestestvenniye proizvoditel'nye sily Rossii [Natural production forces of Russia] Vol. I, Part 1, is characterized by the following values (in m/sec). /332

In the lower layer, the winds follow the local relief. The irregularities of the surface encountered by the wind cause turbulence, which is unfavorable for the work of wind engines. The instability of the wind with regard to both velocity and direction extends up to a height of approximately 80 m above the ground.

1 Подстилающая поверхность	2. Высота (в м)				
	1	2	3	4	5
3 Снежный покров	4,31	5,25	5,48	5,50	5,(9)
4 Снежный покров сошел (апрель-май)	4,65	5,50	5,80	5,95	6,00
5 Среднее значение скорости за весь промежуток времени с 8/II по 24/V 1917 г.	4,88	5,85	6,23	6,40	5,6

Key: 1. underlying surface
2. height (in m)
3. snow cover
4. with snow cover gone (April-May)
5. average value of the velocity in the period from Feb. 8 to May 24, 1917

47. The Energy of the Wind

According to equation (62), Section 14, the energy of the wind changes proportionally to the cube of its velocity:

$$\frac{mV^2}{2} = \frac{F\rho V^3}{2}.$$

It is of practical interest to determine what amount of the wind energy can be utilized by modern technology. Modern wind technology has given as yet no exhaustive answer to this question. The inconsistency of the wind velocity in time and with altitude, the lack of experience in the exploitation of groups of wind engines, as well as of individual powerful wind engines with a power above 200 hp, do not allow to determine the magnitude of the wind energy which can be put to practical use.

Let us, however, present some theoretical considerations on this matter.

N. V. Krasovskiy distributed the wind engines on the surface of the land in a checkerboard pattern over a distance which was 15 fold the diameter of the wind-driven wheel. This author found that the following amount of wind energy could be obtained per square km of ground surface (Table 18).

The over-all power determined for the USSR can amount to 10,701 million kW with an annual average energy output of 18, 281 billions of kW hours [18].

Approximate theoretical calculation of the wind energy. /333
Adhering to the checkerboard pattern of wind engines on the surface of the ground, let us calculate the amount of wind energy per square km. The area under one wind engine should be equal to:

$$F = 0.785D^2, \qquad (a)$$

where: $D = 15$ D -- diameter of the circular area under one wind engine;
D -- diameter of the wind driven wheel.

The closest disposition of wind engines can be obtained if one assumes that the area under each wind engine has the shape of a regular hexagon. The area of such a hexagon will be equal to:

$$F_{he} = 0.87D^2 = 0.87(15D)^2 = 196\ D^2. \qquad (b)$$

TABLE 18

Annual average wind velocity (in m/sec)	3	4	5	6	7	8	9	10
Steady power in kW for generators working with wind engines per sq. km.	297	435	618	790	1 100	1 480	1 880	2 400
Annual output in 1000 of kW hrs obtained per sq. km.	445	680	1 060	1 550	2 220	3 040	3 950	5 120

Dividing one sq. km. by 196 D^2, we obtain the number of wind engines which can be accommodated per sq. km., i.e.:

$$n = \frac{1\,000^2}{196 D^2} = \frac{5\,100}{D^2}. \tag{249}$$

The power of each wind engine equals [Section 22, equation (137)]:

$$N = 0.000654\, D^2 V^3 \text{ hp}$$

Multiplying this expression by $5100/D^2$, we obtain the determined power per sq. km.:

$$N_{det} = 0.000654 D^2 V^3 \cdot \frac{5\,100}{D^2} = 3.34 V^3 \text{ hp} \tag{250}$$

or

$$N_{det} = 2.46 V^3 \text{ kWt.} \tag{250a}$$

/334

If $\xi = 0.30$ we obtain a simple expression for the steady power:

$$N_{det} = V^3_{det} \text{ hp,} \tag{251}$$

where V_{det} is the velocity of the wind corresponding to the determined or nominal power of the wind engine (see chapter IX).

For determining the annual output of a wind engine, its characteristics and the recurrence of the wind in the region of the wind installation should be known.

Knowing the characteristics, the output coefficient of the wind energy can be determined at various wind velocities. From the recurrence curve, the number of work hours of the wind engine can be determined in the course of the year for each velocity of the wind.

Having this data, the annual output can be calculated by means of the equation:

$$\Sigma N = 0.000654 D^2 \eta \Sigma V^3 t_p, \tag{252}$$

where: D -- diameter of the wind-driven wheel;
η -- mechanical output coefficient of the wind engine;
V -- velocity of the wind at which the wind engine can operate;
ξ -- output coefficient of the wind energy;
t_p -- number of hours of recurrence for each wind velocity.

In working with centrifugal pumps, generators, millstones and several agricultural machines, the coefficient ξ can be assumed to be constant, while it is variable in the case of piston pumps.

In calculating the number of hours of wind recurrence, all the hours t of wind recurrence at a velocity above t_y should be added to the number of hours t_y of wind recurrence at a velocity equal to V_y, up to a V_y at which the power of the wind engine becomes limiting, i.e.:

$$t_p = t_y + t.$$

By means of equation

$$N = 0{,}000654 D^2 V^3 \xi \eta$$

the power of the wind engine can be calculated at velocities of the wind 3; 4; 5; 6; 7 and 8 m/sec, if V_y = 8 m/sec (a wind velocity of 3 m/sec is taken into consideration only for wind-driven pump installations). The number of hours per year in which the wind blows with each of these velocities can be found in Table 16 or 17, which describes the recurrence of the wind. Consequently, by multiplying the power of the wind engine by the number of hours of recurrence at the given velocity and adding up the products, we obtain the annual output of the wind engine. The magnitude of the output coefficient of wind energy and the output coefficient of the engine should be taken from the characteristic of the wind engine which operates with a given machine [45]. /335

Table 19 presents the calculations of the annual output in hp hours for an arbitrary wind engine with a diameter of the wind-driven wheel D = 1 m and different annual average wind velocities. The power was calculated for the shaft of the wind-driven wheel, where η = 1.0 and ξ = 0.30 = const.

TABLE 19

Annual average wind velocities (in m/sec)	3	4	5	6	7	8	9
Annual output of wind engine D = 1 m (in hp hr.)	87	196	314	435	544	628	692

Since the power of the wind engine is proportional to the square of the diameter of the wind-driven wheel, its output for different dimensions can be calculated for any annual average wind velocity by means of equation:

$$\Sigma N = \frac{D^2}{D_0^2}\Sigma N_0 = \frac{D^2}{1^2}\Sigma N_0 = D^2 \Sigma N_0, \quad (253)$$

where the values of ΣN_0 are presented in Table 19 for average annual velocities ranging from 3 to 9 m/sec.

48. Accumulation of the Wind Energy.

The periods of fluctuation in wind energy are of the order of seconds, minutes, hours, months and even years.

As an example, Fig. 213 presents the anemographic tracing of the wind velocity at a height of 190 m during a period of 20 seconds. We can see from the graph that the change in wind velocity in intervals /336 of 2 seconds may reach 10 m/sec. For example, from the 13th to the 15th and from the 20th to the 21st second, the velocity of the wind changed from 5 to 15 m/sec, i.e. increased 3 fold. Consequently, the energy of the wind in this moment increased 27 fold. These fluctuations of energy are ironed out by various regulating devices of the wind engine. The inconsistency of the wind in time, with frequent calm periods extending from 1 to 5 days, requires structures of storage devices which make it possible to accumulate the energy during the calm period. At this moment in time, the matter constitutes an extremely complex problem in the practice of wind energy utilization.

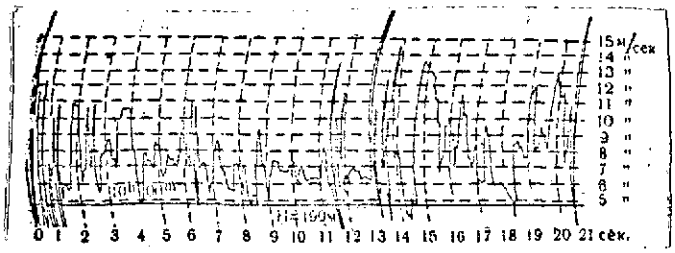

Fig. 213: Anemographic tracing of the velocity of the wind during 20 sec. at the height of 190 m.

Types of storage devices. The changes in wind velocity which take place both in magnitude and in the course of time make it possible to use in practice both buffer and capacitance types of energy storage devices.

The buffer storage devices can accumulate and return to the consumer the stored energy in short periods of time in the order of seconds, minutes, and up to one hour.

The capacitance storage device can store and return to the consumer the energy accumulated in the course of a prolonged time -- from 1 hour to several hours.

According to their principle of operation, the storage devices used in wind technology can be subdivided into the following groups:

1. mechanical 2. electric, 3. hydraulic, 4. thermic, 5. pneumatic and 6. hydrogen storage device.

The mechanical accumulator stores the excess energy and returns it when needed by means of mechanisms such as flywheels, springs, jacks, etc. These mechanisms return the stored energy to the power tool intermittently like the flywheel, or at certain moments in time, like the spring. /337

Of the existing mechanical accumulators the one designed by Ufimtsev-Vetchinkin is well known. This storage device consists of a steel disc with an axis, suspended on ball bearings; the disc is enclosed in a hermetically closed housing. The axis of the disc is connected by means of a special clutch to the generator and is in fact a continuation of the axis of the latter. This generator is set in motion by means of a belt transmission from the vertical shaft of the wind engine. The clutch which connects the axis of the disc to the axis of the generator is designed in such a way that when the number of revolutions increases, like when the wind velocity increases, the disc accumulates kinetic energy just like the flywheel of a steam engine. As soon as the wind slackens and the number of revolutions of the wind engines decreases, the disc continues to rotate with the same number of revolutions which it had in a given moment, and the clutch rotates the generator on account of the energy which it accumulated during the increase in wind velocity. In such a manner, the generator is operated either directly by the wind engine or by the storage device. The frequency at which the clutch is switched over depends on the duration of the wind gusts. As a result, the wind power installation gives to a certain extent an equal amount of energy regardless of the pulsating nature of the wind. This is the buffer type of energy storage device.

The diagram of operation of a wind engine with energy storage device is shown in Fig. 215.

The smallest weight per unit of energy accumulated by the storage device is held by a disc of equal resistance. The weight of the disc per 1 hp equals:

$$q = \frac{2100}{\sigma} \text{ kg/hp. hr.} \quad (254)$$

where σ -- tensile strength per kg/mm^2.

Table 20 presents approximate weights and the main data of energy storage devices, compiled by Prof. V. P. Vetchinkin.

The main drawback of energy storage devices is the losses caused by air friction. With regard to the losses caused by the friction in the bearings, these form an extremely low percentage of the losses of air friction when the bearings are properly made and well lubricated.

TABLE 20

1. The parameter	Ring with a disc instead of spokes	Disc of constant thickness (without openings in the middle)	Disc of equal resistance
2. Theoretical weight of rotor kg/hp hr.	$\frac{5\,700}{\sigma}$	$\frac{4\,700}{\sigma}$	$\frac{2\,850}{\sigma}$
3. Total weight of storage device (with housing, shaft and bearings) kg/hp hr.	$\frac{8\,000}{\sigma}$	$\frac{6\,000}{\sigma}$	$\frac{4\,000}{\sigma}$
4. Material of the rotor	iron	common steel	high quality steel
5. Stress of the rotor kg/mm^2	16	40	80
6. Circular velocity m/sec	140	350	700
7. Weight of storage device per kWt hr of stored energy kg/kWt hr.	500	150	50

In order to decrease the velocity caused by friction of the air, a rotating disc is included in a hermetically closed housing, in which some vacuum had been created. This method was applied by inventor Ufimtsev for the wind installation built by him in the town Kursk. /338

To the mechanical storage devices belong also the elastic energy storage devices in which the elastic properties of bodies are utilized for the accumulation of energy. An example of the simplest buffer storage device are the rubber shock absorbers used in aviation for the undercarriage of airplanes.

Electric energy storage devices -- devices which make it possible to accumulate and preserve the electric energy in the form of constant current for its expenditure according to the graph of consumption. The element of an electric storage device consists of a battery filled with dilute sulfuric acid and the electrodes placed in it, which are lead plates. /339

The number of ampere-hours which the storage device can supply to the net is called the capacitance of the storage device. The capacity depends on the number and dimensions of the plates of each

element and on the intensity of the charged current, under conditions where the dimensions of the plates are the same. Experience shows that the slower the discharge, the larger the capacitance of the storage device, i.e. the larger the number of ampere-hours which it develops, as long as the voltage of each element does not decrease from 2.05 to 1.8 V. For example, if during its discharge the battery can give 70 amperes in the course of 3 hours, it had a capacitance of 210 ampere-hours. When the current of this battery is only 28 amperes, 3 and not 10 hours are needed for it to be charged, i.e. under this condition the capacitance increases up to 28 x 10 = 280 ampere-hours.

The output coefficient of the storage device is called the ratio of the work obtained during complete discharge to the work consumed during the charging. The magnitude of this coefficient varies between the limits 70-80%.

Electric storage devices operate only with constant current. Therefore, in alternating current circuits, the alternating current is transformed into constant current prior to discharge, while during the discharge, the constant current of the battery is transformed into the alternating current circuit. Such a double transformation decreases the output coefficient of the battery and increases the measured losses of the installation.

Hydrostorage devices. The hydrostorage device is a power installation where the energy of the wind or any other energy is transformed into potential energy in the form of water raised to a certain height, which in its fall can perform work. The diagram of a wind installation with hydrostorage device is shown in Fig. 214. The wind engine is situated at the highest point in a place open to the wind and is operated by a generator. Machine building 2 of the hydrostorage device is situated in the vicinity of water source 3 -- a river, pond or lake. The electrical current obtained from the wind-driven installation is transmitted via line 7 and sets in motion the electrical engine with centrifugal pumps which supply the water via a pipe to the forebay pipe. In the absence of wind, the water passes through the same pipe into a turbine, which sets in motion the generator. When sufficient water is available, it can be led into an irrigation system [16]. /340

The amount of water required per 1 hp hr of accumulated energy is determined from the equation for the power of the hydroturbine:

hence:

$$N=\frac{QH\eta 1\,000}{75\cdot 3\,600}=1,$$

$$1000QH\eta=75\cdot 3600\ \text{kg m}$$

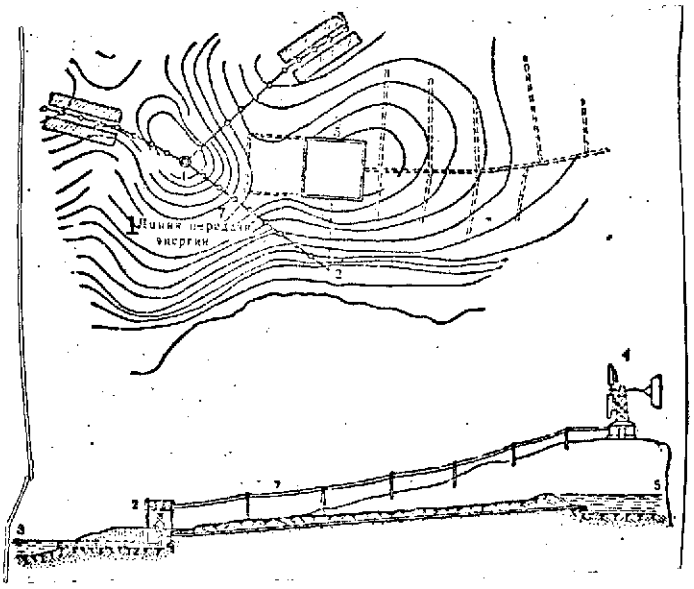

Fig. 214: Diagram of a wind power installation with hydrostorage device.

Key: 1. line of transmission of the energy

This expression yields: /341

$$Q=\frac{75\cdot 3600}{H\eta\cdot 1000}=\frac{270}{H\eta}\ м^3/hp\ hr. \quad (255)$$

where: H -- height from the lower to the upper level of the water in the forebay in m;

η -- efficiency of the hydrostorage device;

Q -- amount of water in $м^3$.

The efficiency of the hydrostorage device is determined by multiplying the efficiencies of the units of the installation, i.e.:

$$\eta=\eta_{tr}\,\eta_{pu}\,\eta_{pi}\,\eta_{tur}\,\eta_{fo} \quad (256)$$

assuming η_{tr} = 0.95 -- efficiency of the transmission from the engine to the pump,

η_{pu} = 0.8 -- efficiency of the pump,

η_{tur} = 0.9 -- efficiency of the pipe,

η_{tur} = 0.85 -- efficiency of the turbine,

η_{fo} = 0.9 -- efficiency of the forebay (evaporation, seepage)

and substituting the numerical values in equation (256), we obtain:

$$\eta=0.95\cdot 0.8\cdot 0.9\cdot 0.85\cdot 0.9=0.525.$$

Substituting η = 0.525 in equation (255), we obtain the volume of water per 1 hp hr.

$$Q=\frac{270}{H\cdot 0.525}=\frac{515}{H}\ м^3 hp\ hr. \quad (255a)$$

The most important structure of the hydrostorage device is the forebay for the storage of water.

At a pressure head H = 10 m per 1 hp hr, the capacity of the forebay should be 51.5 m^2. In such a manner, the hydrostorage device with a steady power N_y = 10 hp per 10 hours of work, should have a forebay with a capacity of:

$$W=\frac{515}{H}\cdot N_y\cdot t=\frac{515}{10}\cdot 10\cdot 10=5\,150\ м^3.$$

It is not convenient to build such a large forebay for a wind installation of low power. Therefore, for building hydrostorage devices, natural water reservoirs have to be sought, which are situated at the required height. It may appear advisable to build dams in ravines and gulleys.

Thermic storage devices are structures in which the energy of /342
the wind is transformed into heat, which is stored either in the form of hot water for the heating of premises or in the form of vapor which is used in steam engines or turbines for central heating.

The thermic storage device which is intended for heating purposes is built according to the following plan. In those periods when the power of the wind-driven installation exceeds the load required by the consumer, the excess electrical energy is directed to electrical boilers in which the water is heated up to vapor formation and is then used in heating systems. An attempt of utilizing a thermic storage device for heating was made by G. A. Ufimtsev at the wind-driven electrical installation in the town Kursk.

The compressed air storage devices make use of the elastic properties of air. The compressed air is stored under great pressure in gas balloons or in reservoirs. In such a manner, the kinetic energy of the wind can be transformed into the potential energy of compressed air by means of a wind-driven compressor installation; the compressed air can be used for the operation of either power tools or air turbines. The work of expanding the air in the engine constitutes not more than 60% of the work spent on compressing this air in the compresssor. Regardless of the degree of compression, the weight of the compressed air storage device equals approximately 18 kg per kg of air.

The hydrogen storage device. G. A. Ufimtsev suggested in 1918 to accumulate the energy of the wind by electric dissociation of water into hydrogen and oxygen. The oxygen is used for industrial purposes, while the hydrogen is used for burning in internal combustion engines. Since the hydrogen can be stored in gas balloons, it is possible to store energy in the form of hydrogen fuel which can be spent according to need on the work of a thermic engine. The diagram of such a wind-driven hydrogen installation is shown in Fig. 215.

The wind engine sets in motion the energy storage device a which is fitted on axis b. The electrical current goes to the storage battery c and the electrolyser d where the process of dissociation of water to oxygen and hydrogen takes place. The oxygen is accumulated in reservoir e and can be used for various purposes. The hydrogen is stored in reservoir f from which it is used for the work of turning engine g which sets in motion generator h. This unit is /343
started in order to cover the excess load. As an example, the same figure shows the daily graph of the load of a wind-driven electric station. Curve I -- I shows the change of this load. The daily income of energy on account of the work of the wind engine is shown by curve k. The consumption of energy during the time from 3 PM to 9 PM is covered by the electrical storage device.

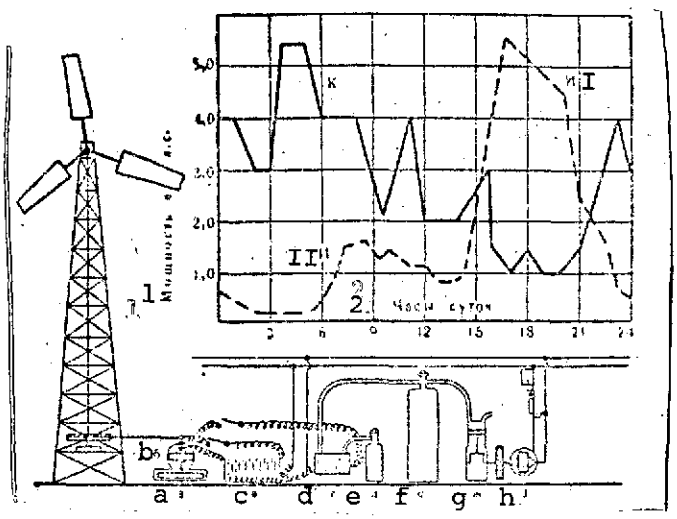

Fig. 215: Ufimtsev's diagram of a hydrogen installation.

Key: 1. power in hp
2. time of day

The reserve hydrogen engine g and the generator are started automatically each time that the charge supply of the storage battery is consumed up to a given limit of its voltage.

The automatic starting is performed by means of the current which passes through the dc generator of the engine. In this case the generator turns into a motor which accelerates the reserve engine during its starting. No practical data on this matter are available to date. It is hard to speak about the prospect of energy storage on account of hydrogen production.

Wind engines are designed according to the conditions of operation of different agricultural machines. The graph of energy utilization and the characteristics of power tools are the conditions which determine the type of wind engine.

Two types of wind engines are available to date; the low-speed -- multi-bladed and the rapid -- sparsely bladed. The output coefficients of wind energy in wind engines of both types with the exception of the rotor type, are almost identical, however the starting moments are largely different. The higher the rapidity the wind engine, the lower its relative moment.

Fig. 216 presents the aerodynamic characteristics of the main types of wind engines; in the upper part of the graph are given the characteristics of the output coefficients of wind energy, i.e. $\xi = f(Z)$, and in the lower part -- the characteristics of the relative moments $\overline{M} = f(Z)$ are given.

The curves in Fig. 216 show the change in the main magnitude of the wind engine characteristics: the initial and working moments, the rapidity of the wind-driven wheel Z_n with load, and synchronal Z_0 -- without load. On the basis of these magnitudes, it is possible to make a correct selection of the wind engine for work with a given machine and to find out the advantages of a certain type of wind engine by comparing the main parameters of its aerodynamic characteristics. For example, comparing the output coefficients of wind energy ξ, we find that winged wind engines are more effective than rotor ones. Comparison of the initial moment M_0 shows that the winged sparsley bladed wind engines are characterized by high rapidity and very small initial moment; the multi-bladed winged wind engines, as well as the rotor type, are distinguished by a large initial moment but very low rapidity, which should be taken into consideration in selecting the type of wind engine. /345

In projecting a wind power installation, the most favorable set of conditions of operation of the wind power unit should be sought for a definite type of work and considering the local wind conditions. In order to perform these tasks in the proper way, in addition to the aerodynamic characteristics, the performance of the wind engine should be known as well as the characteristics of the power tools which are operated at the same time.

49. Performance of Wind Engines and of Piston Pumps

The performance of a wind engine is defined as the relationship between the power of the wind engine at a certain wind velocity

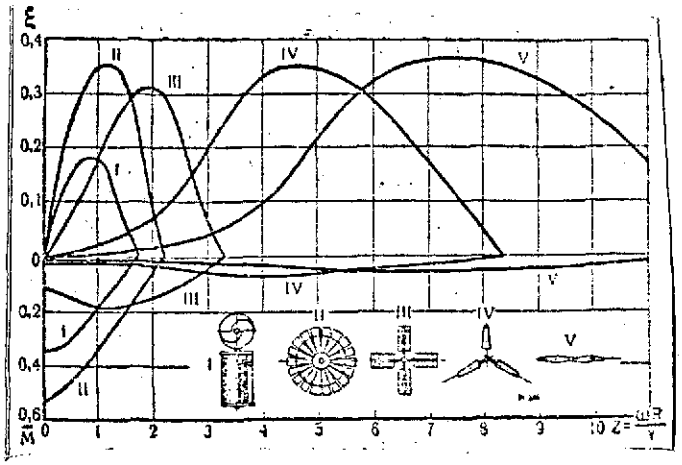

Fig. 216: Aerodynamic characteristics of wind-driven wheels in various systems.

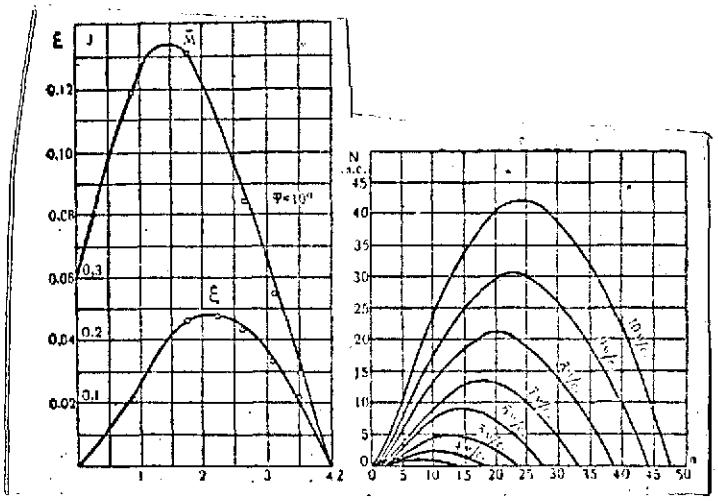

Fig. 217: Aerodynamic characteristics and performance of the VIME D-16 wind engine.

and the number of revolutions of the wind-driven wheel:

$$N = f(n).$$

These characteristics /346 are plotted on the basis of the aerodynamic characteristic $\xi = f(Z)$ by its scaling to the performance $N = f(n)$.

The values of rapidity $Z_1 Z_2$ etc. obtained from the aerodynamic characteristics are written out in a series together with their corresponding output coefficients of wind energy.

The number of revolutions of the wind-driven wheel is determined by means of equation (140) at wind velocities of 3, 4, 5, and 6 m/sec, etc.

$$n = \frac{30ZV}{\pi R}.$$

Further, according to equation (137)

$$N = 0{,}000654 D^2 V^3 \xi$$

the power of the wind engine is calculated for the same wind velocities and their corresponding Z, ξ and n; the result of the calculation is recorded in a table according to which the graph of the performance is plotted.

Example. In Fig. 217 left, the aerodynamic characteristic $\xi = f(Z)$, of the wind-driven wheel is given for an improved type of the VIME D-16 windmill. Let us recalculate this characteristic to the performance $N = f(n)$, as shown above; in Table 21, where V is in m/sec, n is rpm, N is hp on the shaft of the wind-driven wheel.

According to the data of Table 21, let us plot the curve of the /347 power of the wind engine for each working velocity of the wind in relation to the number of revolutions of the wind engine (Fig. 217, right).

TABLE 21

Rapidity of wind-driven wheel or no. of modules Z		0.5	1.0	1.5	2.0	2.5	3.0	3.5	4.0
Output coefficient of the wind energy ξ		0.050	0.125	0.20	0.245	0.230	0.175	0.110	0.020
$V=3$	n	1.80	3.60	5.40	7.20	9.00	10.80	12.60	14.40
	N	0.26	0.56	0.90	1.11	1.04	0.79	0.50	0.05
$V=4$	n	2.40	4.80	7.60	9.60	12.00	14.40	16.80	19.20
	N	0.53	1.34	2.14	2.62	2.47	1.87	1.19	0.12
$V=5$	n	3.00	6.00	9.00	12.00	15.00	18.00	21.00	24.00
	N	1.06	2.66	4.24	5.20	4.90	3.70	2.36	0.24
$V=6$	n	3.60	7.20	10.80	14.40	18.00	21.60	25.20	28.80
	N	1.83	4.60	7.35	9.00	8.50	6.40	4.10	0.41
$V=7$	n	4.20	8.40	12.60	16.80	21.00	25.20	29.40	32.60
	N	2.90	7.30	11.70	14.30	13.50	10.20	6.50	0.66
$V=8$	n	4.80	9.60	14.40	19.20	24.00	28.80	33.60	38.20
	N	4.32	14.30	17.50	21.40	20.20	15.20	9.70	0.98
$V=9$	n	5.40	10.80	16.20	21.60	27.00	32.40	37.80	43.00
	N	6.15	20.40	25.00	30.50	28.80	21.60	13.70	1.38
$V=10$	n	6.00	12.00	18.00	24.00	30.00	36.00	42.00	48.00
	N	8.40	28.00	34.20	42.00	39.40	29.80	18.80	1.89

Examining these curves, we note that the wind engine develops its maximal power corresponding to each wind velocity, only at certain revolutions of the wind-driven wheel. This characteristic should be used in selecting the power tools for a certain wind engine.

It is much more complicated to select the power tool for a wind engine than it is for a thermic engine. The thermic engine works with an almost constant power and number of revolutions, therefore the selection amounts to determining, from a catalogue, the corresponding power of a power tool and its revolutions. The /348 wind engine has both variable revolutions and variable power. The task of selecting a power tool for a wind engine consists in selecting a certain gear ratio of revolutions of the wind engine to fit the revolutions of the power tool, at which the unit can operate the longest time with maximal output coefficient of the wind energy. By means of the characteristics of the wind engine and of the power tool, it is easy to determine the gear ratio at which the unit will have the most favorable operating conditions. These operating conditions are obtained when in trying to superimpose the characteristic of the power tool over that of the wind engine, the former will pass through the peak of the performance curve of the wind engine, as shown by curve A in Fig. 218. Curves B and B' characterize an unfavorable set of operating conditions since in this case, the power consumed by the power tool is smaller than the power of the wind engine developed at each wind velocity. Moreover, curve B characterizes unstable operating conditions. In this case, with the

increase in the number of revolutions, the power of the power tool increases more rapidly than the power of the wind engine; therefore, the load will brake the wind engine in each moment by increasing or decreasing the revolutions with the changes in wind velocity.

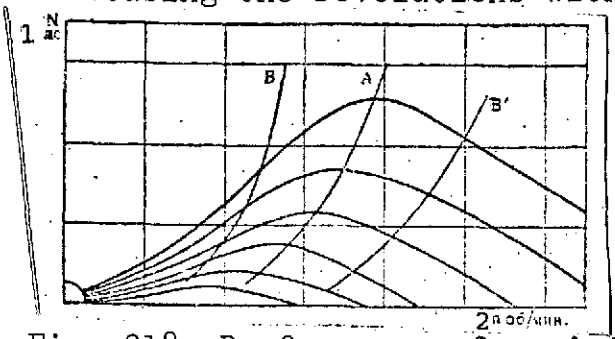

Fig. 218: Performance of a wind power unit under various operating conditions.

Key: 1. hp
2. rpm

The power N required for lifting water by means of a pump is determined by the equation:

$$N=\frac{QH}{75\eta}, \qquad (257)$$

where Q -- output, flow rate or feeding of the water by means of the pump, in liters per second; %349

H -- pressure head in m.

η -- overall efficiency of the pump, which consists of the mechanical efficiency η_m of the pump, accounting for the mechanical losses due to the friction of the piston against the walls of the cylinder, of the bar in the bearings, in the hinges, etc; η_h -- the hydraulic efficiency of the pump, accounting for the degree of faultlessness of the pump in the hydraulic sense, i.e. accounting for the losses in pressure head during the flow through the pump, and finally η_v -- volumetric efficiency of the pump.

$$\eta = \eta_m \eta_h \eta_v \qquad (258)$$

For liquids, the specific weight of which differs from that of water, the factor γ -- specific weight of the given liquid, should be introduced in equation (257). The output of a single acting piston pump is determined by equation

$$Q=hf\eta_v\frac{n}{60}, \qquad (259)$$

where: h -- piston stroke in dm;

-- area of the cross section of the piston pump in sq. dm.;

η_v -- volumetric efficiency or coefficient of filling; its value fluctuates between the limits 0.9 and 0.05;

n -- number of double piston strokes or revolutions per minute of the pump crank;

H -- overall pressure head in m. with which the pump operates or the manometric pressure.

The magnitude H consists of a static or geometric pressure head, H_{st} and of the sum of all the losses in the pressure head Σh_r in the suction intake pipe and in the delivery pipe.

$$H=H_{st}+\Sigma h_r \text{ м}. \qquad (260)$$

Substituting the value of the theoretical output of the pump Q in equation (257), we obtain:

$$N = \frac{hfuH\eta_0}{75 \cdot 60} = \frac{0.785d^2hHn\eta_0}{75 \cdot 60 \cdot \eta}. \quad (261)$$

In this equation the values of hg are constant. Assuming that the pressure head H is also constant, and denoting these magnitudes in equation (261) as C, we obtain: /350

$$N = Cn. \quad (262)$$

This equation shows that the power spent for the operation of the piston pump is directly related to the number of strokes n of the piston or the number of revolutions of the crankcase, at certain values of the piston's stroke h and of the pressure head H without accounting for the losses of pressure during the movement of the water in the pipeline. Hence we see that the characteristics of the pump power, plotted according to n, is a straight line which passes through the origin of the coordinates forming a certain angle with the axis.

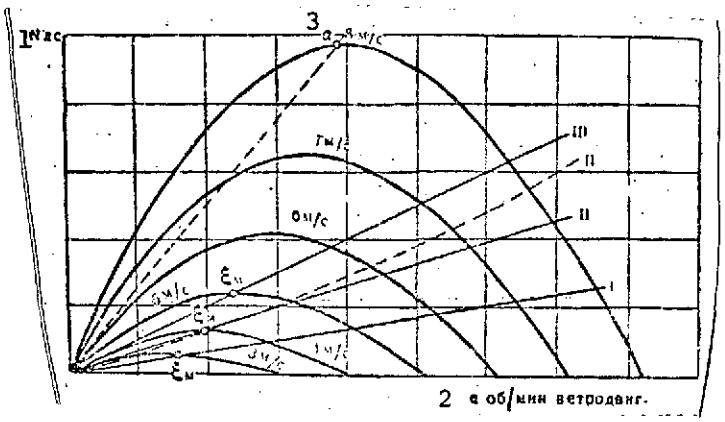

Fig. 219: Congruent characteristics of wind engine and piston pumps of different power.

Key: 1. hp
2. rpm of the wind engine
3. m/sec

Congruency of the performances of piston pumps and wind engines. In designing a wind-driven pump unit, one has to determine the power of the wind engine at which the pump should be connected. If the piston pump were connected at the maximal power of the wind engine, which it develops at the wind velocity of 8 m/sec, the characteristic of such a pump (Fig. 219, dotted straight line), when superimposed on the characteristic of the wind engine would cross it at point a. This straight line does not intersect the characteristic of /351 the wind engine at wind velocities below 6 m/sec., consequently, at this velocity the wind engine will not operate due to overload. However, we know from the tables of wind occurrence that winds with a velocity of 3 to 6 m/sec blow during the largest number of hours per year. In such a manner, a pump computed for the full power of the wind engine would prevent it from operating for the greatest part of the year. The husbandry needs water daily, therefore, the wind engine should work at those wind velocities which occur most frequently. In Table 16 which describes the occurrence of wind we find that most frequent are those winds, the velocities of which are equal to the annual

average velocity. Consequently, by adjusting the pump to the power which the wind engine develops at a wind velocity equal to the average annual value, we permit the wind engine to operate in a wide range of wind velocities and to insure the regular water supply of the husbandry. This means that if the average annual wind velocity in a given region equals 3 m/sec, the characteristic of the pump should intersect the peak of the curve describing the power of the wind engine at a wind velocity of 3/m/sec, as is shown by ray I in Fig. 219. If the average annual wind velocity in a given region is 4 m/sec, the characteristic of the pump should correspond to ray II, and finally, if the average annual velocity of the wind equals 5 m/sec, the characteristic of the pump should follow ray III.

It should be kept in mind, that in calculating the losses in the pipeline which change proportionally to $V^2/2g$, the straight lines I, II, and III assume the shape of a flat curve as shown by the dotted line for ray II.

Determination of the output and of the dimensions of the pump. Let us assume that the most appropriate operating conditions of a wind-driven pump unit corresponding to the average annual wind velocities in a given region, correspond to the characteristic of the pump illustrated by ray III in Fig. 219. The point of intersection of the ray with the peak of the curve describing the power at a wind velocity of 5 m/sec, determines the power of the wind engine which is equal to the power taken up by the pump. Consequently, from equation (255) we can determine the output of the pump:

$$Q = \frac{75 N_\eta}{H} \text{ l/sec} \tag{263}$$

In addition, knowing the diameter of the piston d, its stroke h and the revolutions of the crankcase n, the output of a single acting piston pump Q can be expressed by the equation: /352

$$Q = 0.785\, d^2 h \frac{\eta_v n}{60} \text{ l/sec} \tag{264}$$

From equations (263) and (264) we obtain:

$$\frac{75 N_\eta}{H} = 0.785\, d^2 h \frac{\eta_v n}{60},$$

hence

$$d = 75.6 \sqrt{\frac{N_\eta}{H h n \eta_v}}. \tag{265}$$

The general mechanical efficiency of piston pumps which operate with the wind engine can be assumed to be equal on the average to $\eta = 0.60$, while the volumetric coefficient is equal to $\eta_v = 0.95$. Substituting these values in equation (265), we obtain:

$$d \cong 60 \sqrt{\frac{N}{Hhn}} \text{ dm} \tag{265a}$$

where: H -- total pressure head in m;
n -- number of double piston strokes of the pump or revolutions per minute of the crank mechanism:

h -- piston stroke in dm;
N -- power of the wind engine in hp, which is determined by:

$$N=0.000654D^2V^3;$$

the velocity of the wind V is assumed to be the velocity at which the unit operates with maximal output coefficient of the wind energy (Fig. 219).

The diameter of the piston pump is determined by means of equation (265); pressure head H is computed on the basis of the ground and high level condition of the pump installation, the sites of water consumption, the length of the pipeline and of its parts which cause local losses in pressure head. The piston stroke h is given by construction conditions, as well as by the average velocity of movement of piston d which varies between 0.2 and 1.0 m/sec. The average velocity of the pump piston is determined by means of equation:

$$v=\frac{2hn}{60}=\frac{hn}{30}\ \text{m/sec},\qquad (266)$$

where h -- piston stroke in m.

In solving equation (265), the revolutions of the pump are taken/353 from the performance plotted according to Fig. (219) against the points of intersection of the characteristics of the pump with the peak of the power curve of the wind engine.

In order for the characteristics shown in Fig. 219 for a given pump to remain unchanged during the changes of static pressure head, the piston stroke should be correspondingly changed in such a manner that the product of the piston stroke h by pressure head H should remain constant for a given diameter of the pump piston, i.e.

$$hH=h_1H_1=\text{Const.}\qquad (267)$$

This rule is derived from the main equation of power (261). Denoting by $C=\frac{0.785\eta_n n}{75\eta_1 60}$ we obtain:

$$N=Cd^2hH,$$

and for another pressure head:

$$N=Cd^2h_1H_1,$$

from which we derive equation (267).

In order for the characteristic of the pump to stay unchanged during the changes in the diameter of the piston, h and H for a given characteristic should be correspondingly changed, i.e.:

$$hHd^2=h_1H_1d_1^2=\text{Const.}\qquad (268)$$

Congruency of the characteristics of the moments of wind engine and piston pump. In computing the output of a wind-driven pump installation, the velocity of the wind at which the wind engine starts and stops should be known. The simplest solution of this problem is by congruency of the characteristics of the loading moment of the piston pump with the characteristic of the moment of the wind engine plotted for various wind velocities.

Fig. 216 shows the characteristic of the relative moments $\overline{M}$ of the wind-driven wheel in relation to the rapidity Z. This characteristic is scaled to the characteristic of the dimensional moments M by a method presented on page 243; the moments are determined by the equation:

$$M = \overline{M}\pi R^3 \frac{\rho V^2}{2},$$

where: R -- radius of the wind-driven wheel.

TABLE 22

Rapidity Z		0	0.5	1.0	1.5	2.0	2.5	3.0	3.5	4.0
Relative moment $\overline{M}$		0.060	0.100	0.125	0.139	0.122	0.092	0.058	0.0314	0.005
Velocity of wind m/sec	n	0	3.60	7.20	10.80	14.40	18.00	21.6	25.2	28.80
	M	6.85	11.40	14.30	15.80	13.90	10.50	6.60	3.50	0.57
$V=4$	n	0	4.80	9.60	15.20	19.20	24.00	28.80	33.60	38.40
	M	12.10	20.20	25.30	28.10	24.70	18.50	11.70	6.34	1.01
$V=5$	n	0	6.00	12.00	18.00	24.00	30.00	36.00	42.00	48.00
	M	19.00	31.60	39.60	44.00	38.60	29.10	18.30	9.95	1.58
$V=6$	n	0	7.20	14.40	21.60	28.80	36.00	43.20	50.40	57.6
	M	27.30	45.40	56.70	63.00	45.40	41.80	26.40	14.30	22.80
$V=7$	n	0	8.40	16.80	25.20	33.40	42.00	50.40	58.8	66.60
	M	37.1	61.80	77.00	86.00	75.50	56.80	35.80	19.40	3.10
$V=8$	n	0	9.60	19.20	28.80	38.40	48.00	59.60	67.20	76.40
	M	48.50	80.60	101.00	112.00	98.50	74.20	46.80	25.40	4.04

Table 22 presents a general example of scaling of the relative moment $\overline{M}$ to the dimensional moment M kgm for a 4-bladed wind-driven wheel with a diameter of 8 m. /355

According to this table, a graph (Fig. 220) is plotted, which can be used for comparing the moments of the wind-driven wheel D = 8 m, and of the tool of the corresponding power.

The moment of the piston pump of single action changes during a complete revolution of a crank driven mechanism, proportionally to the sinus of the angle of rotation of the crank (Fig. 221).

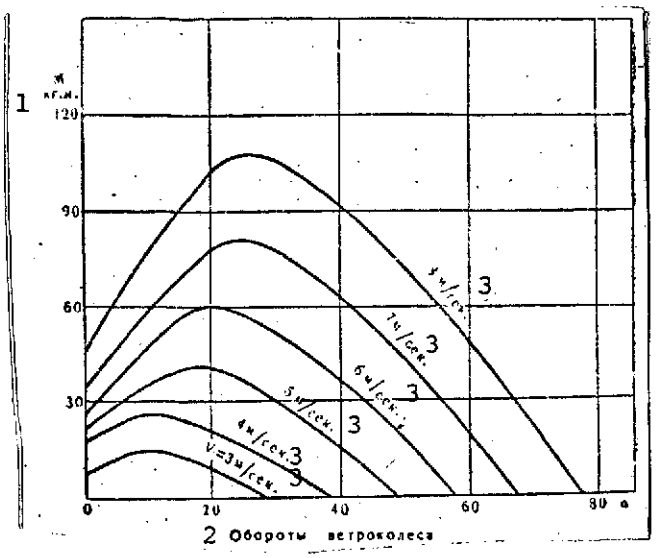

Fig. 220: Characteristic of the dimensional moments of the VIME D-8 wind-driven wheel.

Key. 1. kgm
2. revolutions of the wind-driven wheel
3. m/sec

$$M_{\text{ш}} = Pr \sin\varphi \frac{i}{\eta}, \qquad (269)$$

where: P -- force acting on the bar;
r = h/2 -- radius of the crank;
ϕ -- angle of rotation of the crank, which changes from 0 to π during the forward motion;
i -- gear ratio of crank to wind-driven wheel; /357
η -- total efficiency of the pump determined according to equation (258).

Assuming P = 1, r = 1, i = 1 and η = 1, we obtain the expression for plotting the relative characteristic of the loading moment:

$$\overline{M}_{\text{ш}} = \sin\varphi. \qquad (270)$$

The moment reaches its greatest value when the radius of the crank and rod of the pump subtend an angle $\phi = 90^\circ$. In this case $\sin\phi = 1$, consequently $\overline{M}_{max} = 1$, while at $\phi = 180^\circ$ and $\phi = 0$, the loading moment equals 0.

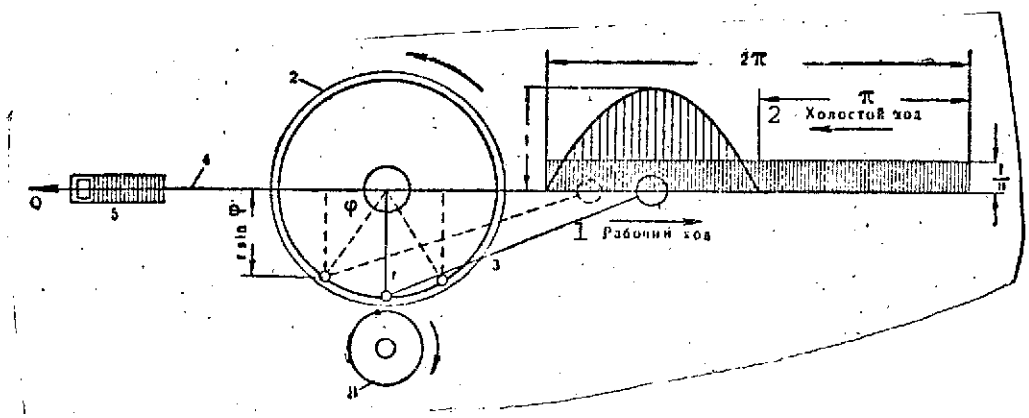

Fig. 221: Characteristic of the moment in the crank of the piston pump: 1-pin on the shaft of the wind-driven wheel; 2-pin of the crank driven mechanism; 3-connecting rod; 4-rod of the pump; 5-pump.

Key: a. forward motion
b. return stroke

During its operation, the wind-driven wheel surmounts the average loading moment, the magnitude of which can be determined by dividing the area circumscribed by the curve of the sinusoid during one stroke by the path made by the pin of the crank during a forward motion and a return stroke, i.e. 2π.

When the angle ϕ changes from 0 to π, the moment area will be equal to:

$$M_F = \int_0^{\pi} \sin \varphi d\varphi = 2. \tag{271}$$

The magnitude of the relative average moment will be equal to:

$$\bar{M}_{cp} = \frac{M_F}{2\pi} = \frac{2}{2\pi} = \frac{1}{\pi}.$$

This moment is shown in Fig. 221 by the hatched area.

Multiplying $\bar{M} = 1$ and $\bar{M}_{av} = 1/\pi$ by the magnitude of the dimensional loading moment from equation (269), we obtain:

$$M_{max} = Pri\frac{1}{\eta}, \tag{272}$$

$$M_{av} = Pri\frac{1}{\eta\pi}, \tag{273}$$

where:

$$P = \frac{\pi d^2 H}{4 \cdot 10} \tag{274}$$

the internal force on the rod of the pump caused by the water column;

d -- diameter of the piston in cm; /358

H -- pressure in m;

η -- total efficiency of the pump [see equation (258)].

Substituting the value of P in equations (272) and (273), we obtain:

$$M_{max} = \frac{\pi d^2 Hri}{4 \cdot 10\eta} = \frac{\pi d^2 Hhi}{4 \cdot 10 \cdot 2\eta} = 0{,}0392 d^2 hH \frac{i}{\eta} \text{ kgm} \tag{272a}$$

$$M_{av} = \frac{\pi d^2 Hri}{4 \cdot 10\eta\pi} = \frac{d^2 hHi}{4 \cdot 10 \cdot 2\eta} = 0{,}0125 d^2 hH \frac{i}{\eta}, \tag{273a}$$

here, d is in cm while h is in meters.

The maximal moment is surmounted by the moment of the wind-driven wheel during the start of the latter if the pressure pipeline is not filled with water, while the average moment is surmounted by the working moment of the wind-driven wheel. Upon matching the characteristics of the moment of wind-driven wheel and pump, the characteristic of the average moment appears in the form of a straight line parallel to the abscissa. The maximal moment is obtained when the revolutions equal 0, i.e. when the wind-driven wheel is set in motion.

Comparison of the characteristic of slow and rapid engines makes it possible to determine which of the two types of wind engines is more suitable to operate with the piston pump. Fig. 222 presents the curve of the working moment: the continuous line corresponds to the multi-bladed slow engine, while the dotted line -- to a 3-bladed

rapid engine. The moment of the piston pump attached to the slow wind engine is shown by the upper straight line 1, while the lower line 2, which is parallel to the horizontal axis, corresponds to the rapid engine. We can see from the figure that in the beginning of the operation, the moment of the slow wind engine is situated above the working moment of the pump, as shownby the continuous curve. The moment of the rapid wind engine during its starting is several times smaller than the moment of the piston pump, as shown by the dotted curve. As a result of this:

1. the slow wind engine starts to operate at a considerably lower wind velocity than the rapid one, and

2. since the piston pump requires a smaller number of movements, the transmission from the wind-driven wheel to the crank of the pump is simpler in the case of the slow wind engine than in the case of the rapid one.

Theoretically, the rapid wind engine could work with the piston pump if it were fitted with:

1. a centrifugal clutch allowing the idle running of the wind-driven wheel and operating a piston pump, when the moment of the centrifugal forces of the clutch is able to surmount the initial moment of the piston pump; /359

2. a reducing gear with large gear ratio for reducing the number of revolutions of the crank-driven mechanism.

Determination of losses of pressure in the pipeline. The characteristics I, II, and III in Fig. 219 were plotted without accounting for the losses of pressure in the pipeline and assuming that the pump operates with a small number of strokes with a short pipeline (up to 30 m), with a small number of joints and without valves along the pipeline. If the pump were to work with a long pipeline, these losses would affect considerably the performance of the pump.

The pressure losses are determined in the following manner:

$$\Sigma h_{\text{л}} = \left(1 + \lambda \frac{l}{d} + \zeta\right) \frac{v^2}{2g}, \qquad (275)$$

where: $\lambda \frac{l}{d} \frac{v^2}{2g}$ -- losses in meters in the suction intake and delivery parts;

$\zeta \frac{v^2}{2g}$ -- local losses in the joints, valves, reducer, etc;

l -- length of the pipeline;

d -- diameter of the pipes;

v -- rate of water movement in the pipes;

λ -- coefficient, which depends on the diameter of the pipes, the roughness of their walls and the rate of water movement in them.

The values of these coefficients in relation to the diameter of iron pipes are presented in Table 23, which was compiled according

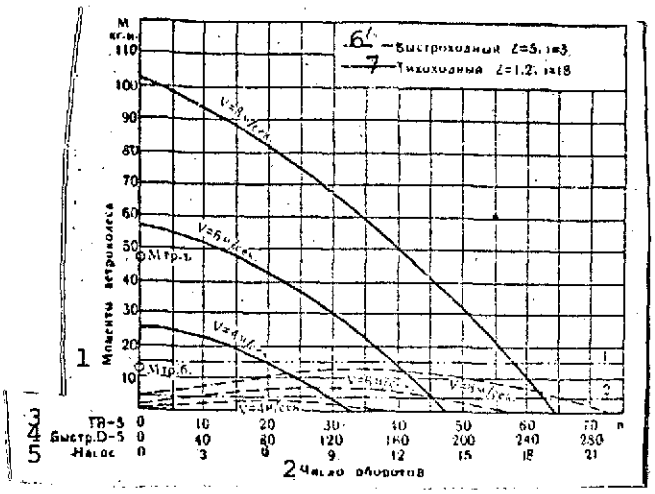

Fig. 222: Comparison of the characteristics of the moments of a slow and rapid wind engine.

Key: 1. moment of the wind-driven wheel
2. number of revolutions
3. TV-5
4. rapid D-5
5. pump
6. rapid
7. slow

to the data of Darcy, Cutter and Manning. This table can be used for rough calculations of the losses in the pipes. The graph of the λ magnitudes according to Darcy resembles that of new pipes with smooth walls; λ according to Cutter approaches pipes with very rough walls and a roughness coefficient K = 0.25, and finally, Manning's data, who assumed a roughness coefficient n = 0.012, correspond to pipes where the walls have a lower roughness [24].

For more accurate calculations of the losses in the pipes, Lang's formula can be used

$$\lambda = \lambda_0 + \frac{1.7}{\sqrt{Re}}, \qquad (276)$$

where λ_0 should be taken equal to 0.01 to 0.021 for smooth pipes, and λ_0 = 0.02, for rough cast iron and iron pipes.

Re — Reynold's number is determined by means of formula (29), where d should substitute ℓ, i.e., $Re = \frac{Vd}{\nu}$; the coefficient of kinematic viscosity for water equals $\nu = 1.10^{-6}$ at t = 20° C.

TABLE 23: THE λ COEFFICIENTS ACCORDING TO DARCY, CUTTER AND MANNING

Diameter of the pipe, mm d	λ according to Darcy	λ according to Cutter at K=0.25	λ according to Manning at K=0.012
40	0.0325	0.0962	0.0524
50	0.0300	0.0820	0.0488
75	0.0266	0.0625	0.0425
100	0.0250	0.0523	0.0386
125	0.0240	0.0458	0.0359
150	0.0233	0.0412	0.0338
175	0.0229	0.0378	0.0321
200	0.0224	0.0352	0.0307
225	0.0222	0.0331	0.0295
250	0.0220	0.0314	0.0285
300	0.0216	0.0287	0.0268

For determining the coefficient ξ of the local losses, the rough /361 estimates presented in Table 24 can be used.

TABLE 24. AVERAGE DATA OF ξ LOCAL LOSSES OF HEAD [24]

Designation of the local obstacle	Resistance coefficient
Pipe inlet with no rounded-off edge of the inlet opening	$\zeta_{in}=0.50$
Same, with well-rounded opening edge	$\zeta_{in}=0.10$
Pipe outlet leads to large capacity reservoir	$\zeta_{ont}=1.00$
Sharp bend of the pipe without rounded-off transition at an angle of the bend of 90°	$\zeta_{bend}=1.25-1.50$
Knee on the pipe forming an angle of 90° at a radius of the knee $R_k > 2d$, where d is diameter of pipe	$\zeta_k=0.50$
Same at optimal relation $R_k=(3-7)d$	$\zeta_k=0.30$
Gate valve on round pipe at medium opening	$\zeta_g=2.00$
Open gate valve on round pipe	$\zeta_g=0.10$
Crane (according to Bakhmetev)	$\zeta_{cr}=5-7$
Inlet to the collection water pipeline (protective grid with locking valve)	$\zeta_{fo}=5-10$

The graph in Fig. 223 shows the pattern of the changes in the losses of head in the valve and grid in relation to the rate of movement of the water in pipes of various diameters. This graph can be used for determining the losses of head in the valve and grid of the given pipeline.

The characteristic of the pump is plotted in relation to the number of revolutions, and therefore the calculation of head should be done for several numbers of revolutions. In order to solve equation (275), the output Q should first of all be determined in relation to the number of strokes of the pump piston.

The output of the pump is equal to:

$$Q = \frac{75Nn}{H}$$

where N -- the power developed by the wind engine at a wind velocity of 3 to 4 m/sec. /362

This power is determined on the work characteristic (Fig. 219) by the point of intersection of ray I or II with the peak of the power curve of the wind engine.

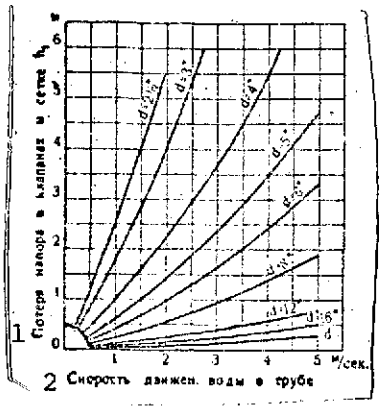

Fig. 223: Graph for determination of the losses in the valves and in the grid.

Key: 1. losses of pressure in the valve and in the grid

2. velocity of water movement in the pipe

In computing the output Q, the static pressure H is assigned.

Since the output of the pump changes proportionally to the revolutions of its crank, at different revolutions, the output will be equal to

$$Q_1 = Q\frac{n_1}{n};\quad Q_2 = Q\frac{n_2}{n},$$

where Q and n without subscript, refer to the power of the pump in the point where its characteristic intersects the peak of the power curve of the wind engine.

With the increase in the number of revolutions, the losses increase as well; their magnitude is determined by means of equation (275).

Introducing these losses in equation (261), the equation of the power spent on the work of the pump, we obtain at different revolutions n_1:

$$N_1 = \frac{0.785 d^2 h_{\text{отв}} n_1 (H + \Sigma h_r)}{75 \cdot \eta \cdot 60}. \qquad (261a)$$

On the basis of equations (261) and (261a), we obtain:

$$N_1 = N\frac{n_1 (H + \Sigma h_r)}{nH} = N\frac{n_1}{n}\left(1 + \frac{\Sigma h_r}{H}\right). \qquad (277)$$

This equation serves to determine the points for plotting the power curve of the pump in relation to the revolutions of its crank-driven mechanism.

The larger the static pressure, the smaller the ratio $\Sigma h_r/H$, which is a term in the multiplier of equation (277) describing the power of the pump. When the number of revolutions of the crank is small, the average velocity of the piston is also small, and consequently the velocity of the liquid moving in the pipe is small, which causes losses in the pressure head, so that the curve of the pump characteristic approaches a straight line. In practice, in order to simplify the calculations, the characteristics of piston pumps are assumed to be straight lines, and a constant pressure head is assumed accounting for the losses caused during normal revolutions of the crank. /363

Method of changing the characteristic of the piston pump according to the charasteristic of the wind engine. Examining the congruent characteristic of a wind-driven pump unit (Fig. 219), we see that rays I, II, and III of the pump characteristic intersect the curve of the power characteristic of the wind engine in the point of maximal power, only at a certain velocity which corresponds to a certain number of revolutions, while at higher wind velocities, these rays intersect the curves in points of lower power. This indicates that the piston pump cannot load the wind engine completely, according to the power developed by it at each wind velocity. This is explained by the fact that the power of the wind engine changes proportionally to the cube of the wind velocity, while the power of the piston pump changes proportionally to the first power of revolutions of the crank-driven mechanism.

Let us draw curve A which obviously corresponds to the highest output coefficient of wind energy ξ (Fig. 218) through the peak of the power characteristic of the wind engine. The curve shows in what manner the power of the machine tool should change, in our case the piston pump, with the change in the number of revolutions, in order for the unit to work at a maximal ξ.

Let us examine whether the piston pump can be induced to work in such a manner that the power required by it should change according to curve A (Fig. 218).

Let us denote by C the constant for the given pump in equation (261) excluding the piston stroke and the revolutions from the constant in this equation; under this condition, the power can be expressed in a simple manner:

$$N = Ch_x n.$$

If we change h or n in this equation, according to the change in the power of the wind engine, i.e. proportionally to the cube of wind velocity, we can obtain instead of a straight line for the power characteristic of the pump, a curve i.e. a cubical parabola. This curve, passes through the peak of the power curve of the wind engine since it is congruent with the characteristics of the latter, as shown in Fig. 218, and consequently for a given wind velocity we can write: /364

$$N = Chn, \tag{278}$$

and for another wind velocity:

$$N_x = Ch_x n_x. \tag{278a}$$

Taking the ratio of these equations we obtain:

$$\frac{N_x}{N} = \frac{h_x n_x}{hn},$$

hence:

$$h_x = h\frac{N_x}{N}\frac{n}{n_x},$$

where N_X, h_X and n_X -- power, stroke and revolutions of the piston crank at different wind velocities.

Since:

$$\frac{N_x}{N} = \frac{V_x^3}{V^3},$$

we can write:

$$h_x = h\frac{V_x^3}{V^3}\cdot\frac{n}{n_x}. \qquad (279)$$

This equation shows that if we change the stroke of the piston pump proportionally to the cube of the wind velocity and inversely to the number of piston strokes, then a power characteristic of the pump can be obtained which corresponds to the work of the wind engine with maximal output coefficient of the wind energy.

Leaving in the equation

$$N = Chn \quad \text{and} \quad N_x = Ch_x n_x$$

the piston stroke constant, we can write:

$$\frac{N_x}{N} = \frac{n_x}{n},$$

hence:

$$N_x = N\frac{n_x}{n},$$

or: /365

$$n_x = n\frac{N_x}{N} = n\frac{V_x^3}{V^3}. \qquad (280)$$

It follows that the characteristic of the pump which corresponds to the characteristic of the wind engine, can be obtained also by changing the number of piston strokes of the pump proportionally to the cube of the wind velocity.

In such a manner, two methods are available for inducing the wind engine to work with the piston pump at maximal values of the output coefficient of wind energy:

1. change of the path of the piston stroke proportionally to the cube of the wind velocity and inversely to the number of piston strokes [equation (279)];
2. the change in the number of piston strokes should be proportional to the cube of wind velocity [equation (280)].

Testing of a wind engine with the device for changing the number of piston strokes, was performed in the former TsVEI in 1935. The characteristic obtained experimentally was very close to the theoretical one. However, this device was not brought up to practical application.

50. Operation of Wind Engines with Centrifugal Pumps

The main advantage of centrifugal pumps over the piston pumps is the absence of a piston with packings which wear out rapidly, high output at low overall dimensions of the pump, and long service life.

However, the operation of wind engines with centrifugal pumps has also certain negative aspects: the centrifugal pump operates with a high efficiency only at certain revolutions, while the wind engine operates with a variable number of revolutions; since the centrifugal pump raises the water with a high efficiency in a small range of revolutions, while the revolutions of the wind engines with load may change two-fold during a change of the wind velocity from 3 to 8 m/sec, the feed system of the pump may prove to be effective only in a small range of wind velocities if the pump is not properly matched to the wind engine. Therefore, for a proper matching of the centrifugal pump to /366 the wind engine, the characteristic of these machines, plotted in relation to the number of revolutions should be known.

Method for recalculating the common characteristics of centrifugal pumps H -- Q, N -- Q and n = const to the characteristics related to n at H = const. Usually the characteristics of centrifugal pumps are plotted in relation to the feed (flow rate) Q, set out on the horizontal axis of the graph; the power N, the pressure head H and the efficiency load r_i are set out on the vertical axis (Fig. 224). In this form, the characteristics n = const, cannot be directly used for matching the pump to the wind engine. Therefore, the given characteristic has to be scaled in relation to the number of revolutions n in order to establish the matching between the operating conditions of the centrifugal pump and the operation of the wind engine.[1]

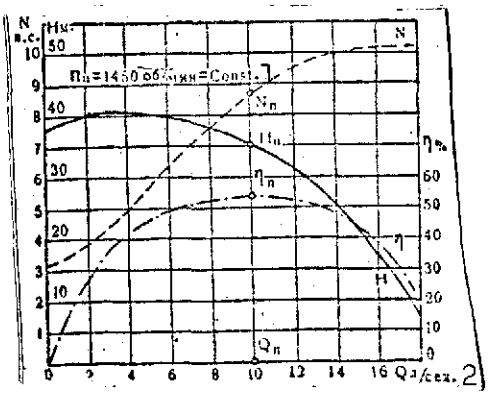

Fig. 224: Characteristic H -- Q and N -- Q with n = const for centrifugal pump.
Key: 1-rpm
2-ℓ/sec

Scaling of the characteristics H -- Q of the centrifugal pump to the characteristics in relation to the number of revolutions is based on the law of dynamic similitude, which establishes a relation between Q, H and N and the /367 number of revolutions n, i.e.:

1. the flow rate is related to the revolutions,
2. the pressure head is related to the square of the revolutions,
3. the power is related to the cube of the revolutions, i.e.:

$$\frac{Q_1}{Q_2}=\frac{n_1}{n_2}=\sqrt{\frac{H_1}{H_2}}, \quad (281)$$

$$\frac{H_1}{H_2}=\left(\frac{n_1}{n_2}\right)^2, \quad (282)$$

$$\frac{N_1}{N_2}=\left(\frac{n_1}{n_2}\right)^3, \quad (283)$$

1. The method of scaling was suggested by engineer S. S. Rudnev.

where Q, H, N and n -- are, respectively, the flow rate, pressure head, power and number of revolutions of the pump.

In order to simplify the scaling of the characteristics to a different set of conditions, it must be assumed that the pressure head is constant during the change in the number of revolutions, i.e. the pump works with a short pipeline. However, the increase in the pressure head may reach 10% of the static pressure even when the pipeline is short.

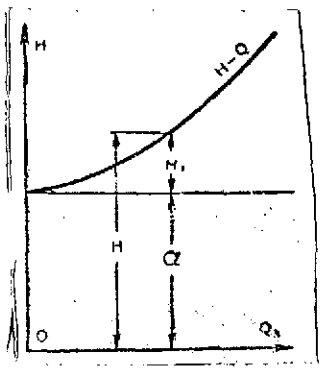

Fig. 225: Characteristic curve of the pipeline.

The change in pressure head during the work of a centrifugal pump is shown in Fig. 225, where Q_x -- flow rate; the ordinate α shows the magnitude of the static pressure; the segment H_r gives the increment in pressure on account of losses in the pipeline. The curves H -- Q showsthe change in pressure depending on the flow rate Q and is called characteristic curve of the pipeline.

In addition, the efficiency of the pump η is assumed to be constant in the scaling operation, which is permissible in practical calculations as it changes to an insignificant degree. Let us examine, for example, the curve of the change in the efficiency (Fig. 226); we see that within the limits n = 900 -- 1300, η = 77-78%, i.e. the efficiency is almost constant /368 and only in the range of 600 to 1500 rpm does it fall to 64-63%.

It is convenient to follow the range within which the efficiency of the centrifugal pump changes with the change in the number of revolutions and other magnitudes of the characteristics, by means of the universal characteristic curve of a centrifugal pump (Fig. 227). The relationships H -- Q and N -- Q are given in this characteristic curve 0.7n, 0.8n, 0.9n, 1.1n and 1.2n. The curves corresponding to identical efficiencies of the pump, have the shape of elongated curves which are closed below and also closed above if continued over a /369 sufficient distance.

The universal characteristic curve of this pump, makes it possible to determine the optimal Q, H, η, and also to determine the values of these magnitudes if one of them is known.

For example, at h_r = const (see horizontal line) and assuming that the pump operates at n revolutions, the work point on the characteristic curve of the pipeline H -- Q will be point A. Under these conditions, the pump requires a power $N_e = N_A$ and creates a pressure head H_A at a flow rate Q_A and an efficiency $\eta = \eta_{max}$. If the conditions of the system change, for example h_r increases to $h_{r'}$, then assuming

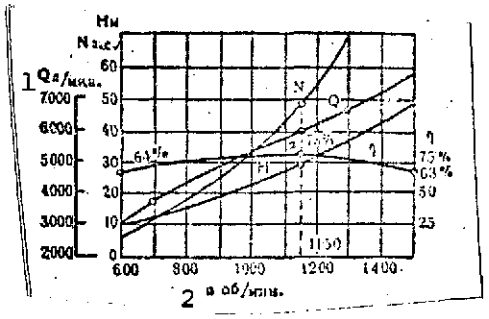

Fig. 226: Characteristic curve of a centrifugal pump in relation to the number of revolutions.

Key: 1. ℓ/min
2. rpm

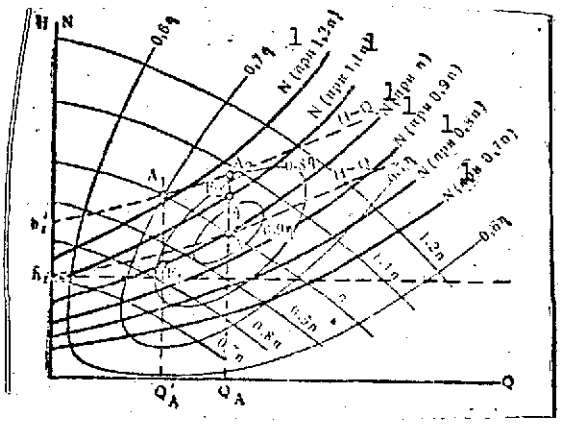

Fig. 227: Universal characteristic curve of centrifugal pumps.

Key: 1.at

that the pump works with a constant number of revolutions, work point A is displaced to A_1, and the flow rate will be $Q_A' < Q_A$, the consumed power $N_e = N_F < N_A$, the created pressure head H_A' at efficiency of the pump an 0.7η. In order to preserve the previous flow rate of the pump, the latter has to operate with a number of revolutions which is 1.09n larger than n. The work point under this condition will be A_2 and the corresponding pressure head will be H'_A. The power of the pump consumed at a number of revolutions 0.09n will be almost equal to N'_A and the efficiency of the pump will be approximately 0.79n. The universal characteristic curve shows that the pump can operate in the range of good efficiency under variable conditions by changing the number of revolutions [51].

In such a manner, with this characteristic curve for determining the type of centrifugal pump, it is possible to determine rapidly the main magnitude of the pump characteristics for various conditions of its operation.

In the absence of the universal characteristic curve of the pump, the characteristics for different sets of conditions can be determined by means of calculations.

On the basis of relations (281)-(284), let us write the equations of scaling the normal characteristics at n_n = const to the characteristics with variable n at constant pressure head H_n = const, which is convenient for matching the pump to the wind engine, i.e.:

hence:

$$\frac{n_x}{n_n} = \sqrt{\frac{H_n}{H}}, \quad n_x = n_n \sqrt{\frac{H_n}{H}}; \quad \frac{Q_x}{Q} = \frac{n_x}{n_n} = \sqrt{\frac{H_n}{H}}, \tag{284}$$

hence:

$$Q_x = Q\sqrt{\frac{H_n}{H}};$$

$$\frac{N_x}{N} = \left(\frac{n_x}{n_n}\right)^3 = \sqrt{\left(\frac{H_n}{H}\right)^3}, \quad (285)$$

hence:

$$N_x = N\sqrt{\left(\frac{H_n}{H}\right)^3}, \quad (286)$$

/370

where n_X, Q_X, N_X -- variable magnitudes at H_n = const.

Solving this equation relative to the magnitude with the subscript x, we can scale the normal characteristics H -- Q (known from the factory catalogue and from data of testing) and plot the curve Q_X, N_X, n_X in relation to n_X at H_n = const.

As an example, let us scale the characteristic of the centrifugal pumps shown in Fig. 224 at n_n = const, to the characteristic under conditions of variable revolutions.

The first point, according to equations (284)-(286), is:

$$n_x = n_n\sqrt{\frac{H_n}{H}} = 1450\sqrt{\frac{35,3}{38,4}} = 1450 \cdot 0,096 = 1390 \text{ rpm}$$

$$N_x = N\left(\frac{n_x}{n_n}\right)^3 3,10\left(\frac{1390}{1450}\right)^3 = 2,74 \text{ hp}$$

The other calculated values are presented in Table 25.

TABLE 25. CHARACTERISTICS OF A CENTRIFUGAL PUMP

number of points	Known values for characteristics H--Q and N--Q for n_n=1450 = const (Fig 224)				Calculated values of characteristics for n variable and H_n = const.		
	Q ℓ/sec	H m	N hp	η %	n_x rpm	Q_x ℓ/sec	N_x hp
1	2	3	4	5	6	7	8
1	0	38,4	3,10	0	1390	0	2.74
2	2	40,1	3,85	27,8	1360	1.88	3.19
3	4	40,6	5,05	42,9	1350	3.73	4.08
4	6	39,6	6,35	49,9	1370	5.67	5.35
5	8	37,9	7,60	53,2	1393	7.72	6.82
6	10	35,3	8,70	54,2	1450	10.00	8.70
7	12	31,4	9,55	52,6	1536	12.72	11.38
8	14	25,8	9,95	48,4	1690	16.35	15.88
9	16	18,2	10,10	38,5	2018	22.26	27.20

The data of Table 25 are plotted on the graph in Fig. 228 which shows the curves of a centrifugal pump in relation to the number of revolutions n at H_n = 35.3 m = const, as assumed in the calculations. /371

In scaling the normal characteristics to another set of conditions, it is convenient to utilize nondimensional characteristics of pumps with various coefficients of rapidity.

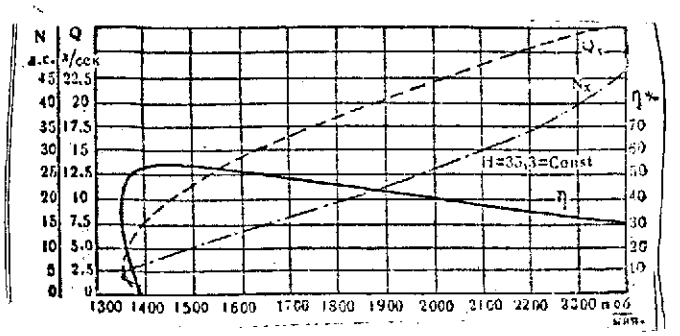

Fig. 228: Scaled characteristic curve of a centrifugal pump in relation to n at H = const.

Let us remember that the rapidity or the specific number of revolutions of the pump is the number of revolutions of a new wheel which in all its details is geometrically similar to the pump wheel of interest. The dimensions of the new wheel are selected in such a manner that the magnitude of the feed equals 75 ℓ/sec at a height of 1 m and an efficient power of 1 hp.

The rapidity is expressed by equation:

$$n_s = 3.65\, n \frac{\sqrt{Q}}{H^{3/4}}, \qquad (287)$$

where n rpm -- number of revolutions of the given centrifugal pump;

Q -- m^3/sec, its feed (for pumps with bilateral suction, Q should be divided by 2);

H -- pressure head in m, corresponding to one stage; consequently, if the pump has several stages (wheels), the head created by each must be divided by the number of stages.

The magnitudes H, Q and n, substituted in equation (287), refer /372 to the optimal conditions of operation of the pump. The expression of the relative magnitudes are obtained by dividing the right and left hand sides of equations (284)-(286); as well as equality $\eta_x = \eta$ by n_n, Q_n, N_n and η_n, respectively, i.e.:

$$\frac{n_x}{n_n} = \sqrt{\frac{H_n}{H}}; \qquad (288)$$

$$\frac{Q_x}{Q_n} = \frac{Q}{Q_n}\sqrt{\frac{H_n}{H}}; \qquad (289)$$

$$\frac{N_x}{N_n} = \frac{N}{N_n}\left(\frac{H_n}{H}\right)^{3/4}; \qquad (290)$$

$$\frac{\eta_x}{\eta_n} = \frac{\eta}{\eta_n}.$$

The values in the right hand side of these formulas are determined by means of the normal characteristics of the pumps H -- Q, and subsequently the characteristics are plotted in relative values at H_n = const in relation to n_x/n. Fig. 229 presents the curves of the /373 nondimensional characteristics of power and flow rate for two pumps with rapidity 82.0 and 76.7, while Tables 26 and 27 present the numerical values of the relative magnitudes for these characteristics.

These tables give the known dimensional values of the characteristics H -- Q and N -- Q at n_n = const (the four columns on the left) and the nondimensional values of the characteristics scaled to equations (288), (289), (290) for variable revolutions at H = H_n = const (the three columns on the right under the letters B, C, and D); column A for η/η_n refers to both the right and the left hand side of the table.

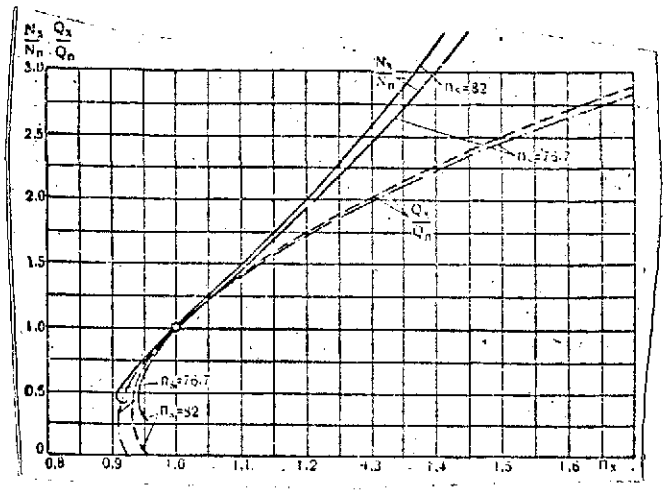

Fig. 229: Known dimensional characteristic curve N_x/N_n and Qx/Qn in relation to n_x/n_n for pumps with various rapidities.

Analogous tables should be computed for a series of pumps with different rapidities. These tables can be useful in calculations performed in practice.

As an example, let us scale the characteristics in (Fig. 224) to another number of revolutions and its corresponding optimal H, Q, and N, in order to show how to use the known dimensional characteristics.

Let us find the main magnitude for the new set of conditions H'_n, Q'_n and N'_n at n'_n = const by means of

TABLE 26. KNOWN DIMENSIONAL CHARACTERISTICS OF THE PUMP WITH A RAPIDITY n_s = 82.0

Known dimensional characteristic H--Q, N--Q at n_n = const.			Known dimensional characteristic at variable n and H = H_n = const			
			A	B	C	D
$\frac{Q}{Q_n}$	$\frac{H}{H_n}$	$\frac{N}{N_n}$	$\frac{\eta}{\eta_n}=\frac{\eta_x}{\eta_n}$	$\frac{Q_x}{Q_n}=\frac{Q}{Q_n}\sqrt{\frac{H_n}{H}}$	$\frac{n_x}{n_n}=\sqrt{\frac{H_n}{H}}$	$\frac{N_x}{N_n}=\frac{N}{N_n}\left(\frac{H_n}{H}\right)^{3/2}$
1	2	3	4	5	6	7
0.0	1.087	0.356	0	0	0.951	0.315
0.2	1.136	0.4425	0.513	0.188	0.939	0.366
0.4	1.150	0.580	0.7915	0.373	0.933	0.470
0.6	1.122	0.730	0.921	0.567	0.945	0.615
0.8	1.074	0.874	0.932	0.772	0.965	0.784
1.0	1.0	1.0	1.0	1.0	1.0	1.0
1.2	0.889	1.093	0.970	1.272	1.060	1.380

equations (284)-(286).

For example, for a pressure head H'_n = 22 m, the values of the other magnitudes corresponding to the optimal conditions of the pump, the characteristics of which are given in Fig. 224, would be equal to: /374

$$n'_n = 1\,450\sqrt{\frac{22}{35{,}3}} = 1\,450 \cdot 0.792 = 1\,150 \text{ rpm};$$

$$Q'_n = 10 \cdot \sqrt{\frac{22}{35{,}3}} = 10 \cdot 0792 = 7.92 \text{ l/sec}$$

$$N'_n = 8.7\left(\frac{1\,150}{1\,450}\right)^3 = 8.7 \cdot (0.792)^3 = 8{,}7 \cdot 0.492 = 4.27 \text{ hp}.$$

TABLE 27. KNOWN DIMENSIONAL CHARACTERISTICS OF THE PUMP WITH A RAPIDITY n_s = 76.7

Known dimensional characteristic H--Q, N--Q at n_n = const			Known dimensional characteristic at variable n and H = H_n = const			
			A	B	C	D
$\frac{Q}{Q_n}$	$\frac{H}{H_n}$	$\frac{N}{N_n}$	$\frac{n}{n_n}=\frac{n_c}{n_n}$	$\frac{Q_x}{Q_n}=\frac{Q}{Q_n}\sqrt{\frac{H_n}{H}}$	$\frac{n_x}{n_n}=\sqrt{\frac{H_n}{H}}$	$\frac{N_x}{N_n}=\frac{N}{N_n}\left(\frac{H_n}{H}\right)^{3/2}$
1	2	3	4	5	6	7
0	1,180	0,521	0	0	0,920	0,405
0,333	1,221	0,689	0,586	0,303	0,908	0,516
0,555	1,200	0,800	0,844	0,508	0,913	0,608
0,777	1,122	0,905	0,963	0,734	0,943	0,758
1,0	1,0	1,0	1,0	1,0	1,0	1,0
1,111	0,931	1,045	0,992	1,153	1,037	1,165
1,333	0,779	1,120	0,928	1,513	1,133	1,630

Multiplying the obtained values by the corresponding ratio for the given pump presented in Table 26 (see the columns on the left), we obtain the normal characteristics H -- Q, N -- Q, for the new number of revolutions n'_n = const. Multiplying the same values by the corresponding ratio in Table 26 right, we obtain the characteristics of the given pump at a variable n and constant H = H'_n = const, which is required for the operation of the wind engine with this pump.

The results of the computations are presented in Table 28.

TABLE 28. SCALING OF THE NONDIMENSIONAL CHARACTERISTICS (TABLE 26) TO THE DIMENSIONAL CHARACTERISTICS

No. of points	Characteristic at n = 1150 = const (obtained by scaling)			Efficiency of pump	Characteristic of pump at variable n and const H'_n (obtained by scaling)		
	Q ℓ/sec	H m	N hp	η %	Q ℓ/sec	n_x rpm	N_x hp
1	2	3	4	5	6	7	8
1	0	23,9	1,52	0	0	1 100	1,35
2	1,584	25,0	1,89	27,8	1,49	1 079	1,56
3	3,17	25,3	2,48	42,9	2,96	1 070	2,01
4	4,75	24,6	3,12	49,9	4,5	1 085	2,63
6	6,35	23,7	3,73	53,2	6,12	1 110	3,35
11	7,92	22,0	4,27	54,2	7,92	1 150	4,27
13	9,52	19,55	4,69	52,6	10,10	1 220	5,60

Let us compare the obtained characteristics with the characteristics shown in Fig. 224 and 228. For this purpose, let us plot the points from Table 28, left in Fig. 224, and the point of the right hand side in Table 28 in Fig. 228; the graphs obtained are shown in Fig. 230 and 231, which give a clear representation of the changes /375 in the characteristics of a centrifugal pump with the change in the parameters of the optimal conditions.

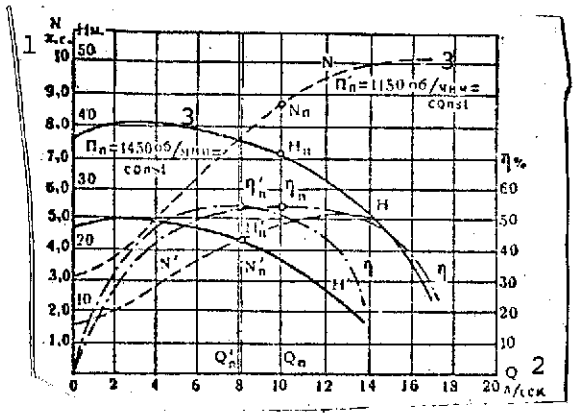

Fig. 230: Characteristic curves H -- Q: N -- Q; η -- Q for 2 sets of conditions n = 1450 rpm and n = 1150 rpm of the centrifugal pump.

Key: 1. hp
2. ℓ/sec
3. rpm

These figures show that the shape of the curves is maintained, while the optimal values are shifted to the left (see points Q'_n, N'_n and η_n on the vertical in Fig. 230 and 231).

The sequence of scaling the /376 normal characteristics of the pump at n = const to the characteristics in relation to the number of revolutions at H_n = const or H'_n = const can be briefly formulated as follows on the basis of what has been said.

1. The main magnitudes of the optimal conditions are found in the catalogue of GOST 2545-46 (see Fig. 239 a and b).

2. By means of equation (287) or graph 239, the coefficient of rapidity n_s is determined, and according to it, the nondimensional characteristics are selected, which are plotted from Tables 26 or 27 with similar rapidity coefficients.

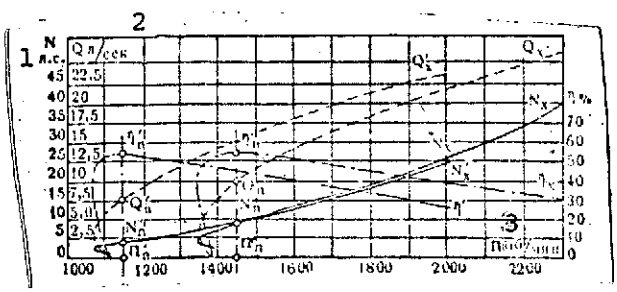

Fig. 231: Recalculated characteristic curve of a centrifugal pump in relation to n at H_n = 35.3 m = const and H = 22 m = const.

Key: 1. hp
2. ℓ/sec
3. rpm

3. The main magnitudes η_n, Q_n, n_n and N_n are multiplied by the measured values of the relative magnitudes presented in the table under letters ABCD for a pump with identical rapidity and the dimensional values of the characteristic N_x, Q_x, H_x and η_x are found for variable n and constant pressure head H.

4. If the main magnitude Qn, H_n, N_n and n_n from the catalogue or the characteristic H -- Q do not correspond to the conditions of the suggested operation of the pump, then these magnitudes are recalculated to a different set

of conditions by means of equations (284), (285) and (286), on the basis of the pressure head H'_n at which it is suggested to operate the pump. Thus n'_n, Q'_n and N'_n are obtained; $\eta'_n = \eta_n$. Computation of the variables n'_x, Q'_x, N'_x and η'_x is made by means of the table of nondimensional magnitudes, i.e.:

$$\eta_x = \eta_n A; \quad \text{(a)}$$

$$Q_x = Q_n B; \quad \text{(b)}$$

$$n_x = n_n C; \quad \text{(c)}$$

$$N_x = N_n D. \quad \text{(d)}$$

The numerical values of ABCD are given in the right hand side of these tables. /377

An example of recalculation of the characteristics of a centrifugal pump to the characteristics as a function of the revolutions. [50].

Let us assume, that we selected a centrifugal pump characterized by the following data for the VIME D-12 wind engine:

$Q_n = 30$ м³/hr $= 0.00834$ м³/sec;
$N_n = 4.6$ hp;
$n = 1\,450$ rpm;
$H_n = 24$ m;
$\eta_n = 0.60$;
$d = 80$ mm;
$k = 2$ step

The rapidity of the pump is equal, according to equation (287), to:

$$n_s = 3.65 \cdot 1\,450 \frac{\sqrt{0.00834}}{\left(\frac{24}{2}\right)^{3/4}} = 3.65 \cdot 1\,450 \frac{0.0915}{6.45} = 75.1.$$

The computed rapidity $n_S = 75.1$ approaches the rapidity of the pump, the nondimensional characteristics of which are presented in Table 27. Let us perform a scaling by means of this table.

For example, the second line of Table 27 gives:

$\eta_{1x} = \eta_n A = 0.60 \times 0.586 = 0.95$;
$Q_x = Q_n B = 30 \times 0.303 = 9.1$ m³;
$n_x = n_n C = 1\,450 \times 0.908 = 1\,410$ rpm;
$N_x = N_n D = 4.6 \times 0.516 = 2.38$ hp, etc.

The results of the computations are illustrated graphically in Fig. 232.

The congruent characteristics of this pump and of the VIME D-12 wind engine, are shown in Fig. 233, where the determination of the

power N, the output Q and of the efficiency are shown by a straight line (dotted line).

Characteristics of a wind-driven pump unit at various pressure heads. Inasmuch as it is possible in practice to have a wind-driven pump unit operate at different pressure heads H, for example, /378 by changing the level of the water in the source (high water), etc, it is useful to know how the selected pump will operate under these new conditions. This makes it possible to determine the limits of the pressure head H, between which effective work of the given wind-driven pump unit is possible.

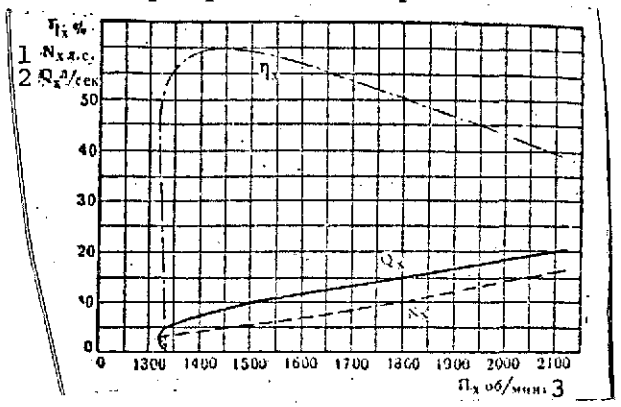

Fig. 232: Recalculated characteristic curve of a centrifugal pump in relation to n at H = 24 m = const.

Key: 1. hp
2. ℓ/sec
3. rpm

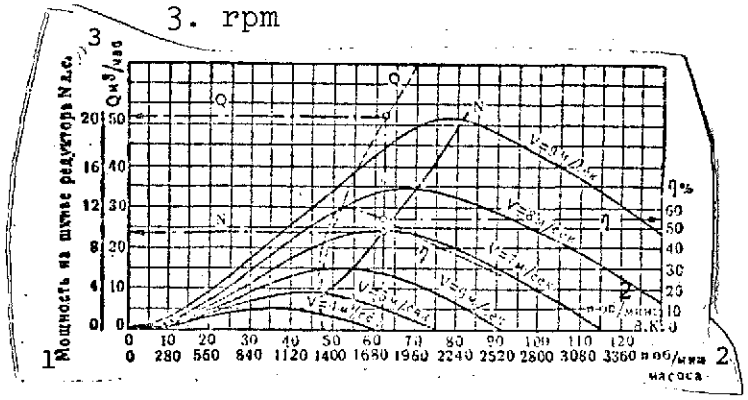

Fig. 233: Congruent characteristic curve of the VIME D-12 wind engine and of the centrifugal pump.

Key: 1. power on the pulley of the reducing gear N hp
2. rpm
3. m^3/hr

These limits can be found /379 either by means of the universal characteristic curve of the given pump or by the characteristics of the pump replotted for other pressure heads. This recalculation is done as shown above with the only difference that in this case we use for the calculation instead of the pressure head H_n, which is given in the catalogue for the given pump, the new pressure head H'_n, and we find the main magnitudes n'_n, Q'_n and N'_n (see Table 29) by means of equations (281)-(283).

The normal conditions for this pump are given in column 5.

Subsequently, we find from Tables 26, 27 or from analogical tables, the values of the parameters for plotting the dimensional characteristics in relation to the number of revolutions: $\eta_x = \eta_n A$; $Q_x = Q'_n B$; $n_x = n'_n C$; $N_x = N'_n D$.

The result of the computations is illustrated in Fig. 234, where the characteristic of the VIME D-12 wind engine is given together with the characteristics of the pump at various pressure heads.

TABLE 29. MAIN MAGNITUDES OF THE CHARACTERISTICS OF A CENTRIFUGAL PUMP AT VARIOUS PRESSURE HEADS H_n

1	2	3	4	5	6	7
Pressure heads under various conditions H_n m . . .	6	12	18	24	30	36
Power N'_n hp	0.575	1.62	2.98	4.6	6.42	8.41
Output Q'_n m^3/hr . . .	4.16	5.9	7.2	8.33	9.30	10.2
Number of revolutions n'_n rpm	725.6	1025	1255	1450	1620	1775

The curves of the power of the pump at various pressure heads, appear in a common bundle which passes through the peak of the power curve of the wind engine. Consequently, the output coefficient of the wind energy can be assumed to be practically constant and equal to maximal output in the operation of a wind-driven pump unit. We shall note further, that a change in the pressure head, i.e. passing/380 to a new set of conditions of operation of the wind-driven pump unit, does not require any change in the gear ratio of the wind-driven wheel to the pump. The change in pressure head effects only the first stage of the water supply by the pump. The smaller the pressure head, the lower the wind velocity at which, at a given gear ratio, the pump starts to feed the water. The characteristic of the beginning of water feeding is shown in these graphs by the dotted curve below [50].

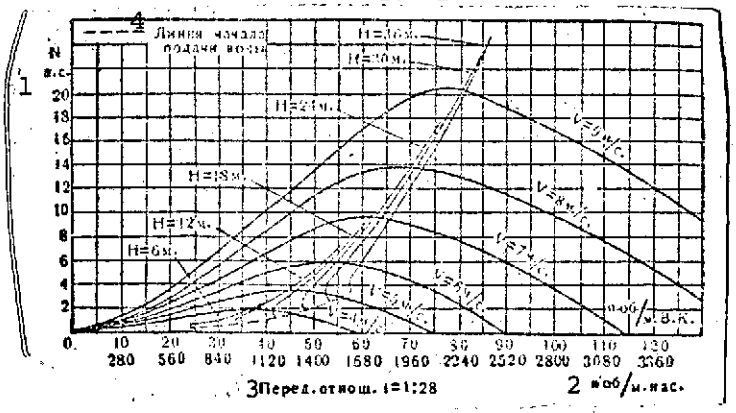

Fig. 234: Congruent characteristic curve of the VIME D-12 wind engine and of the centrifugal pump at various water heads.

Key: 1. hp
2. rpm pump
3. gear ratio 1 = 1:28
4. line of the beginning of water supply

It is convenient to use propeller pumps which are characterized by their high output, for powerful wind-driven pump units which raise the water to small height (up to 5 m). In addition, the small number of revolutions of this pump, makes it possible to solve in a simpler way the problem of designing reducing gears for the mechanical actuator. Fig. 235 presents the nondimensional characteristics of a propeller pump N_n = 183 hp, H_n = 4 m, Q_n = 2.6 m^3/sec, n_n = 500 rpm, n_n = 0.76. This characteristic is shown in dimensional magnitudes in Fig. 236.

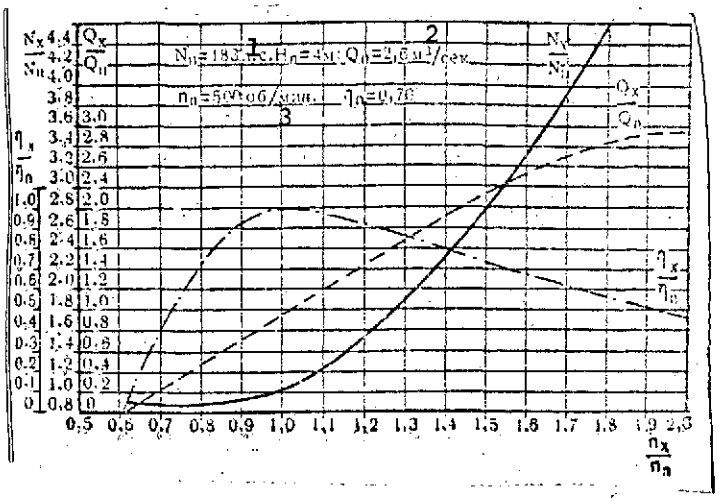

Fig. 235: Nondimensional characteristics of a propeller pump N = 183 hp, n = 500 rpm, Q = 2.6 m^3/sec, H = 4 m; η = 0.76.

Key: 1. hp
2. m^3/sec
3. rpm

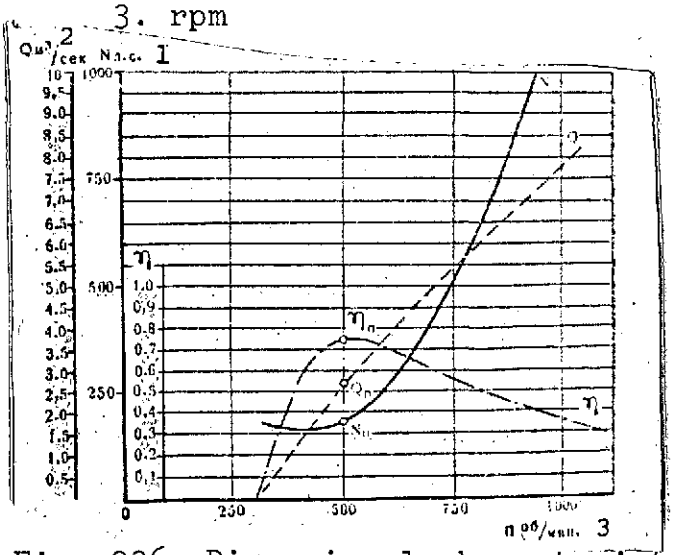

Fig. 236: Dimensional characteristics of a propeller pump N = 183 hp; n = 500 rpm.

Key: 1. hp
2. m^3/sec
3. rpm

Characteristics of a wind-driven pump unit at various gear ratios. In examining the characteristics in Fig. 234, we see that by properly selecting the gear ratio of wind-driven wheel to the pump, the optimal characteristics of the pump can be obtained at various pressure heads without changing the transmission. Let us examine the superposition of the pump characteristics over the characteristics of the wind engine at various gear ratios. Let us superimpose the characteristics of Fig. 232 on the characteristics of the VIME D-12 wind engine, at gear ratios of wind-driven wheel to pump equal to 1:20; 1:25; 1:30; 1:35 and 1:40. The position of this characteristic curve at the indicated gear ratios is shown in Fig. 237. It can be seen that the supply of water starts at higher wind velocities at low gear ratios (see characteristic i = 1:20). Consequently, those wind velocities which occur most frequently i.e. 4-5 m/sec, cannot be utilized in this case. If we induce the pump to work at a large gear ratio (see characteristic at i = 1:40), then with the increase in the number of revolutions corresponding to the wind velocity, its power will change more rapidly than the power of the wind engine; the characteristic of the power of the pump exceeds the limits of the power curve of the wind engine. In this case, the operation of the wind-driven installation will be unstable and the unit will operate at a low ξ. The characteristics at the gear ratio

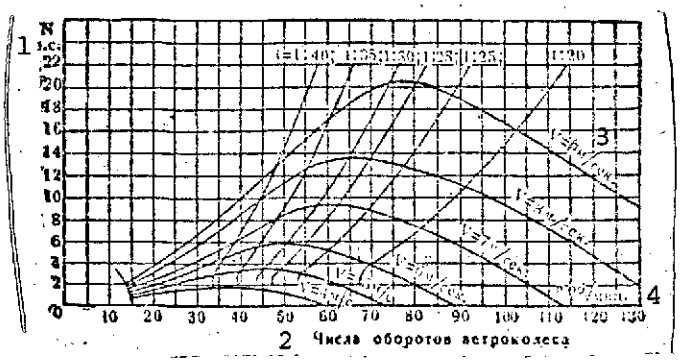

Fig. 237: Congruent characteristic curves of the VIME D-12 wind engine and the centrifugal pump at various gear ratios.

Key: 1. hp
2. number of revolutions of the wind-driven wheel
3. m/sec
4. rpm

1:30 and 1:28 occupy the optimal position. Let us note that the limits of the optimal gear ratio are insignificant, which should be taken into consideration in its determination.

Method of matching centrifugal pumps to the wind engine. /383 It was shown above that the efficiency of the centrifugal pump changes insignificantly with its passage to another set of operating conditions. This makes it possible to utilize centrifugal pumps, the normal power of which is several times higher than the power of the wind engine according to the catalogue.

In selecting the required gear ratio, we can give any number of revolutions to the pump, while the data of the catalogue refer to the number of revolutions of electrical motors, i.e. 2900; 2000; 1450; 960 etc. rpm.

In the selection of centrifugal pumps to wind engines, the problem of the operating conditions of the pump should be solved first. These conditions are caused by the pressure head which the pump is supposed to develop. Knowing this pressure head, it is easy to determine the magnitudes Q'_n, N'_n and N'_n for the new set of conditions of different dimensions of pumps, by means of equations (281), (282) and (283). The next question to solved is what is the power of the pump corresponding to the actual pressure head, with which the wind engine will operate or in other words, what is the velocity of the wind to which the power of the wind engine corresponding to a given pressure head H'_n should be related, in order to obtain the optimal conditions of operation of the entire wind-driven pump unit?

Since the efficiency decreases rapidly to zero (Fig. 232) with a change in the normal number of its revolutions n in the direction of a decrease, the matching of the pump to the wind engine should be done in such a way that the optimal minimal revolutions would correspond to the wind velocity at which the maximal annual energy flowing through the wind-driven wheel is obtained.

In order to find the velocity of the wind corresponding to the maximal annual output, it is sufficient to calculate $V^3 t_p$ for each working velocity of the wind from equation (252) in which all the

magnitudes except for V^3t are constant and the occurance of t_p from M. M. Pomortsev's table. This calculation was performed for annual average wind velocities V_0 from 3 to 6 m/sec. The result of the calculation is presented in the graph of Fig. 238. It appears that there is velocity V_y (see the velocity on the horizontal scale against the point of intersection of the dotted curve with the V^3t_p), /384 at which the maximal annual output of the wind-driven installation is obtained for each average annual wind velocity V_0. This optimal velocity of the wind is approximately 1.5-1.67 times larger than the V_0, i.e.:

$V_0 =$	3	4	5	6
$V_y =$	6	6,5	7,5	8,5
$\frac{V_y}{V_0} =$	1,67	1,62	1,5	1.42

The average

$$\frac{V_y}{V_0} = 1{,}55,$$

hence:

$$V_y = 1{,}55 V_0. \qquad (291)$$

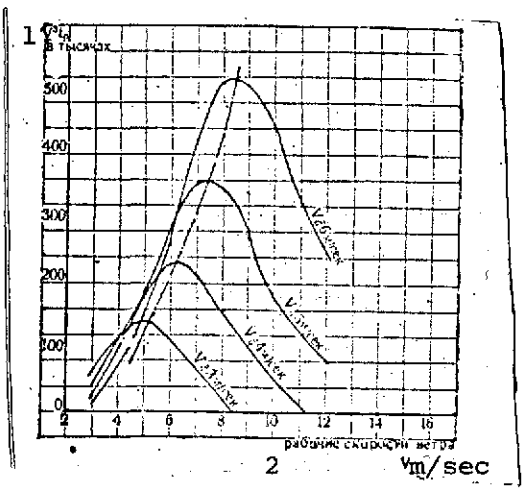

Fig. 238: Graph for the determination of the optimal wind velocity.

Key: 1. in thousands
2. working wind velocities V m/sec

In selecting a set of conditions for the operation of the pump which corresponds to this wind velocity, we obtain the optimal conditions of operation of the wind-driven pump unit.

For example, at an average annual wind velocity of V_0 = 3 m/sec, the maximal output is obtained at wind velocities $V_y \approx$ 5 m/sec. Consequently, /385 the normal power of the centrifugal pump should not be largely different from the power of the wind engine which it develops at a wind velocity V_y = 5 m/sec, i.e.:

$$N_n = N_e = 0{,}000654 D^2 V_y^3 \eta.$$

For TV-8, at ξ = 0.35, η = 0.65, we have:

$$N_n = N_e = 0{,}000654 \cdot 8^2 \cdot 5^3 \cdot 0.35 \cdot 0{,}65 = 1{,}19 \text{ hp}$$

In regions with an annual average wind velocity of V_0 = 5 m/sec, the normal power of the pump working with TV-8 should be determined at a wind velocity

$$V_y = 1.5 \cdot 5 = 7.5 \text{ m/sec}$$

$$N_n = N_e \cong 0{,}000654 \cdot 8^2 \cdot 7{,}5^3 \cdot 0.35 \cdot 0{,}65 = 3{,}94 \text{ hp}$$

In the selection of a centrifugal pump, GOST 2545-46 must be used, where the characteristics of various types of centrifugal pumps are recorded. It is very convenient to use these graphs as

ORIGINAL PAGE IS
OF POOR QUALITY

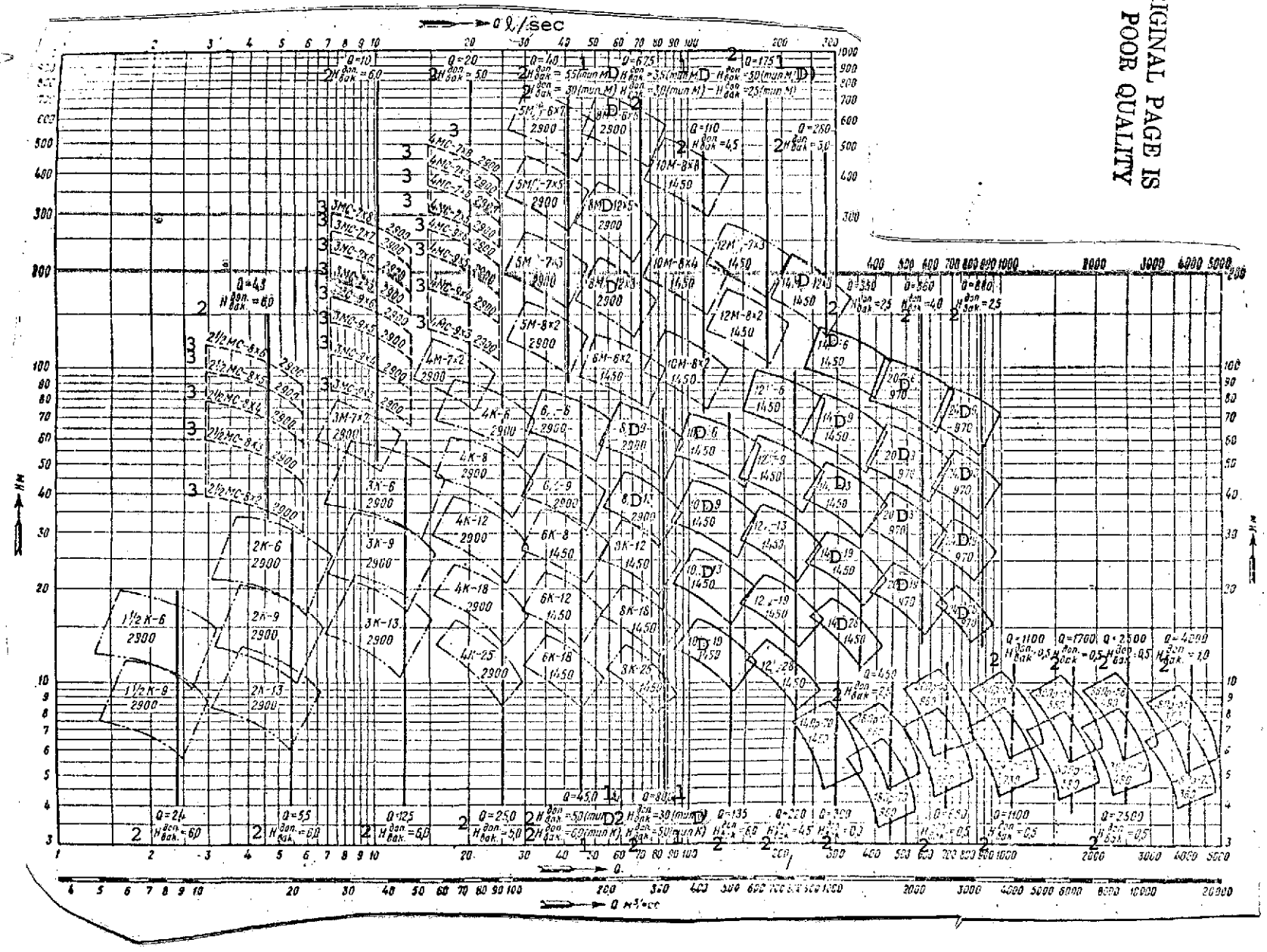

Fig. 239a: Graph for the determination of the performance of centrifugal pumps of type "K", "D", "M", "ND" and "Pr".
Key: 1. type; 2. aux. tank 3. MS

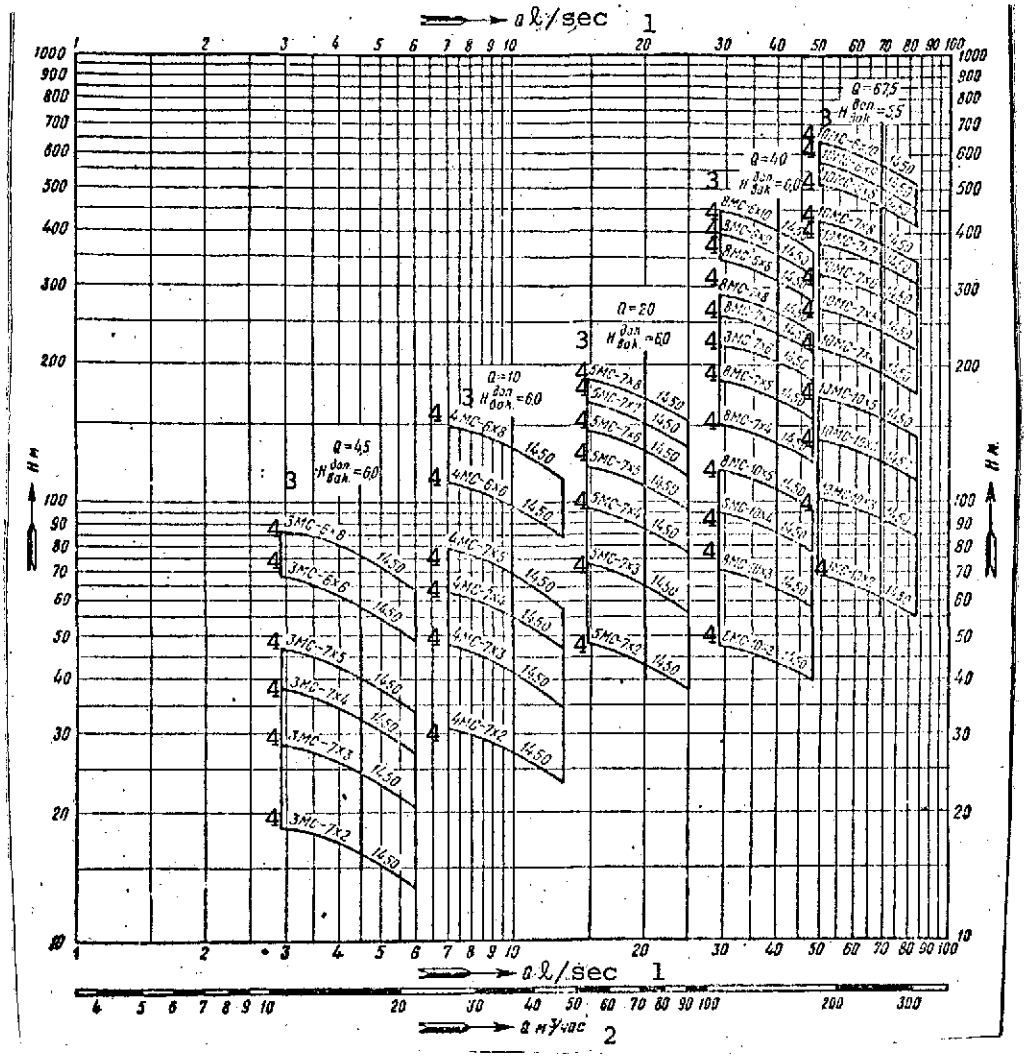

Fig. 239b: Graph for determination of the performance of centrifugal pumps of type "MS".

Key: 1. ℓ/sec
2. m^3/hr
3. aux. tank
4. MS

ORIGINAL PAGE IS
OF POOR QUALITY

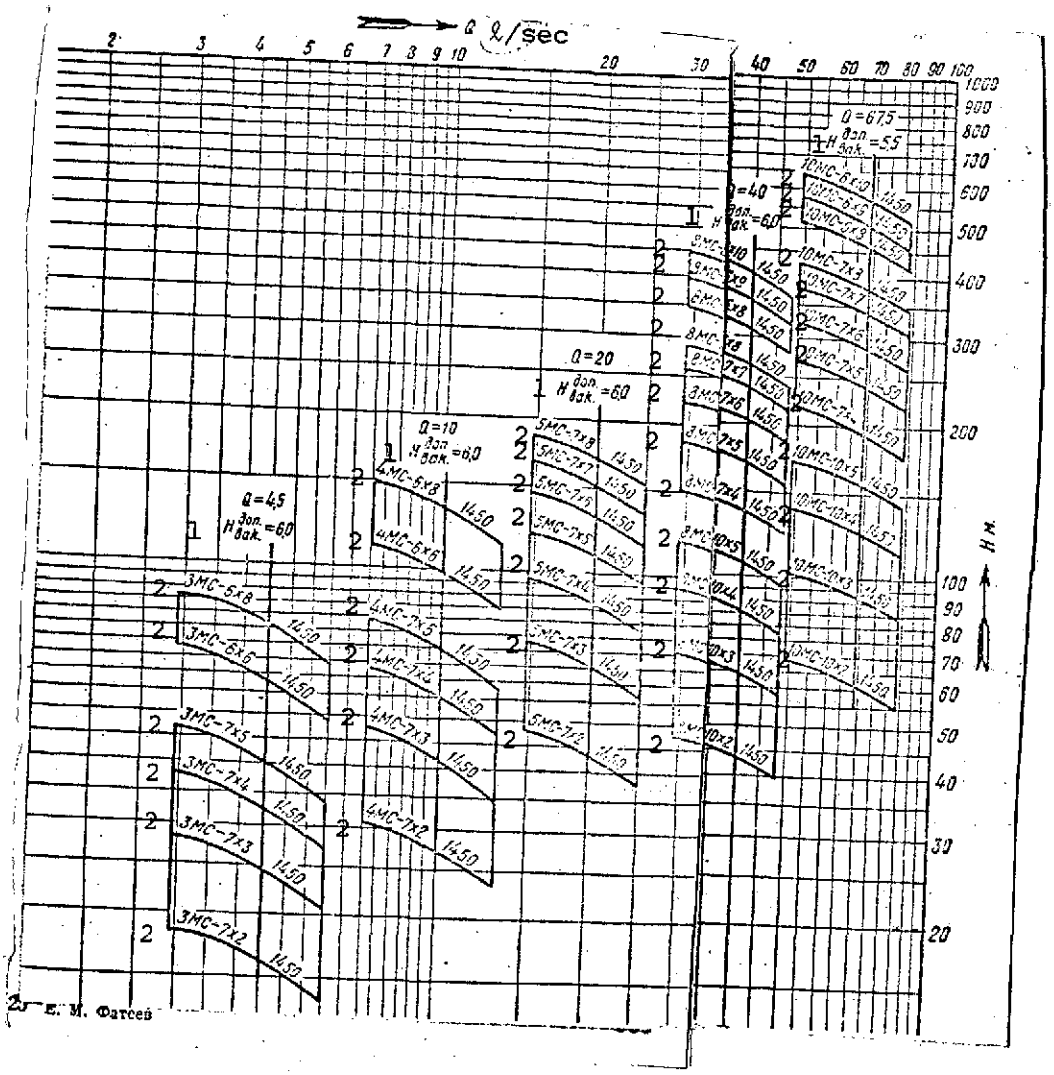

Key: 1. Aux. tank
2. MS

POOR QUALITY

applied to a given standard (Fig. 239 a and b), which gives the tracings of the limits of output Q and pressure head H at n = const. The region Q and H of each pump is traced and inside this region, the make of the pump and its normal revolutions per minute are recorded.

The make (notation) of the pump consists of:
a. letters -- type of the pump;
b. figures before the letter -- diameter of the inlet pipe in mm, 1/25 of the dimension, rounded off;
c. figures after the dash, coefficient of rapidity, 1/10 of the value, rounded off;
d. figures after the multiplication sign in multi-stage pumps -- number of stages.

The types of the pumps are denoted by the following letters:
"K" -- single stage, cantilever, with one-way inlet impeller;
"D" -- single stage with two-way inlet impeller;
"M" -- multiple stage, with horizontal parting in the housing and with one-way inlet impeller;
"MD" -- multiple stage with horizontal parting of the housing, the first impeller with two-way inlet and the other impeller with one-way inlet;
"MS" -- multiple stage ring type, with one-way inlet impeller; /386
"Pr" -- single stage propeller pump.

The total head with which the centrifugal pump actually operates at the site of the installation must be determined by the equation:

$$H = M + V + \frac{v_h^2 - v_s^2}{2g}, \qquad (292)$$

where: M and V are the readings of the manometer and vacuum meter reduced to the axis of the pump in meters of liquid column;

v_h and v_s are the velocities in the head and suction parts of the pump at the sides of junction of the manometer and vacuum meter, in m/sec.

Example. Using the graphs in Fig. 239a, select a pump for operation with a head up to 10 m and an output up to 20 m^3/hr.

Examining the graphs in Fig. 239a, let us find in the left corner below the contour of the field of the recommended limits of head H and output Q of the pump, the make of which -- 2K-13-2900 is given in the contour of the field. This is a single stage overhang type pump with a diameter of the suction pipe of 50 mm, coefficient of rapidity n_s = 130, and normal number of revolutions n_n = 2900 rpm. It can operate with good efficiency in the limit of 6-15 m head and an output of 3 to 6.5 ℓ/sec. The optimal conditions of operation of the pump are marked by means of a thick vertical line. Under these conditions H = 18 m and Q = 5.5 ℓ/sec. In the table of GOST 2545-46, the efficiency of this pump is equal to η = 0.62. The

power needed for the operation of this pump should equal:

$$N_n = \frac{5.5 \cdot 11}{75 \cdot 0.62} = 1.3 \text{ hp}$$

A pump with a different characteristic is needed for an output of 4.5 ℓ/sec at a head of H = 70 m.

In the graph of Fig. 239a, the pump corresponding to this condition is of the make 2 1/2 MS 8 x 4 -- 2900. This is a four-stage pump with a diameter of the suction pipe of 62.5 mm, n_s = 83, n_n = 2900 rpm. According to the table of GOST 2545-46, η = 0.55. The power needed for the operation of such a pump equals:

$$N_n = \frac{4.5 \cdot 70}{75 \cdot 0.55} = 7.65 \text{ hp}$$

Priming of a centrifugal pump working with a wind engine. One /387 of the main operations in starting a centrifugal pump is its priming with water and the removal of air from the chamber of the pump, without which the feeding of the water does not start.

A centrifugal pump with an electrical motor or with an oil engine works at a constant number revolutions, therefore the pump is primed only when it is started. Under these conditions, even manual priming is no difficulty. The situation is different in the case of the pump operating with a wind engine. In the former case, the constant revolutions maintain the pump in operation throughout the whole period, while in the latter case, the pump operates with variable revolutions which decrease in some moments down to zero, according to the changes in wind velocities. The delivery of the water can only start at a certain minimum number of revolutions.

Since the moment of starting of the pump is quite small, the wind engine will rotate the pump without any delivery at all wind velocities below 4-5 m/sec. And if the velocity of the wind does not reach 4-5 m/sec in the course of, let us say, 3-4 hours, then the water may leave the pump. An observer standing behind the wind installation, seeing the rotation of the wind-driven wheel, may not realize that the water is not delivered due to its absence in the pump. He may assume that the water is not delivered by the pump due to an insufficient number of revolutions. Therefore, the manual method cannot fully insure the priming of the centrifugal pump operating with a wind engine. In this case it is necessary either to mount the pump below the level of the water source, so that it would always be primed (see diagram in Fig. 240a), or supply the installation with automatic priming, as shown in Fig. 240b.

In the latter case, during the operation of the pump, the water is partially guided from force pipe A via pipe B into container C with float-type lock D. As soon as the container is full, the float closes the tap. During the leak-off of the water from the pump and the suction pipe, the water flows from the container via pipe E into the suction pipe and fills both it and the pump. Pipe E is fitted with

reflux valve V which does not permit the water to enter the container during the operation of the pump. Valve G is open all the time and closes only when the pump stops working for a longer period of time. The capacity of the container depends on the capacity of the suction pipe and the housing of the pump, as well as on the magnitude of water losses through the foot valve. It should be assumed that a container with a capacity of 0.5 m^3 insures the priming provided /388
that the pump does not stop for more than 24 hours.

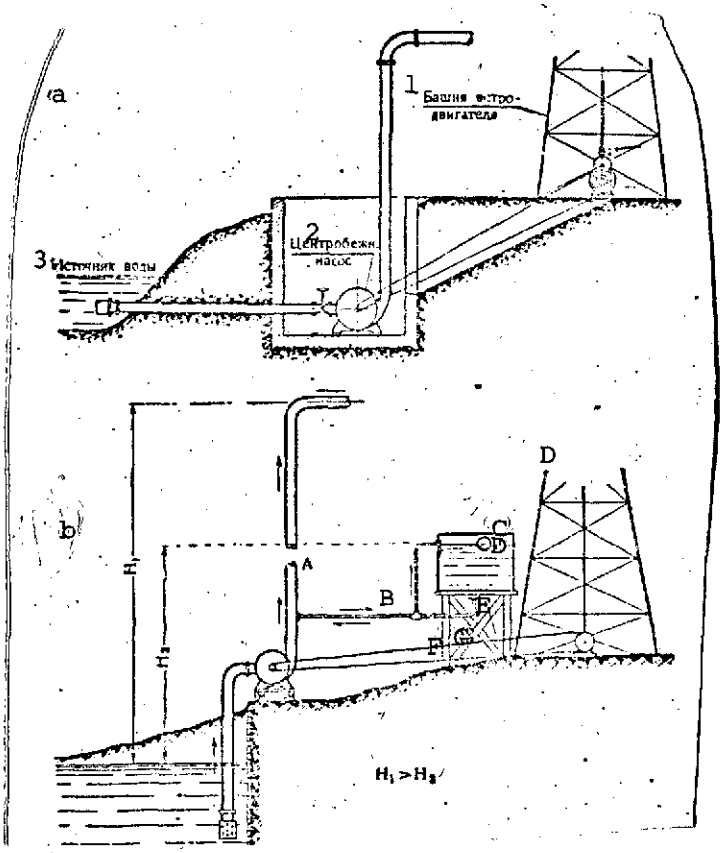

Fig. 240: a) Diagram of the disposition of the pump below the level of the water source.
b) Diagram of the automatic priming of a centrifugal pump.

Key: 1. tower of the wind engine
2. centrifugal pump
3. water source
4. B
5. C
6. D
7. E
8. F
9. G

In addition, the pump will be constantly primed, also in the case that an auxiliary piston pump is attached to the wind engine, as shown in Fig. 241. In this case, as soon as the engine starts operating, /389
the piston pump starts to deliver water and primes the pump. This diagram of operation of a wind-driven pump unit has an additional advantage. The centrifugal pump starts to deliver at wind velocities of 4-5 m/sec, while at lower velocities, the wind engine rotates the pump without delivering water. When the wind engine operates with an additional piston pump, the water delivery will take place as soon as the pump is started, consequently, the flow of water will be continuous even at a wind velocity of 3 m/sec. The power of the piston pump may not be higher than the power at which the centrifugal pump starts to deliver the water.

Unnecessary losses of energy on account of rotation of the centrifugal pump at low wind velocities, can be avoided by means of a device called the automatic connection of the centrifugal pump at certain numbers of revolutions of the wind-driven wheel.

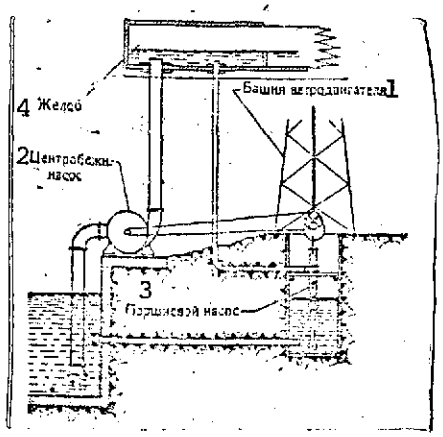

Fig. 241: Diagram of the parallel operation of centrifugal and piston pumps.

Key: 1. tower of the wind engine.
2. centrifugal pump
3. piston pump
4. trough

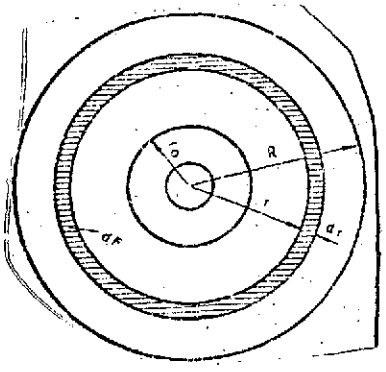

Fig. 242: Elementary area of the working surface of the millstone.

50. Operation of Wind Engines with Millstones and Agricultural Machines.

The utilization of wind engines for operation with agricultural machines is of great importance for sovkhozes and kolkhozes. Grinding, preparation of forage, processing of grain, wood-pulp processing, etc, can be carried out any time during the day, whenever there is a wind, which determines the flexible graph of loading.

Characteristic of the millstone. The torque created by the wind engine must surmount the moment caused by the friction forces of the millstone, which takes place during the grinding of grain into flour.

The forces of friction between the working surfaces of the millstone create a moment M_m which is in fact the sum of the elementary moments dM caused by ring-shaped areas dS, situated at various distances r from the axis of rotation of the millstone (Fig. 242). /390

The elementary ring-shaped area is equal to:

$$dF = 2\pi r dr.$$

The moment of the forces of friction on this ring-shaped area can be expressed as follows:

$$dM = p dF r = p 2\pi r dr \cdot r,$$

hence:

$$dM = p 2\pi r^2 dr,$$

where: p -- drag per unit working surface of the millstone. In the preparation flour for baking and when the millstone operates at top power:

$$p \cong 500 \text{ kg/m}^2.$$

Adding up the moments of the ring-shaped areas on the working surface of the millstone, we obtain the over-all moment of drag of the given machine tool, i.e.:

$$M = \int_{r_0}^{R} p 2\pi r^2 dr = p 2\pi \int_{r_0}^{R} r^2 dr = p 2\pi \left(\frac{R^3}{3} - \frac{r_0^3}{3} \right) = \frac{2}{3} p\pi (R^3 - r_0^3). \quad (293)$$

Here: R -- radius of the millstone including its external circumference; r_0 -- radius of the throat of the millstone, where no grinding takes place but only feeding of the grain into the milling belt.

In this equation, the force p is unknown; it depends on the sharpness of the millstone, on the hardness of the processed material and on the amount of the grain.

Knowing the working moment of the stonemill, we can determine /391 the power which is required for its rotation,

$$N = \frac{M\omega}{75 \cdot \eta},$$

where: η -- mechanical efficiency of transmission;
ω -- angular velocity of rotation of the stonemill.

Substituting in equation (293) the values of the moment and of the angular velocity $\omega = \pi n/30$, while n is the number of revolutions per minute, we obtain:

$$N = \frac{2p\pi(R^3 - r_0^3)}{3 \cdot 75 \cdot 30\eta} = 0{,}00294\, p\, \frac{n}{\eta}(R^3 - r_0^3). \qquad (294)$$

For given dimensions of the stone and for a given type of grain, all the magnitudes in the right hand side of equation (294) are constant, except for the revolutions n. Denoting the constant magnitudes by A, we obtain:

$$N = An.$$

This equation shows that the theoretical power of the stonemill and of similar agricultural machines changes proportionally to the revolutions of the stonemill. Consequently, the characteristics of the theoretical power should be represented graphically by a straight line which passes through the origin and subtends a certain angle with the axes of the abscissa.

In practice, the characteristics differ markedly from a straight line. The drag of the working surface of the stonemill changes along with the change in the feeding of the grain. In addition, this drag can change due to changes of pressure between the working surfaces of the stone mill. In the simplest mills, this pressure is created by the stone mill's own weight; in small grinding mills of the "farmer" type, the pressure is created by a special spring. In such a manner, the characteristics can be changed in any desired manner by changing the feeding of the grain and the degree of its grinding. This makes it possible to adjust to the work of agricultural machines according to the charactertics which are optimal for its operation with a wind engine.

The peculiar feature of operation of wind installations require the construction of characteristics of the power tools in relation to the revolutions. Some of the characteristics can be designed theoretically (piston and centrifugal pumps, generator), others can only be constructed on the basis of experimental data (stone mills, straw cutters, crushers, winnowers, etc.). These characteristics assist in determining the optimal operation conditions of a wind power unit and to design the transmission in accordance with these conditions. /392

For example, only the maximal parameters are given in the catalogues for the existing stone mills of various dimensions. Consequently, each stone mill should have its own engine; this would be all right and in such a case the unit would operate most effectively. However, in the practice of kolkhoz flour milling, several departures have to be made from the choice of such a unit.

If the normal power of the wind engine is smaller than the nominal power of the stone mill, then a certain velocity of the wind should be sought at which the wind engine can develop the required power, while the revolutions should be found from the characteristics of the stone mill at which the power of the stone mill equals the power of the wind engine.

Example. A stone mill of 6/4 arshin with a diameter of 1067 mm requires at full loading a power of N = 16.8 hp; the revolutions of the stone mill amount under these conditions to 176 rpm. What is the velocity of the wind at which a type D-12 wind engine can develop a power of 16.8 hp if at V = 8 m/sec and 28 rpm this wind engine has a power of 12 hp? The velocity is found from the following relations:

$$\frac{N_1}{N_2}=\frac{V_1^3}{V_2^3},\ \text{hence};\quad V_1=V_2\sqrt[3]{\frac{N_1}{N_2}},$$

$$V_1=8\cdot\sqrt[3]{\frac{16.8}{12}}=8\sqrt[3]{1.4}=8\cdot1.12=9\ \text{m/sec}$$

The number of revolutions of the wind engine at a wind velocity of 9 m/sec can be found from the relations:

$$\frac{n_1}{n_2}=\frac{V_1}{V_2},$$

hence:

$$n_1=28\frac{9}{8}=32\ \text{rpm}$$

Consequently, the gear ratio of the revolutions of the stone mill to the revolutions of the wind wheel should be equal to:

$$i=\frac{n_S}{n_W}=\frac{176}{32}=5.5.$$

If we were to solve this problem by means of a characteristic of the stone mill N = f(n) (Fig. 243), then it is easy to see that a power of 12 hp corresponds to 150 revolutions of the stone mill /393

per minute. Dividing 150 revolutions by the number of revolutions of the wind wheel which it develops at a power of 12 hp, we obtain the general gear ratio:

$$i=\frac{150}{28}=5.4.$$

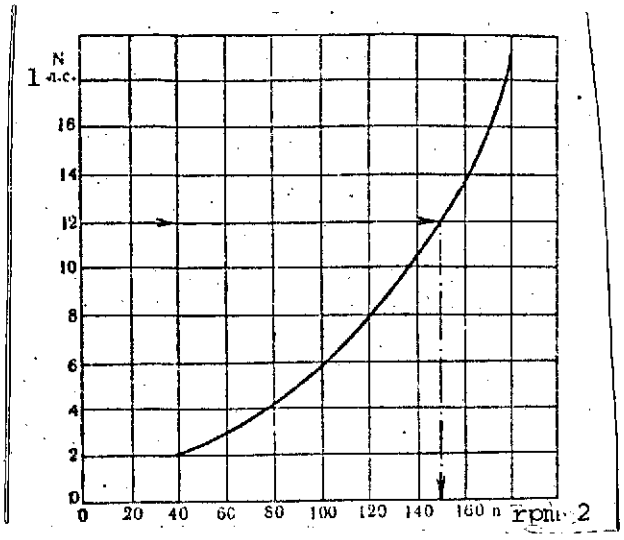

Fig. 243: Characteristics of the stone mill in relation to the revolutions.

Key: 1. hp
2. rpm

Fig. 244 illustrates a nomogram, compiled by the author, in which one can readily find the general gear ratio of the revolutions of various stone mills to the revolutions of wind engines of different power.

The upper part of the nomogram contains approximate characteristics of stone mills (power in relation to revolutions), constructed on the basis of tracings of the output according to revolutions which were recalculated to the characteristics of power according to revolutions. The lower part of the diagram contains rays for wind engines of known power and revolutions, such as VIME D-8, N = 5.3 hp at n = 40 rpm; D-10, N = 8 hp at n = 32 rpm; D-12, N = 12 hp at n = 28 rpm and D-16, N = 20 hp at n = 20 rpm. Only the upper part of the nomogram can be used for wind engines of other characteristics. /394

Example. A VIME D-8 wind engine with a stone mill of diameter D = 550 mm ensures full power of the stone mill at its maximal revolutions 350 rpm. Consequently, in the given case the gear ratio will be equal to: /395

$$i=\frac{n_s}{n_w}=\frac{350}{40}=8.75.$$

If a 6/4 stone mill is connected to the same wind engine, then the transmission must be made in such a way that it can give only 100 revolutions at the full power of the wind engine, which is obtained by passing a line from the scale of the 5.3 hp to the intersection with the characteristic curve of the stone mill 6/4, and then down to the intersection with ray D-8, i = 2.5. In such a manner, the wind engine will mill with any stone mill provided that the transmission is suitably calculated. If the power required for the work of the stone mill is less than the power developed by the wind engine, then the latter will be underloaded and consequently, the wind engine will work with a low output coefficient of wind energy at high wind velocities.

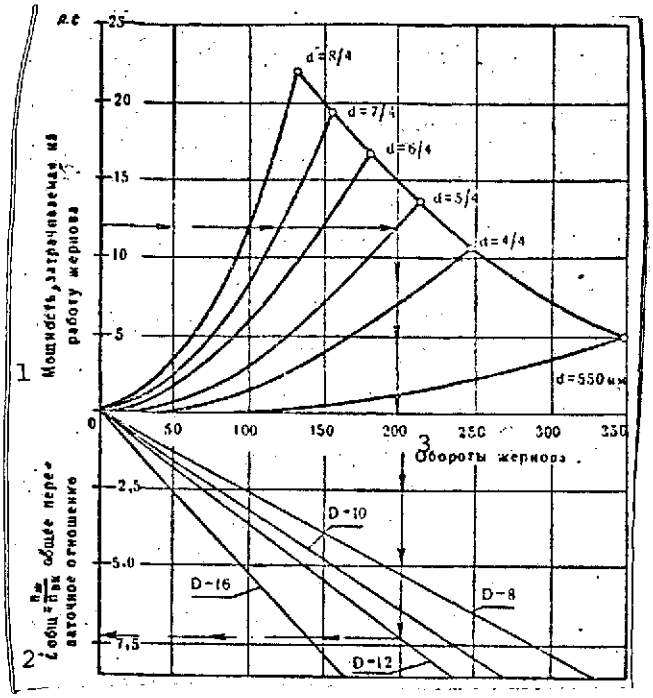

Fig. 244: Ye. M. Fateyev's nomogram for matching stone mills to wind engines.

Key: 1. power spent on the work of the stone mill
2. $i_{gen} = n_S/n_W$ general gear ratio
3. revolutions of the stone mill

Method for regulation of the stone mill. Regulation of the work of the stone mill consists in changing the height of the cleft h between the working surfaces of the stone mill i.e. the runner and the bedstone (Fig. 245). In the common windmills this is done manually by means of wheel A, which is entirely acceptable in the older systems of windmills, since they are not sensitive to sharp changes in wind velocity and the miller has time to adjust the technological process according to the velocity of the wind. However in the rapid wind engine, /396 which has lighter wings, sensitive to even weak wind gusts, this operation is hard to accomplish i.e. the miller would be compelled to stand by the mill and regulate the stone mill. These difficulties can be solved by means of automatic regulation, which is used in the improved models of windmills. The location of the working surface of the stone mill on the belt and the forging of the grooves on the working surface are shown in Fig. 245.

Fig. 246 illustrates the diagram of an automatically regulated windmill with two millstone sets, tested by the author. The action of the centrifugal regulator mounted on the girder in front of the mill, is transmitted through yoke 1-1, the rod 2-2, to levers 3-3 which support the step bearings of the shaft of the stone mill. During the increase in the number of revolutions, the centrifugal loads C come apart and lift the clutch, and together with it the long end N of the yoke 1-1. At this moment, the short external ends h go down at the same time with the shaft and the stone; the height of the cleft h between the stone mills diminishes, and the feeding of the grain increases, which is obtained by increasing the slope of the inclination 4-4, which is connected with yoke 1-1 by means of strings thrown across blocks 5-5.

The ratio of the angular velocity of rotation of the regulator and the angle α which is formed by the lever with the centrifugal /397 loads at their ends is given by N. E. Zhukovskiy's equation:

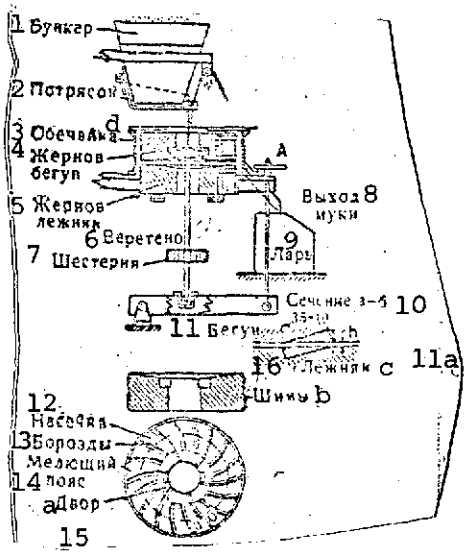

Fig. 245: Manually regulated stone mill.

Key: 1. hopper
2. jolting millstone
3. rim
4. runner
5. bedstone
6. shaft
7. pinion
8. discharge of flour
9. bin
10. section a-b
11. runner
11a. bedstone
12. ragging
13. grooves
14. grinding belt
15. throat
16. shims

$$\omega = \sqrt{\frac{g}{OM\cos\alpha}\left(1+\frac{Q}{P}\cdot\frac{OD}{OM}\right)}, \qquad (295)$$

where: ω is the angular velocity of rotation of the regulator;

$g = 9.81$ m/sec^2, acceleration of the terrestrial gravitation.

Other indications are given in Fig. 247.

By means of this equation, it is easy to determine the height of the cleft h between the working surfaces of the stone mill in relation to the wind velocity at any point in time.

The height of the cleft h changes proportionally to the travel of the clutch H of the regulator. Since the travel of the clutch H changes proportionally to cos α, assuming that the maximal initial height of the cleft between the stone mills is equal to h_0, we obtain the change in the height of the cleft in the following form:

$$h = h_0 \cos\alpha. \qquad (296)$$

The cos α is found from equation (295).

$$\cos\alpha = \frac{g}{\omega^2 OM}\cdot\left(i+\frac{Q}{P}\cdot\frac{OD}{OM}\right). \qquad (297)$$

All the magnitudes in this equation, with exception of ω, are known from the construction of the regulator. For wings of known characteristics, ω is also known for each wind velocity. In such a manner, a complete computation of the regulator for windmills can be made by means of equations (295), (296) and (297).

In determining the magnitudes which enter equation (297), one should use the dimensions of the system of regulation which were determined on the basis of constructional considerations. According to the symbols shown in Fig. 246:

$$Q/2\ L = S\ell;\quad G\ell_1 = S(L_1 + L_1),$$

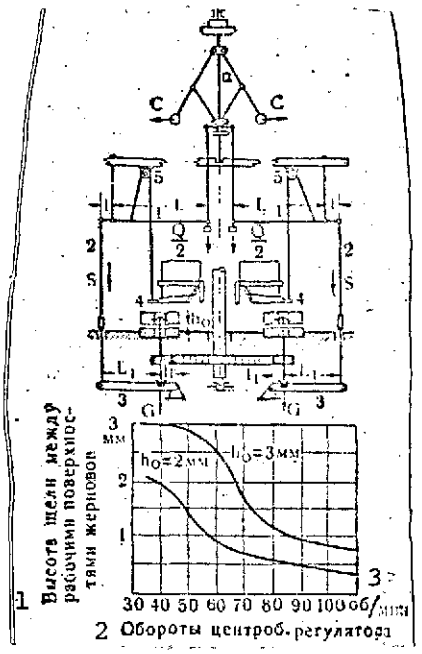

Fig. 246: Diagram of automatic regulation of stone mills.

Key: 1. height of the cleft between the working surfaces of the stone mill
2. revolutions of centrifugal regulator
3. rpm

hence:

$$\frac{Q}{2} \cdot L = Sl;\ Gl_1 = S(L_1 + l_1),$$

$$Q = 2\frac{G l l_1}{L(L_1 + l_1)}. \qquad (298)$$

Example. For a stone mill 6/4 with a weight G = 700 kg and the following dimensions of the arms of the levers (Fig. 246): l = 0.12 m; l_1 = 0.10 m; L = 1.5 m; L_1 = 1.3 m, the magnitude Q will be equal to:

$$Q = 2\frac{700 \cdot 0{,}12 \cdot 0{,}1}{1{,}5(1{,}3 + 0{,}1)} = 9{,}6 \text{ kg}$$

The centrifugal loads M are chosen with a weight P of 5-8 kg each.

Substituting these values in equation (297) at constructional dimensions of the centrifugal regulator adjusted to the type VIME D-16 windmill (Fig. 247), we obtain cos α for various revolutions of the windmill and the corresponding clefts between the working surfaces of the stone mill 6/4.

The computation is presented in Table 30.

The relation between the height of the cleft h and the revolutions is shown in Fig. 246.

This simple automatic construction not only permits regulation of the work of the stone mill but makes it possible to correct the conditions of operation of the windmill unit, i.e. to confer to the stone mill the characteristics which pass through the peak of the power curve of the wind engine.

We know from what has been said above that the theoretical characteristics of the stone mill change as a function of the revolutions in a linear manner, the straight line forming a certain angle with the horizontal axis; the curve is obtained by changing manually the load, i.e. the larger the load, the steeper the curve.

In the case of a centrifugal regulator, the slope of the curve changes according to the automatic change of the load depending on the magnitude of the gear ratio of the revolutions of the wind wheel

1. [Translator's note: Errata checked and found to be illegible.]

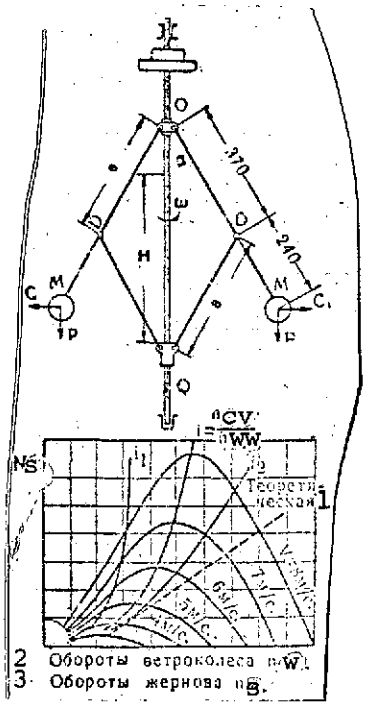

Fig. 247: Centrifugal regulator and its effect on the characteristics of the stone mill.

Key: 1. theoretical
2. revolutions of the wind wheel n_W
3. revolutions of the stone mill n_S

to the revolutions of the regulator. The larger the gear ratio the steeper the power curve of the stone mill.

By determining the various gear ratios between wind wheel and regulator, we obtain a series of curves, one of which will pass through the peaks of the power curves of the wind engine as shown by curve i in Fig. 247 below. Hence we see that at a correct gear ratio i of the centrifugal regulator to the wind wheel, the stone mill will operate under optimal conditions if the transmission between wind wheel and stone mill is properly selected. /399

Let us recall that in the manual method of regulation like in the automatic ones, one has to utilize the nomogram shown in Fig. 244 for determining the gear ratio of the revolutions of the wind wheel to the revolutions of the stone mill.

Operation of the TV-8 wind engine with ZD corn mill. The ZD corn mill-fodder crusher (Fig. 248) is used in animal husbandries for the grinding or crushing of grain for the preparation of fodder. The serrated rolls of the machine grind the grain during the rotation of the main rolls which takes place at a rate of 133-150 rpm. When one couple of pinions is disengaged from the transmission of the machine, both rolls work with the same number of revolutions i.e. 400-450 rpm, and in this case the machine works as a crusher. /400

The experimental performance of the corn mill is presented in Fig. 249. The output is obtained in relation to the wind velocity and the revolutions at a variable feeding of the grain, which makes it possible for the wind-driven unit to work under optimal conditions.

Table 31 presents the output of this machine with regard to grinding and crushing, with indication of the quality of the product and the specific output i.e. the output per hp/hour.

TABLE 30: DETERMINATION OF THE HEIGHT OF THE CLEFT h BETWEEN THE WORKING SURFACES OF THE STONE MILLS OF A VIME D-16 WINDMILL

Computed parameters	Wind velocity (m/sec) 4	5	6	7	8	9	10
Revolutions of the wind wheel	13	17	20	23	26	29	32
Revolutions of the vertical shaft	39	51	60	69	78	87	96
Revolutions of the centrifugal regulator	39	51	60	69	78	87	95
Angular velocity of the centrifugal regulator $\omega = \pi n/30$	4.1	5.3	6.25	7.2	8.8	9.1	10
$\cos\alpha = \frac{9,81}{\omega^2 OM}\left(1+\frac{Q}{P}\cdot\frac{OD}{OM}\right)$ ($OD=0,37$ м; $OM=0,61$ м)	—	0.99	0.71	0.535	0.36	0.33	0.278
$h=h_0\cos\alpha$ at.							
$h_0=3$ мм	3.0	2.96	2.14	1.6	1.08	1.0	0.83
$h_0=2$ мм	2.0	1.48	1.07	0.8	0.54	0.5	0.41

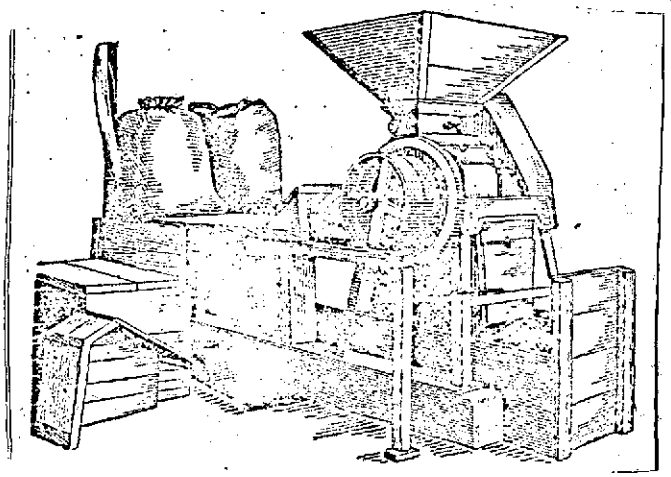

Fig. 248: The ZD corn mill-fodder crusher.

The overall output presented in Table 31 was given by the corn mill-fodder crusher at a wind velocity of 8 m/sec. Its revolutions under these conditions were 390-400 per minute.

Operation of the VIME D-12 wind engine with No. 2 "Farmer". The No. 2 "Farmer" (Fig. 250) is widely used for coarse milling in animal husbandry.

As a result of the processing of testing materials for wind engines and "No. 2 Farmer", the output characteristics of the unit presented in Fig. 251 and 252 were obtained. In the left hand side of the figure, the output curves are given for various degrees of coarseness of grinding in relation to wind velocity, while in the right hand side, in relation to the revolutions of the wind wheel. /402

Since the stabilizing regulation of the wind engine ensures the constancy of the revolutions at any wind velocity above 8 m/sec, the load can be increased in such a way as the wind velocity increases that the curve becomes a vertical, overloading the wind engine without increasing the number of revolutions so that it is not possible to determine by eye the extent of overloading of the wind

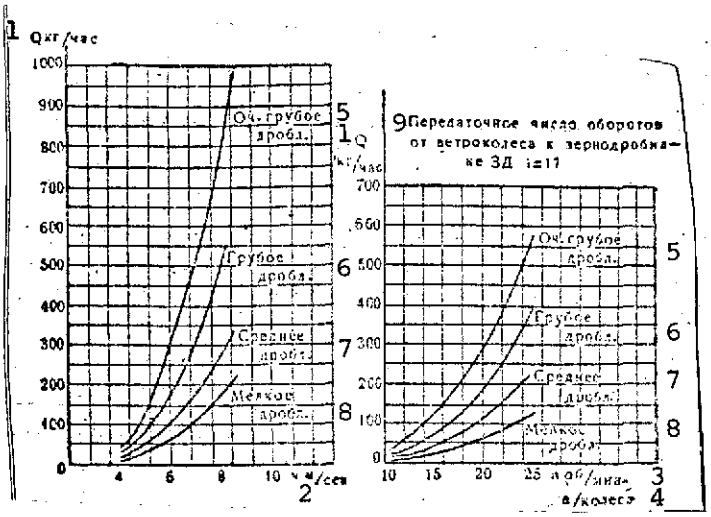

Fig. 249: Performance of the corn-mill in relation to wind velocity and revolutions of the wind wheel.

Key: 1. kg/hour
2. m/sec
3. rpm
4. wind wheel
5. very coarse grinding
6. coarse grinding
7. medium grinding
8. fine grinding

engine. Therefore at wind velocities above 8 m/sec, the load should not be increased to a larger extent than corresponding to the power of the wind engine at a wind velocity of 8-9 m/sec.

The output of the unit in relation to the coarseness of milling is presented in Table 32.

Performance of the wind engine with straw cutters. /403

Tests with the straw cutters of the "Goliaf" system show that the power and output of the machine depends on many factors, i.e.: moisture content of the straw, length of the cut, sharpness of the knives, etc. The effect of these factors on the performance of the machine is illustrated graphically in Fig. 253 and 254.

TABLE 31. OUTPUT OF THE ZD CORN MILL OPERATING WITH THE TV-8 WIND ENGINE

Characteristic of the grinding of barley		grinding		crushing	
Type of Grinding	When more than 50% per weight of the particles in the milling have a diameter (mm)	Output Kg/hr at V=8 (m/sec)	Specific output (kg/hp per hr)	Output (kg/hr)	Specific output (kg/hp·hr)
Fine grinding	0,5 и 1,0	175	35	—	—
Medium grinding	0,5 и 1,5	310	62	—	—
Coarse grinding and crushing	1,0 (1,5 / 2,0)	500	100	825	117
Very coarse grinding and crushing	2,0 (2,5 / 3,0)	800	160	1,700	238

TABLE 32. OUTPUT OF THE VIME D-12 WITH THE NO. 2 "FARMER"

Characteristic of milling		Output (kg/hr) at V=8 m/sec	Specific output (kg/hp·hr)
Type of milling	Diameter of particles (in mm) when they form more than 60% of the amount milled by weight		
Fine milling	0,5 до 1	320	24,5
Medium milling	0,5; 1,0 до 1,5	600	46,0
Coarse milling	1,0; 1,5 до 2,0	910	70,0
Very coarse milling.	2,0; 2,5 до 3,0	1400	107,0

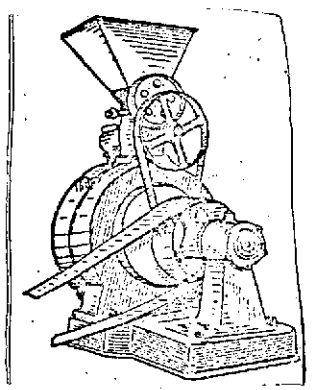

Fig. 250: The "No. 2 Farmer" grinding mill.

The power characteristics as a function of the revolutions is represented by a straight line: by superposing it on the characteristic curve of the wind engine, we obtain a set of unfavorable conditions which are similar to those obtained with the wind engine operating with a rotary pump i.e. the wind engine can only work with maximal ξ at low wind velocities. However, while a complex mechanism is required in order to increase the effectiveness of the wind-driven pump unit working with a rotary piston, no special mechanism is required in the given case in order to improve the characteristics. /404

Since in the case of the straw cutter, loading of the material to be processed is performed manually, smaller amounts of straw can be fed at low wind velocities; in this way the work performed by the straw cutter is smaller and consequently the wind engine is in a position to cope with the load. As the wind velocity increases, the loading of the straw can be increased as well. In such a manner, in the range of velocities 4-8 m/sec, we obtain /405

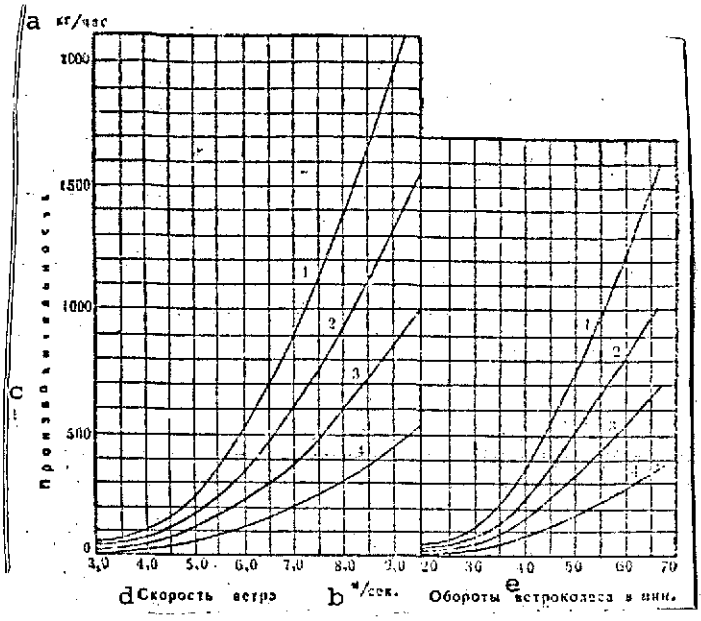

Fig. 251: Characteristics of the output of the VIME D-12 wind engine with "Farmer" at various degrees of grinding in relation to wind velocity

Fig. 252: Characteristics of the output of the VIME D-12 wind engine with "Farmer" in relation to the number of revolutions.

Key. 1. very coarse milling;
2. coarse milling;
3. medium milling;
4. fine milling.
a. kg/hr
b. m/sec
c. output
d. wind velocity
e. revolutions of the wind wheel per minute.

a characteristic curve of the machine which passes through the point of maximal power of the wind engine, i.e., a similar characteristic is obtained to that shown in Fig. 247, below, for the stone mill.

Generally speaking, the characteristic curves of the straw cutters, root cutters, saw, etc. have no definite shape which could be obtained by means of computations. This is explained by the fact that the main parameter, i.e. revolutions and output which characterize the work of similar machines, are not as closely related as for example the revolutions of a pump with its output.

In most of these machines, the feeding of the material to be processed is performed manually, and the output depends on the feeding. Therefore, naturally, the correspondence of the given power output of the wind engine depends on the individual habits of the servicing personnel.

Another factor which affects to a great extent the characteristics of agricultural machines is the tool which performs the processing of the material, i.e., the knife in the case of the straw cutter, the sharpness of the working surfaces of the stone mill in grinding mills, the teeth in the case of the saw, etc. The properties of these tools changes in the course of time and consequently the performance of their work

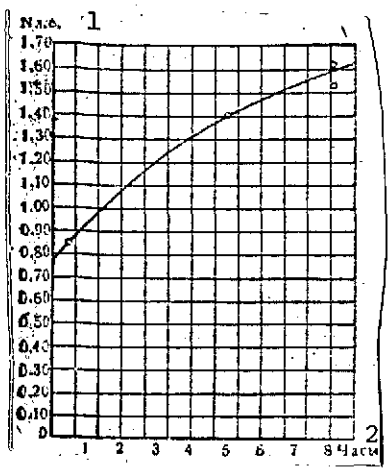

Fig. 253: Power expenditure on the straw cutter in relation to the time of operation from the moment of sharpening of the knives.

Key: 1. hp
2. hr

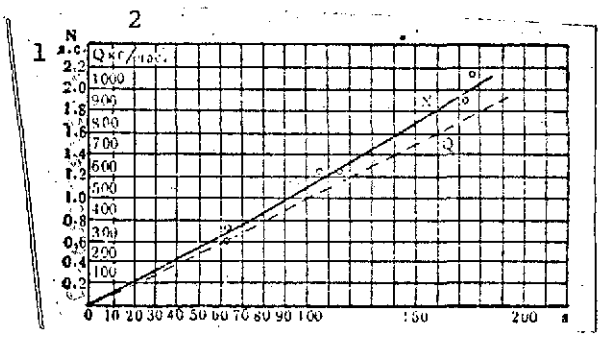

Fig. 254: Power expenditure on the work of the straw cutter in relation to revolutions and output (fresh, dry straw).

Key: 1. hp
2. kg/hr

changes and along with it the required power for their movement.

For example, the power expenditure of the straw cutter "Goliaf" during 8 hours of operation following sharpening of the knives increases twofold (see Fig. 253). With sharp knives the power expenditure was 0.8 hp while at the end of 8 hours of work, it increased to 1.6 hp while the output stayed the same.

Adjusting the agricultural machines to the wind engine. The initial parameters in adjusting agricultural machines to wind engines are their power N and the number of revolutions n. The normal power of the machine should correspond to that value of power of the wind engine at which it gives the maximal output throughout the year in a given region characterized by a given annual average of the wind velocity. Therefore, in selecting a certain machine, the graph illustrated in Fig. 238 should be used which indicates the wind velocities V_y at which the wind engine gives its maximal output during the year in a region with a given average annual wind velocity V_0. /406

Table 33 presents the power values on the shaft of the wind wheel in wind engines VIME D-5, TV-8 and VIME D-12 for wind velocities V_y which were calculated by means of equation (291) and were rounded off. The same table gives the values of the power of the tools at which they give the highest annual output when connected to the wind engine at a given average annual wind velocity. In order to determine the gear ratio of the revolutions of the tool to the revolutions of the wind wheel, the number of revolutions of the wind engine corresponding to the power are also presented.

TABLE 33. POWER OF THE WIND ENGINES AT OPTIMAL WIND VELOCITIES V_y IN RELATION TO AN ANNUAL AVERAGE WIND VELOCITY V_0

Parameter	Average annual wind velocity V_0 (m/sec)			
	3	4	5	6
	Optimal wind wind velocity V_y			
	5	6	8	9
VIME D-5, Rapid				
Power on the shaft of the wind wheel N(hp)	0.5	1.2	2.2	2.7
Power of the machine corresponding to a given power of the wind engine (hp)	0.32	0.73	1.5	1.75
Number of revolutions of the wind wheel	130	150	190	200
TV-8, Low Speed				
Power of the wind engine (hp)	1.2	3.0	5.8	7.0
Power of the machine (hp)	0.78	2.0	3.8	4.5
Number of revolutions of the wind wheel	16	20	22	25
VIME D-12, Rapid				
Power of the wind engine (hp)	2.5	6.1	12.0	14
Power of the machine (hp)	1.6	4.0	7.8	9.5
Number of revolutions of the wind wheel	40	50	60	70

The power of agricultural machines is determined by the relation:

$$N\mu = N\eta,$$

where η is assumed to be equal to 0.65, the mechanical efficiency.

Table 33 makes it possible to determine the wind engine in combination with which the work of a given agricultural machine will be optimal knowing its normal power, as well as to determine the gear ratio of the revolutions of the wind wheel to the revolutions of the machine if the latter are known. /407

Example 1. Determine the wind engine which will operate optimally with a root cutter with a power N = 0.75 hp at n = 80 rpm, and determine the gear ratio.

Examining Table 33, we find that this machine works in a region with an average annual velocity of the wind V_0 = 4 m/sec with a wind engine VIME D-5, while the gear ratio of revolutions of the wind wheel to the revolutions of the machine is equal to:

$$i = \frac{n_1}{n_2} = \frac{150}{80} = 1.9.$$

It is not advisable to connect this machine to a VIME D-5 wind engine in a region with an annual average wind velocity V_0 = 3 m/sec, since under these conditions it would only work a small number of hours per year. At a wind velocity V_0 = 3 m/sec, it would be more convenient to connect this machine to a TV-8 wind engine. In this

case the gear ratio will be:

$$i=\frac{16}{80}=0.2.$$

Example 2. Determine the type of wind engine which would be fully loaded with an oil cake breaker, the normal power of which equals 5 hp. In Table 33 we find that this power corresponds to a power of the TV-8 wind engine as V_0 = 5-6 m/sec. This machine can give a satifactory loading also with type VIME D-12 wind engine as V_0 = 4-5 m/sec.

When the wind engine works with several agricultural machines, it is not required that the power of the machine corresponds to the maximal annual output of the wind engine, since in this case the wind engine works simultaneously with several machines.

Thus, in adjusting a certain power of the machine to the wind engine, not only the type of the wind engine should be considered, but also the average annual wind velocity at which the machine will operate. The same machine will require different dimensions of wind engines at different values of the annual average wind velocity.

CHAPTER 14: WIND-DRIVEN PUMP INSTALLATIONS /408

Wind engines are widely utilized both in the USSR and abroad for the lifting of water from pits, wells and resevoirs.

Wind-driven pump installations can be divided according to their purpose into:

1. wind-driven pump installation for water supply; these lift the water for drinking and domestic needs;
2. wind-driven irrigation installations, which lift the water for irrigating plots of land;
3. wind-driven pump installations for draining marshy lands or deeply-flooded land.

52. Wind-Driven Pump Installations for Water Supply

The main components of a wind-driven pump installation are:

1. the wind engine, designed for operation with a piston or centrifugal pump, Archimedean screw etc.;
2. pump equipment consisting of a pump, suction intake and delivery pipes and various devices which ensure the correct and most effective operation of the pump installation (air chamber, balancer, devices for priming and discharging the water, etc.);
3. resevoir or tank for storing the water on calm days;
4. net of distributor pipes which feeds the water to the places where it is consumed.

For designing wind-driven pump installations, it is imperative to know the amount of consumed water for the needs of a given husbandry, the nature of the source and its output and finally, the relief and wind conditions of the place where it is suggested to set up the wind-driven pump installation. /409

The constructional diagram of the commonest type for the water supply of animal husbandries is shown in Fig. 255.

The deep bedding of the water in pits or wells requires a piston pump for its lifting to the surface, while lifting of the water from open resevoirs or small pits which have a large output can be performed by means of a centrifugal pump. In the first case, a multi-bladed low speed wind engine is required which is characterized by a large moment of stopping and small number of revolutions, while in the second case a sparse-bladed rapid wind engine is required which is characterized by a large number of revolutions and small stopping moment.

The wind and topographical conditions of the place determine the system of regulation of the wind power unit and the type of equipment (the intake, net of pipes, actuatator, etc.)

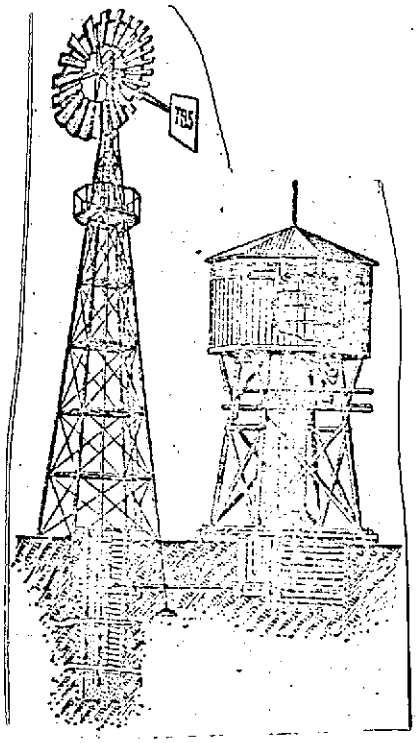

Fig. 255: Constructional diagram of a wind-driven pump installation.

The daily expenditure as well as the output of the water source determine the power of the wind-driven pump installation.

The wind-driven pump unit should be/410 chosen in such a way that the inflow of water from a given source should cover the expenditure. A water deficiency in the source can disturb the normal operation of the wind engine and may be the reason for cluttering of the well by engulfed sand. The expenditure of the water Q should be equal or smaller than the output of the source Q_0 i.e.:

$$Q \leq Q_0 \qquad (299)$$

In such a manner, the following rule is obtained:

a. in adjusting a certain wind-driven pump unit to a source with a limited output, the power of the unit should be established on the basis of the output of the water source and when the latter is deficient, in order to ensure the supply of the husbandry, other water sources should be considered where other wind-driven pump units can be set up:

b. in adjusting the wind-driven pump unit to a water source with an unlimited output, the power of the unit should be determined on the basis of the required amount of water for the given husbandry.

Usually the water from open resevoirs which have a large output are used for production and irrigation purposes. Water from pits and wells with a limited output is usually hauled only for drinking needs. The latter type is most common in steppe regions. Their characteristic feature is a small output, from 0.2 to 2.0 m^3/hr. However in certain regions of our South, wells with a very high output are found, reaching 30 m^3/hr. The water from such wells can be lifted not only for drinking purposes but also for irrigation.

The amount of water which can be supplied by a wind-driven pump installation per day, taking into account a water reserve for 1-2 calm days, is determined according to the existing standards of water requirements q liters per day. Multiplying the standard per consumer by their number n and adding up, we obtain the daily water expenditure Q:

$$Q = \Sigma q n. \qquad (300)$$

For example, according to the standards of the Ministry of Agriculture of the USSR, the daily water consumption of animals including watering places, preparation of fodder and sanitary-hygienic measures is determined by the following figures given in Table 34.

TABLE 34: WATER CONSUMPTION BY ANIMALS [15]

Animal	Daily water consumption per head (ℓ)	
	with internal water pipe	without water pipe
milking cows	75—90	60
calves up to 6 months of age	20	15
calves from 6-18 months of age	24	20
dry cow	45	35
bull-sire	60	50
working ox	60	60
working horse	60	50
foal from 6-12 months of age	40	30
sow with piglets up to 2 months (in the summer)	75	54
same, in the winter	64	38
piglets from 2-6 months (in summer)	17	12
same, in the winter	14	9
fattened pigs, 9 months	35	20
male swine	59	40
sheep	12	8
sheep with lamb	15	10
sheep goat	15	10
rabbit	3	2
chicken	1.5	0.75

The distribution of water consumption in the course of one day /411 is shown in the graph in Fig. 256, which illustrates the water consumption in a cattle yard in the presence of an automatic drinking bowl.

In order to fully supply the consumers with water by utilizing the energy of the wind, the power of the wind-driven pump installation should be calculated not per daily water feed, but per the amount which would ensure the consumer with supply on both windy and calm days. On windy days, the wind installation should ensure the daily water consumption and should store the water for the subsequent calm periods, the length of which may be 1-2 days.

The calm period is defined as days with an average wind velocity of 2 m/sec and below, with a duration of 1 day and more.

Let us assume that for a given region, the variation in the average daily wind velocities during a certain period of time took place as illustrated in Fig. 257, where the hatched areas give a /412 picture of the fluctuations in wind velocities, τ is the number of days with an average wind velocity higher than 2 m/sec between two adjacent calm periods, t is the number of days in the calm period.

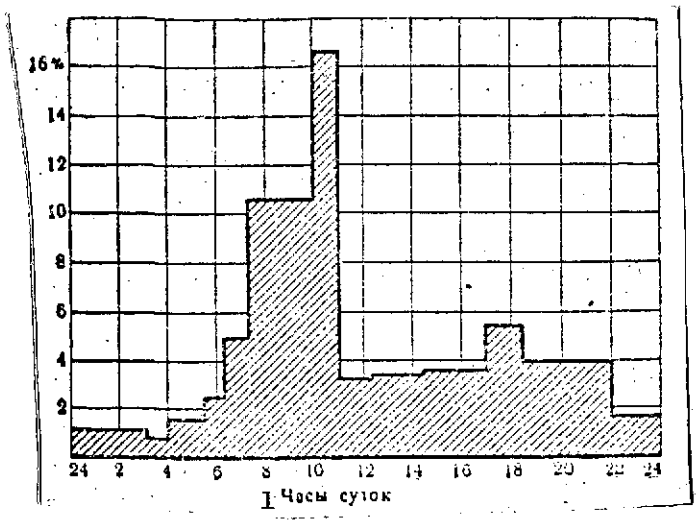

Fig. 256: Daily graph of water consumption for animals.

Key: 1. hour of the day

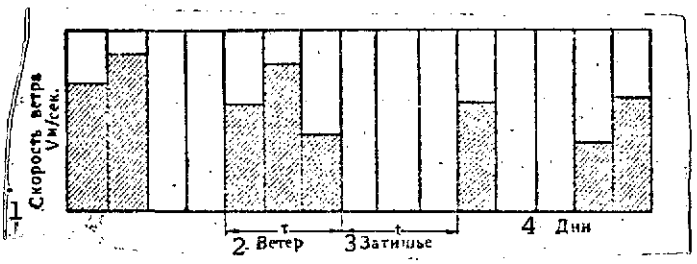

Fig. 257: Graph of the possible fluctuations in average daily wind velocities.

Key: 1. wind velocity V m/sec
2. wind
3. calm
4. days

Such a graph is entirely possible since the sequence and duration of the calm periods do not obey a certain law. There are regions, where the calm /413 periods may last from 2-3 days, but in the same regions, there are cases when the average daily wind velocity does not exceed 2 m/sec for a whole month. This is a rare occurrence but it does happen.

According to the graph in Fig. 257, water can be fed to the wind-driven pump installation in an amount which would ensure the supply to the consumer under less favorable conditions of wind, when the period of calm days t is longest, and the number of windy days τ is smallest. Under these conditions, the amount of water stored in the reservoir can be determined in the following way.

The wind installation should ensure a daily water consumption or a daily expenditure Q m^3/day; in addition, it should haul the water into the stock during the period of calm days; the magnitude of this stock is determined by the expression:

$$\frac{Qt}{\tau}. \qquad (301)$$

In such a manner, disregarding the water expenditure required for covering the peaks of the graphs of water consumption, the power of the wind-driven pump installation should be calculated for an overall amount of water which is equal to:

$$Q_1 = Q + \frac{Qt}{\tau} = Q\left(1 + \frac{t}{\tau}\right). \qquad (302)$$

If there is a large variation in the daily water consumption, the installation can haul water into the stock the amount of which we shall assume to be equal to the daily requirement; consequently the amount stocked per day will be equal to Q/τ.

In this case, the overall amount of water is:

$$Q_1' = Q + \frac{Qt}{\tau} + \frac{Q}{\tau} = \frac{Q}{\tau}(\tau + t + 1). \qquad (303)$$

Power of the wind-driven pump unit. The power of the wind-driven pump unit required for supplying the daily water expenditure is determined by equation:

$$N = \frac{Q \cdot H \cdot 1000}{75 \cdot 3600 \cdot t_p \eta}, \qquad (304)$$

where: Q is the daily water consumption in m^3; /414
t_p is the number of working hours of the wind engine per day;
H is the pressure head in m, which is determined by accounting for the losses in pressure heads;
η is the efficiency of the pump.

If in addition the unit is supposed to feed water into the stock in order to be consumed on calm days, the power will be expressed according to equations (302) and (303), by:

$$N_1 = N\left(1 + \frac{t}{\tau}\right), \qquad (305)$$

or accounting for the inconstancy of the consumption:

$$N_1' = \frac{N}{\tau}(\tau + t + 1). \qquad (306)$$

In addition, the volume of the tank should correspond to the volume of water supplied by the wind-driven installation over and above the daily consumption.

If the amount of supplied water is determined by means of equation (302), then the volume of the tank should equal:

$$W = \left(Q + \frac{Qt}{\tau}\right)\tau - Q\tau,$$

hence

$$W = Qt. \qquad (307)$$

If the water in the tank must suffice also for covering the peak of the graph of water expenditure, according to equation (303), then the volume should equal:

$$W' = \left(Q + \frac{Qt}{\tau} + \frac{Q}{\tau}\right)\tau - Q\tau,$$

hence

$$W' = Q + Qt = Q(t + 1). \qquad (308)$$

However, it should be stressed that a wind-driven pump installation which ensures complete water supply to the consumer on account of the wind energy, is practically unsuitable in regions with long calm periods.

Let us assume that in a certain region where it is planned to set up a wind-driven pump installation, the duration of calm periods averages 5 days, while the number of windy days between two calm periods is $\tau = 2$ days. Determining the required power by means of equations (305) and (306), we obtain: /415

$$N_1 = N\left(1+\frac{5}{2}\right) = 3.5N.$$
$$N_1' = \frac{N}{2}(1+2+5) = 4N.$$

In such a manner, for a 5-day calm period which was preceded by two windy days, the power of the wind-driven pump installation should be 3.5 times larger than the power needed to lift the water in the course of one day, and 4 times larger if the peak of the consumption graph has to be covered.

Under these conditions, the tanks for storing the water should have the following capacity:

$$W = Qt = 5Q.$$
$$W' = Q(t+1) = Q(5+1) = 6Q.$$

How will the wind-driven installation operate if two windy days will be followed by let us say two calm days? In this case the required power will be:

$$N_1 = N(1+\frac{2}{2}) = 2N.$$
$$N_1' = \frac{N}{2}(1+2+2) = 2.5N.$$

The examined examples show that a wind-driven installation calculated for 5 calm days would stand still during calm periods which last less than 5 days and would not supply the required water to the consumer if calculated for a smaller number of calm days. Our conclusion is that in regions with low wind velocities, it is not advisable in practice to design wind-driven pump installations to cover the water supply of the consumer only on account of the wind energy.

Evidently the wind-driven pump installation can supply the consumer with water only in those regions where the calm periods do not exceed 2-3 days while the windy periods between them lasts no less than 1-2 days.

A wind-driven pump installation with a reserve engine which does not work with wind energy would be more advisable. A suitable reserve engine for wind-driven pump installations under rural conditions is a horse-drawn actuator.

In this case the tanks for storing the water can be much smaller i.e. to contain no more than a one-day supply.

53. Water Tanks and Water Towers in Wind Pump Installations /416

Wind pump installations can not operate without a resevoir or a tank for storing water. In the absence of a tank, the wind engine would have to work only at the time of water consumption i.e. with interruptions; the wind installation would have to stop as soon as the consumption of the water stops, and it would have to start again when the requirement for water is renewed. However, in order to start a wind engine which is charged by means of a rotary pump, a wind velocity of at least 4 m/sec is required, while the operation can take place at a velocity of 3 m/sec. The initial loading moment is approximately 3 times larger than the working moment. In such a manner, the intermittent operation of the wind installation as a result of the absence of a tank or a water stock, would be the reason for frequent idle periods in the operation of the wind engine not only when there is no need for water but also when it is needed. Such an installation would be of little use in practice.

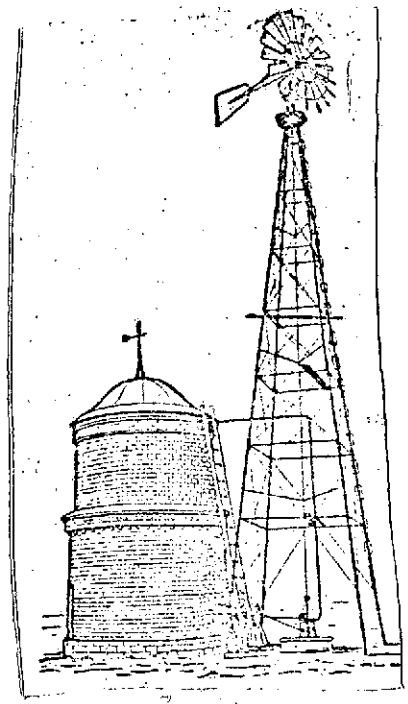

Fig. 258: Wind installation with a 20 m^3 metallic tank in brick walling.

The water tank is the main element in any wind pump installation. The wind energy can be accumulated in the form of the water stored in the tank on calm days. As a result of this, the idle periods of the wind installation are shortened and at the same time the production becomes cheaper, which pays the expenses for the /417 construction of the water tank. The daily water consumption is characterized by large fluctuations as shown in Fig. 256: for example, the water consumption from 12 md until 2 pm is much higher than between 6 am and 10 am. This maximal consumption within a short period of time can of course not be ensured by the wind installation. The presence of water stored in the tank makes it possible to cover the peak consumption regardless of whether the wind installation works or not in the given moment.

Let us present a few examples of the construction of resevoirs and tanks used with wind pump installations. Fig. 258 illustrates a wind pump installation with a tank of 20 m^3 capacity. The cylindrical tank made of iron sheets has a diameter of approximately 2.5 m and a height of about 2.8 m. It is surrounded by brick walling up to a height of 2 m. The brick wall prevents the water from freezing in the winter.

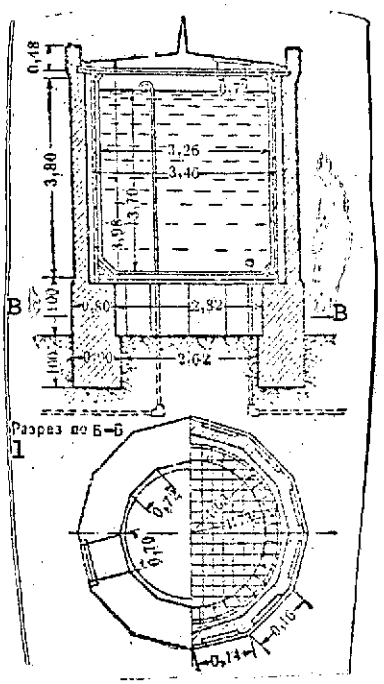

Fig. 259: A 30 m^3 iron-concrete storage tank.

Key: 1. section at B-B

Iron-concrete storage tanks the construction of which is shown in Fig. 259, are quite common. Approximately 8 tons of cement and about 600 kg of iron are needed for the construction of such a storage tank with a capacity of 30 m^3; these are distinguished by their great durability. The construction and computations of iron-concrete storage tanks are presented, for example, in the book of B. A. Shebuyev, Zhelezobetonnye rezervuary, bunkery i silosy, [Iron-concrete resevoirs, bunkers and silos] Moscow, 1935.

Stone resevoirs are durable and can be . . . .

[Pages 418 and 419 are missing in the available copy of this book.]

In the woody regions of the northern /420 and central strips of the European part of the USSR and in Siberia, it is most convenient to build wooden water towers. The height of these towers is determined depending on the losses in pressure head in the distributor net and on the height of the points of water consumption. If the water from the tank is also utilized for extinguishing fires, then its height is taken as 12-18 m. If the water is only used for drinking, then the height of the water tower is taken as 8-10 m.

For the sake of illustration, Fig. 261 presents the general view of the construction of a wooden water tower. Wooden tanks are most commonly used with such towers. An example of a wooden cylindrical tank with an internal diameter of 3.7 m, a general height of /421 2.35 m, and a filling height of 1.85 m is shown in Fig. 262. The tank is made of boards 5 cm thick and is fastened with rings made of round iron with a diameter of 16 mm.

If the tank is fastened with packed rings, then it is given a conical shape, as shown in Fig. 262, right.

In order to prevent the water from freezing, the tank is encased in a skeleton frame cabin with double casing filled with a heating material which may be sawdust or another cheap heat isolating material.

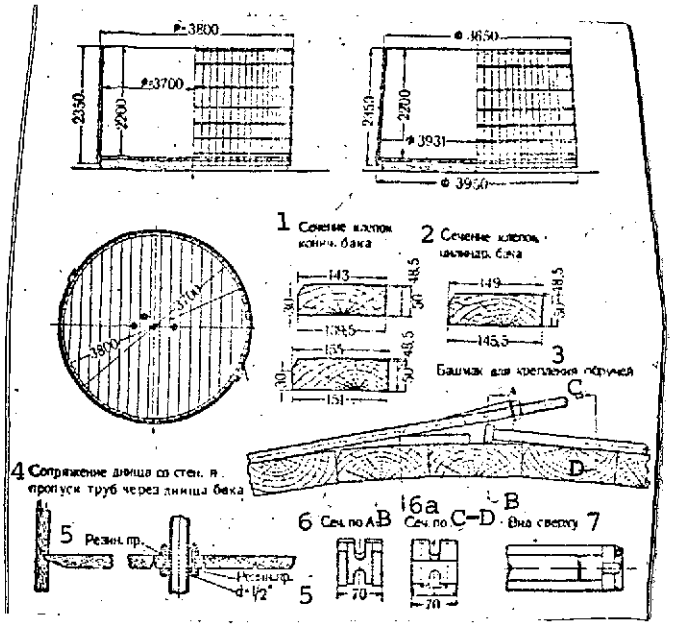

Fig. 262: Cylindrical and conical wooden tanks.

Key: 1. cross section through the riveting of the conical tank
2. section through the riveting of the cylindrical tank
3. socket for fastening the rings/
4. adjoining bottom with the walls and passage of the pipesthrough the bottom of the tank.
5. rubber spring
6. sections along A-B
6a. sections along C-D
7. top view

All the wooden elements of the main construction of the tower are connected by means of grooves and bolts. Below, the feet of the tower are supported on foundations made of rubble or concrete blocks and are fastened to them by means of connecting bolts which pass through the rods consisting of two logs for each pair of feet (Fig. 263).

The upper area of the tower has a planking and a lining: the space between these is filled with a heating layer which protects the tank from the cold coming from below. A duct passes along the axis of the tower from the floor of the cabin to the well, consisting of a skeleton frame with double casing; a heating filling fills the space between the walls. The duct serves for heating the feeding and outlet pipes. The pipe provided with valves for switching the water into the direction of the tank or directly to the consumer and it is mounted in a timbered pit situated at the base of the tower under the duct. /422

The tentative requirement in materials for the wooden tank shown in Fig. 263 with different capacities, is presented in Table 35 (see also Fig. 264). The table was compiled according to the data of the laboratory for wind power utilization VIME.

54. Standard Designs of Wind Pump Installations. /423

The mass distribution of wind pump installation in the USSR dates back to 1936, when about 1300 installations with the wind engines TV-5 and TV-8 were constructed in various regions for the lifting of water. Let us characterize two of the most common installations in more detail.

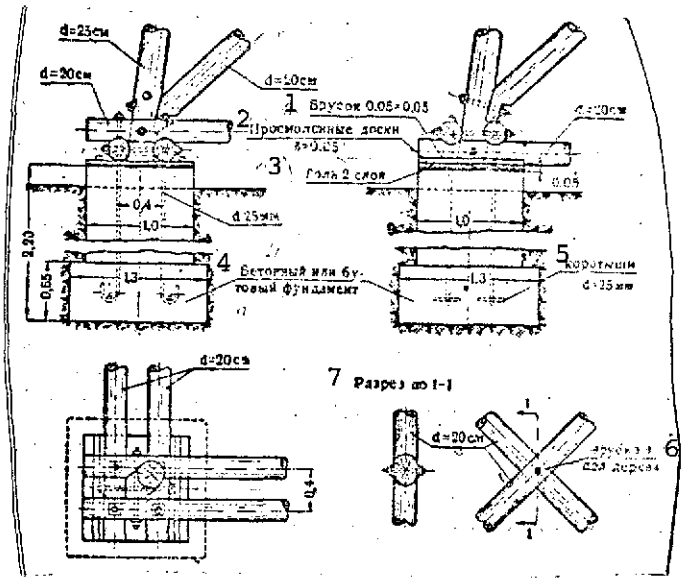

Fig. 263: Foundation under the feet of the water tower.

Key: 1. bar
2. boards covered with tar
3. bare layers
4. concrete or rubble foundation
5. bolsters
6. groove in the floor of the wood
7. cut along 1-1.

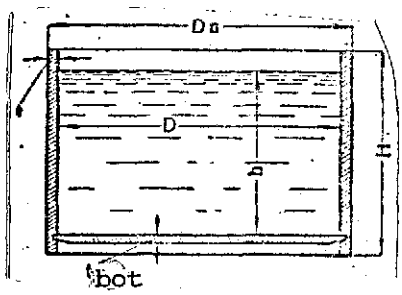

Fig. 264: Main dimensions of wooden tanks.

The wind pump installation with the TV-5 wind engine. The wind pump installation with the TV-5 wind engine (Fig. 265) is one of the most common installations in the USSR. Due to its power it is suitable for use in many kolkhoz and sovkhoz husbandries. /424

The TV-5 wind installation is mainly found in the steppe regions and is used for supplying water to the cattle in the field. It is recommended also to build these wind pump installations in animal husbandries when the water sources are at relatively large distances from the cattle yard. The output of this installation with a rotary pump was computed by means of equation (264) and the characteristics constructed according to Fig. 219, on the condition that the characteristic of the pump follows ray I. The result of the computation is presented in Table 36.

The measured expenditure on a type TV-5 wind pump installation consists of the following losses:

1. Wind engine with pump equipment.....k_1
2. Tank for the storage of water with heated cabin.....k_2
3. Construction of cap and base under the wind engine.....k_3
4. assembly and hoisting of the wind engine....k_4

The sum of the major investments equals $K = \Sigma k$.

The annual expenditures for exploitation consists of the following elements:

TABLE 35. TENTATIVE REQUIREMENTS FOR MATERIALS FOR WOODEN TANKS

Effective capacity (m^3)	Internal diameter (m) D	Height of the tank (m) H	Thickness of walls (cm) t	Thickness of bottom (cm)/bot tom/bot	Number of rings on wall n	Diameter of rings (mm) d	Overall weight of the matter kg	Required volume of lumber m^3
10	2.94	1.82	4.0	4.0	8	12	131.8	1.49
15	3.38	2.04	4.5	4.5	6	16	187.7	2.15
20	3.70	2.20	5.0	5.0	7	16	225.9	2.74
25	3.86	2.47	5.5	5.5	9	16	284.8	3.65
30	4.10	2.61	6.0	6.0	8	19	376.3	4.40
35	4.34	2.74	6.0	6.0	9	19	438.3	4.91
45	4.52	2.83	6.5	6.5	9	19	494.6	5.93
50	4.88	3.03	7.0	7.0	9	22	646.6	7.16
60	5.18	3.20	8.0	8.0	10	22	804.8	9.11

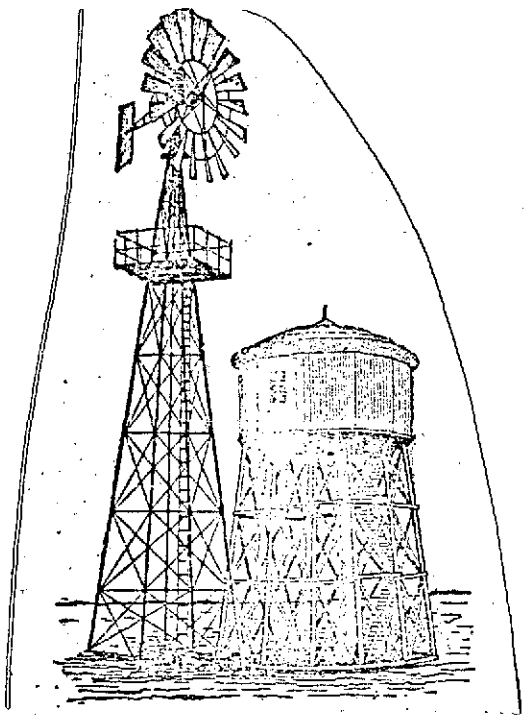

Fig. 265: Wind pump installation with TV-5 wind engine.

/425

1. Damping of the structural part

$$y_1 = 0.054\ k_2.$$

2. Damping of the equipment

$$y_2 = 0.07(k_1 + k_2)$$

3. Routine maintenance of the tank forry$_3$ = $0.02\ k_2$.

4. Routine maintenance of the equipment

$$y_4 = 0.05(k_1 + k_4).$$

5. Maintenance of the windmill installation.....y_5

6. Lubrication and cleaning materials.... y_6

Sum of the annual expenditures: Σy

The cost of 1 m^3 of lifted water is obtained by dividing the annual exploitation expenditure by the amount of water lifted in the course of the year

$$C = \frac{\Sigma y}{Q_y}\ \text{rubles}/\text{m}^3,\quad C' = \frac{\Sigma y}{Q_y'}\ \text{etc.}$$

where Σy is a constant magnitude, while the annual production (Q_y) changes with the change in the average annual wind velocity.

$$\frac{C'}{C} = \frac{Q_y}{Q_y'},$$

ORIGINAL PAGE IS
OF POOR QUALITY

TABLE 36. OUTPUT OF THE TV-5 WIND PUMP INSTALLATION WITH ROTARY PUMP d = 3 3/4"

Total head (m)	wind velocities (m/sec)					
	3	4	5	6	7	8 and more
	liter/hour					
10	2 121	4 000	5 600	7 200	9 000	10 230
20	1 060	2 000	2 800	3 600	4 500	5 125
30	710	1 330	1 860	2 400	3 000	3 400
40	530	1 000	1 400	1 800	2 250	2 560
50	425	800	1 120	1 440	1 800	2 040
60	355	670	930	1 200	1 500	1 710
70	303	570	800	1 030	1 285	1 460
80	266	500	700	900	1 125	1 280

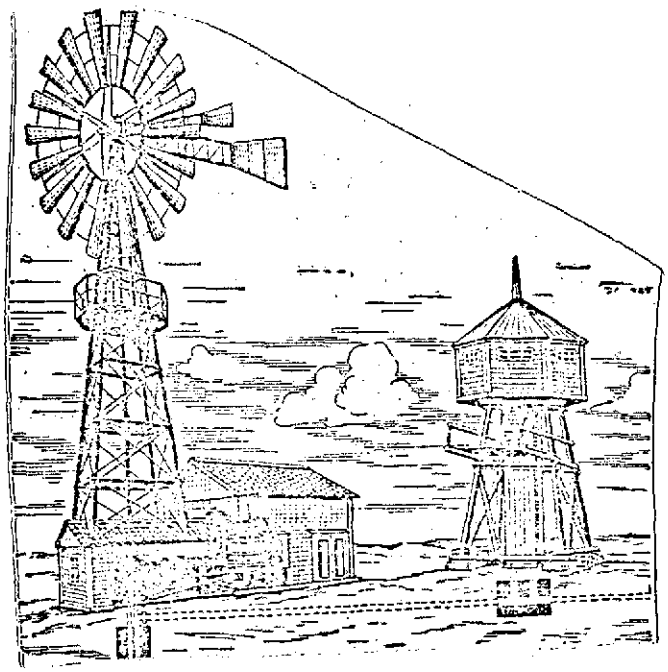

Fig. 266: The TV-8 wind installation for water supply and milling.

Consequently, we can write:

$$C = \frac{\Sigma y}{Q_y}$$

relating the cost C to an average annual wind velocity of 3 m/sec and a head H = 10 m, we find the costs in relative magnitudes for other average annual wind velocities and head values (see Table 37).

The cost in rubles is obtained by multiplying 422, calculated for an annual average wind velocity of 3 m/sec and a head H = 10 m, by the derived values given in Table 37.

The TV-8 wind installation for water supply and milling. The work of the wind engine for water supply and milling represents one of the most rational methods of utilization of the wind energy. The work required for the water supply of medium kolkhozes can not fully load a TV-8 wind engine; more than 60% of the annual power remains unutilized. In order to decrease the cost per unit production, this excess should be utilized on some other type of work for which no particular location of the wind installation is required. Milling is one of those types of work which can be carried out in any kolkhoz farm. Therefore, the TV-8 wind installation is recommended to be set up in combination with a mill for the water supply of kolkhozes. The general view of such a wind installation is shown in Fig. 266. The wind engine sets in motion a rotary piston, the diameter of which is established independently of the head, and a grinding wheel with stone of a diameter 550 or 710 mm. The water is fed into a /427

TABLE 37. RELATIVE MAGNITUDES OF THE COST OF 1 m^3 OF LIFTED WATER IN RELATION TO THE ANNUAL AVERAGE WIND VELOCITIES AND TO THE HEAD

Total head (in m)	Annual average wind velocity (m/sec)			
	3	4	5	6
10	1	0.62	0.46	0.37
20	2	1.24	0.92	0.74
30	3	1.86	1.38	1.11
40	4	2.48	1.84	1.48
50	5	3.10	2.30	1.85
60	6	3.70	2.76	2.22
70	7	4.35	3.22	2.58
80	8	4.95	3.70	2.96

tank with a capacity of 20 m^3 mounted on a wooden tower with a height of approximately 8 m. The station of a grinding mill has dimensions 6 x 6 x 3.5 m and is a very simple construction with log or framework walls, or adobe walls in the southern steppes regions.

When the wind engine works with a rotary piston and with a characteristic curves passing through ray 1 (Fig. 219), the output is obtained from Table 38.

TABLE 38. OUTPUT OF A TV-8 WIND PUMP INSTALLATION WITH ROTARY PUMP

Total head (m)	Wind velodity (m/sec)					
	3	4	5	6	7	8 or more
	Liters per hour ℓ/hr					
10	7 030	13 100	20 000	25 400	29 000	33 400
20	3 500	6 550	10 000	12 700	14 500	16 700
30	2 340	4 350	6 700	8 500	9 700	11 100
40	1 750	3 260	5 000	6 340	7 250	8 350
50	1 400	2 620	4 000	5 080	5 800	6 680
60	1 170	2 180	3 340	4 230	4 820	5 570
70	1 000	1 870	2 860	3 640	4 140	4 770
80	880	1 630	2 500	3 180	3 630	4 180

The TV-8 wind installation used for the preparation of fodder. The TV-8 wind engine can supply energy in excess for the work of fodder-preparing machines which is sufficient for 160 head of cattle, 175 horses, 150 pigs and about 50 sheep. The wind engine operates /428 with a transmission (Fig. 267), by means of which an oil cake breaker

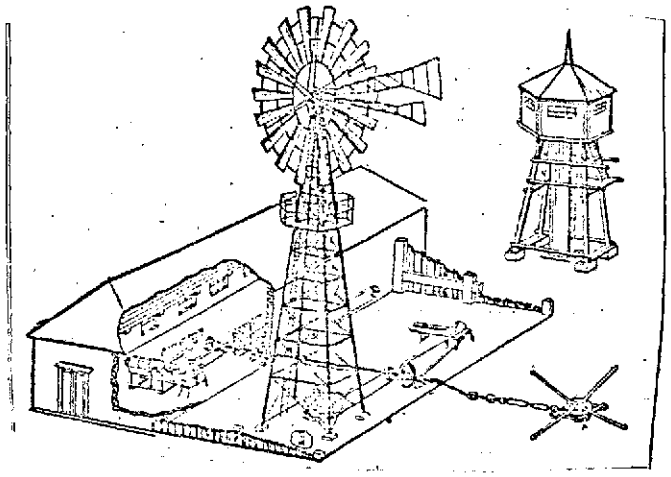

Fig. 267: The TV-8 wind installation operating in a fodder workshop.

and a corn mill situated in a separate building on one side of the gear exit are set in motion by means of belt transmissions, as are a root cutter and root washer situated in another building on the other side of the gear exit. Other agricultural machines situated in separate buildings are set in motion by means of a counter shaft. The straw cutter is set up outside the building under an awning which covers part of the transmission to which the shaft of a horse-drawn actuator is connected by means of a Hooke's joint. The latter is set up as a reserve for operation of the root cutter and root washer on calm days, since it is not possible to do the cutting of the root crops in stalls due to the possibility of damage. A water tower with a 20 m^3 tank was constructed in order to feed water directly to the automatic drinking bowl in the stalls.

The amount of energy required for preparation of fodder in the workshop, without washing of the grain, amounts to 4940 hp hr. The TV-8 wind engine can supply up to 8620 hp hr in a region with an annual average wind velocity of V_0 = 4 m/sec and up to 19200 hp hr in regions with V_0 = 6 m/sec. Since the excess power of the wind engine during its operation in the fodder workshop accumulates mainly during the night hours, this power can obviously be utilized conveniently for milling. Therefore, a mill with a diameter of 550 or 710 mm should be added to the fodder workshop. /429

The wind engine can operate simultaneously with the fodder workshop and with a rotary pump, if the head does not exceed 50 m. The transmission and the rotary pump should be disconnected during the operation of the wind engine with the grinding mill. Under strong wind, 7 m/sec and above, the rotary pump can be connected in addition to the grinding mill. /430

The amount of milling supplied by a TV-8 wind installation operating in a medium animal husbandry workshop, in relation to the average annual wind velocity, is presented in Table 39.

One can see in this table that in a wind installation which operates with several machines, which however do not load the wind engine throughout the day, milling of the grain assumes the role of a storage

TABLE 39. PERFORMANCE OF THE TV-8 WIND INSTALLATION IN AN ANIMAL HUSBANDRY

Name of the processed product	Amount of the consumed product (pump)	Amount of consumed energy (hp/hr)	Energy expenditure for the processing of each type of product in % of the overall energy which can be supplied by the wind engine depending on annual average wind velocity V_0		
			m/sec	5 m/sec	m/sec
Grain milling.....	158.4	2 642	30.60	19.30	13.80
Oil cake milling.....	185.8	926	10.70	6.80	4.80
Cutting and washing of root crops.....	233.5	380	4.40	2.78	1.98
Cutting of straw.....	75.7	340	3.90	2.50	1.76
Lifting of water.....	2 920	658	7.50	4.75	3.40
Total		4 940	57.10%	36.13%	25.74%
Milling grain by means of the unutilized energy in the fodder work shop at V_0=4 m/sec .	98	3 680	42.90	—	—
Same at V_0 = 5 m/sec.....	238	8 889	—	63.87	—
Same at V_0 = 6 m/sec.....	390	14 464	—	—	74.26
Total	—	—	100%	100%	100%

battery of the wind energy, which is stored in the form of the finished product i.e. the flour.

55. Experience with Exploitation of Wind Pump Installations for Water Supply in Agriculture

When properly mounted and with suitable maintenance, wind installations have a long life and a high productivity.

For example, in the kolkhoz "Sotsstroyka", of the Plastunov region, Krasnodar territory, a TV-8 wind installation operating on a mill producing farm with 250 head of cattle promoted a 25% increase in the milk yield of cows and gave an economic gain in manpower amounting to 21000 rubles.

The No. 612 sovkhoz in Donskoy stanitsa[1], krasnodar territory, which had an installation of three TV-8 wind engines for water supply and preparation of fodder for 3000 head of cattle, had an economic gain amounting to 32400 rubles due to the decreasing expenditures in manpower. An approximately similar economic gain is obtained in other kolkhozes and sovkhozes which have wind engines installed on their farms [46].

[1][Translator's note: a large Cossack village]

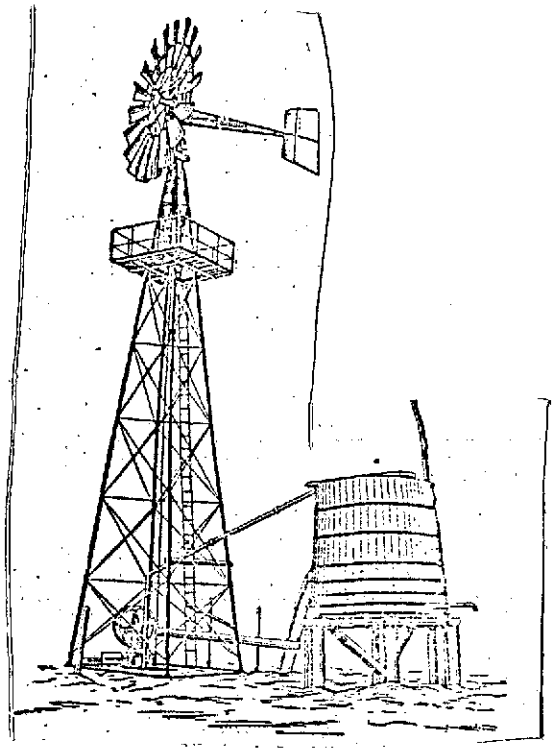

Fig. 268: The TV-5 wind pump installation in the Leski village, Kiev region.

Fig. 268 illustrated a wind pump installation with a TV-5 wind engine, constructed in the kolkhoz of the Leski village, Kiev region, on the stopping place of a field team. Due to proper use, this wind installation has been operating effectively for several years. A wind engine with a 3 3/4" rotary pump, during a travel of the piston of 400 mm, lifts the water from the well into a 19.5 m^3 capacity tank. The well has a depth of 51 m; 25 m of this is formed by a concrete pit and 27 m by the well. The height of the water column is 25.5 m, the lifting height is 30 m, counting from the dynamic level. During prolonged calm periods, the water is /431 lifted by means of a horse-drawn actuator mounted on two horses. The shaft of the horse-drawn actuator is directly connected with the shaft of the grinder by means of a Hooke's joint. The travel of the pump piston during its operation from the grinder amounts to 200 mm.

The water supplies the drinking needs of about 700 kolkhoznics working in field teams as well as for watering places of 260 head of cattle. In addition, the water is used for irrigation of vegetable cultures (top dressing) during one month in spring.

Prior to the construction of the well and of the wind pump installation, 22 horses had been used for the daily transportation of the water to the consumer. After construction of the wind pump installation, 7 horses were sufficient in order to supply the water to the consumers. The VIME wind power laboratory carried out observations on this installation in the course of one year. The output was determined by counting the number of travels of the pump rod and /435 determining the wind velocity by means of an anemometer four times daily.

The observations were processed in the form of graphs which are presented in Fig. 269, for a period of 12 months starting with Oct. 1 through Sept. 30. The daily output of the installation is shown by the hatched areas. The broken lines above the hatched areas show the change in the average daily wind velocity.

ORIGINAL PAGE IS
OF POOR QUALITY

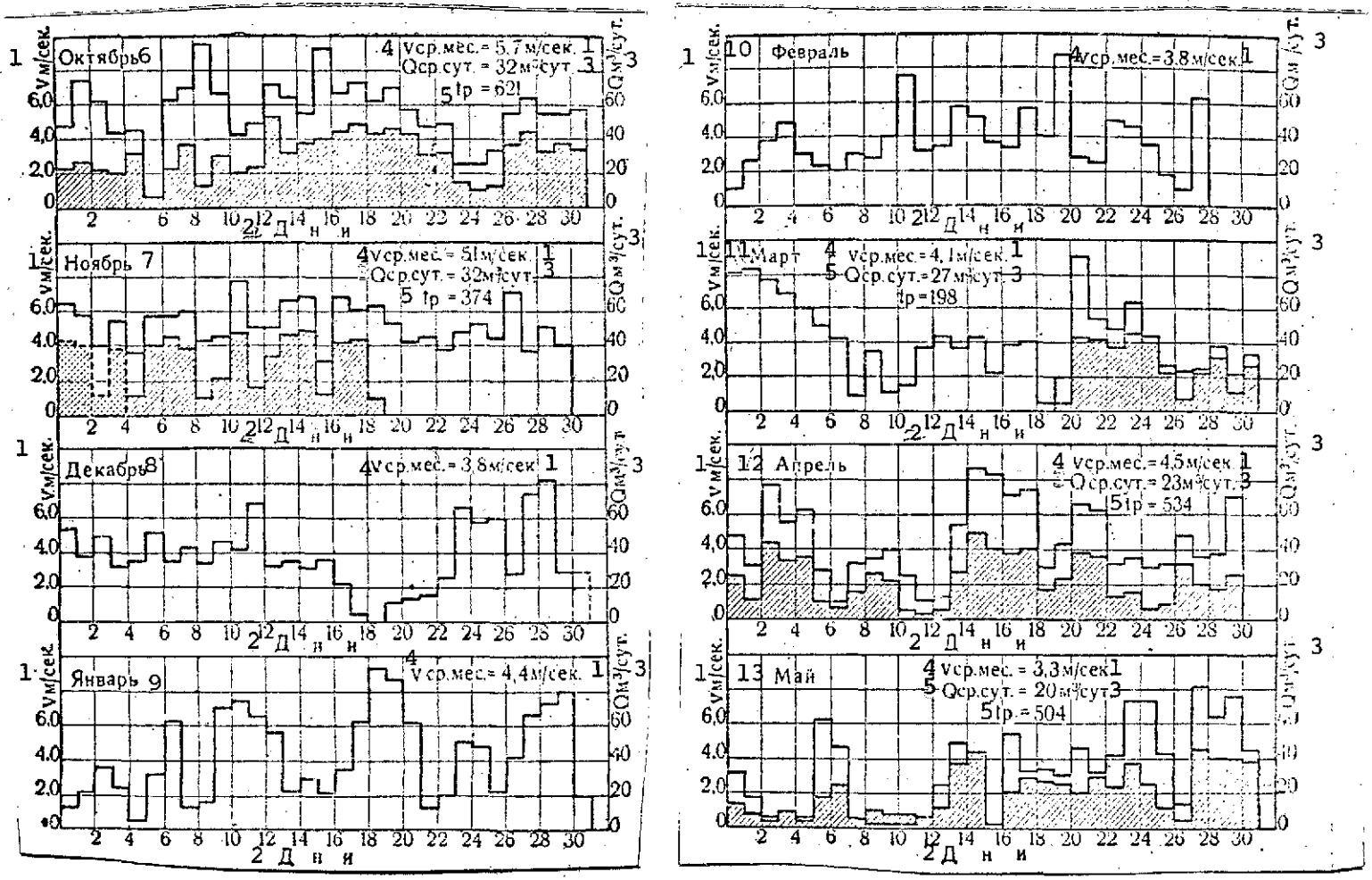

Fig. 269: Graph of the annual operation of the TV-5 wind pump installation shown in Fig. 268.

Key: 1. m/sec 2. days 3. m^3/day 4. average monthly 5. average daily
6. October 7. November 8. December 9. January 10. February
11. March 12. April 13. May

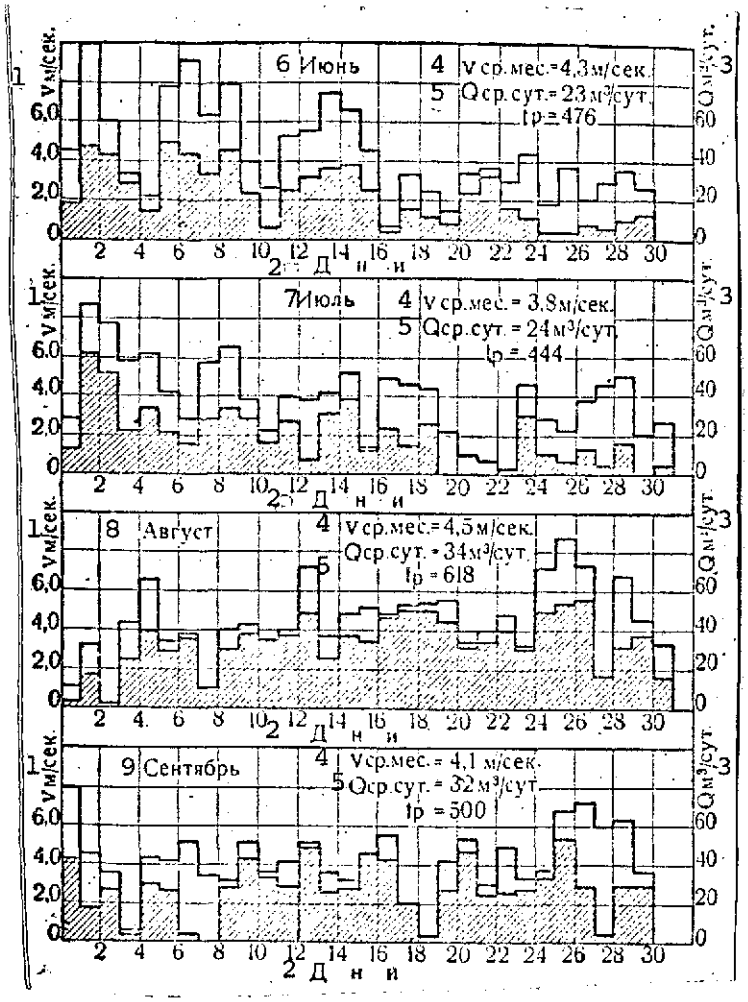

Fig. 269: Graph of the annual operation of the TV-5 wind pump installation shown in Fig. 268 (continuation).

Key: 1. m/sec
2. days
3. m^3/day
4. average monthly
5. average daily
6. June
7. July
8. August
9. September

The average daily output of this wind installation amounted to approximately 30 m^3 at an average monthly wind velocity of 5 m/sec. The work of two horses connected to a horse-drawn actuator amounted to approximately 7.5% of the time of the annual number of work hours of the wind engine; the output coefficient of the wind installation amounted to 73%.

Wind pump installations are sometimes used in agriculture for the transfer of fuel by pumping.

For example, one of the agricultural machine stations in the Stalingrad region has a wind pump installation with a TV-5 wind engine for the transfer of fuel by pumping into storage tanks (Fig. 270). The husbandry needs approximately 1000 tons of fuel while the wind engine can transfer up to 15000 tons per year. In spite of this small loading of the wind engine, it is nevertheless convenient for the husbandry to exploit this installation. In addition, the wind installation presents no fire hazard.

Wind pump installations are also used for production purposes in local industries. For example, in one of the brick factories in the Kiev region, there is a wind pump installation for the feeding of water for clay mixing. The overall amount of water consumed per day is 14 m^3. The TV-5 wind engine with a 30 m^3 tank can cover the water supply of the industry almost completely. /436

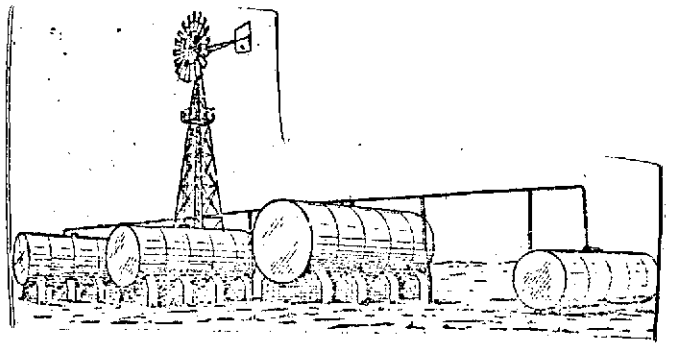

Fig. 270: TV-5 wind installation for fuel transfer by pumping.

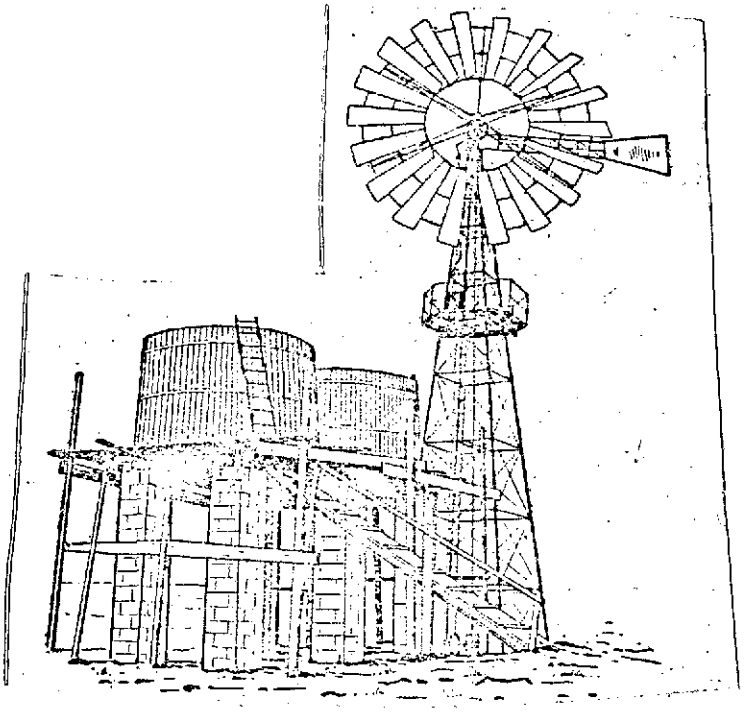

Fig. 271: The TV-8 wind pump installation in a kolkhoz of the Chesmenskiy region, Chelyabinskaya province.

The TV-8 wind engine is used for supplying large amounts of water from wells with a high output to the kolkhozes. Fig. 271 shows a wind pump installation type TV-8, set up in a kolkhoz in the Chesmenskiy region, Chelyabinskaya province. This wind installation lifts the water by means of a d = 5 3/4", h = 450 mm rotary pump from a well with an output of 11 m^3/hr into two 28 m^3 wooden tanks. These tanks are mounted on fixed iron concrete columns with a height of 4 m and have a skeleton frame cabin with heated walls (when the picture was taken, the cabin was not yet ready, therefore it does not appear in the figure). This wind installation supplies with water a kolkhoz with 63 cattle yards, which has 353 head of large cattle, 98 head of young stock, 163 head of pigs, 8-9 head of /437 sheep and 77 horses. The total amount of water consumed per day amounts to about 55 m^3. The TV-8 wind pump installation satisfies entirely the required water consumption; with an actual head of 17 m, it feeds the following amounts of water:

1. at wind velocities of....

3	4	5	6

2. output in m^3/hour.....

4	6.5	9.18	12.5

56. Wind-Driven Irrigation Installations

Depending on the nature of the water source, the disposition of the irrigated area with respect to these sources, the climatic and soil conditions as well as the agricultural works and the economic possibilities, the following types of water management can be distinguished [14].

I. Constant irrigation from rivers, storage lakes or ground water by gravitation or mechanically.

II. Periodic irrigation (high water) performed by means of irrigation channels (in the period of high water in the river) and by liman water by holding back the spring waters.

III. Wetting works, i.e. the retention and utilization on the spot of atmospheric precipitations.

IV. Irrigation of the terrain by the construction of storage lakes (ponds) to be used for domestic needs and for irrigation.

The permanent irrigation management can be divided into two main systems depending on the location of the irrigated area with regard to the water source; by gravity and mechanical.

The gravitational system can be set up in the vicinity of rivers whereby the water is collected into a main irrigation channel which is tracked at a certain inclination so as to promote gravitational feeding of the water to the lands situated between the channel and the river.

The irrigation system in which the lifting of the water to the land to be irrigated is performed by means of pump installations is called mechanical irrigation system. This system makes it possible to adjust to the complex topographical conditions and to utilize the ground water which is extremely important in the steppe regions /438
which are removed from rivers, and where the only water source are wells and pits.

The utilization of wind engines for irrigation has not yet received full development, nevertheless wind engines may play a very important role in this matter.

It cannot be stated that wind engines will be widely utilized for the irrigation of agriculture, since many cultures require regular watering schedules and a certain magnitude of hydromodules which wind engines cannot supply due to the inconstancy of wind energy. The construction of tanks for storing the water to be used on calm days requires great investments. Therefore, in the present state of wind technology, wind engines should be recommended for the irrigation of cultures which do not have a rigorous watering schedule. Small plots of 10-25 hectares as well as gardens are most suitable for irrigation by means of wind engines. Such plots can be irrigated from rivers and open resevoirs as well as from wells and pits if the output of the latter corresponds to the required amount of water for irrigation.

The water expenditure for irrigation in various regions and for various cultures is determined on the basis of existent agrotechnological standards. The amount of water in m^3 which is

required for the irrigation of one hectare of a given culture per season is called standard irrigation requirement. The magnitude of this requirement changes depending on the region and the irrigated culture. For example, in the Ukrainean-Crimean regions, the net standard irrigation requirement for wheat amounts to 2500 m^3 per hectare, while for Central Asia and Southern Kazakhstan, it amounts to 4200 m^3 per hectare. The net standard irrigation requirement for vegetables in the same regions is 3000 and 5000 m^3 per hectare, respectively.

The standard irrigation requirement is fulfilled in several stages at the determined time of watering.

The amount of water in m^3 per hectare in one watering is called irrigation rate.

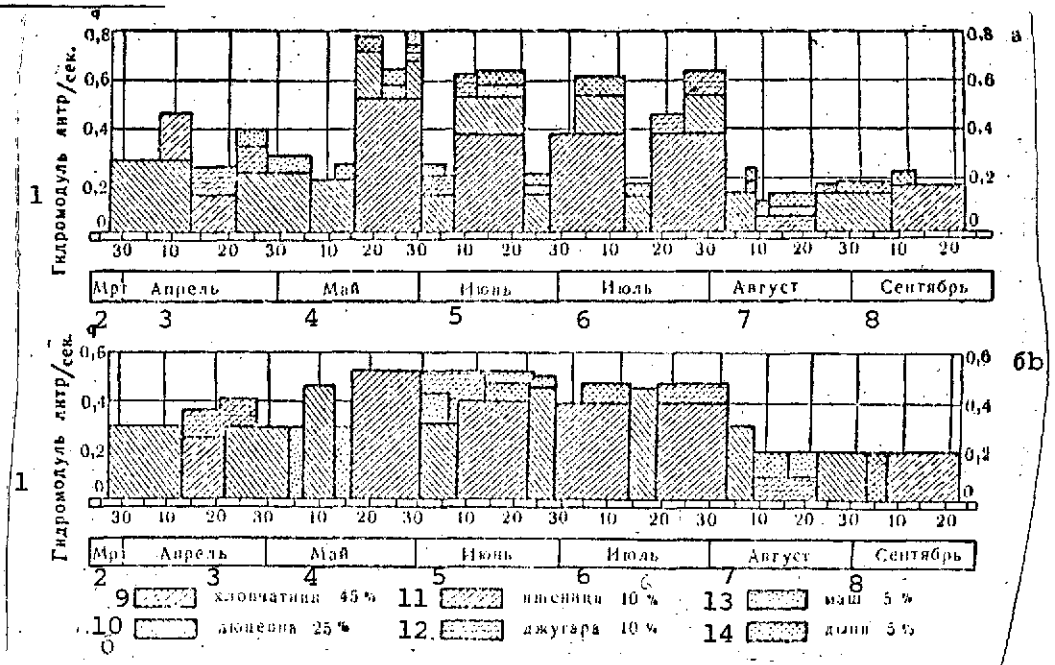

Fig. 272: Graphs of hydromodules: a-nonfitted; b-fitted.

Key: 1. hydromodule, liter/sec
2. March
3. April
4. May
5. June
6. July
7. August
8. September
9. cotton
10. alfalfa
11. wheat
12. sorghum
13. green gram
14. cantaloupe

The magnitude of the irrigation rate is variable and depends on many factors such as climate, soil, natural classifications, cultures, etc. For example, in Crimea, the irrigation rate for clay and loamy soils amounts to 400-600 m^3 per hectare, while it is 300-400 m^3 per hectare of alkaline clay soil. The irrigation rate for

tomatoes equals 300-500 m^3 per hectare, while for potatoes it is 400- /440
600 m^3 per hectare.

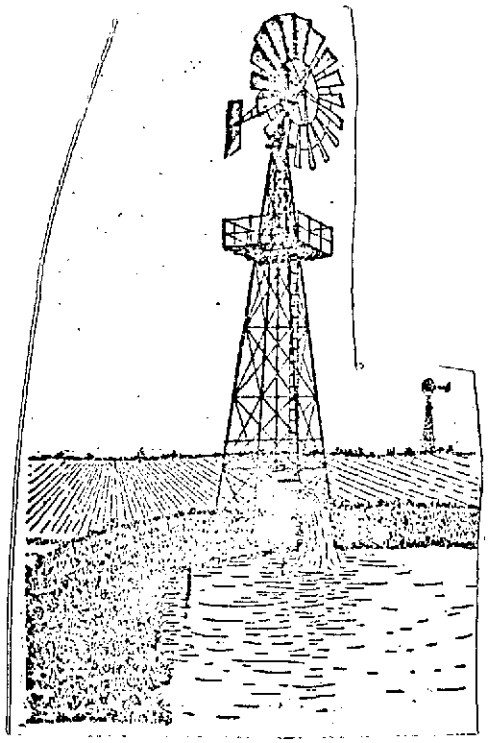

Fig. 273: Low-power wind-driven irrigation installation.

The water expenditure per second, obtained by dividing the irrigation rate by the duration of watering in seconds is called the watering module. Multiplying this magnitude by the composition of the given culture in the crop rotation in per cent, we obtain the irrigation module or hydromodule of the given culture.

The hydromodule for a complex of irrigated cultures is represented graphically in Fig. 272. The water expenditure per second in simultaneous time intervals is laid out on the ordinate, while on the abscissa the time of watering is indicated; as a result, a preliminary watering graph is obtained. Since the peaks of water expenditure on the preliminary graph are not suitable for loading the net of channels and of the pump station (see upper graph a), this graph is fitted i.e. it is leveled by eliminating as far as possible the peaks and dips of water expenditures. As a result, a more uniform hydromodule graph is obtained, as shown in Fig. 272. This graph shows in addition to the time schedule which should be observed in watering, also the characteristics of loading of the pump station. In determining the power of the station, this graph /441 should be used as a guide.

In determining the overall power of a wind-driven pump installation, the power should be distributed among the separate irrigated plots taking in consideration the location and relief of each plot. The availability of wind engines produced by our industries should guide the selection of a certain type of wind engine.

The VIME D-12 rapid wind engine with a power of 14 hp and the VIME-GUSMP-D-18 are most suitable for irrigation purposes of all the existent types of wind engines for operating at a wind velocity of 8 m/sec. These types can be adjusted for operating with centrifugal pumps of any system.

The TV-8 wind engine is most suitable for the irrigation of small land plots up to 5 hectares; this wind engine can set in motion

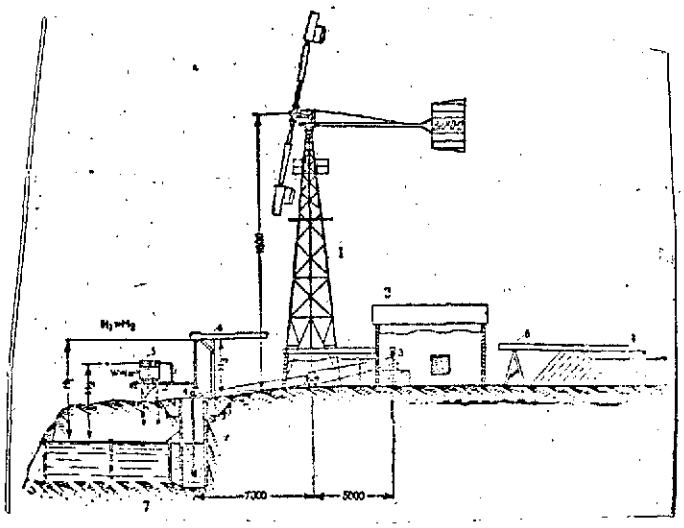

Fig. 274: Construction diagram of a wind-driven irrigation installation with the VIME D-12 wind engine: 1-wind engine; 2-mill; 3-grinding mill "No. 2 Farmer"; 4-centrifugal pump; 5-construction for automatic priming of the pump; 6-trough for transfer of the water to the waterbed; 7-intake; 8-waterbed.

at the same time a rotary and a centrifugal pump. The presence of the rotary pump ensures priming of the centrifugal pump without any additional accessories. /442

Fig. 273 shows a low-power wind-driven irrigation installation with a power of 2-3 hp which lifts the water to the waterbed, whence it is distributed to the plot. Similar wind installations operate with rotary pumps and collect the water from wells.

Such wind installations were used in the southern regions of the USSR for irrigating gardens. They are found in large numbers in the United States.

One of the structures of the wind-driven pump installation is a basin for storing the water, with pipes which transfer the water to the plot.

The construction diagram of a wind-driven irrigation installation with a D-12 wind engine which feeds water from an open waterbed to a trough through which it is transferred by gravitation to a basin situated at a higher point of the irrigated plot is shown in Fig. 274.

An open trough made of planks for feeding water by gravitation is a cheap construction but suffers from great shortcomings. As a result of the intermittent character of the operation, the planks of the trough dry out and slits are formed in the joints between them through which the water leaves the trough so that the latter works with large losses.

Sometimes a wooden pipe or a galvanized iron pipe is added for delivering the water from the basin.

The basin for water storage is a no less complicated matter in irrigation. The capacity of the basin as well as the power of the wind engine should be extremely high if they are to cover fully the water supply on calm days, according to the computations presented in Section 53 [see equation (308)].

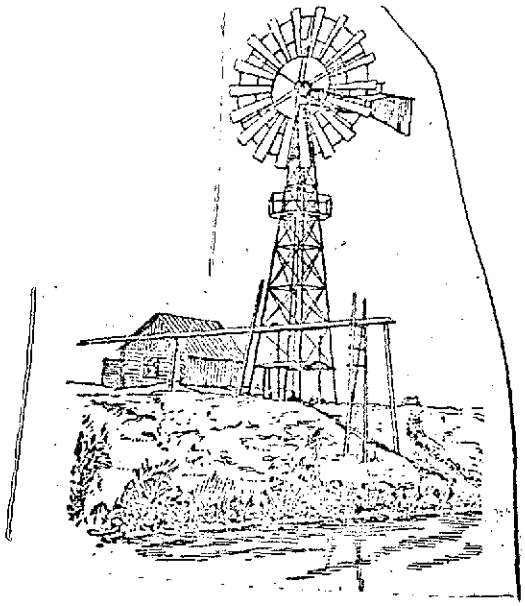

Fig. 275: The TV-8 wind-driven irrigation installation in the Saratov region.

The capacity of the storage lake is large even in the case that it is calculated per one watering, by multiplying the irrigation rate by the number of hectares of the irrigated plot.

The main drawback of open storage lakes is in addition to infiltration of the water into the ground, the large volatility which averages from 500-1000 mm of the thickness of the water surface per season, depending on the climate.

These losses can be diminished if the storage lake is protected from the wind by means of some plantations. However, it is not recommended to plant trees on the barrage forming the wall of the storage lake, since the roots of the trees can weaken the ground and increase the losses due to seepage of the water. /443

The experience of utilizing wind engines for irrigation in the USSR has been obtained from garden and vegetable cultures on small plots only.

For this purpose, a well is dug on an area which rises above the plot of the garden or vegetable garden; a multi-bladed wind engine is set up above the well and a waterbed is built next to it.

The water moves in the wind engine as long as the wind has a sufficient velocity, and stops only for examination and maintenance of the wind installation. In such a manner, the wind engine can store water long before the beginning of the irrigation season.

Fig. 275 shows a TV-8 wind-driven irrigation installation built in the "Proletarskaya volya" kolkhoz in the Saratov region. The wind engine works with a rotary pump d = 4" and a piston pump d = 5 3/4", which works alone when the wind is weak, and together with the centrifugal pump, in strong winds. The river water is fed into a wooden trough from which it goes by gravitation to a 10 hectare plot of the garden to be irrigated. When the wind installation feeds water for irrigation, the wind engine works with a stone mill with a diameter of 8-10 mm (Fig. 276). /444

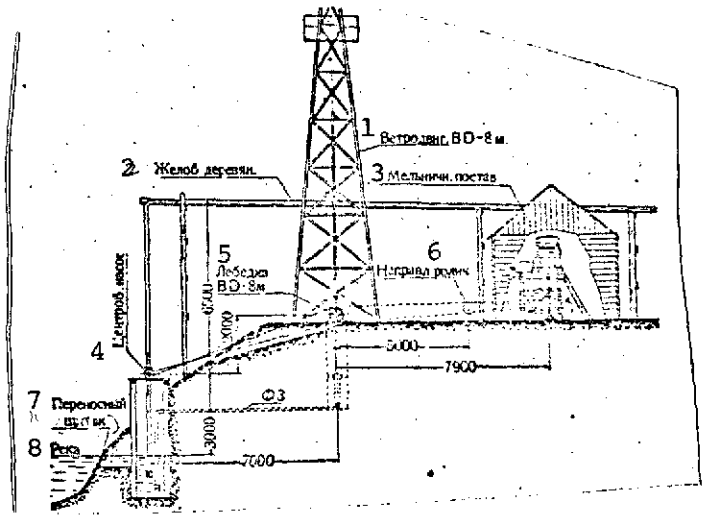

Fig. 276: Construction diagram of the wind installation shown in Fig. 275.

Key: 1. VD-8 m wind engine
2. wooden trough
3. grinding mill
4. centrifugal pump
5. VD-8 m winch
6. guide rods
7. movable gate
8. river

Worth mentioning is the experiment of irrigation of vegetable cultures performed in the Gur'yev region along the river Ural where more than 800 homemade wind-driven irrigation installations were set up. Low-power homemade wind engines guide the water from the river by means of rotary pumps directly to the irrigated plots.

57. Types of Windmills

Wooden wind installations which are homemade and operate with one or two stone mills are called windmills.

There are two main types of windmills: goatskin and tent-shaped.

The goatskin windmill (Fig. 277) has the following constructional features.

1. The building of the mill with the milling equipment is freely supported by its lower girders on a foundation with a stanchion in the center. The mill can be rotated about this stanchion when the wind wheel has to be adjusted to the wind or when it has to be removed from the wind. In some old small windmills, the foundation was made in the shape of a goatskin or of tilted stools between which the stanchion was fitted. Hence the name goatskin windmill.
2. The rotation of the wind wheel is transmitted to the stone mill through a simple transmission. The main cam-operated wheel of the main shaft is connected to a pinion which fits directly on the shaft of the stone mill.
3. During adjustment of the wind wheel to the wind, the whole building of the mill with the milling equipment is turned, which requires a large muscular effort during rotation of the mill to the wind or its removal from the wind.
4. The building of the mill, which is freely supported on the foundation is unstable and this hinders lifting of the wings to a larger height and the increase of their span.

The virtue of goatskin windmills is the simplicity of their construction. Very few metallic details are required in one transmission from the wind wheel to the stone mill; there is no vertical shaft and therefore the construction of such mills can be performed by the kolkhoznics themselves. /446

The main drawback in the construction of goatskin windmills is the requirement for rotating the entire building of the windmill together with the equipment during the adjustment of the wings to the wind. The following shortcomings and inconveniences of this construction result from the above facts. /447

1. Large expenditure of effort in rotating the windmill to the wind.
2. When the wind wheel is adjusted to the wind, with simultaneous rotation of the building together with the whole system of transmission, the fine adjustment of the various part of the windmill is disturbed and so are the supports of the stone mill.
3. Limitation of the height at which the shaft of the wind wheel is situated, since with increase of this height, the entire

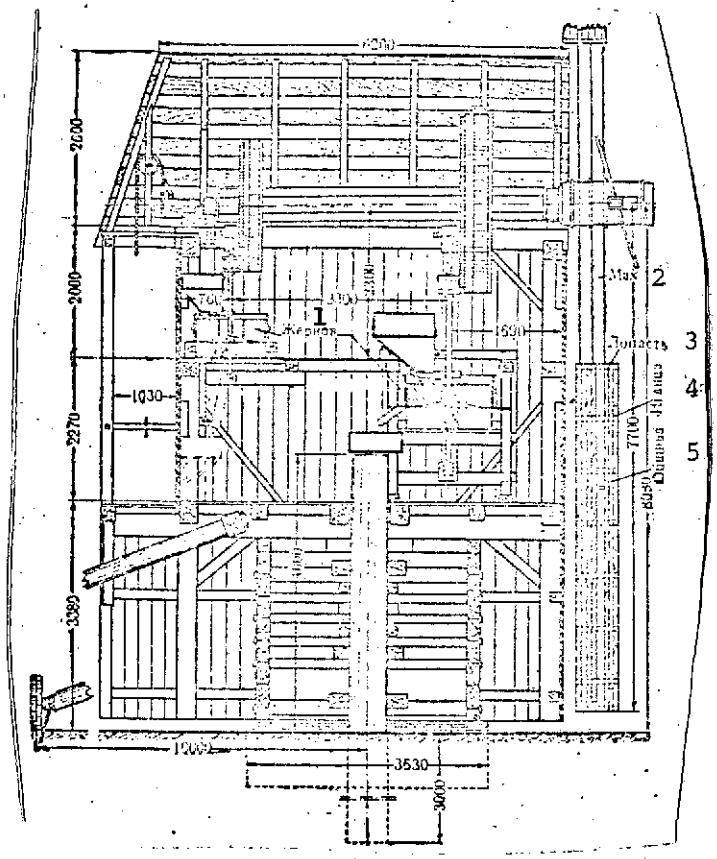

Fig. 277: Section through a goatskin windmill.

Key: 1. stone mill
2. flap
3. vane
4. fastening post
5. casing

building has to be made taller which diminishes its stability. The diameters of the wind wheels of this mill are therefore made not larger than 15 m.

4. Due to its constructional design, the goatskin windmill cannot be made with open walls which would allow free flow of the wind.

The tent-shaped windmill (Fig. 278) usually has a 8-side tower which is covered on the outside with a 1/2 inch board. All the milling equipment is placed inside this tower. The tower ends upward in a rim on which a frame made of thick bark is freely supported. The shaft of the wind wheel with the bearings is mounted on the frame and the rafters of the roof are fastened; the latter are built in the shape of a tent hence the name of the tent-shaped windmill. The tent can be rotated during the adjustment of the wind wheel to the wind or during its removal from the wind.

The construction of the tent-shaped windmill has the following characteristics.

1. The tent is lighter than the body of the goatskin windmill, therefore less effort is required in rotating the tent during adjustment of the wind wheel to the wind than in the case of the goatskin windmills.

2. The tower of the tent-shaped windmill permits the lifting of the wind wheel to a large height.

3. The rotation of the stone mill in most tent-shaped windmills is accomplished by a two-stage transmission.

58. Technical Characteristics of Windmills

Tent-shaped windmills are much more sophisticated than the goatskin windmills from the standpoint of construction. Due to this

fact, it is easier to rotate the tent than the whole building of the /449
windmill, especially if the tent is placed on rolls; tent-shaped windmills can be automatized with regard to adjustment of the wind wheel to the wind by means of a tail or by means of windroses and other devices. In addition, the wind wheel in these windmills can be raised to a large height due merely to a tower constructed in the shape of a girder, which is not feasible in the goatskin windmill. This makes it possible to leave the tower of tent-shaped windmills open, and close only the building below where the milling equipment is mounted. However, the fact that an open tower is less durable should be taken in consideration. Therefore, the wood should be protected from premature destruction by covering it with iron sheets, with a roofing, etc. If no covering is made, it is advisable to putty in and paint those parts which are exposed to the effect of atmospheric precipitations.

Tent-shaped windmills differ merely by the method of rotating the tent and by the disposition of the windmill.

In some of the simpler windmills, rotation of the tent is performed manually by means of a so-called lead. Usually, the tent in such windmills glides during its rotation on wooden bars; the tower undergoes the longest trip. The torque which surmounts the resistance caused by friction in the support of the tent loosens the joints of the tower, twists the supports, etc.

An improved windmill is one in which the tent has a rail supported on rolls or, contrarily, rolls which are supported on rails; the rotation is performed by transmission with 2-3 pairs of pinions. This transmission is rotated either manually or as in the windmill shown in Fig. 278, by windroses mounted on brackets behind the tent, (Fig. 279).

The windroses which are usually used only for adjusting the wind wheel to the wind, are suitable only for windmills which have either sail wings or wings with folds which make it possible to reduce their working surfaces or finally, wings with vanes which are adjusted edge-on to the wind.

If the wind wheel is built with rigidly fastened vanes, it is advisable to rotate the tent manually, since in such a case it is possible to remove the wind wheel from the wind also when the windmill is not required to operate. However, in this case the windmill, being removed from the wind, should have its brake put on because when it stops, the wind may pass in front of the wind wheel which if not being slowed down, may overspeed. The wind load affects /450
badly the wind wheel, especially if it works in the absence of any wind and besides it is not desirable to have the windmill stop under the wind. Therefore, when the operation of the windmill is properly organized, the brakes are obviously used only under exceptional circumstances. Hence we see that in the given case, the manual

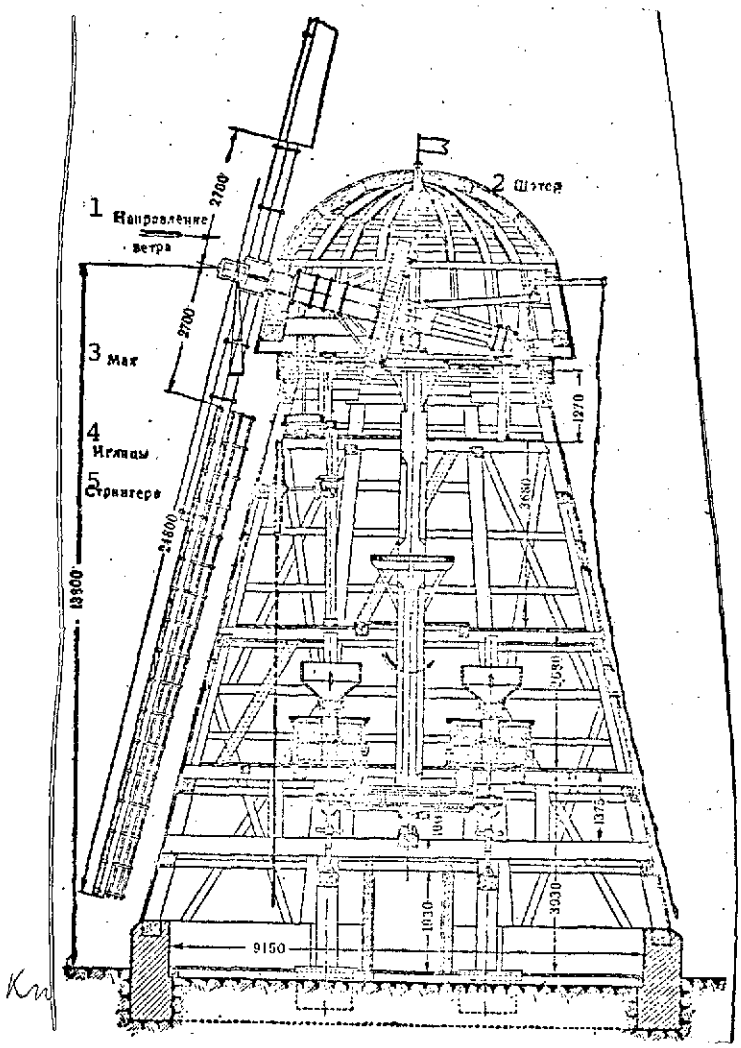

Fig. 278: Section through a tent-shaped windmill.

Key: 1. direction of the wind
2. tent
3. flap
4. fastening post
5. stringers

method makes it possible to regulate the work of the windmill better than the wind-roses which can only adjust the windmill to the wind. The wind wheel can be put into any position with regard to the wind by the manual method, which is convenient when the power of the windmill has to be regulated under strong winds.

Shortcomings of the wings of windmills. In the simplest windmills, the wings are made with a constant rigging angle of the vane, which has a magnitude of 14-15°. The output coefficient of the wind energy of such wings is approximately 1/1.5 of the value of wings with propeller blades. However it is much simpler to make wings with a constant rigging angle.

A certain shape of wings was selected not on the basis of theoretical considerations, but rather depending on the knowledgeability of the farmer who built the given windmill. /451

In some tent-shaped mills, the wings are made with a variable rigging angle; at the tip from 0-10° and at the base from 16-30°, i.e.:

at the external tip of the wing.....//.....10°
at a distance of 2/3 R..15°
at a distance of 1/3 R..20°
at the internal tip, about 1/5 R.....30°

where R is the length of the wing counting from the axis of the shaft up to the tip of the wing.

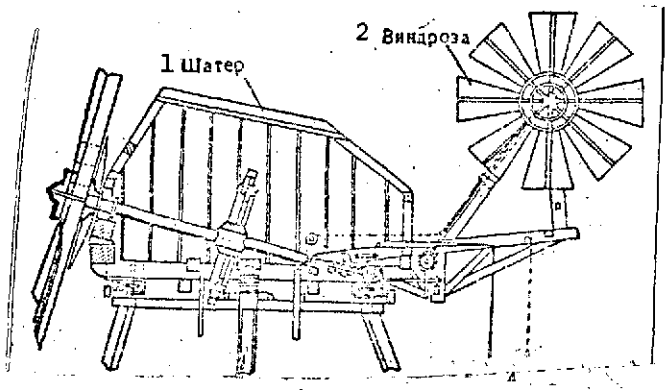

Fig. 279: Windroses for adjusting the windmill to the wind.

Key: 1. tent
2. windrose

The wings are the main part of a windmill. The better their condition, the higher the output of the mill if of course the other parts (stone mill, transmission) are also in good condition. However, one can often see wings in poor shape with cracks, coarse, closely fitted (1/2 in) boards on the planking of the wing, torn linen on the sail wings, etc. which decrease several times the lifting force of the wings and consequently, decrease to the same extent the output of the windmill. By merely bringing the shape of the wings in working windmills to the designed shape, the output could be considerably increased without any complicated constructional transformations. The output can be increased more than two fold by placing the wing with the right rigging angles of the blade transfer bars which are called fastening posts, forming a propeller blade. Wings with streamlined profiles and right rigging angles of the blades can increase the output 3-4 fold in accordance with the required rapidity.

59. Increasing the Power of Old Windmills

The power of existing old windmills can be increased by simple reconstruction of the wings. Testing of several operating windmills with measurements of the wind velocity, revolutions of the wind wheel and of the output showed that these work with a very low output coefficient, i.e. from 4-10%.

The results of tests performed with 3 windmills are presented in Table 40.

The main cause for the low output of existing windmills is the unsatisfactory condition of the wings. Proper maintenance of these wings or their replacements by new wings of a better shape could increase the output of old windmills more than 3 fold. /453

The results of tests with old windmills created the impetus for the task of reconstructing old windmills in order to increase their power.

TABLE 40. PERFORMANCE PARAMETERS OF OLD WINDMILLS

Parameter	Wind velocity (m/sec) 4	5	6	7	8	9	10	11	12
Goatskin windmill D = 15.4 m									
Output (kg/hr)	6.0	30	60	96	138	180	—	—	—
Revolutions of the wind wheel rpm	6	8	10	12	13	15	—	—	—
Revolutions of stone mill 8/4	50	74	90	108	122	135	—	—	—
Tent-shaped windmill D = 24.8 m with sail wings									
Output (kg/hr)	—	—	90	108	125	165	198	246	300
Revolutions of wind wheel rpm	—	—	5.6	6	6.4	7.0	8.2	8.8	9.8
Revolutions of stone mill 8/4	—	—	55	59	63	69	81	87	97
Wooden-metallic tent-shaped windmill D = 20 m									
Output (kg/hr)	72	108	150	192	246	300	—	—	—
Revolutions of wind wheel rpm	8	10.5	12.7	14	15	15.8	—	—	—
Revolutions of stone mill 6/4	45	58	70	78	83	88	—	—	—
Revolutions of stone mill 8/4	38	50	61	67	72	76	—	—	—

An experimental reconstruction of windmills was performed under /454
the author's supervision in 1941-1942 in the Chuvash ASSR; new wings of the simplest construction were elaborated at VIME, which were distinguished by low rapidity and relatively high output coefficient of the wind energy. Models of these wings were tested in the wind tunnel of VISKhOM and in the tower of TsAGI.

Fig. 280 illustrates the construction of wings with plane propeller blades, while Fig. 281 shows the construction of wings with semi-streamlined profile. The aerodynamic performance at rigging angles /455
of the blade tip $\pi = 0°$, $\pi = 10°$ and $\pi = 20°$ for semi-streamlined wings are presented in Fig. 282. Understandably, it is easy to make wings without coefficients of the wind energy between 0.35 and 0.40, but such wings would be distinguished by high rapidity and would have to be factory-made. The existing windmills are distinguished by low rapidity; their transmission with wooden teeth of the gear wheel and pin teeth of pinions is calculated for a rapidity of the wind wheel $Z_n = 2.0-2.5$.

The simplest new wings (Fig. 280 and 281) were mounted during the reconstruction of windmills, and forging of the stone mills was performed i.e. grooves were notched on the working surfaces according to Fig. 245, below. Tests were performed prior to and after reconstruction of these windmills, the results of which are presented in Table 41.

One can see from a comparison of the figures obtained during the testing prior to and after reconstruction that the output of existing windmills can be increased 2-3 fold when the old

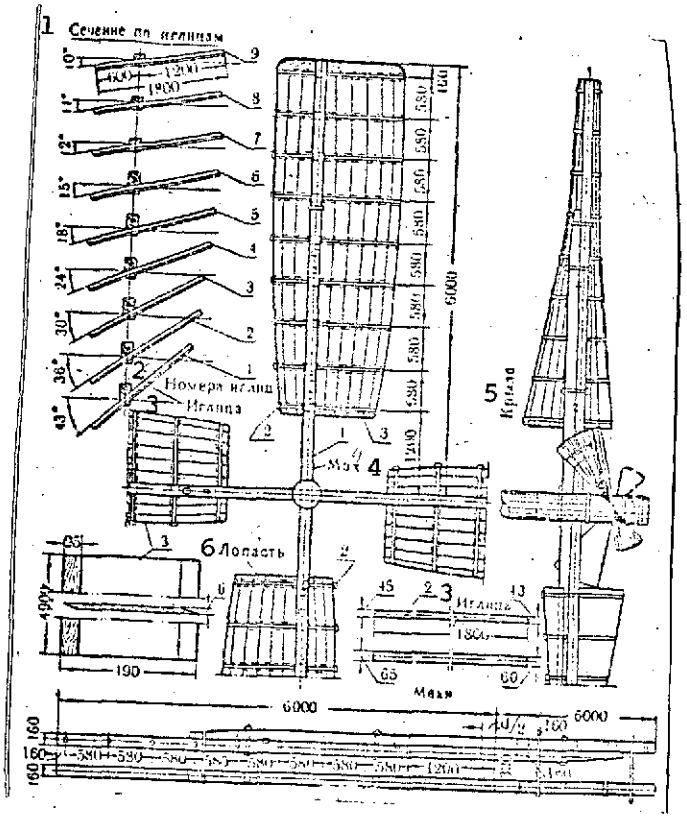

Fig. 280: Construction of wings with plane propeller blades.

Key: 1. section through fastening posts.
2. number of fastening posts
3. fastening posts
4. flap
5. wing
6. blade

wings are replaced by new wings which are as simple as the old ones but have the right shape of the blade.

60. The New Type of Windmill /456

Many kolkhozes take the initiative of constructing windmills on their own, which has a great economic importance.

The number of wind engines required by agriculture is so large that the industry cannot supply all the kolkhozes with factory-made wind engines within a short time. Therefore, the construction of windmills by the kolkhozes out of local materials may increase considerably the rate at which wind power is utilized.

VIME, under the author's supervision, designed the construction of simplified windmills of a new type VIME D-8, D-10 and D-12, in order to help in such a manner the kolkhozes. Simplification was achieved by eliminating the automatic devices on the basis of experience with exploitation of old windmills which were manually controlled. These windmills are made entirely of wood with the exception of fastenings, axis of the bush and rods (Fig. 283)

The wind wheel has four wings, where the blades have a semi-stream-/457 lined profile (Fig. 281). The wing flaps are fastened in lugs of the main shaft by means of wedges. A gear wheel is fastened on the main shaft behind the vertical axis and it is engaged with a lantern wheel pinion fitted on the vertical shaft. The main shaft makes an angle of 8° with the horizon, which is caused by the inclination of the legs of the tower. The head of the wind engine is built on the principle of tent-shaped windmills. The tent with a four-sided roof covers the upper transmission and protects it from atmospheric precipitations.

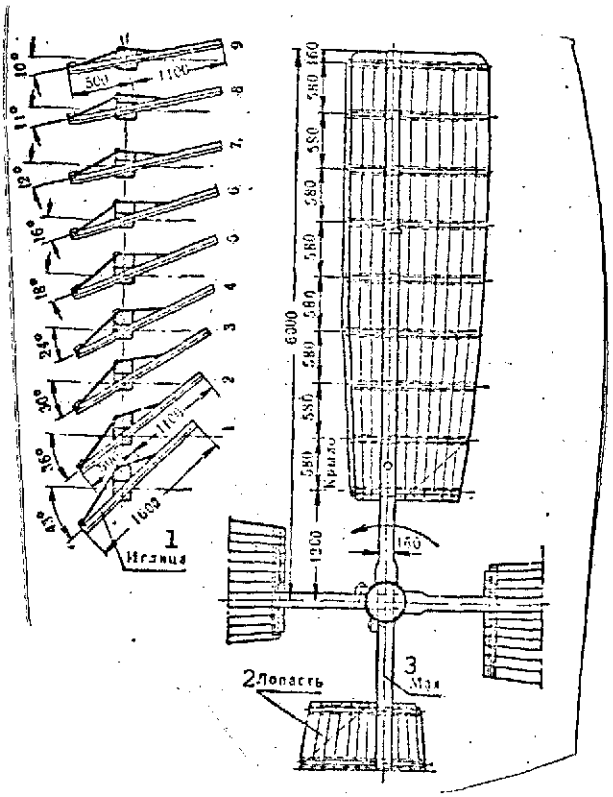

Fig. 281: Construction of wings with semi-streamlined profile.

Key: 1. fastening post
2. blade
3. flap

Transmission of the rotation from the vertical shaft to the stone mill is performed by means of a second pair of gear engagement, mounted below under the platform of the mill. The gear wheel fitted on the vertical shaft is engaged with the lantern wheel pinion of the stone mill.

The wind engine is started /458 by manual adjustment of the wind wheel to the wind. For this purpose, a lead is fastened behind the tent on bars of the supporting frame; the lead consists of three poles which are joined at the base of the tower into a unit and are suspended on bolts made of 3/4" iron bars.

Limitation of the number of revolutions of the wind wheel is performed by its removal from the wind; for this purpose, when there is a strong wind, the tent is rotated by means of the lead as long as the wind wheel performs the right number of revolutions.

The wind engine is mounted on a wooden tower of lattice construction with a height of 9.5 m. The tower is covered with a 1/2 in board below the plane of rotation of the wind wheel. In such a manner, all the milling equipment is placed in a closed building. A skeleton frame building with a four-sided roof and the tower of the /459 wind engine in the center of the building is constructed, when sufficient lumber is available.

For the sake of convenience in servicing the milling equipment, an annex is built in the front part of the skeleton frame which increases the area of servicing. These wind installations are intended for grinding the grain in kolkhozes. However, they can also be utilized for other types of work which requires low power such as preparation of fodder, grain cleaning, thrashing etc. Such windmills are built in the Ryazan, Kursk, Kiev and other regions of the USSR. The exploitation parameters of these windmills are presented in Section 61.

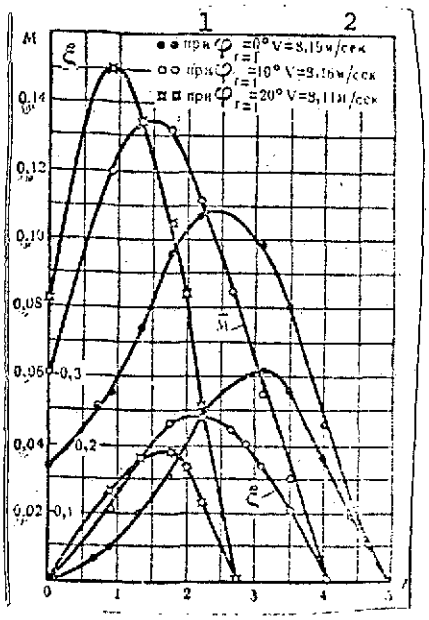

Fig. 282: Characteristics of wings with semi-streamlined profile.

Key: 1. at
2. m/sec

The VIME D-16 windmill (Fig. 284) is distinguished from the above described simplest windmill of VIME design by the fact that its power supplies two windmills. When the wind wheel is adjusted to the wind, the tent rotates by means of a transmission situated in the tower. The wings have a straight blade with semi-streamlined aerodynamic profile (Fig. 285) and are distinguished from the simple wing by the fact that the fastening post passes through the flap and the submast support forming a skeleton frame to which ribs are fastened by means of nails to the sides, forming the streamlined profile of the wing. The casing of the blade is made of a board with the thickness of 6 mm and a width of 100 mm which is nailed onto the ribs through a strip of galvanized iron, which encircles the blade opposite the ribs.

Attachment of the flaps to the shaft

TABLE 41. OUTPUT OF WINDMILLS BEFORE AND AFTER RECONSTRUCTION

Output (kg/hr)	Wind velocity (m/sec) 3	4	5	6
Windmill with D = 15.5 m wings				
With stone mill 6/4	did not work	30	40	65
Before construction	25	55	90	115
After construction				
With stone mill 6/4	did not work	20	76	120
Before construction	"	60	160	280
After construction				
Windmill with D = 12.5 m wings				
Before construction	did not work	–	30	55
After reconstruction with reforged stone mill	"	45	90	155

of the wind wheel is made by means of wedges just like in the simplest windmills.

The wings of this mill can also be made with a semi-streamlined/460 profile (Fig. 281) by forming a rigging angle at the tip of $\pi = 5\%$.

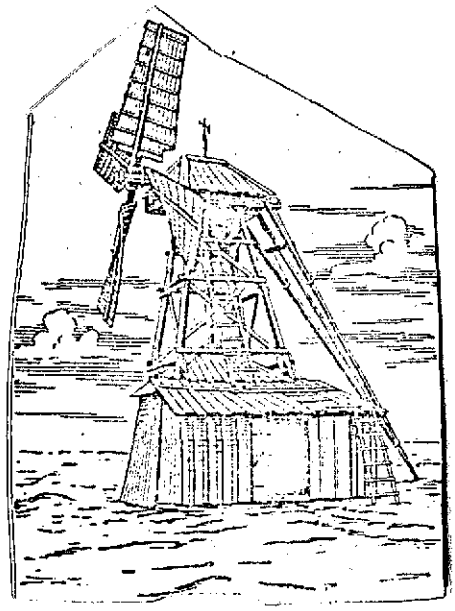

Fig. 283: Simplest windmill of VIME type.

Fig. 284 shows a general view of wings with a semi-streamlined profile.

Technical Characteristics of D-16 Windmill

Diameter of the wind wheel	16 m
Number of wings	4
Width of wings	2 m
Power on the shaft of the wind wheel at a wind velocity of 8 m/sec	25 hp
Coefficient of the wind energy	0.30
Rapidity	2.9
Number of revolutions of the wind wheel at V = 8 m/sec	26 rpm
Height of the tower	11 m

Construction of the main details for VIME D-16 windmill. A large number of windmills which have been built in the USSR have parts and details which are almost identical to the design. Any deviation from the generally convenient construction forms are usually caused by local circumstances such as availibility of materials, experience of the foreman, etc.

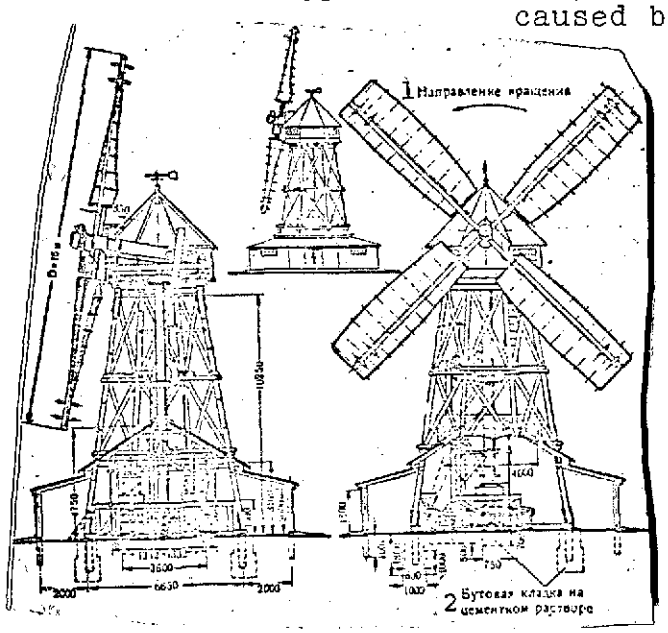

Fig. 284: The VIME D-16 windmill.

Key: 1. direction of rotation
2. rubble walling on cement mortar

In order to get acquainted with the construction of certain details of windmills, we present the description of the main parts for the VIME D-16 windmill which are representative of the construction of homemade and semi-homemade windmills.

The shaft of the windmill is /461 made entirely of wood (oak) with a diameter of 550 mm in the bulging butt. The front bearing is made of cast iron and has an oil pocket. From this pocket the oil is fed to the journal of the shaft by means of a small scoop which is fastened to t/462 the front side of journal (Fig. 286). It is more advisable to make the front bearing on a roller support as shown in Fig. 287. The ring attached to the shaft moves on two rollers fitted on the axis by means of two ball bearings each. The rear ball bearing is thrust radially and m mounted in a cast iron shell which is fastened to the frame by means of 4 bolts (Fig. 288).

The wheel and pinions are wooden of standard type like in the existing windmills (Fig. 289).

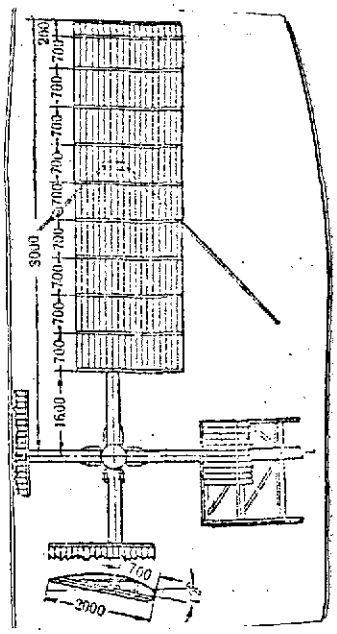

Fig. 285. Wings of the VIME D-16 windmill with streamlined profile.

The gear ratio of the upper couple equals 1:3 while that of the lower couple of pinions is 1 : 2.34. The overall gear ratio equals 1 : 7. In such a manner, at a wind velocity of 8 m/sec, the stone mill will make 182 revolutions per minute, which is quite normal for 6/4 stone mills as mounted here.

The tent (Fig. 290) is a large skeleton frame casing planked with a board. The stanchions of the skeleton lean on 8 angles which are suspended by 2 squares; the latter are made of bars and are shifted with respect with each other in the horizontal plane at an angle of 45° (Fig. 291). The frame of the tent lies above these squares; on it are mounted the bearings of the horizontal and vertical shaft while below, the rim of the tent is attached to the bars of the squares by means of bolts; the rim leans on the roller support attached to the rim of the tower.

The roller support of the tent consists of 16 horizontal roller supports and of 8 supports which /463 are made of both horizontal and lateral rolls (Fig. 292). Thesuch a manner, the vertical loads are perceived by 24 rolls while the lateral loads are perceived by 8 rolls. In such a system of supports, the moment required for rotating the tent amounts to about 1010 kgm.

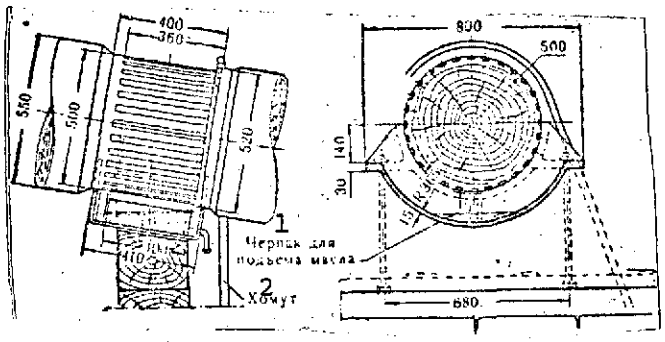

Fig. 286: Front bearing of the main shaft in a windmill.

Key: 1. scoop for lifting the oil
2. yoke

The mechanism of rotation of the tent is built in the following way (Fig. 293): the conical pulley 2 is attached to vertical shaft 1; the pulley is frictionally engaged with a similar pulley 3, fitted on horizontal shaft 4, which has conical pinion 5 at its other end.

This pinion is engaged with a large conical pinion 6 which is fitted on vertical shaft 7, the rotation of which through a couple /464 of cylindrical pinions 8 is transmitted to toothed rack 9, attached to the internal wall of the tent rim.

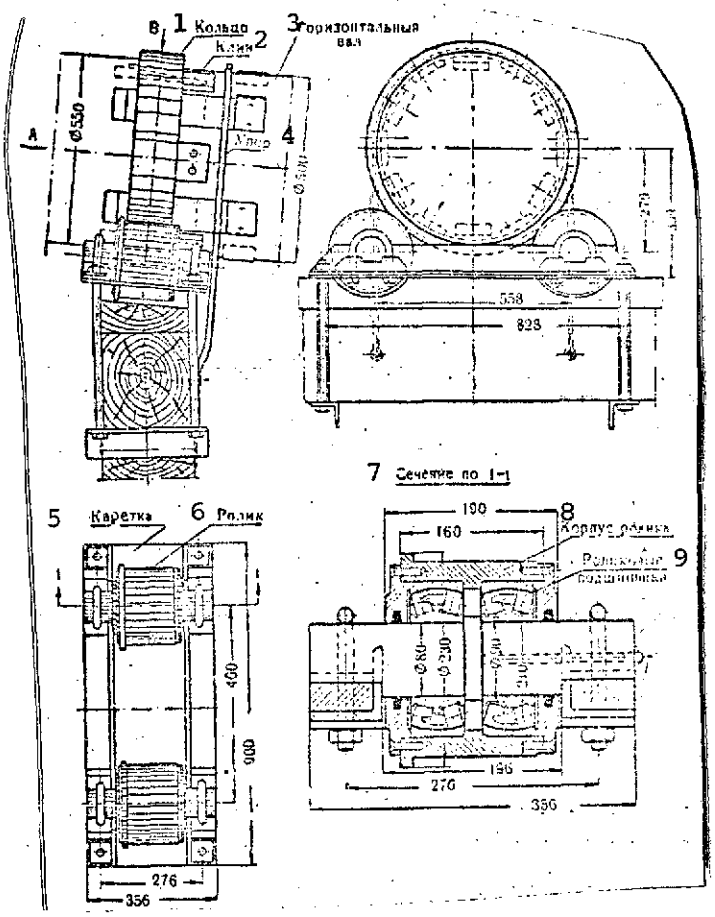

Fig. 287: Roller support of the front bearing on the main shaft.

Key: 1. ring
2. wedge
3. horizontal shaft
4. stop
5. carriage
6. roller
7. section along I-I
8. body of the roller
9. roller bearing

A special branch 10 mounted on the bush of the frictional pulley which is fitted to the horizontal shaft connects and disconnects the frictional pulleys. Cast iron pinions can be used instead of the frictional pulleys. In this case the transmission must be connected when the wind wheel is at standstill. When the wind wheel is adjusted to the wind, this mechanism is set in motion manually; for this purpose, a wooden wheel 11 which is rotated from below by means of cable 12, is fitted on the same horizontal shaft which carries the conical frictional pulley. This construction makes it possible for the wind wheel to remove itself from the wind, which protects it from breaking in storms. This mechanism is not characteristic and /465 is used here for the first time in windmills.

The experience of exploitation of the first D-16 windmill constructed with this mechanism in the village Kolonshchino, Kiev region, showed that the frictional transmission with wooden pulleys is acceptable when the tent rotates easily on rollers. In the opposite case the pulleys may slide through which may cause their ignition. It is better to replace the wooden pulleys by cast iron conical pinions with a gear ratio of 1 : 2 (small pinion on a vertical shaft). In this case, /466 the pinions must be connected when the wind engine is at rest.

The tower of the wind engine has 8 legs (Fig. 294), by means of which the following is achieved: 1. a high resistance to torque, due to the convenient disposition of the horizontal clamps and 2. a more convenient situation of the wings with regard to the legs of the tower, which makes it possible to decrease the distance

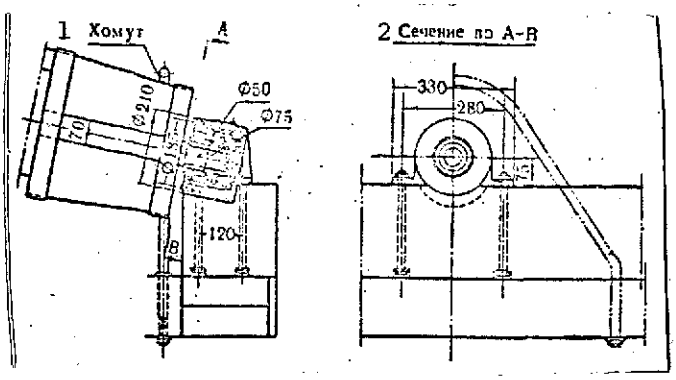

Fig. 288: Rear bearing of the main shaft.

Key: 1. yoke
2. section at the level A-B

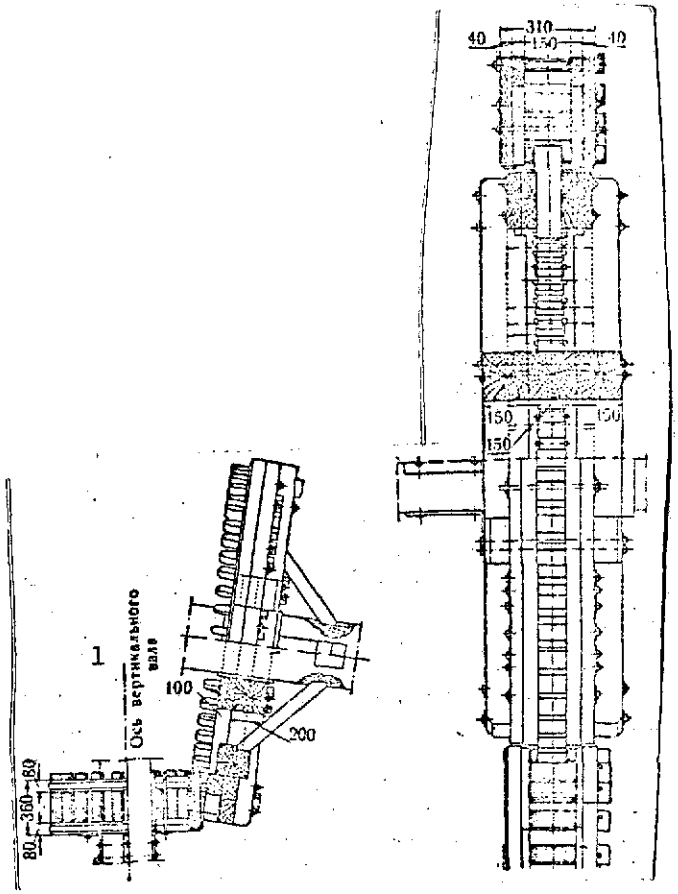

Fig. 289: Uppper and lower transmission of the windmill.

Key: 1. axis of the vertical shaft

between the support of the front bearing on the shaft and the axis of the flaps. Increasing this distance leads to increased load on the front bearing which is not desirable.

The UNDIM D-10 windmill. /467

The Ukrainian Institute for Agricultural Mechanization (UNDIM) built the D-10 windmill of wooden-metallic construction in 1945 according to S. B. Perli's project (Fig. 295). Regulation of the revolutions of the wind wheel is automatic and is performed by means of controlled flaps (according to a suggestion of B. B. Kazhinsky) which are built into the wings; the latter rotates with a large number of revolutions by the action of centrifugal loads, like the blade in the regulation system of V. S. Shamanin.

The windmill operates with a 6/4 stone mill.

The head of the wind engine is made of cast iron and the supports of the ball bearings on the main shaft as well as the upper conical transmission are mounted in it. The test of the first model of this mill gave satisfactory results and hence, the production of the first series of mills was started.

The TsAGI D-10 windmill.

This mill was built by TsAGI engineer M. G. Sorokin in 1945 in a kolkhoz of the Moscow region. /468 The wind wheel has a diameter of 10 m and has 3 wings with streamlined blades. The rear reduction gear of an automobile is used for transmission of the rotation from the wind wheel to the vertical shaft.

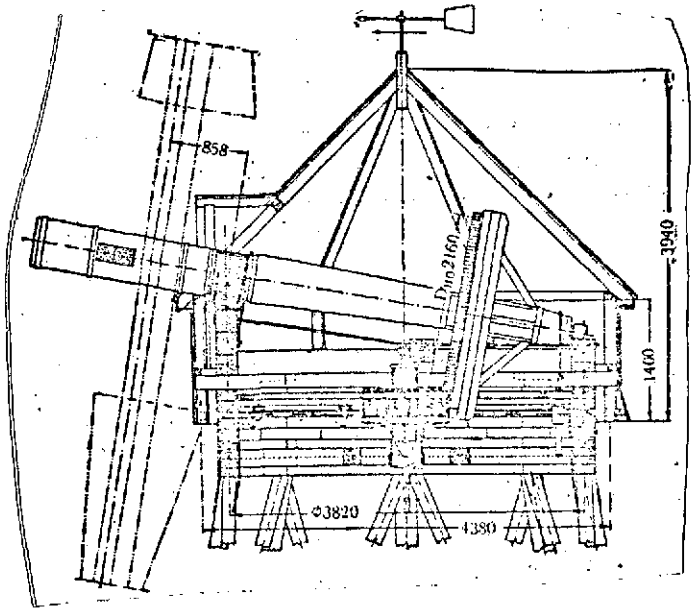

Fig. 290: Tent of a windmill

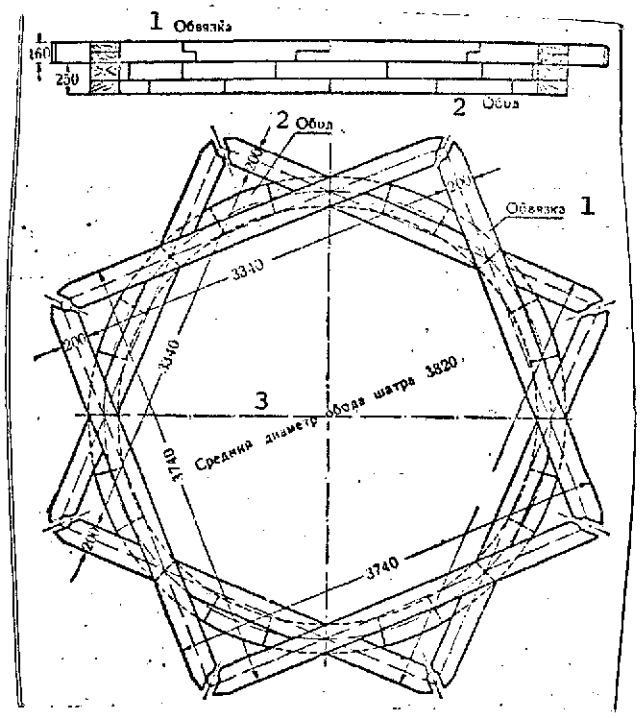

Fig. 291: Frame work and rim of the tent.

Key: 1. frame work
2. rim
3. average diameter of the tent rim.

This reducer is mounted on a small iron carbide girder, fastened to the support with balls which are placed on the ring of the upper corona of the tower. A lead made of two poles is situated behind the girder; this lead leans with its lower end on a rail which surrounds the building of the mill. The lead serves to rotate the head during the adjustment of the wind wheel to the wind or during its removal from the wind.

A pulley is fitted on the lower end of the vertical shaft; from it, a 6/4 stone mill is set in motion by means of a belt transmission.

An improved type of windmill. An experimental windmill of an improved type with the above described VIME D-16 wind engine was constructed in 1945 in the village Kolonshchino, Makarov region, Kiev province (Fig. 296).

The building of the wind-/469 mill is made of brick and has a cylindrical shape. The equipment is distributed on the three floors of the building. Two "No. 2 Farmers", a hulling mill, a separator and the first transmission are situated on the third floor; the second transmission and two revolving wings are situated on the second floor, while the outlet of the flour is situated on the first floor. The first floor also contains the transmission with a pulley situated outside the building for utilization of the windmill with other machines such as thrasher, etc.

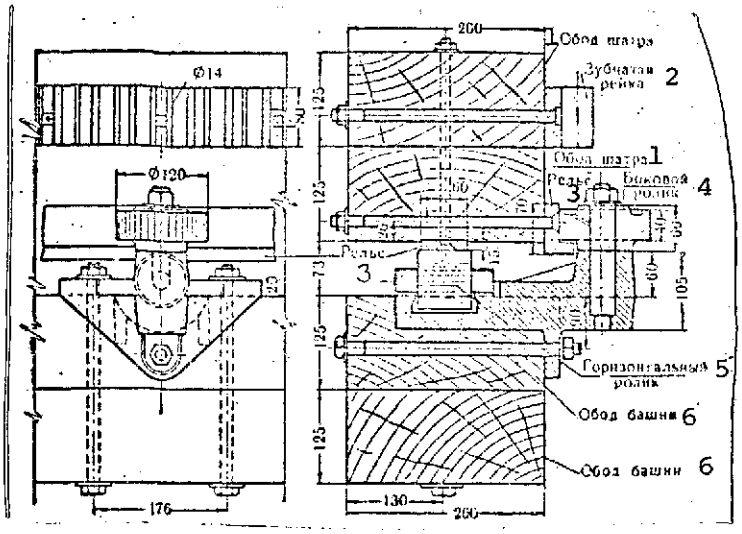

Fig. 292: Roller support of the tent of VIME D-16 windmill

Key: 1. rim of the tent
2. toothed rack
3. rail
4. lateral rolls
5. horizontal rolls
6. rim of the tower

saw, etc. A belt transmission going from the vertical shaft of the wind engine to the transmission and generator of an automobile type with storage battery are situated on the fourth floor. The electricity is consumed only for lighting of the mill building.

Lifting up the grain to the "Farmer" and to the hulling mill is performed by means of four drag conveyors.

The practice of exploitation showed that the "Farmers" which do not have regulating devices are less convenient in operating with the windmill/470 than the stone mills.

In order to limit the number of revolutions of the wind wheel and to protect it from over-speed, air brakes designed by the author are placed on two wings. These consist of 12 streamlined stub wings with an overall area of 2.25 m^2, fastened to axes with a diameter of 20 mm, which are directed downward through the flap. The axes rotate in the bearings under the action of the centrifugal forces of a flyweight and of a rod which are hinged with small levers attached to the axis of the surfaces. When the number of revolutions is a normal number, the brake areas go edge-on in the direction of rotation, while when the number of revolutions exceeds the normal number, the centrifugal forces of the flyweight and of the rod overcome the force of the primary tie-beam and rotate the surfaces with the plane in the direction of movement. A spring is fastened with one end to the rod connecting the brake surfaces and with the other end to the flap of the wing in the vicinity of the shaft (Fig. 297). The diameter of the spring is 140 mm, the diameter of the wire is 3 mm, while the number of loops is 115. The overall surface of the brakes develops a braking moment M_T which equals the excess moment of the wind wheel and can be determined by means of the following equation:

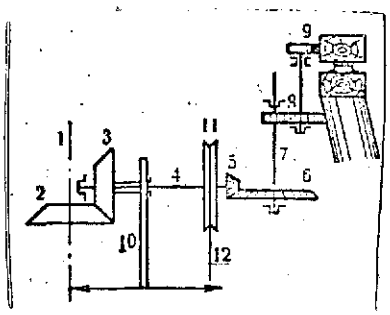

Fig. 293: Diagram of rotation of the tent by means of transmission.

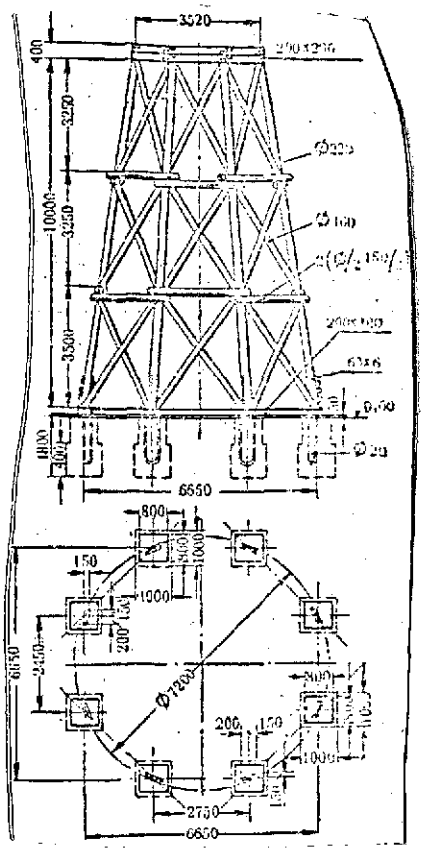

Fig. 294: 8-legged tower.

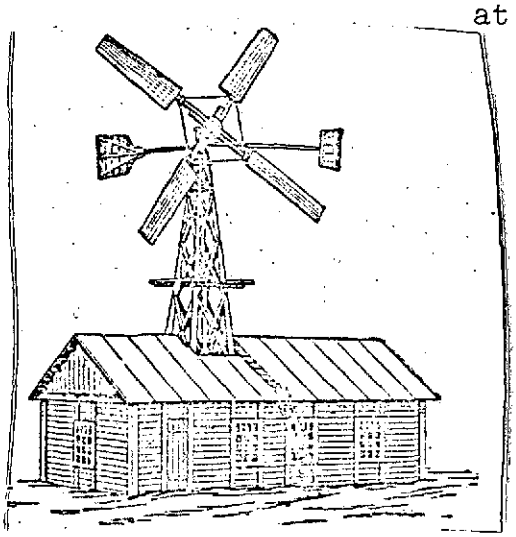

Fig. 295: The UNDIM D-10 windmill.

$$M_{\text{ф}} = \overline{M}\pi R^3 \frac{\rho V_2^2}{2} - \overline{M}\pi R^3 \frac{\rho V_1^2}{2} = \overline{M}\pi R^3 \frac{\rho (V_2^2 - V_1^2)}{2}. \quad \text{(a)}$$

/471

In addition:

$$M_{\text{ф}} = C_x S \frac{\rho W^2}{2} R_1. \quad \text{(b)}$$

The overall surface is obtained from equations (a) and (b):

$$S = \frac{\overline{M}\pi R^3 (V_2^2 - V_1^2)}{C_x W^2 R_1}, \quad (309)$$

where: V_1 is the velocity of the wind at which the number of revolutions of the wind wheel should be limited;

V_2 is the maximal velocity of the wind at which the windmill is supposed to operate up to its removal from the wind;

W is the relative velocity of the air flow which dashes over the stub wings of the aerial brake, situated on radius R_1:

$$W = \sqrt{\omega^2 R_1^2 + V_2^2};$$

C_x is the drag coefficient.

Substituting the value of W^2 in equation (309), we obtain:

$$S = \frac{\overline{M}\pi R^3 (V_2^2 - V_1^2)}{C_x R_1 (\omega^2 R_1^2 + V_2^2)}. \quad (309a)$$

Assuming that the maximal number of revolutions of the wind wheel is n = 32 rpm at a wind velocity V_2 = 12 m/sec, let us determine the overall area of the brakes S for the VIME D-16 windmill. We assume a wind velocity of 12 m/sec on the basis of the fact that when the wind has a higher velocity, the wind wheel must be removed from the wind at the angle γ at which the power of the wind wheel does not increase.

Subsequently let us assume that the angle suspended by the stub wings and the flow is $\alpha = 90°$, and $C_x = 1.28$.

For the wings VIME D-16, R_1 = 7 m and $\overline{M}$ = 0.1. The lowest wind velocity at which the number of revolutions has to be limited is V_1 = 8 m/sec. Substituting numerical values, we obtain:

$$S = \frac{0.10 \cdot 3.14 \cdot 8^3 (12^2 - 8^2)}{1.28 \cdot 7 \left[\left(\frac{3.14 \cdot 32}{30} \right)^2 \cdot 7^2 + 12^2 \right]} = \frac{12\,900}{6\,200} = 2.25 \text{ м}^2.$$

When 6 stub wings are mounted /472
on each of the two wings, the area of each equals:

$$S_1 = \frac{2.25}{12} = 0.188 \text{ м}^2.$$

When two pieces are mounted on /473
each of the four wings:

$$S_1 = \frac{2.25}{16} = 0.14 \text{ м}^2.$$

These brakes work entirely satisfactorily upon starting the windmill.

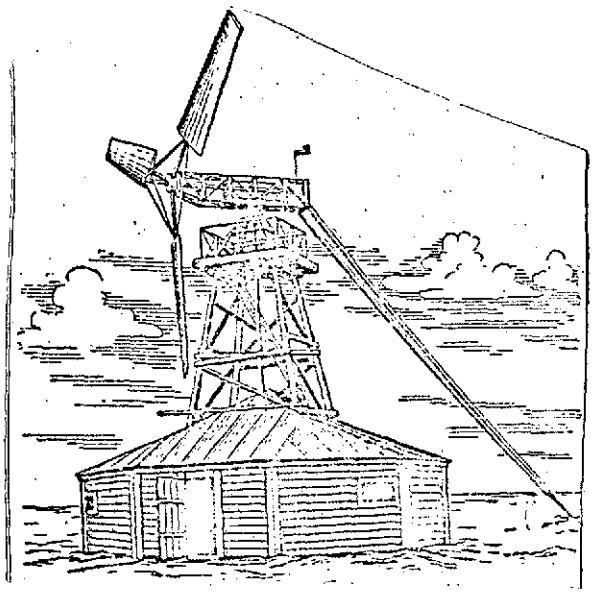

Fig. 295a: The TsAGI D-10 windmill.

61. Performance Characteristics of Windmills

In the exploitation of wind installations, it is imperative to strive for utilization of the working velocities of the wind throughout the year. The idle periods of a windmill in the presence of a wind lead to a decrease in the annual productivity and consequently increase the cost of milling. Hence, it follows that the exploitation of windmills should be organized in such a way that the latter should operate all the time when there is a wind.

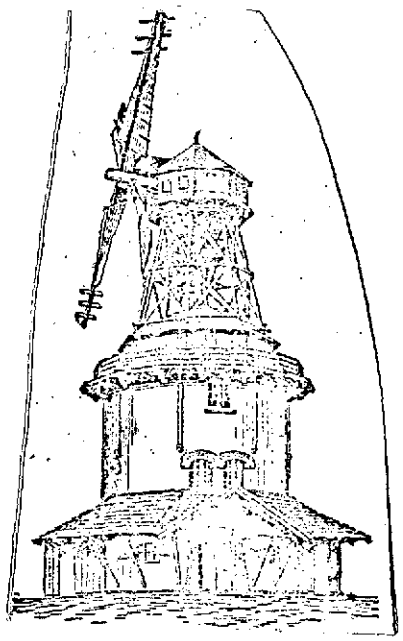

Fig. 296: An improved type of windmill of of the Promzernoproyekt with the VIME D-16 wind engine.

Table 42 presents computations of the power of VIME D-8, D-10, D-12 and D-16 windmills, as well as their output and number of revolutions depending on the velocity of the wind, while Table 43 presents the potential annual output of these mills depending on the average annual wind velocity.

The hours of the annual operations presented in Table 43 are given for:

1. the VIME D-8 windmill assuming that it starts working at a wind velocity of 4 m/sec;
2. for D-10, D-12 and D-16 wind engines, on the assumption that they start to work at a wind velocity of 3 m/sec.

The testing of windmills in operation was performed by VIME in various regions of the USSR.

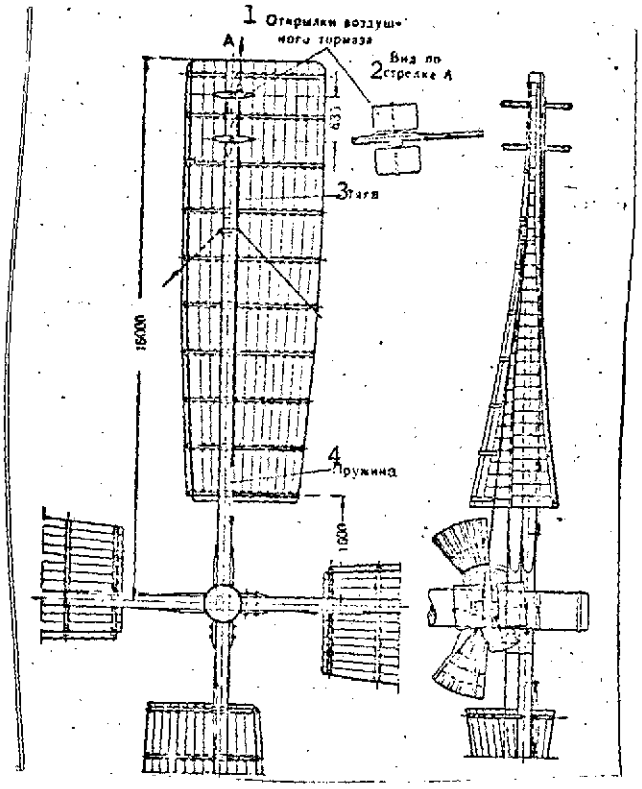

Fig. 297: Wings with aerial brakes of the windmill shown in Fig. 296.

Key: 1. stub wings of the aerial brake
2. view from arrow A
3. rod
4. spring

As an example let us present the results of short time tests performed in kolkhozes with windmills VIME D-8 and VIME D-10. The following measurements were performed during the tests, at the same time (by signaling):

V is the wind velocity which was measured every 2 minutes with an anemometer;

Q is the output which was measured every 2 minutes by weighing,

n is the number of revolutions of the wind wheel.

The data of these tests are presented in Table 44 and in graphs 298 and 299.

The calculated outputs of these /475
windmills were presented above, in Table 42.

The VIME D-10 windmill was tested in the beginning with a stone mill which had been running without forging and then with the same stone mill which had been newly forged. This was done in order to find out the effect of forging of the stone mill on increasing the output.

The graph in Fig. 299 shows that after forging, the stone mill increases considerably its output, while this increase is not noticeable at low wind velocities; at wind velocities above 5 m/sec, the curves are noticeably divergent, i.e. the output increases up to 50%.

The exploitation parameters of three windmills of VIME type, /477
obtained as a result of prolonged observations of their operation in kolkhozes of the Ryazan, are presented in Table 45.

According to Pomortsev's data on the occurrence of wind, the possible number of working hours at average monthly wind velocities of 3-4 m/sec should amount to 400-500 hours a month. Hence we obtain the actual and calculated (potential) coefficient of exploitation /478
(see Table 46).

TABLE 42. CALCULATED TECHNICAL CHARACTERISTICS OF WINDMILLS

Name of characteristic	Working wind velocity (m/sec) 3	4	5	6	7	8	9	10
Windmill VIME D-8								
Power on shaft of wheel (hp)	—	0.65	1.3	2.2	3.5	5.3	7.5	10.3
Revolutions of wind wheel rpm	—	21	27	32	38	40	45	50
Output (kg/hr)	—	20	40	70	100	130	180	230
Windmill VIME D-10								
Power on shaft of wheel (hp)	0.43	1.01	2.03	3.42	5.46	8.26	11.7	16.7
Revolutions of wind wheel rpm	13	17	22	26	30	32	38	43
Output (kg/hr)	13	30	60	108	150	175	218	310
Windmill VIME D-12								
Power on shaft of wheel (hp)	0.63	1.47	2.92	4.95	7.90	12.0	16.9	23.0
Revolutions of wind wheel rpm	10	14	18	21	25	28	32	36
Output (kg/hr)	19	45	90	158	220	270	360	520
Windmill VIME D-16								
Power on shaft of wheel (hp)	1.5	3.2	6.3	11.0	17.5	25.5	37	50
Revolutions of wind wheel rpm	10	13	17	20	23	26	29	33
Output (kg/hr)	32	76	144	264	420	615	880	1 200

TABLE 43. CALCULATED ANNUAL OUTPUT OF WINDMILLS

Type of Windmill	Diameter of wind wheel (m)	Annual average wind velocity 4 m/sec: Possible no. working hr/yr	4 m/sec: Annual Output (t)	5 m/sec: Possible no. working hr/yr	5 m/sec: Annual Output (t)	6 m/sec: Possible no. working hr/yr	6 m/sec: Annual output (t)
VIME D-8	8	5 310	185	6 522	290	7 325	408
VIME D-10	10	6 755	289	7 525	452	8 025	638
VIME D-12	12	6 755	416	7 525	649	8 025	909
VIME D-16	16	6 755	1 224	7 525	2 029	8 025	2 609

TABLE 44. ACTUAL OUTPUT OF VIME WINDMILLS (kg/hr) IN RELATION TO WIND VELOCITY

Type of Windmill	Wind velocity					
	4	5	6	7	8	9
VIME D-8	10	25	50	100	170	270
VIME D-10	26	50	95	155	—	—

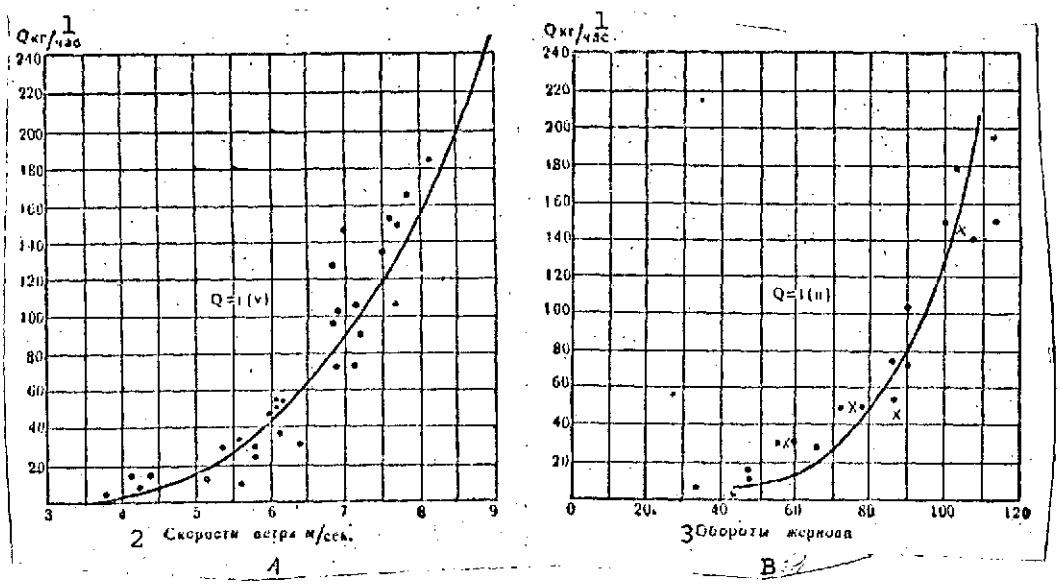

Fig. 298: Characteristic of the output in VIME D-8 windmill: A-output in relation to wind velocity; B-output in relation to the number of revolutions of the stone mill.

Key: 1. kg/hr
2. wind velocity m/sec
3. revolutions of the stone mill

TABLE 45

Type of Windmill	No. of working hrs/mo.	Average wind velocity (m/sec)	Milling per month (kg)	Average output per hour (kg/hr
VIME D-8	June—116	4.18	8 230	71
	July—58	3.30	3 707	64
VIME D-10	Oct. 15 to Nov. 15—82	3.70	4 467	55
VIME D-12	Oct. 15 to Nov. 15—127	4.28	7 875	62

TABLE 46

Type of Mill	Coefficient of exploitation	
	actual	Calculated (possible)
VIME D-8	0.161	0.70
VIME D-10	0.114	0.55
VIME D-12	0.176	0.70

TABLE 47. COMPARISON OF THE EXPLOITATION PARAMETERS OF EXISTING OLD WINDMILLS WITH THE PARAMETERS OF NEW WINDMILLS TYPE VIME.

Type of Windmill	Output at a wind velocity of 8 m/sec (kg/hr) Q	Nominal power on shaft of wind wheel at a specific output of 20 kg/hp. hr.	Output coefficient of wind energy at nominal power of previous column	Output per m^2 of area marked off by wind wheel (kg/m^2)
Goatskin windmills D-15.4 m, Baryshev region, Kiev province, built in 1910	138	6.9	0.087	0.74
Tent-shaped windmill D-24.8 m, Mensk region, Chernigovskaya province, built in 1904	125	6.2	0.03	0.26
Tent-shaped windmill D-20 m, Ol'shansk region, Kiev province, built in 1937	246	12.3	0.117	0.79
VIME D-8 windmill built in 1943 in the Ryazan region, Ryazan province	130	6.5	0.304	2.6
VIME D-10 windmill in 1944 in the Solotchinsk region, Ryazan province	200	10	0.30	2.5

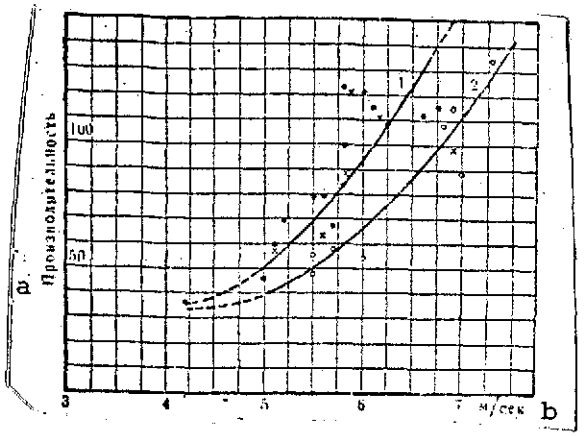

Fig. 299: Characteristics of the output in the VIME D-10 windmill: 1. after forging of the stone mill; 2. prior to forging of the stone mill.

Key: a-output
b-m/sec

It should be assumed that the tested windmills worked with a low coefficient of exploitation not because of slow wind but rather because the daily working wind velocity was not fully utilized. Obviously, the mechanics had no obligation to operate the windmill during the night, when the wind had sufficient strength.

In order to show the increase in the output of new windmills above the output of the old ones, Table 47 presents the exploitation parameters of old windmills, tested by the author in 1940, and of new ones constructed in the Ryazan province and tested by the same method in 1944. For the sake of a more convenient comparison, the last column of Table 47 presents a calculation of the output per m^2 of the area marked off by the wind wheel.

CHAPTER 16. WIND POWER STATIONS

/480

Although wind power installations have not yet received wide distribution, the theoretical and experimental elaboration of this method in the USSR makes it possible to solve already the practical problems of building wind power stations of both low and high power.

The main obstacle in applying wind engines for obtaining electric energy is the irregularity of the wind energy. However, the use of special generators (compound generators) which are suited to variable numbers of revolutions, as well as of automatic voltage regulators makes it possible to elaborate in wind power stations a current which is suitable for practical purposes of lighting and for power loads. Fig. 300 and 301 illustrate one of the first automatic switches.

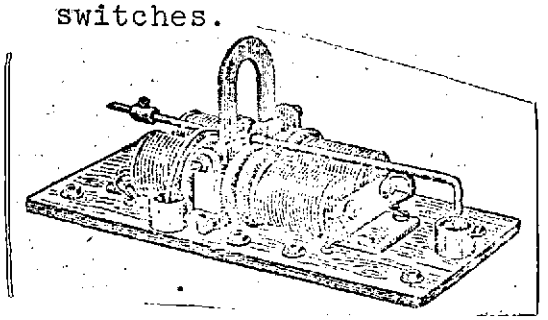

Fig. 300: Automatic cut-out.

The exploitation of the following wind power stations -- Crimean TsAGI D-30, VIME D-12, and of the Kursk system of Ufimtsev-Vetchinkin makes it possible to accelerate markedly the practical construction of wind power stations.

The parallel operation of wind and thermal or hydraulic power stations is now being investigated experimentally.

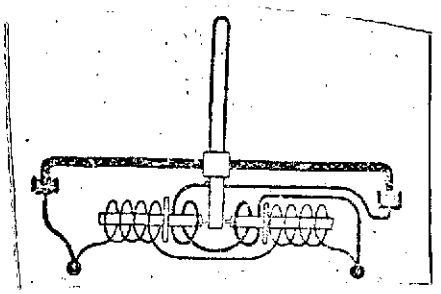

Fig. 301: Diagram of the switch.

The main elements of a wind power station of the average type are the following:

1. wind engine;
2. special type generator suited for operating with a variable number of revolutions;
3. storage battery which ensures the /481 supply of electrical energy to the consumer in short periods of calm weather; the storage battery is supplied with an automatic cutout;
4. reserve unit with thermal engine for operation in periods of prolonged calm weather, when the storage battery is insufficient.

There are 10 to 40% calm days and days with nonworking wind velocities per year; it is not possible to forecast their alternation nor can the number of successive calm days be foreseen.

Therefore it is hard to build a storage battery with a capacity which can supply the consumer with electric energy in a satisfactory

manner. Due to this fact, the wind power stations should have a reserve engine which is not dependent on wind energy.

62. Types of Generators for Operation With Wind Engine and Voltage Regulator /482

Usually, wind engines work at low wind velocities, 4-8 m/sec, with variable number of revolutions, while at wind velocities above 8 m/sec, the number of revolutions is constant if the wind engine is automatically regulated. The irregular revolutions fluctuate within the limits of 3-15% depending on the regulation system of the given wind engine.

In such a manner, the generator connected to the wind engine should ensure the constancy of the voltage during the fluctuations of the number of revolutions. This condition is fulfilled by constant current generators which are mounted as a rule in low-power wind power stations.

Alternating current generators of synchronal and asynchronal types can be used in high-power wind power stations for operation in parallel with other powerful thermal or hydraulic power stations in the general circuit.

Shunt generators of constant current are used for operation with wind engines.

This generator may be of a purely shunt excitation type, the diagram of which is illustrated in Fig. 302, or with mixed excitation, in which an additional series excitation winding is found aside from the the main shunt winding.

The additional winding is connected in such a way that its magnetic current adds up to the main current of the shunt winding and we obtain the diagram of a generator with compound excitation (Fig. 303).

Generators which are usually mounted on tractors and automobiles are used for low-power wind power stations, 100-1000 W. Since these machines work with a variable number of revolutions, the generators used with them are made with a large magnetic saturation and they are also supplied with voltage regulators. Due to this fact, they permit fluctuations of the number of revolutions within large ranges and this corresponds entirely to the irregularity of the operation characteristic of wind engines. The shortcoming of these generators which are known under the trademarks GPT, GAU and GBF, is their low efficiency.

GBT generators are mounted on STZ and KhTZ tractors and have a /483 power of 60-85 W, a voltage of 6 V, bipolar shunt winding of

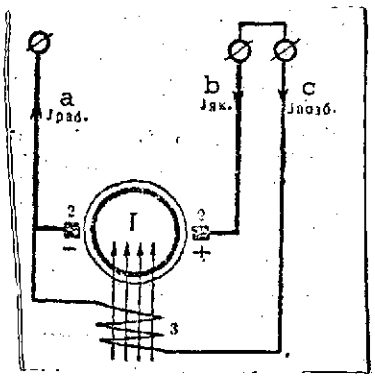

Fig. 302: Diagram of a constant current shunt generator: 1-generator; 2-brushes; 3-excitation shunt winding.

Key: a-work
b-arm
c-excit.

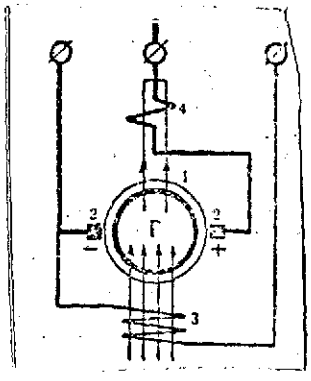

Fig. 303: Diagram of the shunt generator with compound excitation. 1-generator; 2-brushes; 3-shunt winding of excitation; 4-additional series excitation winding

excitation and they operate with an automatic voltage regulator. The regulator permits changing the number of revolutions when working with a load from 1100-2100 rpm, while the voltage is maintained constant.

GBF 3-brush generators are mounted on passenger automobiles M-2 and ZIS-101. Their power is 60-80 W, their voltage 6 V; they are bipolar with shunt winding of excitation.

The advantage of the 3-brush generator is that it can work in charging the storage battery without any special voltage regulator in a range of revolutions from 700-4500 rpm. The plus end of the shunt winding of excitation is connected to a special third brush which is displaced with regard to the neutral by an angle of about 60°. The effect of the reaction of the armature winding on the distribution of the magnetic current in the poles of the generator is used in this case. /484 The current created by the winding of the armature has a function which is analogous to that of the current in the anti-compound winding i.e. it demagnetizes the poles. Due to this fact, the voltage in the clamps of the generators changes little even at large variations in number of revolutions. It should be mentioned that the limitation of voltage will occur only in that case that the generator works with a storage battery or under great loads. The voltage will change greatly under incomplete loads or under conditions of either operations, since in this case there is no working current and consequently no reaction of the armature. The change in the power of the charging current at variations of the number of revolutions in the range of 600-3200 per minute is shown in Fig. 304.

The GA 250/12 generator, of the shunt type, 4-pole, with a power of 250 W and a voltage of 12 V is intended for working on autobuses. It operates with an automatic voltage regulator of type RRT. This regulator ensures constancy of volatge in a range of revolutions form 1300-3000 rpm with load. The generator can be used with a wind engine with a diameter of the wind wheel of 3 m.

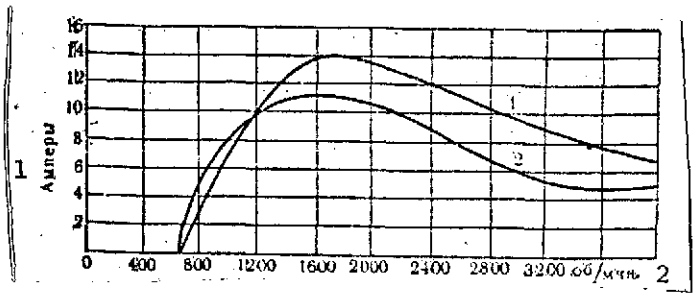

Fig. 304: Characteristic curve of the GBF generator.

Key: 1. amperes
2. rpm

The GT 1000/24 generator with a power of 1000 W and a voltage of 24 V works with a RRT voltage regulator and ensures the constancy of the voltage in a range of revolutions of 950-3000.

This generator can be used with wind engines which have a diameter of the wind wheel from 3-3.5 m and are intended for working in regions /485 with high annual average wind velocities, as well as with wind engines which have a diameter of the wind wheel of 5 m, and are intended for work in regions with an annual average wind velocity below 5 m/sec.

Constant current generators intended for general use have a magnetic system with normal fluctuations, as a result of which their characteristic curve has a large slope (with respect to the horizontal) and is distinguished by a low range of fluctuation of the number of revolutions. Such generators can work with wind engines which are characterized by a lesser irregularity of operation and a higher power.

Conditions of operation with constant resistance in the circuit of excitation[1]. The characteristic of the shunt generators in relation to the number of revolutions at constant voltage is represented graphically as a straight line which makes an angle with the horizontal axis of coordinates; this angle is determined by the magnitude of the excitation current in the circuit of the shunt winding of the generator.

By introducing a resistance in the shunt of the generator, we shift the characteristic curve to the right and thereby decrease the slope, as shown in Fig. 305.

Curve I corresponds to a maximal current of excitation. Curve II corresponds to a medium magnitude while curve III corresponds to the minimal value of the excitation current.

It is desirable to have constant voltage in the operation of a wind power unit, and this is obtained by regulating the load of the generator.

---

1. According to data of the wind power laboratory VIME elaborated by electrical engineer I. B. Vershinin and G. A. Pechkovskiy.

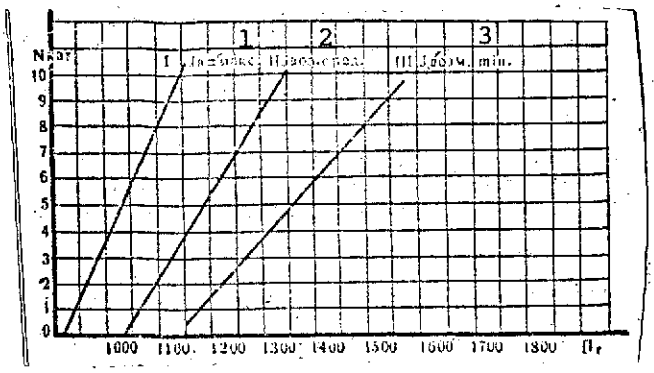

Fig. 305: Characteristic curve of a shunt generator with different excitations.

Key: 1. maximum
2. medium
3. minimum

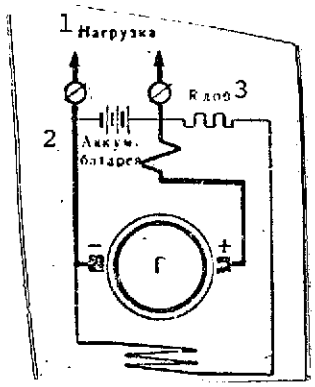

Fig. 306: Connection of the storage battery to the clamps of the generator (with buffer)

Key: 1-load
2-storage battery
3-R_{fr}

The simplest way of achieving such a regulation is by connecting the storage battery in parallel to the clamps of the generator (Fig. 306). The role of the storage battery in the given case is to level off the fluctuations in the power of the wind engine and to maintain a normal magnitude of the voltage in the clamps of the generator. With the decrease in the number of revolutions of the wind engine, the voltage in the clamps of the generator falls, and if the storage battery is in a state of normal charge, its voltage is higher than the voltage of the generator.

Due to this fact, the storage /486 battery assumes a part of the load at the extent of relieving the wind engine. At the same time its revolutions increase in number and the voltage of the generator is restored. If the number of revolutions of the wind engine decreases so much that the generator passes to operating under the conditions of a motor, then it has to switch off automatically. With the increase in the power and the number of revolutions of the wind engine, the voltage of the generator appears to be higher than the voltage of the storage battery, as a result of which it goes over to conditions of charging.

Maintenance of normal voltage can also be /487 performed by means of automatic connecting and disconnecting of a part of the load in rhythm with the fluctuations in the power of the wind engine. It is suitable to take for such a work a shunt generator with anticompound winding. This generator has a softer characteristic $N = f(n)$ and it limits the maximal charging current of the storage battery. The voltage of the generator increases with the increase in the number of revolutions and the current of loading, and the current in the anticompound series winding increases at constant resistance of the external circuit. The increase in the current passing through the compound series winding enhances its counteracting effect.

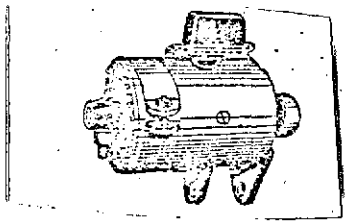

Fig. 307: Voltage regulator for a dc generator.

effect on the main current of excitation and consequently limits the increase in voltage.

Voltage regulator. A vibrational VR regulator is used for operation with the GBT and GAU generators, and it is mounted on the generator itself (Fig. 307). The action of the regulator consists in the following. When the voltage of the generator is below the normal value, the spring approaches armature 2 to contact 1 (Fig. 308); this leads to an increase in the additional resistance of the excitation winding of the generator. As soon as the voltage rises above the normal value, electromagnet 3 surmounts the force of the spring and pulls armature 2 to its own side; at the same time resistance R_n will be removed from the shunt circuit, the current of excitation decreases and the tension in the generator starts to fall, etc. As as result of this, the armature starts fluctuating with a frequency of up 30 periods per second, and consequently the fluctuations of the voltage become so small and frequent that the voltage can be considered practically constant. /488

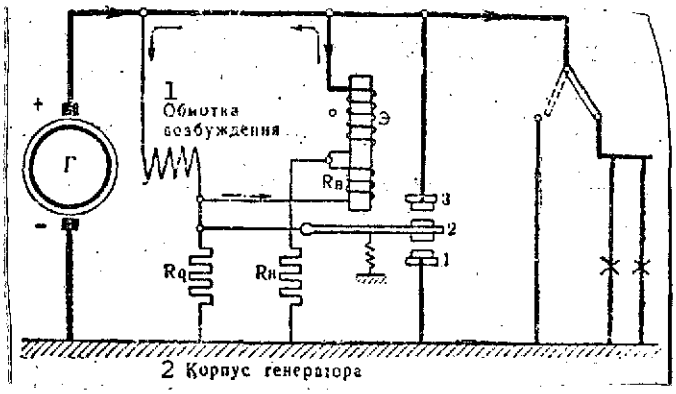

Fig. 308: VR voltage regulator

Key: 1. winding of excitation
2. body of the generator

The RR regulator-relay (Fig. 309), is also of the vibrational type; in addition to its own regulator 3, it has inverse current relay 2 of type TsB, which protects the storage battery from discharging in the generator. The regulator relay is intended for operation with GA 250/12 generator. It is manufactured as an independent instrument and is mounted separately from the generator.

63. Wind Charging Units

Low-power wind power installations intended for charging storage batteries are called wind charging units. For wind charging units, rapid wind engines of low-power and a diameter of the wind wheel between 1.5 and 3.5 m are used, while the generators are of the automobile type, as described above. Charging of the storage batteries is the most convenient load for a wind engine. Let us examine a few examples of wind power units. /489

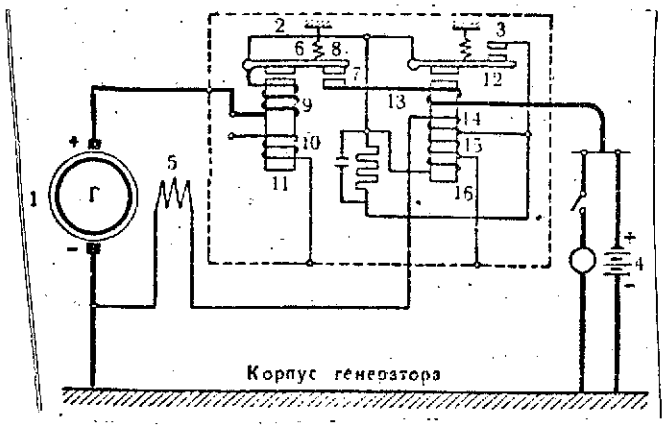

Fig. 309: Electrical circuit of the RR relay-regulator: 1-autobus generator; 2-inverse current relay; 3-voltage regulator; 4-storage battery; 5-generator excitation winding; 6-relay armature of inverse current; 7-conduit; 8-coil; 9-current winding; 10-shunt winding; 11-core disc; 12-voltage regulator armature; 13-current winding; 14-equalizing winding; 15-starter winding; 16-main winding.

The VISKhOM D-3.5 wind power unit. This unit (Fig. 310 and 311) has a rapid wind engine with a two-blade wind wheel. The wind engine is regulated by removal of the wind wheel from the wind. For this purpose, the wind wheel is somewhat displaced from the vertical axis. A GA 250/12 type generator with a power of 250 W and voltage 12 V is attached to the head of the wind engine. In regions with high average annual velocities, above 5 m/sec, the unit is equipped with a type GT 1000 24 type generator with a power of 1 kW and a voltage of 24 V. The electrical part of this unit envisages its use as a charging installation for low-power radio stations. The installation is intended for /491 charging two groups of storage batteries, 12 V and 160 V. Each battery consists of two sets. When one of them feeds the instrument of the station, the other is being charged. The connecting for charging of the 160 V storage battery to a 12 V source of current is performed by resolving it into 13 groups. During the charging, the groups are united in parallel while during the operation under load, they are connected in series in the general circuit.

In order to ensure sufficient voltage in charging the battery, the generator is given a voltage of up to 18 V which is reduced in the beginning of charging in the rheostats which are found in each group of storage batteries.

The VISKhOM RD-1.5 wind charging unit. The 100 W RD-1.5 wind charging unit has a two-blade wind wheel with a diameter of 1.5 m. In the process of regulation of the flaps, the blades rotate in the bush under the action of centrifugal weights which are mounted on a rod fastened to the flap at an angle 90° with the cord of the profile in the lower section of the blade. This system of regulation was suggested by V. S. Shamanin. The electrical part of the unit was elaborated by I. B. Vershinin. The wind wheel is attached directly to the axis of the generator of type GAU with a power of 100 W and a voltage of 6 V. The general appearance of the unit is shown in Fig. 312; the electrical circuit is given in Fig. 313.

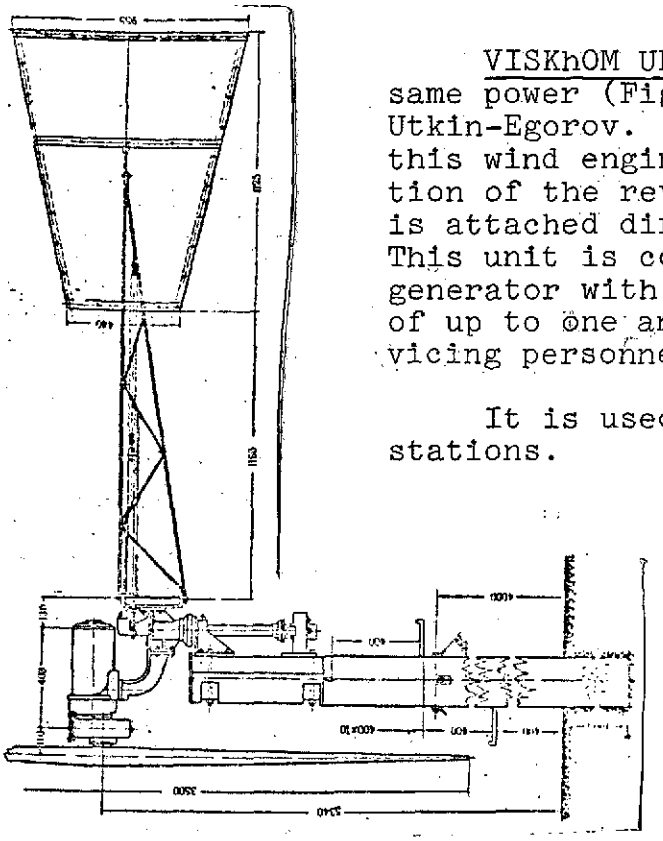

Fig. 310: The VISKhOM D-3.5 wind power unit.

VISKhOM UD-1.5 wind charging unit of the same power (Fig. 314) was designed by V.VV. Utkin-Egorov. The characteristic feature of this wind engine is the highly accurate regulation of the revolutions of the wind wheel which is attached directly to the axis of the generator. This unit is computed for operation with a generator with variable current in the course of up to one and a half years without any servicing personnel. /492

It is used for automatic meteorological stations.

64. Low-Power Wind Power Stations

The winds which blow on the shores of seas and oceans are distinguished by their high velocities and they represent a powerful source of energy.

The first wind power station in the Mediterranean region of teh USSR which worked with a TsVEI D-8 wind engine, gave an electrical current with small fluctuations of voltage despite the absence of automatic electrical equipment. This wind power station worked 6200 hours per year at full power out of the possible 8760 per year. It is understandable that such a number of hours per year with full load is only possible in a region with high wind velocities. With regard to the small fluctuations in the voltage of the electric current, this achievement is due exclusively to the regulation system of G. Kh. Sabinin and N. V. Krasovskiy, used in wind engines of this type (see Chapter IX, Section 35, Fig. 129). /493

Due to the high wind velocities, many wind power stations work several months without any reserve. The extent of loading of the reserves in one station throughout the year can be seen in the operating schedules (Fig. 315, a and b): VES D-12 corresponds to the lower graph, while VIME D-5 corresponds to the upper figure, whereby the output of the reserve is shown by black columns, while the output of wind engine is illustrated by the hatched columns.

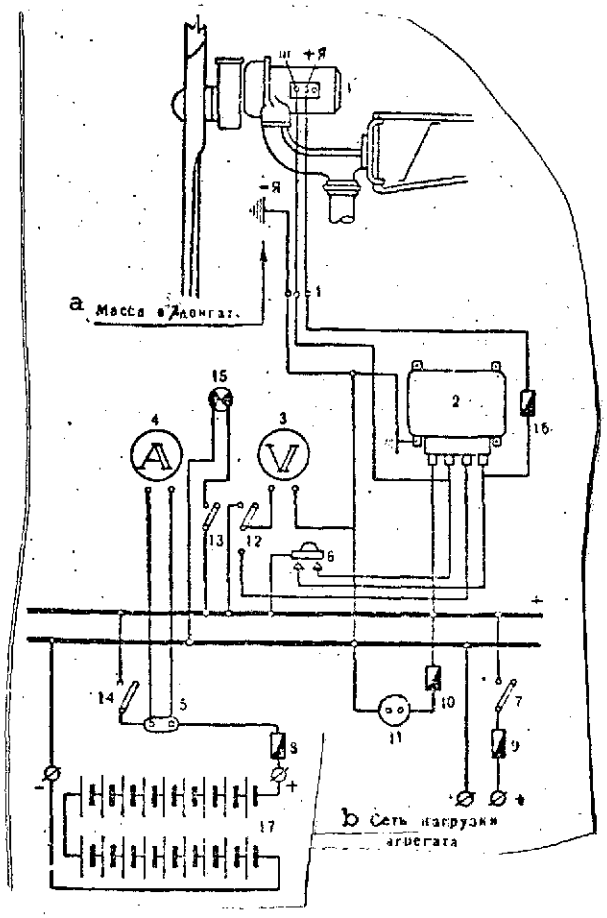

Fig. 311: Electrical circuit of the VISKhOM D-3.5 wind power unit: 1-generator; 2-regulator relay; 3-voltmeter; 4-ammeter in the ciruit of the storage battery; 5-storage battery connection clamps; 6-wind engine starter button; 7-line cutout for unit charger; 8-storage battery fuse; 9-line fuse of unit charger; 10-fuse in switchboard outlet; 11-portable lamp outlet; 12-voltmeter transfer switch; 13-instrument lamp switch; 14-storage battery switch; 15-switchboard or instrument panel light; 16-generator circuit fuse; 17-storage battery.

Key: a-mast of the wind engine
b-loading circuit of the unit

The construction of wind power/494 stations in regions which are far removed form thermic energy re- sources makes it possible to reduce considerably the transport of fuel which is usually fraught with large difficulties [39].

65. Parallel Operation of Wind Power/495 Stations in a General Circuit with Large Thermic Stations and Hydropower Stations

The wind power station working alone has an important shortcoming which consists in the fact that in order to ensure uniform feeding of the energy, storage batteries and a reserve thermic engine have to be set up. As a result of this, powerful wind stations working with constant current are hard to realize and the cost of the obtained energy is very high. Wind power installations working alone should be built wherever the cost of other energy sources is very high. However, these wind installations have advantages if they operate with a mechanical actuator and the electrical energy is utilized for auxillary purposes such as lighting of service buildings, charging, etc.; in this case large capacity storage batteries are not required.

A wind installation which is used for servicing electrical lighting and mechanical loading will have losses in both mechanical and electrical machines i.e. it will be less avantageous.

The useful power of a wind installation working with a mechanical actuator is expressed by the following equality:

$$N_n = N_r \eta_{\mu}$$

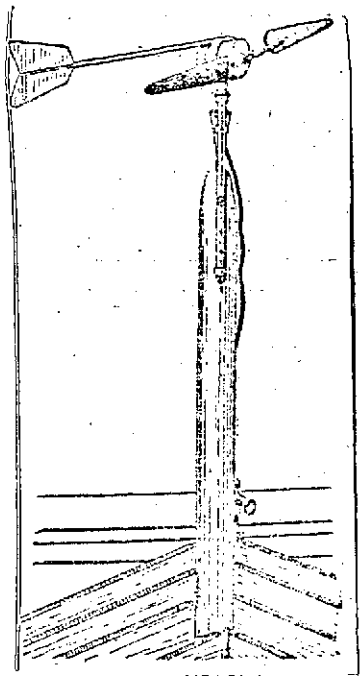

Fig. 312: The VISKhOM RD-1.5 wind charging unit.

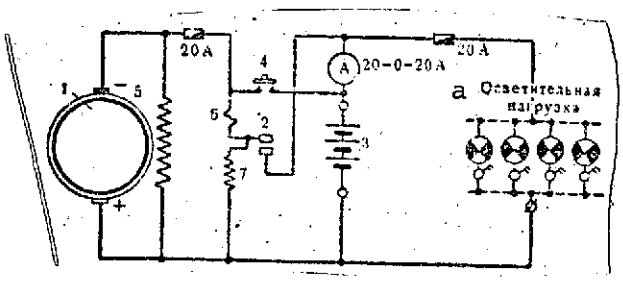

Fig: 313: Electrical circuit of the VISKhOM RD-1.5 wind charging unit: 1-generator 100 W, 6-8 V; 2-inverse current relay; 3-storage battery 6 V, 144 A-hr; 4-pushbutton of motor starter; 5-shunt winding of the generator; 6-series winding of the relay; 7-shunt winding of the relay.

Key: a-lighting load

If the wind installation supplies electrical energy for power loading, then its useful work will be equal to:

$$N'_n = N_w \eta_m \eta_g \eta_e$$

where N'_n is the useful power;

N_w is the power of the wind engine;

η_m = 0.6 to 0.8, the mechanical efficiency of transmission from the wind wheel to the tool;

η_g = 0.7 to 0.8, the efficiency of the generator;

η_e = 0.7 to 0.8, the efficiency of the electrical engine.

If we will take the upper limits of the efficiencies of the machine, we obtain:

$$N_n = N_w 0{,}8$$
$$N'_n = N_w 0{,}8 \cdot 0{,}8 \cdot 0{,}8 = N_w \cdot 0{,}512.$$

In such a manner, our wind installations would give in the second case 0.8 : 0.512 = 1.56 i.e. 1/1.56 useful power. /496

Of extraordinary interest for the electrification of the socialist economy are the wind power stations of high power which work in the general electric circuit in parallel with the thermic and hydropower stations. The general circuit of large power stations is in this case an enormous storage battery which absorbs the excess electrical energy and covers the load of the wind power station on calm days. In this case it is not necessary to have storage batteries with low efficiency added to the installation which increase the cost of the energy obtained in wind power stations.

By parallel operation of the wind power stations, it is possible to solve problems related to the stable operation of the station, without overloading the wind engine and the generator and excluding the

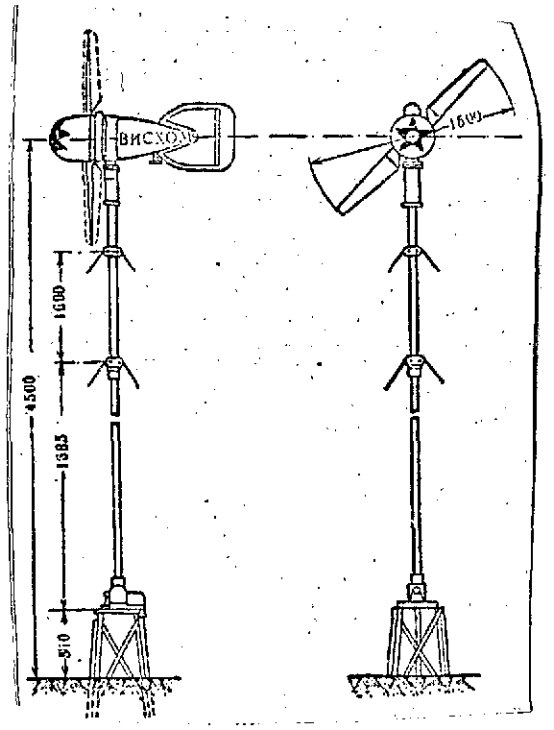

Fig. 314: The VISKhOM UD-1.5 wind power unit.

movements in the system so as to obtain a reliable operation. All this requires the creation of mechanical electric devices for automatic regulation of the wind power station.

Generators for parallel operation in the general circuit. Both synchronal and asynchronal generators can be used in parallel operations of wind power stations with alternating current.

The former has a strictly determined constant number of revolutions which depends on the frequency of the circuit.

The asychronal generators allow a certain small fluctuation in the number of revolutions at constant frequency of the circuit.

Asynchronal generators have a number of advantages over the synchronal one, i.e. they are cheap and of simple construction, do not requires an additional exciter and are stable under overloads. A drawback of these generators is that they charge the circuit with reactive current. Their efficiency decreases markedly with the decrease of the load.

Synchronal generators require for connecting into a net of alternating currents a complete preliminary synchronization of the generator with the net. This can be performed by an automatic synchronizer. The reliability of this generator consists in the fact that it works in the circuit without deterioration of the latter and has a high power coefficient cos ϕ. The load has little influence /497
on the magnitude of the efficiency. This generator is less suitable for operation in wind power stations due to the following reasons: elaborate synchronization; the generator requires a separate exciter; danger of overload, which is hard to prevent electrically.

Operation of the wind engine with asynchronal generator. Complete correspondence of the characteristics of the wind engine with those of the generator is required in order to obtain satisfactory operation of the wind power unit. The power supplied by the asynchronal generator into the circuit equals 0 at a number of revolutions which is lower than the synchronal number. When the number of revolutions

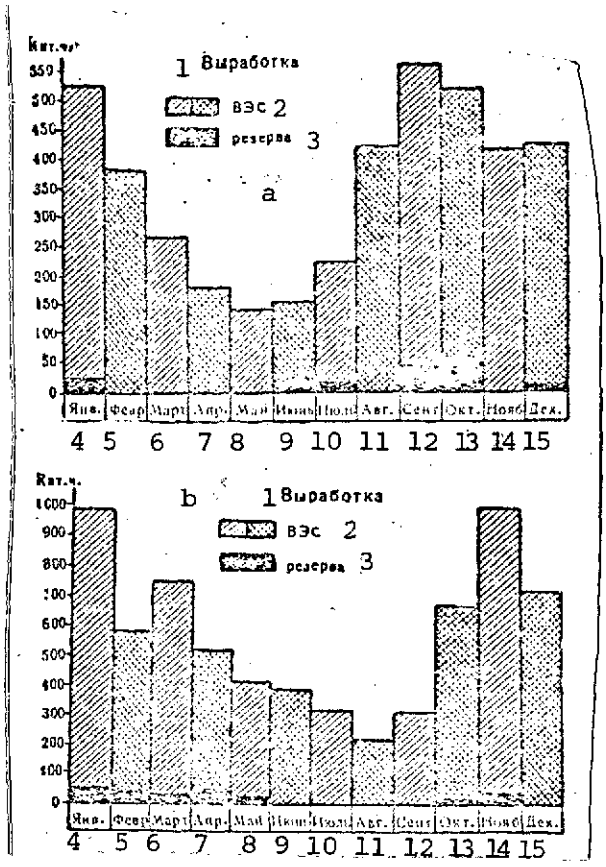

Fig. 315: Operating schedule of a wind power station: a-VIME D-5 wind power station; b-D-12 wind power station.

Key: 1. output
2. wind power station (WPS)
3. reserve
4. January
5. February
6. March
7. April
8. May
9. June
10. July
11. August
12. September
13. October
14. November
15. December

exceeds the synchronal number, the power increases rapidly and reaches its maximum by a 5% slip. The power fed into the circuit by the generator decreases when the number of revolutions increases above this value.

In such a manner, the operation of the asynchronal generator takes place between the highest power which changes proportionally to the slip and 0 power which corresponds to the synchronal number of revolutions. The wind engine and asynchronal generator should be calculated for a possible overload of up to 60%.

The operation of a wind power station which asynchronal generator takes place in the following sequence. The wind engine which is started at a certain wind velocity picks up [illegible] revolutions and as soon as the synchronal number is reached, a circuit breaker connected with a centrifugal regulator connects the circuit of the power station to the general circuit by means of an oil switch; subsequently the wind power station feeds current into the general circuit until the wind velocity decreases below a certain value. The inverse current relay disconnects at this point the electric engine in its role of generator.

Operation of the wind engine with synchronal generator. The operation of a wind engine with synchronal generator requires a regorously constant number of revolutions.

The overload of a synchronal generator is permitted to a much lesser degree than in the case of the asynchronal generator. As a result of this, reliable regulation of the wind power station is required either by regulation

of the wind engine or by regulation from the electrical circuit of the station. In the opposite case, the generator may lose its synchronicity under conditions of overload. In such a manner, automatization of the wind power station is more complicated with the synchronal generator. /498

In the operation of wind power stations with regulation of the wind engines, both with asynchronal and with synchronal generators, the wind engine must be regulated so that the number of its revolutions does not fall below the synchronal number. If the wind engine is regulated in such a manner that the number of its revolutions is limited and does not reach the synchronal number, then neither the synchronal nor the asynchronal generators can feed enough energy into the circuit at any wind velocity.

Loading of the synchronal generator can take place only at synchronal velocity and is determined by phase shift.

However, when regulation of the wind engine is performed, the latter as well as the generator must be protected from overload. Since the power of the generator grows according to an almost vertical curve, with the increase in wind velocity, the wind engine which is regulated under the effect of centrifugal weight, while maintaining its number of revolutions, will develop a power which is proportional to almost the cube of wind velocity, and cause overloading of the unit. Therefore, an additional device is required which would protect the unit from overloading at high wind velocities.

The operation of wind power stations with synchronal generators is performed according to a diagram which is analogous to the asynchronal generator. The only difference is that the wind power station working with synchronal generator must have a synchronal automatic device which acts on the maximal switch of the circuit only after a certain number of revolutions of the generator as well as coincidence of the phases is reached.

In addition, automatic regulation of the excitation, connected with a power factor meter should be introduced in order to improve the conditions of the circuit. Protection from overloading can be accomplished either by corresponding regulation of the wind engine or by additional mechanical device (hydraulic slip clutch).

The electrical protection from overloading is made by switching from the synchronal generator to the asynchronal one, which permits slipping during the increase in the number of revolutions.

66. Experimental Testing of the Operation of Wind Power Stations Connected Parallel in the Circuit [53] /499

The experimental investigations on the parallel operation of wind power stations were carried out for the first time under the

guidance of G. Kh. Sabinin in the TsAGI wind power laboratory. The wind power apparatus by means of which these investigations were performed consisted of a rapid wind engine and an inductive machine which worked in the capacity of a generator under asynchronal and synchronal operating conditions with a steady power of 5 kW at 220 V in the circuit.

The computation diagram of the experimental installation elaborated by I. B. Vershinin is presented in Fig. 316. This diagram allows operation under both asychronal and synchronal conditions however it is inadequate for a powerful wind power station since it lacks several elements of automation and protection.

The operation of the instrument, according to the diagram, is performed in the following order.

a. Asynchronal operating conditions.

According to the diagram in Fig. 316, the knife switches, the circuits of the bcd rotor and knife a of the stator circuit should be connected prior to starting the wind engine with inductive generator.

As soon as the wind engine conveys to the rotor a synchronal velocity, which is measured by tachometer 3 and 4, the circuit is closed by means of knob 6 of the automatic switch 2. The automatic device connects the generator to the circuit and if the number of revolutions of the rotor increases, the generator intercepts the load in the circuit according to the given slip.

When the wind velocity decreases, and consequently, the power supplied by the generator is below the calculated one, the relay of the reverse current is automatically disconnected.

The diagram illustrates the manual connecting of the generator by means of knob 6 which acts on the solenoid of automatic circuit breaker 2. Protection of the generator from overloading in the absence of a maximally depending relay, is performed by means of fuses.

When the wind power station works with a limited power of the generator which is achieved by automatic slip regulator 9, the sequence of operation of the instrument in connecting the generator is maintained the same as in the case of the shorted-out rotor. The only difference is that knife switch d which shorts out the rotor must in this case be disconnected. /501

b. Synchronal operating conditions.

The transition of the inductive generator to synchronal conditions (Fig. 316) is performed by means of the automatic frequency relay 7. Knife switches a, b, and e are connected while b and c

are switched on prior to starting the wind power station. Subsequently, inductive generator 1 is connected to the net. Changeover switch f is placed in the left position, corresponding to the connecting of the excitation rails of the reel in frequency relay 7. The current of the slipping frequency flows around the second reel of the frequency relay which is connected in circuit 1 of the rotor phase while the knife switch is disconnected; when the current of the slipping frequency assumes its maximal value of the negative wave, a current is created which has the same direction as the flow of the reel. Under the effect of the overall flow of the reel, the frequency relay 7 closes its left working contacts, and thus connects the rotor to the constant current machine. As a result of this, the inductive generator becomes synchronal and continues to work synchronally. If the generator ceases to be synchronal as in the case of a considerable load jerk, the diagram provides for automatic switching off of the generator.

Protection of the wind power station from overloading by regulation of the wind engine. When the wind engine works in parallel with the synchronal generator, the centrifugal regulator which limits the number of revolutions of the wind wheel cannot limit the power of the wind engine. This is explained by the fact that under conditions of a steady synchronal number of revolutions, which are maintained constant by the circuit, the centrifugal regulator cannot act on the mechanism which rotates the blades at the required angle of attack. In order to prevent the wind power station from getting overloaded, one has either to act on the mechanism which changes the angle of the blade by some kind of device from the side which is not related to the revolutions of the wind wheel, or else the wind engine must be connected to the generator not directly but rather by means of an intermediate hydraulic clutch. In the latter case, the power of the wind engine will be limited by its regulation since in this case, the revolutions of the wind wheel may increase by 1.5-2% and set in motion the centrifugal regulator. The power of the generator is limited by the /502
operation of a hydraulic clutch which can only transmit a limiting torque established depending on the power of the machine tool. Any extra moment causes slipping of the clutch.

In studying the operation of D-10 wind engine with stabilizing regulation to synchronal conditions of a wind power station, connected in parallel, tests were performed with three devices which acted on the mechanism of rotation of the blade tip without being connected with the revolutions of the wind wheel:

1. with the "Askaniya" oil regulator;
2. by rotation of the stator;
3. by means of an additional small wind engine whose blade can be longitudinally displaced along the axis of the flap under the /503
action of its centrifugal forces (Fig. 317) (suggestion of V. S. Shamanin).

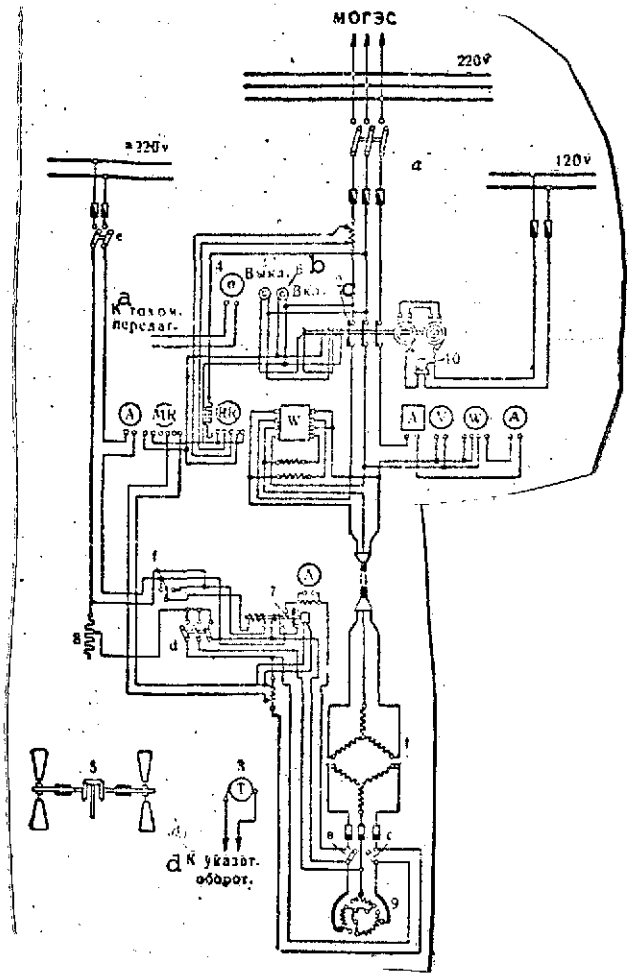

Fig. 316: Commutation circuit of an experimental windpower station for studying parallel operations in the general circuit: 1. asynchronal generator; 2-automatic circuit breaker; 3-tachometer-transmitter; 4-tachometer-gauge; o-measuring instrument; -recorders; 5-wind rotors; 6-on-off button; 7-automatic synchronization device; 8-excitation rheostat; 9-slipping regulator; 10-motor of tie beam of the spring for automatic cut-out.

Key: a. to the tachometer gauge
b. current breaker
c. switch
d. to the tachometer gauge

Each one of these mechanisms is connected to the regulating clutch which rotates the stabilizers and along with them the blade tip under the required angle of attack.

In such a manner, the position of the rotating blade tip was determined entirely by the magnitude of the linear displacement of the regulating clutch a in millimeters, which is kinematically connected with the wing stabilizers.

By means of the experimental characteristics M and $\xi = f(a,Z)$, obtained for various positions of the regulating clutch, the dependence of the power of the wind wheel on wind velocity at each α at a constant number of revolutions can be plotted. Such a plot is presented in Fig. 318 for α= 10, 13, 15, 17 and 20.

The wind engine works /504 most efficiently at a = 10, i.e. at the smallest inclination angle of the blade. However at this a, the power of the wind engine overloads the generator by 100% starting with wind velocities of 9.3 m/sec, which is inadmissible.

In order to prevent overloading of the installation, the wind wheel must be changed to less efficient operating conditions when the wind velocity exceeds 8 m/sec, i.e. the regulating clutch connected with the rotating blade tip must be displaced with respect to its initial position by more than 10 mm.

It is easy to determine the magnitude of a at which

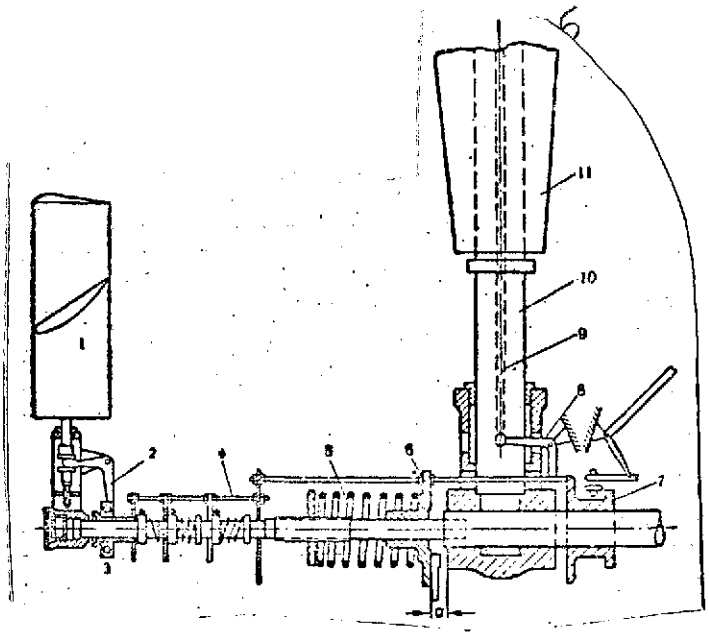

Fig. 317: V. S. Shamanin's device for limitation of the power of wind engines which are regulated by rotation of the blades under the action of centrifugal forces: 1-fly; 2-lever; 3-slip clutch; 4-rod; 5-spring; 6-clutch, the course of which is measured by magnitude a; 7-regulating clutch; 8-lever; 9-rod to the stabilizer; 10-flap; 11-wing of the wind wheel.

the regulating clutch must be shifted depending on the wind velocity in order to maintain the constancy of the installation power by means of the graphs in Fig. 318; as an example, the plot was made for a 4 kW power generator.

When the wind engine operates with stabilizing regulation to an asynchronal generator with slipping regulator, the revolutions of the wind wheel may increase by 1.5 to 2% as compared to the normal number. This increase in the number of revolutions immediately leads to a shift in the centrifugal flyweight of the regulator which acts on the stabilizer and turns the blade. In such a manner, no additional device for shifting the clutch by magnitude a is needed in the given case.

The results of the tests yielded recordings where the course of the regulating clutch is illustrated as a function of wind velocity during operation of a wind power unit with the indicated above 3 additional regulating devices. The tracings of the course of the clutch during operation with the first and second regulator showed that these regulators do not give the required change of a as a function of V for maintaining the constancy of the wind engine power.

Continuous variation of wind velocity must be accompanied by a corresponding change in the magnitude of a; nevertheless, the fluctuations in a, the course of the clutch, assumed the pattern of a course with peaks. The pattern of the clutch fluctuations depending on wind velocity is shown in Fig. 319 where the upper curve shows the change of a during the operation with "Askaniya"; the change in wind velocity is shown by the lower curve.

More satisfactory results were obtained in the work with the fly suggested by V. S. Shamanin. Fig. 320 depicts the curves of wind velocity (lower curve) and of the clutch course a corresponding to these velocities. The even pattern of variation of the /505

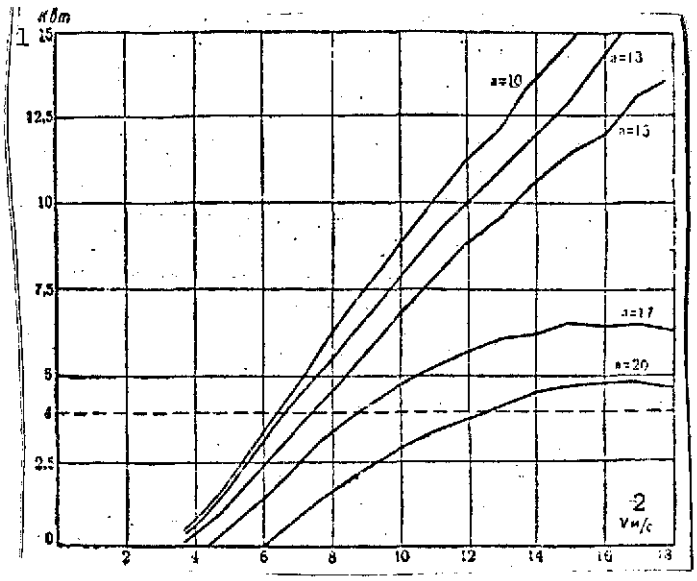

Fig. 318: Variation of the power of the wind wheel at various positions of the clutch depending on wind velocity.

Key: 1. kW
2. V m/sec

clutch course shows that this device provides for constancy of the wind engine power with fluctuations between more or less narrow limits relative to the given magnitude.

In such a manner, the problem of automatic protection of the wind engine from overloading in the case of operation with a parallel synchronal generator in a high power circuit and with wind velocities exceeding the calculated values, is technically solvable.

Although the causes for the pulsation of the moment are not entirely known, the following assumptions can be forwarded on this matter. The wind velocity which pulsates in magnitude and direction causes a greater pulsation of the forces which rotate the wind wheel. But since the revolutions of the wind wheel during the operation with a synchronal generator are maintained reasonably constant, the pulsating action of these forces is manifested in a sharp pulsation of the torque of the wind wheel as can be seen from the equation of the power of the wind engine N, expressed by means of the torque M and the angular velocity ω: /506

$$N = M\omega \text{ kg/m/sec}$$

Since ω = const, the pulsation of the power on the whole corresponds to the pulsation of the torque.

When the wind engine is loaded in such a manner that insignificant fluctuations in the angular velocity of the wind wheel are permitted, as for example during operation with an asynchronal generator, the peak of the torque decreases to a smaller or greater extent, which is immediately reflected in the power curve which assumes a more smooth course. When the wind engine operates with a synchronal generator in the general circuit, it is extremely important to exclude the possibility of transmission of the pulsating moment to the generator.

Such operating conditions of the wind wheel can be fully provided for by the hydraulic clutch connected in the transmission

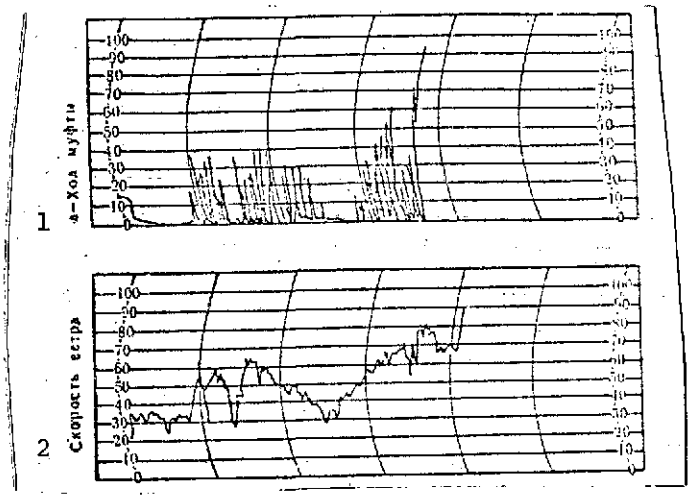

Fig. 319: Tracings of thecourse a of the clutch during operation of the wind wheel with the "Askaniya" device acting on the clutch, in relation to wind velocity.

Key: 1. a -- course of the clutch
2. wind velocity

between the reduction gear and the generator. This clutch permits slipping of the leading mechanism of the wind engine relative to the main shaft of the generator. Consequently, the number of revolutions of the wind wheel will slightly increase without disturbing the strictly constant revolutions of the generator. /507

It should be assumed that the operations of the wind engine with synchronal generator in the presence of a hydraulic clutch can be entirely satisfactory without any additional devices for limiting the power of the wind wheel which is regulated by means of centrifugal flywheels.

Operation of a wind engine connected in parallel without regulation. On the basis of a series of theoretical and experimental studies, G. Kh. Sabinin arrived at the conclusion that it is absolutely superfluous to regulate the torque at wind velocities exceeding the calculated values in the case of a winged type rapid wind engine (Z_n = 6) which is connected in parallel. This assumption was experimentally tested in the wind power laboratory of TsAGI on a wind wheel model D-10, i = 3, Z_n = 7. It appears that starting with wind velocities about 12 m/sec, the power on the wings of the wind wheel not only does not increase but even decreases. At the same time the number of revolutions is limited by the circuit itself, whose overall power is several times greater than the power of the wind engine. The characteristic of a D-10, Z_n = 7, i = 3 wind engine connected in parallel and operating without regulation is illustrated in Fig. 321. /508

In such a manner, during the operation of a rapid wind engine connected in parallel, the danger of excessive overloading of the generator and of the racing of the wind wheel with increasing wind velocity is excluded. What is needed in this case is merely a simple device which acts only during accidents in the circuit or following sudden removal of the load.

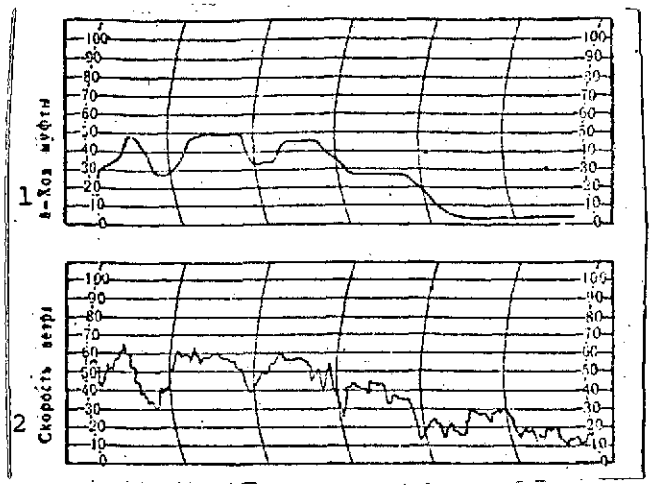

Fig. 320: Recording of the course a of the clutch during operation of the wind wheel with a fly which acts on the clutch, as a function of wind velocity.

Key: 1. a-- course of the clutch
2. wind velocity

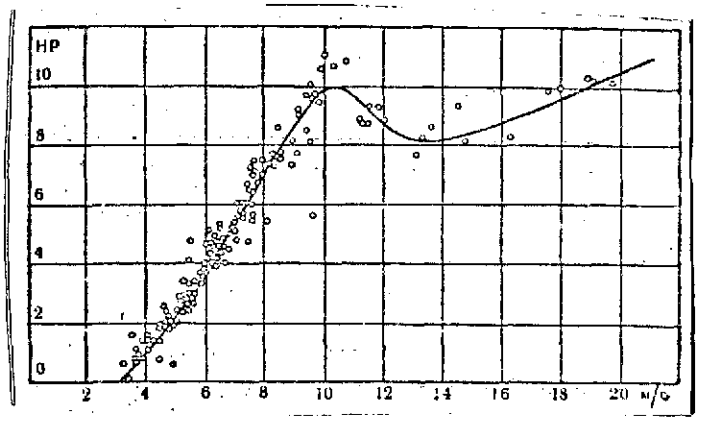

Fig. 321: Characteristic of the power of a wind power installation working in the general circuit without regulation.

67. High-Power Power Stations Connected in Parallel

The Crimean wind power station TsAGI D-30. The wind power station in Crimea (Fig. 322) had a purely experimental value and was constructed with the purpose of investigating the operation of a wind power station in parallel with a thermal power station in the same region. By the dimensions of the wind wheel D = 30 m and the power of about 100 kW at 30 rpm, this station had no equals in the USSR or abroad. In 1942, the station was destroyed by the German fascist aggressors.

The height of the wind engine tower was 23.3 m, the distance between the legs was 6.0 m. The cabin of the head which contained the generator and the electrical apparatus had the length of 13.7 m, a width of 3.5 m and the height of 3.8 m. The overall weight of the wind engine metal amounted to 49.1 tons. The volume of the foundation was 60 m^3.

The wind wheel has a diameter of 30 m and has three blades which rotate freely about their flaps under the action of stabilizers of the G. Kh. Sabinin and N. M. Krasovskiy's regulation system. The blades had a streamlined profile, analogous to the profile of an airplane wing. The blade was 11 m in length, 2 m wide at the base and 1 m wide at the tip. The flapswwere made of steel pipes with a diameter of 350 mm and were connected by means of a light girder made of iron carbide and and iron channels and pipes. A steel rim with a diameter of 3.4 m was secured to the flaps by means of bolts. On its internal side, the rim had a rolling surface which was supported by two steel rolls

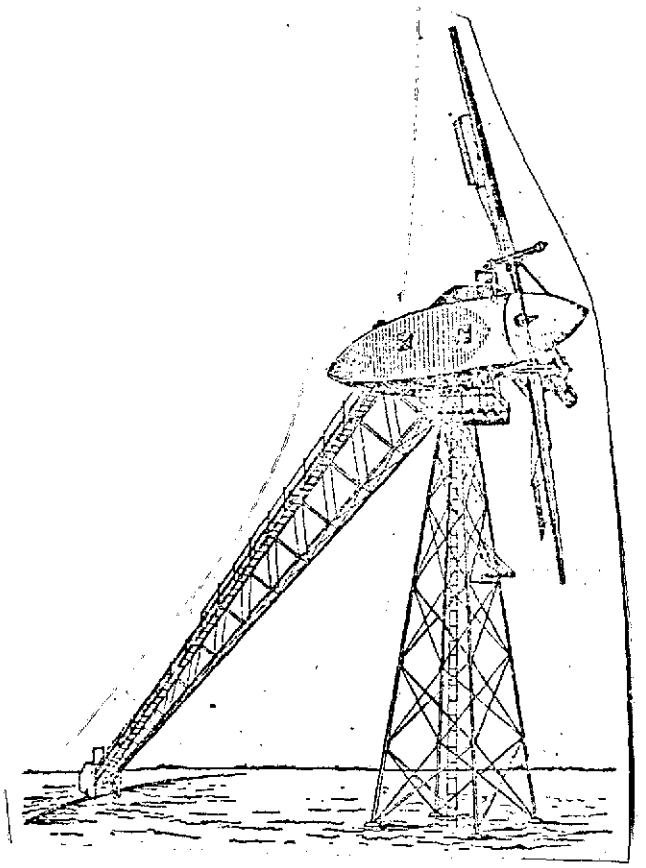

Fig. 322: The Crimean TsAGI D-30 wind station.

rotating on ball bearings fastened to the girder of the head. The wind wheel with the rim turn on these rolls. In addition, along with a smooth surface the rim has a surface with openings which contain /509
wooden teeth made of hornbeam. The teeth of the rim are engaged with two cast iron pinions situated inside the wing. The pinions are fitted on the two shafts which transmits the rotation to the differential gear and from the latter to the shaft of the generator. The differential gear is used in the transmission for a uniform distribution of the power between the two transmission shafts. The overall gear ratio of the two gears equals 21 : 4. The plane of rotation of the wind wheel has an inclination of 12° with respect to the vertical which is caused by the requirement of decreasing the gap between the wind wheel and the tower. The head of the wind engine is mounted on iron carbide and iron channels and leans through a spherical pivot on a spherical support secured on top of the tower. The wind engine turns about the vertical axis on this support during adjustment of the wind wheel to the wind. The girder of the head is hinged with the inclined tail girder, to which a carriage with motor and winch are hinged at the lower end. The tail girder serves for regulating /510
the wind wheel to the wind during changes in its direction. The carriage is supported on a rail which surrounds the tower along a circle with a radius of 20.5 m. The movement of the carriage on the rail is performed by means of an electrical motor with a power of 1.5 kW with worm gearing. Connecting of the motor takes place automatically during changes in the direction of the wind. For this purpose, a wind vane with a size of 400 x 700 mm is mounted on top of the cabin. During changes in direction of the wind, the wind vane connects one of the rolls of the electromagnetic change-over switch which is found in the circuit of the motor of the tail carriage. The motor moves the carriage around the rail as long as the wind wheel does not stand into the wind and the wind vane does not open the contact. A ladder is used in order to climb the tower and the tail girder.

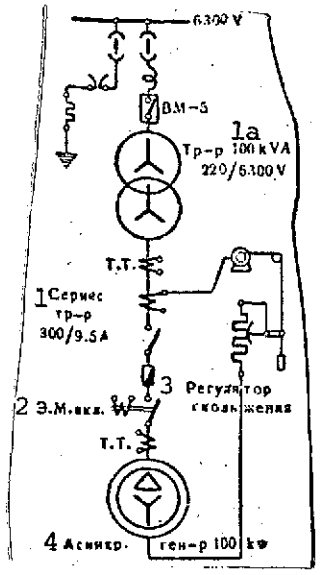

Fig. 323: Electrical diagram of the D-30 wind power station.

Key: 1. series transformer
1a. transformer
2. electromagnetic switch
3. slip regulator
4. asynchronal generator

The asynchronal generator of the unit is a normal 3-phase motor of type D-125 hp at 600 rpm.

The nominal power of the generator is 93 kV. The voltage of the starter phase is 220 V, the connection of the winding of the starter is made by means of a triangle, the linear current is 300 amperes, $\cos \phi_n = 0.83$. The weight of the generator is 2040 kg.

An aerial line of power transmission of 6.3 kV with a cross section of the copper 3 x 10 mm and a length of 2600 m passes from the building of the wind power station; it is connected in the line of electrical transmission and works in parallel with a thermic power station.

The electrical diagram of the unit is shown in Fig. 323; the basic diagram of automatic connection and protection of the generator is shown in Fig. 324. The automatic device and the relay protection work with an alternating current of 220 V. Automatic switching on and off of the generator on the side of low voltage is performed by means of a two-pole electromagnetic switch of type MSW-34. In the third phase, a one-pole knife switch is seen. The contact of each of the circuit breakers, calculated for 150 A, are connected in parallel to a 300 A current of the generator. The connecting takes place automatically, as soon as the synchronal number of revolutions is obtained. Closing of the switch contact is performed by means of a centrifugal mechanism which is turned by means of one of the intermediate transmission shafts of the wind engine.

Tests for exploitation of the wind power station D-30 were performed under two sets of operating conditions: at 19 and 30 rpm of the wind wheel. It appears that the operating conditions of a wind power station working with 30 rpm is considerably better. The characteristics obtained in the tests are shown in Fig. 325. The maximal output coefficient of wind energy of the wings $\xi = 0.242$ was obtained at the rapidity $Z_n = 4.75$ which was in good agreement with the results of tests performed with the D-10 model on the tower of the wind power laboratory. /511

The characteristics were taken in the following manner. The observed values of the power fed into the circuit at a low level

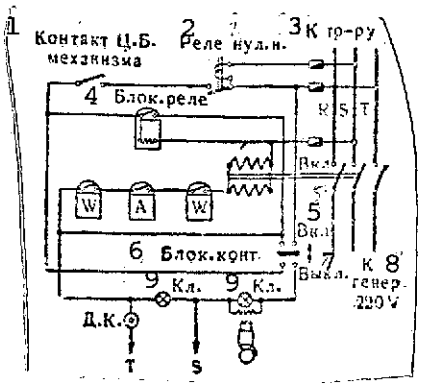

Fig. 324: Basic diagram of automatic connection and protection of the generator.

Key: 1. contact of the centrifugal mechanism
2. relay of the zero lever
3. to the transformer
4. block relay
5. switch
6. control block
7. circuit breaker
8. to the generator
9. key

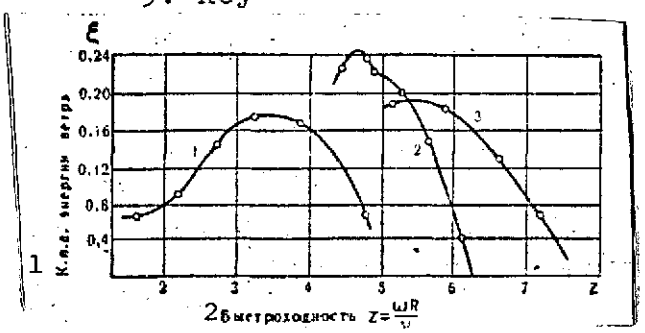

Fig. 325: Aerodynamic characteristics of the wings in the D-30 wind power station.

Key: 1. efficiency of the wind energy
2. rapidity

of the step up transformer 220/6300 V were averaged for 20 minutes. These values were determined by the difference in the counter readings in kilowatt hours and were checked with the recordings of the wattmeter. The average wind velocity for the 20 minute time interval was measured on a mast at a height of 25 m, corresponding to the center of the rotation of the wind wheel. The mast was set up at a distance of 50 m from the wind engine.

The recordings of wind velocity were performed by means of the recording anemometer with an electric contact after 500 m of path crossed by the wind. /512

The recorded power over an interval of 7 minutes is presented in Fig. 326. The curve shows that the power fluctuations of the asynchronal generator over this short interval of time did not exceed 30% in the limits of permitted overload.

The performance tests revealed the entirely adequate operation of the installation and of the automatic device [38].

Description of the project of the wind power station with the D-50 m wind engine. Worth mentioning is the project of the wind power station with the D-50 m wind engine which was intended for parallel operation in the general circuit with a thermic power station with a power of 7500 kW and with a hydropower station with a power of 48000 kW.

The general view of this wind power station is illustrated in Fig. 327. The cabin of the generator is situated on top of the tower and can turn about its vertical axis during adjustment of the wind wheel to the wind. /513

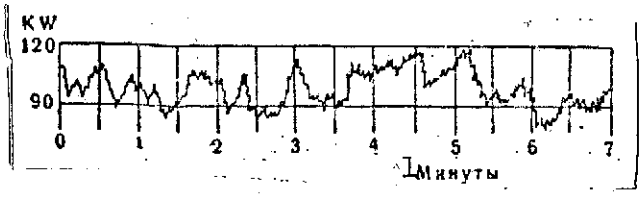

Fig. 326: Recording of the power of D-30 wind power station during operation with asynchronal generator connected in parallel.

Key: 1. minutes

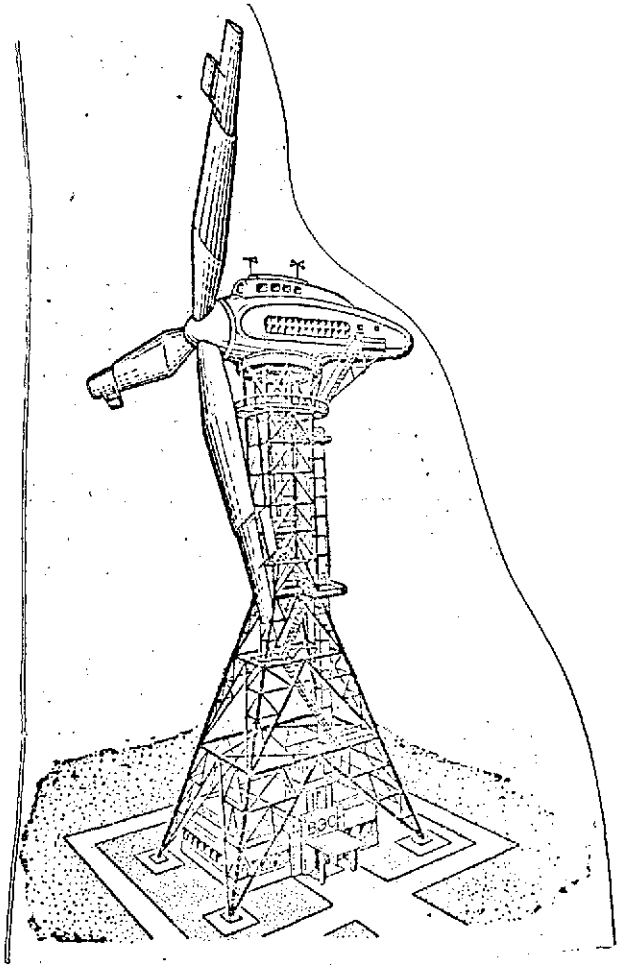

Fig. 327: The TsVEI D-50 wind power station, 1000 kW (project).

The transmission of rotation from the shaft of the wind wheel to the generator is performed through a 2-stage reducing gear with a gear ratio of 1 : 25. The wind wheel /514 makes 24 rpm, while the generator makes 600 rpm. The cutaway of the cabin in its general view is shown in Fig. 328. In addition, the cabin of the wind engine contains the motor of the adjustment to the wind and the on/off motor of the wind engine. All the remaining electrical equipment is situated below under the tower in the substations.

The voltage of the synchronal generator equals 6300 V and 600 rpm; the power of the wind power station equals 1000 kW at 14 m/sec wind velocity. The annual average wind velocity in the region where it is suggested to build the wind installations amounts to 7-8 m/sec. The number of working hours per year of the wind power station was calculated to be 2380 hours with the output of 10 D-50 units being 2.2 million kW hr per year. The project cost per kW hr is 1.8 kopecks, while the cost of steady kW of power is 425 rubles.

The three-blade rapid (Z_n = 6) wind engine of the power station with aerodynamic regulation of the blade tip rotation by means of stabilizers was suggested by G. Kh. Sabinin and N. V. Krasovskiy.

Use of this type of regulation has enormous advantages in the sense of reliability of operation, which is known from the practice of operation of the D-12 wind engine regulated by this system, as well as in the simplicity of construction and low weight of the regulating device. /515

Adjustment of the wind wheel to the wind is performed by means of an electromotor which is mounted on a cramp iron girder in the

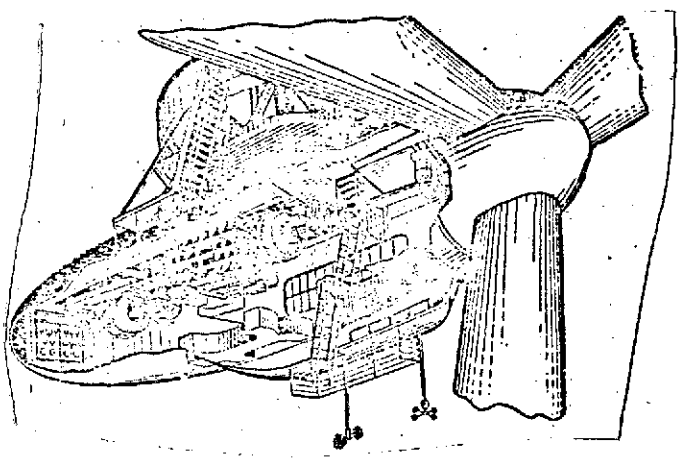

Fig. 328: Cabin of the TsVEI D-50 wind power station.

lower part of the cabin. This motor is connected by means of a worm gearing with two long shafts which carry a second worm gearing, the latter engaged with pins of the rim fastened to the tower.

The cabin contains the small wind engines with vertical plane passing through the axis of the shaft which rotates during the changes in wind direction; the stop motor is connected by means of an electrical transmission and it operates as long as the wind wheel does not stand into the wind; in that moment the small wind engine is turned off.

The height of the tower is 50 m; dimensions of the base 25 x 25 m. An elevator goes to the upper balcony of the tower. In addition, there is a ladder incase the elevator is out of use.

At the base of the tower a building is situated, which contains the main distributing installation of the electrical parts.

The pulsating nature of wind energy and its lack of constancy with regard to velocity and direction, as well as the complete automation of the controls were the consequence of complicating the commutation diagram. The following main elements were elaborated in the general commutation circuit:

1. automatic start and stop of the wind power station, determined by the presence or absence of wind;
2. automatic synchronization;
3. automatic regulation of voltage by a rapid voltage regulator;
4. automatic disconnecting of the wind power station by actuation of one of the accident protection devices without repeated connection of the automatic device;
5. automatic adjustment of the wind engine to the wind;
6. limitation of the power at strong wind gusts by means of a hydraulic clutch permitting slipping of the main shaft.

For the sake of illustration, we present the weight of the wind engine parts:

Wind wheel	35 t
Girder of the head	20 t
Mechanical part of the wind engine	63 t
Tower, ladder and elevator	52 t
Overall weight	160 t

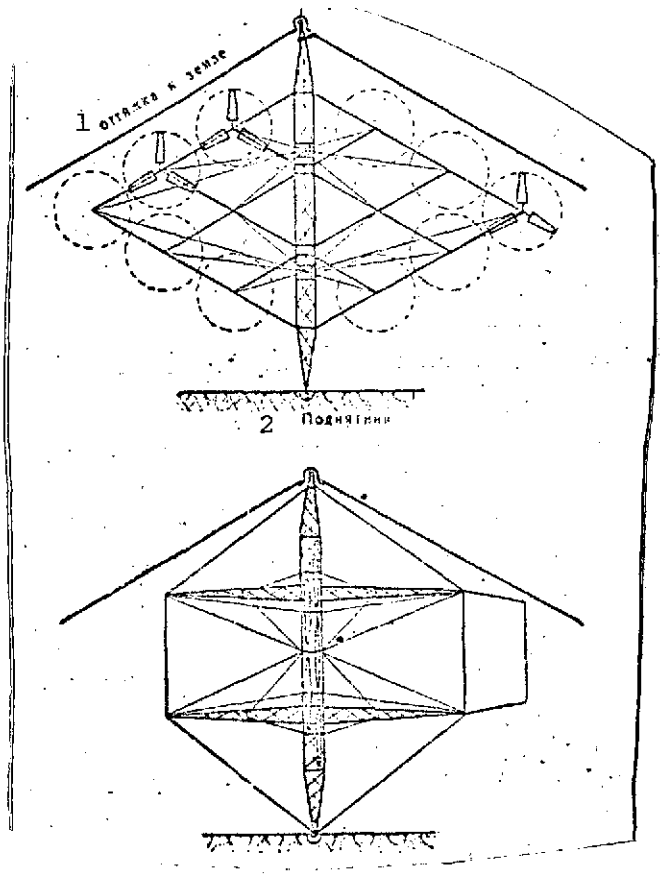

Fig. 329: Diagram of a wind power station with many wind engines in the A. G. Ufimtsev and V. P. Vetchinkin system.

Key: 1. guide rope to the ground 2. hoist

The wind power station with many wind engines. A. G. Ufimtsev and Prof. V. P. Vetchinkin suggested to solve the problem of a powerful wind power station not by increasing the dimension of the wind wheel's diameter but rather by means of a large number of wind wheels with relatively small diameters, mounted on the general tower of a frame construction (fig. 329). /516 /517

The frame with a chessboard distribution of the wind wheels is mounted on a girder rotating tower. Tie beams coming from the upper support maintain the tower in vertical position. Twelve wind engines with a diameter of the wind wheel of 20 m each are mounted on the frame. The overall power is about 500 hp at the wind velocity of 8 m/sec. A similar power can be given at the indicated wind velocity by a wind engine with a single wind wheel having a diameter of 70 m. But while it is very hard to make 70 m wind wheels, wind wheels with a diameter of 20 m are available in practice. This circumstance was the motive to suggesting a wind power station containing many wind engines. There are as yet no such wind power stations in practice.

68. Brief Data on Foreign Wind Power Stations

Fig. 330 illustrates a wind power station with a power of 30 kW manufactured by the general electricity company, with a wind engine of the Kumme system.

A motor power of 45 kW is large for the indicated wind power station and requires a secondary machine; for this purpose a dc generator is used with parallel excitation, 44 kW, which is set in motion by means of a reserve engine which is started in parallel with the wind engine during maximal energy comsumption i.e. during thrashing. The operation of both machines is quite adequate with the diagram shown in Fig. 331. Here a 3-wire system 2 x 230 V /518

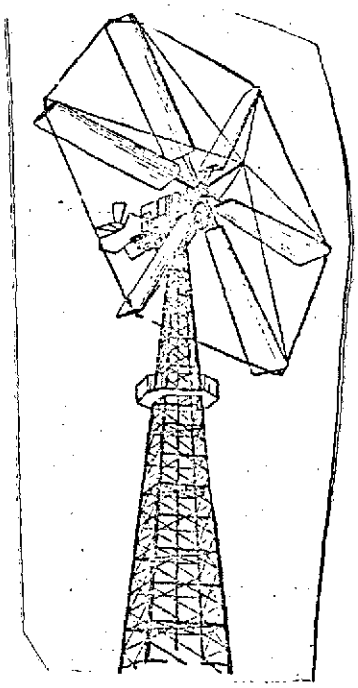

Fig. 330: The 30 kW wind power station with wind engine of the Kumme system.

is used with distribution of the voltage through a battery. The charging unit consists of a model with parallel excitation and a voltage augmenter. The storage battery contains 240 elements of type AK for the highest power of the charging current of 36 amperes.

In the United States, low power wind charging units with two-blade propellers fitted directly on the axis of the generator of a special low speed type are widely distributed.

The dc generator of the "wind charger" low power wind charging unit gives a voltage of 6 V, while the current in relation to the number of revolutions is illustrated below:

Revolutions of the dc generator	330	370	440	500	600
Amperes	1	2	4	5	8

/519

Revolutions of the dc generator	700	860	1060
Amperes	10	12	14

A two-blade propeller with the length 1.5 to 1.8 m can give 300 to 1000 rpm if the width of its blade and the rigging angle are computed for a rapidity $Z_n > 7$.

Wind charging units with a power exceeding 100 W are manufactured with a reducing gear since the propeller with a diameter exceeding 1.8 m cannot develop the number of revolutions required for the dc generator at a wind velocity of 8 m/sec.

Fig. 332 shows the general view of the "Wincharger" wind charging unit with a 32 V dc generator. The power of the wind charging is 650 W. The gear ratio of the revolutions of the dc generator to the revolutions of the propeller equals about 5. Limitation of the revolutions is achieved by means of an aerial brake, secured to the shaft of the wind wheel. At a certain radius from the axis of rotation, surfaces which have a curvature along the radius of its rotation are secured, in order to obtain smallest resistance during normal revolutions of the propeller. As soon as the wind wheel picks up in the number of revolutions and reaches a value above normal, these surfaces are deflected under the effect of

/520

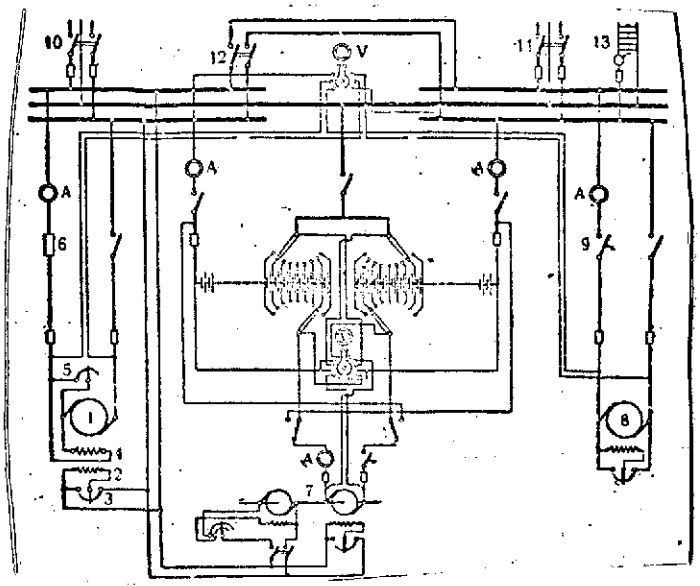

Fig. 331: Diagram of connection of the wind engine and of the reserve model.

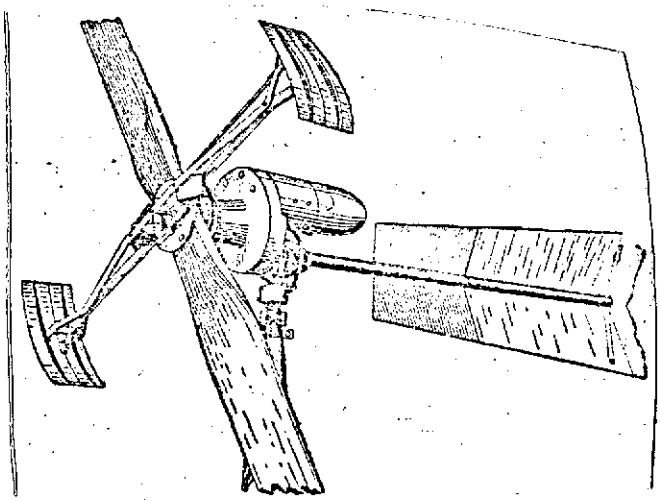

Fig. 322: The "Winchanger" wind charging unit.

centrifugal forces. When fully deflected, these surfaces become perpendicular to the direction of movement and create a resistance. In the reverse position, the surfaces are stopped by the force of the spring. The structure of the reducing gear and of other parts of the unit are illustrated in Fig. 333.

The "Wind-Impeller" company releases wind charging units (Fig. 334) of the same power as the "Wincharger" with the only difference that the aerial brake used for limiting the number of revolutions of the propeller is made of surfaces which rotate in the plane of rotation of the wind wheel (Fig. 335). The braking surfaces lie in the plane of rotation in normal revolutions (see illustration, a); when the number of revolutions exceeds the normal value under the effect of centrifugal forces of their own weight, the blades start to move along the radius and may overcome the force of the spring shown in position b. These surfaces are fitted with their bushes on the axis, which is disposed in the plane of rotation of the wind wheel perpendicularly /521 to the propeller. Pins c pass through helical cuts a in the bushes, due to which the surface turns about the axis during the movement of the bush along the axis and is stopped by a plane in the direction of movement, as illustrated in Fig. d, and a resistance is created.

These wind charging units are released with a power 100 W to 5 kW.

In recent years, attention has been accorded in the United States to high-power wind power stations.

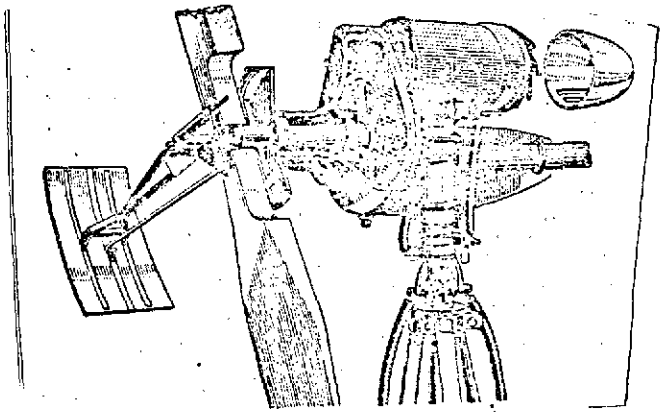

Fig. 333: Head of the wind charging unit shown in Fig. 332.

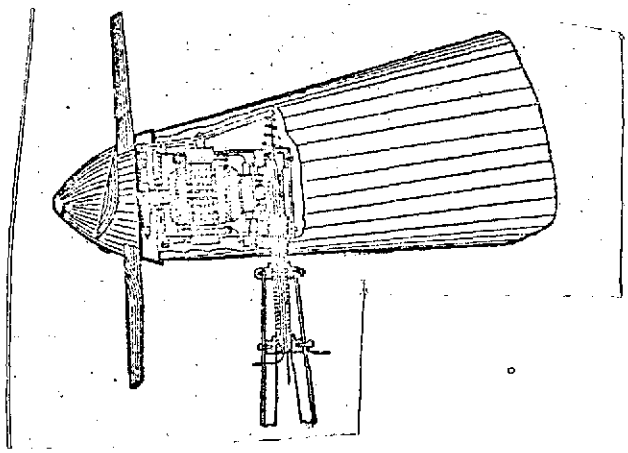

Fig. 334: The "Wind-Impeller" wind charging unit.

Fig. 336 illustrates a 1000 kW wind power station built near the town of Rutland in the state of Vermont on top of the Grantpass Mountain, the height of which is about 610 m above sea level.

The tower of the wind engine is of girder construction, has a height of 35 m and is fastened to a steel lattice which is laid in a concrete foundation at a depth of about 7 m. The two-blade wing wheel with a diameter of 53 m has a blade length of 20 m and a width of 3.7 m, which is uniform throughout the length. The power developed at a wind velocity of 14 m/sec and 28.7 rpm is 1000 kW. The circular velocity of the blade tip is 80.3 m/sec which results in a rapidity of Z = 5.72. The overall weight of the wind wheel is 20 t. Regulation of the revolutions is achieved by rotation of the blade about the axis of the flap. The flaps of the wings are hinged to the shaft in such a manner that during wind gusts they deviate in the direction of the wind by 20° under the effect of the impact load, which helps the regulator to limit the number of revolutions of the wind wheel. The centrifugal forces of the blade turn to maintain it in the plane of rotation of the wind wheel. The generator developes a nominal power of 1000 kW at cos ϕ = 80%, voltage 230 V, 60 periods of 3-phase current. The electrical wiring from the generator goes down through central openings in the girder of the head and joins the contact rings mounted on the hollow shank of the contact rings. The brushes on these contact rings join the cables which guide the current to the transformer group where the voltage is increased for the purpose of connection with the line of transmission of the electrical power system. /522 /524

The shaft of the wind wheel has a diameter of 61 cm and rotates on two double roller bearings mounted at a distance of about 3.7 m from each other on the supporting frame of the head. The bearing situated directly behind the wind wheel is radial, while the bearing near the clutch for regulation of revolutions intercepts both loads, the radial and the head load. The shaft of the wind wheel is

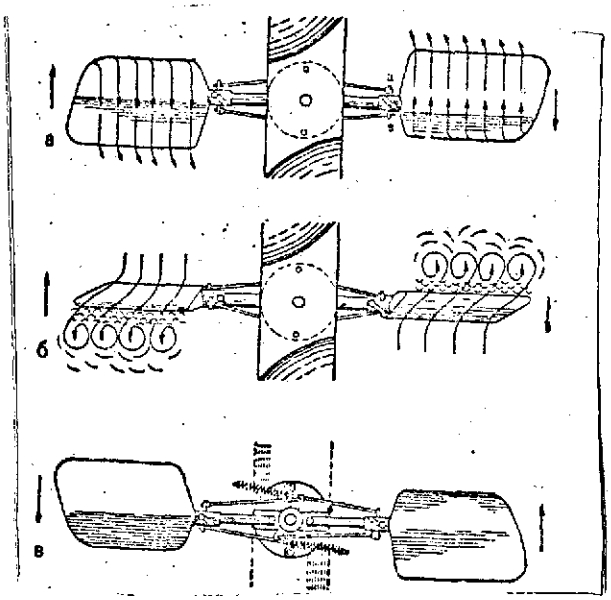

Fig. 335: Regulation of "Wind-Impeller" by changing the position of the braking surfaces of the wind wheel; a-at normal number of revolutions; b-braking surfaces turn under the effect of centrifugal forces; c-kinematic connection of the surfaces.

connected to a two-stage reducing gear with chevron gearing, which increases the number of revolutions given by the generator to 600 per minute. In the first stage, the revolutions are increased by means of teeth which are geared with the notches on the wall from each side in one plane which passes through the shaft axis. The shaft of the second stage of transmission is connected with the shaft of the generator of a hydraulic clutch released by the American Blower Company. On the external side, the generator is directly connected with the exciter. The standard velocity regulator with additional electrical conduct is set in motion through a tooth-gearing from the main shaft of the wind wheel.

Adjustment of the wind wheel to the wind is performed by means of a hydraulic mechanism which sets in motion the transmission mounted on the girder of the head which is engaged with a large gear wheel, fastened to the upper crown of the tower. The connecting and disconnecting of the mechanism of adjustment to the wind is performed by means of a wind vane which is constantly adjusted to the wind.

The wind engine is stopped by means of a braking device with frictional transmission which is set in motion by means of an electric motor.

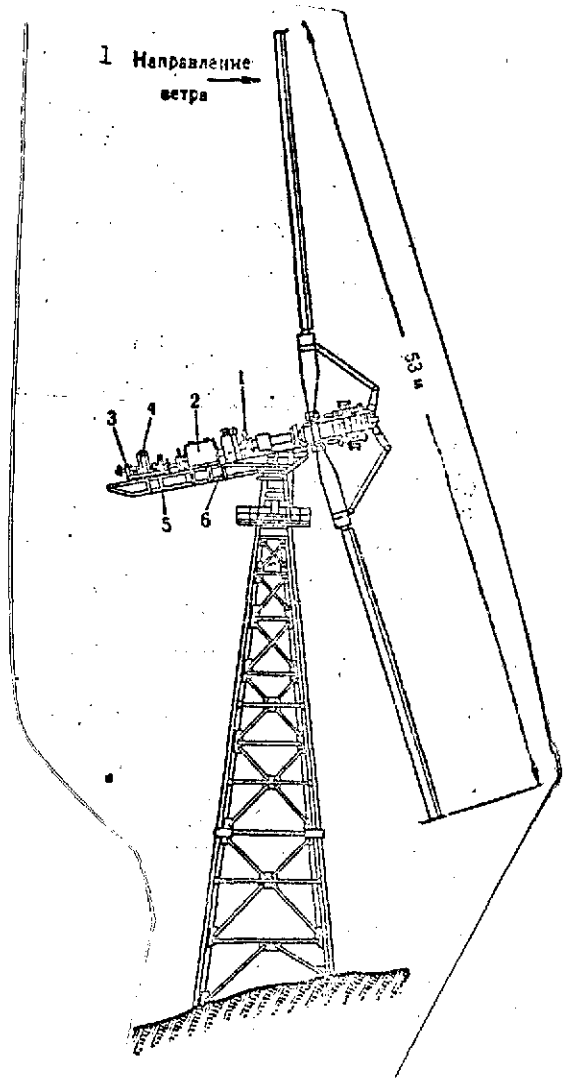

Fig. 336: The 1000 kW American wind power station.
1-velocity regulator
2-reducing gear
3-exciter
4-generator
5-hydraulic clutch
6-oil tank

Key: 1. wind direction

From October 1941 through March 1945, this wind power station yielded 360, 000 kW hr. During this period it worked for 1030 hours, of which the installation worked for 838 hours with an average power of 431 kW while connected in parallel. In March 1945, an accident took place in the wind engine, the 7 ton blade of the wind wheel broke during the run. The accident occurred due to the inadequate system of regulation.

CHAPTER 17. BRIEF DATA ON THE INSTALLATION AND MAINTENANCE OF WIND ENGINES /525

The installation of factory made wind engines has an extraordinary importance for the introduction of wind engines in agriculture. Poor fitting of the parts of wind engines during the installation may cause not only poor operation of the wind installation but the latter may become entirely unserviceable.

Detailed instructions on the sequence of installation of various types of wind engines are given in the instructions compiled either by the manufacturer for each type of wind engine released or by the organization which designed the wind engine.

69. Installation of a Low-Power Wind Engine, from 1 to 15 hp.

The installation team usually consists of 5 or 6 workers and one qualified foreman.

The first work of the team consists of unpacking and checking the assembly parts of the wind engine which are supplied locally. During the checking they have to make use of the specifications contained in the instructions on installation which come together with the given set of wind engine. If insufficiencies or unserviceable parts are discovered, a document is immediately compiled and sent to the manufacturer for timely completing of the set.

Subsequently the foreman takes the measurements of the foundation pit under the legs of the tower in the place selected for setting up the wind installation. If the wind engine is built for the lifting of water, then the position of the pit with respect to the vertical axis of the tower is taken into account.

Installation of the wind engine is started with assembly of /526
the tower. The main angle bars of the legs in one of its panels is laid out on logs in such a manner that after lifting the tower, its axis would correspond exactly with the mark made for the center of the tower at its base. If the axis of the tower does not coincide with the mark of its center on the foundation, then considerable labor is required in order to shift the lifted wind engine.

After assembly of the tower, the head and the vertical shaft of the wind engine are assembled. Dirty parts of bearings and of the necks of axis and shaft are washed with kerosene and lubricated with fresh grease. The engaging of the upper transmission, which is assembled in the head of the wind engine, is checked by several rotations about the hub of the wind wheel. During this operation, the head is turned with the axis of the wind wheel pointing upward. The wind wheel and the mechanism of adjustment of wind engines with a power of up to 10 hp are assembled below at the same time with the assembly of the head.

The assembled wind engine is lifted in a tilted position and laid with the upper compartment on bounces (Fig. 337), and it is supplied with the rigging equipment. For the sake of reference, Table 48 presents data of the rigging equipment used in practice for lifting the TV-8 wind engine. /527

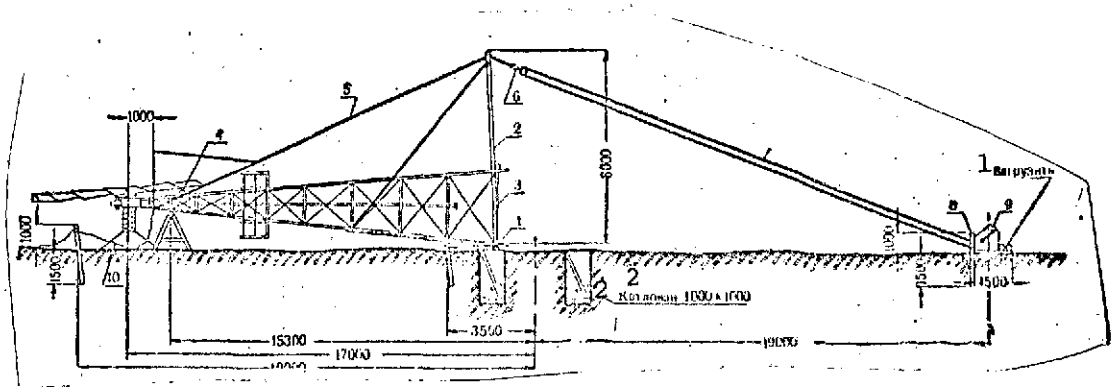

Fig. 337: Equipment of the wind engine with the rigging equipment prior to lifting.

Key: 1. apply load
2. foundation pit

Prior to lifting the wind engine, the strength of its rigging is checked; for this purpose the wind engine is lifted to several centimeters above the support by means of the loading winch and, leaving it in this position, an additional load is placed on the head of the wind engine. Usually this load is formed of 4 to 5 people who stand on top of the tower (Fig. 338). By this means, the fitting and the checking of the equipment takes place since it is in this position that the forces directed along the cable are the largest. The general aspect of the lifting of a TV-8 wind engine is illustrated in Fig. 339. /528

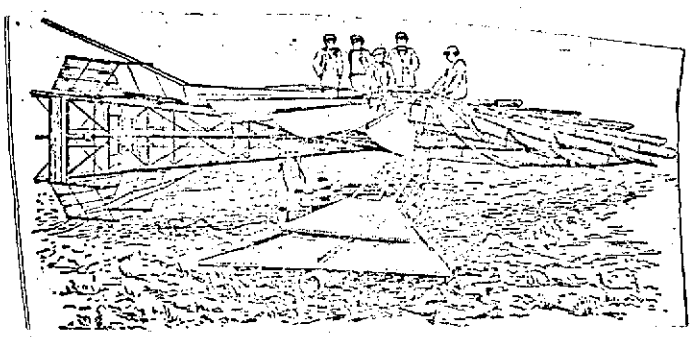

Fig. 338: Checking the equipment of the wind engine.

If the wind engine is intended for lifting the water from a pit, then an excavation is made under the pit in order to set up the pump equipment between the legs of the tower; the walls of the pit are made of brick or rubble walling in cement mortar. Fig. 340 shows the foundation and the pit of the pump equipment for the TV-8 wind engine with main installation dimensions. /529

TABLE 348. RIGGING FOR LIFTING OF THE TV-8 WIND ENGINE

Name of Part and Accessory	Dimension of the material	Amount
1. Loading winch, 3 t	-	1
2. Single-drop block, 5 t	-	1
3. Block rollers under cable 17.5 mm	-	2
4. Anchor log for rear guide rope	Pine d=22 cm ℓ=2 m	1
5. Derricks	Pine d=22 cm ℓ=8 m	1
6. Cross beams	Pine d=25 cm ℓ=6 m	2
7. Log for supporting the legs of the tower	Pine d=12 cm ℓ=5 m	2
8. Foundation pit	Pine 13x13 cm ℓ=1 m	8
9. Anchor log of lower cross beam	Pine d=25 cm ℓ=5 m	1
10. Anchor log of winch	Pine d=25 cm ℓ=3 m	1
11. Loading steel cable	d=17.5 mm(6x37x0.8+1) ℓ=100 m	1
12. Anchor cable of winch	Steel (6x37x0.8+1) d=17.5mm ℓ=15m	1
13. anchor cable for cross beam	Steel (6x27 8+1) d=17.5m, ℓ = 20 m	1
14. Bracing wire of cable derrick	Steel (6x30x0.5,5+1) d=10 to 12 mm, ℓ=20 m	1
15. Guide rope of cable	Steel (6x30x0.5+1) d=10-12mm, ℓ=50m	2
16. Support cramp for rollers	Bar-iron 100x12 mm	1
17. Axis with nuts	Round-iron d=30mm, = mm[1]	1
18. Stud bolts with nuts	d=3/4" ℓ= 36 cm	4
19. Washer	Bar-iron 10x80 mm	2
20. Yoke of junction	Round-iron d=3/4",	1
21. " " "	Bar-iron 10x60 mm	4
22. " " "	Round-iron 10x60 mm	1
23. Steel block cable	d=17.5mm, (6x37x0.8+1) ℓ=8m	1
24. Bolts with nuts	d=3/4", ℓ=5m, Round iron	8
25. Support log for rear guide rope	d=32 cm, ℓ=120 cm	2
26. Cross log under wind wheel	d=15 cm ℓ=6 m	1

More powerful wind engines are also lifted in the assembled form, but without wind wheel and tail. These parts are lifted after the tower is secured to the foundation, for which purpose the girder with two blocks is set up on the head of the wind engine (Fig. 341). A cable is thrown around these blocks to which first the wind wheel is secured which is lifted with the winch, and then the tail. /530

1. [Number in original illegible]

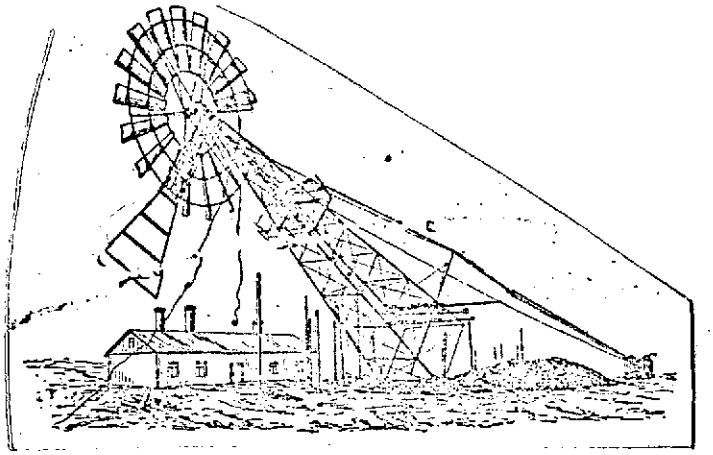

Fig. 339: General view of TV-8 lifting.

After setting up the wind engine, the transmission from the wind engine to the power tool is assembled.

Wind engines with a power above 25 hp are assembled in parts. The tower is assembled from scaffolding. The individual parts of the wind engine assembled below are lifted by means of a "derrick" crane. Fig. 342 illustrates the installation of the D-30 m Crimean wind power station by means of the "derrick" crane (for description of the station, see Section 67).

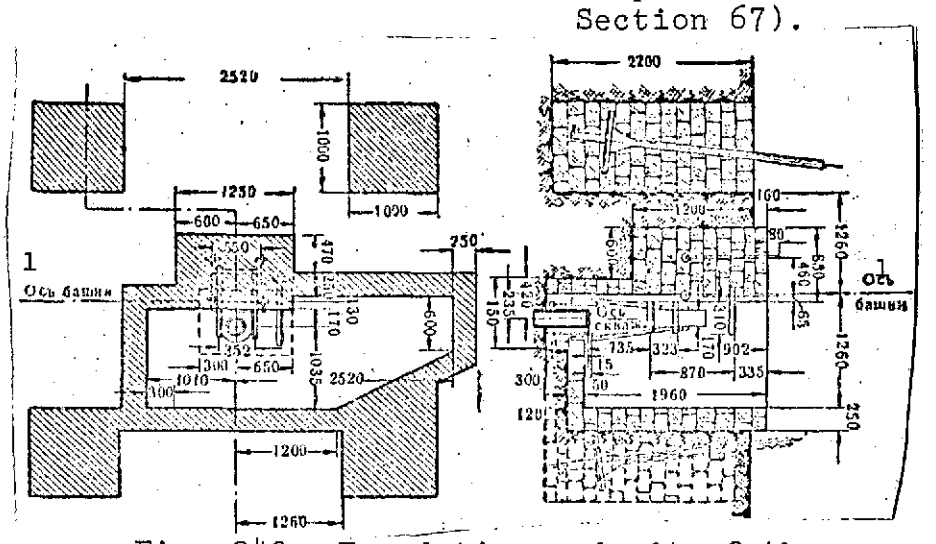

Fig. 340: Foundation and pit of the pump equipment.

Key: 1. Tower axis

Checking the installation and setting up the wind engine for operation. Upon completion of installation, the transmission, regulation and adjustment to the wind are checked. The wind engine has to be regulated in such a manner that the mechanism starts to limit the revolutions at a given wind velocity. For example, in regions with an annual average wind velocity of 4-5 m/sec, the wind engine should start limiting the revolutions at a wind velocity of 8 m/sec. By means of a larger or smaller tie beam of the regulating spring it is achieved that the wind engine starts to limit the revolutions at the required wind velocity. /531

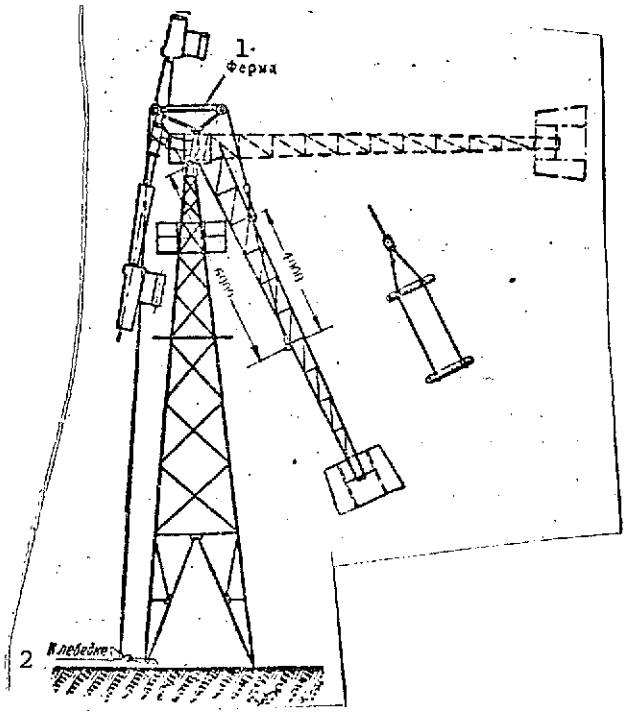

Fig. 341: Lifting of the wind wheel and of the tail by means of blocks.

Key: 1. girder
2. to the winch

Checking of the regulation is performed by starting the wind engine. Those wind engines which are regulated by removal of the wind wheel from the wind are started under load. If the removal of the wind wheel is performed by the pressure of the wind either on the side blade or on the wind wheel which has a certain eccentricity, than this checking must be performed at wind velocities which vary from 7 and above 8 m/sec in order to check the wind velocity at which the regulating mechanism is actuated. /532

If the wind engine is regulated under the action of centrifugal forces, than the check must be performed also at low wind velocities but without load, since in the given case the centrifugal regulator starts to operate at a certain number of revolutions which has to be found out during the checking.

Measurement of the wind velocity during the checking of regulation is most conveniently performed by means of an anemometer which shows the instantaneous fluctuations in wind velocity. For this purpose, it is convenient to use an instrument with a voltmeter the scale of which is calibrated to wind velocity. At the same time with checking the regulation, the precision of the transmission and of other parts of the wind installation is checked.

The installation team releases the wind installation to the farm after checking its operation in the course of 24 hours. If any imprecision in the operation of the different mechanisms is observed during this time as a result of unsatisfactory installation, than the detected shortcoming should be removed, and only after this can the wind installation be sent to the farm with the document for putting in operation.

70. Maintenance and Servicing of Wind Engines

As compared to other engines, the wind engine is under more difficult conditions of operation. Atmospheric precipitations (ice crust), gusty winds and storms create variable loads wh

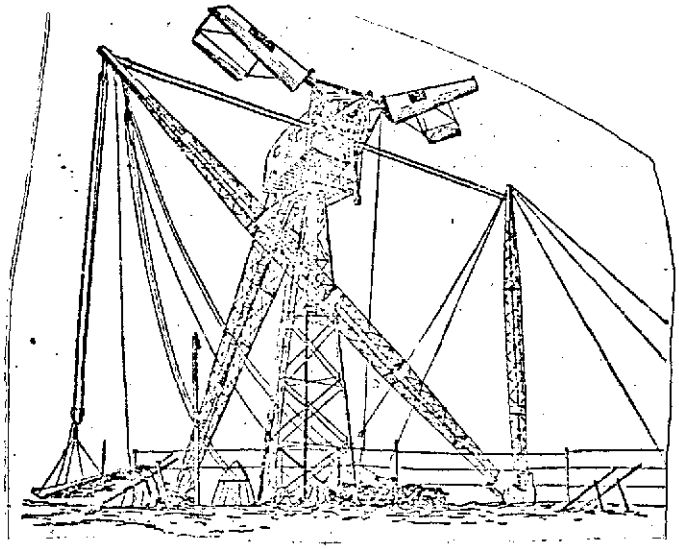

Fig. 342: Installation of the wind engine by means of the "derrick" crane.

which acts on its parts both during operation and during standstill. In order to prevent breakage of the wind wheel and to keep the wind installation in good condition, the man in charge should be acquainted with the mechanism and should be able to remove any trouble noted during operation of the engine.

The duties of the man in charge of the wind installation are compiled in instructions which should be hung up in the building of the installation. The same building contains a set of the following tools: fitting hammer, cold chisel, 0.5 ℓ oil can, 10 kg can for grease, 15 kg. can for oil, spanner and adjustable wrenches, fire-fighting belt with spring and rope with a length of 4 m and a thickness of 45 mm, an oil lamp -- hurricane lamp, and a set of overalls. The duties of the man in charge which are common for all wind installations consist in the following. /533

Daily examination of the bolt joints, tightening loosened nuts, bolts and wood screws. During the examination, all the places where parts rub against each other must be lubricated. The oil used for automatic lubrication must be renewed once in six months. Processed and dirty oil should not be used for lubrication.

The man in charge should not allow any outside people to climb on the tower. The following should also be kept in mind. The wind wheel must not be tied to the tower. If it has to be slowed down, then it may be tied only to the tail or to the head. The wind wheel may be tied to the tower only in the case that it is adjusted to the wind manually instead of by the tail.

The wind engine should be loaded only to the power for which its transmission was calculated. If the wind engine is regulated by the action of centrifugal forces, then it can be overloaded at high wind velocities. The excess load will lower the increasing number of revolutions; under these conditions, it will be able to operate with a load which corresponds to the power of the wind engine increasing proportionally with the cube of the wind velocity. For example, if a D-12 wind engine with a calculated power of 15 hp at

a wind velocity of 8 m/sec were to be loaded with the increase in wind velocity above 8 m/sec, then at 16 m/sec it could provide for work with a load corresponding to 120 hp at an insignificant increase in the number of revolutions. Naturally, such an overload would cause breakage of the transmission mechanism.

Maintenance of the wind engines, as of other machines, consists in repairing old worn or broken parts and their replacement with new parts. No standard has been yet set out for wind engines which would allow usage of a known system of periodic preventive maintenance, and therefore, in order to prevent accidents caused by excessive wearing of parts, the general method of trouble shooting common for all machines are used in the maintenance practice of wind engines. With regard to the organization of maintenance in wind engines, this has its own specific features which result from the conditions of operation of these machines. Undoubtedly, when wind engines will be introduced at a large scale, an improved maintenance system will be introduced, like those which are now used in the tractor and automobile business. /534

Periodic preventive maintenance is used wherever the intervals after which a certain repair has to be performed can be established in advance and a definite maintenance plan can be set up. This maintenance system can be divided into current, medium and major maintenance.

Technical maintenance is intended for removing insignificant defects in the equipment and is carried out by the servicing personnel without participation of the maintenance workshop or of the maintenance team.

The current repair includes the repairs of parts which are accessible to examination as well as of parts which require immediate repair or replacement without involving complete dismantling of the machine. These repairs should remove any detected deficiency as long as this is not reflected in other parts. In such a manner, current maintenance plays an important role during the service life of the wind engine as is the case for other machines.

Medium repairs are distinguished from the current repairs by a more advanced dismantling of the machine. For example, for the maintenance of the wind engine, this includes removal of the wind wheel, replacement of the rods or of pinions, etc. At the same time other accessories are repaired including all the operations of the current maintenance.

Major repairs are performed after a certain period of operation of the machine when the latter is in a condition that neither the current nor the medium repairs can remove deficienies due to wearing of the machine. All the parts and accessories are checked and maintenance of the wind engine involves its "knocking down" to the ground.

In this case, participation of the entire team is required with rigging equipment and a complete set of tools which are used in maintenance and installations. During maintenance, the wind engine is put out of operation for a long period of time.

Accidental defects of the machine are removed either by the medium repairs or the major ones depending on the degree of the damage and on the general condition of the machine after the accident. In the practice of wind engine maintenance, two types of repairs are used, the current and the major repairs.

The wind engine is subjected to wearing not only during its operation when the transmission and the bearings are exposed to /535
wearing but also during standstill of the wind engine as a result of the constant action of wind gusts. During standing, the support in the head, the hinges in the tail, the supports of the rotating blades etc. are being worn out.

The constant action of the wind as well as of atmospheric precipitations on the working parts which are usually in the strongest wind flow, place the wind engine under quite difficult conditions of operation.

Therefore, examination and current repairs of the wind engine must be performed daily. This maintenance includes several preventive measures which make it possible to decrease considerably the wearing of the parts and to reduce to a minumum the various troubles and accidents. In order to perform the major maintenance, the construction of the nuts and of the mechanisms of the wind engine should be known as well as of the interaction of its parts. Consequently, the leader of the maintenance should be qualified in the field of wind installations.

It is advisable to organize maintenance of the wind engine from mobile installation and maintenance workshops. This is a closed truck equipped with all the required mechanical equipment such as wall-mounted manual drilling machines, vice, a set of fitting and forging tools, etc. The truck should contain a store for reserve parts and small maintenance materials.

71. Safety Measures During Installation and Servicing of Wind Engines

The devices and structures which provide for the safety of the worker can be divided into: 1-individual protective devices, 2-barriers and 3-preventive equipment.

The individual protective devices are intended for every worker, here belong the preventive (protective) glasses, overalls and working boots, helmets and gloves for electrical welding, life belts and climbing irons for those who work at height.

The barriers are used in order to forbid the access of people to the dangerous sites as well as to protect them from dangerous objects and possible falls from high places.

Preventive structures are intended for signaling the advent of danger or for removing danger in the due moment. /536

Work at a high level takes place mainly during installation, maintenance and servicing of the wind engines. These works are performed by people who underwent medical examinations. It is forbidden to allow people suffering from giddiness, epilepsy, cardiac diseases etc. to work at high levels. Wherever it is possible, constant areas of sufficient dimensions, with rails having a height of no less than 1 m and a continuous sheathing below must be provided for works at heights in order to prevend disabling injuries to someone passing by from an object which might fall from the area.

A ladder with hand rails should lead to the area situated at the high level.

For work to be performed on the head of the wind engine, life belts should be used on grounds of safety. Safety of the work depends on the reliability of the belt and of the rope to which it is attached. Prior to use, the belt and the rope should be tested with a weight of 100 kg which is thrown five times from a height of 2 m; the length of the rope for tying up the worker should be 2 m. The belt and the rope should be preserved in a dry place in the store house.

Sound climbing irons must be used in work to be performed on telephone poles and on wooden masts of the wind engines.

The most dangerous moment during the installation of the wind engine is its lifting from the ground (Fig. 339). Careless and hasty assembly of the equipment (Fig. 337) as well as incorrect organization of the installation may be the cause of serious accidents in which apart from the inevitable breaking of the wind engine, misfortunes involving people may occur.

The foreman of the installation team should strictly observe the following elementary rules for a successful and safe lifting of the wind engine:

1. To use logs which correspond to the timber forseen by GOST for the rigging equipment. When used logs are utilized, such logs which are weakened by cuts, holes, kerfs as well as rotten logs should not be used. The thickness of the logs should not be less than the thickness indicated in the specifications of the dimensions which refer to the upper end of the log and not to the butt. /537

2. The loading winch should have frictional brakes. Winches of the old model with band brakes should not be used.

It is forbidden to do the lifting or lowering of the flyweight with put off trigger since under these conditions the frictional brakes of the winch cannot operate. Lowering of the flyweight by means of the winch is performed by turning the handles to the side opposite to the direction of lifting.

3. In joining the wooden units of the lifting equipment, wide washers should be placed under the nut of the bolts.

4. It is not allowed to have sharp bends in the steel cable at the knot where it is fastened to the lifted flyweight. If the cable lays on sharp angles of the flyweight to be lifted or on its wooden part, then special hempen mats or at least rags, pieces of boards, plywood, etc. should be placed under it.

5. It is forbidden to have the cable rotate during the winding of the winch on the drum since lasting twists in the wires cause an additional stress which may cause rupture. During the winding of the loading cable on the drum of the winch, one has to take care that it is disposed in even rolls without forming bulges, since slipping of the cable from the bulge is accompanied by vibrations of the lifted weight with an impact effect on the equipment which may cause breakage of the weakest knot.

6. In order to prevent rupture of the cable or of the knots in the equipment during the lifting, the strength of the equipment must be checked prior to lifting. The head of the wind engine is lifted by means of the winch to a height of 10 cm above the supports, the lifting unit is secured and the wind engine is left in the raised position. This position causes the greatest stress in the equipment. Subsequently an additional load is placed by having 4-5 people mount on the wind wheel (Fig. 338). Under such a load (about 300 kg), the cables of the equipment are tightened and if they do not rupture under these conditions then no rupture will occur during the subsequent increase of the tilt since with the increase of the angle of inclination between the tower and the wind engine, the stress decreases and approaches zero when the tower assumes a vertical position. No load is admitted during the lifting or under the tower /538 when the latter is in an inclined position.

7. It is desirable and preferable to do the lifting in calm weather; if there is a wind, its velocity should not exceed 5 m/sec.

8. In winter time it is not possible to do the lifting at a temperature below 12-15°, since at low temperatures the equipment becomes brittle and less durable.

Practice shows that even in the southern regions of the USSR, the installation works cost more in the winter and their quality suffers.

9. Use of the ladder for both climbing and descending is permitted without any load. Light objects must be placed in the pockets or hung on the belt. Heavy accessories must be lifted or lowered by means of a rope or cable.

10. The guide rope and the loading cable should be released only after the tower is fully secured.

11. When the wind engine is started, no one should be in the area on top of the tower.

12. The leader of the lifting operation should give his instructions to the workers near the loading winch by means of prearranged signals. The workers near the winch are obliged to receive only those signals which are given by the leader of the lifting operation. In order to avoid confusion in the work, no other instructions should be given.

A specially assigned man who is acquainted with the requirements of safety measures should be servicing the wind installation. This requirement can be reduced to the following:

a. examination and lubrication of the wind engine parts when the wind engine is at standstill;

b. foreign people and especially children should be prohibited from access to the tower. A barrier should be made at the base of the tower which will prevent children from going under the tower to the mobile mechanism;

c. for stopping the wind engine, special devices should be used in all cases which are available for this purpose in every wind engine. Stopping the wind engine by slowing down the wind wheel of the pinion or pulley by means of a lever is forbidden since an accident may occur with breakage of parts of the wind engine and possibly a misfortune.

REFERENCES

1. Aleksandrov, V. L., Tekhnicheskaya gidromekhanika [Hydromechanical Technology], Moscow, 1946.

2. Vershinin, I. B., Primeneniye malomoshchnykh vetroelektricheskikh agregatov v sel'skom khozyaystve, [Utilization of Low-Power Wind Power Installations in Agriculture], 1946.

3. Vetchinkin, V. P. and Polyakov, N. N., Teoriya i raschet grebnogo vinta [Theory and Computation of Screw Propellers], Moscow, 1940.

4. Vetchinkin, V. P., "Principles of Wind Utilization Elaborated by A. G. Ufimtsev," Proceedings of the First All-Union Conference on Aerodynamics, Moscow, 1932.

5. Vetchinkin, V. P., Akkumulyatory vetrovoy energii. Materialy po Kurskoy vetroelektrostantsii, [Storage Batteries of Wind Energy. Data of the Kursk Wind Power Station], 1935.

6. Vetchinkin, V. P. and Fateyev, E. M., Energetika i tekhnika vetroispol'zovaniya. Materialy Akademii nauk USSR, [Energetics and Technology of Wind Utilization. Papers of the Academy of Sciences of the USSR], 1936.

7. Zhukovskiy, N. E., Vetryanaya mel'nitsa NEZh. Polnoye sobraniye sochineniy N. E. Zhukovskogo, [The NEZh Windmill. Complete Collection of N. E. Zhukovskiy's Works], Vol. VI, 1937.

8. Zhukovskiy, N. E., Teoreticheskiye osnovy vozdukhoplavaniya, [Theoretical Principles of Aerostatics], Moscow, 1925.

9. Kazhinskiy, B. B. Rukovodstvo po ustanovke, remontu i ekspluatatsii vetrodvigateley v sovkhozakh, [Manual for the Installation, Maintenance and Operation of Wind Engines in Sovkhozes], Moscow, 1943.

10. Kazhinskiy, B. B., Gidroelektricheskiye i vetroelektricheskiye stantsii maloy moshchnosti, [Hydro- and Wind Power Stations of Low Power], Moscow, 1946.

11. Karmishin, A. V., Vetrodvigatel' TV-8. Sborka, pod'yem i ukhod za nim, [The TV-8 Wind Engine. Assembly, Lifting and Maintenance], 1937.

12. Karmishin, A. V., Vetrodvigatel' TV-8 (pravila ukhoda i tekhnicheskoy ekspluatatsii), [The TV-8 Wind Engine -- Maintenance Rules and Operation], 1947

13. Karmishin, A. V., Vetrodvigatel' TV-5 (pravila ukhoda i tekhnicheskoy eksploatatsii, [The TV-5 Wind Engine -- Maintenance Rules and Operation], 1947.

14. Kostyakov, A. N., Osnovy melioratsii, [Principles of Land Reclamation], Moscow, 1940.

15. Krasnov, V. S., Mekhanizatsiya trudoyemkikh protsessov v zhivotnovodstve, [Mechanization of Laborious Processes in Animal Husbandry], "Sel'khozgiz" Press, 1940.

16. Krasovskiy, N. V., "Method for the Computation of Wind Power Stations," Trudy TsAGI 43, (1929).

17. Krasovskiy, N. V., Kak ispol'zovat' energiyu vetra, [How to Utilize Wind Energy], "Energoizdat" Press, Moscow, 1936.

18. Krasovskiy, N. V., Vetroenergeticheskiye resursy USSR i perspektivy ikh ispol'zovaniya, [Wind Energy Resources of the USSR and Prospects of their Utilization], 1935.

19. Krasovskiy, N. V., "A New Wing for the Russian Windmill," Trudy TsAGI 4, (1923).

20. Makarevskiy, A. I., O raschete na prochnost' samoustanavlivayushchikhsya kryl'yev vetrodvigateley, [Strength Computation of Self-Adjusting Wind Engines], Materialy b. TsVEI, [Materials from the Central Wind Energy Institute], 1935.

21. Makarevskiy, A. I., Eksperimental'no-teoreticheskiye raboty Tsentral'nogo vetroenergeticheskogo instituta (TsVEI), [Experimental and Theoretical Studies of the Central Wind Energy Institute (TsVEI)], Byulleten' TsAGI, [Bulletin of the Central Institute of Aerohydrodynamics], 1933.

22. Makarevskiy, A. I., Sverkhmoshchnyi vetrodvigatel'. Sotsialisticheskiy zakaz izobretatelyam energokhozyaystva, [A Super-Powerful Wind Engine. Socialist Order to Inventors in the Energy Economy], 1932.

23. Molchanov, P. A., Aerologiya, [Aerology], MOscow, 1931.

24. Pavolovskiy, N. N., Gidravlicheskiy spravochnik OITI, [Hydraulic Manual of OITI], 1937.

25. Perli, S. B., Vetroelektricheskiye i vetronasosnyye agregaty, [Wind Power and Wind Pump Installations], Khark'kov, 1938.

26, Popov, S. G., Izmereniye vozdushnykh potokov, [Measurement of Air Flow],"Gostekhnizdat" Press, OGIZ, [Association of State Publishing Houses], 1947.

27. Pomortsev, M. M., "Concerning the Law of Distribution of Wind Velocities," Zapiski po gidrografii 15, (1894).

28. Proskura, G. F., Eksperimental'naya gidroaerodinamika, [Experimental Hydroaerodynamics], "Gosenergoizdat" Press, Khar'kov, 1933.

29. Rogozhkin, N. S., Remont i eksploatatsiya vetrodvigateley, [Maintenance and Operation of Wind Engines], Rostov on the Don, 1947.

30. Rozentul, S. L., Problema akkumulirovaniya pri vetrosilovykh ustanovkakh, [The Problem of Energy Storage in Wind Power Installations], Materialy b. TsVEI, [Materials from the Central Wind Energy Institute], Manuscript, 1934.

31. Sabinin, G. Kh., "Wind Engines with Self-Adjusting Blades," Trudy TsAGI 2.

32. Sabinin, G. Kh., "Theory of the Ideal Wind Engine," Trudy TsAGI 32, (1927).

33. Sabinin, G. Kh., "Performance of a Wind Engine in Relation to the Direction of the Wind," Trudy TsAGI 28, (1926).

34. Sabinin, G. Kh., "The Gyroscopic Effect of Wind Engines and Computation of Rotary Wind Engines," Trudy TsAGI 22, (1926).

35. Sabinin, G. Kh., "Theory and Aerodynamic Analysis of Wind Engines," Trudy TsAGI 104, (1931).

36. Sabinin, G. Kh., "Experimental Testing of the Theory of Wind Engines," Trudy Tsentral'nogo instituta eksperimental'noy gidrologii i meteorologii I(43), (1934).

37. Sabinin, G. Kh., "The TsAGI Wind Power Lagoratory," Trudy TsAGI 164, (1934).

38. Sektorov, V. R., "The Balaklava Experimental Wind Power Station," Elektrichestvo 19, (1938).

39. Sektotov, V. R., Energeticheskiye kharakteristiki VES s asinkhronnym generatorom, rabotayushchikh na obshchuyu set' [Energy Characteristics of Wind Power Stations with Asynchronous Generator, Operating in the General Circuit], 1947.

40. Smirnov, I. V., Inertsionnyi metod ispytaniya modeley vetryakov v aerodinamicheskoy trube, [The Inertia Method for Testing Models of Wind Engines in the Wind Tunnel], Materialy b. TsVEI, [Materials from the Central Wind Energy Institute], 1935.

41. Smirnov, I. V., Eksperimental'naya proverka klassicheskoy teorii vetryaka, [Experimental Testing of the Classical Theory of Wind Energy], Materialy b. TsVEI, [Materials from the Central Wind Energy Institute], 1931.

42. Ufimtsev, G. A., Problema anemofikatsii, [The Problem of Wind Energy Use], "Kurskiy Gubplan" Press, 1927.

43. Fabrikant, N. Ya., Kurs aerodinamiki, [Course in Aerodynamics], Part I, Moscow, 1938.

44. Fateyev, E. M., "Systems of Wind Engines," Energoizdat, 1933.

45. Fateyev, E. M., Vetrodvigateli v sel'skom khozyaistve [Wind Engines in Agriculture], "Sel'khozgiz" Press, 1939.

46. Fateyev, E. M., "Röle of Wind Engines in Animal Husbandries" Vestnik mekhanizatsii i elektrifikatsii 1, (1940).

47. Fateyev, E. M. and Shamanin, V. S., Rukovodstvo k izgotovleniyu kryl'yev vetryanykh mel'nits, [Instruction Manual for the Manufacture of Windmill Wings], NKZ RSFSR, [People's Commissariat of Public Health, Russian Soviet Federative Socialist Republic], 1941.

48. Fateyev, E. M., Kak povysit' moshchnost' suchchestvennykh vetryannykh mel'nits NKZ SSSR, [How to Increase the Power of Available Windmills of NKZ USSR], 1943.

49. Fateyev, E. M., "Windmills," Moskovskiy Bol'shevik, 1945.

50. Fateyev, E. M., "Wind Engines," Energoizdat, Moscow, 1946.

51. Florinskiy, M. M., Nasosnyye ustanovki i stantsii, [Pump Installations and Stations], "Sel'khozgiz" Press, 1946.

52. Chirkov, M. M., "Investigation of Wind Engines in the TsAGI Wind Power Laboratory," Trudy TsAGI 164, (1934).

53. Chirkov, M. M. and Vershinin, I. B., Eksperimental'naya proverka raboty VES parallel'no v set', [Experimental Testing of the Operation of Wind Power Stations Connected in Parallel], Materialy b. TsVEI, [Materials from the Central Wind Energy Institute], 1934.

54. Shirmanov, P. M. and Gorskiy, V. S., Atlas aerodinamicheskikh kharakteristik aviatsionnykh profiley, [Atlas of the Aerodynamic Characteristics of Aviation Profiles], "Gosaviaizdat" Press, 1932.

55. Yur'yev, B. N., Eksperimental'naya aerodinamika, [Experimental Aerodynamics], Part I, Moscow, (1939).

56. Yur'yev, B. N., Eksperimental'naya aerodinamika, [Experimental Aerodynamics], Part II, Moscow, (1938).

57. Yur'yev, B. N. and Lesnikona, N. P., Aerodinamicheskiye issledovaniya, [Aerodynamic Investigations].

58. Yur'yev, B. N., Vikhrevaya teoriya vintov, [The Turbulence Theory of Propellers], Publishing House of the Military-Aerial Engineering Academy N. E. Zhukovskiy, (1947).

Note: The references are given in the text in square brackets in numerical order.

PAGE IS
OF POOR QUALITY